



Geotechnique and Natural Hazards



A symposium sponsored by
The Vancouver Geotechnical Society and
The Canadian Geotechnical Society
May 6 - 9 , 1992

Geotechnique and Natural Hazards

A symposium sponsored by
The Vancouver Geotechnical Society and
The Canadian Geotechnical Society
May 6 - 9, 1992

GeoHazards '92 Organizing Committee

Alan Imrie	Chairman	B.C. Hydro
Debra Bowman	Conference Arrangements	Bowman Technical Services
Peter Byrne	Publications	University of B.C.
Bob Gerath	Technical Tours	Thurber Engineering Ltd.
Bruce Hutchison	Treasurer	B.C. Hydro
Graham Rawlings	Exhibits	Golder Associates Ltd.
Mike Roberts	Technical Program	Simon Fraser University
Wayne Savigny	Technical Program	University of B.C.
Bill Seyers	Secretary and Conference Arrangements	B.C. Hydro
Adrian Wightman	Publicity and Communication	Klohn Leonoff Ltd.

Printed and bound in Canada

Published 1992

Published and sold by:
BiTech Publishers Ltd.
903-580 Hornby Street
Vancouver, British Columbia
Canada V6C 3B6

ISBN 0 921095 24 4

Table of Contents

First Canadian Symposium on Geotechnique and Natural Hazards

Keynote Addresses

P.W. CAVE

**Natural Hazards, Risk assessment and land use planning
in British Columbia: Progress and Problems. 1**

L. S. CLUFF

Politics of seismic safety decision making 13

C.J. HICKSON

Volcanism in the Canadian Cordillera: Should we worry? 31

S.G. VICK

Risk in geotechnical practice 41

Session 1 - Seismic Hazards

G.C. ROGERS

The earthquake threat in southwest British Columbia 63

D.D. CAMPBELL and J.L. ROTZIEN

Deterministic basis for seismic design in B.C. 71

T.S. MURTY

Tsunami threat to the British Columbia coast 81

Session 2A - Landslides

N.A. SKERMER and D.F. VANDINE

Catastrophic impact of some historical mountain landslides. 91

D.P. MOORE, B.D. RIPLEY, and K.L. GROVES

Evaluation of mountain slope movements at Wahleach 99

K.L. MYERS

Landslide mechanisms in the cordillera 109

Session 3A - Landslides (continued)

V.A. DIYALJEE, and K. LI

Landslides caused by highway construction activity in slide prone terrain. 119

H.S. RADHAKRISHNA, M. BECHAI, K.C. LAU, K.T. LAW, and I. HALE

Nipigon River Landslide. 127

O. HUNGR

Runout prediction for flow-slides and avalanches: Analytical methods 139

Session 2B - Seismic Hazards (continued)

B.D. WATTS, W.C. SEYERS, and R.A. STEWART

Liquefaction susceptibility of greater Vancouver area soils. 145

E. NAESGAARD, A. SY and J.J. CLAGUE

Liquefaction sand dykes at Kwantlen College, Richmond, B.C. 159

J.D. BRAY, J-L. CHAMEAU, and S.GUHA

Seismic response of deep stiff clay deposits 167

R.J. DESCHAMPS, D.R. PUTZ and K.G. SUTTERER

Seismic hazard analysis for San Juan, Puerto Rico 175

Session 3B - Seismic Hazards (continued)

T.E. LITTLE, D.F.VANDINE and A. SUTHERLAND-BROWN

An airphoto study to locate ground surface rupture caused by the 1946 earthquake on Vancouver Island, British Columbia. 183

D.F. VANDINE and S.G. EVANS

Large landslides on Vancouver Island, British Columbia 193

K.W. SAVIGNY, D.C. SEGO and K.L. MACINNES

The Little Doctor Lake landslide, an example of coseismic reactivation of a landslide in permafrost terrain. 203

Session 4A - Risk Assessment and Land Use Planning

E.M. TIPPETT and M.C. ROBERTS

Natural hazards in mountainous environments: French and Austrian approaches to planning and zoning 211

<i>S.O.D. RUSSELL</i>	
Engineering decisions and natural hazards	219
<i>G.C. MORGAN G.E. RAWLINGS and J.C. SOBKOWICZ</i>	
Evaluating total risk to communities from large debris flows	225
<i>D.M. McCLUNG</i>	
Engineering aspects of land-use planning in snow avalanche terrain	237
<i>S. THOMSON, D.M. CRUDEN and J. De LUGT</i>	
Setbacks from the crests of slopes	243
<i>R.S. VON SACKEN, K.W. SAVIGNY, I. OLSEN and G. DAVY</i>	
A seismic risk assessment methodology for comparative assessment of multiple sites	251
 Session 6A - Risk in Geotechnical Practice	
<i>P.M. BYRNE and T. SRITHAR</i>	
Assessment of foundation treatment for liquefaction	263
<i>R.C. LO and E.J. KLOHN</i>	
Behavior of embankment dams in earthquakes	273
<i>P.M. BYRNE, H. JITNO and J. HAILE</i>	
A procedure for predicting the seismic response of tailings impoundments	281
<i>M. STEPANEK and H.F. McALPINE</i>	
Landslide dams at Clinton Creek	291
 Session 4B - Surface Hydrology and Debris Flows	
<i>V.J. GALEY, K. ROOD and O. HUNGR</i>	
Dynamics of hazards within watersheds	299
<i>M.J. BOVIS and T.H. MILLARD</i>	
Precipitation thresholds for debris flow initiation in the southern coast mountains of British Columbia	309
<i>R.J. FANNIN, T.R. ROLLERSON, D. HOGAN and D. DAUST</i>	
Characteristics of a large debris flow channel	311

Session 5B - Surface Hydrology and Debris Flows (continued)

D.E. CASS, B.F.I KENNING and G. RAWLINGS

The Philpott Road debris failures - Kelowna, BC 1990. The impacts of geology, hydrology and logging activities 319

B.C. ANDERSON, T.R. HAIGH, and C.D. SMITH

Geogrid reinforced soil and lock-block debris deflector for transmission towers 331

M. MILES, R. KELLERHALS and A.H. RICE

Performance of buried fibre optic telecommunications cable subjected to debris torrent events, Coquihalla corridor, British Columbia. 339

A.H. RICE, L.H.E. WERAN, K. SAVAGE and M. MILES

Relocation of buried high pressure oil pipeline subjected to potential flood hazard, Coquihalla River valley, British Columbia 347

Session 6B - Hydrology

P.R.B. WARD, N.A. SKERMER

The 50-year flood in Fitzsimmons Creek, Whistler, British Columbia 355

B.S. HART, D.B. PRIOR, T.S. HAMILTON, J.V. BARRIE and R.G. CURRIE

Patterns and styles of sedimentation, erosion, and failure; Fraser River delta slope, British Columbia. 365

L. JIANG and P.H. LeBLOND

Surface water waves generated by submarine landslides. 373

F. MOUTTE, J. LOCAT and P. THERRIEN

Numerical modeling of physical aspects of submarine debris flows 381

J. LOCAT

Viscosity, yield strength, and mudflow mobility for sensitive clays and other fine sediments. 389

J. VAUNAT, S. LEROUEIL and F. TAVENAS

Hazard and risk analysis of slope instability 397

S. EVANS

Landslides and river damming events associated with the Plinth Peak volcanic eruption, southwestern British Columbia. 405

Program

First Canadian Symposium on Geotechnique and Natural Hazards

08:00 08:15 **INTRODUCTORY REMARKS - Wednesday, May 6, 1992**

KEYNOTE ADDRESSES

08:15 09:00 J. COSTA - Landslide Dams

09:00 09:15 Discussion

09:15 10:00 L. CLUFF - The Politics of Seismic Safety Decision Making

10:00 10:15 Discussion

10:15 10:45 Coffee

Session 1 - Seismic Hazards

10:45 11:15 ROGERS, G.C. - The earthquake threat in southwest British Columbia

11:15 11:45 CAMPBELL, D.D. - Deterministic basis for seismic design in B.C.

11:45 12:15 MURTY, T.S. - Tsunami threat to the British Columbia coast

12:15 13:30 Lunch

Session 2A - Landslides

13:30 14:00 SKERMER, N.A. and VanDine, D.F. - Catastrophic impact of some historical mountain landslides

14:00 14:30 EVANS, S.G. - Landslides and river damming events associated with the Plinth Peak volcanic eruption, southwestern British Columbia

14:30 15:00 MOORE, D., Ripley, B.D. and Groves, K.L. - Evaluation of mountain slope movements at Wahleach

15:00 15:30 MYERS, K.L. - Landslide mechanisms in the cordillera

15:30 16:00 Coffee

Session 3A - Landslides (continued)

16:00	16:30	DIYALJEE, V.A. and Li, K. - Landslides caused by highway construction activity in slide prone terrain
16:30	17:00	RADHAKRISHNA, H.S., Bechai, M., Lau, K.C., Law, K.T. and I. Hale - Nipigon River landslide
17:00	17:30	LOCAT, J. - Viscosity and mudflow mobility for sensitive clays and other fine sediments
17:30	18:00	HUNGR, O. - Runout prediction for flow-slides and avalanches: Analytical methods

Session 2B - Seismic Hazards (continued)

13:30	14:00	WATTS, B.D., Seyers, W. and Stewart, R. - Liquefaction susceptibility of greater Vancouver area soils
14:00	14:30	NAESGAARD, E., Sy A., and Clague, J.J. - Liquefaction sand dykes at Kwantlen College, Richmond, B.C.
14:30	15:00	BRAY, J.D., Chameau, J-L. and Guha, S. - Seismic response of deep stiff clay deposits
15:00	15:30	DESCHAMPS, R.J., Putz, D.R., and Sutterer, K.G. - Seismic hazard analysis for San Juan, Puerto Rico
15:30	16:00	Coffee

Session 3B - Seismic Hazards (continued)

16:00	16:30	LITTLE, T.E., VanDine, D.F. and Sutherland-Brown, A. - An airphoto study to locate ground surface rupture caused by the 1946 earthquake on Vancouver Island, British Columbia
16:30	17:00	VANDINE, D.F. and Evans, S.G. - Large landslides on Vancouver Island, British Columbia
17:00	17:30	SAVIGNY, K.W., Segó, D.C. and MacInnes, K.L. - The Little Doctor Lake landslide, an example of coseismic reactivation of a landslide in permafrost terrain.

08:00	18:00	TECHNICAL TOURS - Thursday, May 7, 1992
-------	-------	--

08:00 08:15 **INTRODUCTORY REMARKS - Friday, May 8, 1992**

KEYNOTE ADDRESSES

08:15 09:00 S. VICK - Risk in geotechnical practice
 09:00 09:15 Discussion
 09:15 10:00 P. CAVE - Natural hazards, risk assessment and land use planning
 10:00 10:15 Discussion
 10:15 10:45 Coffee

Session 4A - Risk Assessment and Land Use Planning

10:45 11:15 TIPPETT, E.M. and Roberts, M.C. - Natural hazards in mountainous environments, French and Austrian approaches to planning and zoning
 11:15 11:45 RUSSELL, S.O.D. - Engineering decisions and natural hazards
 11:45 12:15 MORGAN, G.C., Rawlings, G.E. and Sobkowicz, J.C. - Evaluating total risk to communities from large debris flows
 12:15 13:30 Lunch

Session 5A - Risk Assessment and Land Use Planning (continued)

13:30 14:00 McCLUNG, D.M. - Engineering aspects of land-use planning in snow avalanche terrain
 14:00 14:30 THOMSON, S., Cruden, D.M. and de Lugt, J. - Setbacks from the crests of slopes
 14:30 15:00 VAUNAT, J., Leroueil, S. and Tavenas, F. - Application of risk analysis to slope instability evaluation
 15:00 15:30 VON SACKEN, R.S., Savigny, K.W., Olsen, I. and Davy, G. - A seismic risk assessment methodology for comparative assessment of multiple sites
 15:30 16:00 Coffee

Session 6A - Risk in Geotechnical Practice

16:00 16:30 BYRNE, P. and Srithar, T. - Assessment of foundation treatment for liquefaction
 16:30 17:00 LO, R.C. and Klohn, E.J. - Behavior of embankment dams in earthquakes
 17:00 17:30 BYRNE, P., Jitno, H. and Haile, J. - A procedure for predicting the seismic response of tailings impoundments
 17:30 18:00 STEPANEK, M. and McAlpine, H.F. - Landslide dams at Clinton Creek

Session 4B - Surface Hydrology and Debris Flows

- 10:45 11:15 GALEY, V.J., Rood, K. and Hungr, O. - Dynamics of hazards within watersheds
- 11:15 11:45 BOVIS, M.J. and Millard, T.H. - Precipitation thresholds for debris flow initiation in the southern coast mountains of British Columbia
- 11:45 12:15 FANNIN, R.J., Rollerson, T.R., Hogan, D. and Daust, D. - Characteristics of a large debris flow channel
- 12:15 13:30 Lunch

Session 5B - Surface Hydrology and Debris Flows (continued)

- 13:30 14:00 CASS, D.E., Kenning, B.F.I. and Rawlings, G. - The Philpott Road debris failures - Kelowna, BC 1990. The impacts of geology, hydrology and logging activities
- 14:00 14:30 ANDERSON, B., Haigh, T.R. and Smith, C.D. - Geogrid reinforced soil and lock-block debris deflector for transmission towers
- 14:30 15:00 MILES, M., Kellerhals, R. and Rice, A.H. - Performance of buried fibre optic telecommunications cable subjected to debris torrent events, Coquihalla corridor, British Columbia
- 15:00 15:30 RICE, A.H., Weran, L.H.E., Savage, K. and Miles, M. - Relocation of buried high pressure oil pipeline subjected to potential flood hazard, Coquihalla River valley, British Columbia
- 15:30 16:00 Coffee

Session 6B - Hydrology

- 16:00 16:30 WARD, P.R.B., Skermer, N.A. - The 50-year flood in Fitzsimmons Creek, Whistler, British Columbia
- 16:30 17:00 HART, B.S., Prior, D.H., Hamilton, T.S., Barrie, V.B. and Currie, R.G. - Patterns and styles of sedimentation, erosion, and failure; Fraser River delta slope, British Columbia
- 17:00 17:30 JIANG, L. and LeBlond, P.H. - Surface water waves generated by submarine landslides
- 17:30 18:00 MOUTTE, F., Locat, J. and Therrien, P. - Numerical modeling of physical aspects of submarine debris flows
- 18:00 22:00 **BANQUET ADDRESS - Friday May 8, 1992**
- HICKSON, C.J. - Volcanism in the Canadian Cordillera: Should we worry?

Saturday, May 9, 1992

Session 7 - Panel Discussion

- 09:00 Chairman: Professor N.R. Morgenstern

Keynote Addresses

stage following the completion of the previous one. In practice, of course, all four components tend always to move ahead together with new information and experience in one area leading to revisions and improvements in others.

This paper summarizes the program developed in Fraser-Cheam, drawing attention to major substantive and methodological issues. Based upon this experience, it then makes recommendations for improvement and assistance directed at both the scientific and engineering community and at the provincial and other governments.

Hazard Identification

Hazard identification in Fraser-Cheam is essentially a two-step process, the rationale for which has been described in greater detail elsewhere[1]. Under the Community Planning budget, and in the context of section 945 of the Municipal Act, it begins with an **overview geotechnical study** which is commissioned to identify those areas of land which appear to be free from the types of hazards listed in the Act. These overview studies are quite preliminary and are based largely on air photo interpretation with supplementary field reconnaissance. Therefore, the geotechnical engineer must draw the "safe line" cautiously and well clear of natural hazards. This is the area on which development is normally allowed to proceed without further geotechnical investigation unless building foundation conditions on site require special attention.

Outside of this "safe" area is a more

problematical "geotechnical study area" or "geologically sensitive area" within which exposure to risk may vary from virtually none to extremely high. Where portions of this "study area" are already developed, especially for residential uses, such that they may be exposed to existing hazards, Fraser-Cheam will normally proceed to the next investigative step which is the **secondary geotechnical study**. Typically, this will involve hip-chain and clinometer foot traverses, detailed geologic observations, topographic mapping, test pitting and specialist geotechnical skill in slope hazard investigation. Unlike the overview study, the secondary study will specifically identify those lands which are subject to hazards of various kinds and will assign return period probabilities to events of different magnitude. It tends to be the most elaborate and expensive phase of geotechnical investigation. Normally, the secondary study will increase the extent of the safe area as improved knowledge allows the geotechnical engineer to be more definitive.

Under B.C. statute, the onus falls upon the developer to undertake **site-specific geotechnical studies** prior to receiving development permits or building permits[2]. These studies are more limited and focused, but also much more numerous, with over 150 examples in Fraser-Cheam compared with 7 overview and 12 secondary studies. Generally, they contain recommendations respecting hazard avoidance or mitigation measures, some of which can be fully implemented during the construction phase while others relate to on-going maintenance or monitoring.

Evaluation

Evaluation of these hazards, once identified, is essentially a matter of determining the levels of risk which are acceptable for various types of development. These **hazard acceptability thresholds** will depend upon the specific nature of the hazard and upon the density of use of the land and hence upon the level of exposure or risk. Where risks exceed these thresholds, hazard mitigation measures have to be considered, including protective engineering and, under certain circumstances, legal devices designed to transfer liability. Because complete hazard avoidance (zero exposure) is less realistic in some areas than in others, acceptability thresholds have to be determined regionally, or perhaps provincially, and cannot yet be expected to be consistent from one geological and climatic zone to another.

In Fraser-Cheam, acceptability thresholds have been defined in some detail for eight different types of natural hazard[3]. They represent a codified summary of the many previous decisions of the elected Regional Board which in turn were based partly on limited provincial guidelines (respecting flood hazards and subdivision approvals), partly upon legal precedent[4], and particularly upon advice from engineers and staff. Typical examples are shown in Figure 2, which describes the regulatory response to various types of applications for residential development in the face of rockfall, debris flood, catastrophic landslide, and Fraser River flood hazards. Other thresholds are applied to stream avulsion, debris flow, minor landslip and snow avalanche hazards. Thresholds are higher for those applications which involve

higher densities of use, and therefore greater risk (i.e. higher overall exposure to the hazard), and for those hazards which pose a greater threat to life. Note also that a spectrum of conditions may be attached to any given approval to reflect strategies of hazard prevention, avoidance, mitigation, protection and liability transfer, as appropriate to the situation.

Policy, Regulation, Approval and Enforcement

Five separate sections of the **Municipal Act** empower local governments to develop policies and regulations to implement these hazard acceptability thresholds[5]. Each must be adopted by a bylaw as opposed to a resolution, permit, agreement, contract or administrative procedure. Public and provincial government input into the process, including a public hearing where necessary, is specified in Part 29 of the Act. Community plans, development permit areas, zoning bylaws, flood-plain and tree-cutting bylaws all form part of an integrated policy and regulatory program. Its components should be clearly spelled out in the bylaws and should be made understandable to the public through appropriate brochures and information packages directed at those who may be affected. Otherwise, consistent implementation of the program and public support or compliance is almost impossible to achieve.

Development approval through rezonings, development permits, subdivision approvals, building permits and agreements is a complex technical field involving the use of a whole array of legal

Type of Project	Rockfall: Small-Scale Detachment					Debris Flood			
	Annual Return Frequencies					Annual Return Frequencies			
	1:100	1:100-1:500	1:500-1:1000	1:1000-1:10000	<1:10000	1:50	1:50-1:200	1:200-1:500	1:500-1:10000
Minor Repair (<25%)	5	2	1	1	1	2	2	1	1
Major Repair (>25%)	5	4	2	1	1	4	4	1	1
Reconstruction	5	4	2	1	1	4	4	3	1
Extension	5	5	4	1	1	4	4	3	1
New Building	5	5	4	1	1	4	4	3	1
Subdivision (infill/extend)	5	5	5	4	1	5	5	4	2
Rezoning (for new community)	5	5	5	5	1	5	5	5	3

Type of Project	Major Catastrophic Landslide					Inundation by Fraser River			
	Annual Return Frequencies					Annual Return Frequencies			
	1:200	1:200-1:500	1:500-1:1000	1:1000-1:10000	<1:10000	1:40	1:40-1:200	1:200-1:500	1:500-1:10000
Minor Repair (<25%)	5	2	1	1	1	2	1	1	1
Major Repair (>25%)	5	5	2	1	1	4	3	3	1
Reconstruction	5	5	5	1	1	4	3	3	1
Extension	5	5	5	1	1	4	3	3	1
New Building	5	5	5	1	1	4	3	3	1
Subdivision (infill/extend)	5	5	5	5	1	5	4	4	1
Rezoning (for new community)	5	5	5	5	5	5	5	5	1

1. Approval without conditions relating to hazards.
2. Approval, without siting conditions or protective works conditions, but with a covenant including "save harmless" conditions.
3. Approval, but with siting requirements to avoid the hazard, or with requirements for protective works to mitigate the hazard.
4. Approval as (3) above, but with a covenant including "save harmless" conditions as well as siting conditions, protective works or both.
5. Not approvable.

Figure 2. Hazard-related Responses to Development Approval Applications.

instruments. For the most part, final approval is an administrative process, as opposed to a political one, such that the applicant is required to satisfy the concerns and meet the standards identified in the policies, and relatively little discretion is involved.

Having issued a development approval, enforcement proceedings or remediation measures must be taken if the project deviates from the geotechnical safety conditions imposed in the permit. Unfortunately, this is an area of statute in which there remain some gaps in B.C., particularly with respect to hazardous situations induced by unsound earth-moving or similar activity and with respect to the locus of liability following public sector intervention. Perhaps these gaps are more apparent than real and reflect only the recency of the statutes. As case law develops, the extent of local government's duty of care for geotechnical hazards will become better defined and only then will the full implications of the amendments enacted in the 1980's become clear.

II. Problems

Based on experience with integrated programs such as the one in Fraser-Cheam, it is possible to identify those aspects of the system which remain inadequate. The analysis and recommendations which follow are grouped in terms of the improvements which are necessary in data collection, data distribution, interpretation, program design and implementation. Overall, this review of the strengths and weaknesses of

the system suggests that the regulatory framework is somewhat ahead of the science and its institutional support system.

Data Collection

Academic research in the field of natural hazards tends to focus on process, rather than on place, in the hope of developing an understanding which would have general applicability in other situations. As a result, there are many examples of potentially hazardous situations which have not been subject to intensive study despite their significance from a public safety point of view. Moreover, there is no agency with a clear mandate and funding to remedy this deficiency and systematically review the extent to which each area may be exposed to hazards.

A case in point was the research conducted into the possibility that Mt. Breakenridge, on the shores of Harrison Lake in Fraser-Cheam, could perhaps be the source area for a future catastrophic landslide and resultant tsunami-type wave which could devastate the shoreline[6]. Helicopter reconnaissance seemed to suggest that the threat may be real; but there was no institutionalized system for assessing the need for action and in any case the costs of a meaningful investigation were far beyond the local government's resources. To its credit the provincial government provided special funding under the Provincial Emergency Program and, fortunately, the study found the mountain to be more benign than first feared. Despite good science and responsible actions by the Province, however, the exercise revealed serious

flaws in the system.

First, the linkage between PEP and geotechnical research is not a good one from a public relations perspective, at least until the existence of a serious hazard is proven, because it only lends weight to the many sceptics who doubt the value of any such work on the predictability of natural hazards. The positive findings, rather than prompting critical review and feelings of relief, tended to be disparaged and the whole study cited as an example of bureaucratic over-anxiety. Furthermore, once the prospect of an emergency was dispelled, it was very nearly impossible to obtain the funding necessary to return to the site and take readings from the extensometers which had been installed to monitor the tension cracks.

Secondly, the lack of any routine, objective, scientific, comparative review process necessarily forced an *ad hoc* decision on whether to devote scarce resources to research this one particular problem, as opposed to any one of several dozens of other potentially hazardous situations in the Province. Matters of liability and political credibility inevitably factor into such decisions, but there is no doubt that the system would be served better if there existed a standing committee of qualified professionals whose role it was to review the merits of, and assign priorities to, research directed at public safety.

These problems could be remedied by the establishment of a structured and on-going program of research, with objectively defined priorities, under the auspices of the B.C. Ministry of Environment. This is not to argue that local government's existing mandate for geotechnical study in official community plans should be changed, or

that developers should not be required to undertake site-specific studies when there is a known problem. Rather, the analogy is drawn to seismic and geophysical hazards, and to meteorological hazards, for which it is generally agreed that the public sector has the primary responsibility to identify zones of risk. The B.C. government has accepted this position with respect to flood hazards and has taken a lead role in regulation, but responsibility for other geotechnical hazards has been delegated to local government without the benefit of systematic research having been undertaken.

Data Distribution

The need to establish some form of central registry for geotechnical reports was one of the principal recommendations to flow from the provincial Geologic Hazards Workshop in 1991 which brought together more than 130 experts on various aspects of geologic hazards and public safety from B.C, Yukon, Alberta and Washington State for a meeting at the University of Victoria[7]. The workshop reviewed existing knowledge, on-going research, current legislation and implementation techniques and concluded that the B.C. Geological Survey should establish and operate the registry as a central data-base for this vital information. For its own area, Fraser-Cheam already maintains such a data-base, but there is no doubt that ready access to a more comprehensive reference source would enhance the quality of site-specific studies while limiting their cost. Indeed, one of the principal shortcomings of these limited-budget private commissions is their failure to consult

previous relevant work on a consistent basis.

Professional Standards

Recognition of the professional significance of the 1985 legislation has been rather slow to develop within the engineering community. It remains an alarming fact that some professionals are still not fully aware of the statutes, and of the implications of the requirement for "certification"[8]. Amongst the great preponderance of good reports, for example, Fraser-Cheam has received too many which are either substantively incompetent, prematurely presented (with inadequate evidence) or otherwise fatally flawed. The results are almost always difficult and embarrassing both for the client and the regulator. Examples include a study which denied the possibility of an erosion hazard at a proposed building site on the active soft alluvial floodplain of a fast flowing mountain river, a study which identified a serious landslide hazard affecting private land which later proved to be false, and reports insensitive to the regional geotechnical context of their subject because of failure to consult previous work. Even the method and timing of reporting, not simply the matter of substance, is critically important in the light of present legislation. The guiding principles for any report affecting public safety must be prudence and caution, but premature announcements of negative findings, unless supported by irrefutable evidence, can be almost as destructive as unwarranted optimism and can easily attract liability.

This is not the place to recommend any specific actions which should be taken by professional associations to remedy these problems. However, there is clearly a need for these organizations to increase the level of awareness of the legislation and to define some standards for geotechnical reports to meet. In their absence, Fraser-Cheam has compiled a preliminary list of criteria against which to evaluate the acceptability of geotechnical reports[9], including the requirement that the engineer show evidence that previous work has been consulted. This does not, however, provide a proper substitute for guidelines from a professional association.

Methodology

Given the rapidly developing state of knowledge in the science, it is perhaps inevitable that geotechnical reports display an inconsistency of methodology which makes them difficult to compare and to implement. This diversity may be creative rather than negative; convergence cannot be anticipated until a consensus has developed within the scientific community. Nevertheless, there are certain methodological principles which could be agreed upon immediately if professional leadership were present.

One source of confusion, for example, is the distinction for subdivisions between those geotechnical reports which detail "hazard free" or "safe building areas" and those which identify "safe building sites". The one type of study will review geotechnical conditions over the entire parcel to be subdivided and will demarcate a "safe line" which is then locked in by

means of a covenant against further re-subdivision or future development of the lands beyond the surveyed safe line. The simpler and cheaper, "safe building site" study is more suitable for one- or two-lot subdivisions particularly in areas where future re-subdivision is unlikely. In these studies, the engineer restricts his report and certification to the future proposed building site, and the geotechnical conditions which may affect it, leaving remaining areas to be studied at some date in the future. In this case, the covenant will require that the new building occur only within the approved site and will commit a future owner to undertake additional geotechnical study before any other portion of the land can be developed.

A second and more profound source of confusion concerns the use of probability statements to express the uncertainty inherent in predicting natural hazards. From a regulatory perspective there is a clear need to distinguish between those probability statements which describe uncertainty as to the **timing** of an event which is considered to be virtually inevitable to occur in the long run and those in which the probability statement expresses uncertainty as to whether the event will **ever** occur. The latter has scientific value and may accurately describe the (uncertain) state of knowledge, but it provides no credible basis for land use regulation. Too often are these types of statement presented as equivalent when in reality they are fundamentally different.

Finally, in terms of specific methodology, professional engineers and geoscientists should make a particular effort to incorporate Quaternary geologic and geomorphologic evidence and, where

necessary, they should provide the same level of detailed support mapping for these surficial features as is normal for structural elements. Reports should be set in a regional geomorphological context and should contain lines of reasoning and judgement in sufficient detail to allow an independent professional review, where necessary, by the approving authority.

Interpretation

Despite the success in applying the acceptability thresholds adopted locally by Fraser-Cheam Regional District, there is no doubt that thresholds defined provincially would be preferable and easier to administer. Already the provincial government has provided guidance in the context of flooding and subdivision. A more complete set of guidelines would make it easier for local authorities to obtain compliance and would assist the professional community in standardising the content of reports. It would also help to clarify such matters as liability and the effect of hazards on property values in relation to insurance and mortgage equity. Given all the other problems in the geotechnical field, it may still be somewhat premature to expect definitive guidelines from the Province. In the long run, however, acceptability thresholds will not be set by local government. They will be defined at the provincial level either by the government or by the courts, and the latter would involve a much longer and more painful process.

Program Design

Amongst the shortcomings of the hazard land management and development control program illustrated in Figure 1 is the fact that it is conceived as a linear and a "one time" decision process. This limitation is not surprising because it reflects the statutory basis of the program in regulating new development. Inherently this fails to recognise that hazards do not exist only at one point in time. Their probabilities are not static; they are dynamic and will change along with geotechnical conditions (such as the quantity of debris in a stream channel) and with science's ability to predict.

Although most geotechnical engineers will recommend some form of monitoring as an integral part of their certification, few agencies at the local level are able to commit to such a program over the long term. Noteworthy is the fact that the Ministry of Environment, which oversees the flood protection program, routinely monitors the snow-pack prior to the spring freshet, and the Ministry of Highways monitors and scales unstable rock slopes and potential snow avalanches which pose a threat to provincial roads. Techniques are becoming increasingly sophisticated and reliable and there is no doubt that monitoring is a valuable adjunct to hazard avoidance and protection. Local governments, on the other hand, do not have the resources to do the same kind of monitoring even of those slopes which may have been given only conditional safety certification prior to development.

This deficiency must be corrected if the hazard land management program in the Province is ever to become reliable,

consistent and fully accepted by the population. An established monitoring program will permit a more flexible, sensitive and "common sense" response to development applications. As an aid to its establishment, it would be useful if geotechnical reports would be more specific as to the nature, frequency and cost of the monitoring which is recommended. Local governments might then be able to seek an endowment fund at the time of development, or might introduce a tax levy against the new development sufficient to pay the costs of the required monitoring.

Implementation

The recent review of geotechnical programs completed for the Ministry of Municipal Affairs identified surprisingly few gaps and inconsistencies in the statutory framework[10]. A hazard land management program would certainly be easier to implement if there were clear authority to intervene in situations where earth-moving (for driveway construction or any other reason) was creating a condition of instability which did not previously exist. Such activity rarely requires a permit, and in its absence intervention and remediation is not mandated. Implementation would be easier, too, in difficult cases where things have gone wrong, if local government were empowered to recover the costs of enforcement and remediation on the taxes against the property and if there were protection from liability in the event that the best efforts of the municipality to effect a solution prove ultimately to be unsuccessful. Perhaps the statutes could help, too, by making explicit reference to

the funding and liability issues of long-term monitoring activities.

Nevertheless, these are not the primary difficulties in regulating development in the context of risk from natural hazards. Much more problematical is the relatively primitive state of geotechnical science today, the lack of funding to permit adequate research and the lack of agreement as to methodology and as to hazard acceptability thresholds. Certainly some of the work being undertaken in B.C. is exemplary and some geotechnical reports are penetrating and profound. However, given the inconsistent quality of reports, the number of differing opinions and the variable state of knowledge available to the decision-maker at the critical time, it is sometimes easy to believe that the geotechnical community as a whole is not yet ready to have its advice form the basis for statutory regulation. For those planners and politicians who dread the alternative, and for the sake of public safety as a whole, the hope must be that these problems will be rapidly overcome.

References

1. Cave, P.W., H. Sloan, R.F. Gerath. Slope Hazard Evaluations in Southwest British Columbia, Procs. Canadian Geotechnical Conference, Tome I, Univ. Laval, October 1990.
2. Municipal Act, Sections 976(8) and 734(2).
3. Cave, P.W. Hazard Acceptability Thresholds for Development Approvals by Local Government, B.C. Geologic Hazards Workshop, Victoria, February 1991.
4. Berger, T.B., Reasons for the judgement of the Honourable Mr. Justice Berger on the matter of the Land Registry Act - and an application for approval of a proposed subdivision by Cleveland Holdings Ltd., Supreme Court of British Columbia, 1973.
5. Cave, P.W., Legal Instruments and Techniques for Implementing Hazard Land Planning Policies in British Columbia, report to the Ministry of Municipal Affairs, January 1992.
6. Mount Breakenridge Slide Phase 2 Study, Thurber Consultants, February 1990.
7. Jackson, Lionel E., Ed., Recommendations of the Geological Hazards Workshop, July, 1991, available from Geological Survey of Canada, Vancouver office.
8. Municipal Act, Section 734(4) which requires "certification".
9. Cave, P.W., 1992, op. cit.
10. Cave, 1992, *ibid.*

Politics of Seismic Safety Decision Making

Lloyd S. Cluff

*Commissioner, California Seismic Safety Commission
San Francisco, California*

Abstract

California and British Columbia have much in common: economic vitality, spectacular natural beauty, and attendant natural hazards, including earthquakes. Earthquakes have the potential to cause catastrophic losses, particularly when buildings and structures are located, designed, and built without taking earthquake forces into consideration. Although most of our modern buildings and structures have considered the potential effects of earthquakes, many of the older ones have not. One of the most vulnerable classes of hazardous buildings in California is state-owned buildings. This class of buildings has been the focus of significant attention since about 1979, when state-owned buildings were identified as a crucial problem that needed immediate attention. Unfortunately, competing social needs have taken priority over funding of seismic safety improvements, and progress to improve state buildings has been slow. The occurrence of damaging earthquakes has been the prime motivating factor in causing the formulation of earthquake safety policy. During the legislative session following the 1989 Loma Prieta earthquake, 443 bills were introduced that addressed seismic safety—more than 20 times that of previous sessions.

Background

California and British Columbia have much in common. Both are lands of economic vitality and cultural diversity. Both have great natural beauty, drawing residents and international visitors alike to their mountains, lakes, forests, and coastal areas. California and British Columbia also have another thing in common. Along with their natural beauty come natural hazards, particularly from earthquakes, volcanic eruptions, and landslides.

I would like to focus on earthquakes, and how earthquakes have affected California, particularly from the viewpoint of providing opportunities for improving seismic safety. Many of the difficult lessons Californians have learned, the successes we have had, and the mistakes we have made may be of value to British Columbians in making improvements in their seismic safety.

Everyone in California is affected by the occurrence of a major earthquake, whether due to direct damage, or

indirectly, due to increased taxes, loss of utilities and infrastructure, or reduced economic activity. In 1980, the National Security Council [1] estimated that a single large California earthquake would potentially cost tens of thousands of lives, and from \$20 to \$80 billion in damage. In terms of today's values, total damage costs are estimated to run much higher; the combined direct and indirect losses could exceed \$120 billion for a major earthquake near a highly populated region.

Recent scientific research [2, 3] tells us there is a high probability of one or more major earthquakes striking either Southern or Northern California within the next three decades. Given this high likelihood of destructive earthquakes and the estimated huge losses, prudence dictates that actions be taken to manage and minimize the risks. However, recognizing that California must mitigate earthquake vulnerabilities and be better prepared for future damaging earthquakes is not enough to cause corrective actions to be taken.

One of my primary messages is that implementation of earthquake safety measures often depends on *timing*. Destructive earthquakes can be viewed as an asset in that they motivate decision makers to take swift and positive action for the long term improvement of seismic safety. When an earthquake occurs, there are tremendous advantages to being able to get the right information to the right people at the right time.

Most of California's legislation to improve seismic safety was enacted following destructive earthquakes. For example, the San Francisco earthquake in 1906 was the impetus for the

formation of a state commission to investigate the causes and effects of earthquakes and how these effects could be considered in future construction [4]. The 1933 Long Beach earthquake, which caused the collapse of many schools, resulted in the passage of the Field Act requiring that all California public elementary schools be properly designed to resist earthquakes. Following the 1964 Alaska and 1967 Caracas, Venezuela, earthquakes, California formed a Joint Legislative Committee on Seismic Safety. The purpose of the committee was to evaluate seismic safety improvements and make recommendations to the Legislature. The 1971 San Fernando earthquake damaged hospitals and freeways, triggering passage of a state hospital act that required all new hospitals to be designed to resist earthquakes and remain functional. Funding was also made available for research on highway bridges and overpasses [5]. In 1975, these activities culminated in the formation of the California Seismic Safety Commission.

Following the Mexico City earthquake in 1985, California's State Legislature enacted the California Earthquake Hazards Reduction Act of 1986. This act directs the California Seismic Safety Commission to prepare and administer the California Earthquake Hazards Reduction Program [6]. The program is aimed toward the development and implementation of new and expanded activities to significantly reduce the risk of earthquakes to the citizens of California by the year 2000. This program is now in its sixth year of development and implementation, and continues to evolve through a series of initiatives to achieve results. Initiatives are modified and added as knowledge is

gained, and each year a progress report is prepared for the Governor and the Legislature. The second five-year plan was presented to California public-policy makers in September 1991.

Statewide expenditures by state agencies for earthquake hazard mitigation, emergency planning, and disaster preparedness during 1987 was \$75 million. After the occurrence of the Loma Prieta earthquake in 1989, the annual expenditure was doubled. This excludes about \$700 million the California Department of Transportation has been appropriated to improve the seismic safety of California's bridges and overpasses. The program has identified several crucial seismic safety issues where a combined price tag could be on the order of \$10 billion before significant progress can be claimed. Given the current unfortunate condition of the California budget deficit, it is likely that we will be far from achieving the goals of the Earthquake Hazards Reduction Act by the year 2000. Even so, much progress has been achieved and many lessons have been learned.

State-Owned Buildings; One of the Greatest Risks

Efforts to identify hazardous buildings began in earnest in the aftermath of the 1971 San Fernando earthquake, where 65 lives were lost and economic losses exceeded \$500 million. In a 1979 study by the Seismic Safety Commission [6], unreinforced masonry construction, nonductile concrete frame buildings, and buildings designed prior to the introduction of adequate seismic codes were identified as potential collapse hazards. Many of the existing hazardous

buildings are owned by the State of California and the federal government.

A significant number of state-owned buildings are owned by the University of California. In 1975, the University worked closely with the Seismic Safety Commission to develop a method for evaluating and classifying their buildings into categories of expected performance during earthquakes. The ratings were expressed in subjective terms:

Rating	Expected Life-Safety Impact
Good	Minimal effect on life safety
Fair	Low life-safety hazards
Poor	Significant structural hazard and appreciable life-safety hazards
Very Poor	Extensive structural damage, collapse resulting in high life-safety hazards

It was felt that this way of evaluating buildings was more useful than calling buildings *safe* or *unsafe*.

The study of the University buildings found that at least 20 percent rated poor or very poor and urgently needed strengthening or demolition. In 1980, cost estimates to improve the seismic safety of University buildings exceeded \$500 million. Progress has been slow due to a lack of funds and competing demands on the short supply of resources. This point is well-illustrated by the proceedings of a public hearing that focused mostly on the University portion of state-owned buildings.

Public Hearing on the Seismic Vulnerability of State-Owned Buildings

Ten years after the Seismic Safety Commission's report on state-owned buildings, and one month short of one year before the occurrence of the Loma Prieta earthquake, the California Seismic Safety Commission held a public hearing on the seismic vulnerability of state-owned buildings. The hearing was conducted as part of the Commission's regular monthly meeting, and was held on the UCLA campus, one of the University campuses having a significant number of buildings in the poor and very poor categories [8].

As Chairman of the Commission in 1988, I chaired the hearing. I reiterated that the problem of collapse-hazard buildings in California is a major Commission concern, and stated that the hearing would focus on the buildings owned and operated by the state, especially those in the University of California system. The hearing was to illustrate the process of deciding what level of safety is acceptable. One of my objectives was to assure that the Commission focused on the process, and stimulated positive action. The Commission was to help define the problems, determine why the problems existed, identify the likely consequences if the problems were not corrected, and help define what could be done and how much it might cost. The objective was to decide the level of risk that was acceptable.

I noted that, looking at past efforts to strengthen state-owned buildings, it was clear that not a lot had been accomplished. Consequently, it could be concluded that the state believed that the

existing level of seismic risk was acceptable. Most would agree this is not the case; however, individuals in responsible positions did not clearly understand the magnitude of the problem or how it could be corrected. One of the purposes of the hearing was to cause these individuals to better understand the problem, and to try to motivate them toward giving seismic safety a higher priority.

The test of acceptability should be a process of considering the level of safety that is acceptable once the likelihood of earthquakes and the consequences are clear. (The occurrence of destructive earthquakes often assists in this understanding.) One must assume the earthquake will occur today, and then consider whether the consequences would be acceptable.

The following excerpts from the minutes of the meeting illustrate some of the difficulties California is facing with regard to deciding what level of seismic safety is acceptable.

University of California, Statewide - I introduced Mr. Jack Burnett, Director of Facilities Management and Construction, Office of the President, University of California. Parts of his testimony follow.

The 1971 San Fernando earthquake created interest in hazard mitigation. In that same year, the Office of the President directed University of California campuses to conduct preliminary studies and report on the structural soundness of existing buildings. The state budget for 1974-75 contained an appropriation of \$10 million for

seismic and other life-safety hazard mitigation projects. However, only \$1.5 million was used to complete two seismic projects.

In January of 1975, the Regents adopted a seismic safety policy intended to provide an acceptable level of safety for students, faculty, employees, and the public who occupy and use university buildings and facilities. Key points addressed in the policy include:

- Establishing responsibilities of university administrators,
- Developing a program for abatement of seismic hazards,
- Using a consulting structural engineer for review,
- Establishing standards for rehabilitation projects and new structures.

The University of California policy requires independent review of each major capital improvement project by a credible structural engineer well-versed in seismic engineering. "Value engineering" (project quality management) is practiced on major projects. This review involves architectural and structural aspects as well as cost. The initial 1971 survey looked mostly at older buildings, those that were suspected of not being structurally sound. The 1977 study was a preliminary seismic evaluation of the principal buildings in the University of California system. The report, completed in June 1978, reviewed 750 buildings with about 45

million square feet of space. Buildings were rated according to the expected performance of the structure during an earthquake. About 20 percent of the buildings were rated poor and very poor.

Since the 1974-75 budget appropriation, the University has continued to work with the State Department of Finance, the Legislative Analyst, and the Seismic Safety Commission to more clearly identify seismic safety problems that exist in University structures. A list of state buildings in priority order was developed by the Seismic Safety Commission in April 1981. Twenty-six of the top 50 buildings listed, and 14 of the top 25 buildings listed, were University of California structures. In 1981, the Budget Act appropriated funds for more detailed engineering and cost studies of the first seven buildings on that list. These studies have been completed and a request for project funding to correct the seismic hazards has been included in the annual Regents' budget for the last several years. The request includes projects involving seismic structural corrections only, and general renovation projects that include seismic structural corrections.

Progress on the elimination of seismic hazards in state-funded buildings has been limited because of a lack of funds. The University has continued to work on seismic correction problems in its nonstate-funded facilities over the years, and has taken upon itself

the responsibility to correct nonstructural seismic problems, such as falling hazards, using the operational budget. The University intends to continue working diligently to make seismic corrections. A bond issue of \$350 million will not come close to solving the University's seismic problems. It is estimated that it would cost in excess of a billion dollars to solve the University of California's statewide seismic safety problems.

University of California, Los Angeles - I introduced Chancellor Charles E. Young of UCLA. Portions of his testimony follow.

The seismic risk on the UCLA campus is not acceptable. We have been trying to reduce the unacceptable risks since 1972, with little success. UCLA's problems include buildings built before 1933, a number of buildings built between 1933 and 1972, and three active faults close to the campus. In 1972, UCLA developed a plan to improve dangerous buildings to a level where they would not be dangerous, or where the danger was substantially mitigated. A decision was made at that time that nothing could be done until the state's total earthquake problem was surveyed, analyzed, and reviewed.

It is interesting to note the rationalization used here to justify why UCLA could not correct the problem. Their strategy was to defer the issue until the state as a whole dealt with it.

In the meantime, UCLA decided to deal with all the buildings we could deal with; that is, buildings funded by nonstate sources. We have a timetable that will bring certain buildings, such as the student union, to a level where the danger to inhabitants and individuals around the buildings will be at a minimum.

UCLA has done a number of analyses over the years, but the most recent and important determined what could be done to eliminate or substantially mitigate the danger to persons who inhabited the buildings or were around the buildings, even though the work might not be enough to save the buildings. The study concluded that we could do the kind of mitigation that would reduce dangers to individuals, but not save buildings to the point of being able to use them after the earthquake, for substantially less money than it would cost to bring the buildings up to a higher standard.

UCLA has developed a plan to do this, and we have proposed to seek funding from the state through a bond issue for a multi-year, multi-project program. This gives us legislative approval to retrofit one building after another. We have prepared a 15-year program to accomplish the work required, scheduled according to the danger involved. When completed, this program would result in a level of risk where there is minimal likelihood of endangering the persons inhabiting the buildings,

or in the proximity of the buildings.

UCLA hopes that the program will be included in the University of California building program approved by the Governor and the Legislature as part of the bond-financed program so the work does not compete with UCLA's academic program needs. New facilities are needed for new programs on all of the campuses. When seismic safety programs compete with those other needs, quite often the seismic safety programs do not get funded.

We have moved forward on the residence halls, student union, student activities buildings, and parking structures by making minor capital improvements such as seismic anchoring. We have invested several hundreds of thousands of dollars into that program over several years, and in the last week or two have added substantially more funds to the program.

Chancellor Young said UCLA would appreciate the Commission's help in getting others to understand the importance of seismic projects, and in helping UCLA to obtain funds. He believes the risk is one that cannot be ignored; however, he is in a difficult position. Campus teaching and research programs must be continued, and it is impossible to abandon the buildings that are seismically below par. As a result, they take the risk. He believes they should not have to take that risk.

Chancellor Young wanted the Commission to understand the continuing work of UCLA's Earthquake Safety Committee, which he had appointed five years previously. He introduced Professor Aroni, Chairman of the Committee. Excerpts from Professor Aroni's testimony follow.

The task of the Earthquake Safety Committee has been to review seismic safety on the campus, make recommendations, and monitor progress. The Committee has been expanded to include representatives of the undergraduate and graduate student governments and staff assembly. The committee has investigated many things, including the possible failure of an old earthfill dam above the campus. The campus has ten pre-1933 buildings. One-third of all buildings on campus are either poor (nine) or very poor (fifteen), and all are high on the statewide benefit/cost priority list.

The Committee recommended a study of chemical, biological, radiation, and fire dangers associated with earthquakes. This study has been completed, and recommendations are being implemented. The Committee also recommended development of a comprehensive earthquake preparedness plan that includes the medical center and critical facilities on campus.

The Committee's unanimous conclusion is that UCLA is a campus at risk, facing a potentially devastating catastrophe in the next

great Southern California earthquake, unless energetic measures are taken, particularly with respect to the vulnerable buildings. An estimated 1500 to 2000 deaths could be caused in these buildings. Many more would be injured, and UCLA's ability to function would be destroyed. Approximately \$150 million is needed to strengthen the 24 state-owned University buildings.

Professor Aroni concluded with four points I thought interesting:

1. *Studies are essential, but they are unimportant. Only by implementing the conclusions of the studies can safety be achieved.*

2. *Three weeks earlier, UC President David Gardner had presented to the Board of Regents a study on the future of the UC system. By the year 2005, an estimated 63,000 additional students would be added to the 154,000 currently attending the nine UC campuses. Three new campuses are needed within the next 12 years, at a cost of \$300 million each. Under these circumstances, it makes sense for the state to invest \$100 or \$150 million to save a great campus.*

3. *All segments of the campus community support the efforts of seismic upgrading. Resolutions have been passed unanimously by the legislative assembly of the Academic Senate and the undergraduate and graduate student associations. The*

resolutions called for permitting seismic corrections to proceed expeditiously, without necessarily undertaking other life-safety requirements.

4. *He urged the Commission to provide its full vocal and energetic support for legislation to authorize needed bonds to finance the seismic upgrading as soon as possible.*

I asked the UCLA representatives if UCLA would be willing to sponsor legislation, with the Commission in a supporting role. Professor Aroni said that he would hope that a whole array of bodies—the UC President's Office and representatives of the rest of the state educational system—would sponsor such legislation, which the Commission then could endorse. He noted that the Legislature recognized earthquake safety problems when it upgraded the State Capitol. He expressed concern that a state that requires private owners to seismically upgrade their buildings would put its people, citizens, visitors at risk. We should not have to have a catastrophe to do something. He quoted figures from Japan where, in 1980, they spent \$100 per person on seismic upgrades, versus California's \$0.65 per person. He said that it is difficult to put actual numbers on the impact on society and the economy if educational facilities are lost.

University of California, Berkeley - I introduced Mr. Gene Cross, a representative of the Berkeley campus, who said:

More funding is needed to accomplish necessary studies and

renovation. A more in-depth classification of the buildings would allow limited funds to be used strategically on buildings with the greatest risk.

There are secondary matters of asbestos, PCB, chemicals, and nuclear materials to be considered in seismic renovation. Seismic renovation cannot be done without running into asbestos in almost any building. Asbestos abatement can cost millions of dollars in a building, and employee relations and union problems arise when seismic projects move employees to other inferior buildings, or expose employees to asbestos.

The University would support bonds in concept, as long as it would not be in lieu of other funding needs on the campuses. Programmatic needs on the campus are to serve the community by teaching, doing research, and providing public service. If all their funds were spent on making buildings safe, they wouldn't be able to provide programs.

In answer to questions regarding the possibility of funding seismic retrofit with private donations, Mr. Cross said:

After 30 years' experience in facilities management and construction in higher education, my opinion is that it is very difficult to solicit private donations from individuals and groups for infrastructure-type projects. UC Berkeley is doing

everything it can within the budgetary limits and competing priorities set after comprehensive and ongoing reviews of the total campus needs.

The UC Berkeley campus is unique in that it straddles the Hayward fault. Memorial Stadium and other buildings are located directly on the fault; in fact, the stadium is slowly being sheared by tectonic fault creep. Recent reports by the U. S. Geological Survey [2, 3] indicate there is a 50 percent chance of a large earthquake striking the Bay Area within the next 30 years, and the Hayward fault is a likely source. This high probability should cause the Berkeley campus to place a higher priority on those buildings judged seismically unacceptable. Mr. Cross agreed:

The campus did a full evaluation of the need, and requested and received funds for improvements to three of the buildings rated highest on the benefit/cost analysis priority list. Berkeley will ask for funds to work on the next three buildings on the list. When those funds are allocated, the work will be accomplished.

It was clear that the impact of an earthquake and the effect it would have on UC Berkeley's ability to carry out teaching and research programs had not been fully considered. Seismic repairs could help to avoid the loss of use of buildings and equipment that will result during the forthcoming earthquake. UC has plans, people to evaluate the plans, and seismic needs have been identified in priority order. The campus is seeking funds; there is no schedule for

renovation, as the schedule will depend on when funding becomes available.

Other State Buildings - Testimony on behalf of other state-owned buildings was given by Mr. Michael Bocchicchio, the California State Architect. Mr. Bocchicchio provided the Commission with information on the state's infrastructure retrofit program, which is administered by the Office of the State Architect.

The Department of General Services owns and operates 43 office buildings throughout the state, most of them in densely populated areas. Some of these buildings date back to 1919, and many are reaching an age where there is a great amount of retrofit work required to bring the facilities up to standard. Over the years, maintenance has been deferred. Now, roofs need to be replaced, elevators need maintenance and upgrading, space must be reconfigured to meet tenants needs, several buildings have been cited by the Fire Marshall for life-safety violations, and other deficiencies need correcting. Some buildings are not accessible to the handicapped, and asbestos has been found in just about every one. Most of the structures predating 1933 are not capable of resisting the seismic loads that we know about today. Most do not comply with energy standards.

A piecemeal approach to budgeting for building repairs has been taken in the past. Since

building systems are inter-dependent, they often were trapped in a circular situation where certain improvements could not go forth until the Fire Marshall's concerns were addressed, yet there was no money for addressing the Fire Marshall's concerns. To resolve this problem, the State Architect's office reviewed the total inventory of 43 state office buildings, and prioritized the buildings for further study. Infrastructure studies incorporated detailed structural analysis. The next step was to devise a master plan for the retrofit of each building, seek funding, and implement the master plan.

Four studies have been completed (Oakland office building, San Francisco state office building, and two buildings in Sacramento). The Los Angeles state office building will be studied this year [1990]. A seven-year master plan has been completed for the San Francisco state office building, and legislation is being sought for bonds to finance the work.

The in-depth structural studies indicated that some of the buildings have only 10 to 12 percent of the strength required by present seismic standards. Also, there are materials in some buildings that could be hazardous in moderate earthquakes.

The Commission's bond proposals in the 1990 legislative session would not have been adequate to cover the work needed on the

state-owned buildings. Retrofitting of the buildings, including seismic strengthening, is a costly project. The least expensive way to accomplish the work is to move tenants into leased space, do the work, and move them back once work is completed.

The Office of the State Architect is sponsoring legislation that would propose the use of lease-purchase revenue bonds. This would allow the State Public Works Board to take title of the property from General Services, lease it back to General Services, and sell bonds. The bonds would be paid off through the lease payments that General Services makes to the Public Works Board. This project has not been easy to get through; both houses of the Legislature turned it down last session.

The Office of the State Architect needs support for legislation to repair the San Francisco state office building; it would be a crime to leave this building in the condition it is in, in the location it is in, with what is known about it. The cost to strengthen the 600,00-square-foot state office building is \$143 million over seven years for design, construction, and implementation.

Loma Prieta Earthquake

The magnitude 7.1 Loma Prieta earthquake of October 17, 1989, occurred in a somewhat remote and sparsely settled portion of the greater San Francisco Bay Area. The earthquake

resulted in 63 deaths, 350 hospitalized injuries, and approximately \$10 billion in direct damage and indirect losses. The collapse of buildings and structures in San Francisco and Oakland, including the collapsed I-880 viaduct which took 41 lives, occurred as far away from the earthquake energy release as 60 miles. The Loma Prieta earthquake caused damage to over 23,000 residential structures, 3500 commercial businesses, and 140 public buildings in the ten counties affected. The cost of the Loma Prieta earthquake represents an expenditure of \$1700 per person for the Bay Area's six million people. The state-owned buildings in San Francisco and Oakland were severely affected and, at this time, more than two years later, these buildings are standing vacant.

The Loma Prieta earthquake was but one in a series of recent damaging earthquakes striking California; others since 1970 include the San Fernando (1971), Oroville (1975), Morgan Hill (1979), Coalinga (1983), and Whittier Narrows (1987). Each of these earthquakes, even though of only moderate magnitude, caused important structures to fail. Most of the structures that failed could have been identified as being high-risk structures prior to the earthquake. Each of these recent earthquakes was serious and locally catastrophic to those directly affected, even though each was relatively minor when compared with the earthquakes that have the potential of occurring near metropolitan areas in both Southern and Northern California. A large earthquake striking a major California urban center would cause damage, losses, and social disruption ten to twenty times greater than those resulting from the Loma Prieta earthquake.

The Seismic Safety Commission's Investigation - Following the Loma Prieta earthquake, the California Seismic Safety Commission made recommendations based on an investigation of the earthquake and its aftermath. The Commission recognized the importance of timeliness and the fiscal limits that affect hazard reduction efforts, and recommended some less costly advances that could be made quickly by local and state agencies. They advocated promoting public understanding of the risks, protective actions citizens can take, development of programs that reduce the level of relief and recovery demands, and routine exercising of emergency response plans and plans for other short-term relief efforts.

Governor Deukmejian's Board of Inquiry - Because of the large losses from the Loma Prieta earthquake, California's Governor George Deukmejian appointed a Board of Inquiry to assess why failures occurred, and to recommend what the state should do to protect its citizens from further earthquakes.

The Board's comprehensive report [9] resulted in Governor Deukmejian issuing an Executive Order (Attachment) establishing California policy that seismic safety is a priority consideration in the allocation of resources for all state structures. The Governor, in acting so quickly and decisively, had taken to heart the Board of Inquiry's assertion that:

The Loma Prieta earthquake should be considered a clear and powerful warning to the people of California. Although progress has been made during the past two

decades in reducing earthquake risks, much more could have been done, and awaits doing. More aggressive efforts to mitigate the consequences of earthquakes are needed if their disastrous potential is to be minimized and one of the most fundamental responsibilities of government is to be fulfilled—to provide for public safety.

University of California's Building Retrofit Program Reassessed - In light of the Governor's Executive Order, and due to the urgency of the University of California's seismic safety needs, President David Gardner appeared before the Seismic Safety Commission at the regular Commission meeting on January 11, 1990 [10] for the purpose of seeking assistance from the Commission toward improving seismic safety on the University of California's nine campuses. Excerpts from President Gardner's testimony follow:

Seismic safety is of utmost importance to the University of California, and I am personally committed to moving as expeditiously as possible to correct seismic and other life-safety hazards in University facilities. I also am committed to ensuring the safety of staff, faculty, and students, as well as the thousands of people who visit the campuses each year.

I will be recommending, at the Regents' meeting next week, that the University borrow \$50 million to perform work needed to correct the most seismically vulnerable buildings. The plan developed

will go a long way toward speeding up corrections of the University's seismic problems. It reasonably allocates the burden among interested parties; improves the level of preparation for earthquakes; affords assurance to students, staff, and faculty that the university has acted responsibly and expeditiously on this problem; and permits the University to proceed immediately with corrections. Considering state funds, nonstate funds available on the campus, and the funds I plan to set aside, I anticipate spending about \$30 million a year, on an average, for seismic improvements for the University of California as a whole, which should allow the University to improve the seismic safety of buildings, especially those rated poor and very poor.

President Gardner introduced Vice President William Baker, who said:

The first seismic correction project included in the University of California budget appeared in 1974, following the San Fernando earthquake of 1971. Of the \$20 million requested at that time, only half was approved by the Legislature and only \$1.5 million was actually released by the state for two projects at the Santa Barbara campus. Both were completed. The University continued to request funds each year to strengthen seismically substandard facilities; however, no state funds were provided until the early 1980s. In 1974, the Legislature established the Seismic

Safety Commission and in January of 1975 the Board of Regents adopted a policy calling for acceptable levels of seismic safety in University facilities.

Each year in the late 1970s and early 1980s (a ten-year period), the Board of Regents was asked to approve an authorization for the President to amend the budget to include the highest priority projects, and to request appropriate state funding should the state indicate a willingness to provide funds for correction of seismic deficiencies. In the early years of that period, the state advised that it was not prepared to fund such projects, pending completion of a report by the Seismic Safety Commission and an evaluation of state-owned buildings. In later years the state was spending relatively little capital outlay for the University projects or for the minor amounts of money for studies and planning. During these years, serious consideration was given to posting signs on buildings thought to be seismically substandard indicating each building's relative safety.

Seismic Safety Commission Report on the Executive Order - The Governor's Executive Order D-86-90 directed the Seismic Safety Commission to review and report to the Governor, by December 1, 1990, on the adequacy and status of the efforts in response to the order, as well as on the responses to the recommendations of the Governor's Board of Inquiry on the 1989 Loma Prieta

Earthquake [11]. The Seismic Safety Commission concluded that responses must address five elements to demonstrate an effective seismic safety program. These five elements are:

1. *Policy Statement.* A statement of policy that states goals, expectations, and deadlines, and explains the ranking of seismic safety in the agency's responsibilities.

2. *Seismic Safety Program.* A seismic safety program with a plan and process to identify earthquake hazards to people and to the organization's functions, to abate the unacceptable hazards, and to prudently manage the risks that cannot be eliminated.

3. *Responsible Staff.* A management-level agency official having the clear responsibility for meeting the goals in the policy statement, and an appropriately sized staff that has the administrative and technical knowledge and experience needed to carry out the program.

4. *Adequate Funds.* Funds adequate to carry out the program or a plan to raise the funds needed.

5. *Accountability.* A way to measure and report progress to the person or organization legally responsible for the agency, and to the Governor and the Legislature, and a way to ensure technical performance in carrying out the program.

Although great strides had been made to lessen the state's exposure to earthquake risks, we still have a long way to go. Only the California Department of Transportation responded to the executive order with an adequate program. Although the Department of General Services made considerable progress in making seismic safety a priority consideration, it still must find a solution to its fiscal resources problem. The University of California began to address seismic safety long before the Loma Prieta earthquake, but has not reexamined or accelerated its existing program since the issuance of the executive order. Because of the lack of funding and a structure for accountability, UC's program is not adequate to meet immediate, existing seismic safety needs.

Discussion

California now has a different governor, Pete Wilson. Gubernatorial orders from previous governors exist at the pleasure of the incumbent. Although Governor Wilson has not rescinded Executive Order D-86-90, he has not made a public statement in support of it.

In addition to the loss of life, injuries, damage, disruption of operations, and impact on the economy that a damaging earthquake would cause, the state also must recognize the potential liability exposure that the state risks if seismic safety remains just another competing factor in resource allocation. The state did not know that the Cypress viaduct was a collapse hazard, but it is paying millions of dollars in damages to the victims of that collapse during the 1989 earthquake. This could be miniscule

compared to the claims that could occur after the failure of state buildings that are known to be potential collapse hazards in an earthquake.

It is also important to note that despite the limited immunities conferred upon the Regents of the University of California and the Trustees of the California State University system, as well as the top management officials of both universities, the potential remains for them to be held personally liable, along with the State of California, for failure to mitigate known dangerous conditions, such as earthquake hazards. In determining whether an administrator, regent, or trustee is personally liable for an act or omission, the courts apply the *reasonable person* standard, which excuses honest errors in judgment, but not the intentional ignoring of significant problems. Although fear of liability should not be the driving force, the potential for liability is an important consideration for the state in providing funding and setting priorities to abate earthquake hazards.

The most clear representation of public policy to address earthquake hazards is the enactment of public laws to address seismic safety concerns. California has led the nation and the world in the passing of earthquake safety laws.

The Seismic Safety Commission monitors the legislative process and assists the legislators by either sponsoring, supporting, or opposing bills. During a normal legislative session, there are about 15 or 20 bills that require diligent monitoring. Destructive earthquakes stimulate this process by increasing the awareness of decision

makers and providing an opportunity for new laws to be considered. During the 72-year period from 1906 to 1988, 112 seismic safety bills were passed into law in California.

The Loma Prieta earthquake resulted in the most prolific legislative session (1989-90) of all time for seismic safety. About one month prior to the Loma Prieta Earthquake, on September 1, 1989, the Commission submitted to the Governor and the legislators the Commission's annual report, *California at Risk* [12], outlining 72 separate initiatives where decision-makers could take action to improve seismic safety. When the earthquake occurred, the Governor and the legislators were acutely aware of earthquake issues and had the language to address them. During the legislative session following the Loma Prieta earthquake, a total of 443 bills were introduced addressing seismic safety. When the 1989-90 session finally closed, 164 bills had passed the legislative process and were sent to the Governor for signature. The Governor signed most of the bills into law; however, he vetoed those that required substantial financial commitments. During this short period, California law makers more than doubled the body of seismic safety laws.

It is interesting to note that the issue of lack of funding for earthquake studies in California was a problem in 1906. On May 31, 1906, only six weeks after the San Francisco earthquake, the Earthquake Commission submitted a Preliminary Report to the Governor. In this report, the details of the organization of the Commission, the program of its work, and the results attained to that date were put forth. But

although the Commission acted under the authority of the Governor of the state, no money was provided by the government for the conduct of its work. The embarrassment arising from this lack of funding was relieved about June 1, 1906, by a subvention from the Carnegie Institution of Washington,, which enabled the Commission to prosecute its program as it had been planned. It seems they set a precedent for programs that lacked funding that is still with us and not as easily or quickly resolved as it was in 1906.

References

- [1] Federal Emergency Management Agency, 1980, *An assessment of the consequences and preparation for a catastrophic California earthquake—findings and actions taken*: Washington, DC, 59 p.
- [2] U. S. Geological Survey, 1988, *Probabilities of large earthquakes occurring in California on the San Andreas fault*: by the Working Group on California Earthquake Probabilities, Open-file Report 88-398, 51 p.
- [3] U. S. Geological Survey, 1990, *Probabilities of large earthquakes in the San Francisco Bay Region*: by the Working Group on California Earthquake Probabilities, USGS Circular 1053, 84 p.
- [4] Lawson, A. C., 1908, *The California earthquake of April 18, 1906*: Report of the State Earthquake Commission, Carnegie Institution, Washington, DC, 2 vol. and atlas.
- [5] Joint Committee on Seismic Safety, 1974, *Meeting the earthquake challenge—Final report to the Legislature*: California Legislative Committee, Sacramento.
- [6] California Seismic Safety Commission, 1986, *California at risk—reducing earthquake hazards, 1987 to 1992*: Sacramento, 92 p.
- [7] California Seismic Safety Commission, 1979, *Evaluating the Seismic Hazard of State-Owned Buildings*: SSC Report 79-01, Sacramento.
- [8] Minutes of the November 10, 1988, meeting of the California Seismic Safety Commission.
- [9] Housner, G. D., Chairman, 1990, *Competing Against Time: Report of the Governor's Board of Inquiry on the 1989 Loma Prieta Earthquake*.
- [10] Minutes of the January 11, 1990, meeting of the California Seismic Safety Commission.
- [11] California Seismic Safety Commission, 1990, *Report to Governor George Deukmejian on Executive Order D-86-90*: SSC Report 90-06, Sacramento, 25 p., 7 appendices.
- [12] Seismic Safety Commission, 1989, *California at risk—Reducing earthquake hazards, 1987-1992*: Report SSC 89-02, Sacramento, 178 p.

ATTACHMENT

EXECUTIVE DEPARTMENT
STATE OF CALIFORNIA

Executive Order D-86-90

WHEREAS, on October 17, 1989 a major earthquake occurred in Northern California, causing deaths, injuries, and widespread damage to transportation facilities and other structures; and

WHEREAS, an independent Board of Inquiry was formed in November 1989 to investigate the reasons for the collapse of transportation structures and to recommend actions to reduce the danger of tragic structural failures in future earthquakes; and

WHEREAS, the Board of Inquiry found that there is a high probability that one or more major earthquakes will strike heavily populated areas in Northern and Southern California in the future; and

WHEREAS, California's state of earthquake readiness needs improvement to better protect the public safety and our economy from potentially serious impacts of future earthquakes;

NOW, THEREFORE, I, GEORGE DEUKMEJIAN, Governor of the State of California, by virtue of the power and authority vested in me by the Constitution and Statutes of the State of California, do hereby issue this Order, to become effective immediately:

- 1. It is the policy of the State of California that seismic safety shall be given priority consideration in the allocation of resources for transportation construction projects, and in the design and construction of all state structures, including transportation structures and public buildings.*
- 2. The Director of the Department of Transportation shall prepare a detailed action plan to ensure that all transportation structures maintained by the State are safe from collapse in the event of an earthquake and that vital transportation links are designed to maintain their function following an earthquake. The plan should include a priority listing of transportation structures which will be scheduled for seismic retrofit. The Director shall transmit this action plan to the Governor by August 31, 1990.*
- 3. The Director of the Department of Transportation shall establish a formal process whereby the Department seeks and obtains the advice of external experts in establishing seismic safety policies, standards, and technical practices; and for seismic safety reviews of plans for construction or retrofit of complex structures. The Director shall transmit a summary of this process to the Governor by August 31, 1990.*
- 4. The Director of the Department of Transportation shall assign a high priority to development of a program of basic and problem-focused research on earthquake engineering issues, to include comprehensive earthquake vulnerability evaluations of important transportation structures and a program for placing seismic activity monitoring instruments on transportation structures. The Director shall transmit a description of the research program to the Governor by August 31, 1990.*

5. *Local transportation agencies and districts are encouraged to review the findings and recommendations of the Board of Inquiry on the 1989 Loma Prieta Earthquake and to adopt policies, goals, and actions similar to those proposed for Caltrans.*
6. *The Director of the Department of General Services shall prepare a detailed action plan to ensure that all facilities maintained or operated by the State are safe from significant failure in the event of an earthquake and that important structures are designed to maintain their function following an earthquake. The plan should include a priority listing of facilities which will be scheduled for seismic retrofit. The plan shall further propose measures by which state agencies constructing new facilities or retrofitting existing facilities would:*
 - a. *be governed by the provisions of a generally accepted earthquake resistant code for new construction;*
 - b. *secure structural safety review and approval from the Office of the State Architect;*
 - c. *seek independent review of structural and engineering plans and details for those projects which employ new or unique construction technologies; and*
 - d. *have independent inspections of construction to insure compliance with plans and specifications.*

The Director shall transmit the plan to the Governor by August 31, 1990.

7. *The Department of General Services shall, when negotiating leases of facilities for use by state employees or the public, consider the seismic condition of the facilities and shall initiate leases only for those facilities which demonstrate adequate seismic safety.*
8. *The Seismic Safety Commission shall review state agencies' actions in response to this executive order and the recommendations of the final report of the Board of Inquiry and provide a report to the Governor on the adequacy and status of actions taken by December 1, 1990.*
9. *The University of California and the California State University shall give priority consideration to seismic safety in the allocation of resources available for construction projects. The University of California and the California State University shall prepare and transmit to the Governor by August 31, 1990 a description of their plans to increase seismic safety at facilities which they maintain or operate.*

IN WITNESS WHEREOF I have here unto set my hand and caused the Great Seal of the State of California to be affixed this 2nd day of June 1990.

*George Deukmejian
Governor of California*

Volcanism in the Canadian Cordillera: Should We Worry?

Catherine J. Hickson
*Geological Survey of Canada
Vancouver, British Columbia*

Abstract

The Canadian Cordillera encompasses a geologically dynamic region which includes subduction zones, major transcurrent faults, areas of crustal rifting and high heat flow. As a consequence of this dynamic environment, some 100 volcanoes and volcanic fields have formed. These are arranged in five broad belts: the Garibaldi, Anahim, Alert Bay, Stikine, and Wrangell volcanic belts; plus other less-well-defined volcanic regions. The tectonic forces that produced these volcanic belts are still active and thus the potential for a volcanic eruption in the Canadian Cordillera continues to exist. Much remains to be done to assess the risk of a volcanic eruption in the Cordillera due to numbers and remoteness of volcanoes. Studies to date, suggest that small localized basaltic eruptions producing tephra that covers limited areas, and more infrequent violent explosive events, severely impacting vast areas are both possible. Basaltic eruptions may occur with little or no warning, but will only pose a hazard if the eruption occurs close to a populated area or a transportation corridor. Explosive eruptions usually have associated earth tremors that will be picked up on the regional seismic network. Unfortunately, however, some significant events elsewhere in the world have occurred where precursor seismicity commenced only hours before the volcano erupted explosively.

Apart from the hazard posed by the eruption of a volcano, a continuing hazard is posed by the extreme relief of many vent areas and the unstable nature of volcanic deposits. Landslides and debris flows from volcanoes pose a very real threat. Comparable debris flows generated in volcanic areas have much greater run out distances than those generated in nonvolcanic areas, in part, because of a greater percentage of fine material in "volcanic" debris flows. Where human development is pushed into volcanic areas, this hazardous aspect of Cordilleran volcanoes must be taken into consideration during planning. Should an eruption occur, the impact would be much wider reaching.

Introduction

Canada has been spared the almost ceaseless volcanism characteristic of such places as Hawaii, Japan, or Indonesia, but it has not escaped volcanism completely. We are part of a continuous line of subduction zones and transform faults that encircle the Pacific Ocean. Our global position on this dynamic sphere gives rise to not only subduction zone volcanoes, but to volcanoes formed where the crust is weakened and stretched by extension, and additionally by

plumes in the underlying mantle creating upwelling of hot mantle material. These forces have produced five broad belts of volcanoes plus other less-well-defined volcanic regions (Figure 1). The Garibaldi and Wrangell Volcanic Belts owe their origin to subduction; the Stikine Volcanic Belt to crustal extension, and the Anahim Volcanic Belt to a mantle plume or "hot spot". Deep faults and crustal dynamics in other regions formed volcanic fields such as Wells Gray-Clearwater and other isolated cones, or cone fields, in British Columbia and Yukon. But, what of the risk? Do these volcanoes pose a

threat to our Society?

Volcanic Hazards

Volcanoes, when they erupt, produce a number of hazardous events (Table 1). What hazard will occur at which volcano will depend to large degree on the composition of the erupting magma (Table 2). Basaltic eruptions [basaltic magmas are low in silica, an essential building block element of minerals] pose a minimal hazard in comparison with explosive felsic eruptions [felsic, or the older term 'acid', magmas are high in silica]. Similarly, an andesitic eruption is less hazardous than a dacitic eruption. A number of caveats must be applied. Basaltic eruptions occurring during winter months in regions of heavy snow pack could produce devastating debris flows (lahars) or floods from rapidly melting snow. Some basaltic eruptions in Canada have been in mountainous terrain near glaciers. Subglacial volcanism has occurred in British Columbia in the past (2),(3). This form of volcanism can produce potentially destructive jokulhlaups and water-magma interactions (phreatic or phreato-magmatic eruptions) can potentially produce very large explosions -- even if the magma is basaltic. Such an explosion,

during the 1924 explosive phreatic event at Kilauea, caused the only recorded fatality of a Hawaiian eruption.

Hazards from the eruption of intermediate to high silica content magmas can be moderate to extreme - depending on the size of the eruption. The size of an eruption is quantified using a scale called the Volcanic Explosivity Index (VEI, (4)). The VEI takes into consideration the volume of eruptive products, height of eruption cloud, duration of the main eruptive phase, and other parameters to assign a number from a linear, 0 to 8 scale. The May 18, 1980 eruption of Mount St. Helens, which destroyed 632 km² of land, expelled 1.4 km³ of magma (dense rock equivalent, DRE) and produced an eruption column which peaked at an elevation of 24 km, had a VEI of 5. Mount Pinatubo, in the Philippines, ejected about 3 km³ (DRE) of material and had a VEI of 6. The actual size of the eruption does not have a direct relationship to the number of lives lost, however, it is directly proportional to the economic losses sustained by the region.

No modern man or woman has witnessed a truly cataclysmic eruption and lived to tell the tale. The 1813 eruption of Tambora, ejected 50 km³ (DRE) of pyroclastic material into the

TABLE 1 -- Volcanic hazard summary (modified from (1), Table 1.4, p. 12)

Volcanic hazard	Frequency of Adverse Effect/Damage/Death					
	Less than 10	10-30	30-100	100-500	500-1000	Greater than 1000
	Distance (km)					
Lava flows	F	C	VR			
Ballistic projectiles	C					
Tephra falls	VF	F	F	C	R	
Pyroclastic flows and debris avalanches	A	F	R	VR		
Lahars and jokulhlaups	F	F	R	VR		
Seismic activity and ground deformation	C	C	VR			
Tsunami	A	F	C	R	VR	
Atmospheric effects	C	C	R	VR	VR	
Acid rains and gases	F	F	R	R	VR	VR

* Hazard level is based on the relative frequency of deaths given that the specific type of activity occurs.
A = Always; VF = Very Frequent; F = Frequent; C = Common; R = Rare; VR = Very Rare.

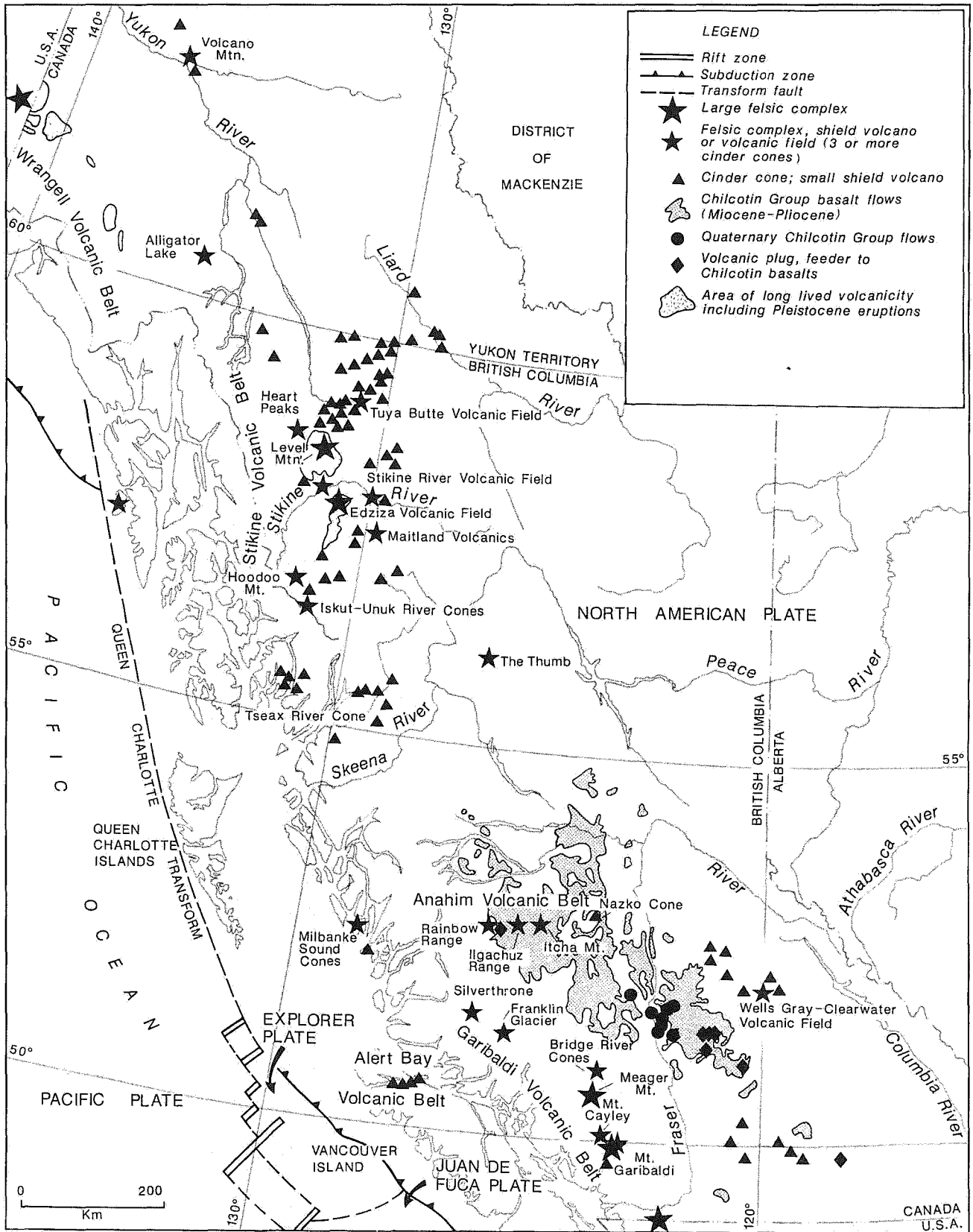


Figure 1 -- Quaternary volcanic vents in the Canadian Cordillera.

TABLE 2 -- General relationships between volcano types, predominant lava, eruption styles, and common eruptive characteristics (from {5}, Table 1.1, p. 2)

Volcano type	Predominant lava Composition	Relative Viscosity	Eruption style	Common Eruptive Characteristics
Shield ¹	Basaltic (mafic)	Fluidal	Generally non-explosive to weakly explosive	Lava fountains, lava flow (long), lava lakes and pools
	Andesitic	Less fluidal	Generally explosive but sometimes non-explosive	Lava flows (medium), explosive ejecta, tephra falls
Composite ²	Dacitic to rhyolitic (felsic)	Viscous to very viscous but can be non explosive	Typically highly explosive but can be non-explosive, especially after a large explosion	Explosive ejecta, tephra falls, pyroclastic flows and surges, and lava domes

¹ Generally located in the interior of tectonic plates ("intraplate") and presumed to overlie "hot spots," but also may occur in other tectonic settings (eg., Anahim Volcanic Belt, Galapagos, Iceland, Kamchatka).

² Generally located along or near the boundaries of convergent tectonic plates (subduction zones); also called strato-volcanoes (eg. Cascade-Garibaldi Volcanic Belt, Wrangell Volcanic Belt).

atmosphere cooling the global climate by 2°C for two years following the eruption. This cooling caused considerable hardship and famine in temperate areas of the Northern hemisphere. We can only speculate upon the consequences of an eruption of the scale of Toba, Sumatra, which expelled 2,500 km³ (DRE) of tephra and as a consequence may have brought about the last ice age (6).

Volcanic Risk

Erupting volcanoes only become a risk when there is something valued that may be destroyed - either lives, property or resources. Risk is usually assessed on the basis of the number of human lives which may be lost as a result of a hazardous event (7). But, in actual fact, natural disasters throughout history have taken only a small fraction of the lives that have been lost in armed conflict. In 1,000 years of record keeping, volcanoes have taken less than 300,000 lives (5). The death toll from the recent Gulf War probably took at least a third that number of lives in just a few short weeks. Why then do we concern ourselves with the risk of death from natural hazards? The reason probably has more to do with the unexpectedness of the deaths and the belief that if more had been known or done, then perhaps, these lives could have been spared.

Yokoyama *et al.* (8), devised a method for assessing risk at a volcano (Table 3). High risk volcanoes "score" 10 or above. Using this scheme and our present knowledge level, no Canadian volcano falls into the high risk category. Growing populations, however, increase the risk posed by volcanos both here and abroad. For example, Mount Ruiz, Columbia, was not considered a high risk volcano, yet, its eruption on November 13, 1985, killed 25,000 people - the greatest volcanic disaster since the eruption of Mount Pelée at the turn of the century. A poignant point brought out in Voight's (9) retrospection of this event, was the observation that in 1845, a similar event wiped out 1,400 people - all those that lived in the town at that time. In 1985, 30,000 people now lived in the same area and a repeat of the 1845 event resulted in an order of magnitude escalation in the loss of life. In a similar vein, the Philippine

volcano of Mayon produced pyroclastic flows during its 1814 eruption which killed 1,200 people - 800,000 people now live in the same area (9).

TABLE 3 -- Proposed criteria for identification of high-risk volcanoes (8). A score of 1 is assigned for each rating criterion that applies; 0 if the criterion does not apply.

HAZARD SCORE

- 1) High silica content of eruptive products (andesite/dacite/rhyolite)
- 2) Major explosive activity within last 500 yr
- 3) Major explosive activity within last 5,000 yr
- 4) Pyroclastic flows within last 500 yr
- 5) Mudflows within last 500 yr
- 6) Destructive tsunami within last 500 yr
- 7) Area of destruction within last 5,000 yr is >10 km²/
- 8) Area of destruction within last 5,000 yr is >100 km²
- 9) Occurrence of frequent volcano-seismic swarms
- 10) Occurrence of significant ground deformation within last 50 yr

RISK RATING

- 1) Population at risk >100
 - 2) Population at risk >1000
 - 3) Population at risk >10,000
 - 4) Population at risk >1 million
 - 5) Historical fatalities
 - 6) Evacuation as a result of historical eruption(s)
-

In Canada we are blessed with a country still relatively unpopulated so a volcanic eruption, with few exceptions, will probably result in no direct casualties (or at least very few). How then do we assess the risk if no lives are to be lost?

How do we figure into our equations of risk the loss of a forest, of spawning streams, of a river, and of people displaced? These will be the legacy of any large explosive volcanic eruption in Canada.

Preparing for an Eruption

Despite infrequent natural disasters in Canada, we should not ignore the fact that we live in a tectonically active region in which future earthquakes and volcanic eruptions are a certainty. Peterson and Tilling {10} have shown that countries experiencing many small eruptions are best able to cope with them, no matter what the economic status of the region. However, they find that countries faced with infrequent events, even when that country is scientifically advanced, have extreme difficulty dealing with volcanic events. "Unrest at long-quiescent volcanoes is particularly difficult to diagnose: such unrest does not necessarily culminate in an eruption, but if an eruption does occur, it may be particularly violent. Either outcome poses difficult challenges to scientists, not only in their study of the volcano, but in their public relations." {10}.

Monitoring unrest at a volcano is a complex exercise that does not necessarily result in easy or straight forward answers. Figure 2 shows the relationship of scientists monitoring a volcano to a few of the groups that would become involved in any volcanic emergency. Communication between the groups and emergency planning are the key to effective response to a natural disaster.

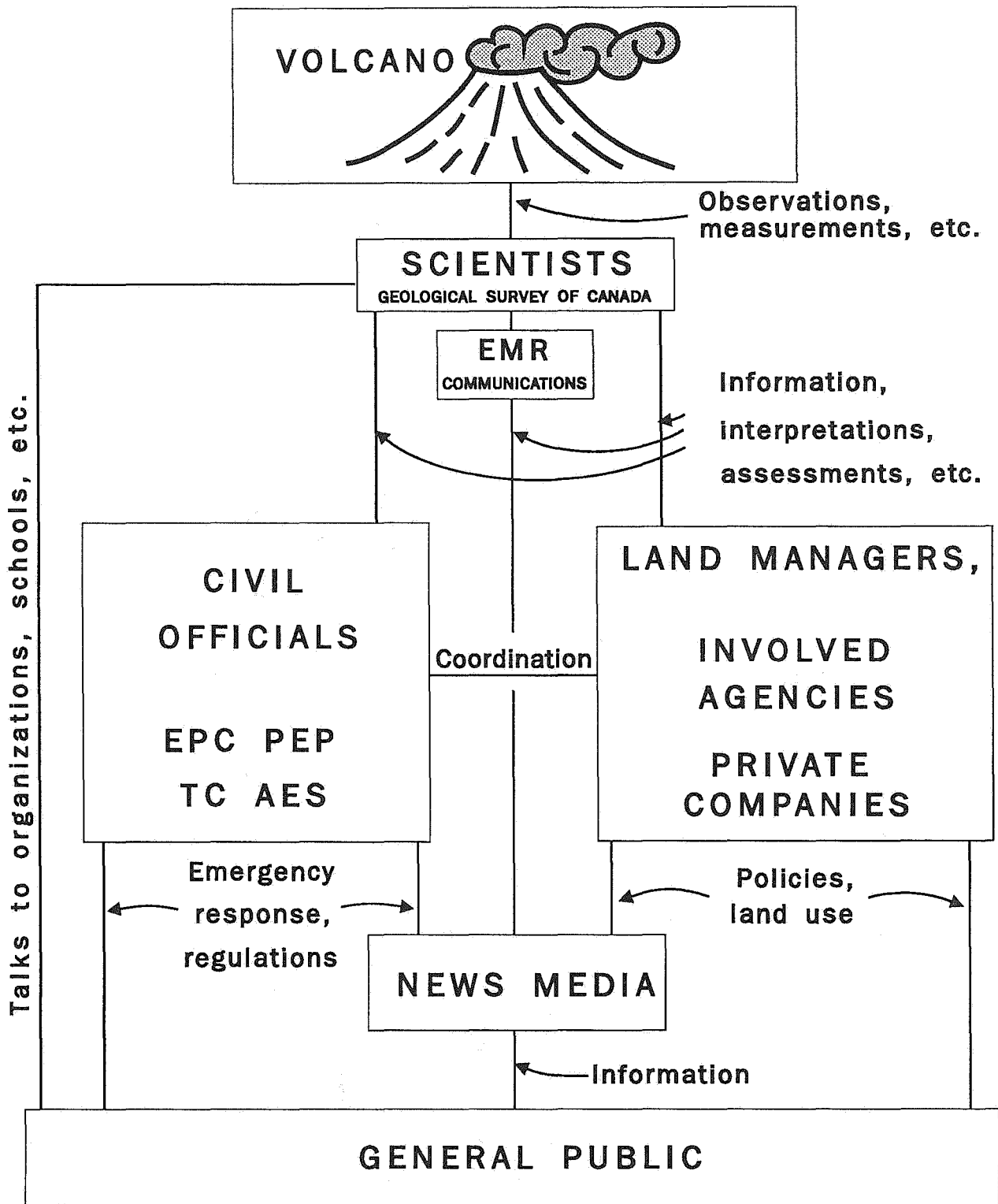
Emergency planning is carried out in British Columbia by the Provincial Emergency Program (PEP) and Emergency Preparedness Canada (EPC). The responsibilities of both these agencies is outline by Dalley {11} and Pollard {12}. A critical review of emergency planning in British Columbia can be found in Anderson *et al.* {13}. At present, the level of preparedness for a volcanic eruption consists of a notification network set up between the agencies involved (Figure 3). Each agency has specific responsibility to pass information on to other involved agencies and to respond according to its individual mandate. In the case of Transport Canada, its responsibility will be to reroute aircraft away from the eruption and set up safe routes around the trouble area. PEP will be responsible for notification of the municipality and people living in the region affected. The Geological Survey of Canada (GSC) assumes responsibility for hazard warning {14},

monitoring and passing information on to the other involved agencies as outlined in its 'Statement of Responsibility' {14}. Assessment of potential volcanic activity will be handled by a committee called the 'Volcanic Activity Evaluation Committee' (VAEC). The guidelines and mandate of this committee are given in Hickson {14}.

In addition to possible future volcanic eruptions, the Garibaldi Volcanic Belt, in particular, poses a considerable threat in the form of large rock failures {15, 16, 17 and 18} and catastrophic debris flows {19}. In fact, several deaths have already occurred from landslides in this region. The volcanoes are extremely rugged regions of high relief underlain by unstable, poorly consolidated and/or strongly jointed volcanic rocks. These conditions have already lead to a number of failures and debris flows. Comparable debris flows generated in volcanic areas have much greater run out distances than those generated in nonvolcanic areas, in part, because of a greater percentage of fine material in "volcanic" debris flows {19}. These factors must be taken into consideration before any development in the vicinity of the volcanoes.

Conclusions

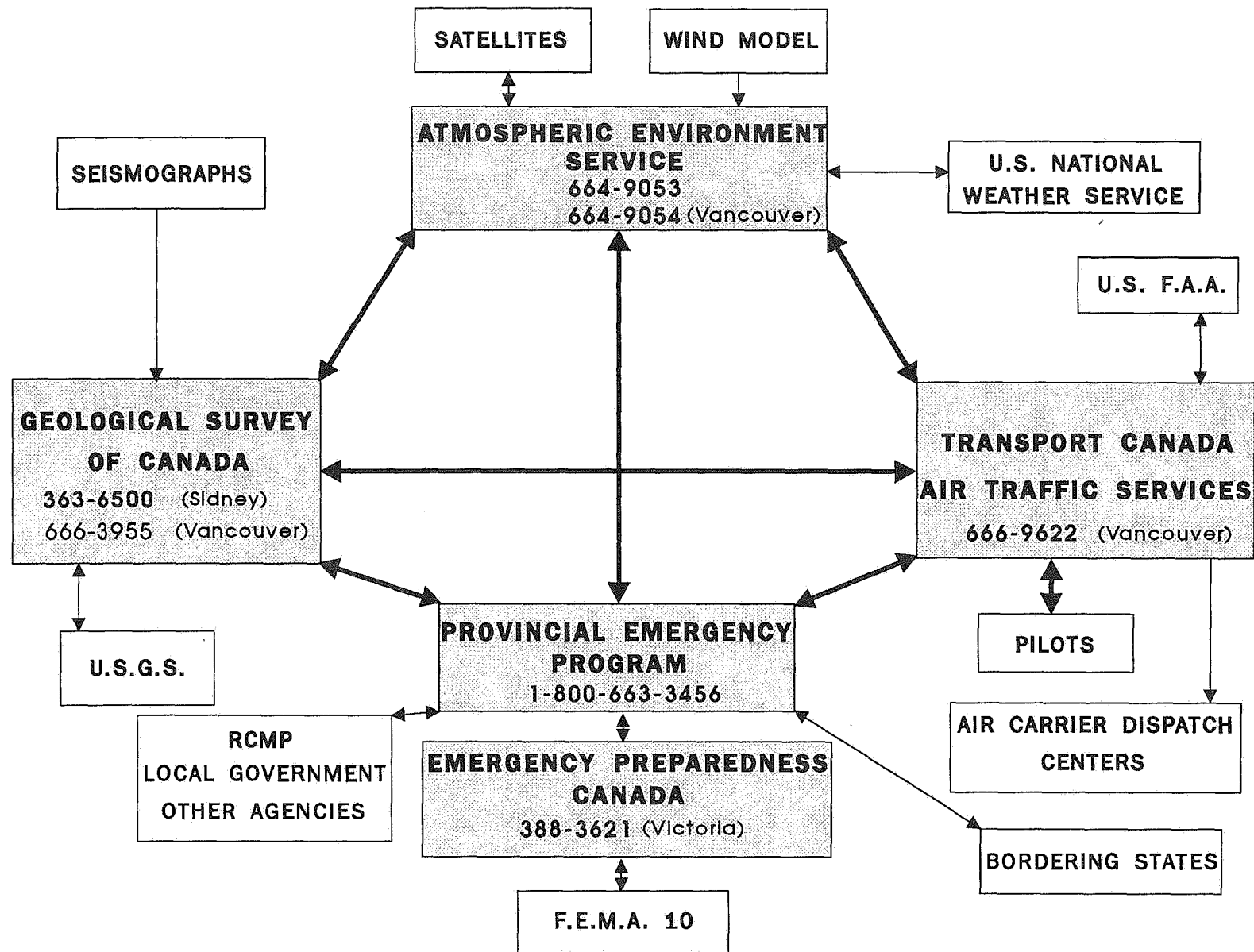
British Columbia and Yukon are blessed with some of the most spectacular scenery in the world - but we must not forget this scenery owes its origins to cataclysmic events in the earth's interior. Uplift, mountain building, earthquakes and volcanoes are all part of our heritage. Although the Canadian Cordillera has been spared continuous volcanism on a human time-frame - it has not on a geological one. We must try to look beyond the short recorded history of the human species when we are dealing with geologic hazards which have recurrence intervals longer than 50 years. Hazard zonation and planning must be an integral part of our future if we are to save lives and property. In the area of emergency planning for volcanic eruptions we can help by increasing public awareness and putting into place well thought out emergency plans. Detailed geological work at specific volcanoes that potentially threaten populations would help quantify the risk from future



EPC = Emergency Preparedness Canada
 PEP = Provincial Emergency Program

TC = Transport Canada
 AES = Atmospheric Environment Service

Figure 2 -- Organizational plan for dissemination of information about volcanic eruptions (modified from 17).



All telephone numbers in bold are 24 hours

Figure 3 -- Communication pathways for notification, coordination and response of government agencies.

eruptions, rock failures and debris flows. This work should be carried out before rezoning or major shifts in population occur. We may not see an eruption in Canada in our lifetime, on the other hand we may - shouldn't we be prepared?

Acknowledgements

Some of the work and thinking about volcanic hazards and their risk started when I was asked to prepare a talk for a workshop on Geological Hazards held in Victoria, February 20-21, 1991. This paper is a shorter version of the paper prepared for that workshop. I. Alarie, N. Striemer and B. Vanlier helped with preparation of the manuscript. Dr. L. Jackson provided a thoughtful review of the manuscript.

References

- 1) Blong, R.J. 1984
Volcanic hazards: Academic Press, New York, 424 p.
- 2) Mathews, H.W. 1947
"Tuyas," flat-topped volcanoes in northern British Columbia. *American Journal of Science*, v. 245, p. 560-570.
- 3) Hickson, C.J. 1986
Quaternary volcanics of the Wells Gray-Clearwater area, east central British Columbia: Ph.D. Thesis, University of British Columbia, Vancouver, 357 p.
- 4) Newhall, C.G. and Self, S. 1982
The volcanic explosivity index (VEI): An estimate of explosive magnitude for historical volcanism. *Journal of Geophysical Research*, v. 87, p. 1231-1238.
- 5) Tilling, R.I., ed. 1989
Volcanic Hazards: American Geophysical Union, Short Course in Geology, v. 1, 123 p.
- 6) Chesner, C.A., Rose, W.I., Deino, A., Drake, R., and Westgate, J.A. 1991
Eruptive history of Earth's largest Quaternary caldera (Toba, Indonesia) clarified. *Geology*, v. 19, p. 200-203.
- 7) Morgan, G.C. 1991
Quantification of Risks From Slope Hazards: Geological Hazards Workshop - 1991, Victoria, February 20-21.
- 8) Yokoyama, I., Tilling, R.I., and Scarpa, R. 1984
International mobile early-warning system(s) for volcanic eruptions and related seismic activities. UNESCO (Paris), FP/2106-82-01(2286), 102 p.
- 9) Voight, B. 1989
The 1985 Nevado del Ruiz volcano catastrophe: anatomy and retrospection. *Journal of Volcanology and Geothermal Research*, v. 44, p. 349-386.
- 10) Peterson, D.W. and Tilling, R.I. 1991
Interactions between scientists, civil authorities, and the public at hazardous volcanoes in "Handbook for Monitoring Active Lavas," U.S. Geological Survey, 34 p.
- 11) Dalley, W.C. 1991
The role of the Provincial Emergency Program in geological hazards management and mitigation. Geological Hazards Workshop - 1991, Victoria, February 20-21.
- 12) Pollard, D. 1991
The role of Emergency Preparedness Canada. Geological Hazards Workshop - 1991, Victoria, February 20-21.
- 13) Anderson, P., Edelson, N., Hansen, B., Harding, R., Huhtala, K., and Laughy, L., 1990
Hazard Management Planning in British Columbia: Issues and Challenges. Emergency Preparedness Planning, UBC Centre for Human Settlements, 32 p.

- 14) Hickson, C.J. 1991
Volcanic Hazards and volcanism in the Canadian Cordillera. Geological Hazards Workshop - 1991, Victoria, Feb. 20-21.
- 15) Evans, S.G. 1990
Massive debris avalanches from volcanoes in the Garibaldi Volcanic Belt, British Columbia. GAC/MAC, Annual Meeting, Program with Abstracts, v. 15, p. A38.
- 16) Clague, J.J. and Souther, J.G. 1981
The Dusty Creek landslide on Mount Cayley, British Columbia. Canadian Journal of Earth Sciences, v. 19, p. 524-539.
- 17) Peterson, D.W. 1985
Mount St. Helens and the Science of Volcanology: A five year perspective. *in* Mount St. Helens: Five Years Later, ed. S.A.C. Keller, Eastern Washington University Press, p. 3-19.
- 18) Read, P.B. 1978
Geology, Meager Creek geothermal area, British Columbia. Geological Survey of Canada, Open File Report 603.
- 19) Jordan, P. 1990
Dynamic behaviour and material properties of debris flows in southern Coast Mountains, British Columbia. GAC/MAC, Annual Meeting, Program with Abstracts, v. 15, p. A66.

Risk in Geotechnical Practice

Steven G. Vick
Consulting Geotechnical Engineer
Bailey, Colorado

Communication of Geologic Uncertainty

Karl Terzaghi was the originator, and certainly the master, of integrating the theories of soil mechanics with the realities of geology. In tracing the evolution of Terzaghi's thinking, Einstein [1] expresses a central idea that emerges late in Terzaghi's career: that the geotechnical engineer should apply theory, but temper it in the context of the uncertainty of nature. Translated into practice Terzaghi introduced this idea as the observational procedure, long at the core of the profession's ability to cope with extreme uncertainties in geologic conditions. As Terzaghi recognized, geologic uncertainties are endemic to geotechnical engineering. Even after geologic unknowns have been evaluated as thoroughly as possible within pragmatic project constraints, some degree of residual uncertainty inevitably remains, which may be related either to incomplete knowledge of geologic conditions and material properties or to imperfect understanding of the processes and mechanics involved. To the extent that these uncertainties may give rise to adverse consequences, risk results.

If the profession has advanced since Terzaghi's day in its ability to reduce risks through such techniques as the observational approach, its progress in expressing the risks and uncertainties that remain has been less impressive. In his 1964 Terzaghi lecture "Role of the 'Calculated Risk' in Earthwork and Foundation Engineering" Casagrande [2] saw the process of dealing with risk as containing two elements, the first having to do with geologic uncertainty and the second with acceptable risk:

- (a) The use of imperfect knowledge, guided by judgment and experience, to estimate the probable ranges for all pertinent quantities that enter into the solution of the problem.
- (b) The decision on an appropriate margin of safety, or degree of risk, taking into consideration economic factors and the magnitude of losses that would result from failure.

Despite use of the word "probable," Casagrande did not advocate the use of numerical probability to quantify unknowns, and instead relied on verbal descriptions such as "grave" risks and "great" uncertainties. While the significance of these terms to practicing engineers and geologists might be immediately evident, they are too ambiguous to allow for accurate communication to others. By contrast, if uncertainty is to be accurately communicated then it must be quantified, and this in turn requires that verbal descriptors be translated into probabilistic statements.

In 1964, it is safe to say that there was little need to accurately communicate geologic uncertainties to those beyond the design or project team. The second step of Casagrande's process clearly implies that decisionmaking about appropriate margins of safety and acceptable degrees of risk was then within the sole purview of the same engineers or geologists who assessed the uncertainties. But the realities of engineering geology practice almost 30 years later are vastly different, and neither Casagrande nor other practitioners of his day could have foreseen such developments as the adversary process that now surrounds most significant engineering projects, the need to address environmental as well as public safety risks, the current degree of regulatory and public involvement in the design process, the trend toward competitive bidding for professional services that invariably increases uncertainty and risk, and the accountability through litigation for risk judgments.

All of these factors go to the issue of determining what degree of risk in a project is acceptable, and while engineers and geologists have long relied on satisfying codes and standards of practice within the profession itself, this is not sufficient to address risk concerns of other parties to the decisionmaking process. Engineers and geologists can indeed assess the degree of geologic uncertainty, but they can no longer act as the sole arbiter of whether the resulting risk level is acceptable. Decisions regarding acceptable risk are more and more frequently undertaken by clients, project owners, regulatory bodies, competing interest groups, and the public at large. Essentially then, the need for probabilistic quantification of uncertainties derives from the need to communicate risk judgments between the parties involved in the two separate steps of Casagrande's process, who no longer are the same.

Rationale for Probabilistic Approaches

More concrete justification for probabilistic characterization can be provided in the context of natural hazard assessment. Consider the example of a potentially unstable rockmass situated above a group of residences, where quantifying the probability of loss of life due to a rockslide might be warranted by the following:

- (1) The meaning of verbal descriptors of likelihood is often different from one person to another, for example when both geologic and engineering time scales can be applied. A rockslide could legitimately be characterized as "imminent" by a

geomorphologist and "unlikely" by an engineer concerned only with the lifetime of the structures, but the probability of a rockslide within a defined period does not depend on this context.

- (2) Expert opinion communicated to a public authority considering evacuation of the residences might have very different implications for a rockslide characterized as "possible" versus a rockslide probability given as, say, 0.5. Probabilistic characterization may make such actions or decisions more defensible by more clearly documenting the expert opinions expressed at the time they were made.
- (3) Allocation of resources for hazard mitigation depends on a consistent measure of relative risk. Stabilization measures for several rockslopes having similar failure consequences would logically be applied first to those with highest failure probability. In addition, probabilistic characterization provides the basis for more formal methods of decision analysis whereby the need for slope stabilization, various means to accomplish it, and alternative measures such as warning systems, can be evaluated.
- (4) A probability statement may reduce the liability of the engineer or geologist by explicitly identifying the possibility of an adverse outcome and providing an unambiguous expression of opinion regarding its likelihood. Whereas a conventional assessment might conclude that "a rockslide is unlikely to occur" (or worse, neglect to mention the possibility altogether), a statement of rockslide probability given as 0.1 supports the same conclusion while explicitly acknowledging uncertainty in the assessment and allowing others the opportunity to make informed judgments about the degree of risk and whether actions to reduce it may be warranted.

Possibly the most important justification for probabilistic characterization is the irreplaceable heuristic it provides for understanding potential failure modes and gauging the relative importance of various necessary steps in the failure sequence. In reviewing geotechnical failures, Peck [3] found that they usually result from multiple deficiencies whose effects coincide. Assigning probabilities to these component failure events requires that they be individually considered and thought through, and the exercise of defining and decomposing failure modes is often more important than the individual probability values themselves. Once the key elements in the failure process are defined and those with greatest uncertainty are isolated, potential steps to make the design more robust often become immediately apparent. For any important geotechnical structure or natural hazard that embodies significant risk, the value of performing such an imaginary post-mortem prior to failure, rather than an actual one afterwards, is evident.

Failure Mode Decomposition

The previous landslide example can be explored more fully to better develop the principles of decomposition and introduce the symbology of fault trees. To eliminate some of the intentional oversimplification of the previous discussion, suppose now that the rockslope in question is situated above a suburb of Vancouver and that the residences are unoccupied during daytime hours. If loss of life is to result then not only must a rockslide be triggered, but the debris must travel a distance sufficient to reach the houses, and the rockslide must occur at night. A fault tree using this simple decomposition as a first approximation is given on Figure 1(a), and the probability of the "top event" (loss of life) would be derived from probabilities assigned to each of the three component events shown.

However, realistic estimates of rockslide probability might not be possible without discriminating among various triggering mechanisms including earthquakes, high pore pressures induced by extraordinary rainfall, and other causes under normal conditions not directly attributable to extreme events. The first refinement to the fault tree on Figure 1(b) reflects these mechanisms. Here the probability of "normal" triggering might be estimated from the failure frequency of adjacent slopes at similar inclinations, and the probability of extreme earthquake and rainfall failures from seismic hazard and rainfall frequency analyses to determine the likelihood of critical ground motion and pore pressure values causing failure in stability analyses. Even further refinement, if warranted, is shown on Figure 1(c), which recognizes that there are no unique "critical" ground motion and pore pressure values at which a rockslide will or won't be triggered with certainty. Rather, failure probability varies in proportion to the level of ground motion or rainfall. In this case, ranges of extreme loadings are defined. The probabilities that these conditions will occur and the corresponding probabilities that the slope will fail in response are discrete approximations to continuous probability distributions for demand (or hazard) and capacity (or fragility) used in system reliability fields.

As Figure 1 shows, the complexity of the fault tree, the number of individual probabilities that must be estimated, and the analytical effort to support these estimates, all increase geometrically with the level of decomposition. On the other hand, it may not be possible to estimate probabilities for complex failures without some minimum level of disaggregation. In geotechnical applications, a central element in representing the failure process is to achieve a degree of decomposition in the failure sequence that sufficiently identifies key sources of uncertainty without reaching a level of complexity that obscures the relationships between component events and sacrifices the clarity that systematic probabilistic approaches can provide. Irrespective of the level of decomposition adopted, fault trees, event trees, or related approaches, are essential to systematically identifying the derivative sources of uncertainty in a geologic process and communicating the results.

Probability Interpretations

If probabilistic expression of uncertainty were as straightforward as the above example suggests, probability applications would have long ago achieved the same acceptance in geotechnical practice that they enjoy in structural engineering, where the field of structural reliability constitutes a recognized subspecialty. Whereas steel and concrete can be statistically sampled, tested, and characterized, geotechnical engineers and geologists have long argued (not without irony) that geologic conditions are too variable to allow such probabilistic approaches to be applied, and that these approaches would ignore the element of judgment that constitutes the essence of geotechnical practice. These objections stem from the dichotomous concepts of probability itself that trace their roots to the philosophy of science and the foundations of logical inference. While most geologists and geotechnical engineers recognize the statistical interpretation of probability and its shortcomings, few have been familiarized with the use of probability as the quantified expression of judgment. It is this alternative but equally admissible probability interpretation that is fundamental to expressing and communicating geologic uncertainty.

"Statistical" Probability

The most widespread definition of probability, the relative frequency concept, is based on the relative number of times a certain outcome will occur in a series of trials performed either by inference or actual experiment. According to this concept (called "statistical" probability here because of its usual connotation) one would infer a 50% probability that the toss of an unbiased coin would come up heads if a sufficiently large number of trials were performed; likewise, soil strength would be probabilistically characterized by obtaining a sufficient number of laboratory or field measurements.

The use of statistical probability is well developed in geotechnical engineering for such problems as slope stability where statistical data on strength can be obtained from the laboratory [4], or liquefaction where statistics can be derived directly from field case histories [5]. The problem with the statistical interpretation of probability arises in connection with an unknown state of nature where repeated trials are not meaningful, or where suitable analytical models of the phenomenon do not exist. For example, the probability that a fault is present at a specified location cannot be determined by repeated sampling: either the fault exists or it does not. Similarly, the probability of piping in a dam foundation cannot be directly derived from statistical analysis of soil gradation because too many other factors influence the process whose relationships are not quantified by any available procedure of analysis: statistically characterizing an input parameter is not by itself sufficient if the principal unknowns involve the process itself. In both of these circumstances, judgment of the engineer or geologist is paramount, and is not accounted for by statistical probability interpretations. This has led some

to reject probabilistic methods as inapplicable to many areas of geotechnical practice, when in fact the deficiency lies in the statistical interpretation of probability rather than in the method itself.

"Judgmental" Probability

Another interpretation, the subjective degree-of-belief approach, defines probability as the measure of one's confidence in the prediction of a particular outcome. This interpretation holds that probability is a measure of an individual's belief based on all information available, be it statistical and data-based, or empirical and experience-based. Relevant statistical data, while admissible, need not be formally incorporated in the probability estimate. Perhaps the best example is provided by the weatherman who predicts an 80% chance of rain in a certain forecast. In making this prediction, statistics indicating rain on this date for, say, 55% of the past years of record may indeed be relevant. In addition, however, particular aspects of frontal patterns and the weatherman's past experience with similar situations are essential elements in formulating his 80% degree-of-belief that it will rain today. In a similar way, an engineer's evaluation of piping failure probability for a dam may be made with an awareness of, but not necessarily directly derived from, piping failure statistics for other dams.

Judgment is therefore a fundamental element in the subjective degree-of-belief probability interpretation, so much so that the term "judgmental probability" is adopted here to avoid the pejorative connotation of the term "subjective" among engineers and laymen alike which would suggest that it is unscientific and therefore somehow inadequate. In fact, judgmental probability is the quantified expression of opinion, and as such may be expected to vary from one individual to another in the same way as judgment itself. Far from being non-rigorous, this property of judgmental probability captures and quantifies the essence of individual experience, and by doing so directly addresses the shortcomings of statistical probability in geotechnical engineering.

This is not to deny the role of statistical probability, and in fact the two interpretations are complementary. The calculus of probability does not depend on the interpretation adopted, and risk characterizations in geotechnical practice that utilize both are usually the most useful, as the subsequent case histories will show. As just one example, it is widely recognized that in most places the historic earthquake record is too short to justify the use of statistical data alone in seismic hazard analyses. These data are consequently supplemented by judgmentally-derived assessments of maximum magnitude and other important factors such as attenuation and source zonation, which themselves are subject to geologic uncertainty. The more sophisticated applications of seismic hazard analyses assign judgmental probabilities to these uncertainties [6], thus combining statistical and judgmental probability to evaluate ground motion probability more accurately than would be possible using either interpretation alone.

Judgmental Probability Assessment

Inasmuch as quantifying geologic uncertainty through judgmental probability is so vital to the understanding of risk in geotechnical practice, the common reluctance of geotechnical engineers to do so must be addressed. Casagrande [2] for example viewed "calculated risks" as those "which at present defy quantitative analysis," although he did not hesitate to advocate the application of judgment in qualitative form to them. Also, geologists often protest that geologic uncertainties are too great to be quantified, which is much like objecting to estimating large numbers because of their magnitude. These misgivings have much to do with the fact that an entire body of statistical theory provides numerical rules for statistical probability determination, while little related guidance is available for judgmental probability assessment. Although procedures involving artificial bets and lotteries are sometimes used in decision theory applications to elicit judgmental probability statements, geotechnical engineers often perceive such techniques as trivializing the uncertainties and the judgmental process used to derive them. Instead, explicit guidelines have been found useful to those being asked to assess judgmental probabilities for geologic uncertainties. By providing background and structure, such guidelines elevate the probability assessment process above that of just an armchair guess. This guidance is reproduced below in unabridged form, essentially as it has been provided to those asked to assess judgmental probabilities in geotechnical practice.

Guidelines for Judgmental Probability Assessment in Geotechnical Practice

The art of geotechnical engineering has been described as the ability to make rational decisions in the face of imperfect knowledge. Geotechnical decisions almost always incorporate uncertainty to one degree or another, and the engineer must rely on judgment - the difficult to define but nonetheless very real interpretive process that derives from the sum total of one's experience, insight, and intuition.

Assessing judgmental probabilities requires that one apply this ability together with available theory to quantify uncertainties that accurately express one's degree of belief in the state of nature, engineering properties, or outcome of a process. You have been asked to assess your judgmental probabilities for aspects of the conditions at hand where recognized uncertainties exist. In expressing these opinions, you may feel that there is insufficient information, or that you do not qualify as an expert in the field. However, these probabilities are based on your personal understanding of the site with information currently available to you, and the object is to elicit your opinion about how much uncertainty exists. Do not be intimidated that there are those with greater technical expertise. Right now there is nobody who knows more about both this site and the processes involved, and it is for exactly this reason that your expressions of uncertainty are sought. There is no correct or incorrect answer, only a numerical probability

statement that quantifies your judgments and uncertainty in these judgments as accurately as possible.

The assessment of judgmental probability is a systematic process of self-questioning, and it is important that you interrogate yourself about all of the possible outcomes that might occur without discarding any prematurely. Ask why you presently believe a particular outcome will occur or state of nature exists, what the support for your belief is, and how strongly you believe it. At the same time, carefully consider the evidence that now exists for alternative outcomes and the quality of the information incorporated in your assessment.

Research has been conducted using both experienced scientists in general and geotechnical engineers in particular whereby judgmental probabilities of measurable properties are assessed, then testing or experiments are performed for comparison [7, 8, 9]. Observations derived from these studies and from experience can be summarized as follows:

- (1) overoptimism. Geotechnical engineers are often overoptimistic in their best estimates of a particular parameter, state of nature, or probability. In providing a best estimate or most likely value, it is important to recognize that many engineers incorporate a bias for favorable outcomes even though most of us feel ourselves to be conservative. Some engineers tend to be consistently pessimistic in their estimates, but they are probably the minority. The point of judgmental probability assessment is to be neither conservative nor unconservative, as either will skew the outcome. With this in mind, it may be appropriate to calibrate your probabilities for any bias that you feel may apply.
- (2) overconfidence. Geotechnical engineers often display more confidence in their estimates than they should, and this tendency may increase the more experienced an engineer becomes. Overconfidence is not the same as overoptimism: rather than a bias in the mean value of a parameter, overconfidence is represented by insufficient dispersion about the mean. Stated differently, the best estimate may be accurate, but there is insufficient recognition of the possibility of higher or lower values. Even though your probabilities may accurately reflect the most likely value or outcome, do not underestimate the possibility that other outcomes may be more likely than you suspect.

Experience shows that the following techniques are helpful in the process of assessing judgmental probabilities.

- (1) Decomposition. Most people have an intuitive grasp of probabilities only in the range of about 0.1 to 0.9, and for events considered to be "very unlikely," it may be quite difficult to differentiate between assigned probabilities of, say, 0.01 and 0.001. Decompose a complex or very unlikely event into a sequence of simpler component events each having a probability within some more limited range (such as 0.1 to 0.9) you feel comfortable in assessing. Component probabilities can

then be aggregated provided that each is "conditional," or predicated on the occurrence of the preceding event in the sequence.

The more a complex event can be decomposed, the less need there is for precision in estimating probabilities of the individual components. When there are more than a few component events having probabilities in the range of 0.1 - 0.9, reasonable variations within this range usually produce aggregated results in the same order of magnitude, which represents the overall level of accuracy to be expected in virtually any probability assessment. It is almost always easier to make rough estimates of probabilities for many simple events than to make a single precise estimate for a highly complex and very unlikely one.

- (2) Consistency. Suppose that shear strength can fall within three possible ranges and that you assign a probability of 0.3 to each one. Something is inconsistent because the sum of the probabilities of all possible outcomes must be 1.0. Either one or more strength is more likely than you estimated, or there remains another possible strength range that is unaccounted for.

Proportional likelihoods are sometimes easier to estimate than absolute ones, and proportional ranking of outcome probabilities can provide another consistency check. If the first strength is twice as likely as the second and ten times more likely than the third, this statement can be algebraically translated into probabilities that sum to 1.0. These can be compared to your initial probabilities and adjusted accordingly until the final result is consistent with basic probability rules and your judgment.

- (3) Limits. Suppose some state of nature has only two possible outcomes - say that either liquefaction-susceptible soils exist at a site or they don't. If you are completely and totally uncertain, then either outcome is equally likely and the probability of each is 0.5. But if you feel the presence of such soils is more likely than not, then the probability that they exist is something greater than 0.5. If you are not completely sure they exist, then the probability is something less than perhaps 0.9. Questioning yourself about the upper and lower bounds of your uncertainty may help you to converge on your best probability estimate. It is sometimes more useful to think in terms of simple chance ratios such as one-in-three or four-out-of-five than the corresponding decimal fractions.
- (4) Normalizing. Whether we realize it or not, much of our accumulated experience and resulting judgment relies on case history data, either published or personal. Consciously search both literature and memory for case histories (or better yet case history compilations) of circumstances similar to those you are addressing. You may be able to evaluate to what extent your situation is better or worse than "typical" conditions represented by the case history database and normalize your judgmental probability accordingly. For example, the historical dam failure

frequency due to piping is about 10^{-5} per dam per year. If you believe your dam to be 10 times safer against piping than most, a normalized probability estimate would be 10^{-6} . Whether used directly or as a check on other techniques, comparisons with statistical data help to establish that your judgmental probability is in the right ballpark.

These techniques should help demonstrate that judgmental probability assessment is quite similar to the ordinary application of judgment in geotechnical engineering and differs from it only in requiring more explicit statements and careful reflection about all possible conditions and their likelihoods. Experience has shown that a written description providing the rationale in support of probability estimates and describing the experience upon which it is based forms an essential element of the probability assessment process.

Case Histories

Case histories provide perhaps the best way to illustrate how judgmental and statistical probability interpretations are integrated to express uncertainty in geotechnical practice, and three such cases are described below. The illustrations have been selected with emphasis on natural hazards and their effects on engineered structures. In addition, how the assessments were used and interpreted is discussed to provide the basis for lessons learned.

Sinkhole Risk Assessment

The Ocala Uplift in central Florida provides one of the few high quality limestone deposits in the state sufficiently above the water table to allow for large-scale conventional mining. Unfortunately these same circumstances have promoted extensive karstification, and both ancient infilled (paleokarst) sinkholes and active sinkhole collapses are common throughout the area. Expansion of one such mining operation required the construction of a dyke 10m high and 1200m long to retain fresh water. Although they were not revealed by conventional exploration and geophysical surveys, the potential for sinkholes in the dyke foundation, and the resulting risk due to dyke failure from sinkhole collapse, were clear.

A troubling indication of this potential was provided by slimes ponds in an adjacent area containing tailings from rock washing operations as shown on Figure 2(a). Periodic drops in fluid level of up to 1m in these impoundments provided evidence of sinkhole activity. Yet curiously, no sinkhole-related damage or failure of these dykes had ever occurred despite their total length of some 13 km. The dilemma was then whether to proceed with construction of the proposed dyke in the face of the risks posed by the known presence of sinkholes in the area, or

to carry out a costly program of intensive sinkhole exploration or mitigation in spite of the entirely satisfactory performance of the existing tailings pond dykes. In this case the geotechnical engineer elected to probabilistically characterize sinkhole uncertainties in order to elicit the owner's informed involvement in the decision. Details of the geologic conditions and probabilistic formulation have been provided elsewhere [10].

The typical sinkhole spacing and diameter was established from geologic mapping and regional information. Assuming sinkhole likelihood to be spatially independent, the probability of sinkhole occurrence within the area of the proposed dyke foundation was determined to be about 0.45. Also, the frequency of observed sinkhole collapses from records maintained in the area allowed a conditional probability of sinkhole collapse of 0.08 to be estimated. Both of these represent statistical probability interpretations of the kind derived from easily collected or readily available geologic data.

However, the performance of the existing tailings pond dykes suggested that even if sinkhole collapse were to occur, dyke breach would not necessarily result. This inferred resistance was decomposed into component events related to cracking resistance, piping resistance, and dam breach characteristics, and judgmental probabilities were estimated for each. The fault tree showing component events and estimated probabilities, both statistical and judgmental, is shown on Figure 2(b). The resulting probability of uncontrolled reservoir release due to foundation sinkholes was calculated as about 0.01, and comparison of this probability to dam failure frequencies from other causes was used to confirm the judgmental reasonableness of this result.

This probabilistic formulation of geologic uncertainty was extended to a formal decision analysis by estimating failure consequences and identifying alternative measures to reduce either consequences or failure likelihood that included performing additional exploration, implementing a warning system, or constructing a secondary dyke. This analysis concluded that constructing an inexpensive secondary dyke of mine waste to retain floodwaters that might be released by dyke breach had the lowest expected cost of the alternatives evaluated. Even so, the owner elected to accept the risks associated with constructing the water-retention dyke without the benefit of any supplementary risk-reduction measures. A factor in this decision was that the incremental risk added by the new dyke would not materially increase his risk exposure already present from the existing tailings ponds. Upon subsequent dyke construction, difficulties in reservoir filling were encountered which, while not unanticipated, required time-consuming sinkhole treatment. Nevertheless, performance of the dyke proved to be satisfactory on first filling and has remained so over the past five years with no signs of sinkhole-related distress.

The outcome of this case history was favorable insofar as probabilistic characterization helped to address conflicting inferences that could not likely have been resolved by informal processes alone. In addition, geologic uncertainties and risk were effectively communicated by the geotechnical engineer to the owner. This allowed the owner to become involved in an important design decision, and by being willing accept project risks, to avoid the costs of risk-reducing contingencies that might otherwise have been adopted.

Earth Fissure Risk Assessment

Groundwater withdrawal from alluvial basins in the Southwest U.S. can cause substantial consolidation of sediments. Surface tension cracks may develop in response to the resulting subsidence, especially near valley margins and other abrupt bedrock irregularities where horizontal tensile strains are concentrated. These "earth fissures" frequently form en-echelon patterns, with lengths of the individual features up to 1 km and an initial width of about 1 cm prior to enlargement by erosion from intercepted surface runoff. While geologic information provides some basis for understanding earth fissure development, neither the time nor location of future fissures can be predicted with certainty. The presence of earth fissures near the site of a proposed lined landfill was identified as a potential permitting issue. Although geologic evidence indicated that fissure development and consequent liner rupture at the site would be very unlikely, a probabilistic assessment was undertaken to better support this view before permitting authorities and the public.

Geologic records, detailed surface mapping, and historic airphotos identified the number and locations of fissures near the site and showed that they had developed over the 30-year period corresponding to the term of agricultural development and aquifer drawdown in the valley. The fissure source zone delineated on Figure 3(a) from observed fissure patterns, bedrock topography, and drawdown data, provided the fissure development rate per unit area assuming a simple Poisson process. The probability that a fissure would develop beneath the area of a lined landfill module while it contained leachate was then estimated to be about 0.002, according to this statistical interpretation.

For a leak to result from such a fissure would also require that the geomembrane liner be unable to sustain the induced deformations, and both wide-strip tensile tests and pullout-box tests were performed. Neither was capable of producing rupture to the limits of the device, and the material was still well within the elastic range under simulated fissure widths. As a result, it was not possible to base liner reliability on statistical evaluation of test results. Instead, judgmental assessments by the geotechnical engineers responsible for liner testing and design yielded a liner rupture probability of 0.1 under field fissure conditions. This resulted in a probability of 2×10^{-4} , or one chance in 5000, that leachate would be released from the landfill due to a fissure-induced liner rupture, as represented by the leachate leakage event on the fault tree of Figure 3(b). This probability reflects geologic and geotechnical uncertainty regarding fissure occurrence and liner reliability, but it does not represent risk. To do so requires that the consequences of liner rupture be accounted for.

The analysis and the fault tree were therefore extended by assuming that all leachate would reach and enter the groundwater some 60m below, and that continuous human consumption of this water would occur from hypothetical wells located at the site boundary. Given these conditions together with the aquifer characteristics, and EPA algorithm accounting for health effects of landfill leachates was used to estimate a probability of 7×10^{-10} that adverse human health effects would result [11]. The overall probability that earth fissure development at the site could

produce adverse health effects is therefore about 10^{-13} , or 1-in-10 trillion, as represented by the top event on the fault tree of Figure 3(b).

Although the analysis clearly demonstrated that health risks due to fissure development were negligible, the permitting authority nevertheless expressed a preference for further structural reinforcement by adding a geogrid to the liner system. The results of the risk analysis were not a material factor in establishing this preference. In this case, probabilistic methods were successful in expressing both the geologic uncertainties and resulting risks, but the incomprehensibly small risk value and the vagaries of the added health risk assessment may have detracted from the clarity, and therefore the credibility, of the analysis. A simpler version limited to evaluating only liner leakage probability might have been more effective in addressing the geologic and geotechnical uncertainties at issue.

Seismic Tailings Dam Risk Analysis

Rich lead deposits in the central U.S. have been extensively exploited for over a century, but only recently has the seismic hazard of the region become well known. This awareness led to concern for the seismic stability of an abandoned tailings dam constructed at one such mine between 1942 and 1965 by the "upstream" method. In this case, the usual practice of evaluating seismic dam safety according to a single established ground motion criterion produced a misleading impression of failure potential, which was clarified by a more formal probability and risk analysis.

Research of mine records and interviews with former personnel revealed that tailings in later years of mill operation were discharged mostly from the rear of the impoundment, resulting in extensive deposits of saturated, liquefaction-susceptible slimes near the embankment face as shown on Figure 4(a). A two-dimensional dynamic response analysis determined that liquefaction of these slimes would be triggered under the 0.20g peak bedrock acceleration specified by state regulations for dam safety assessment. This value has a recurrence interval at the site of roughly 2500 years.

Post-earthquake stability analyses assigning residual undrained shear strength to the liquefied slimes showed the critical feature to be a slimes layer at about mid-height of the dam, and seismic stability was controlled by the extent to which this layer approached the embankment face, indicated by the distance \bar{X} on Figure 4(a). Although the slimes layer was penetrated in borings drilled from the dam crest, the steep downstream slope precluded drillrig access to the critical region beneath the embankment face. Available information was limited to historic accounts of dam construction indicating that slimes could have been deposited as close as 20m from the slope. Therefore \bar{X} was taken as 20m in the analysis, which from Figure 4(b) resulted in post-earthquake FS of 0.5.

This result was presented to the dam owner as the conclusion that the dam would fail under the specified ground motions having an annual probability of 4×10^{-4} . Whereas the computed FS clearly indicates to the geotechnical engineer that failure would also occur under much smaller and more likely ground motions, the dam owner erroneously inferred that 4×10^{-4} was the annual probability of seismic failure, and consequently that the need for remedial measures might not be especially urgent.

A probabilistic analysis was therefore undertaken to estimate what the actual seismic failure probability would be. The previous dynamic response analyses predicted little amplification of base motions at the location of the critical slimes layer. Under this condition, and neglecting any effects of initial static shear stress as a first approximation, level-ground liquefaction assessment procedures were applied using the program PROLIQ [12]. By integrating a conventional seismic hazard analysis with level-ground SPT-based liquefaction criteria, this procedure accounts for uncertainty in both earthquake acceleration and magnitude, although both the input soil properties and the liquefaction criteria are still deterministic. These simplifications notwithstanding, PROLIQ provides a statistical-type probability of liquefaction triggering, which for the critical slimes layer was found to be 0.009 per year.

The other principal uncertainty in seismic failure probability was the extent of the critical slimes layer. From Figure 4(b), $\bar{X} = 35\text{m}$ corresponds to post-earthquake $FS = 1$, and distances greater or less than this value were believed to be equally likely. Hence, the corresponding fault tree event on Figure 5(a) was assigned a judgmental probability of 0.5. The probability of seismic dam failure is therefore about 5×10^{-3} per year, about 10 times greater than the probability of the ground motions specified as the criterion for the original dam safety assessment. Providing this information to the dam owner effectively clarified the initial misimpression and pointed to the need to consider remedial measures for seismic dam stabilization. To aid in this assessment, a risk and decision analysis was performed by accounting for the consequences of failure and defining various alternatives that might be used to reduce failure risk.

An analysis of potential tailings flowslide runout from seismic failure of the dam [13] showed the consequences of failure to be those associated with tailings cleanup, environmental restoration, and dam repair, and allowed the related economic costs to be estimated. Also, several feasible remedial measures for dam stabilization were identified, conceptual designs were prepared, and construction costs were estimated. By using PROLIQ, the reduced failure probability associated with each of these options was estimated.

The total cost of any option (including the existing conditions) can be taken as the cost of implementing the option plus its "risk cost," defined as failure probability multiplied by failure cost. Figure 5(b) shows annualized total, construction, and risk costs for four different methods of seismic tailings dam stabilization. In this case, the total cost of a berm is the lowest for the remedial options considered, and does not greatly exceed that associated with accepting the risk of current conditions. While a remediation decision for this project has yet to be made, the failure probability and risk characterization was well-received by the dam owner and state dam

safety authorities, and proved to be instrumental in the accurate assessment of geotechnical and geologic risks that might otherwise have remained misconstrued.

Lessons Learned from Case Histories

These three case histories represent the spectrum of the author's experience in the degree to which geotechnical probability and risk characterizations have influenced project outcomes and decisions, ranging from largely irrelevant to essential. Yet in all cases the uncertainties associated with the various geologic hazards were fairly portrayed and accurately communicated to the owners and regulatory authorities with ultimate responsibility for accepting or mitigating the resulting risks.

Both statistical and judgmental probability interpretations were adopted in each case, and it is doubtful that the nature of the uncertainties could have been adequately represented by either one alone. Statistical models such as those applied to sinkhole and fissure occurrence were very simplistic, and many embellishments related to spatial distribution, size, and occurrence rate are easily envisioned. Likewise, the judgmental unknowns associated with earthquake and liquefaction phenomena are legion, and many of these were not formally addressed in the tailings dam case. Nevertheless, simple statistical models and decomposition of judgmental likelihoods at a relatively crude level captured the key uncertainties to a degree consistent with the level of information available and the geologic or geotechnical understanding of the problem.

If the object of a probabilistic assessment is to communicate uncertainty and risk, then it cannot be presented to a decisionmaker as a "black box" to be accepted at face value like many other types of geotechnical analyses or geologic evaluations. The key to communication is imparting understanding, and an important lesson to be derived is that simplicity rather than analytical detail is perhaps the key factor determining the usefulness of probabilistic methods in geotechnical application. Although essential geologic unknowns cannot be neglected, attempting to extend the analysis to the full universe of uncertainties may be counterproductive and detract from the credibility of the results.

Conclusions

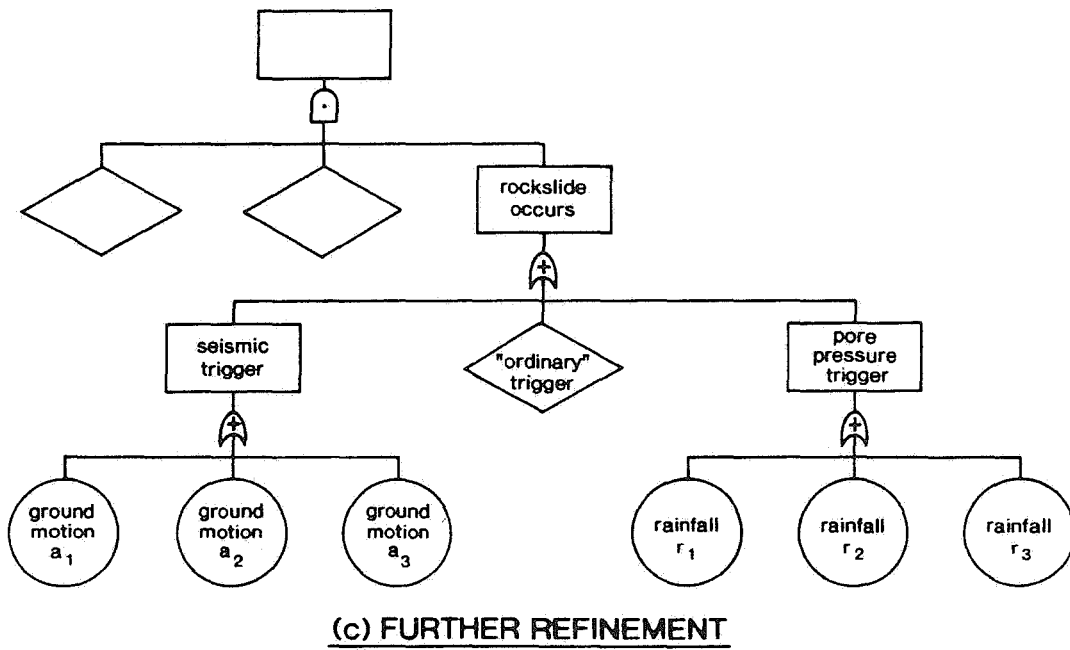
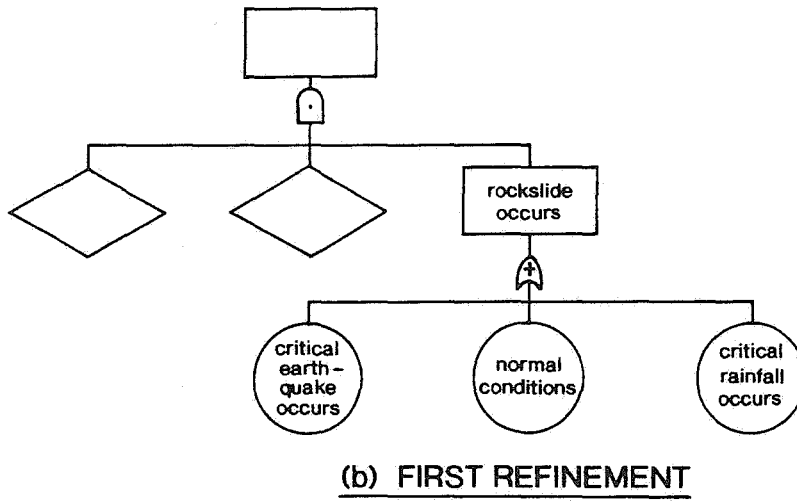
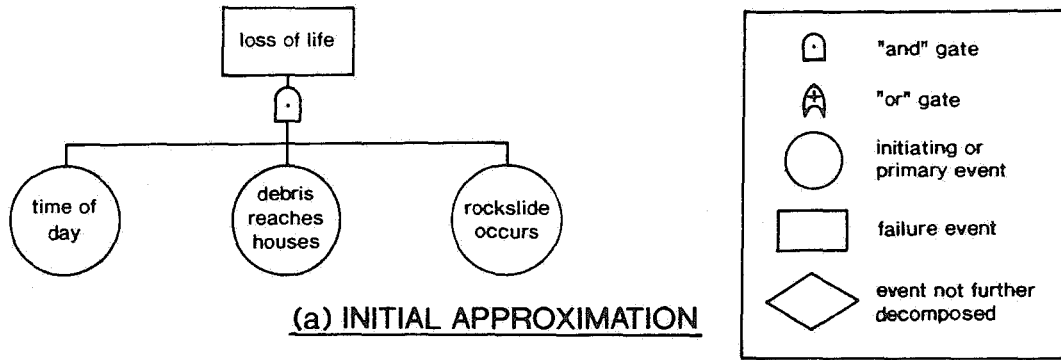
Geologic and geotechnical uncertainties, particularly those related to natural hazards, are often considered unquantifiable, and therefore not amenable to probabilistic treatment. A major reason is that only the statistical interpretation of probability is acknowledged, and statistics are frequently viewed as anathema to the exercise of judgment so undeniably fundamental to geotechnical practice.

On the other hand, judgmental probability has equally legitimate origins and is ideally suited to the expression of geotechnical judgment as the degree of belief in the state of nature or outcome of a process. That this interpretation has largely failed to cross interdisciplinary boundaries into geotechnical/geologic fields, where it is perhaps more useful than in any other, may be ascribed at least partially to the unfortunate vernacular in the parent fields of probability and mathematics (such as "subjective" in relation to belief and "indifference" in connection with equal degrees of uncertainty), as well as to such technically sound but artificial devices as the imaginary lotteries devised by decision theorists. Missing have been translations of terminology into geotechnical and geologic language, guidelines providing structure to the probability assessment process, and case history examples to guide application in practice. This paper is an effort toward addressing these deficiencies, and in so doing attempts to show how judgmental interpretations can complement statistical probability in applications relevant to ordinary geotechnical practice. A related aim has been to show that useful applications of probabilistic methods need not necessarily involve complex manipulations performed only by those conversant with statistical or decision theory, and to thereby encourage more widespread application of these methods by practicing engineers and geologists.

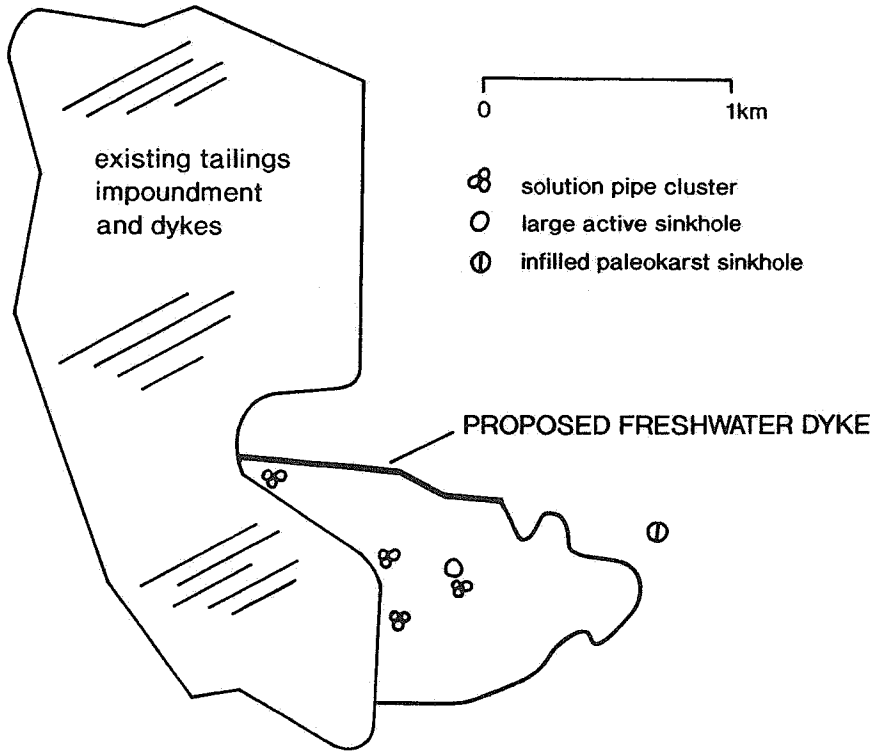
It has been said that for any new technique to become established in engineering practice, it must either be demonstrably more efficient than available methods, or be able to analyze physical conditions that existing procedures cannot address. Were these the sole standards, then probabilistic methods might justifiably reside in the shadows of geotechnical practice. However, in contemporary society it is unrealistic to believe that either engineers or scientists can continue to exercise their former authority in defining the degree of risk or safety that is acceptable in the technologies they apply. Public demands for explanation and accountability for these risk decisions are expressed by requirements for regulatory involvement in project decisionmaking, and enforced by the hammer of legal liability for those who fail to comply. Probabilistic expression of geologic and geotechnical uncertainty provides an important vehicle by which the application of professional judgment can remain intact in this environment. To this extent, probabilistic methods deserve to be viewed as the natural evolution of such established approaches to uncertainty as the observational method and the concept of calculated risk that trace their origins to Terzaghi, Casagrande, and the inception of modern geotechnical practice.

References

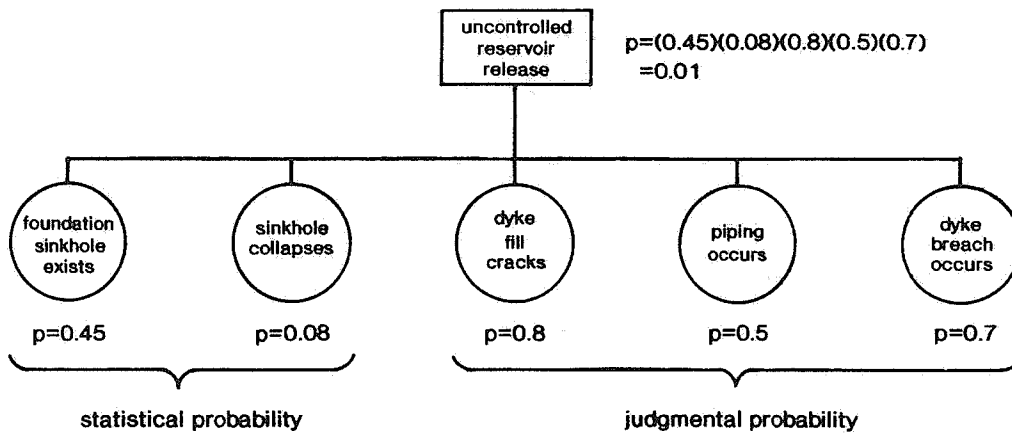
- [1] Einstein, H., 1991, "Observation, Quantification, and Judgment: Terzaghi and Engineering Geology," J. Geotech. Eng., ASCE, v. 117, no. 11.
- [2] Casagrande, A., 1965, "Role of the 'Calculated Risk' in Earthwork and Foundation Engineering," J. Soil Mech. Div., ASCE, v. 91, no. SM4.
- [3] Peck, R., 1984, "Where Has All the Judgment Gone?" Judgment in Geotechnical Engineering, J. Duncicliff, and D. Deere, (eds.), John Wiley & Sons.
- [4] Vanmarke, E., 1977, "Reliability of Earth Slopes," Journ. Geotech. Eng., ASCE, v. 103, no. GT11.
- [5] Liao, S., Veneziano, D., and Whitman, R., 1988, "Regression Models for Evaluating Liquefaction Probability," Journ. Geotech. Eng., ASCE, v. 114, no. 4.
- [6] Youngs, R., Swan, F., Power, M., Schwartz, D. and Gray, R., 1987, "Probabilistic Analysis of Earthquake Ground Shaking Hazard Along the Wasatch Front Utah," Assessment of Earthquake Hazards and Risk along the Wasatch Front, Utah, P. Gori and W. Hays (eds.), USGS open file Report 87-585, v. II.
- [7] Baecher, G., 1972, "Site Exploration: A Probabilistic Approach," Ph.D thesis, Massachusetts Institute of Technology.
- [8] Folayan, J., Hoeg, K., and Benjamin, J., 1970, "Decision Theory Applied to Settlement Predictions," J. Soil Mech. Fdn. Eng., ASCE, v. 96, no. SM4.
- [9] Rubin, J., 1989, "The Dangers of Overconfidence," Technology Review, v. 92, no. 5, July.
- [10] Vick, S. and Bromwell, L., 1989, "Risk Analysis for Dam Design in Karst," J. Geotech. Eng., ASCE, v. 115, no. 6.
- [11] U.S. Environmental Protection Agency, 1988, Proposed Rules, RCRA Subtitle D, Federal Register, Vol. 53, no. 100, Aug. 30, 1988, pp. 33356-33363.
- [12] Atkinson, G., Finn, W., and Charlwood, R., 1984, "Simple Computation of Liquefaction Probability for Seismic Hazard Applications," Earthquake Spectra, EERI, v. 1, no. 1.
- [13] Vick, S., 1991, "Inundation Risk from Tailings Dam Flow Failures," Proc. IX Panamerican Conf. on Soil Mech. and Fdn. Eng., v. III.



ROCKSLIDE EXAMPLE
FIGURE 1

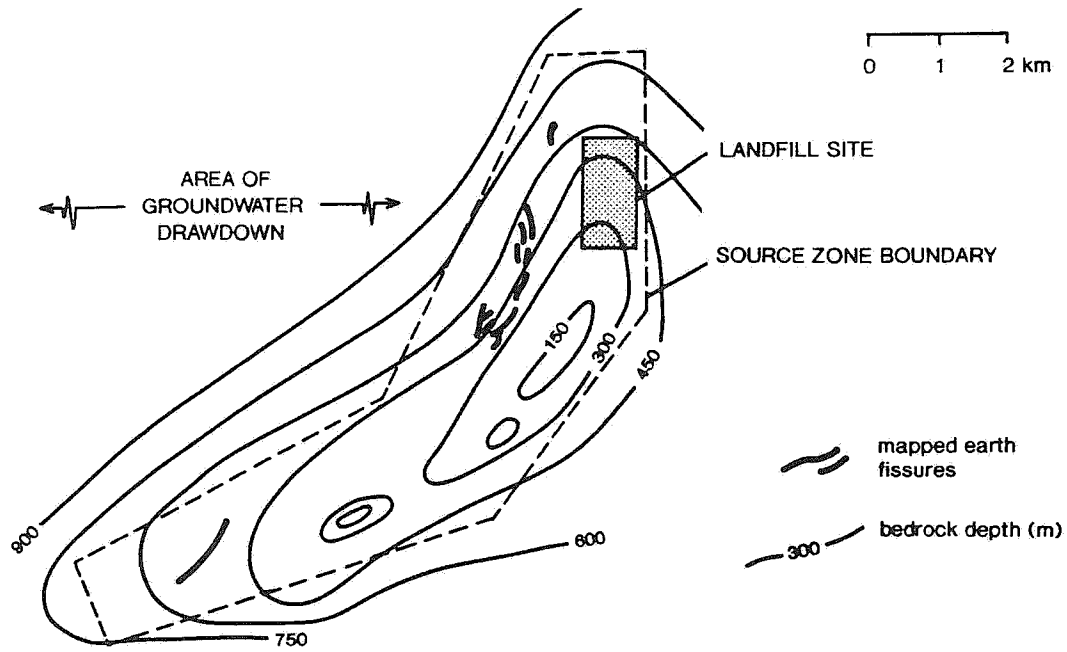


(a) PROJECT FEATURES

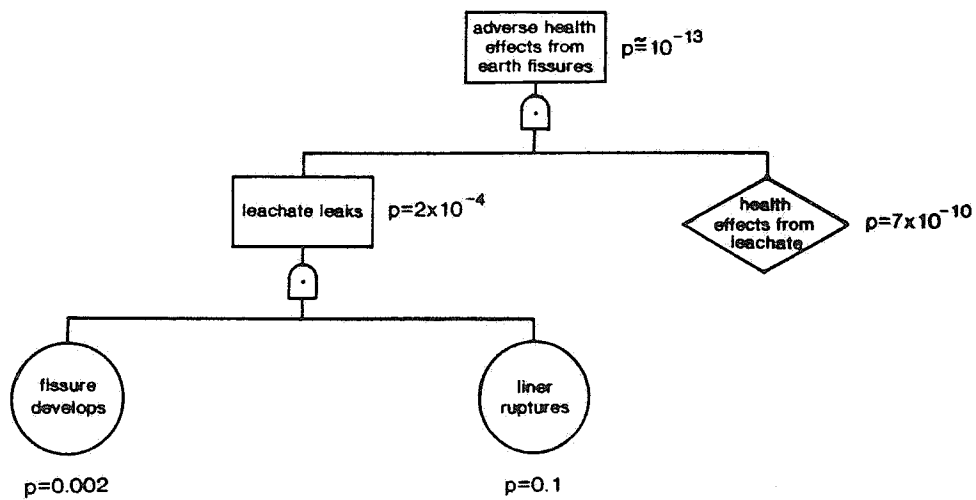


(b) DYKE FAILURE FAULT TREE

**SINKHOLE
CASE HISTORY
FIGURE 2**

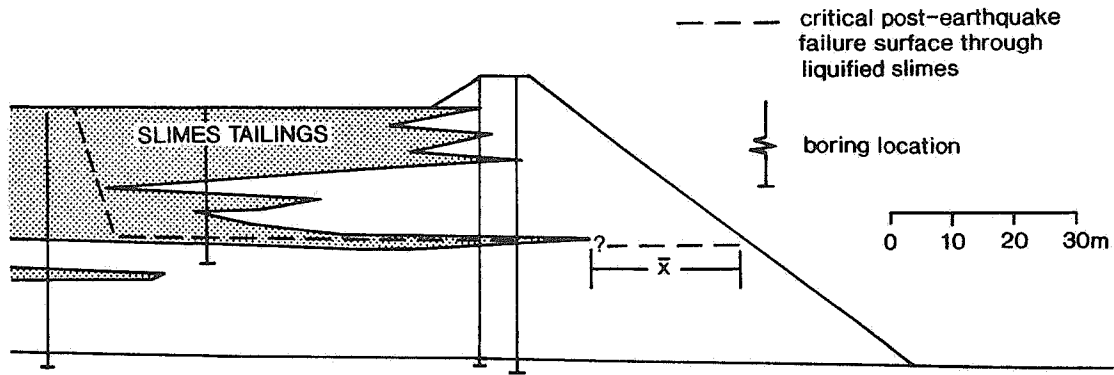


(a) PROJECT FEATURES

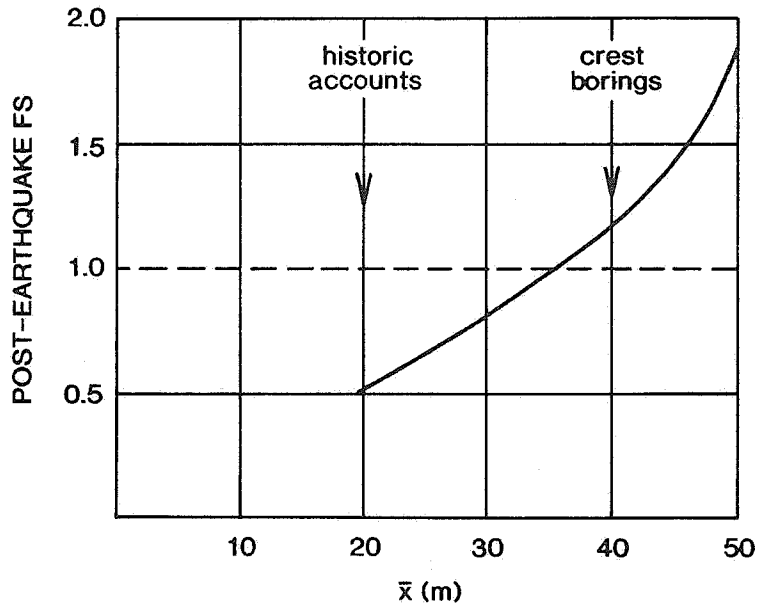


(b) FAULT TREE

**EARTH FISSURE
CASE HISTORY
FIGURE 3**



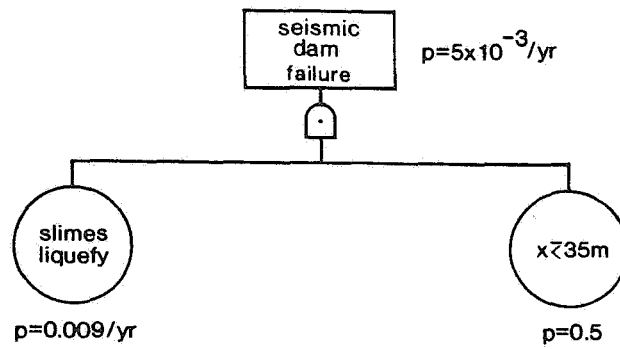
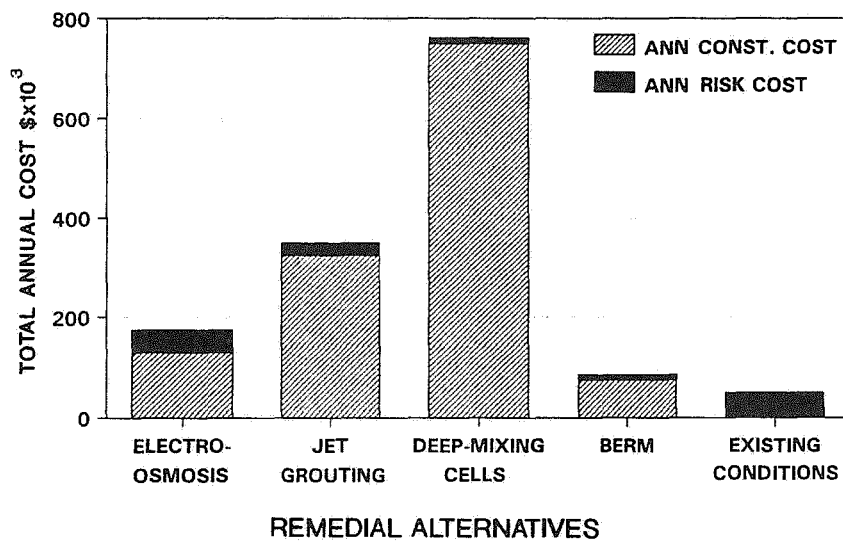
(a) EMBANKMENT CROSS SECTION



(b) SEISMIC STABILITY RESULTS

TAILINGS DAM STABILITY ANALYSIS

FIGURE 4

(a) FAULT TREE(b) DECISION ANALYSIS RESULTS

**TAILINGS DAM
SEISMIC RISK
FIGURE 5**

Session 1

Seismic Hazards

the pattern of small earthquakes.

There is a subset of the ongoing small earthquakes that do occur in the upper 10 km of the crust. Some of the larger of these very shallow events had long aftershock sequences typical of California earthquakes and may have occurred on faults that ruptured the surface. The November 30, 1975 earthquake ($M=4.9$) in central Georgia Strait [4] and the April 13, 1990 Deming, Washington earthquake ($M=4.8$), just south of Abbotsford [5], are two such events. Such extremely shallow earthquakes are rare, but represent the greatest source of uncertainty in assessing seismic hazard in the region because their distribution and maximum magnitude are difficult to assess, but such near surface sources can have very high accelerations in close proximity to them. There is a growing amount of geological evidence that is interpreted as a prehistoric earthquake in the magnitude 7 range about 1100 years ago [6] that ruptured the surface in central Puget Sound near Seattle.

Subcrustal Earthquakes

Subcrustal earthquakes in this context refer to earthquakes within the subducting Juan de Fuca Plate. This is the best quantified earthquake source region. Ongoing microearthquake activity positions the subducted plate precisely (Fig. 3). The maximum size of earthquake is well constrained to the 7 to 7.5 magnitude range because of the known thickness of the young subducting plate and hence an upper limit to rupture area for typical rupture lengths.

The earthquakes within the Juan de Fuca plate are concentrated in two regions as the plate descends. The first is in the coastal region where a bend occurs as the plate goes from horizontal in the deep ocean to a shallow dip of ten to twenty degrees beneath Vancouver Island. The band of seismicity straddling the coast in Figure 1 represents this seismicity.

The next concentration is below the Strait of Georgia and Puget Sound where the plate bends further to a steeper dip of about thirty degrees. This is the region where the subducting plate is transferred from positive to negative buoyancy by phase changes in the rocks of the oceanic crust. It is marked by a band of seismicity mainly in the 45 km to 65 km depth range beneath Georgia Strait and Puget Sound. This seismicity is also concentrated in a north-south sense between 47°N and 49°N but continues both to the north and south. The arching of the plate in this region [7] to accommodate the bend in the coast line forces this north-south concentration.

All of the larger subcrustal earthquakes in historic time have occurred within the boundaries of the present day concentration between 47°N and 49°N . Damaging earthquakes occurred 1949 and 1965 at the south end of Puget Sound and have provided accelerograms of strong ground motion. At the north end of the concentration, earthquakes near the damage threshold (in the magnitude 5 to 6 range) occurred in the Gulf Islands/San Juan Islands region in 1864, 1904, 1909, 1920 and 1976.

Subduction earthquakes

The potential for large earthquakes on the subduction interface in the Cascadian subduction zone has been discussed in the scientific literature for less than a decade [8], [9], [10] but the wide ranging evidence for their occurrence has convinced most of the geoscience community that the hazard is real [11], [12]. Geological deposits in coastal estuaries [13] and deep sea sediments [14] spaced centuries apart, that are attributed to these earthquakes, are convincing pieces of evidence. Tree ring dating of trees killed by submergence of coastal regions has placed the last event at about 1700 AD [15]. The ongoing and uniform strain buildup parallel to

the direction of subduction on Vancouver Island and on the Olympic Peninsula in northern Washington is another key piece of evidence [16], [17].

Subduction events are rare but can be quantified. Constraints on potential ground motion can be made because the position of the plate interface is known from the microearthquake seismicity [18], seismic reflection [19] and seismic refraction results [20], and information from other subduction zones can be used to obtain a realistic range of estimates on rupture behavior and thus surface ground motion. The most important parameter for hazard estimates is the down-dip extent of the seismogenic zone. Simplistically, this surface is defined by the length of contact between the brittle portion of the overlying continental crust (about 30 km - see Fig. 3) and the subducting plate. The down-dip end of the potential rupture surface is roughly in the region of the outer coast of Vancouver Island. Recent subduction earthquakes in 1985 in Mexico and Chile [21] have had significant seismic energy coming off the subduction fault to depths of about 40 km. The surface of the subducting plates is slightly older and colder in these instances and thus the seismogenic zone may be expected to be slightly deeper than in the Cascadia region. Recent thermal modelling of the Vancouver Island region [22] suggests the maximum depth of the seismogenic region may be slightly less than 30 km.

One study that generated simulated accelerations for the Cascadia subduction zone predicts ground motions at the distance of Vancouver from the seismogenic zone would be smaller than those that would be expected from larger subcrustal earthquakes [23]. The main difference in hazard from subduction earthquakes is the long duration of strong shaking associated with large ruptures and the large area of shaking involved. The long duration can adversely affect certain types of structures and the liquefaction potential of saturated soils.

Good examples of the kinds of effects that a subduction earthquake will have can be seen in examining the damage caused by the great 1964 Alaska earthquake ($M = 9.2$) in the city of Anchorage [24] which is about the same distance from the down dip end of the Alaska seismogenic zone as Vancouver is from the Cascadia seismogenic zone. The estimated three minutes of strong shaking during the Alaska earthquake damaged numerous larger structures. Single family wood frame dwellings and other similar small wood frame structures performed excellently as a class of construction, when not located in an areas subject to soil failure.

References

1. Cassidy, J.F., Ellis, R.M. and Rogers, G.C. 1988. The 1918 and 1957 Vancouver Island earthquakes. *B. Seis. Soc. Am.*, **78**, 617-635.
2. Rogers, G.C. and Hasegawa, H.S. 1978. A second look at the British Columbia earthquake of 23 June, 1946. *B. Seis. Soc. Am.*, **68**, 653-676.
3. Malone, S.D. and Bor, S. 1979. Attenuation patterns in the Pacific Northwest based on intensity data and the location of the 1872 North Cascades earthquake. *B. Seis. Soc. Am.*, **679**, 531-576.
4. Rogers, G.C. 1979. Earthquake fault plane solutions near Vancouver Island. *Can. J. Earth Sci.*, **16**, 523-531.
5. Qamar, A. and Zollweg, J. The 1990 Deming, Washington earthquakes: a sequence of shallow thrust earthquakes in the Pacific northwest. (Abstract) *EOS, Transactions, American Geophysical Union*, **71**, 1145.
6. Bucknam, R.C. and Barnhard, T.P. 1989. Evidence of sudden late Holocene uplift in the central Puget Lowland, Washington. (Abstract)

- EOS, Transactions, American Geophysical Union, **70**, 1332.
7. Crosson, R.S. and Owens, T.J. 1987. Slab geometry of the Cascadia subduction zone beneath Washington from earthquake hypocenters and teleseismic converted waves. *Geophys., Res. Let.*, **14**, 824-827.
 8. Heaton, T.H. and Kanamori, H. 1984. Seismic potential associated with subduction in the northwestern United States. *B. Seis. Soc. Am.*, **74**, 933-942.
 9. Heaton, T.H. and Hartzell, S.H. 1987. Earthquake hazards on the Cascadia subduction zone. *Science*, **236**, 162-168.
 10. Rogers, G.C. 1988a. An assessment of the megathrust earthquake potential of the Cascadia subduction zone. *Can. J. Earth. Sci.*, **24**, 844-852.
 11. Rogers, G.C. 1988b. Seismic potential of the Cascadia subduction zone. *Nature*, **332**, 17.
 12. Heaton, T.H. 1990. The calm before the quake? *Nature*, **343**, 511-512.
 13. Atwater, B.F. 1987. Evidence for great Holocene earthquakes along the outer coast of Washington State. *Science*, **236**, 942-944.
 14. Adams, J. 1990. Cascadia subduction zone: evidence from turbidites off the Oregon-Washington Margin. *Tectonics*, **9**, 569-583.
 15. Atwater, B.F., Stuiver, M. and Yamaguchi. 1991. Radiocarbon test of earthquake magnitude at the Cascadia Subduction zone. *Nature*, **353**, 156-158.
 16. Dragert, H. and Lisowski, M. 1990. Crustal deformation measurements on Vancouver Island, British Columbia: 1976 to 1988. Proc. 125th Anniversary Meeting of the International Association of Geodesy, D. R. Vyskocil, C. Reigber and P.A. Cross, editors, Springer-Verlag, New York, 241-249.
 17. Savage, J.C., Lisowski, M. and Prescott, W.H. 1991. Strain accumulation in Western Washington. *J. Geophys. Res.*, **96**, 14493-14507.
 18. Rogers, G.C., Spindler, C., and Hyndman, R.D. 1990. Seismicity along the Vancouver Island Lithoprobe corridor. Proceedings of the Lithoprobe Southern Cordillera Symposium, University of Calgary, 166-169.
 19. Hyndman, R.D., Yorath, C.J., Clowes, R.M. and Davis, E.E. 1990. The northern Cascadia subduction zone at Vancouver Island: seismic structure and tectonic history. *Can. J. Earth Sci.*, **27**, 313-329.
 20. Drew, J.J. and Clowes, R.M. 1990. A re-interpretation of the seismic structure across the active subduction zone of western Canada. in: *Studies of Laterally Heterogeneous Structures Using Seismic Refraction and Reflection Data*, A. G. Green, editor, Geol. Surv. Canada Paper 890-13, 115-132.
 21. Somerville, P., Sen, M. and Cohee, B. 1991. Simulation of strong ground motions recorded during the 1985 Michoacan, Mexico and Valparaiso, Chile, earthquakes. *B. Seis. Soc. Am.*, **81**, 1-27.
 22. Wang, K. and Hyndman, R.D. 1991. Thermal constraints on the zone of possible major thrust earthquake failure on the Cascadia Margin. (Abstract) EOS, Transactions, American Geophysical Union, **72**, 314.
 23. Cohee, B.P., Somerville, P.G., and Abrahamson, N.A., 1991. Simulated ground motions for hypothesized M=8 subduction earthquakes in Washington and Oregon, *B. Seis. Soc. Am.*, **81**, 28-56.
 24. Wood, F.J. 1967. The Prince William Sound, Alaska, earthquake of 1964 and aftershocks. (in 3 volumes), Coast and Geodetic Survey Pub. 10-3, U.S. Dept. of Commerce.

Vancouver Island Earthquakes
Jan 1982 - Dec 1991

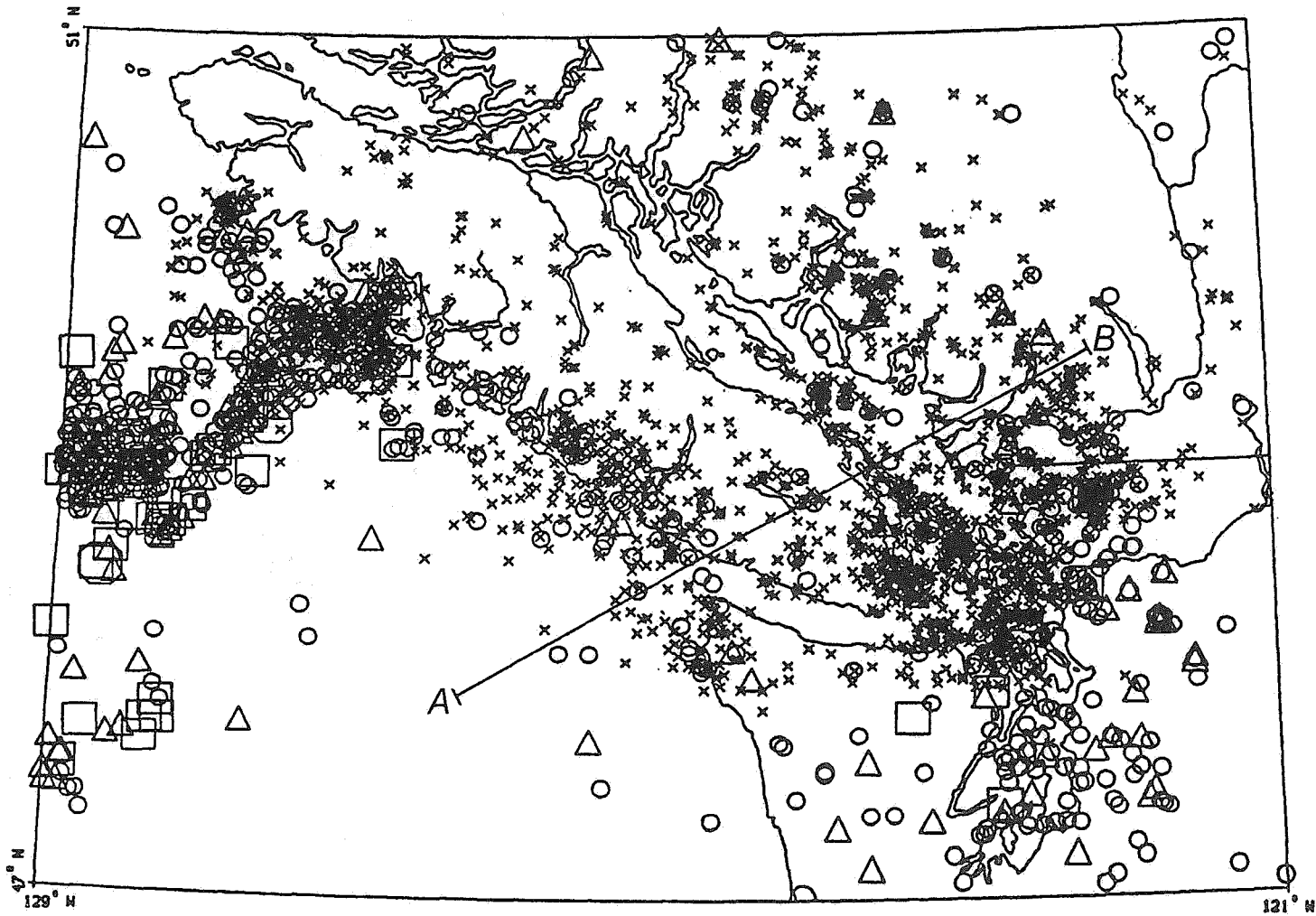


Figure 1. A ten year sample of seismicity in the Vancouver Island region. Seismicity is not complete in the United States. Crosses are events less than magnitude 2, circles between 2 and 3, triangles between 3 and 4 and squares 4 and greater. Line AB is the cross section shown in Figure 3.

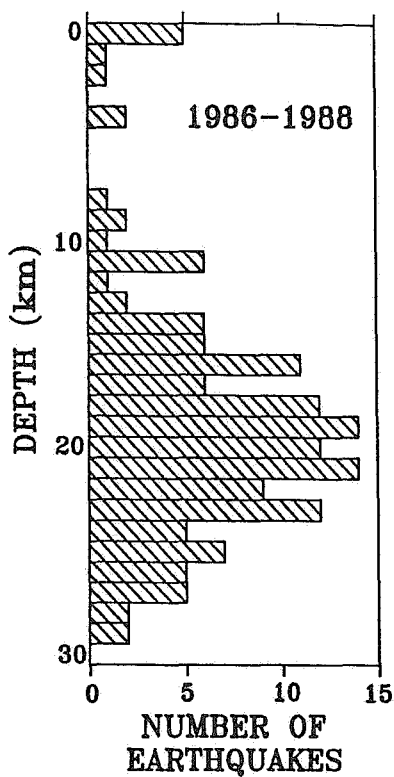


Figure 2. Depth distribution of a three year sample of crustal earthquakes in southern Georgia Strait.

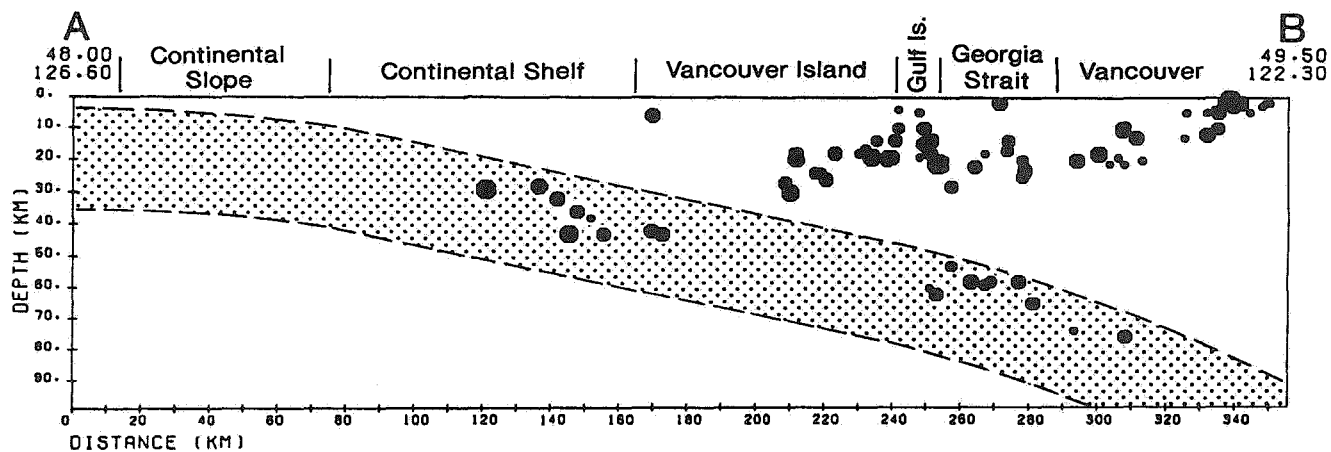


Figure 3. A 50 km wide corridor projected on to the cross section shown in Figure 1. Earthquakes continue to the west within the subducting plate but do not meet the plotting criteria of less than 5 km in standard error of depth used here.

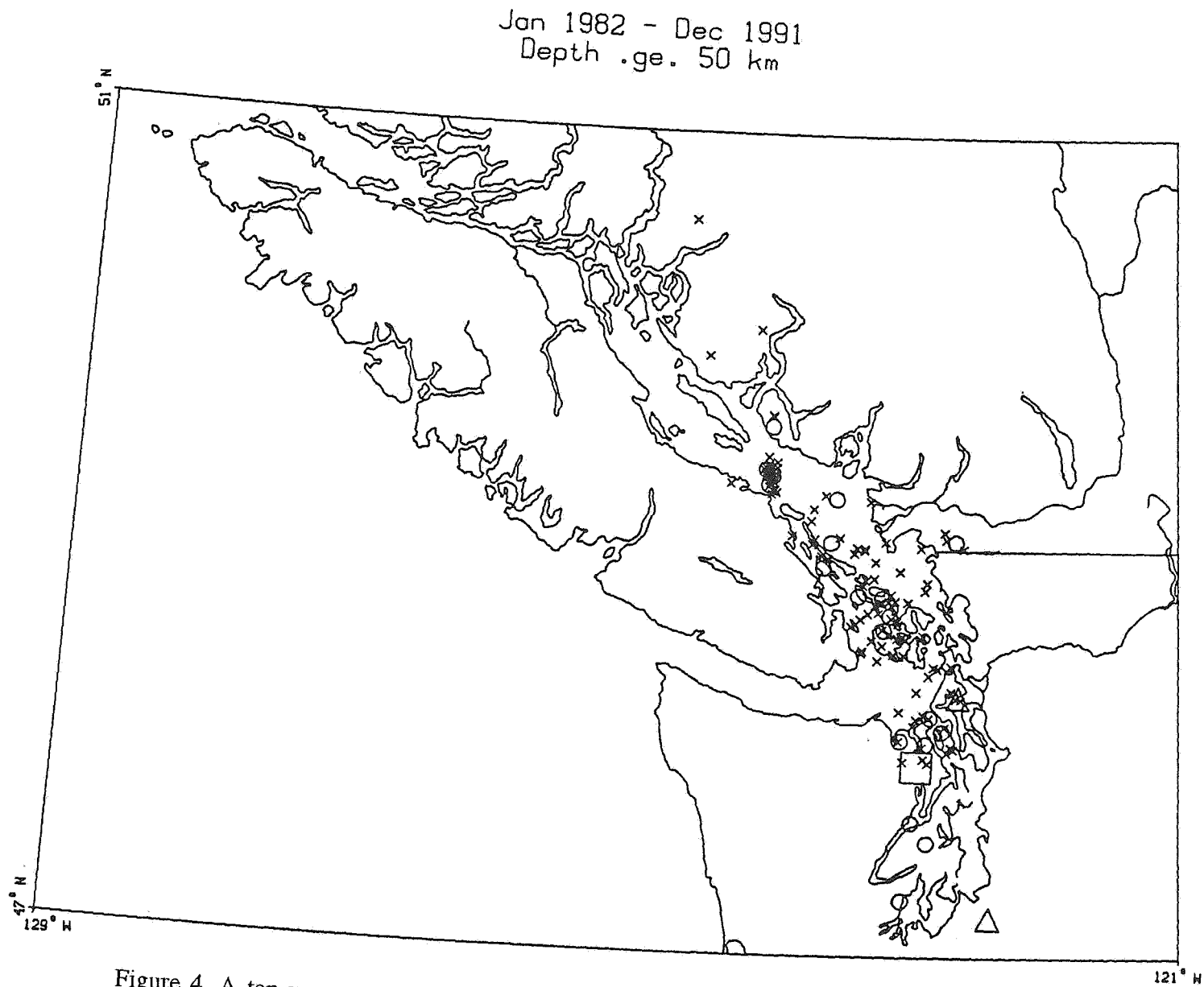


Figure 4. A ten year sample of subcrustal earthquakes beneath Georgia Strait. Symbols are as in Figure 1. Data incomplete in the United States.

Deterministic Basis for Seismic Design in B.C.

D.D. Campbell & J.L. Rotzien
Dolmage Campbell Ltd.
Vancouver, British Columbia

1 Abstract

Seismic design in Canada has been based upon probabilistic models which have produced judgemental design parameters ranging widely in both accuracy and practical sensibility. Advances in seismic monitoring, measuring and understanding of the earth's crust everywhere now make it possible to establish specific deterministic seismic design criteria throughout most of North America. In particular the active crustal tectonics of British Columbia are now reliably and accurately known and therefore form a dependable framework for deterministic analyses. This paper presents a seismic hazard zoning map for British Columbia that is based upon peak ground accelerations (PGA) that can be expected to be generated by the maximum credible earthquakes (MCE) that will occur on the specific seismically active geologic structures in the crust. The attenuation relationship between PGA and MCE (Schnabel and Seed), has been strongly verified by records from the 1989 Loma Prieta earthquake.

The degrees of certainty are not everywhere uniform in this analysis and time will doubtless present new data that will require adjustments to be made in the maps; however, it is anticipated that such adjustments will be more in the nature of fine tuning of the instrument rather than major repairs. The intent of the compilation of this seismic hazard map is to provide a technically dependable, valid and sensible basis for seismic design in British Columbia.

The validity of a so-called "mega-subduction earthquake" (M9+) proposed in 1988 for the subducting Cascadia plates is negated on the basis of physical plate geology and seismic records.

2 Introduction

Earthquakes are elastic shock waves in the earth originating from brittle failures of the earth's crust. They are caused by the release of compressive and/or tensional strains built up as various segments of the crust interact to the rotational forces of the earth and the changing heat fluxes in the hot plastic mantle below the crust. There are two types of crust, continental and oceanic, which are primarily differentiated by

widely contrasting specific gravities and density. The oceanic crust is derived directly from molten magma that rises from the underlying mantle through fissures in the crust. This magma is a mix of heavy elements that solidifies at the (oceanic) surface to form dense oceanic crust of basic to ultrabasic rock. The continental crust is made up primarily of lighter elements that have risen to the surface of the original molten earth and have coalesced into the present continents. Continental crust rarely recycles into the mantle,

the oceanic crust with minor exceptions, always does.

Because the continental crust is lighter than the oceanic crust, when the two collide the oceanic crust is generally forced down under the continental crust and eventually sinks into the mantle. This type of plate interaction, termed subduction, generates the largest number of large magnitude earthquakes in the crust. Where crustal plates collide obliquely or break into segments that slide past one another, the sliding occurs along steeply dipping transcurrent faults. Such transcurrent faults presently generate the second largest number of major earthquakes in the world. Thrust faults occur where crustal rocks fail or collide under compression and one segment overrides the other. This can occur in all types of crust and is the primary element in subduction zones. Normal faults are the opposite of thrust faults in that the crust fails and separates in tension, resulting in the down-dropping of blocks. This type of rock failure is the principal cause of earthquakes in rift valleys and in intracontinental relaxation zones.

3 Zoning of Seismic Hazard in B.C.

There are two methods for estimating the maximum possible earthquake ground motions that will affect specific sites: (i) The deterministic method, which is applicable where crustal seismic mechanisms are located, understood and monitored, and (ii) The probabilistic (Cornell) method which has been developed for areas where the seismic mechanisms are not clearly identified.

The deterministic method is primarily based on the Maximum Credible Earthquake (MCE). The MCE is derived from an evaluation of known tectonically active crustal structures and related measured seismicity. The MCE on each active fault structure is commonly taken to be the highest recorded magnitude plus one half a magnitude. This methodology for seismic analysis has successfully stood the test of long term application in cordillera-type crusts similar to B.C. for transcurrent faulting and for subduction generated thrust faulting. The

deterministic evaluation of seismic hazards also requires the development of a relationship between the MCE within the target region and the site ground motions. Seismic ground motion diminishes with distance from the source earthquake hypocenter because of geometric spreading and non-elastic attenuation. The ground motion parameters of peak ground acceleration (PGA), velocity (PGV) and frequency response spectra of the spreading seismic waves can be derived from the magnitude and distance relationships of earthquakes within all types of the earth's crust, [2].

The seismic parameter used most often to define ground motion for design purposes, the PGA, can be derived for different types of earth crust from empirical relationships between measured earthquake magnitude and distance to the earthquake hypocenter. Increasingly dependable PGA attenuation curves have been derived from magnitudes and hypocentral distances in the earth's crust. Those developed by Schnabel and Seed [3], and subsequently modified and substantiated by the Loma Prieta data, have proven to be most dependable for Cordillera-type crust and have been adopted for the present study. With the great increase in installations of seismograph stations throughout North America in the 1980's, it is now possible to locate active earthquake source structures in the crust, to determine their mode of failure and to develop a reasonably dependable specific earthquake location map for those areas of British Columbia that experience significant seismicity. Specific zones of PGA can now be developed in B.C. to fit this framework of identified active earthquake structures.

The U.S. National Building Code produced a zoned acceleration coefficient earthquake map, in January, 1992, that covers the entire continental U.S.A. and is to be the guide for seismic design of all future structures in the U.S.A.

This paper presents a PGA zonation map for British Columbia as derived from the geological structural framework (Fig. 1) and the recorded seismicity of the province (Fig. 2), which matches

very well with the U.S. earthquake zoning map. This PGA zone map of B.C. (Fig. 2) is intended for use in the definitive determination of seismic hazard and required design parameters in B.C. The seismic database for eastern B.C. is not as clearly defined as that to the west, due to apparent industrial seismic overprint. Continued monitoring of seismically suspect crustal structures in the eastern half of the province will be required to verify the activity in these areas. The application of conservatively high seismic parameters for local areas may be required until the seismic record is sufficiently refined to permit a specific deterministic analysis.

4 Seismotectonics of B.C.

Coastal British Columbia and the Alaska Panhandle together represent a seismotectonic mirror image of California. The northern two thirds of the B.C. coast, including the Alaska Panhandle, is seismically dominated by the highly active Queen Charlotte Fault (Fig. 1). This transcurrent fault is the boundary of the Pacific Plate (oceanic) and the North America Plate (continental) along which earthquakes in excess of M 8 occur over a length of about 2000 km. The most significant difference between the San Andreas and the Queen Charlotte faults is that the San Andreas Fault is largely on-shore, while the Queen Charlotte Fault is off-shore. If, for comparison, the San Andreas is transposed as a mirror image to the Queen Charlotte location we find that the seismic frequencies and intensities of these two plate boundary faults are essentially identical, with somewhat more recorded M 8 events along the Queen Charlotte than along the San Andreas. The Queen Charlotte Fault extends southward (off-shore) to the northern tip of Vancouver Island, where it in effect terminates the north end of the Cascadia Subduction zone, as does the northern San Andreas Fault at the south end of Cascadia.

The only other known active faults in B.C. are related to the north tip of the Cascadia subducting plate, beneath the southern third of

Vancouver Island. One of these faults is the east-dipping subduction zone itself, the other is the Nootka Fault, which is a normal fault that is cutting off the north remnant of the subducting Cascadia Plate along the sea floor west of Vancouver Island as well as beneath the Island and east to the vicinity of Powell River, (Fig. 1). The subduction related faults in southwest B.C. occur relatively deep within the crust, none have been found that break the surface on land. They occur at three geological structural types of sites: (1) as shear and/or thrust faults within the overriding North America Plate; (2) as shear failures along the interface zone that spans the top of the subducting Pacific Plate and the bottom of the overriding North America Plate; and (3) as tension failures of the subducting Pacific Plate as it breaks up against and beneath the North America Plate. The foci of these failures range in depth from 5 to 50 kilometers, depending on which plate they occur within. All of the recorded earthquakes in southwest B.C. greater than magnitude 3 appear to have been of these subduction-related types.

The mainland coast of B.C. is bordered by a belt of granitic intrusive rocks that forms a tectonic barrier 200 kilometers in width and over 30 kilometers in depth (Fig. 1) that is virtually aseismic, except for the possible subsurface Terrace Zone and the eastern extremity of the subsurface Nootka Fault Zone, (Fig. 1).

The interior of the province from the east boundary of the Coast Range batholith (intrusive) belt to the Rocky Mountain Trench is essentially aseismic except for a scattering of M 3-M 4 epicenters in the south end of the Okanagan Valley, and in the southeast corner of the province, and a line of four pre-1942 events of about M 5 that have been arbitrarily located along the Yalakom Valley that forms the southeast boundary of the Coast Range batholith.

At least two of the Yalakom events are clearly mislocated and probably belong along the line of the Nootka Fault to the west. The other two occurred when the west coast population was too sparse to provide dependable seismic intensity

reports and the recording seismographs were distant and the events have therefore been arbitrarily located. The complete absence both of minor seismicity and of geological evidence for active faulting in this area negates the probability of these events having been accurately located.

At present, the Rocky Mountain Trench comprises a suspect seismic structure east of Prince George and in the Kinbasket (Mica) Reservoir on the basis of the location of isolated events.

The northeast (Peace River) corner of the province, east of the Rocky Mountains, is in the Plains which have no significant seismic hazard potential (Fig. 2).

The north coast mainland and near-shore islands of B.C. are virtually devoid of recorded seismic events greater than M 3. The active Queen Charlotte Fault is too far offshore to transmit significant ground tremors to the mainland, even for magnitude 8.5 events. Only two land areas on the north coast are susceptible to major earthquake hazard, these are, (Fig. 1): the St. Elias mountain range in the extreme northwest corner of B.C. that is bracketed by the active Fairweather and Denali faults; and the Queen Charlotte Islands, immediately flanking the Queen Charlotte transcurrent fault to the west. One other area that has minor possible exposure to seismic hazard is a very local linear seismic zone immediately west and north of Terrace. This zone has experienced one recorded M 4, one M 3 and at least six M 2 events; however, there is no surface expression of active faulting in the area. The presence of hot springs and proximity of recent volcanism in this region may indicate that the seismicity is related to structural post-volcanism adjustments in the crust.

Vancouver Island is the most populous area of B.C. affected by seismic events. The south end of the Queen Charlotte Fault is offshore of the north tip of Vancouver Island (Fig. 1). The structural interaction between this transcurrent fault and the fragmented oceanic plates at the north edge of Cascadia Subducting Plate is not clearly defined by the seismic record and sea

floor studies; however, the present evidence indicates that the Queen Charlotte Fault is continuing to extend southward, cutting off the subducting plates in the process. [4,5] Geological evidence indicates that in the last 10 million years it has advanced at an overall average rate of 4 meters per 100 years. Earthquakes offshore at the south end of the QC Fault present very low earthquake hazard to the north tip of Vancouver Island.

There are no known active surface faults on Vancouver Island; however, there is a linear zone of strong subsurface seismicity between Gold River and Campbell River (Fig. 1). The alignment of this linear seismic zone exactly matches the projection of the active Nootka Fault, which has been identified in the seafloor oceanic crust to the west, extending about 150 km seaward from the island. The Nootka Fault appears to separate the subducting oceanic Juan de Fuca Plate to the south from the remnant, non-subducting Explorer Plate to the north, (Fig. 1). The projection of this fault alignment suggests that the subsurface seismicity beneath this part of Vancouver Island originates from the breaking up of the subducted portion of the Explorer plate which now appears to be detached from the active Cascadia subduction system to the south, (Fig. 1). There is no known surface rupture from the four or five significant earthquakes that have occurred along this alignment beneath Vancouver Island and the Mainland. The instrumented events have originated at depths of 25 km or more, near or below the bottom of the continental crust.

The other potential seismic hazard zone on Vancouver Island is that portion of the island south of Nanaimo and Tofino. That part of the Island is underlain by the northern extremity of the subducting Juan de Fuca plate portion of Cascadia. Lithoprobe surveys [6] indicate that the subducted plate is at a depth of 60 km below Nanaimo and that subduction has probably ceased at and north of that latitude. Recorded sporadic seismicity identifies that the subduction zone is active beneath Victoria and southeastward beneath Puget Sound. The subduction surface is approximately 40 kilometers

beneath Victoria and comprises the principal source of seismic hazard for the south end of Vancouver Island, (Fig. 2).

The only source of seismic hazard for the Lower Mainland is the down-dip terminus of the subduction surface to the west of Vancouver and south of the U.S. border. This subduction surface has an anticlinal configuration between Nanaimo and Portland (Fig. 2), which appears to be related to the termination of active subduction north of Nanaimo. The recorded seismicity of the subduction zone is highest in frequency and intensity within about 100 km north and south of the axis of this anticlinal form, which lies along latitude 48°, about 50 km north of Seattle and south of Victoria. In shallow-dipping subduction zones such as Cascadia, the high fluid content of both the subducting and overriding plates, as well as the thin loading by the leading edge of the overriding continental plate, result in aseismic sliding for the initial 100 kilometers or so downdip from the subduction trench. Thus, landward subduction seismicity along the Cascadia zone begins approximately at the outer coastlines of Vancouver island and Washington, at which location the subduction zone is 25-40 kilometers deep and much of the nascent fluid content has been forced out of the rocks. Although the magnitudes of the earthquakes down-dip on the subduction zone increase, so also does the distance from the surface and the resulting attenuation of the seismic wave. From this depth seismic waves attenuate appreciably before they reach the surface. The B.C. Lower Mainland lies beyond (east of) the down-dip termination of the Cascadia Subduction zone and about 70 kilometers above it, well beyond significant seismic hazards from that source.

From Puget Sound south to northern California, where the subducting plate is cut off by the San Andreas Fault, the Cascadia seismic zone is consistently active with earthquakes of magnitudes of M3-M7, indicating that subduction is progressing in an orderly manner and not storing the energy required for a megathrust earthquake.

5 Deterministic seismic risk zoning of B.C.

The proposed peak ground acceleration (PGA) zoning for western B.C. has been constructed by taking the maximum credible earthquake (MCE) for each active fault structure and, by means of the Loma Prieta verified acceleration attenuation curves, determining the distance that the selected boundary PGA's would extend from the causative fault plane and be projected to the surface.

In the present analysis the writers have selected two zones of values of peak ground acceleration. These two adjacent zones bracket decreasing values of PGA away from each of the active seismic source structures described in the preceding section. (Fig. 2). The highest PGA zone is directly adjacent to the causative fault and extends away from both sides of the fault to a distance equivalent to a PGA of 0.30 g. (For an MCE of 7.5 on the Cascadia subduction surface and an MCE of M 8.5 on the Queen Charlotte Fault.) The next zone, adjacent to the first zone and more distant from the source, spans the distance from the 0.30 g boundary outward to the 0.15 g boundary, (Fig. 2). These PGA boundaries have been selected for the present study because they represent boundaries of generally worldwide distinctive earthquake hazard effects. For example, many dams of all types have experienced ground accelerations of 0.30 g with no significant damage; whereas, above that level some dams have been appreciably damaged. An Earthquake Intensity Scale recently developed for Papua New Guinea demonstrates the relationship between zonation and damage thresholds. The intensity index of VI is at the 0.30 g threshold, below which physical damage is minimal. Highlights of the description for Intensity Zone VI are: "General excitement, some roaring sounds. Minor household breakages, heavy furniture moves. Church bells ring. No damage to normal buildings but at the threshold of minor damage to water tanks and weak dwellings. Minor landslides." The next higher intensities, (VII, VIII), indicate a marked material damage change: "Most water tanks burst, buildings sway violently, threshold of structural damage to "well

built" structures, seiches on lakes and reservoirs, extensive landslides, liquefaction occurs ..., etc."

Local foundation materials of course have a pronounced impact on intensities and the amplification of ground acceleration, but for bedrock foundations the selection of a zone boundary of 0.30 g PGA represents a boundary for seismic zoning above which threshold structural damage has proven to be increasingly critical in most seismic locations in the world. The boundary limits of 0.30 g and 0.15 g PGA have also been very well corroborated by the Loma Prieta damage data for both bedrock and soil foundations.

The zones of highest seismic risk (+0.30 g) in B.C., as projected at the surface (Fig. 2), do not underlie highly populated or developed areas except for the southwest corner of Vancouver Island and mid Vancouver Island. Victoria, Campbell River and Powell River are the only large municipalities that are possibly exposed to relatively high seismic risk damage, based on the conservative procedure of adding one half a magnitude to the largest event recorded on the subduction zone (for Victoria) and the Nootka Zone (for Campbell River and Powell River). Most of the Queen Charlotte Islands and all of the northwest St. Elias appendage of B.C. are under high risk of earthquake damage; however, they are presently devoid of large man-made structures.

The 30 km-wide Nootka seismic risk zone that crosses Vancouver Island at Campbell River is zoned as high seismic risk; however, because the monitoring period of that area has been relatively short and the magnitude of one of the three large events is only estimated this categorization could change significantly, up or down, with additional future monitoring of seismic events.

The north tip of the Cascadia Subduction Zone that underlies Vancouver Island south of Nanaimo comprises a source of moderate to high seismic damage risk to Victoria and the southwest coast of the island. Victoria lies approximately at the 0.30 g PGA boundary for a

M 7.5 event on the subduction zone at depth. This ground acceleration should not present serious structural design problems for most of the south end of the Island where foundations are generally firm glaciated bedrock and glacial till. Foundation problems could arise however in areas of local glacial and post-glacial clays and outwash deposits.

Vancouver and the Lower Mainland lie beyond the 0.15 g eastern edge of the seismic risk zone of the Cascadia Subduction. The sharp decrease of seismic activity on this subduction zone north of the 49th parallel strongly suggests that subduction of the slab has drawn to a close in that region (6). In any case, assuming that the subduction zone is capable of producing an MCE of M 7.5, (M 7 + 0.5), north of the 49th parallel and immediately west of Vancouver, because of the long distance (+60 km) from the top of the seismic zone up to the surface at Vancouver, the PGA at Vancouver would be a little over 0.1 g. On the bedrock and till foundations of most of the metropolitan area 0.1 g may hardly be noticed by many people and would not be significant to the integrity of even only reasonably well built structures. The many dams, structures and industrial installations in and east of the Vancouver environs would definitely not be affected. The above levels of cited bedrock acceleration are also generally too low to induce liquefaction, unless resonance is built up in unconsolidated material by reflection of seismic waves off surrounding bedrock, as in the destructive 1985 earthquake in Mexico City. In the Lower Mainland concern has been expressed regarding liquefaction of parts of the Fraser Delta. Various agencies are studying this potential problem. Most of the deposits that make up the delta are glacial and glacial-fluvial in origin and are not susceptible to liquefaction. Sample borings [8, 9] indicate that a number of locally distributed near-surface deposits may be prone to liquefaction. The assessment presented in this paper indicates a bedrock PGA at the delta of 0.10 g, or less, with no closed bedrock configuration to induce local resonance, as occurred at Mexico City. Borings of the delta deposits indicate no evidence of liquefaction disturbance of the deeper (glacial) deposits in

the last 13,000 years, indicating either that there has been no major earthquake effects on the delta in that period or that the deeper material in the delta deposits is not liquefiable.

6 Giant Subduction Earthquakes

Five years ago an hypothesis was postulated by a California seismologist that the Cascadia subduction zone beneath the U.S. Pacific Coast could perhaps be capable of generating a giant earthquake, (+M 9). The basic reasoning was that since three other subduction zones around the Pacific Rim have produced such "mega" earthquakes in historical times and since Cascadia has not, then Cascadia must be "stuck" and will therefore "catchup" by means of a giant dislocation. In 1988 a technical paper by Dr. G. Rogers [10] suggested that the Cascadia zone could be capable of a M 9.2 earthquake, even though most Cascadia geological and seismological characteristics differ markedly from those of the known circumPacific giant earthquake zones. The critical fallacy of the postulation of a "megasubduction earthquake" is that the comparison of the Cascadia subduction zone with the three existing circumPacific giant earthquake subduction zones virtually ignores not only the geological and physical (mechanical) differences between these zones and Cascadia but also the fact that many other subduction zones throughout the world, much larger than

Cascadia, have far more similarities to the existing megaequake zones, yet have long seismic histories of very well recorded earthquakes, none of which have exceeded M 8.5. The significant differences between the three large earthquake subduction zones and Cascadia are summarized in Table 1. The comparison of the oceanic plate characteristics in Table 1 clearly indicates that the Cascadia subduction plate is a very poor candidate for a giant earthquake. It strongly suggests that the recorded level of seismicity that exists on the Cascadia zone is most likely precisely what "we" will get for the next 5-10 million years. The preponderance of geological, geophysical, seismic and physical evidence strongly indicates that the Cascadia subduction zone is expiring (in geological time scale terms) and is incapable of storing the necessary energy to generate a giant (M9) earthquake. In addition, the assertion that the Cascadia zone is "stuck" belies the high, consistent seismicity of the zone as recorded in the last ten years. Large earthquakes are common on Cascadia, for example, in one week ending August 23, 1991, four earthquakes of M 5.9, 5.6, 6.9, and 4.4 occurred on the subduction zone, distributed along a 600 km distance from northern Oregon south to northern California. These very significant large earthquakes occurring on the same zone within one week certainly do not suggest that the source zone is "stuck", but rather that it is progressing very satisfactorily.

TABLE 1 --

Characteristics of subducting Pacific plates

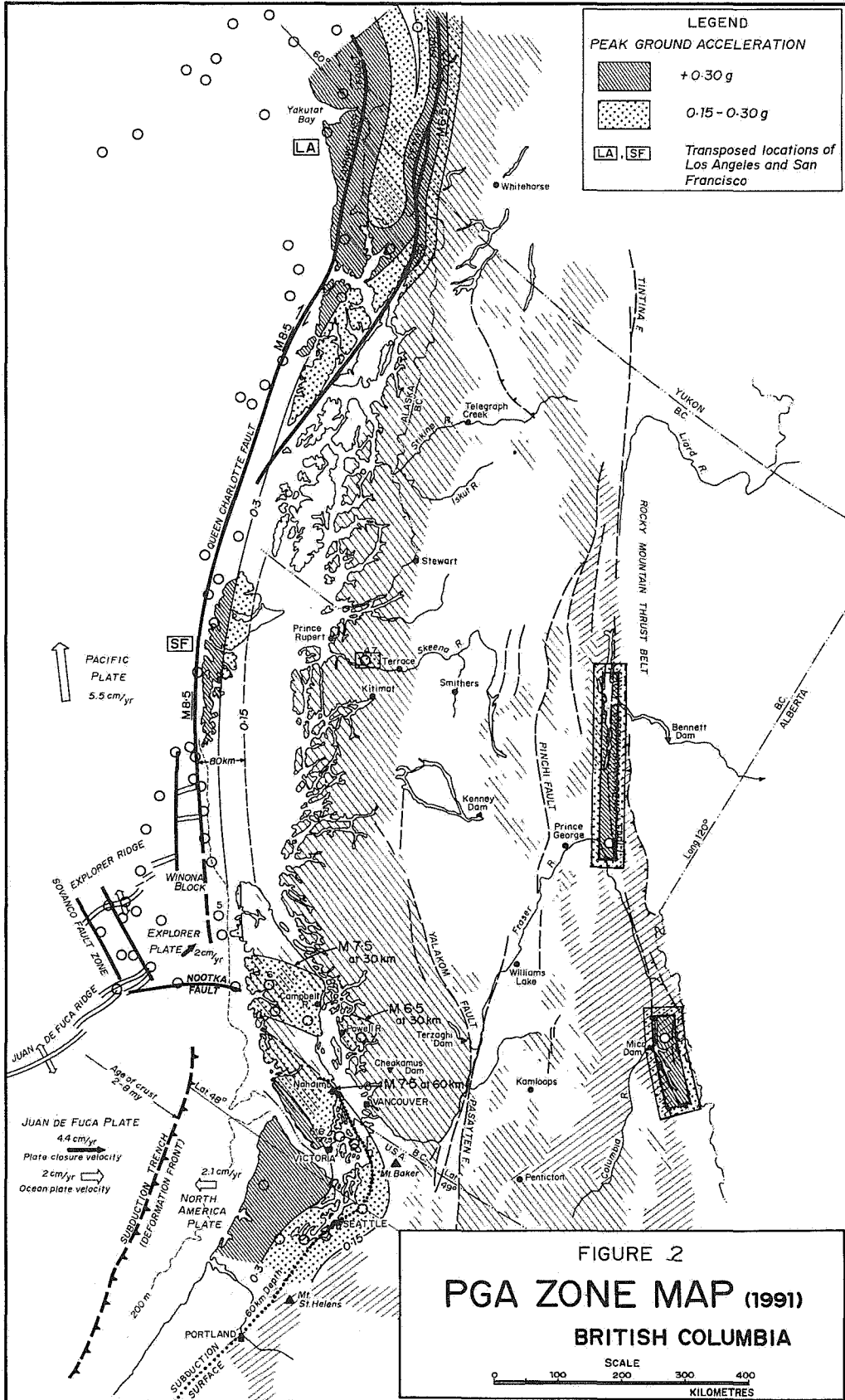
<u>Plate</u>	<u>Age (my)</u>	<u>Thickness (km)</u>	<u>Surface Roughness</u>	<u>Closure Rate cm/yr</u>	<u>Maximum Magnitude</u>
Cascadia	10	8	Smooth	2-4	7.0
Nazca (Chile)	60	60	High	8-10	9.5
Aleutian	60-100	50	Extreme	8	9.1
Nankai (Japan)	140	40	Extreme	5+	8.5

In view of the above summarized technical evidence against it, the writers consider that the hypothesis of a possible giant earthquake occurring on the Cascadia is not technically valid. Therefore, it is considered that the likelihood of a giant earthquake ("mega-subduction") occurring on the Cascadia zone does not warrant consideration in a seismic hazard analysis for British Columbia.

It should be appreciated that even if this hypothetical anomalous megaequake event did occur, the attenuation from the subduction zone (plane) to the bedrock foundation of the Lower Mainland (Vancouver) could result in a PGA of about 0.18 g in that area. This would be felt and could liquefy near-surface deposits of the delta, but it would certainly not comprise a significantly destructive event for structures founded on the bedrock or glacial till that underlies most of the Lower Mainland.

References

- [1] Crouse, C.B., Determination of seismic design parameters, Seminar on Geotechnical Aspects of Earthquake Engineering, American Society of Civil Engineers, March 31, 1990.
- [2] Benioff, H., Orogenesis and deep crustal structure, additional evidence from seismology. *Bull. GSA* v. 85, May, 1954.
- [3] Schnabel and Seed, Accelerations in rock for earthquakes in western United States, *Bull. Seis. Soc. Amer.*, 63, 1973.
- [4] Barrash, W., Timing of Late Cenozoic volcanic and tectonic events along the western margin of the North America plate. *GSA Bull.*, v. 93, Oct. 1982.
- [5] Dumitru, T.A., Major quaternary uplift along the northernmost San Andreas Fault, King Range, northwestern California, *Geology*, v. 19, May 1991.
- [6] Yorath, C.J., Sutherland-Brown, A., et al, Lithoprobe, southern Vancouver Island: seismic reflection sees through Wrangellia to Juan de Fuca plate. *Geology*, v. 13, Nov. 1985.
- [7] Tepel, R.E., The Morgan Hill earthquake of April 24, 1984 - Effects on facilities of the Santa Clara Valley Water District, *Earthquake Spectra*, vol. I, May, 1985.
- [8] Berger, G.W., Clague, J.W., Zeroing tests and application of thermoluminescence dating to Fraser River delta sediments. *Can. Jour. of Earth Science*, v. 27, 1990.
- [9] Williams, H.F.L., Roberts, M.C., Holocene sea-level change and delta growth; Fraser River delta, British Columbia, *Can. Jour. Earth Science*, v. 26, 1989.
- [10] Rogers, G.C., An assessment of the megathrust earthquake potential of the Cascadia Subduction Zone. *Can. Jour. Earth Science*, v. 25, 1988.



Tsunami Threat to the British Columbia Coast

T.S. Murty

*Department of Fisheries and Oceans
Sidney, British Columbia*

Abstract

Tsunami threat to the coast of British Columbia due to tsunamis originating in distant sources as well as local sources is considered and reviewed. Most past studies ignored the important aspect of flooding of land by the tsunami waves, mainly for mathematical convenience in the numerical models. Such omission of land flooding tends to over-estimate the tsunami amplitudes and through the related continuity equation, underestimate the horizontal velocity field. Some recent studies have made attempts to include land flooding, although it is fair to say that this problem is far from being solved.

1. Introduction

Maximum tsunami water levels and currents along the British Columbia outer coast have been computed (Dunbar et al. (1989, 1991) [1,2] for waves originating from Alaska, Chile, the Aleutian Islands (Shumagin Gap), and Kamchatka. Three computer models have been developed to generate and propagate a tsunami from each of these source regions in the Pacific Ocean to the continental shelf off Canada's west coast, and into twenty separate inlet systems. The model predictions have been verified against water level measurements made at tide gauges after the

March 28, 1964 Alaska earthquake. Simulated seabed motions giving rise to the Alaskan and Chilean tsunamis have been based on surveys of vertical displacements made after the great earthquakes of 1964 (Alaska) and 1960 (Chile). Hypothetical bottom motions have been used for the Shumagin Gap and Kamchatka simulations. These simulations represent the largest tsunamigenic events to be expected from these areas. Maximum wave and current amplitudes and travel times have been tabulated for each simulated tsunami at 185 key locations along the British Columbia coast. On the north coast of British Columbia, the Alaska tsunami generated the largest amplitudes. In all other regions of the west coast, the largest amplitudes were generated by the Shumagin Gap simulation. Wave amplitudes in excess of 9 m were predicted at several locations along the coast and current speeds of 3 to 4 m/s were produced. The most vulnerable regions are the outer coast of Vancouver Island, the west coast of Graham Island, and the central coast of the mainland. Some areas, such as the north central coast, are sheltered enough to limit expected maximum water levels to less than 3 m.

Strong evidence suggests that the Cascadia subduction zone, off the west coast of Canada

and the United States, is strongly seismically-coupled and that a possible megathrust earthquake might occur in that area in the near future. Numerical simulations of tsunami generation and propagation have been carried out using three models based on shallow water wave theory. Three cases of ground motion representing the ruptures of different crustal segments in the area have been examined. Computed results provide information on tsunami arrival times and a general view of the wave height distribution. The outer coast of Vancouver Island was found to be the most strongly affected area. At the head of Alberni Inlet, wave amplitudes reached up to three times the source magnitude. Inside the Strait of Georgia the wave heights are significant enough to receive closer attention, especially in low-lying areas (Ng et al., 1990, 1991) [3,4].

Maximum tsunami amplitudes that will result from major earthquakes in the Pacific Northwest region of North America are considered (Hebenstreit and Murty, 1989 [5] and Murty and Hebenstreit, 1989 [6]). The modeled region encompasses the coastlines of British Columbia in Canada, and Washington and Oregon in the United States. Three separate models were developed for the outer coast and one model for the system consisting of the Strait of Georgia, Juan de Fuca Strait, and Puget Sound (GFP model). Three different source areas were considered for the outer coast models and the resulting tsunami was propagated to the entrance of Juan de Fuca Strait. Using the output from the other models, the GFP model was run. The results showed that large tsunami amplitudes can occur on the outer coast, whereas inside the GFP system, unless the earthquake occurs in the system itself, no major tsunami will result.

2. Summary of the work of Dunbar et al. (1989, 1991 [6,7])

The various inlet systems modelled for tsunami effects from distant earthquakes are listed in Table 1.

TABLE 1--British Columbia Inlet systems included in tsunami simulations (from Dunbar et al., 1989)

System	Areas Included	System	Areas Included
A	Portland Canal Observatory Inlet- Hastings Arm Alice Arm Khutzeymateen Inlet Work Channel	K	Mereworth Sound Belize Inlet Nugent Sound Seymour Inlet
B	Prince Rupert Inlet	L	Holberg-Rupert Inlets Quatsino Sound- Neroutsoos Inlet Forward Inlet
C	Rennell Sound	M	Klaskino Inlet
D	Tasu Sound	N	Quoukinsh Inlet
E	Douglas Channel Kildala Arm Gardner Canal Sheep Passage- Mussel Inlet	O	Nuchalitz Inlet
F	Spiller Channel Roscoe Inlet Cousins Inlet Cascade Inlet Dean Channel Kwatna Inlet South Bentinck Arm	P	Port Eliza Espinosa Inlet Tahsis Inlet Cook Channel- Tlupana Inlet Zuciarie Channel- Muchalat Inlet
G	Laredo Inlet	Q	Sydney Inlet Shelter Inlet Herbert Inlet
H	Surf Inlet	R	Pipestem Inlet
I	Rivers Inlet Moses Inlet	S	Effingham Inlet
J	Smith Inlet	T	Alberni Inlet

Table 2 summarizes the extreme tsunami amplitudes. Note that these values are an over-estimate, especially at the head of inlets, where more realistic values can be obtained by multiplying these with 0.7. We will return to this runup problem in later sections.

TABLE 2--Summary of extreme tsunami amplitudes (from Dunbar et al., 1989)

Location	Maximum Tsunami Height	Source
North Coast	3.5m near the head of Khutzeymateen Inlet	Alaska
	3 to 3.5m throughout Hastings Arm (north end of Observatory Inlet)	Alaska
	3.5 to 4m near Stewart	Alaska
North Central Coast	3.5 to 4.5m west of Princess Royal Island	Shumagin
	4.2m in Cousins Inlet	Shumagin
	7.2m at the head of Spiller Channel	Alaska
	5.6m at the head of Laredo Sound	Shumagin
South Central Coast	3.3 to 9.2m at the heads of Rivers and Moses Inlets	Shumagin
	6 to 9.3m in Smith Inlet (increasing toward the head)	Alaska
Northwest coast of Vancouver Island	5.5 to 7.2m in Quatsino Sound	Shumagin
	Up to 9m in Neroutsos Inlet	Shumagin
	8 to 8.5m in Quatsino Narrows	Shumagin
	3.4m at the head of Holberg Inlet	Shumagin
	6 to 7m in Forward Inlet	Shumagin
	5 to 6m in Klaskino Inlet	Shumagin
Central Coast of Vancouver Island	> 10m at the head of Quoukinsh Inlet	Shumagin
	3.5m to 4.5m in Nuchalitz Inlet	Shumagin
	4.5 to > 10m in Muchalat and Tlupana Inlets (increasing toward the heads)	Shumagin
	3.5 to 4.5m at the south end of Tahsis Inlet	Shumagin
	3m at the head of Tahsis Inlet	Shumagin
	3.6 to 7.6m in Port Eliza and Espinosa Inlet	Shumagin
	3.5m in Nootka Sound	Shumagin
Southern coast of Vancouver Island	3 to 4m in Sydney Inlet	Shumagin
	4 to 8m in Pipestem and Effingham Inlets	Shumagin
	3 to 8m in Alberni Inlet (increasing toward the head)	Shumagin

Table 3 summarizes the extreme currents due to the tsunamis under discussion. Note that in contrast to the tsunami water levels (listed in Table 2) which are deliberately over-estimated, the currents listed in Table 3 are under-estimated. In reality, the extreme currents in actual tsunami events could be at least this strong.

TABLE 3--Summary of extreme tsunami wave current speeds (From Dunbar et al., 1989)

Location	Maximum Tsunami Current	Source Area
North Coast	2.3 m/s at entrance to Observatory Inlet	Alaska
North Central Coast	currents less than 2 m/s	n/a
South Central Coast	currents less than 2 m/s	n/a
Northwest Coast of Vancouver Island	2.5 to 4.7 m/s in Quatsino Narrows	Shumagin
	2.5 to >5 m/s near Port Alice on Neroutsos Inlet	Shumagin
	3 m/s at entrance to Forward Inlet	Shumagin
	3 m/s at entrance to Klaskino Inlet	Shumagin
	2 m/s in Quoukinsh Inlet	Shumagin
Central Coast of Vancouver Islands	2.7 m/s at entrance to Muchalat Inlet	Shumagin
	2.5 to 3.5 m/s near entrance to Tlupana Inlet	Shumagin
	2.3 m/s at south end of Tahsis Inlet	Shumagin
Southern Coast of Vancouver Island	3.7m at entrance to Pipestem Inlet	Shumagin
	2 to 3.5m in Alberni Inlet	Shumagin

3. Summary of the work of Ng et al. (1990, 1991)

The similarity of the Cascadia subduction zone's tectonic features to those of other subduction areas in the world, together with results from recent geodetic surveys of the ground motion as well as records of prehistoric large earthquakes in the area, suggest that a megathrust earthquake may occur in western British Columbia in the near future. The compelling evidence for a large seismic event off British Columbia has prompted the study of the local tsunami response. Three numerical hydrodynamical models covering different areas of the studied region were used to calculate tsunami generation and propagation. Computed results

include tsunami travel times and sea surface displacements and may provide useful information for the emergency planning response to tsunami hazards.

Three cases of source motion were studied. Simulated wave amplitudes have been plotted for major tide gauge locations and some densely populated areas along the British Columbia coast. The wave pattern observed at each location depends strongly on local topography, such as the width of the continental shelf, and the shoreline configuration, both of which affect wave refraction and reflection, the amount of shoaling and the excitation of resonance.

Results have shown that the most affected area was along the outer coast of Vancouver Island because of its proximity to the source. Particularly at the head of Alberni Inlet, the waves are seen to be drastically magnified through resonance, with magnitudes about three times those in Barkley Sound.

The travel times of the first positive wave to Victoria and Vancouver, the two main business and commercial centres in British Columbia, are 94 and 187 minutes respectively if all three segments break as a whole and are correspondingly 127 and 226 minutes if only the Winona and Explorer segments rupture together. With the exception of those locations that are very near the source, the largest waves usually come after the leading waves, as is seen in the Strait of Georgia system. The wave amplitudes observed there, although the area is sheltered by Vancouver Island and the wave is attenuated by friction, are still significant. Around the Vancouver area, the maximum wave amplitude is approximately 1m. Low-lying areas such as Richmond are therefore subject to threats of flooding when the tsunami arrives at high tide.

The major limitation of the tsunami amplitude computations comes from the uncertainty in specifying the source. A more confident description of source parameters such as the dimension of the displacement zone would enhance the accuracy of the computed results. The wave models, on the other hand, could also be improved in a number of ways.

1. The area of computation should be extended southwards to include the entire Cascadia zone. The Gorda plate and the lower portion of the Juan de Fuca plate were not considered in this study, which might result in different wave forms if any of these two segments were to rupture.
2. The present model has omitted a detailed study of most of the inlet systems along the British Columbia coast. Only Alberni Inlet was treated in detail in the inlet computation. The results from the deep-ocean model therefore represent only the wave response adjacent to the mouths of the inlets. Finer resolution models are required to improve the results' accuracy in bays and inlets.
3. The treatment of Alberni Inlet under the present scheme is, however, not yet complete. The results only provide the wave amplitudes at the shoreline; it does not give the runup heights. The latter information is considered to be more important because flooding by tsunami waves causes most of the damage. The modelling of the runup process, which may include bore formation, breaking and rushing-up, requires modification of the present assumption of zero mass transport at the coastline and development of high-resolution models to account for complex structures such as small islands and narrow branches at the head of the inlet.

A better scheme of coupling the shelf and inlet models may also be required.

4. Sea level changes and currents due to astronomical tides might have to be taken into consideration. In inlets and low-lying areas such as Richmond, the inclusion of tidal effects could provide a better estimate of the maximum wave heights. Including tidal currents with those of the tsunami wave could also give a better estimate of energy dissipation in near-shore areas.

4. Summary of the work of Hebenstreit and Murty

Heaton and Hartzell (1986) [7] have divided the Cascadia subduction zone into three subzones. The northernmost zone consists of the Explorer Plate, the southernmost zone of the Gorda South Plate, and the intervening Juan de Fuca Plate makes up the remaining zone. Rogers (1988) [8] includes the Winona Block in his reckoning of the structures that make up the Cascadia zone, but the likelihood of subduction earthquakes in that complex is unclear.

Following Heaton and Hartzell's definition of the Cascadia subduction zone, the Gorda South Plate (shortened to Gorda Plate hereafter) is the smallest of the three main zones, being only 150-200 km long. It is subducting at a rate that is possibly 25% slower than the Juan de Fuca zone (3.3 cm/year versus 4.0 cm/year according to Heaton and Hartzell, 1986, and may be less likely to experience subduction earthquakes. Indeed Spence (1988) [9] suggests that subduction under the Gorda Plate has effectively stopped. However, in the absence of evidence to the contrary, it seems prudent to examine an event in this zone. Rogers (1988) provides estimates of the various source parameters for all of the zones

he examined. For the Gorda zone, he suggests a fault width of 100 km, a length of 150 km, and a vertical displacement under maximum rupture of approximately 3.0m. Using the Wyss (1979) [10] relationship for maximum expected magnitude

$$M = \log(\text{length} \times \text{width}) + 4.15 \quad (1)$$

this fault could produce an earthquake of magnitude 8.3.

The Explorer Plate is somewhat larger than the Gorda Plate (200 km), although the width of the fault can also be estimated at 100 km. Rogers estimates a vertical displacement of 2.0m (maximum Wyss magnitude of 8.5). Riddihough (1984) [11] estimates that this plate is subducting at a much slower rate than the Juan de Fuca Plate (as low as 2 cm/year), although it is not clear what this means in terms of its potential for subduction earthquakes.

The Juan de Fuca plate is on the order of 800-900 km long. It is subducting at a rate of 4-4.5 cm/year. Of the three areas being examined, it is probably the one most likely to experience large subduction zone earthquakes. A rupture along the full length of the plate would produce a magnitude in the range of 9.1. One difficulty with such an event, however, is that the rupture would have to "turn the corner" along the Washington coast. Although this is not completely unreasonable, it would seem more likely that the plate would be subject to two separate ruptures, one in the northern half and one in the southern half. Either such event, given a length of roughly 400-500 km, would have a magnitude of roughly 8.8. Rogers (1988) estimates that the vertical displacement of a rupture in this region would be on the order of 18m.

To use the Mansinha-Smylie model, the dip angle of the fault plane and the depth of the

fault must be specified. Heaton and Kanamori (1984) [12] indicate that the Juan de Fuca Plate is dipping at approximately 10° below the North America plate. We use this value for all of the events studied. For convenience, an arbitrary focal depth of 30 km was chosen.

Hebenstreit and Murty (1989) numerically simulated the tsunamis from these above sources. It is generally believed that the probability of an occurrence of a major tsunami-generating earthquake inside the GFP system (Straits of Georgia-Juan de Fuca-Puget Sound) is small. Nevertheless, simulations of a tsunami that might result from a small earthquake such as the one that occurred on Vancouver Island on June 23, 1946, were made. Hypothetical earthquakes were assumed to occur off Victoria (in Juan de Fuca Strait), off Vancouver (in the Strait of Georgia), and off Seattle (in Puget Sound). The bottom motion used in these simulations to approximate that for the 1946 event was taken from Rogers and Hasegawa (1978) [13].

As to be expected, earthquakes occurring off the three respective cities produce tsunami amplitudes that are greatest within their immediate areas. Little wave energy passes through to locations in the Strait of Georgia from the Victoria area earthquake simulation, although some effects can be felt farther along Juan de Fuca Strait and in Puget Sound.

The Vancouver area earthquake simulation produces the most moderate effects of the three simulations. Amplitudes tend to be smaller at Little River even though it is closer to the earthquake source than Campbell River, indicating the effect that shallow water plays in damping waves at the former location. The Gulf and San Juan Islands effectively block entry into Juan de Fuca Strait and Puget Sound. The simulated earthquake off Seattle has little impact anywhere but in the Puget

Sound, where resonance tends to amplify the waves in Seattle's harbor.

It should, however, be noted that, unlikely as it might be, if a major earthquake (Richter magnitude greater than 8.0) occurs in the GFP system, a major tsunami (with amplitudes almost 3m) could result. Also, submarine slides, e.g., in the foreslope hills in the Strait of Georgia (an 11×6 km area on the face of the Fraser River delta), whether occurring independently or in association with earthquakes, could generate tsunamis that could be significant locally. Submarine slides into Howe Sound also could generate local tsunamis.

5. Tsunami Runup

Kowalik and Murty (1992) [14] numerically simulated the runup and flooding at Port Alberni due to the 1964 Alaska earthquake tsunami. Following Harbitz et al. (1991) [15] we present a simple analytical technique for runup computations; this method was originally proposed for tsunamis generated by submarine slides. Let h_0 be a typical water depth, b a typical wavelength and " a " a typical amplitude for the tsunami. Let η denote the amplitude of the surface wave, A and B are amplitude functions, k and ω are wavenumber and frequency and t is time. For simple analytical calculations, Harbitz et al. (1991) assume a simple geometry defined by a depth function $h(x)$

$$h(x) = \begin{cases} h_0 & \text{for } x > x_L > 0 \\ 0 & \text{for } x = 0. \end{cases}$$

For the incident and reflected waves in the region $x > x_L$ one can write

$$\left. \begin{aligned} \eta_{in} &= Ae^{i(k(x-x_L)+\ell y+\omega t)} & A \in \mathbb{R} \\ \eta_{ref} &= Be^{i(-k(x-x_L)+\ell y+\omega t)} & B \in \mathbb{C} \end{aligned} \right\} (2)$$

where R is the total horizontal displacement during time T , and where k , ℓ and ω fulfil the dispersion relation and the real parts, only, have physical significance. For all x we correspondingly write:

$$\eta = \zeta(x)e^{i(\ell y+\omega t)} \quad (3)$$

Assuming $t = 0$, eliminating u and v from the momentum and continuity equations, and finally inserting the expression (3) we arrive at the ordinary differential equation (here u and v are the components of horizontal velocity):

$$\frac{d}{dx} \left[gh \frac{d\zeta}{dx} \right] + (\omega^2 - \ell^2 gh) \zeta = 0 \quad (4)$$

From (2) we obtain as offshore boundary conditions:

$$\frac{d\zeta}{dx} + ik\zeta = 2ikAe^{ik(x-x_L)} \quad (5)$$

which can be applied whenever $x \geq x_L$. We define $F(x; x_0)$ as the solution of (4) that also fits the conditions $F(x_0; x_0) = 1$ and $dF(x_0; x_0)/dx = 0$ if $x_0 > 0$. The first requirement suffices to determine F uniquely if $x_0 = 0$, due to the singularity of (4). In terms of F the solution for ζ becomes (Harbitz et al., 1991):

$$\zeta(x) = \frac{2ikA}{F'(x_L; x_0) + ikF(x_L; x_0)} F(x; x_0) \quad (6)$$

where F' denotes the derivative of F . The maximum runup height, R_u , becomes accordingly:

$$\frac{R_u}{A} = \frac{2k}{\sqrt{F'(x_L; x_0)^2 + k^2 F(x_L; x_0)^2}} \quad (7)$$

It can be seen that R_u/A is a continuous function of x_0 , also for $x_0 = 0$. This implies that the solution of the "rigid wall problem" becomes a close approximation to the solution of the "true runup problem" for small x_0 . To prove the continuity of R_u/A we write the general solution of (4) as a linear combination of $F(x; 0)$ and another function, $R(x)$, that inherits a logarithmic singularity at $x = 0$, as can be shown by standard application of the Frobenius method. Thus, we may write $F(x; x_0) = \gamma(x_0)F(x; 0) + \kappa(x_0)R(x)$ where γ and κ are determined through the boundary conditions: $F(x_0; x_0) = 1$ and $F'(x_0; x_0) = 0$. This implies that κ/γ tends to zero sufficiently fast for $F(x; x_0)$ to approach $F(x; 0)$ for all $x \geq x_0$ as $x_0 \rightarrow 0$.

The solutions for the case $x_0 = 0$ and linear bottom profile, $h(x) = h_0 x/x_L$ for $x < x_L$, is discussed by Pedersen (1985) [16]. For this bottom topography F may be expressed in terms of confluent hypergeometric functions, that may be derived from Bessel functions when $\ell = 0$. The latter case is analyzed for more general incident waves by Pedersen and Gjevik (1983) [17].

Next, following Harbitz et al. (1991) we will consider the discrete runup calculations. Even though the two boundary value problems are nicely related, additional difficulties may arise during the discretization. Most considerations concerning accuracy and convergence of numerical methods of the present type, rely on Taylor series expansion. Unfortunately, the use of this expansion may be inappropriate in runup calculations where Δx is larger than or comparable to x_0 , which equals the radius of convergence for ζ at $x = x_0$. We will thus

analyze the discrete problem along the lines of the previous subsection.

We assume that the geometry is discretized with u-nodes at the boundary $x = x_0$. The arithmetics run almost as for the analytical case. Again we assume (2), but this time k , ℓ and ω have to obey the numerical dispersion relation:

$$\tilde{\omega}^2 = gh_0(\tilde{k}^2 + \tilde{\ell}^2) \quad (8)$$

where

$$\begin{aligned} \tilde{k} &= \frac{2}{\Delta x} \sin \left[\frac{k\Delta x}{2} \right] & \tilde{\ell} &= \frac{2}{\Delta y} \sin \left[\frac{\ell\Delta y}{2} \right] \\ \tilde{\omega} &= \frac{2}{\Delta t} \sin \left[\frac{\omega\Delta t}{2} \right] \end{aligned} \quad (9)$$

The discrete analogue to (3) defines discrete values ζ_j which have to be determined. Elimination of velocities from the discrete equations of momentum and continuity, followed by separation of variables (introduction of ζ) yields in analogy to (4):

$$[\delta_x(g\bar{h}^x\delta_x\zeta) + (\tilde{\omega}^2 - \tilde{\ell}^2gh)\zeta = 0]_j \quad (10)$$

where the position number $j = 1/2$ corresponds to $x = x_0$. The offshore boundary condition now reads:

$$[m\delta_x\zeta + i\tilde{k}\bar{\zeta}^x]_{j+1/2} = 2im\tilde{k}Ae^{ik(j\Delta x + x_0 - x_L)} \quad (11)$$

where $m = \cos 1/2 k\Delta x$. When $x_0 > 0$ the discrete F is defined through:

$$[\delta_x F = 0]_{1/2} \quad F_1 = 1 \quad (12)$$

where F_0 is introduced as a fictitious value. The analytical case $x_0 = 0$ has a proper

numerical counterpart only if $[\bar{h}^x]_{1/2} = 0$, which implies that the fictitious value ζ_0 does not enter the difference equation (10). A unique solution for F can then be obtained by requiring $F_1 = 1$ and solving the tridiagonal system (10). As a consequence the discrete method automatically reproduces the nonsingular solution for F . Defining ζ_1 as R_u^* one then finds:

$$\frac{R_u^*}{A} = \frac{2m\tilde{k}}{\sqrt{[m^2(\delta_x F)^2 + \tilde{k}^2(\bar{F}^x)^2]_{j-1/2}}} \quad (13)$$

where $(j - 1/2)\Delta x + x_0 > x_L$. A study of calculated solutions by Harbitz et al. (1991) shows that the discrete results generally are in excellent agreement with the analytical results in spite of the singularity at $x = 0$.

References

- [1] Dunbar, D., P.H. LeBlond and T.S. Murty (1989): Maximum tsunami amplitudes and associated currents on the coast of British Columbia. *Sci. Tsunami Hazards* 7(1): 3-44
- [2] Dunbar, D., P.H. LeBlond and T.S. Murty (1991): Evaluation of tsunami amplitudes for the Pacific coast of Canada, *Progress in Oceanography*, 26, 115-177.
- [3] Ng, M., P.H. LeBlond and T.S. Murty (1990): Numerical simulation of tsunami amplitudes on the coast of British Columbia due to local earthquakes, *Science of Tsunami Hazards*, 8(2), 97-127.
- [4] Ng, M., P.H. LeBlond and T.S. Murty (1991): Simulation of tsunamis from great earthquakes on the Cascadia subduction zone, *Science*, 250, 1248-1251.

- [5] Hebenstreit, G.T. and T.S. Murty (1989): Tsunami amplitudes from local earthquakes in the Pacific Northwest region of North America - Part 1: The outer coast, *Marine Geodesy*, 13, 101-146.
- [6] Murty, T.S. and G.T. Hebenstreit (1989): Tsunami amplitudes from local earthquakes in the Pacific Northwest region of North America - Part 2: Strait of Georgia, Juan de Fuca Strait and Puget Sound, *Marine Geodesy*, 13, 189-209.
- [7] Heaton, T.H. and S.H. Hartzell (1986): Source characteristics of hypothetical subduction earthquakes in northwestern United States, *Bull. Seismol. Soc. Amer.*, 76(3), 675-708.
- [8] Rogers, G.C. (1988): Megathrust potential of the Cascadia subduction zone. *Can. J. Earth Sci.*, 25(6), 844-852.
- [9] Spence, W. (1988): Anomalous subduction and the origins of stresses at Cascadia. Presented at the Workshop on Evaluation of Earthquake Hazards and Risk in the Puget Sound and Portland Areas, Olympia, WA., 12-15 April, 1988.
- [10] Wyss, M. (1979): Estimating maximum exceptable magnitude of earthquakes from fault dimensions. *Geology*, 7, 336-340.
- [11] Riddihough, R. (1984): Recent movements of the Juan de Fuca Plate system. *J. Geophys. Res.*, 89(B8), 6980-6994.
- [12] Heaton, T.H. and H. Kanamori (1984): Seismic potential associated with subduction in the northwestern United States. *Bull. Seismol. Soc. Amer.*, 74(3), 933-941.
- [13] Rogers, G.C. and H.S. Hasegawa (1978): A second look at the British Columbia earthquake of June 23, 1946. *Bull. Seismol. Soc. Amer.*, 678(3): 653-676.
- [14] Kowalik, Z. and T.S. Murty (1992): Numerical simulation of two dimensional tsunami runup, (in preparation).
- [15] Harbitz, C.B., G. Pedersen and B. Gjevik (1991): Model simulations of large water waves due to landslides, *Tech. Rept.* ISBN. 82-553-0734-6, No.3, April 1991, Matematisk Institutt, University of Oslo, Norway, 54 pages.
- [16] Pedersen, G. (1985): Runup of periodic waves on a straight beach, Preprint Series, Dept. of Math., Univ. of Oslo, No.2.
- [17] Pedersen, G. and B. Gjevik (1983): Run-Up of solitary waves, *J. Fluid Mech.*, 135, 283-299.

Session 2A

Landslides

mining of this "Lavezstein", or "Ofenstein" as it was also called, had helped to make Piuro rich, and the stone was used in the production of pots, ovenware and firebricks. The mine was said to have been very old. The richest seam dipped into the mountain, striking roughly west to east along the valley. The workings were about 500 m above Piuro. The adits can be seen on Scheuchzer's engraving. Heim doubts that the workings were ever backfilled. He was convinced that mining was the cause of the rockslide. The seat of the sliding may have been perpendicular to the Lavezstone, but the quarries and adits sunk into it would finally have loosened the mass above.

A striking feature of this catastrophe is the comparatively small volume of rock involved. The length of the debris has been estimated to be 20 m or so, and the total volume no more than 3 to 4 Mm³. Piuro, however, was in the direct path of the falling rock.

The surface of the debris is hummocky. Some of the blocks of rock are the size of a house. The city was never rebuilt, and the area is overgrown with chestnut trees. In fact, after 360 years it has become obscure, and it is difficult to believe that it was once a flourishing city known all over Europe. There is a moral in this story of the proud city dwellers of Piuro - like Humpty Dumpty, who all the king's horses and all the king's men couldn't put back together again.

The Himalayas and the Middle East

The Army to the Rescue

The rockslide at Gohna in the Garhwal Himalayas in 1893 occurred in the valley of the Birahi Ganga, which flows westwards to join the Alaknanda a main tributary of the Ganges. As the crow flies Gohna is about 311 km northeast of Delhi, and about 240 km along the river upstream of Hardwar. It lies 12 km above the confluence with the Alaknanda. The rocks in the Birahi Ganga valley are dolomitic limestones and shales dipping generally southeast and in places oversteepened.

Rockslides in this valley are common. About 13 km upstream of Gohna a small lake known as the

Gudyar Tal was formed by a landslip, and in the rains of 1869 a second slip fell into the lake, sending a disastrous flood down the valley. Part of Srinagar downstream was washed away.

Rockfalls at Gohna commenced in early September 1893. They fell from the north side of the valley. The main slide came on September 22 falling between the villages of Gohna on the north side of the valley, which it narrowly missed, and Durun on the south. The total height of fall was over 1000 m. The slide blocked the valley. The slide was immediately investigated and full topographic surveys made. From this data and making some assumptions about the pre-slide profile of the valley the calculated volume of the slide is roughly 230 Mm³. The tonnage was said to be 800 million. The length of the debris along the valley was about 3 km.

The filling of the lake was carefully observed. It was estimated that overflow of the dam would be in the middle of August 1894, the actual commencing date being 25th of that month. The volume of water released was about 300 Mm³, most of it during the night of August 26. Thorough preparations were made for the deluge, so that by the time it did arrive everyone had been evacuated out of the valley bottom and no lives were lost - a tribute to the foresight and planning of the army engineers and civil officers.

Although the slide is often mentioned in the literature and the references to it are readily accessible, details of the resulting débâcle are hidden away in an old government report, Pulford (6). The document is difficult to access, but the description of the collapse of the dam and resulting débâcle is very interesting.

Although no lives were lost during the flood, the property damage was enormous. Immediately following the slide tremendous efforts were made by British Army Engineers to minimize the impact. Even so Pulford estimated nearly 100,000 rupees of damage to public property, including roads, bridges and buildings. The city of Srinagar 125 km downstream was destroyed including the Raja's palace. The deluge there reached a maximum height of 13 m above the ordinary flood level. Similarly at Nandpryag and Karnpryag, and at the smaller

villages near the river banks "the flood swept away all vestiges of habitation." By the time it reached Hardwar it was 3.3 m above ordinary flood level and damage was minor.

Grand Cataclysm of the Indus

Almost, but not quite, legendary accounts exist of the collapse of the giant rockslide dam on the Indus River in June 1841. The dam 220 m high was formed in December 1840 by a rockslide off a spur of Nanga Parbat, at a point on the river said by one observer to be "perhaps one of the most savage and deepest valleys in the world", a nearly 5000 m deep gorge.

By the time the dam failed the lake behind was 65 km long. It seems that the entire volume, estimated at 3 Gm³, emptied in the space of about 24 hours. The result downstream was an enormous deluge - the grand "Cataclysm of the Indus". Abbott (7) quotes from the mouth of an eyewitness:

"Suddenly some one cried out, the "Rivers come!" And I looked and perceived that all the dry channels were already filled and that the river was racing down furiously in an absolute wall of mud, for it had not at all the colour or appearance of water. They who saw it in time easily escaped. They who did not, were inevitably lost. It was a horrible mess of foul water, carcasses of soldiers, peasants, war-steeds, camels, prostitutes, tents, mules, asses, trees and household furniture, in short, every item of existence jumbled together in one flood of ruin. For Raja Goolab Singh's army was encamped in the bed of the Indus at Koolaye, 3 koss above Torbaila, in check of Poynda Khan."

Torbaila was probably the site of present day Tarbela Dam!

The event has been researched and described in more detail recently by Code and Sirhindi, and published in Schuster (5).

The Mountain of the Ark

Do earthquakes "cause" rockslides? People usually like to blame them. Heim (2), however, saw little reason for this. He distinguished between the cause of a rockslide and the final triggering. An earthquake can be the cause of small rockfalls - the

mountains "shake off their loose rinds". But in the case of large rockmasses, they are too well-embedded, he claimed. An earthquake can do no more than put the finishing touches to a rockmass that has already reached a precarious state. The real cause of major rockslides according to Heim was to be found in deep-seated instability processes that had been going on for years. Heim often talked of the landslide slowly "preparing itself". Little by little the bonds break, and at the moment of the fall the alleged caused, like heavy rainfall or earthquakes, are no more than the trigger.

A most spectacular example comes from the Middle East. It is the slide off Mount Ararat triggered by a catastrophic earthquake in the summer of 1840. Ararat is close to the border of Turkey and Iran. Because it is the biblical mountain of the Ark, the slide aroused the interest of many European writers, see for example Parrot (8). It originated above snow-line on the north-east face of the mountain, and formed a mixed avalanche of rocks, ice and mud, similar to the avalanches off Huascaran in Peru. Mount Ararat is 5170 m high. Nearly halfway up stood the village of Arghuri, consisting of some 200 houses and a population of around 1000. The 800-year old Christian monastery of St. Jacob was close by. The huge avalanche completely obliterated the village, the monastery and the monks, together with 30 families of Kurds camped nearby. The debris lodged in a ravine. Shortly after when the snow and ice melted an enormous debris flow swept a further 20 km or so into the valley of the Araxes destroying four other villages. It deposited huge blocks of rock. Because Ararat is a volcano, the dust sent up by the avalanche was mistaken for smoke, leading to some false reports that the mountain had erupted.

Japan

Landslides have affected the Japanese people from their earliest periods of history. The oldest landslide legend dates back to the Kamakura Period (1190-1333 AD) when the Sarukuyoji landslide site in Niigata Prefecture was a continual hazard to the local residents. The earliest recorded mitigative measure was attempted during the 12th Century, when the local residents sacrificed a travelling Buddhist monk in an attempt to ward off further landslide disasters.

Eight centuries later, in 1938, the remains of this monk were accidentally uncovered during an excavation in the area and were subsequently enshrined at the site. Some doubt, however, lingers about the present applicability of this early technology! Landslides are still a problem in the area and the Sarukuyoji landslide is used as a field experimental station by the Public Works Research Institute of the Ministry of Construction.

Fix it and Damn the Cost

And today, as the population of Japan continues to grow and development spreads into more marginally stable terrain, landslides have become a greater problem in this relatively small and mountainous country, which experiences 10% of the world's seismic activity each year and contains approximately 10% of the world's active volcanoes. The following case history, largely abstracted from Araya et al 1985 (9), is an example of a fairly recent landslide problem associated with volcanic activity.

Mount Usu, located on the north island of Hokkaido, is a stratovolcanic mountain that has erupted every 30-50 years since 1663. It is 500 m high and approximately 7 km to 8 km across at its base. The volcano last erupted between October 1977 and March 1978. Composed of dacite and andesite, Mount Usu's eruptions are of the explosive, Mount St. Helens, variety.

Much of the Mount Usu area is a national park and Toya, located at the base of the volcano, is a spa or tourist city of 80,000, visited by approximately 4.5 million tourists annually. The City of Toya lies along the scenic shoreline of Lake Toya, a Pleistocene caldera approximately 10 km in diameter.

As a result of the 1977-1978 eruption, Toya was immediately covered with a metre or so of volcanic ash and 35,000 people had to be evacuated for about a month. The peak of the volcano slowly moved 200 m horizontally and the associated crustal movements destroyed 266 houses, two hospitals, several hot springs hotel and office buildings, disrupted roads and underground utilities, locally increased slopes from 25 degrees to 34 degrees and precipitated many landslides and debris slides.

Numerous periods of debris flow and mud flow

(lahars) activity followed. A total of 130 such events occurred on 14 creeks with one creek witnessing 21 separate events. The worst period of debris and mud flow activity occurred on October 24, 1978 when rainfall, with an intensity of 14.5 mm/hr, caused a total of 176,000 m³ of debris to flow down six creeks destroying four houses, damaging 21 and flooding over 100 others. Fortunately only three deaths resulted.

The Japanese philosophy with regard to mitigation of Mount Usu has been that since future volcanic activity and associated crustal movements can not be mitigated, efforts will be made to defend Toya against future debris flows and mud flows. Initially, the volumes and locations of "unstable debris" and "hazardous debris" were mapped. "Unstable debris" was considered to be all unconsolidated material that could easily be eroded by water, while "hazardous debris" was a subset of "unstable debris" and included unconsolidated material that could be eroded only by a "large-scale flood".

Between 1977 and 1982 emergency measures were carried out, and subsequently permanent works were constructed. Up to 1984, mitigative measures, included:

- on the mountain top and side slopes;
 - 302 ha of helicopter seeding and hillslope works
 - 13 km of erosion fences
 - 7 km of retaining walls
- along the creek and drainage paths;
 - 293 check dams
 - 646 groundsels (groundfills, also called consolidation dams)
 - 11 slit dams (to stop the movement of large boulders)
 - 29 sabo (erosion) dams
- and on the creek fans
 - 7 sand pockets (sediment basins)
 - 5 km of dykes
 - 11 km of channelization.

In addition, regular surveillance of the entire mountain area is carried out by helicopter, airphoto interpretation and automatic monitoring devices including remote television cameras and rain gauges.

Up until 1984, mitigative works involved 1 million man-days, and the costs were approximately \$480 million or \$6000 for each permanent resident of Toya. These are thought to be the most concentrated and costly natural hazard mitigative works in the world. They very likely are so! Riviere and Kamomura (10), rationalized that:

"Although the considerable amount of money involved remains a surprise for many people, the general opinion is that it is justified in Japan, a developed country where the employment is highly protected, and where a solution such as evacuation is mostly avoided".

Conclusions

Landslide hazards result from excess precipitation earthquake activity, volcanic eruption, mining activities and other sources. Man's relentless development of the earth's surface together with increase in world population is likely to intensify rather than diminish this hazard, despite our understanding of processes and technological innovation. A knowledge of historical events should, however, tend to lead to some improvements.

References

1. Montandon, F., 1933. *Chronologie des Grands Éboulements Alpains. Matériaux pour L'Étude des Calamités.* Société de Géographie, Genève.
2. Heim, A., 1932. *Bergsturz und Menschenleben.* Naturforschenden Gesellschaft in Zurich. Translated by Nigel Skermer (Landslides and Human Lives) published by Bitech, Vancouver, 1989.
3. Eisbacher, G.H., and Clague, J.J., 1984. *Destructive Mass Movements in High Mountains: Hazard and Management.* Geological Survey of Canada, Paper 84-16.
4. Bjerrum, L., and Jørstad, F., 1968. *Stability of Rock Slopes in Norway.* Norwegian Geotechnical Institute, Publication No. 79.
5. Schuster, R. L., (editor) 1986. *Landslide Dams: Processes, Risk, and Mitigation.* American Society of Civil Engineers. Geotechnical Special Publication, No. 3.
6. Pulford, R. R., 1893. *Report on the Gohna Landslip, Garhwal: The measures undertaken for the protection of life and property from the flood which ensued on the bursting of the barrier.* Records of the Government of India, Public Works Department, No. CCCXIV, PWD Series No. 30, Calcutta.
7. Abbott, J., 1848. *Inundation of the Indus, taken from the lips of an eye-witness, A.D. 1842.* Journal Asiatic Society of Bengal, XVII.
8. Parrot, F., 1845. *Journey to Ararat.* Translated by W.D. Cooley, London.
9. Araya, T., Nakasuji, A., Yamagishi, H., Matsuda, T., Miyasaka, S. and Ohzu, K. (editors), 1985: *Usu Volcano - disasters and measures; Guidebook for the 4th International Conference and Field Workshop on Landslides, August 27, 1985, DPW, Hokkaido Prefectural Government.*
10. Riviere, A. and Kadomura, H., 1984: *Impact of erosion control works on the environment - a case study on Usu Volcano; A Follow-up Survey of Environmental Changes Caused by the 1977-1978 Eruptions of Mt. Usu and Related Events, Graduate School of Environmental Science, Hokkaido University.*

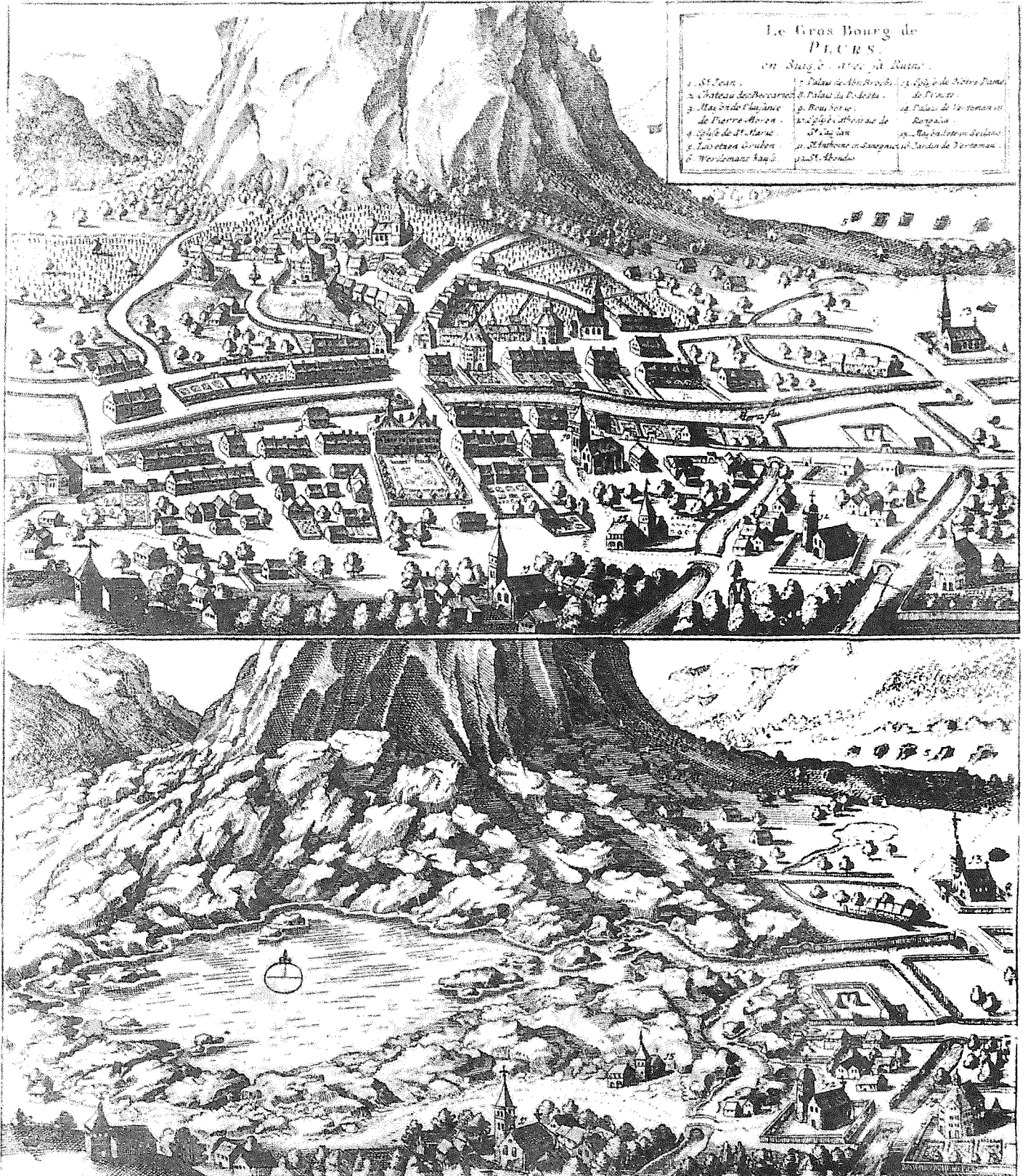


Figure 1. Destruction of Piuro. (Photo courtesy of John Rylands University Library, Manchester, England)

Evans, S.G.

**Landslides and river damming events associated
with the Plinth Peak volcanic eruption,
southwestern British Columbia**

Paper to be found on page 405

Evaluation of Mountainslope Movements at Wahleach

D.P. Moore, B.D. Ripley, K.L. Groves
B.C. Hydro
Vancouver, B.C.

Introduction

The mountainslope containing the western end of the power tunnel for the Wahleach hydroelectric project has been intensively investigated and monitored since 1989 when slope movements ruptured the steel lining of the tunnel and released water into the slope [1,2]. The steel lining ruptured in axial extension at one location in the upper tunnel and buckled in axial compression at eight locations in the shafts (Fig.1).

Movement monitoring during the last three years and surveys of the displacement of the steel lining since construction in 1951-52 provide a rare opportunity, not only to understand the style of deformation and evaluate the hazard of this slope, but also to gain insight into the deformation and hazard of other similar slopes.

A summary of the Wahleach deformation data within the context of the physical setting is provided, followed by a discussion of the evaluation of this data.

Project Layout

In 1951-52 the Wahleach hydroelectric project was built about 120 km east of Vancouver, B.C. to develop the power

potential between Wahleach Lake and the Fraser River.

The western end of the power conduit includes a nearly horizontal upper tunnel, a surge shaft, an inclined shaft and a lower, nearly horizontal tunnel. These excavations are nominally 3 m in diameter and mostly lined with a 2 m diameter steel lining. The annulus between the steel lining and the rock is backfilled with concrete.

In 1990, construction began on a replacement tunnel and shaft to bypass the portions of the original (1951-52) conduit located in the deforming area of the slope [3].

Physiography

The Wahleach slope rises from the Fraser River at Elevation 21 m to a ridge crest at Elevation 1100 m in the Cascade Mountains (Fig. 2). The surface profile along the tunnel is characteristic of a glacially oversteepened slope having increasingly steeper bedrock slopes towards the toe. Alluvial/colluvial fans burying the toe of the bedrock slope have been derived mainly from two steep-sided creek valleys which incise the main slope of the Fraser Valley to vertical depths up to 125 m isolating the

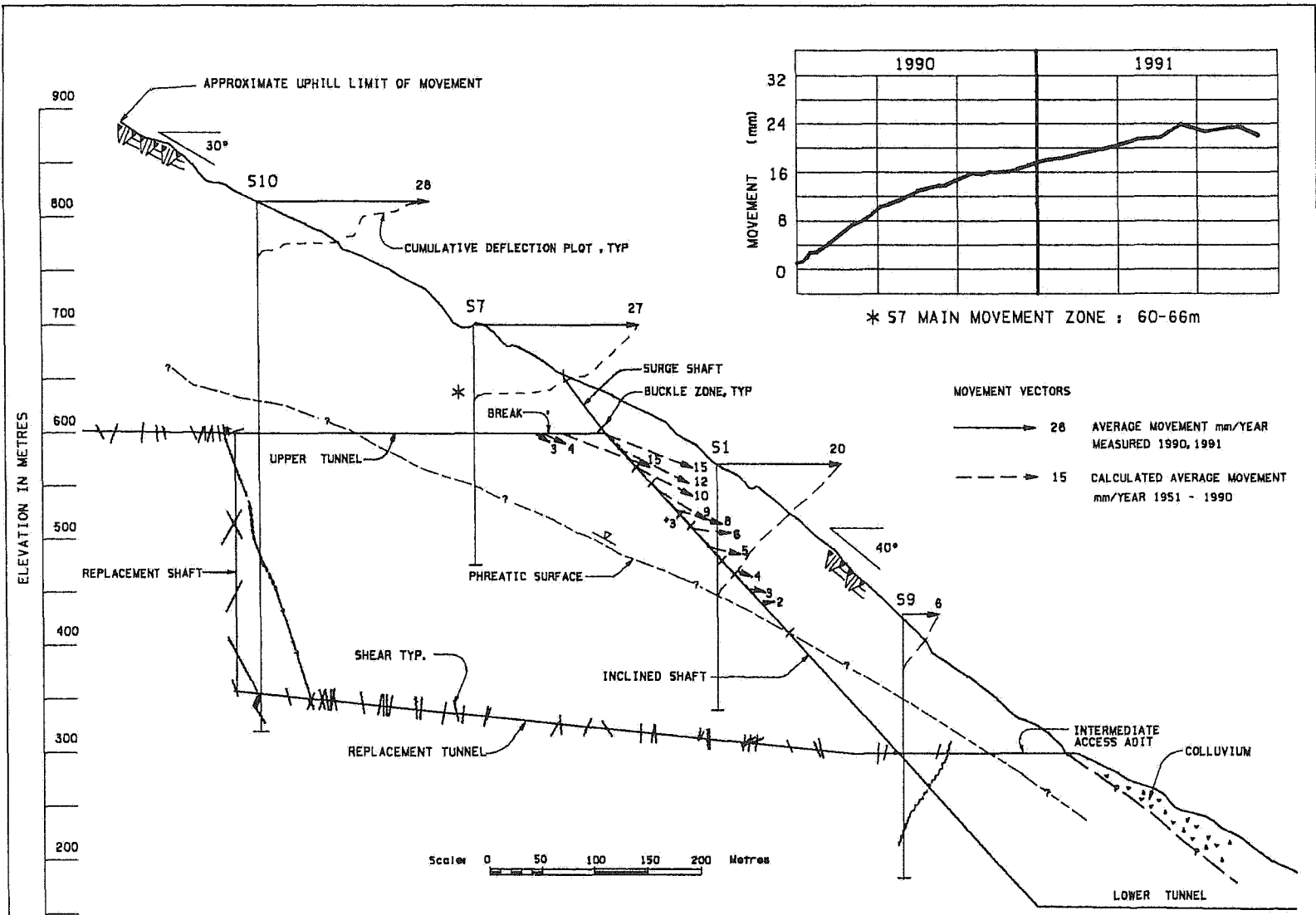


FIGURE 1
WAHLEACH - SECTION SHOWING MOVEMENT AND GEOLOGY

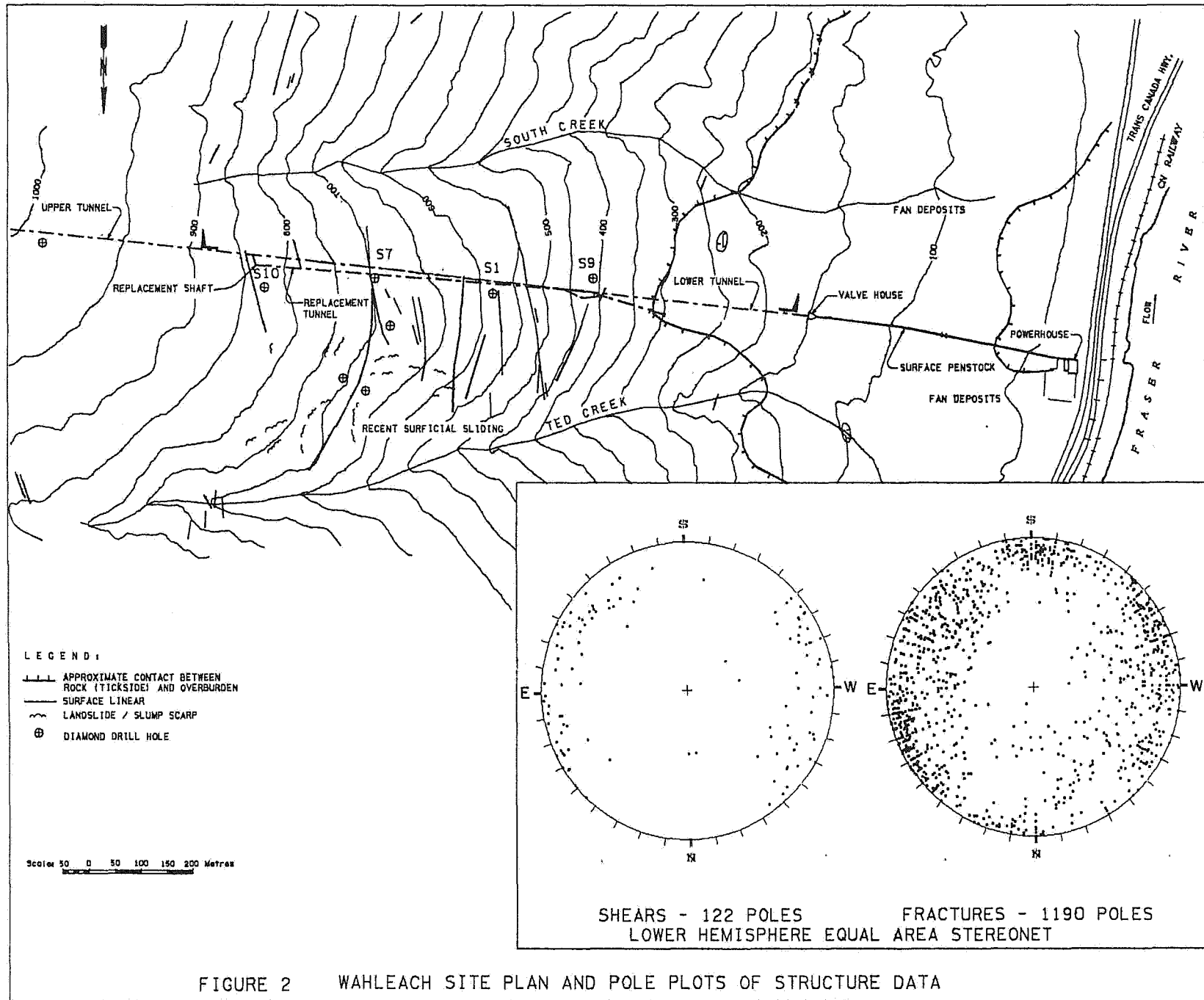


FIGURE 2 WAHLEACH SITE PLAN AND POLE PLOTS OF STRUCTURE DATA

prominence of rock containing the tunnel system.

Linear ridge-trough couplets up to 10 m deep trend along the contours of the main slope and cross the steeper portions particularly towards the north side of the prominence. These features are similar to those associated by many investigators with gravitational spreading or creep [4]. The trees growing in the troughs and along the ridges are often over one hundred years old and do not show any consistent evidence of tilting during their life.

Regional Geology

The Wahleach slope is located in a 16 to 24 million year old granodiorite pluton in an area of northwest, north, and northeast trending regional faults. No regional faults are known to offset the pluton, but small offsets would not necessarily have been detected.

Lithology

The slope is formed of generally hard and strong granodiorite which is cut by minor felsic and mafic dykes. There is nothing particularly unusual about the lithology except that locally the rock breaks easily into sand-size material when squeezed or lightly struck. In surface exposures, this rock has the appearance of highly weathered granite, but on closer inspection it is apparent that the mineral grains are fresh. The breakdown is likely due to a myriad of both inter and cross grain microfractures which have been seen in thin sections. The cause of these microfractures has not been determined.

Most of this weak rock occurs outside of the main prominence of the Wahleach slope. Within this prominence, the weak rock occurs locally in outcrops and adjacent to some fractures at depth.

Fractures and Shears

Rusty fractures, often with soft coatings or granular infillings, are spaced an average of 0.2 m apart near the ground surface in vertical drillholes (Fig. 3). Near the surface, the infillings are often different from the fresh wall rock of the fracture indicating some transport of material. The block sizes seen in surface exposures are typically less than 0.2 m on edge. A gradual trend to fewer fractures, less rust, less soft or granular material, less core loss and tighter interlocking of the fracture surfaces is evident with depth in the drillholes. At depth, as seen in the replacement tunnel and shaft, the average block size is closer to 0.5 to 1.5 m on edge. The general rock quality is characterized by transitional rather than abrupt changes with few if any exceptions.

The fractures have a wide range of orientations with two vague concentrations: one strikes roughly across the slope, the other strikes roughly downslope and both dip within 20° of vertical (Fig. 2).

Shear zones spaced 20 to 40 m apart are generally less than a few metres in thickness but can be continuous for hundreds of metres. Irregular, discontinuous, clayey, gouge zones less than 10 mm thick within a zone of increased fracturing and/or soft granular rock less than a few metres thick are characteristic. The shear zones strike roughly across the slope (+- 45°) and dip steeply. Where seen at depth, the apparent

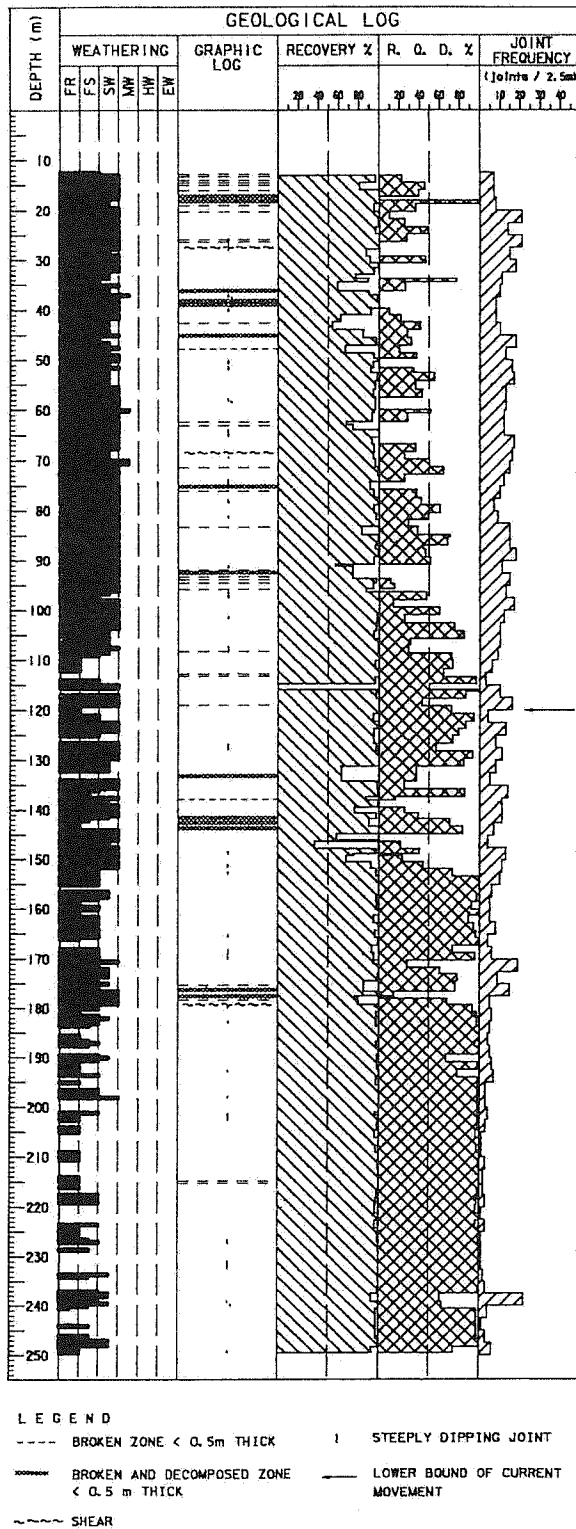


FIGURE 3
TYPICAL GEOLOGICAL LOG
VERTICAL DRILL HOLE (S1)

offsets on these shears have been typically less than a few metres.

Slickenside orientations observed in the drill cores and tunnel excavations range widely but 40% plunge less than 30° and 77% plunge less than 60°.

Thus, the rock mass at Wahleach is characterized by closely spaced, steep fractures, steep shear zones spaced 20 to 40 m apart, and gradual changes in rock quality. Of note is the lack of throughgoing discontinuities with downslope dips less than 45°.

In Situ Stresses

Hydraulic jacking tests were performed to determine minimum in situ stresses across fractures and shears for use in the design of the replacement water conduit. The tests showed that the lower bound of the jacking pressures is equivalent to 35% of the theoretical vertical stress based on vertical cover [5]. This result is consistent with the steep topography of the site for which more stress relief is expected compared to flatter topography [6]. Relief has presumably occurred through deformation and is promoted by the erosion of the main valley and incision of the side creeks.

Of interest is that the measured lower bound of the jacking pressures is approximately equivalent to the calculated minimum principal stress assuming that the friction angle of the rock mass is equal to the slope angle. This suggests that the slope is approximately at the angle of repose for the rock mass, which is consistent with the highly fractured, loose appearance of the near surface rock.

Groundwater

Piezometric measurements show that the phreatic surface is generally below the zone of slope movements, but local transient pressures build up within the zone during rainfalls and possibly also during snowmelt.

Piezometers indicate that prior to the recent excavation of the replacement tunnel and shaft, the unlined portion of the upper tunnel acted as a drain rather than a source of groundwater. Construction of the replacement tunnel and shaft in 1990-91 caused further widespread decreases in groundwater pressures. When the replacement system begins operating in 1992, these decreases could reverse.

Slope Movements

The slope movements at Wahleach fall into three general categories: near-surface sliding of local areas, current movement, and ancient movement.

Near-surface sliding of local areas is important as it contributes to the debris torrent hazard and is an indication of deeper deformations. Ancient movement is indicated by the very loosened appearance of the rock mass to average depths of 150-200 m, i.e. well below the currently monitored movements. About 60 million cubic metres of rock have this appearance. Possibly this material is still moving at rates too slow to be measured or possibly it moves intermittently as a result of some external influences such as earthquakes. The current movement involves about 20 million cubic metres of rock to depths of about 60-120 m and is the subject of the following discussion.

Since 1989, current movements have been monitored by a variety of methods including: visual inspections, electronic distance measurements from the north side of the Fraser valley, global positioning surveys, conventional ground surveys, wire and pulley extensometers, level meters, bore hole extensometers, strain meters on the steel lining of the tunnel, and inclinometers.

Of these methods, the inclinometers provide the best overall picture of the movements as they are accurate, extend from surface to depth, measure the largest component of movement, are widespread, and their results are generally consistent with the other methods.

Current Movements

During 1989 to early 1992, the inclinometers have shown that current movements of the rock at Wahleach have the following characteristics (Fig.1):

1. Generally within the moving rock mass the movements are diffuse but at a few locations they are concentrated;
2. Towards the uphill part of the slope the movements tend to be more concentrated within zones and the greatest rates of deformation tend to be at the base of the moving rock mass;
3. The movements generally are not associated with any notable or unusual geological features in the drill core;
4. The movements are seldom, if ever, associated with down slope dipping discontinuities;

5. The movements at depth have resulted in the larger cumulative displacements being at the ground surface and near the uphill boundary of the moving rock mass;
 6. The rates of movement have been relatively constant during 1990 to 1992 and are slower than they were in 1989;
 7. The movements in 1990-1992 have resulted in surface displacements ranging from 4 to 40 mm/year;
 8. The movements in the inclinometers do not exhibit an annual cycle;
 9. The movements are above the long term phreatic surface, but are within an area where where transient water pressures exist locally during rainfalls;
 10. To date, the rate of movement has not been linked to precipitation, drainage resulting from construction of the replacement conduit, or to operation of the existing conduit.
1. The largest measured movement of the steel lining of the inclined shaft is near its intersection with the upper tunnel and is about 600 mm , which is equivalent to an average of about 15 mm/year;
 2. The movement gradually diminishes down the inclined shaft;
 3. If this trend is extrapolated to the surface it would amount to 850mm at the collar of the surge shaft which is equivalent to an average of 22mm/year;
 4. The movement is generally downslope toward the Fraser Valley at azimuths between 250° and 270°;
 5. The inclinations of the movements in the upper shaft are between -20° and -30° but below buckle zone 3 they are about 15° flatter. This is equivalent to a 10 mm drop of the up-shaft portion relative to the down-shaft portion;
 6. An abrupt decrease in the total and vertical component of displacement also occurs near the break in the lining in the upper tunnel.

The movement of the steel lining since construction has been determined by comparing its present surveyed position with its estimated original position. This method is not accurate enough to determine present rates of movement but provides a good estimate of the cumulative movement that has taken place during the last 39 years (Fig.1). This survey also provides the vertical component of movement as well as the horizontal components provided by the inclinometers. The steel lining survey has confirmed the style of movement shown by the inclinometers at Wahleach and has indicated the following additional characteristics:

Styles of Movement

Diffuse movement not associated with throughgoing weaknesses is a major component of the movement at Wahleach. This is consistent with gravitational creep more akin to "flow" than to movement of large intact blocks relative to each other by rotation or sliding. This "flow" is facilitated by shear stresses due to the steep topography; by the large number of individual fractures and shears, most of

which are much steeper than the ground surface; and by the lack of throughgoing discontinuities weaker than the rock mass and oriented conducive to sliding.

The evidence from the upper parts of the slope of more concentrated movements is consistent with sliding, but clearly no throughgoing displacement surface has pre-existed or developed as a result of these movements. The poorer quality of the rock and the relatively more concentrated movements near the top of the slope indicate that the failure has progressed further in this area and probably began there rather than at the toe of the slope.

The series of ridge-trough couplets and the abrupt change in the inclination of the movements in the inclined shaft are consistent with relative movement of large blocks along steep, throughgoing discontinuities. This could result from rotation or from downdropping of wedges combined with dilation of the rock mass.

At Wahleach, all three styles of movement; flow, sliding, and block rotation or downdropping, are contemporaneous. This could well be true for many other similar slopes throughout the world.

Similar styles of movement during the last 40 years as exist today suggest that no other mechanism such as earthquake induced movement need to be found to explain the present physical condition of the slope. Nevertheless, the performance of the slope under earthquake loading is uncertain.

Slope Evolution

One process of slope evolution at Wahleach is by skin shedding in a series of small

slides, by ravelling and by "normal" near-surface erosion which tend to flatten the slope. Some of this material builds up at the toe and also tends to flatten the slope. In competition with this process is the tendency for the movement to develop concentrated displacement surfaces and for the slope to move "en masse". The steep topography and downcutting of the side creeks promotes both processes by reducing confinement.

The first process would lead to gradual stabilization whereas the second process could lead to sudden massive sliding. Both processes could be accelerated by earthquakes or extremely adverse weather conditions. Future monitoring will indicate which of these processes will eventually prevail.

However, at the present time the geological conditions, especially the lack of throughgoing, adversely oriented discontinuities; the long history of diffuse, slow movements; and the insensitivity of these movements to groundwater indicate the present processes will continue for a considerable time and that a large rockslide is not imminent.

Acknowledgements

The authors wish to thank A.S. Imrie and D.G. Baker of B.C. Hydro, and E. Hoek and A.H. Merritt who served on an Advisory Board for the Project, for their contributions in evaluating the slope behaviour.

References

1. Baker, D.G. 1991. Wahleach Power Tunnel Monitoring. Proc. of 3rd International Symposium on Field Measurements in Geomechanics, Oslo, Norway.
2. Moore, D.P., Imrie, A.S. and Baker, D.G. 1991. Rockslide Risk Reduction Using Monitoring. Proc. 3rd Canadian Dam Safety Conference, Whistler, B.C.
3. Ripley, B.D., Banks, P.A. and Imrie, A.S. 1991. Design Aspects for the Wahleach Conduit Replacement. Proceedings Canadian Electrical Association, Hydraulic Power Section, Toronto.
4. Varnes, D.J., Radbruch-Hall, D.H., Savage, W.Z. 1989. Topographic and Structural Conditions in Areas of Gravitational Spreading of Ridges in the Western United States. USGS Professional Paper No. 1496.
5. Ripley, B.D., Doe, T.W., Baker, D.G. 1991. Hydraulic Jacking Testing at the Wahleach Power Tunnel Project. Proc. 8th Canadian Tunnelling Conference, Vancouver.
6. Ripley, B.D., Brawner, C.O. 1991. Case Histories of the Influence of Steep Topography on In-Situ Stresses in Rock. Proc. 43rd Canadian Geotechnical Conference, Quebec.

Landslide Mechanisms in the Cordillera

Kenneth L. Myers
Welsh Engineering, Inc.
Reno, Nevada

Abstract

Landslides in the United States alone are responsible for more than \$1 billion in economic losses and in excess of 25 fatalities annually. Because of the nature of the steep terrain and climate, many of these slides occur in the mountainous regions of the Appalachians in the east, and the Cordillera of western North America. With few exceptions landslides are initiated by changes in the groundwater conditions. Patterns of groundwater flow in mountainous areas are often very complex being influenced concurrently by infiltration rates from rainfall and snowmelt, slope, landform morphology, rock outcrop patterns, joint and fracture patterns, accumulation of colluvial soils, etc. This paper will review some of the geomorphic controls on mass wasting in the mountains and describe some of the more common types of slope failure complexes (usually groupings of different types of slope failures with linked failure mechanisms). These findings are based on numerous observations throughout the western United States from New Mexico to Montana and Colorado to California involving projects ranging from subdivisions to mines and ski resorts to dams.

Slope Profiles

Geomorphologists are frequently concerned with the geometry of slopes and the angles developed on different parts of the slope profile. The general slope profile will contain three major components; 1) a convex crest slope section; 2) a straight mid-slope section consisting of either a steep cliff face (or fall face) and/or a flatter "transportational" mid-slope; 3) a concave foot slope. Some investigators have suggested a more detailed classification system involving nine distinct units [1]. A graphical representation of the nine units that comprise the full land surface model will be found in Figure 1. The predominant geomorphic processes associated with each of these nine units are listed in Table 1.

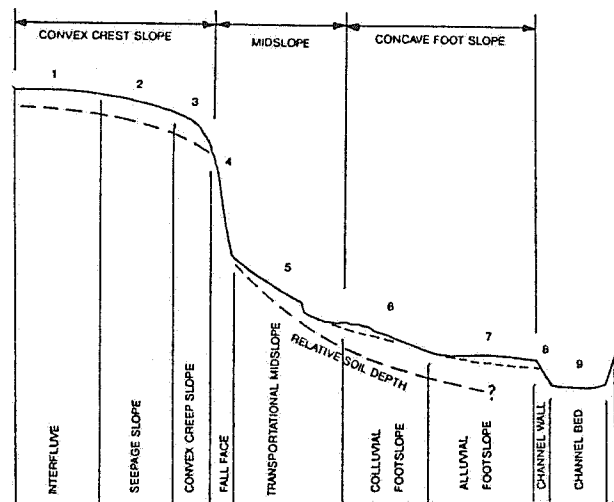


FIGURE 1 -- Nine unit landsurface model

TABLE 1 -- Predominant Geomorphic Processes Within Slope Components

Component	Geomorphic Processes
1. Interfluve 0-1°	Pedogenic processes associated with vertical subsurface soil water movement.
2. Seepage Slope 2-4°	Mechanical and chemical eluviation by lateral subsurface water movement.
3. Convex Creep Slope	Soil Creep: terracette formation.
4. Fall Face (minimum angle 45°, normally over 65°)	Fall; slide; chemical and physical weathering.
5. Transportational Midslope (frequently occurring angles 26-35°)	Transportation of material by mass movement (flow, slide, slump, creep); terracette formation; surface and subsurface water action.
6. Colluvial Footslope	Redeposition of material by mass movement and some surface wash; fan formation. Transportation of material; creep; subsurface water action.
7. Alluvial Toe slope 0-4°	Alluvial deposition; processes resulting from subsurface water movement.
8. Channel Wall	Corrasion, slumping, fall.
9. Channel Bed	Transportation of material down valley by surface water action; periodic aggradation and corrasion.

Hydrologic Cycle in the Mountains

Hydrologic systems common in mountainous environments are often quite complex with surface water and groundwater systems closely tied together. Figure 2 illustrates schematically the type of hydrologic system often present on mountain slopes. Mountain environments typically contain near-surface bedrock with frequent outcrops and surface exposures sometimes mantled with a thin veneer of residual and/or colluvial soil. Basins typically have steep slopes and correspondingly high surface and groundwater gradients. Geomorphically the ratio of mechanical weathering to chemical weathering is relatively high and the weathering products will either remain in place or be transported over very short distances. All of these effects will commonly produce fairly coarse-grained soils with relatively low clay contents and, therefore, high permeabilities and high infiltration rates.

If the predominant rock types involve igneous extrusive or igneous intrusive rocks they will be characterized by low porosity and low storage. The rocks themselves will have virtually no primary permeability with virtually all permeability resulting from secondary

sources (i.e., joints and fractures). Since the permeability of these rock masses are controlled by joints and fractures, they tend to have higher permeability near the surface where joints and fractures have been widened by weathering and opened by creep and other slope movements. Permeabilities will tend to dissipate with depth as fractures begin to tighten and close or sometimes dissipate entirely. The result is a complex system dominated by fracture flow in the upper portions of the bedrock profile and with frequent interaction between the surface and groundwater system.

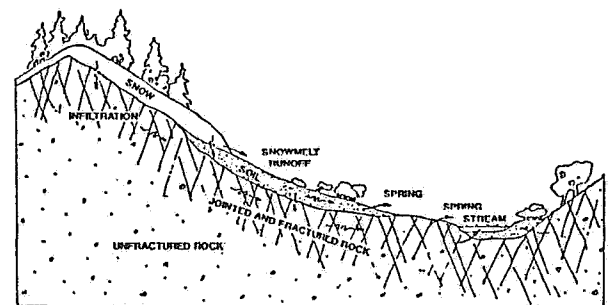


FIGURE 2 -- Mountain slope hydrology

Another important aspect of mountain hydrologic systems is that the majority of the precipitation occurs during the winter months in the form of snow. Therefore, the majority of the water in the basin is stored at the ground surface and not released until spring. The rate of release is controlled more by fluctuations in air temperature than by any specific meteorological event. The presence of the snowpack tends to promote a higher ratio of infiltration to runoff by retarding the overland flow of melt water, clogging surface drainage structures, and detaining surface flows in the early stages of the melt.

Mountain Mass Wasting Overview

The western mountains contain a wide range of environments that vary with location, altitude and aspect. Every ascent of 1,000 feet corresponds roughly to a northward advance of 300 miles at sea level. Five so-called "life zones" are used to describe the diverse environments in the mountains, each named after the continental region which it ecologically resembles. From highest to lowest, these zones consist of the Arctic-Alpine zone, the Hudsonian zone, the Canadian zone, the Transition zone and the Upper Sonoran zone [2].

The Arctic-Alpine zone is basically the area above timberline. Here the landscape is a vast expanse of rock and tundra. Just below this zone is the Hudsonian or Sub-Alpine zone where some vegetation begins to appear consisting largely of gnarled white bark pine and low shrubs. The ground surface in this zone remains wild and rocky. Snow is the predominant form of precipitation in the Arctic-Alpine and Hudsonian zones, and snowmelt the predominant source of water making late spring and early summer the peak time for instability. Few manmade structures will exist in these zones except for the occa-

sional ski lift terminal or maintenance building, or an occasional mine structure. Therefore, mass wasting will usually represent a relatively minor "hazard" which can often be mitigated by relocation for avoidance. Slope components 1 and 2 (interfluvial and seepage slope) are often small or nonexistent. The creep slope predominates in the convex portion of the slope profile. Creep and solifluction processes are common forming small terraces that criss-cross the slope normal to the fall line.

Mechanical weathering processes dominate in the Arctic-Alpine/Hudsonian. Coarse angular clasts with the fines winnowed out are common. The fines will often collect on flat benches and in surface depressions. These depressions which also collect water will sometimes produce translational slides or shallow, large radius rotational slides with multiple springs issuing from their toe. Small debris flows occur in narrow gullies on the fall face which may also serve as avalanche chutes in the winter. Small debris cones grow at the base of each of these gullies when some significant width of foot slope or an alluvial terrace is present to catch the debris. Where these flat spots are not present at the base of the gully, they will discharge their debris load directly into the stream. Where a long continuous fall face exists producing a good supply of debris, these cones will often coalesce into a long apron of debris mixed with talus from rock fall directly off the face. Parallel sets of debris levees sometimes snake down the surface of these aprons, evidence of recent debris flows that create their own channel in order to transport their debris load as far as possible on the otherwise unbroken surface of the fan.

The Canadian zone is where the deep forests of fir and lodgepole pine begin. The climate is cool and wet with abundant snow in the winter and spring giving way to thunderstorms

through late summer. Slightly lower in elevation is the Transitional zone, a still wet but somewhat warmer version of the Canadian zone with the fir and lodgepole pine giving way to ponderosa pine. Both geochemical and pedochemical weathering processes begin to dominate over the mechanical processes of disintegration. Thick soil profiles develop and migrate down the slope to form thick deposits of colluvium. In these two zones the works of man now begin to become more prevalent with subdivisions, ski resorts and roads becoming more frequent targets of mass wasting activities. Mass wasting in these zones represents a more serious "hazard." All types of mass wasting activity are common in this relatively wet soil covered environment. On steep north facing slopes it is not unusual to see a whole series of shallow infinite slope failures, shallow rotational slides, block slides and small flows knitted together in what appears to be an almost continuous sheet of instability (sometimes covering an area of a square mile or more). Often at the head of a deep alpine valley a series of rotational slumps or a large rock slide will line the starting zone of a large earth flow which may extend down valley for a few thousand feet to as much as 2 or 3 miles. On the steep walls of a glacially carved hanging valley, a large slope failure complex consisting of deep rotational slides, planar translational slides and small flows will cut through a series of lateral moraines lying precariously along the oversteepened slope.

The last zone is the Upper Sonoran zone. Here the climate and the slopes are beginning to dry out. On the west slope of the Sierra Nevada this zone will be marked by grasslands with small clumps of live oak and sycamore. However, in the majority of the Rocky Mountain west, this zone is dominated by pinion, juniper and sage. The routine precipitation occurs less frequently and in smaller doses. Mass wasting is more often

associated with extreme precipitation events. Debris flows and debris floods race down canyons and gorges often undermining the toes of the slopes above. Topples and rotational slumps form in the steep canyon walls and large complex translational slides may be released in the more moderate slopes above the canyon.

The following sections will describe the landslide triggering mechanisms of the more common slides and flows found in the wet Canadian and Transition zones and the case history of a large predominately translational failure in the Upper Sonoran zone.

Infinite Slope Failures and Small Debris Flows in Colluvial Soils

Mountain slopes often contain a relatively thin veneer of residual or colluvial soil above a fractured and jointed bedrock. This type of profile lends itself readily to infinite slope failures. For any given depth of soil the stability will depend on the shear strength characteristics of the soil, the groundwater depth and the direction of groundwater flow. The direction of groundwater flow affects the character of pore pressure gradients within the soil profile and also provides body forces which can either add to or detract from driving and resisting forces. Table 2 shows the effect of groundwater depth on the factor of safety of a typical colluvial soil slope. Table 3 shows the effect of groundwater flow direction on the factor of safety.

The subsurface water which affects the stability of these slopes can come from two sources; 1) vertical infiltration of rain water; and 2) pressurized flow in open joints beneath the soil cover. Infiltration is a function of rain fall intensity. The effects of intensity can be examined using the SCS methods for estimating infiltration and runoff. At low

intensities the infiltration rate is controlled directly by the intensity of the storm and the soil profile accepts all moisture producing no runoff. At higher intensities the infiltration and runoff are divided based upon the SCS equation for runoff [3]. Table 4 shows information on the infiltration rate, percent saturation and wetting front velocity estimated based on the SCS equations, simple weight-volume calculations, and the estimation of unsaturated hydraulic conductivity from the saturated hydraulic conductivity and percent saturation [4]. During a long duration low intensity storm, a partially saturated wetting front develops within the soil profile moving slowly downward. It has little impact on the stability of the soil layers since at this point in time no pore pressure exists and it merely adds to the weight involved in the driving forces. It does however take the soil profile from a relatively low moisture content to a moisture content that may be on the order of 80 percent saturated or more. Should the storm intensity increase in the late stages of the storm or should the storm be followed days or weeks later by a higher intensity storm, only the small remaining pore space in the soil must be filled in order to rapidly advance the wetting front and begin building piezometric head within the layer. Failures associated with this pattern of increase in

antecedent moisture from numerous long duration low intensity rain fall events followed by a high intensity storm are numerous in the literature. Campbell [5], in studying a number of debris flow failures in the Los Angeles area during the winter of 1969, concluded that the area had significant debris flow activity when a storm with an intensity exceeding 1/4 inch per hour occurred following a total of at least 10 inches of low intensity rain fall for the season. In 1985, Cannon and Ellen [6] looked at threshold combinations of rain fall intensity and duration producing abundant debris avalanches in the San Francisco Bay area. Okimura, in 1981, examined the effect of fissure water on the timing of superficial slides in the Rokko Mountains of Japan [7]. Slides were observed to occur when rain fall intensities exceeded 50 millimeters per hour following two days of long duration storm events where intensities remained below 20 millimeters per hour.

The second groundwater flow mechanism involved in shallow slides is that of pressurized flow in joints. In the spring of 1986, a valley along the north fork of the Gunnison River in Colorado experienced nearly nine days of steady low intensity rain fall punctuated by a brief period near the end of the storm where intensities exceeded 3 inches per hour.

TABLE 2 -- Groundwater Depth vs. Factor of Safety

	Groundwater Depth (ft.)	FOS
Slope Angle = 34°	0	1.55
$\phi = 37^\circ$	0.5	1.46
$c = 100$ psf	1.0	1.39
$\gamma_s = 120$ pcf	1.5	1.32
Soil layer thickness = 5 feet	2.0	1.25
	2.5	1.19
	3.0	1.13
	3.5	1.07
	4.0	1.02
	4.5	0.97
	5.0	0.93

TABLE 3 -- Groundwater Flow Direction vs. Factor of Safety

	Theta (deg)	FOS
Slope Angle = 34°	-55	-21.56
$\phi = 37^\circ$	-45	-1.12
$c = 100$ psf	-35	-.13
$\gamma_s = 120$ pcf	-25	.24
Soil layer thickness = 5 feet	-15	.44
	- 5	.58
Note: Soil Profile is assumed to be saturated. Negative theta angles indicate a flow direction above the horizontal plane and positive angles below the horizontal plane.	5	.68
	15	.76
	25	.83
	35	.90
	45	.97
	55	1.05
	65	1.13
	75	1.24
	85	1.38

TABLE 4 -- Rainfall Intensity vs. Infiltration Rate, Percent Saturation, and Wetting Front Velocity

Rainfall Intensity (in/hr)	Runoff Volume Q (in/hr)	Infilt. Volume F (in/hr)	Equivalent Seepage Rate (cm/sec)	Required Percent Saturation (%)	Wetting Front Velocity (ft/hr)
0.10	0.00	0.10	7.06E-05	51.6%	0.15
0.20	0.00	0.20	1.41E-04	57.3%	0.23
0.30	0.00	0.30	2.12E-04	61.2%	0.30
0.40	0.00	0.40	2.82E-04	64.4%	0.36
0.50	0.00	0.50	3.53E-04	67.0%	0.41
0.60	0.00	0.60	4.23E-04	69.3%	0.46
0.70	0.00	0.70	4.94E-04	71.4%	0.51
0.80	0.00	0.80	5.64E-04	73.3%	0.56
0.90	0.01	0.89	6.30E-04	74.9%	0.60
1.00	0.02	0.98	6.93E-04	76.4%	0.63
1.25	0.06	1.19	8.38E-04	79.4%	0.72
1.50	0.13	1.37	9.67E-04	81.8%	0.79
1.75	0.22	1.53	1.08E-03	83.8%	0.84
2.00	0.32	1.68	1.19E-03	85.4%	0.90
2.50	0.57	1.93	1.36E-03	88.1%	0.98
3.00	0.86	2.14	1.51E-03	90.1%	1.05
4.00	1.53	2.47	1.74E-03	93.1%	1.15
5.00	2.28	2.72	1.92E-03	95.1%	1.22

Note: Assumes a soil with an SCS Curve Number of 73 and a saturated hydraulic conductivity of 2.4×10^{-3} cm/sec and initial volumetric water content of 10%.

Numerous small debris flows were generated, most of them initiating either immediately above or adjacent to steep fall faces on the slope where bedrock was exposed and the soil cover thinned. As the colluvial soil cover

thins at the top of an outcrop, the relative depth of groundwater flowing through this zone increases and the flow direction is upward relative to the ground surface. This combination of thinning soil cover and

emerging groundwater flow is felt to be responsible for the initiation of these slides many of which began as infinite slope failures which with the addition of water from continued rainfall become fluid debris flows.

Those debris flows which initiated adjacent to outcrop locations typically formed a small arcuate head scarp within the shallow soil layer with a strong flowing spring centered beneath the head scarp, usually emanating from a small patch of fractured rock visible on the failure plane. This water was obviously flowing out of the joint system in the bedrock. In many cases flows from those springs persisted for weeks after the initial failure.

The north fork site was an underground coal mine which provided a unique opportunity to examine the relative impact of the two sources of groundwater for the shallow slides; i.e., infiltration versus pressurized flow in joints. The ventilation or fan portal penetrated a substantial thickness of landslide debris associated with a large slope failure complex on the mountainside. The landslide debris was approximately 80 feet thick. The effects of vertical infiltration from rain water were clear near the surface and the wetting front had progressed approximately 15 feet into the silty to clayey sand soil profile. However, the intervening area between the base of the wetting front and the base of the landslide debris was completely dry. At the interface of the landslide debris in the bedrock, conditions were once again wet with a 1/4 inch diameter stream of water jetting from a joint in the bedrock and landing more than 8 feet from the rib in the middle of the mine floor. The source for this water was obviously considerably higher on the mountain with the water being under considerable pressure.

Modelling the complex groundwater flow in

mountain slopes can be difficult. Depending on the nature of the slope profile suitable techniques may vary from a simple application of Darcy's Law and continuity of mass to an elaborate finite difference model. One of the more interesting approaches to this problem is a technique used by Sugawara. It is an empirical model using a series of tanks with orifices at various locations on the bottom and/or sides of the tanks. The tanks are sized to represent storage within the aquifer and the orifice discharge points can be sized to represent various rates of leakage between aquifers, lateral discharge between aquifers, or surface discharge from springs [7].

Earthflows at the Heads of Alpine Valleys

Large earth flows are relatively common in the soft rock areas of the Rocky Mountains. These flows will usually have a characteristic "dog bone" shape with a large circular bowl at the head of the slide followed by a narrower transportation section and terminating in a more or less circular depositional fan. Once again groundwater is critical to the mobilization of these flows. In these more or less circular areas in the heads of the valleys, groundwater flow is being concentrated geometrically due to the effect of converging flow lines from the slopes above. Even in the absence of converging groundwater flow, the soils located in this portion of the valley floor will naturally be carrying a considerably greater degree of moisture than the remainder of the slopes. Another feature common to these large earth flows is the presence of one or more large rotational slumps originating on the slopes above the source area of the earth flow at the valley head. The two occur together frequently enough that it seems to be more than mere coincidence. It is the author's opinion that the rapid surcharge loading on the soft saturated soils at the head of these valleys is

responsible for a rapid decrease in effective stress which can help push these soil materials into the plastic Bingham flow region of the stress strain curve. Yet another possible factor involved in the mechanics of these large flows is a phenomenon known as static liquefaction (a sudden stress path induced strength loss caused by a low level static surcharge). However, to my knowledge no documented evidence directly linking this phenomena to the initiation of earth flows is yet available.

Landslides Associated With Inverted Topography

Extensive basalt flows cap the mesas in the foothills of the Sangre de Cristo Mountains in southern Colorado. It is speculated that some of the present day mesas are the result of an "inverted topography" (sometimes referred to as exhumed topography). This is where the basalt flows track the low lying valley floor areas on the pre-existing erosional surface. The materials underlying the basalt consist of weakly cemented Tertiary aged sandstones with well developed soil profiles, a significant thickness of alluvial materials in what used to be the valley floor. As erosion progresses, the more easily eroded sedimentary materials along the ridges are removed at a faster rate eventually undermining the edges of the basalt and reversing the topographic trend (i.e., the former higher areas are now low and the former lower areas are now high). As erosion continues to progress, the edges of the mesas are continually kept sharp by the calving of basalt into the deepening valley.

An interesting case history involves a large translational slide in the above described environment which covers more than a square mile in surface area. The landslide rests on the south side of Trinchera Creek and is a slope failure complex. By far the most

dominant mechanism in this complex is translational sliding where the horizontal components of movement dominate over the vertical. The failure plane is located at the interface between the basalt and the underlying soil profiles and weak soft rock of the tertiary sediments.

A commonly held principal with regard to slope stability is that "laying back" a slope or unweighting the slide will improve stability. However, for a site which contains hard competent material overlying weak softer material, precisely the opposite can be true. Those areas which are thinnest or have the least mass above the failure plane will tend to be less stable and therefore more mobile than the thicker heavier areas. This is because the failure plane is restricted to the softer layers at depth and resists passing through the strong more competent materials that overlies them. Reducing the thickness of these competent materials will simply reduce the normal force on the failure plane with a corresponding decrease in the shear resistance along the failure plane. At the Trinchera Creek site the lower or northern most portion of the site appears to have undergone considerably larger movements than the upper or southern edge of the slide implying that the basalt is thinning to the north. This was subsequently confirmed on this site by geophysical surveys using magnetics.

Since the horizontal component of movement dominates in translational sliding, great tension will be produced in the materials above the failure plane. This results in the formation of large "graben" areas within the slide which in this particular case were hundreds of feet wide. In the floor of one of these graben areas a "window" was opened through the basalt to the underlying materials which disclosed a zone of rounded alluvial cobbles more or less centered beneath the axis of the slide. The remnant alluvial valley floor

beneath the basalt can provide a ready conduit for transmitting water and more importantly high pore pressures to the base of the basalt.

Another interesting phenomena observed at this site involved a progressive change in the dip of the basalt near the toe area of the slide. In the upper portion of the slide the basalt dipped toward the valley floor at angles on the order of 15 to 20 degrees. Approaching the toe the dip began to change progressively as one crossed successive scarps until finally at the canyon's edge the basalt dipped away from the valley floor at angle in excess of 30 degrees. It was originally postulated that this change in dip occurred in remnants of rotational slumps in the oversteepened toe area of the slide. However, shallow seismic reflection testing in several lines across the area revealed a "ramping" effect and compressional features (i.e., the upper blocks were tending to force themselves below the lower blocks during the shearing). It became apparent that the sudden reversal in dip was caused by a buckling phenomenon near the toe of the slide. The thin southward dipping slides are remnant limbs of the arches created by buckling during the formation of the original landslide dam when these thin slabs impacted the opposite canyon wall. The entire toe area of the slide along the axis of this arch appears to have been removed by erosion forming the existing canyon of Trinchera Creek.

References

- Ritter, D.F., 1986. *Process Geomorphology*. Wm. C. Brown Publishers.
- Bowen, E., 1975. *The High Sierra, The American Wilderness*. Time-Life Books.
- McCuen, R.H., 1982. *A Guide to Hydrologic Analysis Using SCS Methods*. Prentice-Hall, Inc.
- Todd, D.K., 1980. *Groundwater Hydrology*. John Wiley & Sons.
- Campbell, R.H., 1975. *Soil Slips, Debris Flows, and Rainstorms in the Santa Monica Mountains and Vicinity, Southern California*: U.S. Geological Survey Professional Paper 851, 51p.
- Cannon, S.H. and Ellen, S. *Rainfall Conditions for Abundant Debris Avalanches, San Francisco Bay Region, California*: California Geology, December 1985.
- Okunishi, K. and Okimura, T. 1987. *Slope Stability: Groundwater Models for Mountain Slopes*. pp. 265-285. John Wiley & Sons Ltd.

Session 3A Landslides (continued)

construction of the box culvert. However, shortly after the start of excavation to prepare the bedding for the box culvert, cracking started at a small old scarp and seepage zone just above the creek bank. Due to subsequent large scale retrogressive cracking to the top of the backslope, the box culvert was abandoned.

The extent of the slide measured 400 m in width along the creek valley, 400 m in length and 50 m in height from the creek to the top of the backslope. It appeared that failure along the old slide zone might have been reactivated. The area of this slide was approx. 150,000 sq. m. The mode of failure was observed as translational, semi-circular and retrogressive.

Minor slides at (A) 12+000, (C) 13+540 & (D) 13+980

During the first week of September 1989, slope movements of a lesser magnitude were observed at the above locations of sidehill fill embankments.

Investigation following the slides indicated that flowing groundwater was located in gravel/sand stringers at slide C and one other location at sta 12+980 (not discussed in this paper). As an attempt to alleviate any adverse groundwater conditions, drilled horizontal drains were installed. Surface cracks were also infilled to minimize surface water ingress. The alignment was eventually shifted south towards the backslope away from the 3 minor slides. However, cracking persisted over one year duration and encroached towards the shifted alignment. The modes of failure were semi-circular and retrogressive.

Slide A was located along the outside curve of the alignment at a cut/fill section with approx. 6 m fill at centreline. Sidehill seepage was not evident. The slide was dressed and a toe berm was constructed at the allowable space along

the creek bank. Despite berming and constant crack infilling, a tension creek persisted along the outside shoulder edge.

For the winter 1989, the slide areas were left for natural stabilization and any further remediation in the next year.

Causes of Failures

All instabilities occurring along this alignment at the identified locations resulted as a consequence of construction activity.

Except for Slide B which was considered a reactivated area, the other areas were not considered unstable by themselves, except that the proposed sidehill constructions in these areas created situations which resulted in instability of the fills as well as in the naturally occurring ground.

For areas A, C, and D, the slightly consolidated glacial lake deposit of recent geological age with interspersed sand/gravel laminations and stringers presented seepage zones, in the natural ground. These were considered contributory to instability of sidehill fills, if not properly identified prior to and during fill placement.

Other possible factors contributing to failures in these areas were the inadequate removal of thick surficial vegetative cover prior to fill placement or removal of this weak material and incorporating it to the fill through the benching operations.

Based on investigation of these failure locations and previous experience of behaviour of sidehill fills, it was concluded that lack of drainage of the possible seepage zones prior to fill placement along with the other factors discussed previously were the primary causes of failures occurring in these areas during and

following fill construction.

Remediation

General

Allowing time for the minor slides to stabilize and 'heal' themselves along with the alignment shift towards the allowable space in the backslope direction was attempted with limited success.

Generally, shifting of the alignment away from the slide areas was the first priority option considered. The space restriction of the road corridor, backslope steepness as well as geometric compatibility with the adjoining road sections was addressed in deciding the shifts.

Berming the creek with the installation of an underlying culvert was taken as a second priority recourse if movement persisted even after shifting the alignment from the slides.

During reconstruction of some slopes, benching into native ground and cleaning out of stripping material at the slide toe were carried out. Drainage measures were also implemented at seepage areas.

Major Slide B at 12+750

As it was apparent that an old slide was activated by excavation at the toe of slope during the box culvert installation, massive toe berming was considered a viable remediation. Berming of the creek at the toe of the slide would serve as a toe restraint and buttress against the opposite valley wall. The original box culvert was replaced by a steel pipeline conduit (760 mm dia.) which was installed, within the toe berm. Over 300 m of steel pipeline and corrugated steel pipe (CSP)

culvert were used to replace the creek.

The material from the top half of the slide was removed and used for berming at the toe areas. The alignment was shifted approx. 50 m from the middle to the toe of the slide. Utilizing an embankment of approximately 10 m maximum fill height above original ground, a toe load was accomplished. The volume of earth quantity for berm construction amounted to over 500,000 cu. m. The cross-section of the berm for the creek and roadway as well as the plan of alignment shifts are shown on Fig. 3.

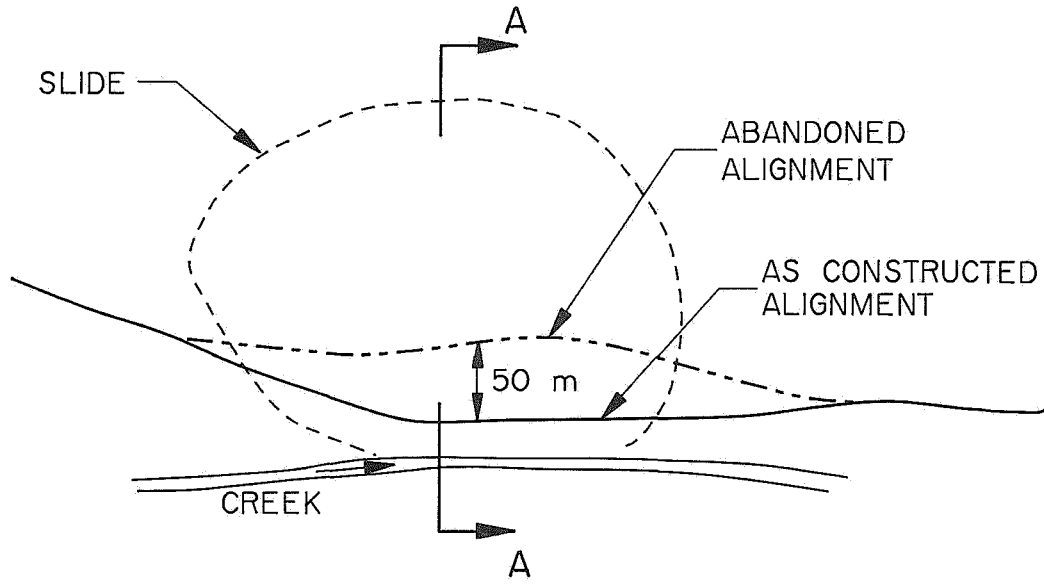
Minor slides C,D at (C) 13+540 & (D) 13+980

Since it was apparent that sideslope seepage and inadequate toe restraint were the major causes of failure, toe berming and subsurface drainage remediations were utilized. Due to the tight space within the creek valley, berming of the slope by filling in the creek was undertaken to achieve a toe restraint. Creek flow was accommodated by the installation of a CSP downdrain beneath the berm.

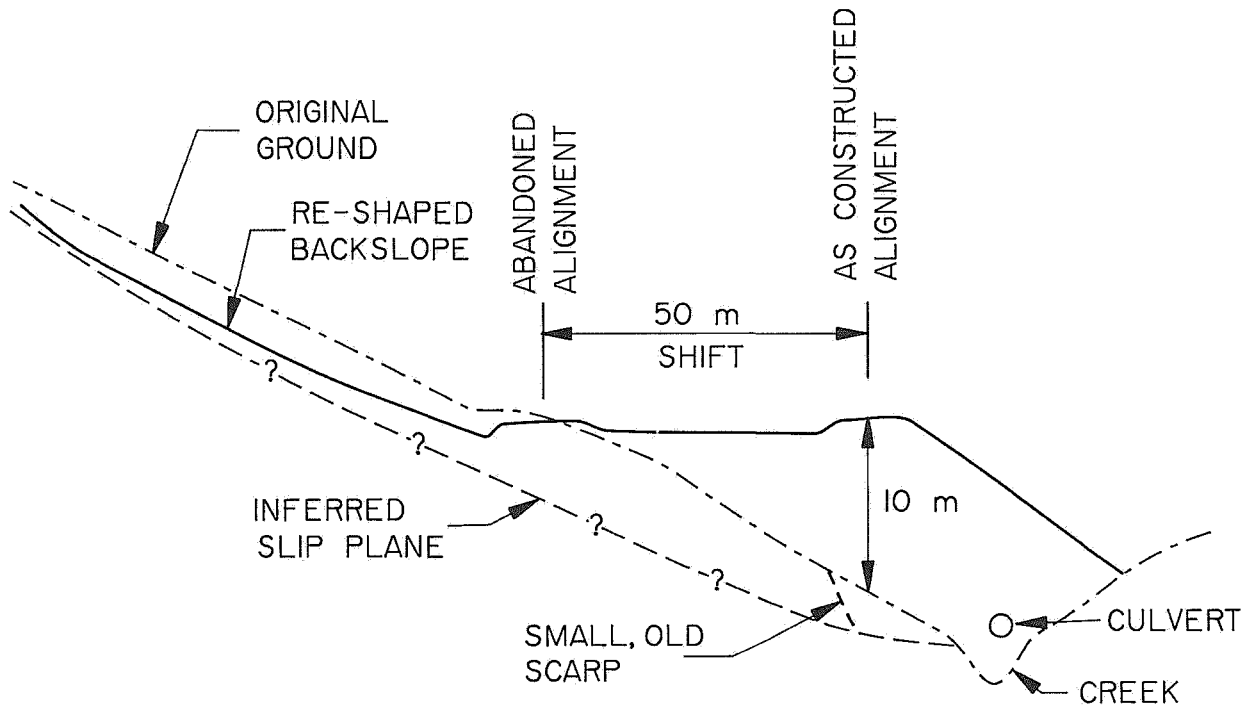
The fills were reconstructed with 3:1 slope and drainage measures. The drainage included: 1) subsurface drains at regular vertical intervals traversing the dip of the slope and 2) a backslope subsurface drain. Such drainage measures were designed to intercept any seepage zones at the cut/fill interface verified through investigative efforts. The drains entailed free-draining granular material and perforated pipe with daylight outlets. The slope reconstruction and drainage remediations are shown on Fig. 4.

Minor slide A at 12+000

The location was a typical sidehill cut/fill construction. Despite berming at the toe of the



PLAN (SLIDE B)



CROSS SECTION A-A

FIGURE 3 ALIGNMENT SHIFT & CROSS-SECTION OF BERMING

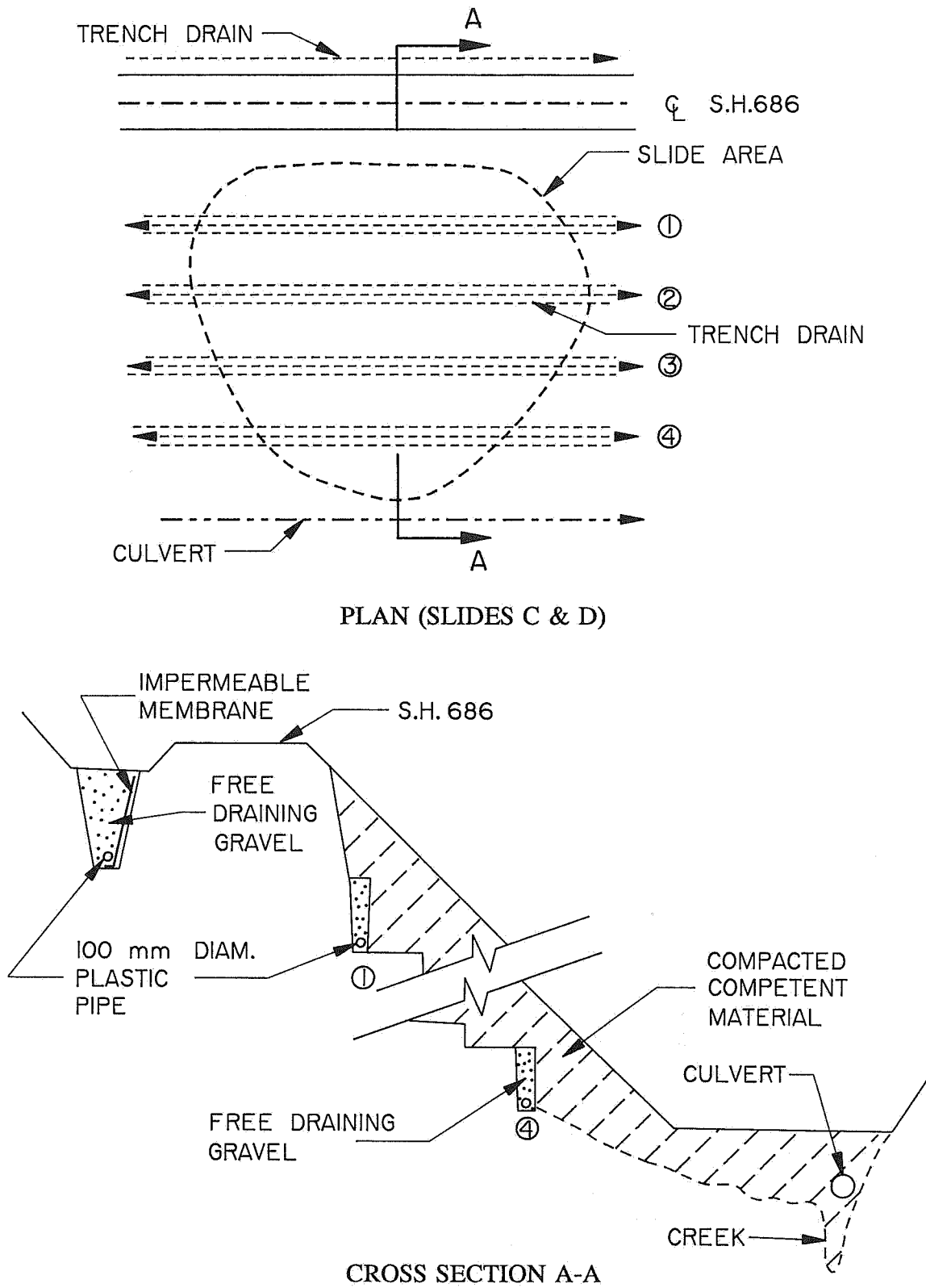


FIGURE 4 SLOPE RECONSTRUCTION & DRAINAGE MEASURES

construction. Despite berming at the toe of the sideslope along the narrow creek bank, tension cracks persisted along the road shoulder edge over a period of one year. Further subsurface investigation revealed that soft foundation material at the toe area was the main contributive cause and that seepage zones were not apparent.

As shifting towards the backslope was prohibitive due to vast cut quantities, a plausible and economical solution was buttressing the slope against the opposite valley wall by berming over the creek. A CSP culvert was installed along the creek path to accommodate the creek flow prior to berming.

Discussions

The alignment SH 686:01 was completed in September 1990 pending completion of the new Peace River Bridge. Slope indicators were installed following construction at all unstable sites and the rebuilt slopes have been monitored since October 1990. To date, general creep movement is prevalent and the rate of movements along the slip plane is approx. 15-20 mm/year. So far the roadway grade is in good shape and no signs of movement can be observed from visual observation. The remedial measures have, therefore, proven very successful.

The lesson learned from the project is that sidehill construction in slide prone terrain needs to be given very special attention during investigation and construction. This type of attention was given to the alignment on the west side of the Peace River where similar terrain conditions also existed. Drainage prior to fill placement was implemented through trench drains and granular blankets. That this was not done on the east side can be considered a shortcoming of both the geotechnical investigation and construction

execution of a modern highway grading project. The result of these failures incurred extra cost to the contract. Such failures are, however, considered, in local experience, to be somewhat unavoidable if one reviews historic evidence of roadway construction in virgin ground in the Peace River Area. Nonetheless, these failures have reinforced the need to pay very careful attention to sidehill fill construction both from a geotechnical and construction perspective.

Acknowledgements

The authors wish to express their appreciation to M. Pariti, Senior Geotechnical Engineer for reviewing the paper during draft stage, T. McDaniel for her assistance in typing this manuscript and to Les Appleby for drafting the figures. This paper expresses the opinions of the authors and does not necessarily reflect the view of Alberta Transportation and Utilities.

Nipigon River Landslide

H.S. Radhakrishna, M. Bechai, K.C. Lau
Ontario Hydro
Toronto, Ontario

K.T. Law
Carleton University
Ottawa, Ontario

I. Hale
Bird and Hale Ltd.
Toronto, Ontario

INTRODUCTION

On April 23, 1990, a landslide (Fig. 1) occurred on the east bank of the Nipigon River about 8 km south of Alexander Generating Station and 8 km north of the town of Nipigon, Ontario. The failure extended about 350 m inshore from the riverbank and had a maximum width of 285 m. A gas pipeline near the headwall was displaced by about 8 m towards the river, and left suspended for a distance of about 75 m. The pipeline did not rupture but required major repairs and restoration. A Bell Canada fibre optic cable which ran adjacent to the gas pipeline ruptured, giving the first alert to the event.

The displaced mass moved into the river, flowed both upstream and downstream (Fig. 1) and created a temporary blockage which caused tail water level just downstream of Alexander GS to rise by almost 2 m. Heavy silting of the river downstream of the slide area affected the water intake for the town of Nipigon. The water intake was relocated at a substantial cost. There were also concerns of the effects of siltation on fish spawning beds.

Following the slide, Ontario Hydro had to reduce its discharge to 113 cms until a preliminary assessment of the slide and relocation of the intake for the town's water supply were completed. This amounted to a loss of revenue of about \$300,000 because of the inefficient operation of the stations. The debris including clumps of trees that floated into Lake Helen had to be removed. The silt load in the water after the slide was a potential cause of difficulties with the boiler feedwater of a paper mill several km downstream in the town of Red Rock. By the spring of 1991 most of the failed material that was mobile, was removed by river flow and things had returned to normal.

There was no loss of life or private property but there were some substantial economic and environmental impacts as a result of this slide. Bank erosion and slides have occurred all along this stretch of the river, but this large slide was the first one in the area that received significant attention, and studies were performed to understand its mechanism and the factors which caused it.

Soon after the landslide the area was visited by the representatives of the Ministry of Natural Resources MNR, Ontario Hydro and Trans Canada Pipelines. In May 1990, a soil investigation commissioned by the Ministry of Natural Resources and Trans Canada Pipelines was performed by Trow Ontario Limited.

Subsequently, Ontario Hydro acquired aerial photography with full stereo coverage of the whole area in the spring and fall of 1990 and spring of 1991 and carried out a study of the event.

This paper presents a description of the landslide and examines the possible contributory factors, both natural and man-made. Results of the simplified stability analysis are presented to explain the initiation of bank failure and a mechanism by which it becomes retrogressive, and resulted in a large landslide is postulated. Particular attention is focused on factors such as groundwater regime and the river level fluctuation which may have affected the stability of the bank slopes.

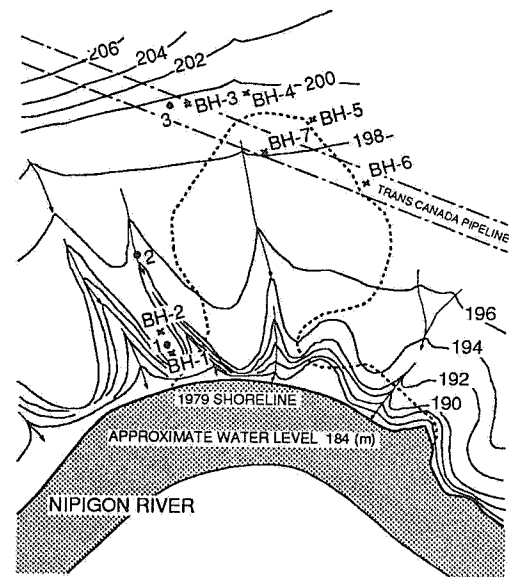


Figure 1

Aerial View Showing the 1990 Landslide Area

General Geology

The Nipigon River Valley is probably formed on a fault and fracture zone which was deepened by the continental ice sheet. Historically, the area was inundated by post glacial Lakes Minong and Houghton, the predecessors of present day Lake Superior, resulting in a thick layer of lacustrine sediment consisting largely of varved silt, fine sand and some clay was deposited. This lacustrine plain exhibits poor site drainage and some discontinuous organic soil cover. Crustal rebound resulted in the retreat of the Lake Superior shoreline to its present location. At that time, two areas around Lake Nipigon (presently Black Sturgeon River Valley and the Orient Bay Valley) apparently served as spillways for water from glacial Lake Agassiz to the west, through Lake Kelvin into (now Lake Nipigon), Lake Minong (now Lake Superior) to the east. Lake Kelvin sat at a much higher elevation and was more extensive than Lake Nipigon is now. The two outlets were subsequently blocked by glacial debris resulting in the opening, in the latter stages of the spillway, of the present day Nipigon River Outlet. It was probably during the latter stages of the ponding and the early stages of the spillway that the surface covering of fine sands in the study area was deposited.



Legend

- Limits of Land Slide
- Contours of ground elevation as seen in 1979 Airphotos
- * Boreholes by Trow, Ontario Ltd. (May 1990)
- Boreholes by Ontario Hydro (July 1991)

Figure 2

Physiography of Failed Area Based on Airphotos of 1979

The present status of the Nipigon River channel is largely a result of erosional processes that have been active after the outlets from Lake Agassiz were blocked. Other than immediately downstream from the Alexander Generating Station, there is no evidence of old river meanders and abandoned channels or oxbows. The Nipigon River is apparently in the early stages of floodplain development (1). The lacustrine sediments which are found in the region of the study area are susceptible to slope failures and erosion. It is believed that the majority of the stream bank erosion and retrogression that were identified during this study are related to the lacustrine sediments, rather than any other geological terrain unit. A steep ridge of granitic and magmatic rock east of the Nipigon River exhibits shallow soil coverings or rock outcrop. Isolated rock outcrops of this type also are found on the west side of the river, particularly in the north half of the Nipigon River area. There is no surface expression of pleistocene tills or glacial-fluvial deposits in the immediate vicinity of the river. Some coarse

grained soil deposits are found at higher elevations on rock outcrops to the east and the west of the river valley.

River Hydrology

Lake Nipigon is the largest enclosed lake in Ontario. It drains via the Nipigon River and Lake Helen to Lake Superior. The hydroelectric development downstream of Lake Nipigon consists of (from north to south); Pine Portage GS (built between 1950 to 1954), Cameron Falls GS (built between 1920 to 1926 with extensions built in 1945 and 1958), and Alexander GS built in 1931 with extensions in 1945 and 1958). The reach under investigation, from Alexander GS to Lake Helen is 12 km long.

Pine Portage GS controls the overflow from Lake Nipigon with a maximum flow of 560 cms imposed to protect a CPR bridge upstream of Lake Superior. A minimum flow of 113 cms is maintained to provide adequate levels for the water intake to the Town of Nipigon. The normal operating pattern is to draw the Nipigon lake down during the fall and winter months to allow for it to fill up during freshet. The optimum discharge for the generating stations on the Nipigon River is 350 cms.

The Nipigon River channel is generally of uniform width for most part of its length. As the river empties into Lake Helen there are several bends and a deltaic fanning. The 1990 landslide was located on an outside bend of the river about 4 km upstream of Lake Helen. There the river levels at the failure site can fluctuate about 2.0 m which corresponds to the difference between the high and low discharge rates of 540 and 113 cms.

Airphoto Analysis

In 1990-91 an airphoto interpretation investigation of the Nipigon River area between Alexander GS and Lake Helen and the shores of Lake Helen between the mouth of the river and the general vicinity of the Town of Nipigon was undertaken (2) for the purpose of: i) defining the general physical terrain characteristics, ii) identifying the major land use changes as they relate to watershed area for each retrogressive failure identified, iii) identifying

and mapping bank failure features on a number of different sets of aerial photographs, iv) analyzing the frequency and distribution of bank failures, associated soil types, bank heights and slopes, v) indicating areas which displayed potential for retrogressive slump failures, and vi) estimating the shape of the ground surface of the 1990 failure area, as it might have been prior to the failure. All available photography was analyzed. Base maps were prepared from a laydown, uncontrolled mosaic using the 1:12000 May 1990 airphoto coverage. Interpreted data were transferred from different years of airphoto coverage to the base maps using local terrain features as reference (3).

The physical terrain characteristics observed by Airphoto Interpretation were consistent with the geological history of the area. The topography ranges from near flat, in the areas of organic and lacustrine deposits to near vertical in some bedrock areas. Steep slopes tend to develop on the banks of tributary streams near their confluence with Nipigon River and on the outside bank of the Nipigon River bends. New steep terrace-like features appeared in some airphotos indicating the eroded surface of the slump scarps.

A number of past bank slope failures and landslides of retrogressive nature were identified and mapped. Table 1 contains a summary of some of the characteristics of the retrogressive failures, including their size, location, watershed characteristics and the photo coverage on which they were first, and subsequently observed. Single event slump failures were identified on approximately 79% of the total shoreline in the study area. The most persistent and rapid erosion was seen on the outside downstream bends in the river. A total of 31 sites of retrogressive failures were tentatively identified (see Table 1), fourteen of which dated between 1931 and 1991. The remainder occurred prior to 1931, and based on the maturity of forest cover, and elevation difference between the suspected failure bases and the existing river, many of them occurred prior to this century. Of these 14, 12 occurred prior to the period from 1979 to the present. With one exception, these failures concentrated on both sides of the lower reaches of the river, invariably on steeply sloping, previously eroding sites, where the river had access to the toe of the slope at least for part of the time, and on the outside, downstream

TABLE 1
Possible and probable retrogressive failures on the Nipigon River

Feature	Location (km)	Date of Photo	Age of Failure	Visible on Photo								Width at Shore (m)*	Inshore Extent (m)*	Bank Height **	Volume (m ³)++	Physiography at head
				1931	1947	1952	1962	1975	1979	1990	1991					
1	8.3 E	1931	old ^x	✓	✓	✓	✓	+	✓	✓	✓	150	120	(8)	82,000	OL
2	8.7 W	1931	old	✓								60	90	(8)	25,000	LP
3	9.0 W	1931	old	✓	✓		✓	✓	✓	✓	✓	160	400	(8)	430,000	OL/LP
4	9.5 E	1931	old	✓	✓					✓	✓	160	350	(6)	280,000	OL
5	9.7 E	1931	old	✓					+	✓	✓	80	100	(6)	29,000	OL
6	9.9 E	1931	recent	✓	✓	✓	✓	✓	+	✓	✓	80	50	8	28,000	OL
7	10.9AE	1931	old							✓	✓	120	60	(2)	8,800	OL
11 (47)	8.5 E	1947	old	✓	✓		✓	✓		✓	✓	200	200	4	97,000	OL
8	1.4 W	1952	old			✓	✓	✓	✓	✓	✓	120	100	16	100,000	LPI
9	7.4 E	1952	old			✓						50	20	(5)	3,000	LP
10	8.1 E	1962	old				✓	✓	✓	N/A		125	70	(8)	34,000	OL
SITE II – was originally seen on 1962 coverage; recently acquired 1947 coverage shows the same feature																
12	8.3 E	1975	recent					✓	✓	N/A		110	60	6	87,000	OL
13	1.4 E	1979	recent						✓	✓	✓	130	30	8	12,000	LP
14	8.9 W	1979	recent						✓	✓	✓	70	60	7	17,000	LP
15	9.6 E	1979	recent						✓	✓	✓	80	50	7	19,000	OL
16	9.9 E	1979	recent						✓	✓	✓	80	50	8	32,000	OL
17	10.0 E	1979	recent						✓	✓	✓	100	30	5	14,000	OL
18	0.8 E	1990	old							✓	✓	450	200	6	270,000	LP/LPI
19	3.3 E	1990	old							✓	✓	350	50	6	56,000	LPI/RO
20	7.3 E	1990	old							✓	✓	130	300	5	280,000	OL/RO
21	7.9 E	1990	recent							✓		385	430	10	910,000	OL/HT
22	8.4 W	1990	recent							✓	✓	70	50	4	15,000	LP
23	9.6 E	1990	recent							✓	✓	70	50	5	8,600	LP
24	10.3 E	1990	recent							✓	✓	200	60	4	16,000	OL/LP
25	7.1 E	1990	recent							✓	✓	60	60	10	27,000	LP
26	8.5 E	1991	old							✓		115	100	5	28,000	LP
27	8.7 E	1991	old							✓		110	110	5	47,000	LP
28	8.9 E	1991	old							✓		120	120	5	30,000	LP
29	9.7 E	1991	old							✓		140	120	6	78,000	LP
30	8.9 W	1991	recent							✓		180	7	7	2,000	LP
31	7.8 W	1991	recent							✓		240	6	6	4,500	LP

* Measurements made on originally interpreted airphotos
 ** By parallax bar except where bracketed
 () Estimated values
 + Site of reoccurring failure
 x Old means prior to the date of photo
 ++ UNESCO 1990

Physiography:
 RO Bedrock outcrop
 LP Lacustrine plain
 LPI Lacustrine plain (incised)
 OL Organic soil cover

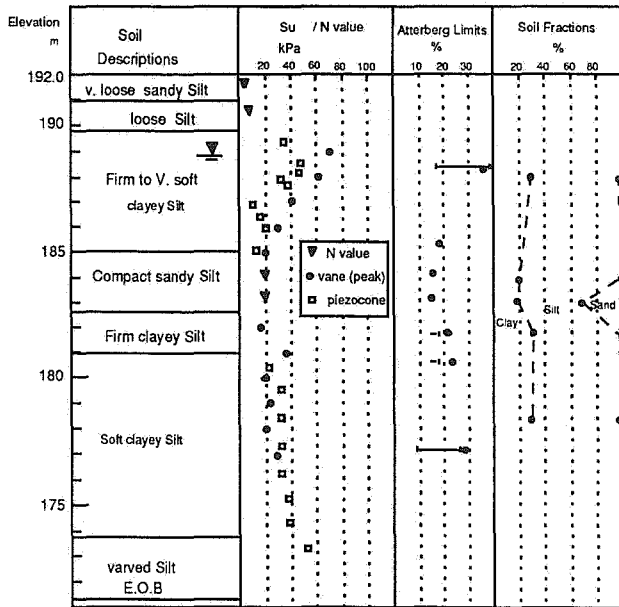


Figure 3a
Borehole 1 Profile

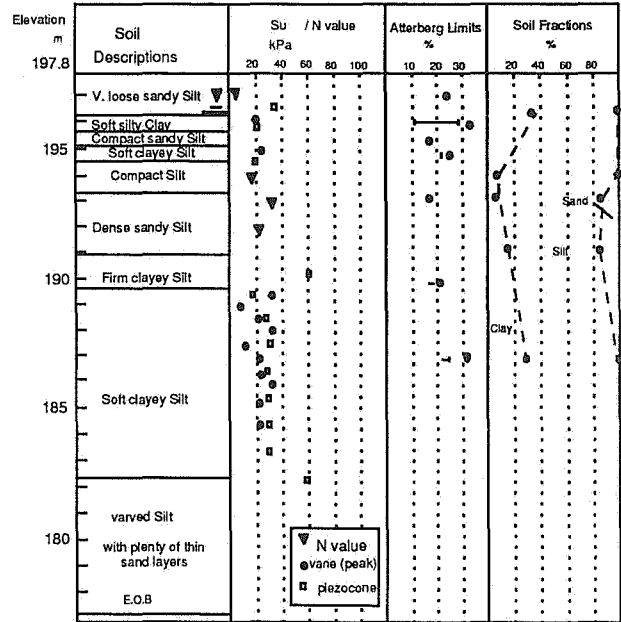


Figure 3b
Borehole 2 Profile

segment of a bend in the river.

Soil Profile Description

A geotechnical investigation of the possible cause of the failure was carried out one month after the landslide, by Trow, Ontario Limited on behalf of TCPL and MNR (3). A total of 7 boreholes were established to the north and east of the failed area. Two 20 m deep boreholes were erected close to the edge of the river bank and the 5 remaining boreholes (10 to 16 m deep) were located around the Trans Canada pipeline at the east limit of the landslide (Fig. 2). Open standpipes were installed in Borehole 2, 4 and 5. Slope indicator casing was installed in Boreholes 1 and 6. The boreholes were put down by washboring and disturbed samples were recovered by means of a split spoon sampler. Vane shear tests and dynamic penetration tests were performed where possible. Because of the very soft and silty nature of the deposit, the sample recovery was very poor. Effective strength parameters had to be assumed for their slope stability analysis. They hypothesized that this massive landslide was initiated by a bank slope failure and because of the very soft nature of the soils and high groundwater conditions present, it

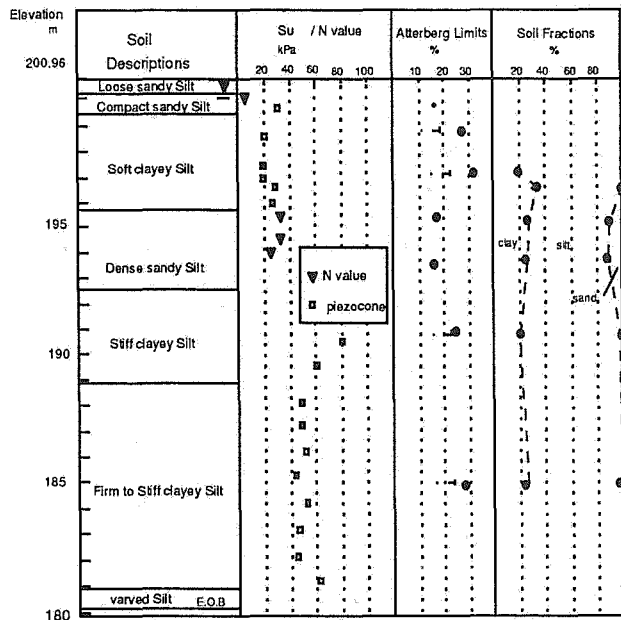


Figure 3c
Borehole 3 Profile

retrogressed eastward until firmer soil conditions were encountered at the Trans Canada Pipelines right-of-way.

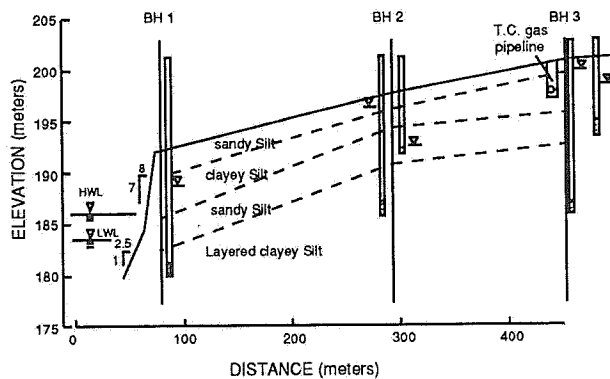


Figure 4
Soil Stratigraphy and Bank Slopes of
the 1990 Landslide

In July 1991, 3 boreholes were put down by Ontario Hydro to delineate the soil stratigraphy in the area and to obtain good quality soil samples for effective strength parameter determination of the soft and sensitive stratas. Undisturbed samples were recovered by means of a piston sampler. The fine detailing of the soil stratigraphy and undrained strength profiling was achieved by means of an electric piezocone and the Geonor shear vane. Borehole 1 was positioned 8 m east of the bank edge and close to Trow's Borehole No 1 (Fig. 2). Borehole 2 was located about 165 m east of Borehole 1 and Borehole 3 was positioned just east of the landslide limit and Trans Canada Pipelines right-of-way. Open type Geonor piezometers were installed at depths of 6 m, 9 m and 12 m at each of the 3 boreholes. A standpipe piezometer was installed at 3 m depth to monitor the perched water table in the surficial sand layer. The piezocone profiling was interrupted when stiff silt or dense sand layers were encountered, which were augered through to continue piezocone profiling. Pore pressure dissipation tests were performed in clayey layers with the piezocone to determine the coefficient of consolidation. The soil stratigraphy and geotechnical parameters of the layers penetrated by each borehole are summarized in Figs. 3a to 3c. The results of the soil analysis indicated that the soil layers involved in the landslide are predominantly soft to very soft clayey silt of medium to low plasticity. The vane shear values were often higher than the piezocone and laboratory triaxial values because of the high silt content.

Based on the results of the 2 soil investigations, a detailed soil stratigraphy and strength profiles for the deposit involved in the landslide were established. The soil profiles, though variable were consistent over the investigated area. The most probable stratigraphy of the landslide area is shown in Fig. 4 as the east-west cross section through Boreholes 1 to 3. The bank geometry was estimated from the analysis of airphotos coverage prior to landslide by Bird & Hale, 1990 (2) and verified by land survey data. The submerged slopes of the river channel in the vicinity of the failed area were measured in the range of 2.5(h):1(v) to 2(h):1(v), and the channel depth was 6 to 8 meters.

The soil deposit in the failed area is of lacustrine origin and can be divided into 4 distinct soil strata as shown in Fig. 4:

Unit 1: A 1 to 2 m thick surficial layer of loose sandy silt having standard penetration values of 2 to 8.

Unit 2: A soft to firm low plastic clayey silt interbedded with thin sand layers. This unit is 2 to 5 m thick with an undrained shear strength of 20 to 40 kPa. The vane shear values in this unit are considerably higher than the piezocone and laboratory triaxial strength values. The sensitivity values ranged from 2 to 4. The effective strength parameters of this unit as determined by the consolidated undrained triaxial compression tests on piston samples are $c' = 12.8$ kPa and $\phi' = 30^\circ$. This unit gently slopes towards the river.

Unit 3: A 3 to 5 m thick compact to dense sandy silt layer underlying the soft clay layers. The standard penetration values in this layer are 18 to 35. This layer is continuous from east to west and probably served as an aquifer or subsurface drainage for the area. This layer of sandy silt also dips gently towards the river from the west.

Unit 4: A thick deposit of laminated soft clayey silt and silty clay. This unit is rich in silt and is non-plastic in behaviour. Its undrained strength values range from 20 to 40 kPa. The liquidity index of this unit is greater than 1.0 with a strong susceptibility for liquefaction upon disturbance. The remoulded strength of this layer ranges from 1.3 to 2.6 kPa showing a high sensitivity of 10 to 15. The river channel is cut into this layer with often steep

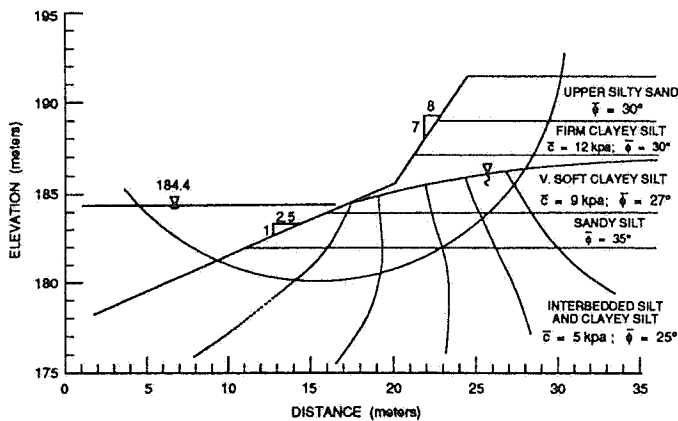


Figure 5

Slope Stability Analysis - Base Case 1

submerged slopes. The effective strength parameters of this unit near its top surface are $c' = 5$ kPa and $\phi' = 25^\circ$. This layer displays a normally consolidated behaviour with its undrained shear strength increasing with depth. This deposit stiffens up with increasing sand content below elevation 174.0 m near the river and below elevation 185.0 m near the failure scarp.

In general the overburden is of lacustrine origin and is predominantly silt based with low plasticity and liquidity often exceeding 1.0. This renders the deposit susceptible for liquefaction by disturbance or by high groundwater conditions.

Groundwater Condition

No data is available on the groundwater regime present in the area prior to landslide. The groundwater levels recorded in the boreholes in the unfailed area after the failure are likely to be effected by the failure scarp, and different sets of weather conditions. The piezometric levels recorded by Trow Ontario Limited on May 1990 are shown in Fig. 3. Even though these measurements were done one month after the failure, they indicate high groundwater conditions. The actual piezometric levels at the time of failure could have been much higher.

Most of the watershed for the 1990 failure site is relatively flat. Well defined stream channels were confined to the lower reaches. About 40 per cent of the watershed was clear cut of trees. In addition, the pipeline trench may have acted as a conduit for the infiltration drainage of the area north

of the failure site resulting in an increase of the watershed area by as much as 50 per cent. These characteristics combined with organic soils which tend to absorb water, indicate a watershed with relatively high infiltration rates.

Prior to the landslide during April 1990, the climatic conditions in the area were such that there was a sudden spring melt in the recharge area which was partly tree cleared, while there was still some frost on the banks and failure area which were tree covered. The sudden snow melt in the recharge area raised the piezometric heads in the sandy silt layer underlying the soft and sensitive clayey silt layers. This effect was particularly significant in view of the clearing of a large portion of the watershed. The sandy silt layer itself being a low pervious aquifer did not drain rapidly enough and probably caused boils in the failure area.

The total pressure heads recorded by piezometers during the investigation indicated a groundwater flow from the clayey silt layers (above and below the sandy silt layer) to the sandy silt layer. This confirmed that the sandy silt layer was acting as a subsurface drain for the area.

The groundwater regime and the pore water pressures in the slope prior to the 1990 failure were estimated by constructing the seepage flow net based on the piezometric levels recorded one month after the event and the river level at an elevation of 184.4 m corresponding to a discharge rate of 250 cms at Alexander GS (Fig. 5). This was the average flow recorded the week prior to failure.

The Postulated Failure Mechanism

From the kinematic considerations and the aerial dimensions of the failure geometry, it is postulated that the 1990 failure occurred in two stages: 1) the initial slide of the bank slope and 2) the subsequent retrogressive failure of the land behind the bank slope. Factors that may have contributed to the initial slide at the 1990 failure site are: the steep geometry, the soft conditions, the high groundwater conditions, and the changing river levels.

Slope geometry - The failure was located on the outside bank of the river where erosion of the bank and toe was active. Also the fluctuation of the river level causes cyclic wetting and drying of the soil

which could induce slumping of the silty banks. These processes can transform the slope profile to a more critical configuration and thus lead to the initial failure of the slope.

Soil conditions - different types of failure mechanisms dominate in different soil types. For example in Eastern Canada, retrogressive type of slope failures are often reported to occur in sensitive clay deposits (4). At the Nipigon site the presence of the soft and low plastic clayey silt layers combined with the high groundwater pressure within the lower sandy silt layer may have led to a retrogressive type failure.

Groundwater condition - the stability of the slope is a direct function of the pore water pressure within the slope. Any increase in pore water pressure due to the changes in hydraulic boundary conditions decreases the stability of the slope. Above the phreatic line, the soils exhibit suction. This suction caused by the capillary action induces negative pore water pressure in the soil and thereby increases the effective shear strength. The change of soil moisture from partially saturated to saturated condition destroys the capillary or matric suction in the soil and reduces the stability of the slope (5).

River level - The change in river level can have dual effects on the stability of the slope: (i) The rise in river level acts as a loading on the toe to improve the stability of the slope. With the lowering of the river level, the hydraulic load on the toe is reduced and the stability of the slope decreases. (ii) The rapid lowering of the river level can create a sudden drawdown condition during which the phreatic surface may not have time to adjust to the new river level, thereby reducing the stability of the slope. However, while the river level fluctuations and drawdowns are present over the full length of the river, only the soil conditions, bank slope and groundwater conditions vary. In the case of rising river levels, the rate of change is not important.

Slope Stability Analysis

The slope geometry, soil conditions, groundwater conditions, and river level prior to the 1990 failure inferred by the available sources of information are presented in Fig. 5. With the uncertainty involved in some of these parameters, a parametric slope stability analysis was carried out to determine their

TABLE 2
Results of parametric analysis
of the slope stability

Case	Parameters Changed from Base Case	Factor of Safety	% Change in F.S. w.r.t Base Case
1 (Base Case)	---	0.989	---
2	Soil Suction Above Phreatic Line Is Ignored	0.915	- 9.2
3	River Level Increased from 184.4 m to 185.7 m	1.003	+ 1.4
4	River Level Decreased from 184.4 m to 183.8 m	0.909	- 8.1
5	Rapid Drawdown of River Level from 184.4 m to 183.8 m	0.898	- 9.3
6	Avg. Bank Slope Above River Level (183.8 m) Changed from 1(v) : 1.15(h) to 1(v) : 1.5	1.085	+ 9.7
7	Avg. Bank Slope Below River Level (183.8 m) Changed from 1(v) : 2.5(h) to 1(v) : 2(h)	0.935	- 5.4
8	Phreatic Surface Rised from 186.9 m to 190.7 m	0.845	- 14.6

impact on the initial bank failure and to rank them. The parameters used for the Base case (Case 1) in this parametric analysis are shown in Fig. 5.

The commercial computer program PC-SLOPE by GEO-SLOPE Programming Ltd. was used for this study (6). (The option of Bishop's simplified method for slope stability analysis was used.) The effect of soil suction or negative pore water pressure was taken into account by invoking the soil suction option in the program. In this program the soil above the phreatic line is assumed to have full suction. In coarse grained soils, this assumption may overestimate the suction effect.

Based on the site conditions, the possible ranges of variation for each parameter were selected (Table 2). In each analysis, only one of the parameters in the base case was changed. The effects of soil suction above the phreatic surface on the stability of the slope were examined in Case 2. The effects of river fluctuation were considered in Cases 3 and

4. In Case 3, the maximum river level, 185.7 m, was used. In Case 4, a river level of 183.8 m corresponding to a discharge rate of 125 cms at Alexander GS was used. For these two cases, the groundwater flow pattern of the base case (Fig. 5) was modified to take into account the changes in the hydraulic boundary condition at the toe of the bank. In Case 5, the effect of rapid river drawdown from elevation 184.4 m to 183.8 m on the stability of the bank was studied. This drawdown condition is similar to the drawdown event that occurred 5 days prior to the 1990 failure. The rapid drawdown of the river created a seepage surface at the face of the bank between elevations 184.4 and 183.8 m. With time, the phreatic surface adjacent to the toe of the bank would drop to its equilibrium position intercepting the bank slope face at elevation 183.3 m. At that time, the groundwater pressure pattern is identical to the groundwater pressure pattern of Case 4.

In Cases 6 and 7, the effects of changing the slope geometry by erosion on the bank stability is examined. In Case 6, the bank slope above the river level is flattened from 1.15(h):1(v) to 1.5(h):1(v) slope. Such flattening of the bank may be caused by the surface erosion of the bank. The scouring effect of the river could steepen the submerged slope of the bank beneath the river level. In Case 7, the effect of steepening of the bank slope beneath the river from 2.5(h):1(v) to 2(h):1(v) on the stability of the bank is examined.

The phreatic surface used in the Base case was based on the field data obtained one month after the occurrence of the 1990 failure. After the failure, some of the excess pore pressures might have been dissipated. Therefore, in Case 8, a higher phreatic surface was used to assess its effect on the bank slope stability. The phreatic surface was assumed to be located at 190.7 m just beneath the weathered zone of the soil as identified by the borehole logs.

From the above analysis it is apparent that the rising of phreatic surface behind the slope to 190.7 m and the loss of suction in the zone between high and low phreatic surfaces accounts for a reduction in the slope stability by about 25%. Steepening of submerged slope by scouring and the river level dropping will decrease the factor of safety of the bank slope by about 5 to 8 per cent respectively from the base case. The effect of the rate of

drawdown of the river level on the stability of the bank slope is very minor. The difference in factor of safety is only 1.2% between Cases 4 and 5.

The Proposed Mechanism of the Initial Failure

The slope stability analysis indicates that prior to the failure the river bank profile was in a relatively critical configuration. Even though the river drawdown event had an effect on the slope stability of the bank, it alone could not have caused the 1990 initial failure, because the slopes in this area had experienced drawdown events of similar magnitude several times without any major slope instability. In addition, the failure occurred 5 days after the drawdown event. Therefore, additional factors must have existed for the failure to occur.

The warm weather began 5 days prior to the failure providing a ground thawing condition at the site. The snow melt water could have destroyed the soil suction in the upper sandy silt layer, particularly where the vegetation cover is absent or reduced and increased the pore water pressure in the lower sandy silt and the clayey silt layers through a recharge boundary in the high-terrace area as indicated by the airphoto study. It is believed that the combined effect of a soil suction destruction in the upper sandy silt layer and an increased pore water pressure in the lower sandy silt and the clayey silt layers provided the additional necessary condition for the occurrence of the failure.

Subsequent Retrogressive Failure

It is postulated that the 1990 failure was initiated by a slope failure at the river bank which retrogressed inland leading to a large scale landslide. A number of retrogressive type of failures have been recorded in very sensitive clays of Eastern Canada (7) and Norway (8). The mechanism of these failures have been analyzed by Tavenas et al 1983 (9). Based on their analysis of several landslides in sensitive clays in Eastern Canada, they proposed 4 criteria to assess the risk and extent of retrogressive slide.

- 1) There must be an initial slope failure,
- 2) there must be a continued backscarp instability ($\text{Stability factor} = \gamma H/c_{uv} > 4$),
- 3) the slide debris must have the ability to

flow when remoulded (remoulded shear strength < 1 kPa or liquidity index > 1.2), and

- 4) the slide debris must have the ability to become remoulded during the slide.

The results of a slope stability parametric analysis of the river bank at the 1990 slide area indicates that conditions were present for the occurrence of the initial slide, i.e. criterion 1 is satisfied. From the profile of the slide area, the height of the retrogressive zone is estimated to be 8 m for which $\gamma H/c_{iv} = 19.0 \times 8 / 30 = 5.0 > 4$ and thus criterion 2 is satisfied. The remoulded vane shear strength of the clayey silt is 1.3 kPa to 6.0 kPa which is close to 1 kPa specified in criterion 3. Also the liquidity index of the clayey silt is in the range of 1.2 specified in criterion 3. This means the failure debris could flow when remoulded.

For this site it is postulated that with the initial slope failure, the drainage path for the lower sandy silt layer at the bank face was blocked by the failed debris, causing a build up of a high hydraulic head. The maximum hydraulic head that could develop in this sandy silt layer is equal to the elevation of the recharge boundary. This high hydraulic pressure propagated into the soft clayey silt layers and reduced its effective stress. The reduction in effective stress in turn reduced the operative shear strength of the clayey silt. In addition, the height of the overburden above the lower sandy silt decreases in the area where the retrogressive failure is occurring. Thus the total stress acting on the lower sandy silt layer is reduced. Such a reduction in total stress, and the high pore water pressure may have been sufficient to create a liquefaction condition in the lower sandy silt, and thereby cause the failure debris to flow to the river and facilitate further retrogression to occur. This hypothesis can also explain why the majority of retrogressive failures identified by airphoto study were located in soft lacustrine deposits having high groundwater conditions with poor surface drainage patterns.

Conclusions

An airphoto study showed that the Nipigon River had a history of bank instability and retrogressive failures predating the construction of Alexander GS.

A total of 31 sites of past retrogressive failure were identified of which 14 occurred between 1931 and 1991.

These sites were concentrated in the lower reaches of the river 7.3 to 10.4 km downstream of Alexander GS. Most of the retrogressive failures took place in the outside banks at the river bends. The 1990 failure site had most of the characteristics that were present at other retrogressive failure sites.

Based on the results of the parametric analysis of the initial bank failure, the following factors are ranked to be the most critical ones in the following order: i) High groundwater pressure regime existed in the site prior to failure, ii) loss of soil suction in the bank slope above the phreatic surface due to surface infiltration from a rapid ground thaw, iii) weak shear strength of the clayey silt deposit, iv) steepening of submerged slope by erosion, and v) lower river levels.

The high groundwater conditions and the loss of suction were both related to the rapid thawing of the ground and high infiltration of snow melt water in the partly clear-cut watershed area. The scour and drawdown conditions also existed at this failure site.

The retrogressive failure was a result of the combined action of high pore pressures in the sandy silt layer and susceptibility for liquefaction of silt predominated soft lacustrine deposits in the area.

References

1. Bell, Dr. Robert 1899. "The Geological History of Lake Superior". Transactions of the Canadian Institute, Vol VI, 1889.
2. Bird and Hale Limited 1990. "Aerial Photography Interpretation - Nipigon River Landslide Study". File No. 90-173.
3. Trow Ontario Limited 1990. "Soils Investigation and Analysis - Nipigon River Landslide". Job Reference No. F-90141-A/G.

4. Eden, W.J., R.J. Mitchell, 1970. "The Mechanics of Landslide in Leda Clay". Canadian Geotechnical Journal, Vol. 7(3), pp. 285-296.
5. D.G. Fredlund, 1984. "Analytical Methods for Slope Stability Analysis". Fourth International Symposium on Landslides, Toronto, Vol 1, pp. 229-250.
6. GEO-SLOPE Programming Limited 1985. "PC-SLOPE User's Manual - Slope Stability Analysis:.
7. Lefebvre, G 1981. "Fourth Canadian Geotechnical Colloquium" Strength and Slope Stability in Canadian Soft Clay Deposits". Canadian Geotechnical Journal, Vol. 183), pp. 420-442.
8. Bjerrum, L., T. Loken, S. Heiberg, R. Foster 1969. "A Field Study of Factors Responsible for Quick Clay Slides". Proc. 7th ICSMFE, Mexico, Vol. 11, pp.531-540.
9. Tavenas, F., P. Flon, S. Leroueil, J. Lebulc 1983. "Remoulding Energy and Risk of Slide Retrogression in Sensitive Clays". Proc. Symp. on Slopes on Soft Clays, Linkoping, SGI Report No. 17, pp. 423-454.
10. UNESCO, 1990. "A Suggested Method for Reporting a Landslide". Bull. (41), International Association of Geology.

Locat, J.

**Viscosity, yield strength, and mudflow mobility for
sensitive clays and other fine sediments**

Paper to be found on page 389

Runout Prediction for Flow-Slides and Avalanches: Analytical Methods

Oldrich Hungr
Thurber Engineering Ltd.
Vancouver, British Columbia

ABSTRACT

Dynamic analysis of rapid slide motion is a tool for predicting the runout behaviour of potential catastrophic landslides or avalanches. Important and expensive decisions are sometimes based on the results of such analyses.

This paper discusses problems inherent in current analytical models of flow-sliding and suggests means of their improvement.

Uses of Runout Analysis

Runout analysis is necessary in every case where engineering or policy decisions must be made with the assumption that a rapidly moving flow-slide or avalanche can occur. A few examples follow.

B.C. Hydro (1981) carried out runout analyses of all potential landslide areas surrounding the proposed Site "C" reservoir in north-eastern British Columbia. The velocities and runout distances derived from the analyses were used for detailed modelling of slide wave generation and possible effects on the dam. Major design provisions are sometimes based on such analyses.

Estimates of areas subject to potential runout of debris flow surges are now routinely required in hazard studies carried out under the B.C. Municipal Act, or in connection with subdivision applications. Typically, on debris flow susceptible alluvial fans in coastal British Columbia, 10 to 80% of the fan surface can belong to the "direct impact" hazard zone, the extent of which depends on runout (Thurber Consultants Ltd., 1983). Since alluvial fans also represent a large proportion of suitable develop-

ment land in coastal B.C., the importance of runout estimates is obvious.

Very large hazard zones result where there is perceived potential for rock avalanches. For example, development prohibitions in the runout area of a possible future rock avalanche at Rubble Creek near Squamish, B.C., encompass 800 ha. Runout analysis has also been used to define hazard zones in the vicinity of Mount Garibaldi in the same region (Thurber Engineering and Golder Associates, 1992). Considering a typical deposition area of a rock avalanche to be of the order of 500 hectares and assigning a value of, say, \$100,000 per ha to rural development land, every two percent change in runout distance estimate costs one million dollars!

Flow-slide runout estimates are increasingly being requested as part of risk analyses for tailings dams and mine waste dumps, both existing and proposed (e.g. - Golder Associates, 1987, Thurber Consultants, 1986). Here, the analysis results can influence siting decisions, with significant economic consequences.

In some cases, runout analyses are used directly to provide input parameters for engineering design of remedial measures. For example, approximately 20 km of state

highway at La Clapière, in the French Maritime Alps were re-routed upslope according to a runout analysis of a potential 50 million m^3 rockslide carried out by the French Ministry of Public Works (Rochet, 1987). The same analysis was used to determine the required length of a diversion tunnel to prevent landslide damming of the river Tinée. At another rockslide site in the French Alps, dynamic analysis was used to dimension a large retention dyke (Antoine - et al., 1987).

Methods of Runout Analysis

Despite the fact that there is frequent need for practical runout estimates, runout analysis is far from being a routine procedure in geomechanics. A survey of the examples mentioned above and much of the other literature on the subject shows that analyses are most often based on "proprietary" techniques which are rarely ported from one worker or agency to another. A great variety of methods are found in the geological literature, most of which apparently receive no practical utilization.

A number of empirical methods exist, but these will not be discussed here. They are very important for practical uses, but their reliability is limited due to the wide range of geometrical configurations of flow-slide paths.

Analytical models can be roughly divided in terms of mathematical framework into lumped-mass ("sliding block") models and fluid-mechanics models.

Sliding Block Models

Sliding block models originated in snow avalanche research and are routinely used in snow avalanche engineering (Perala et al., 1980). The moving flow-slide is considered as a point of mass driven by gravity and resisted by frictional forces dependent on mass, material properties and velocity. Sliding block models have been applied to flow-slides by Koerner (1976), McLellan (1983), Hutchinson (1986) and others.

The problematics of this approach are illustrated by considering the prehistoric Avalanche Lake rockslide in the Mackenzie Mountains described by Eisbacher (1979) and shown in Figure 1. The west branch of the rock avalanche, along cross-section A-A, exhibits the highest runup against adverse slope of any known rockslide, equal to approximately 600 m vertical (Evans, 1989). The east branch of the debris spread out along the base of a valley and travelled for about 4 km away from the source slope on relatively gentle slopes (cross-section B-B).

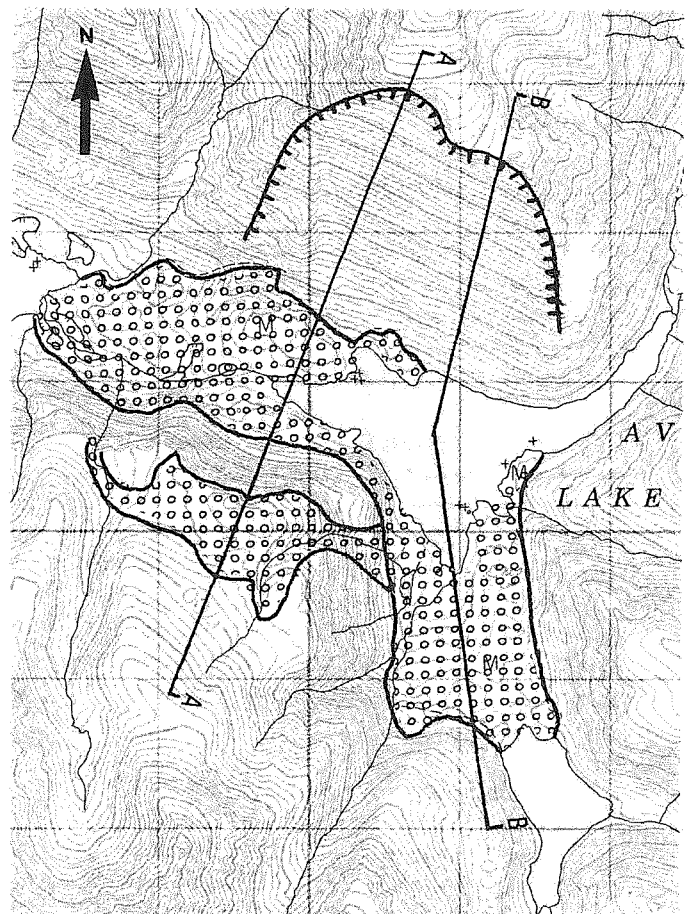


Figure 1. Plan of Avalanche Lake slide deposits at 1:50,000 scale (see Eisbacher, 1979). The scarp symbol outlines the source area. Slide volume is of the order of 500 M m^2 .

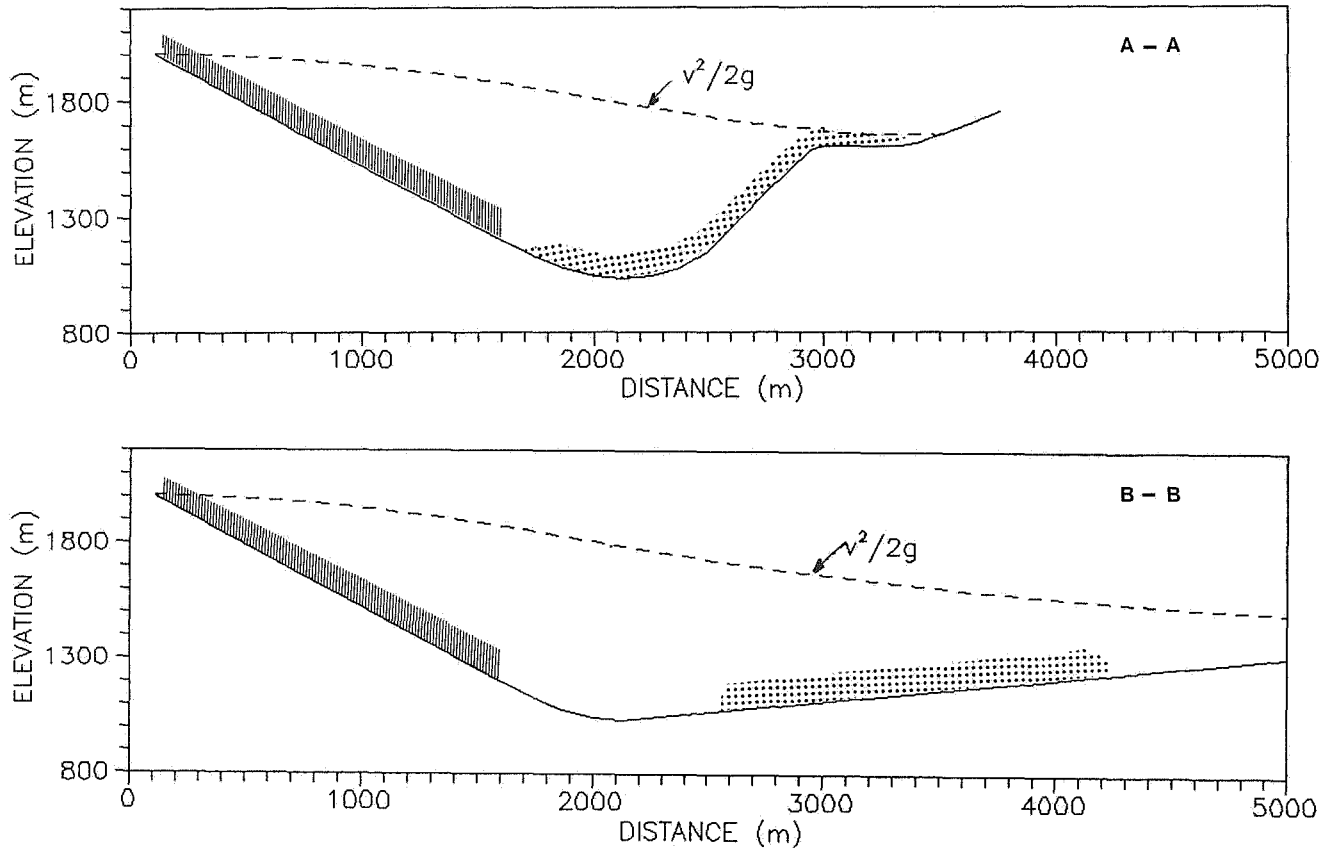


Figure 2. Lumped-mass analysis of the two cross-sections shown in Fig. 1, using the method of Koerner (1976). The resistance parameters used for both profiles are: $k_{si} = 1000 \text{ m/sec}^2$, $\mu = 0.02$, avg. flow depth = 100 m.

Kaiser and Simmons (1989) analyzed the two cross-sections using the Koerner (1976) model, implemented somewhat as shown in Figure 2. As originally proposed by Koerner and done by others, the sliding block was assumed to travel from the crest of the source area to the toe of the deposit. Extremely low flow resistance parameters need to be used in Section A-A to achieve the required runup. When the same parameters are applied in Section B-B, the runout is grossly overpredicted. Kaiser and Simmons concluded that the notion of gravity flow on the two profiles was physically impossible.

However, the lumped mass approach should be applied to this example in a different way as shown in Figure 3. The landslide mass was nearly 2 km long. Should we consider the displacement of the centre of gravity of the mass, both profiles can be

simulated with the same set of resistance parameters, which is moreover in the same range as parameters backcalculated from other cases by McLellan (1983). The phenomenal runup of Profile A-A is simply the consequence of the extreme volume and length of the slide mass.

While the correct application of the approach at the centre of gravity will improve its performance in some cases, nevertheless the sliding block technique is unable to simulate the important effects of lateral and longitudinal spreading. A recent attempt to include internal momentum transfer effects due to changing mass of the block appears to be incorrect (Erlichson, 1991).

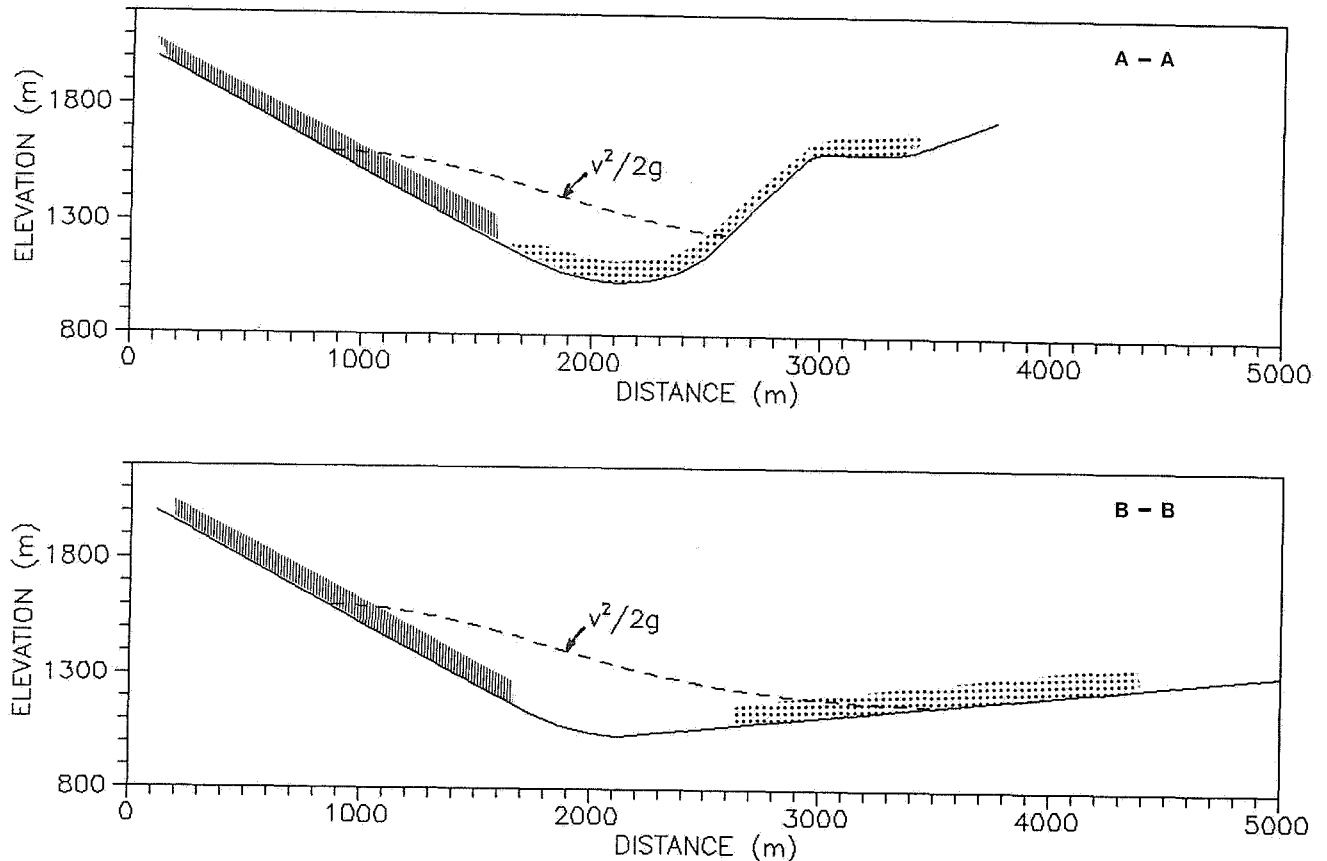


Figure 3.

The same analysis as in Fig. 2, referenced to the centre of gravity of the displaced mass. The resistance parameters used for both profiles are: $k_{si} = 250 \text{ m/sec}^2$, $\mu = 0.02$, avg. flow depth = 100 m.

Fluid Dynamics Models

Fluid dynamics models account for flow and shape changes in two or three dimensions using the governing equations of unsteady flow. The algorithms are generally quite complex (e.g. Trunk et al., 1986, Norem and Locat, 1992).

The author is in the process of developing a similar two-dimensional model based on referencing the unsteady flow equations to a moving frame ("Mass Referenced Flow Model"). The application of the model to Cross-section A-A of the Avalanche Lake event is shown in Figure 4.

The model predicts longitudinal spreading of the slide mass during its descent from the source area. On encountering the steep adverse slope of the opposite valley side, however, the flow front decelerates and thickens rapidly and eventually builds up into a form of standing wave, becoming stationary far below the crest of the runup bench. Similar result is obtained with any value of flow resistance parameters, even with zero resistance such as would apply with an ideal fluid. A fluid simply lacks the internal rigidity, required to sustain the stresses imposed by the dramatic change in path slope. No model based on fluid mechanics, nor a physical model using real fluid, can simulate flow-slide movement on this profile.

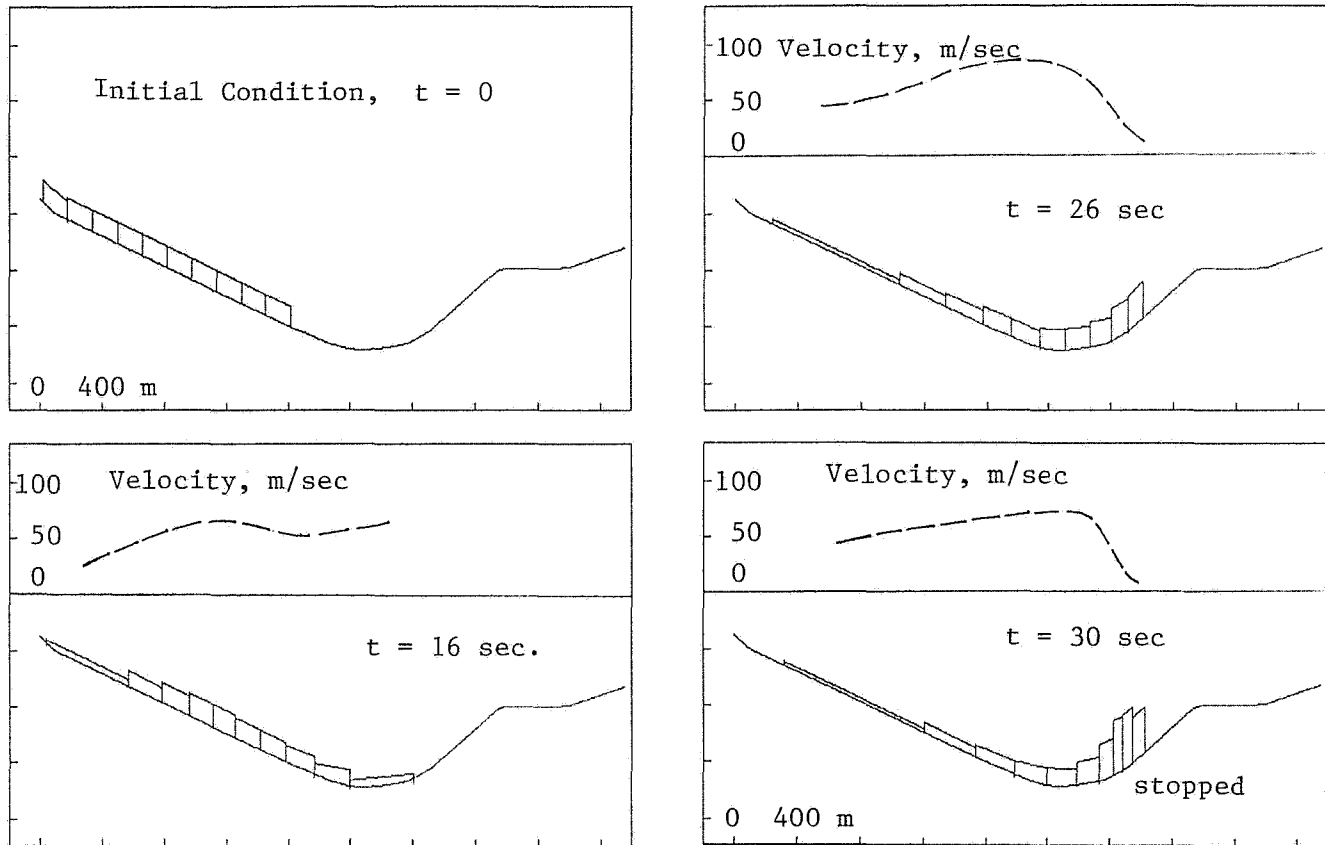


Figure 4.
Fluid dynamics analysis of Profile A-A (Figure 1) using the Mass-Referenced Flow Model, showing the development of a standing wave.

Conclusion

The actual rock avalanche was able to project material onto the shelf only because the slide mass of dry broken angular rock is a relatively rigid sheet, moving on a much weaker lubricated basal layer (probably liquefied valley soils). A successful model for flow slides, whether analytic or physical, will need to integrate fluid mechanics and plasticity so as to simulate the unique compound nature of flowing earth materials. An attempt to incorporate these aspects into the Mass Referenced Flow Model is currently under way.

Until better modelling tools become available, runout and runup estimates must be made carefully using the existing imperfect techniques. Backanalyses must utilize prototypes which are closely similar

to the case under consideration. Otherwise, serious errors could result from biases inherent to the algorithms used.

Acknowledgement

The author's visit to Avalanche Lake was supported by a grant from the Geological Survey of Canada and B.C. Hydro and Power Authority.

References

- B.C. Hydro and Power Authority, 1981. Peace River Development, Site C. Report on reservoir slopes. Unpublished.
- Antoine, P., Camporota, P., Giraud, A., Rochet, L., 1987. La menace d'écroulement aux ruines de Sechillienne (Isere). Bulletin liaison de Laboratoire des Ponts et Chausees, Vol. 150, pp. 55-63, (in French).

- Eisbacher, G.H., 1979. Cliff collapse and rock avalanches (sturzstroms) in the Mackenzie Mountains, northwestern Canada. *Canadian Geotechnical Journal*, Vol. 16, pp. 309-334.
- Evans, S.G., 1989. Highly anomalous run-up of Avalanche Lake rock avalanche, NWT, Canada. *Nature*, Vol. 340, p. 271.
- Golder Associates, 1987. Regional study of coal mine waste dumps in British Columbia. Report to the Federal Panel on Energy R. & D., Supply and Services Canada Ed., (unpublished).
- Erlichson, H., 1991. A mass-change model for estimation of debris flow runout, a second discussion. *Journal of Geology*, Vol. 99, pp. 633-634.
- Hutchinson, J.N., 1986. A sliding-consolidation model for flow slides. *Canadian Geotechnical Journal*, Vol. 23, Number 2, pp. 115-126.
- Kaiser, P.K., Simmons, J.V., 1989. A reassessment of transport mechanisms of some rock avalanches in the Northwest Territories, Canada. *Canadian Geotechnical Journal*, Vol. 27, pp. 129-144.
- Koerner, H.J., 1976. Reichweite und Geschwindigkeit von Bergstürzen und Flies-schneelawinen. *Rock Mechanics*, Vol. 8, pp. 225-256.
- McLellan, P.J.A., 1983. Investigation of some rock avalanches in the MacKenzie Mountains. M.Sc. Thesis, University of Alberta, Edmonton, Alberta, pp. 281.
- Noren, H. and Locat, J., 1992. A dynamic model for rock avalanches. GAC Special Paper - Landslide Hazards in the Cordillera, S.G. Evans Ed., in press.
- Perla, R., Cheng, T.T., McClung, D.M., 1980. A two-parameter model of snow-avalanche motion. *Journal of Glaciology*, Vol. 26, Number 94, pp. 197-207.
- Rochet, L., 1987. Developpement des modes numeriques dans l'analyse de la propagation de eboulements rocheux. *Procs., 6th Congress ISRM*, Vol. 1, pp. 479-484, (in French).
- Thurber Consultants Ltd., 1983. Debris torrent and flooding hazards, Highway 99, Howe Sound. Unpublished report to B.C. Ministry of Transportation and Highways.
- Thurber Consultants Ltd., 1986. Syncrude Tailings Dyke, Analysis of behaviour in the event of failure. Unpublished report to Syncrude Canada, Ltd.
- Thurber Engineering Ltd. and Golder Associates Ltd., 1992. Cheekye Fan Terrain Hazards Study. Unpublished report to B.C. Lands, Parks and Housing.
- Trunk, F.J., Dent, J.D., Lang, T.E., 1986. Computer modeling of large rock slides. *Journal of Geotechnical Engineering*, Vol. - 112 Number 3 ASCE, pp. 348-361.

Session 2B
Seismic Hazards
(continued)

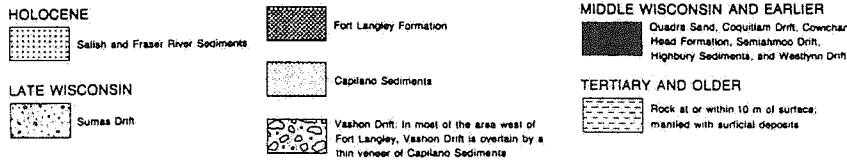
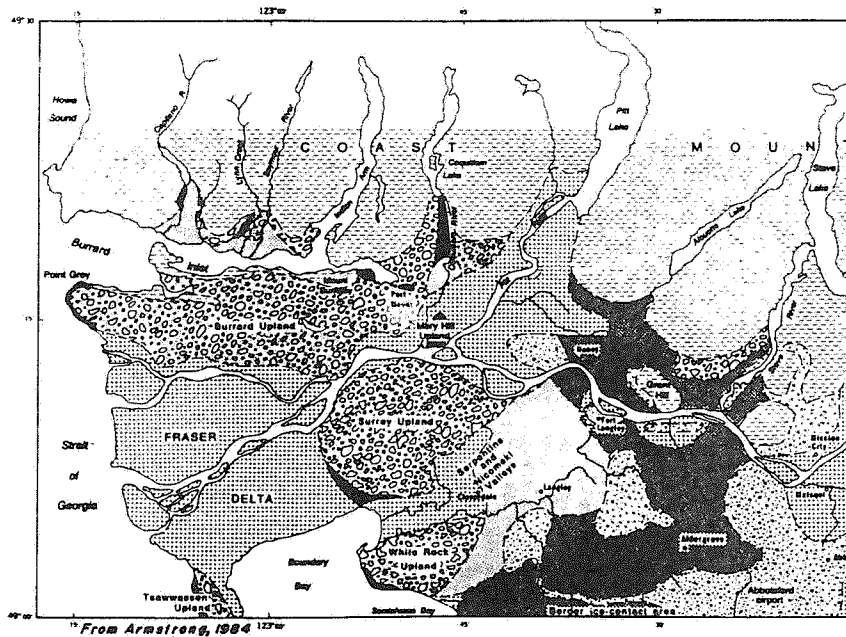


Figure 1A Regional Surficial Geology

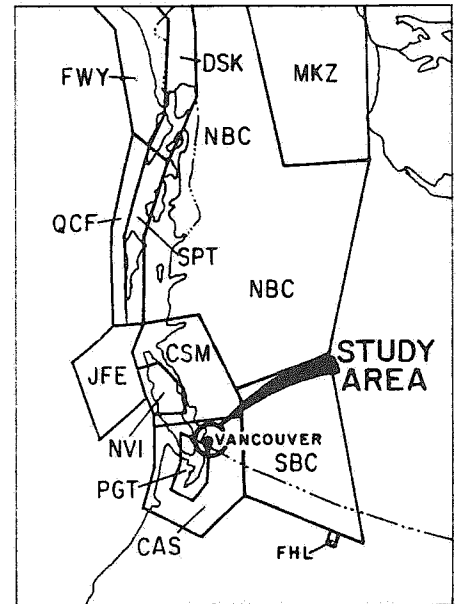


Figure 1B Location Plan and NBCC Seismic Zones

Liquefaction Susceptibility of Lower Mainland Soils

The Fraser Lowlands were covered by glaciers repeatedly during the Pleistocene. Most of the soils filling the lowlands of the region were laid down during the last major glaciation (Fraser Glaciation) and during the preceding nonglacial period. During recession of the ice, between about 13,500 and 10,000 years ago, complex successions of subaqueous outwash, sands, gravels, silts and clays, delta deposits and marine clays were laid down on the coastal lowlands depressed by the weight of the ice. After retreat of the glaciers and completion of isostatic adjustments, deltas, including that of the Fraser River, prograded into the Strait of Georgia. The regional surficial geology of the area is presented on Figure 1A.

The primary source of information on the soils for this study have been the surficial geological maps of the Vancouver and New Westminster area at a scale of 1:50,000 prepared by the Geological Survey of Canada[4,5]. The regional maps were supplemented with site specific drilling data. A preliminary database of subsurface information has been compiled.

Global correlations between the age and mode of deposition of surficial deposits and liquefaction susceptibility have been established by Youd and Perkins[7]. The liquefaction susceptibility of the surficial deposits in the Lower Mainland area has been assessed (Table 1) using the Youd and Perkins approach with some modifications based on local knowledge. The preliminary liquefaction

TABLE 1 Estimated Susceptibility to Liquefaction of Lower Mainland Soils						LIQUEFACTION SUSCEPTIBILITY	LIQUEFACTION SUSCEPTIBILITY
GEOLOGICAL UNIT	AGE	DISTRIBUTION	TYPE OF DEPOSIT	MATERIAL TYPE	WATER TABLE	YOUD & PERKINS MODEL	LOCAL ASSESSMENT
Fraser River Sediments							
Fa	Very recent	Along present river	River channel	Sand	At surface	Very high	Very high
Fb	Holocene	Widespread	Overbank	Sand & silt	Near surface	High	High
Fc	Holocene	Widespread	Overbank	Silt - silty clay	Near surface	High	High
Fd	Holocene	Widespread - 5 - 10m below surface	Deltatic	Mostly sand	Near surface	High	High to low
Fe	Holocene +	Widespread - underlies Fd sands	Estuarine	Sand/silt/clay	Near surface	Moderate - low	Low
Salish Sediments							
SAA	<500 yrs	Variable	Landfill	Variable	Near surface		Low to very high
SAB	Holocene	Widespread	Bog	Peat	At surface		* (See Note)
SAC	Holocene	Widespread	Bog	Peat	At surface		* (See Note)
SAD	Holocene	Variable	Bog	Organic loam	At surface		* (See Note)
SAE	Holocene	Variable	Bog	Peat	Near surface		* (See Note)
SAF	Very recent	Boundary Bay	Marine shore	Sand	At surface	High	High
SAG	Holocene	Local	Marine beach	Coarse sand	Near surface	Moderate	Moderate
SAH	Holocene	Local	Channel fill	Sand - clay	Near surface	High	High
SAI	Holocene	Local +15 m thick	Mountain stream	Gravel	Near surface	Moderate	Moderate
SAJ	Holocene	Local < 8 m thick	Mountain stream	Sand and gravel	Near surface	Moderate	Moderate
SAK	Holocene	Local	Channel fill	Sand and gravel	Near surface	Moderate	Moderate
Capilano Sediments - Fraser Glaciation - 11,000 - 28,000 years BP							
Ca	11-14000 yrs	Locally variable	Raised beach	Sand and gravel	Variable	Very low	Very low
Cb	11-14000 yrs	Locally variable	Raised beach	Coarse sand	Variable	Very low	Very low
Cc	11-14000 yrs	Locally variable	Raised deltatic	Sand to gravel	Variable	Low	Low
Cd	11-14000 yrs	Widespread	Marine	Stoney clay	Variable	Very low	Extremely low
Ce	11-14000 yrs	Locally variable	Marine	Silt to clay loam	Variable	Very low	Very low
Fort Langley Sediments							
FLA	11-13,000 yrs	Rare	Glacial	Sandy till	Variable	Very low	Extremely low
FLB	11-13,000 yrs	Rare	Outwash	Gravel and sand	Variable	Low	Low
FLC	11-13,000 yrs	Widespread	Glaciomarine	Stony clayey silt	Variable	Very low	Extremely low
FLD	11-13,000 yrs	Local	Marine	Silty clay	Variable	Very low	Extremely low
FLS	11-13,000 yrs	Local	Proglacial delta	Gravel and sand	Variable	Low	Low
Sumas Drift							
Sa	11-14,000 yrs	Local	Outwash	Sand and gravel	Near surface	Low	Low
Sb	11-14,000 yrs	Local (2-5 m thick)	Ice-contact	Gravel and sand	Near surface	Low	Low
Sc	11-14,000 yrs	Local (2-5 m thick)	Ice-contact	Gravel and sand	Near surface	Low	Low
Sd	11-14,000 yrs	Local (>5 m thick)	Ice-contact	Gravel and sand	Near surface	Low	Low
Se	11-14,000 yrs	Local	Proglacial delta	Gravel and sand	Variable	Low	Low
Vashon Drift							
VCa	13-18,000 yrs	Widespread <10 m thick	Glacial	Glacial till	Variable	Very low	Extremely low
VCb	13-18,000 yrs	Widespread <25 m thick	Glacial	Glacial till	Variable	Very low	Extremely low
Va	13-18,000 yrs	Locally variable	Glacial	Lodgement till	Variable	Very low	Extremely low
Vb	13-18,000 yrs	Locally variable	Glacioluvial	Sand and gravel	Variable	Very low	Very low
Pre-Vashon Deposits - Range from 18,000 yrs and older							
PVa	18-28,000 yrs	Rare	Channel fill	Quadra sand	Variable	Very low	Extremely low
PVb	18-28,000 yrs	Rare	Glacioluvial	Quadra sand/gravel	Variable	Very low	Extremely low
PVc	18-28,000 yrs	Rare	Marine	Quadra sand/silt	Variable	Very low	Extremely low
PVd	19-23,000 yrs	Rare	Glacial	Coquitlam till	Variable	Very low	Extremely low
PVe	25-38,200 yrs	Rare	Bog	Cowichan Head Fm.	Variable	Very low	Extremely low
PVf	>62,000 yrs	Rare	Glacial	Semiahmoo Drift	Variable	Very low	Extremely low
PVg	Wisconsin	Rare	Fluvial	Highbury sediments	Variable	Very low	Extremely low
PVh	Sangamon	Rare	Glacial	Westlynn Drift	Variable	Very low	Extremely low

Note 1: Peat is not liquefiable but underlying material may be.

susceptibility map for the Lower Mainland is presented on Figure 2.

The evaluation and compilation procedures used to develop this map impose several qualifications and limitations on its use. The map is regional in scope and indicates general areas where susceptible materials are likely to be present. It cannot be used to determine the actual presence or absence of liquefiable soils beneath any specific locality. The boundaries between zones are estimates only. Investigations are required to assure that a correct rating is given for any individual site within or near these boundaries.

The zones shown as having very high, high or moderate susceptibility are expected to be the main areas of liquefaction in future significant earthquakes. Actual occurrence of liquefaction within these zones will depend on local material property variations. Susceptibility boundaries are based on geological criteria only. The next phase of the study will use geotechnical criteria to better map susceptibility boundaries.

Ground water levels in much of the area rise and fall with tides and seasonal rainfall. Susceptibility, which is a function of ground water level, therefore also varies and may also vary with long-term climatic changes.

High to Very High Susceptibility Zones

Fraser Delta

The Holocene sediments of the Fraser River Delta form the largest zone of soils susceptible to liquefaction in the area. Evidence of historical liquefaction has been found in this zone at the new Kwantlen College Richmond site (Figure 2)[8].

The modern Fraser River delta extends from a gap in the Pleistocene uplands at New Westminster into the Strait of Georgia and Boundary Bay. The Strait of Georgia and Boundary Bay sections of the perimeter are separated by the Point Roberts peninsula, a former island composed of Pleistocene sediments. Postglacial Fraser River sediments, which make up the delta, can up to 200 m thick.

The delta has been subdivided into the following major zones:

Unit Fa represents the most recent sediment in the area deposited within the current river channel (Figure 2). These relatively uniform saturated, fine sands, no more than several hundred years old, have a very high susceptibility to liquefaction.

Most of the delta has been subdivided into two general areas: areas covered by overbank deposits Fb and Fc; and, areas covered by peat deposits (SAb,c,d). Although the liquefaction susceptibility rating for the two areas has been assessed as high, the depth of liquefaction in the two areas will be different. In the peat covered area, the liquefiable soils are beneath the peat. The peats are not liquefiable.

Williams and Roberts[9] subdivided the deltaic soils of Lulu Island on the basis of a series of drill holes and developed a longitudinal section (Figure 3). As part of the current study, an attempt has been made to correlate their geological soil units with cone penetration profiles. This has been done to provide some geotechnical characteristics to the units which aid in defining liquefaction susceptibility with depth.

Unit 4 - Peat This organic layer, shown as Units SAb, c, d on Figure 2, varies from 1 to 10 m thick and is found in the eastern portion of the delta. The peat layer typically has a

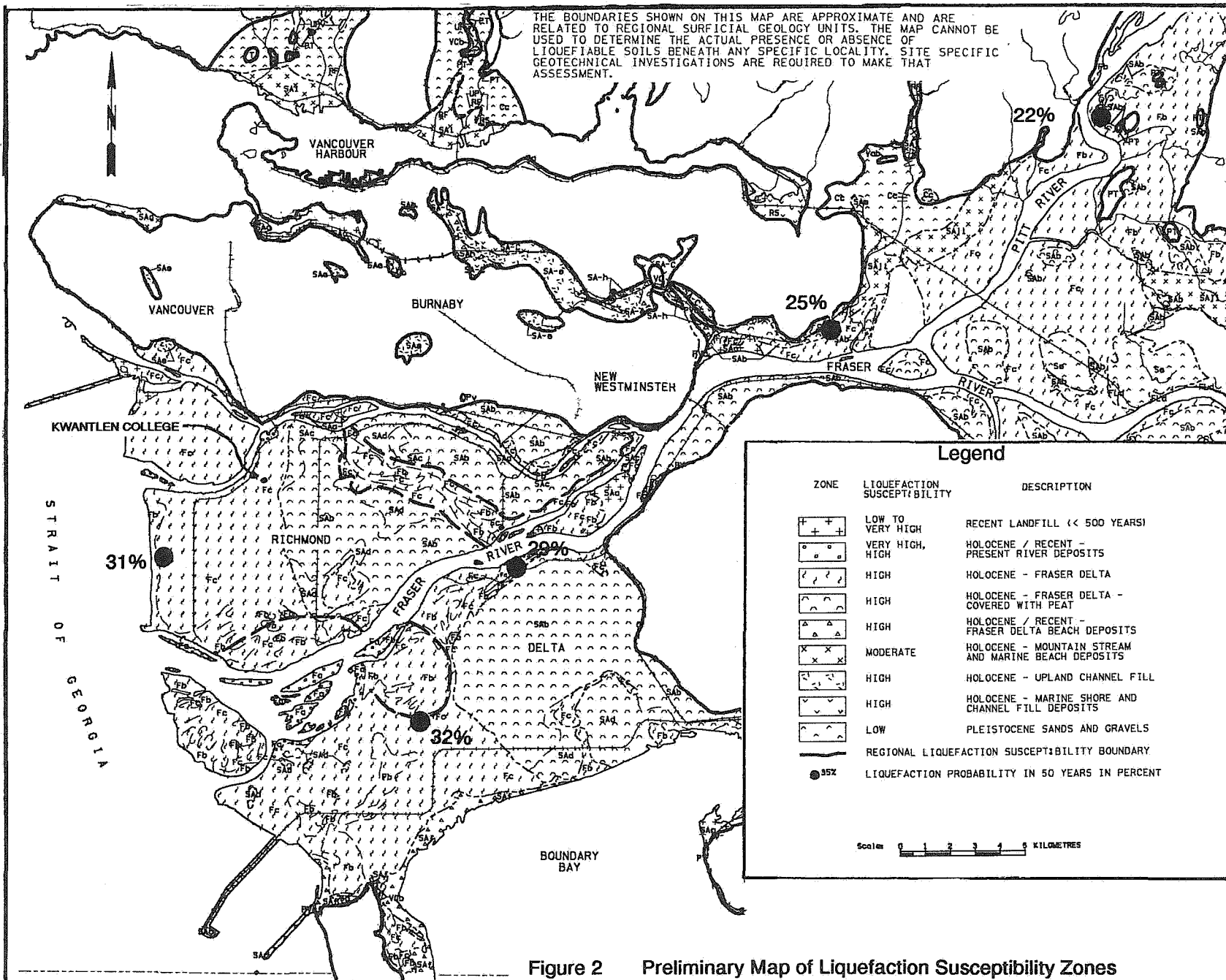
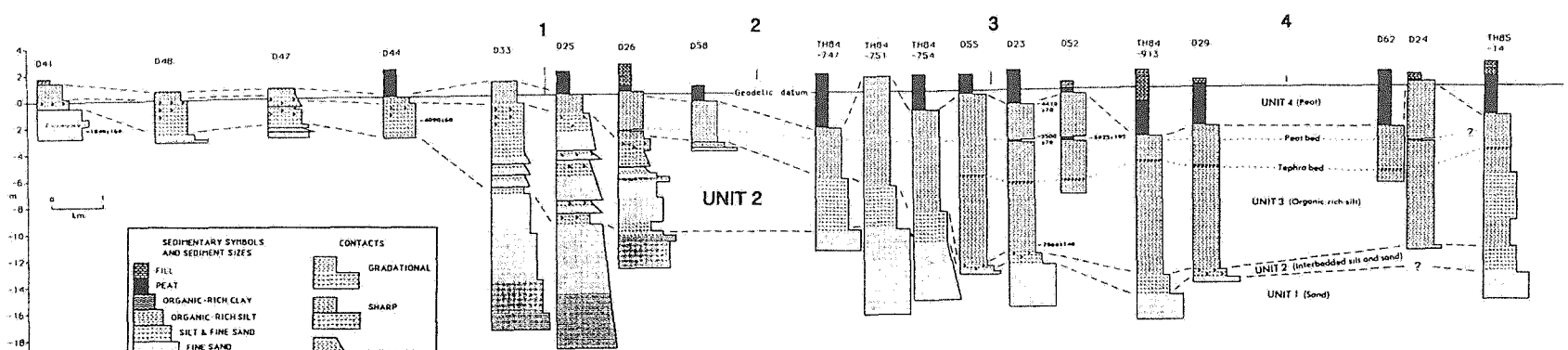
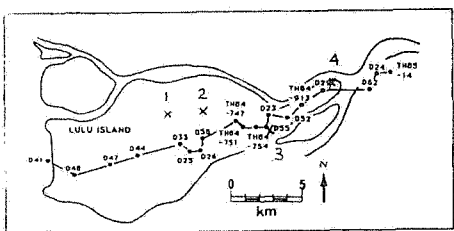


Figure 2 Preliminary Map of Liquefaction Susceptibility Zones



Longitudinal Section Through Lulu Island, Richmond (from Williams and Roberts, [91])



- Sampled hole used in soil section
- x CPT hole

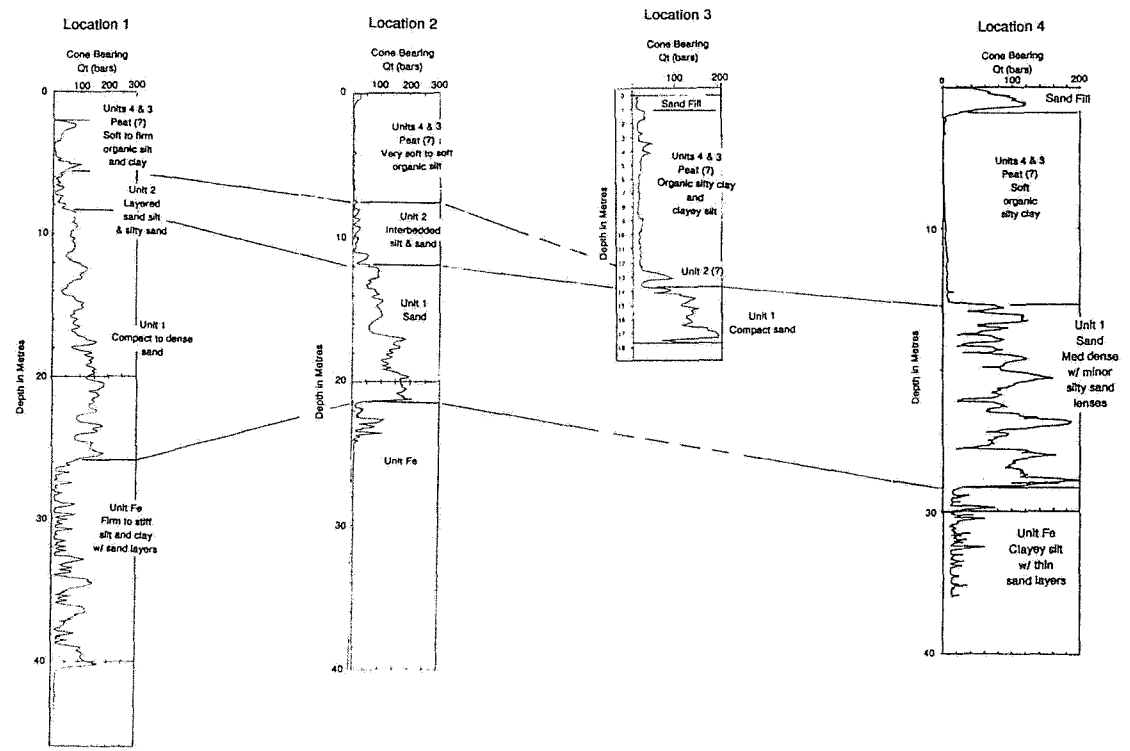


Figure 3 Geological / CPT Profile – Lulu Island, Richmond, B.C.

very low CPT tip penetration resistance and is sometimes difficult to distinguish, on the basis of CPT alone, from the underlying very soft silts.

Unit 3 - Silts This unit (corresponding with Fc on Figure 2) is composed of overbank soils deposited during periodic flooding by the river. Williams and Roberts[9] have subdivided this unit into upper and lower units on the basis of palynological evidence. The upper silt (**Unit 3b**) is composed of organic-rich silt. A 1-2 cm thick tephra bed was found at depths ranging from 4 to 6.5 m below mean sea level. The tephra marker bed was identified as Mazama (ca 6800 years BP)[9]. The lower silt (Unit 3a) is primarily an organic-rich silt although it is sandier than Unit 3b. The unit grades into the underlying soils.

The silts range from liquefiable to non-liquefiable depending on their clay content. It is common practice to determine liquefaction susceptibility using the Chinese criteria[10] and/or cyclic laboratory tests.

Unit 2 - Interbedded Silts and Sands This unit consists of interbeds of silt, sand and silty sand which have a very high susceptibility to liquefaction. CPT tip resistance vary from 10 to 40 bars but is highly variable. These silts and sands are mid-tidal flat sediments.

Unit 1 - Sand This unit (Fd on Table 1) consists primarily of well sorted medium to coarse sand and represents deposits of the lower tidal flat and subaqueous platform environments. These sands, which range in thickness from 15 to 40 m, have much greater resistance to liquefaction than the Unit 2 sand interbeds but are still susceptible to liquefaction. Their density, as illustrated in the CPT logs on Figure 3, is highly variable vertically and horizontally over short distances. It is common practice in

the Richmond area to densify foundations, where required, to depths corresponding approximately with the middle of this sand unit.

The depth to Unit 1 increases from west to east. Unit 2 has a maximum thickness of about 8 m in the central portion of the island and thins to the east and west to about 1 to 2 m or less. At Location 4, Unit 2 could not be identified. Unit 3 thickness (Figure 3) increases substantially to the east.

The sands of Unit 1 are underlain by more than 40 m of marine delta fore slope deposits (Fe) which are very soft to firm, grey, clayey silt with some interbedded silt and fine sand. The penetration resistance characteristics of these deposits are illustrated in the CPT logs at Locations 1, 2, and 4 (Figure 3). The marine delta deposits are underlain by postglacial stiff marine grey clayey silt and silty clay. Liquefaction susceptibility of soils below Unit 1 is not normally considered in engineering practice because of their great depths.

Still Creek/Burnaby Lake

Unit SAh consists of lowland stream channel fill deposits of sandy to clayey silts and organic sediments. It has been found up to 8 m thick along Still Creek in Vancouver and in Burnaby near Burnaby Lake. It is associated with SA-C deposits which consists of marine shore and fluvial sands up to 8 m thick. SA-C and SAh soils are classified as highly susceptible to liquefaction.

Landfill

Landfill consisting of sand, gravel, till, crushed stone and refuse has been used in various areas around the Lower Mainland. Because of its variability,

it's susceptibility ranges from low to very high. Although it has been mapped as a highly susceptible soil site specific investigations are required to determine actual susceptibility.

Moderate Susceptibility Zones

Holocene sand and gravel deposits are found in several areas in the Lower Mainland. Marine shore and beach deposits of medium to coarse sand and gravel up to 8 m thick belonging to Unit **SAg** are found along beaches at Point Grey and Jericho in Vancouver and Crescent Beach in White Rock. At the mouth of the Capilano and Seymour/Lynn rivers in West and North Vancouver deltas consisting of medium to coarse gravel and minor sand (Unit **SAi**) have developed to over 30 m thick. Mountain stream and deltaic deposits of Unit **SAi** and **SAj** are found in the Coquitlam River area and also in an area north of Haney. These Holocene marine beach and deltaic deposits are classified as having moderate liquefaction susceptibility but may have high liquefaction susceptibility zones.

Liquefaction susceptibility of upland soils could be significantly influenced by ground water levels and soil saturation caused by long periods of rain. The extent of liquefaction during the San Francisco earthquake of 1906 is a good example. The earthquake occurred near the end of a very wet season when ground water levels and susceptibility were relatively high. More soils probably liquefied during that event than would have under the dryer conditions that normally occur during summer[11].

Low Susceptibility Zones

The Capilano, Fort Langley and Sumas deposits contain Pleistocene sand and gravels which may be susceptible to liquefaction.

In the North and West Vancouver areas and in the Coquitlam area, raised deltaic and channel fill medium sand and gravel are found over 15 m thick. These Unit **Cc** sediments were deposited by proglacial streams. They are underlain by silt to silty clays of Unit **Cd**.

Liquefaction Potential

Liquefaction potential is a measure of soils propensity to liquefy and depends on its susceptibility and the regional seismicity. The probability of liquefaction was calculated using PROLIQ2[12] and is a direct measure of liquefaction potential. The liquefaction potential was determined at 45 test hole sites in the first phase of the study within the boundaries of the susceptible zones.

PROLIQ2

The liquefaction potential within the study area was determined with the computer program PROLIQ2 which combines the Cornell-McGuire probabilistic seismic hazard procedure with the liquefaction assessment procedure for level ground first published by Seed and Idriss[13]. PROLIQ2 thus incorporates the most widely accepted models for predicting seismic peak ground acceleration and for determining the liquefaction resistance of cohesionless soils.

Seismic source zones, magnitude-recurrence relationships and the attenuation function used in this study are identical to that used for the 1985 and 1990 National Building Code of Canada and which were first published in [14] (see Figure 1B). The influence of large magnitude subduction earthquakes which are postulated to occur off the west coast of Vancouver Island have not been included in the seismic model. This exclusion was made

to be consistent with the current version of the NBCC which does not include large magnitude interplate subduction earthquakes.

The basic steps in a PROLIQ2 analysis are shown in Figure 4. PROLIQ2 starts with the corrected standard penetration resistance, $(N_1)_{60}$, and uses the Seed method to calculate the surface acceleration, A_{crit} , required to just cause liquefaction for a narrow magnitude range, termed a magnitude class. This calculation is independently made for half-magnitude increments from M5 to the maximum magnitude for each source zone. The critical acceleration is then used with a discrete attenuation relationship to calculate the epicentral radius, R_{crit} , within which earthquakes must be to at least cause the critical acceleration for liquefaction at the site.

R_{crit} is used to calculate the annual rate of occurrence of earthquakes that cause liquefaction using the discrete magnitude recurrence relationship. Assuming the rate of occurrence of earthquakes to be a Poisson process, the probability of liquefaction is calculated for each magnitude class and each source zone. The total probability of liquefaction is simply the addition of the probabilities for each magnitude class and for each zone.

The PROLIQ2 procedure considers only the random nature of earthquake ground motion intensity at a test hole location for calculation of the probability of liquefaction. Other uncertainties are the Seed liquefaction model and the variation in blowcount. As important as these variables are, they are second order effects compared to the influence of the random nature of the earthquake ground motions on the probability of liquefaction.

PROLIQ2 was also modified to use the algorithm in [15] for SPT blowcount

overburden correction and the fines correction suggested in [16].

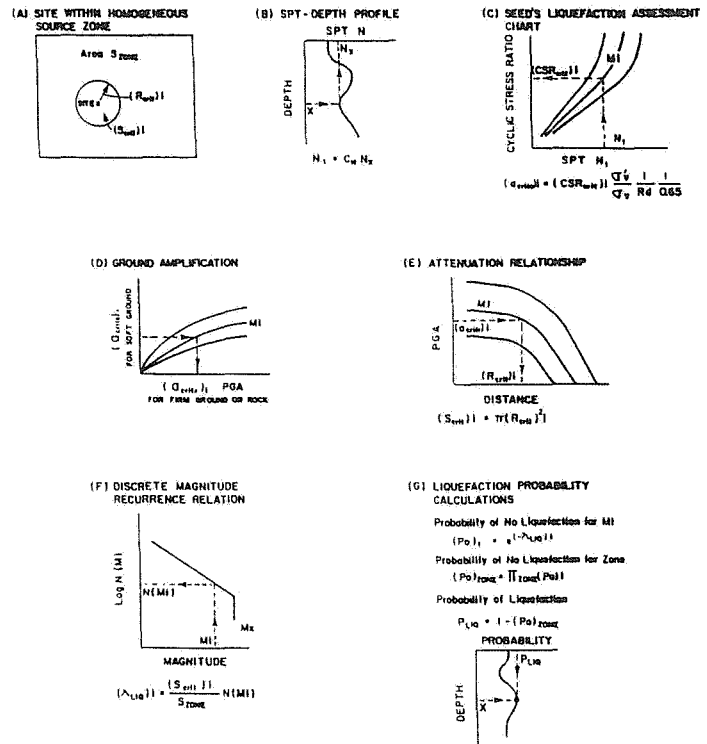


Figure 4 - PROLIQ2 Methodology

Ground Amplification

Recent work by Lo et al [17] suggests that significant amplification of seismic ground motions could occur in the Fraser River delta soils for the predominant earthquake magnitudes contributing to the NBCC risk level of 0.0021 per annum. Also the Richmond Liquefaction Task Force chaired by Dr. P. Byrne of the University of British Columbia recommended that the peak horizontal ground acceleration at an annual risk level of 0.0021 be amplified for liquefaction assessments. This work prompted the development of a simple algorithm to include the surface acceleration for soft sites versus firm ground acceleration amplification curves proposed by Idriss [17] in the

PROLIQ2 model as shown in Figure 4D. Idriss[17] derived curves for earthquake magnitudes 5.5 and 7 only. Curves were constructed for the other magnitude classes in PROLIQ2 by interpolation and extrapolation from these base curves.

The probability of liquefaction results calculated using the curves in [18] were unreasonably high. The results are likely high because amplification of ground motions will not occur at all magnitudes and at all epicentral distances the algorithm Figure 4D requires. Amplification only occurs when the predominant period of the earthquake motions excites the natural periods of the soil profile. Thus the incorporation of amplification in the PROLIQ2 model must consider the natural periods of the soil profile at the test borehole and the change of predominant period of the earthquake motions with distance from the source.

Another factor which could contribute to the unreasonably high values are the widely used magnitude scaling factors proposed by Seed, based on laboratory cyclic tests, which are much higher than those calculated by Ambraseys[19] based on observations. Both of these factors are under consideration in the next phase of the study.

Resolution of the amplification issue for the PROLIQ2 model is important because the calculated results are all greater than the maximum probability calculated from past earthquakes. Thus mapping of liquefaction probability based on site specific test hole data will only be meaningful when this issue is resolved. Calculation of the maximum probability of liquefaction is described in the next section.

Ambraseys Maximum Probability of Liquefaction

Studies of past earthquakes show that the maximum distance at which liquefaction occurs from an earthquake epicentre is a function of earthquake magnitude and soil type. Many researchers [3,8,20,21] have plotted maximum epicentral distance, R_e , of liquefaction occurrence versus causative earthquake magnitude. Liquefied soils at the maximum distance are estimated to have $(N_1)_{60}$ values of about 4[20].

Ambraseys[19] added a large number of data points to previous work, as shown in Figure 5, and proposed the following relationship between earthquake magnitude and maximum epicentral distance of liquefaction occurrence:

$$M_w = -0.31 + 2.65 \times 10^{-8} R_e + 0.99 \log(R_e) \quad (1)$$

where R_e = epicentral distance in km
 M_w = moment magnitude

Equation 1 can be treated as an attenuation function in PROLIQ2 where R_e becomes R_{crit} for each magnitude class. The probability of liquefaction calculated in this manner should be the maximum value possible for an area because Eq. 1 incorporates many data points from soft sites which presumably would have experienced amplification. The probability of liquefaction using Eq. 1 was calculated for all test hole locations and compared with the probability values calculated assuming amplification and no amplification. In virtually all cases the amplified values were greater than the upper bound.

Liquefaction Potential Results

As mentioned above the liquefaction potential calculated using Ambraseys' weak ground model was always lower than the values calculated using the amplified model. Selected,

representative values of the upper bound are plotted on Figure 2.

Ambraseys' relationship gives a probability of liquefaction in 50 years ranging from about 32 percent at the southwest corner of the study area to about 23 percent in the northeast corner of the study area. This trend is reasonable since Ambraseys' liquefaction potential does not depend on the site specific ground conditions

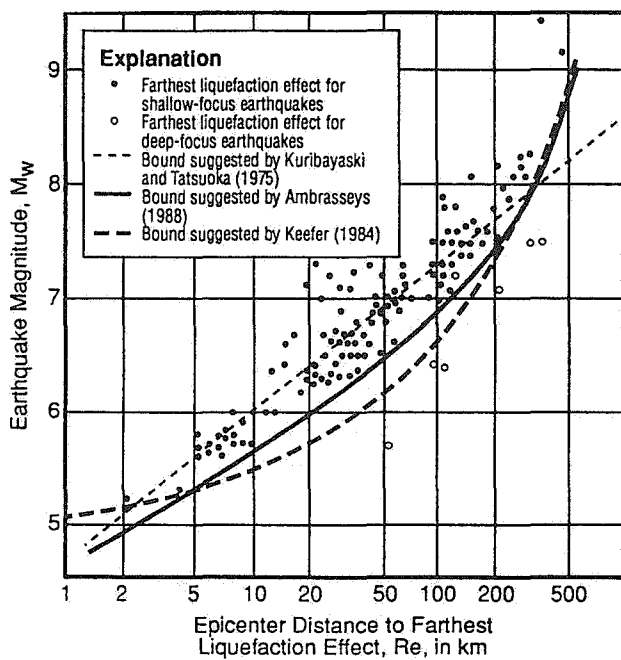


Figure 5 - Magnitude Versus R_e (Youd[3])

but only on the regional seismicity which is dominated by the Puget Sound Zone (PGT) (Figure 1B). This liquefaction probability is equivalent to a recurrence interval for liquefaction of about 130 to 150 years. In the absence of site specific testing and analysis, it is reasonable to assume that this recurrence interval is representative of much of the Fraser Delta area since susceptibility mapping shows that weak and liquefiable layers

extend throughout the area. For comparison, a similar study discussed in [3] for the Los Angeles area gives a recurrence interval of 33 years.

Conclusions

A preliminary liquefaction susceptibility map has been prepared based largely on the regional surficial geology of the Lower Mainland. The zones shown as having very high, high or moderate susceptibility are expected to be the main areas of liquefaction in future significant earthquakes. Actual occurrence of liquefaction within these zones will depend on local material property variations.

The zones on Figure 2 show susceptibility to liquefaction rather than susceptibility to ground displacement, which is the actual damage-producing consequence of liquefaction. Under some conditions, liquefaction can occur without generating significant ground displacement. Consequently, the probability of damaging ground displacement during an earthquake is less than the probability of liquefaction.

The liquefaction potential estimates have been calculated using the PROLIQ2 computer program. As the seismicity across the region is relatively constant, a relatively uniform probability of liquefaction exists for those soils susceptible to liquefaction. This probability ranges from about 23 to 32% in 50 years which represents a return period of 130 to 150 years.

Acknowledgements

The authors are grateful to Mr. G. Salmon, P.Eng. of B.C. Hydro for permission to publish the preliminary results of this study.

References

1. **Armstrong, J.E.**(1981). Post-Vashon Wisconsin Glaciation, Fraser Lowland, British Columbia; Geological Survey of Canada, Bulletin 322.
2. **National Research Council** (1985). Liquefaction of Soils During Earthquakes, National Academy Press, Washington, D.C., 240 p.
3. **Youd, T.L.** (1991). Mapping of earthquake-induced liquefaction for seismic zonation, Fourth International Conference on Seismic Zonation, Vol.1, pp.111-197.
4. **Armstrong, J.E. and Hicock, S.R.** (1980a). Surficial geology, New Westminster, British Columbia; Geological Survey of Canada, Map 1484A, scale 1:50,000
5. **Armstrong, J.E. and Hicock, S.R.** (1980b). Surficial geology, Vancouver, British Columbia, Geological Survey of Canada, Map 1486A, scale 1:50,000
6. **Armstrong, J.E.** (1984). Environmental and engineering applications of the surficial geology of the Fraser Lowland, Geological Survey of Canada, Paper 83-23.
7. **Youd, T.L. and Perkins, D.M.**(1978). Mapping liquefaction-induced ground failure potential, Journal of Geotechnical Engineering Division, ASCE, Vol. 104, No. GT4, pp. 433 - 445.
8. **Naesgaard, E., Sy, A., and Clague, J.** (1992). This volume.
9. **Williams, H.F.L. and Roberts, M.C.** (1989). Holocene sea-level change and delta growth: Fraser River delta, British Columbia, Canadian Journal of Earth Sciences, Vol. 26, pp. 1657 - 1666.
10. **Seed, H.B., and Idriss, I.M.**(1982). Ground motions and soil liquefaction during earthquakes, EERI, 134 p.
11. **Youd, T.L., and Hoose, S.N.** (1976). Liquefaction during 1906 San Francisco earthquake. Journal of Geotechnical Engineering Division, ASCE, Vol. 102, No. GT5, pp.425-439.
12. **Atkinson, G.M., Finn, W.D.L. and Charlwood, R.G.** (1984). Simple computation of liquefaction probability for seismic hazard applications. Earthquake Spectra, Vol. 1. No. 1, pp. 107-124.
13. **Seed, H.B., and Idriss, I.M.** (1971). Simplified procedure for evaluating soil liquefaction potential, Journal of Soil Mechanics and Foundations Division, ASCE, Vol. 97, No. SM9, pp. 1249-1273.
14. **Basham, P.W., Weischert, D.H., Anglin, F.M. and Berry, M.J.**(1982). New probabilistic strong seismic ground motion maps of Canada - A comparison of earthquake source zones, methods and results. Earth Physics Branch Open file 82-83.
15. **Liao, S. and Whitman, R.V.** (1986). Overburden correction factors for SPT in sand, Journal of Geotechnical Engineering, ASCE, Vol.112, No.3, pp.373-377.
16. **Seed, H.B., Tokimatsu, K., Harder, L.F. and Chung, R.M.** (1985). Influence of SPT procedures in soil liquefaction resistance evaluations, Journal of Geotechnical Engineering, ASCE, Vol. 111, No. 11, pp. 1425-1445.
17. **Lo, R.C., Sy, A., Henderson, P.W., Siu, D., Finn, W.D.L., and Heidebrecht, A.C.** (1991). Seismic site amplification study for Fraser delta, British Columbia, Sixth Canadian Conference on Earthquake Engineering, pp. 509-516.

18. Idriss, I.M. (1991). Unpublished data, Evaluation and mitigation of earthquake induced liquefaction hazards seismic short course, San Francisco State University.

19. Ambraseys, N.N. (1988). Engineering seismology, International Journal of Earthquake Engineering and Structural Dynamics. Vol. 17, No. 1, pp. 1-105.

20. Kuribayashi, E. and Tatsuoka, F. (1975). Brief review of liquefaction during earthquakes in Japan, Soils and Foundations, Vol. 15, No.4, pp. 81-91.

21. Seed, H.B., Tokimatsu, K., Harder, L.F. and Chung, R.M. (1984). The influence of SPT procedures in soil liquefaction resistance evaluations, Berkeley, California, University of California, Report No. EERC-84/15, 50p.

Liquefaction Sand Dykes at Kwantlen College, Richmond, B.C.

Ernest Naesgaard
Macleod Geotechnical Ltd.
West Vancouver, British Columbia

Alex Sy
Klohn Leonoff Ltd. & Dept. of Civil Engineering
University of British Columbia
Vancouver, British Columbia

John J. Clague
Geological Survey of Canada
Vancouver, British Columbia

Abstract

Numerous sand dykes were observed during a large foundation excavation at the site of the new Kwantlen College campus in Richmond, British Columbia. The sand dykes are believed to have been caused by seismically induced liquefaction related to one or more moderate to large earthquakes. The sand dykes apparently originated in a shallow fine to medium grained sand unit and intruded into an overlying 3 m thick clay/silt layer. The grain sizes of the sand dykes fall within the gradation envelope of the source sand unit. In-situ tests show that the upper portions of the sand deposits are loose, and liquefaction analyses confirm that these zones are susceptible to liquefaction, when subjected to ground motions even below the 1 in 475 year National Building Code of Canada design earthquake motion for the area.

Introduction

At six sites on and adjacent to the Fraser River delta in southwestern British Columbia, sand dykes, sills and some evidence of vented sand boils have been observed. These features are believed to have been caused by seismically induced liquefaction related to one or more moderate to large earthquakes. The observed features at the six sites, regional tectonics and seismicity, and local geology are described in Clague et al. [1]. At one of the sites, Kwantlen College's new Richmond campus, many sand dykes were found in a large dewatered excavation for foundation preparation. Detailed mapping of the liquefaction features, sampling and in-situ testing were conducted at the site. This paper describes the field observations, summarizes the field and laboratory tests, and presents the results of liquefaction analyses based on the test data. Radiocarbon dates of selected samples to constrain the age of the sand dykes are also presented. Remedial measures used to mitigate the foundation liquefaction risks at the site for the new buildings are also described.

Fraser Delta Geology and Seismicity

The Fraser delta, with an area of approximately 300 km², is located south of Vancouver in the southwest corner of the British Columbia mainland. The inhabited portion of the delta is dyked and lies 0 to 2 m above mean sea level, with the water table within 2 m of the ground surface. The delta is geologically young, having formed since the disappearance of the last ice sheet some 13,000 to 11,000 years ago [2]. The very thick (over 100 m) deltaic sequence of silty clays, silts and sands overlies Pleistocene till and glaciomarine sediments [3].

Most of the seismicity affecting the Fraser delta is associated with the interactions among the North American plate, the Juan de Fuca plate, the Explorer plate, and the Pacific plate as shown in Fig. 1. Historical records of seismicity in the region date back only about 120 years, and they show that no major earthquakes have occurred in the vicinity of the delta. Many minor earthquakes, however, have been recorded in the area and larger earthquakes have occurred in adjacent areas [4].

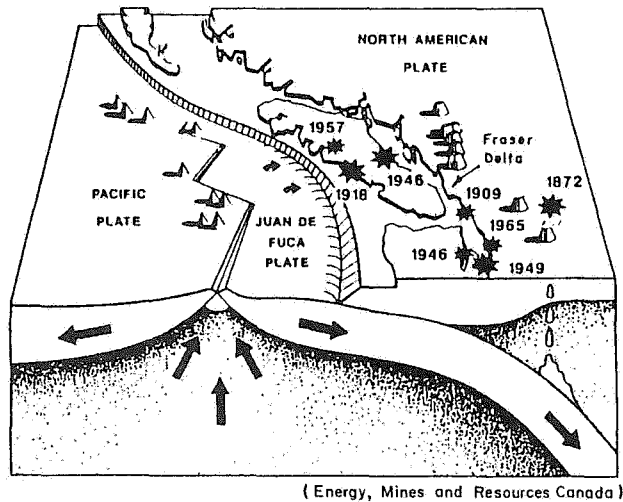


Fig. 1 Regional Tectonic Setting of Fraser Delta

The Fraser delta lies within Zone 4 of the 1990 National Building Code of Canada (NBCC) seismic zoning maps. The maps are based on a probabilistic assessment of the regional seismicity using the Cornell-McGuire method. For a probability of exceedance of 0.0021 per annum, equivalent to a return period of 475 years as adopted in the Code, the peak horizontal ground acceleration (PGA) is 0.21 g and the peak horizontal ground velocity (PGV) is 0.21 m/s over most of the inhabited Fraser delta. These values refer to firm ground or rock sites. The dominant contributions to the NBCC design ground motions come from earthquakes of magnitudes 6.3 to 7.3 at epicentral distances of about 30 to 70 km [5]. For a deterministic evaluation of liquefaction potential as described later in this paper, a design earthquake of Magnitude 7 is assumed.

Site Conditions

As shown on Fig. 2, the Kwantlen site is located in the north-central area of the Fraser delta. The soil profile at the site is typical of much of the delta and excluding recent surface fill, comprises three main stratigraphic units. The upper Unit 1, locally called the "crust", consists of horizontally bedded silty clay, silt, and sandy silt. This unit is 3 to 5 m thick, with the upper 1 to 1.5 m being stiff and over consolidated due to desiccation, and the lower portion firm to soft. Natural water contents are in the range of 35%

to 60%, liquid limits 35% to 49%, and plastic limits 20% to 36%. Vane shear strengths range from over 100 kPa in the upper desiccated portion of Unit 1 to between 25 and 50 kPa in the lower portion of the unit. A 0.15 to 0.5 m thick topsoil or organic soil overlies the clay/silt in some locations, while in others, the topsoil has been completely or partially removed. Fine roots and root holes are common throughout Unit 1.

The contact between Unit 1 clay/silt and the underlying Unit 2 sands is generally sharp, although minor interlensing of the two lithologies was observed at some locations. Unit 2 consists of 20 to 30 m of relatively uniform-graded, fine to medium grained sands with some silty layers. These sands have erratic densities ranging from loose to dense over short distances. Ignoring local density variations, there is a trend of increasing density with depth. Unit 2 is believed to be the source for the sand dykes observed within Unit 1.

Interbedded fine sands, sandy silts and silty clays (Unit 3) underlie Unit 2 sands and likely extend to 150 m depth

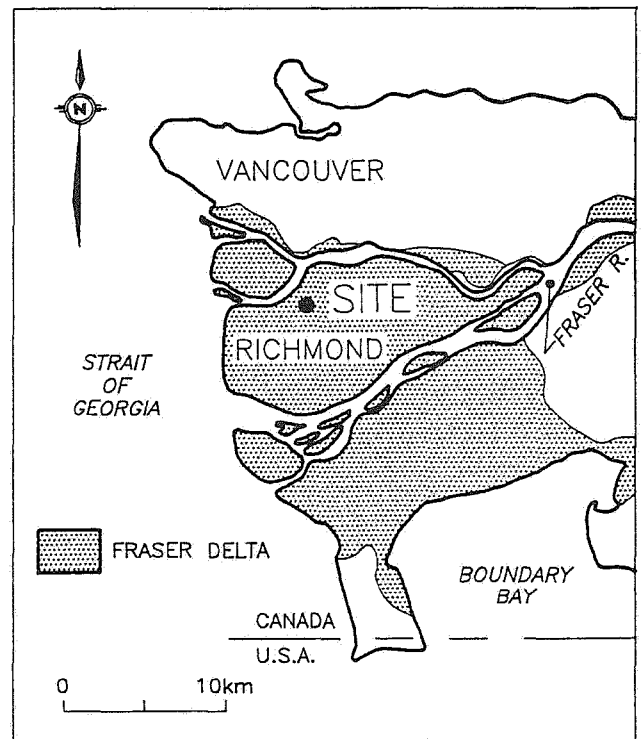


Fig. 2 Site Location

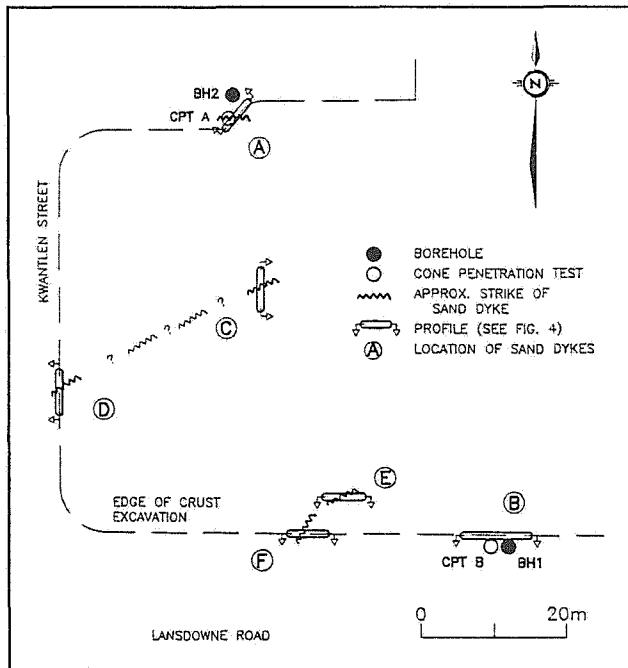


Fig. 3 Site Plan

or more on this part of the delta. The Unit 3 deposits are firm, normally to very slightly over consolidated.

It was realized early in the design stage that the subsoils at the Kwantlen site, like most sites on the Fraser delta, were susceptible to seismically induced liquefaction. The foundation design called for support of the three-storey structure on spread footings founded on sand densified in-place by the dynamic compaction process. In early 1990, foundation site preparation for the new campus commenced. The site preparation work consisted of stripping existing fill and organic soil, dewatering to 4 to 5 m depth below the stripped surface, excavating the 3 m thick Unit 1 clay/silt crust, backfilling the excavation with dumped sand fill, and densifying the sand fill and underlying loose native sands to a depth of approximately 10 m below grade using the dynamic compaction procedure. It was during the excavation phase that sand dykes and other liquefaction features were observed on the vertical cuts through Unit 1.

Observed Liquefaction Features

Detailed mapping and sampling of the sand dykes were conducted at the six

locations, A to F, shown in plan on Fig. 3 and in profile on Fig. 4. The observed sand dykes extend into or through Unit 1 clay/silt. The thickness of the dykes ranged from less than 1 mm to about 300 mm, and in some cases, as shown on Profile A in Fig. 4, it changed over relatively short distances. Generally, the dykes tended to be thicker near the base of Unit 1 and to thin toward the surface. The contact between the dykes and the clay/silt which they cut were sharp. A few lumps of clay/silt were observed in some of the sand dykes. At some locations, the dykes also cut through the upper part of Unit 2, indicating a deeper origin.

Most of the sand dykes had no recognizable internal structure, while others had definite stratification, generally parallel to the margins of the dykes.

At Location A, comparison of bedding strata in the Unit 1 clay/silt indicated a 200 mm heave of the block of clay/silt enclosed by the dykes (Fig. 4). At this location, the sand dyke also cuts through and spreads over a buried topsoil, likely indicative of the venting of a sand boil. At Location C, a sand dyke intruded and heaved a surficial topsoil layer. The dykes at Locations C and D have similar profiles and strikes, and are believed to be different sections of the same structure with a lateral extent of at least 30 m.

Radiocarbon dating was conducted on three wood samples collected from Unit 1 and the top of Unit 2, at Location F (Fig. 4). The dates ranged from ca. 3540 to 3880 years B.P. and are indicative of the time of deposition of the Unit 1 material. The observed sand dykes must, therefore, be younger than 3500 B.P.

As shown in Fig. 5, the grain size distributions of samples from the sand dykes are similar to and within the envelope of those of the underlying Unit 2 sand samples obtained in boreholes BH1 and BH2 (Fig. 3). Fig. 5 also shows that the grain size envelope of the dyke material at Location A is similar to that of the sample recovered from 4.1 m depth in BH2. This depth coincides with a loose zone within the BH2 profile as discussed in the following section (Fig. 6), and suggests that the sand dyke material originated from this zone.

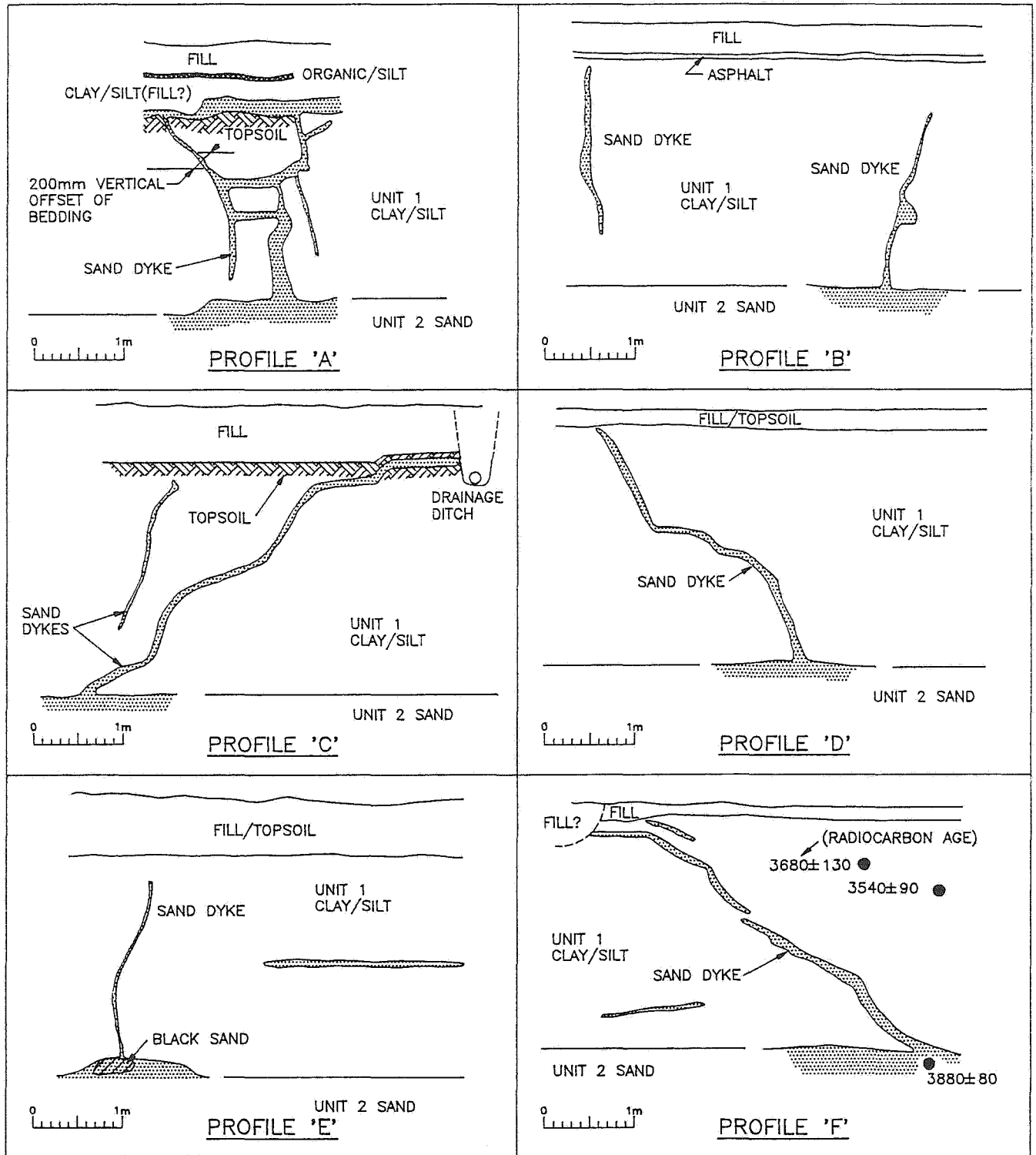


Fig. 4 Profiles of Sand Dykes

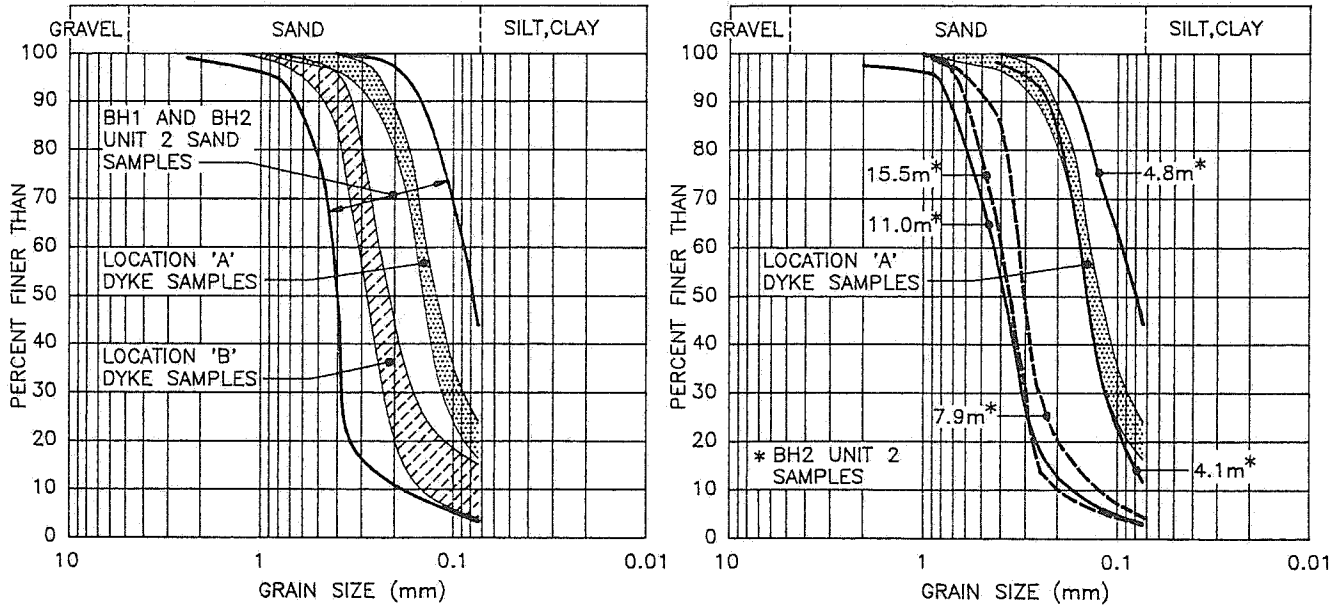


Fig. 5 Grain Size Distribution of Sand Dykes and In-Situ Unit 2 Sands

In-Situ Tests and Liquefaction Assessments

In-situ tests were conducted in the vicinity of the sand dykes. These include Standard Penetration tests (SPT) in mud rotary boreholes, static cone penetration tests (CPT), Becker penetration tests, dynamic cone penetration tests and downhole seismic tests. Samples were collected from the drill holes, and laboratory tests were conducted which included grain size sieve/hydrometer analyses and Atterberg limits, where appropriate. All the tests were conducted prior to densification by dynamic compaction. Due to space limitations, limited data from two locations only are presented in this paper.

Figs. 6 and 7 summarize the pertinent field and laboratory test results at Locations A and B, respectively. The CPT included measurements of cone tip resistance, sleeve friction and pore pressure. The SPT was conducted using the rope and cathead technique and following the procedure recommended in Seed et al. [6]. A donut hammer was used in BH1, while a safety hammer was used in BH2. SPT energy measurements were performed in accordance with ASTM D4633-86 [7]. As shown in Figs. 6 and 7, both the CPT tip resistance and the SPT N_{60} values show that the upper portions of the Unit 2 sand deposit are loose.

The SPT and CPT test results were analyzed to assess the susceptibility of the Unit 2 sands to seismically induced liquefaction. Two basic approaches were employed: deterministic and probabilistic. In the deterministic approach, commonly referred to as the Seed's simplified procedure, the cyclic stress ratio (CSR) caused by the design earthquake was compared to the cyclic resistance ratio (CRR) of the soil, at each depth under consideration, and a factor of safety against triggering liquefaction was calculated: $FS = CRR/CSR$.

The earthquake induced CSR, τ_{av}/σ'_o , was calculated from Seed's formula

$$\tau_{av}/\sigma'_o = 0.65 (\sigma_o/\sigma'_o) A_{max} r_d \quad (1)$$

where τ_{av} is the average shear stress caused by the earthquake, σ_o is the total vertical stress, σ'_o is the effective vertical stress, A_{max} is the maximum ground surface acceleration in gravity units, and r_d is a stress reduction factor which accounts for the flexibility of the soil. Significant amplification of acceleration through the deep Fraser deltaic sequence is anticipated, similar to that which occurred at deep soft soil sites during the 1985 Mexico earthquake and the 1989 Loma Prieta earthquake. For a design peak acceleration on bedrock of 0.21g, the expected peak ground surface

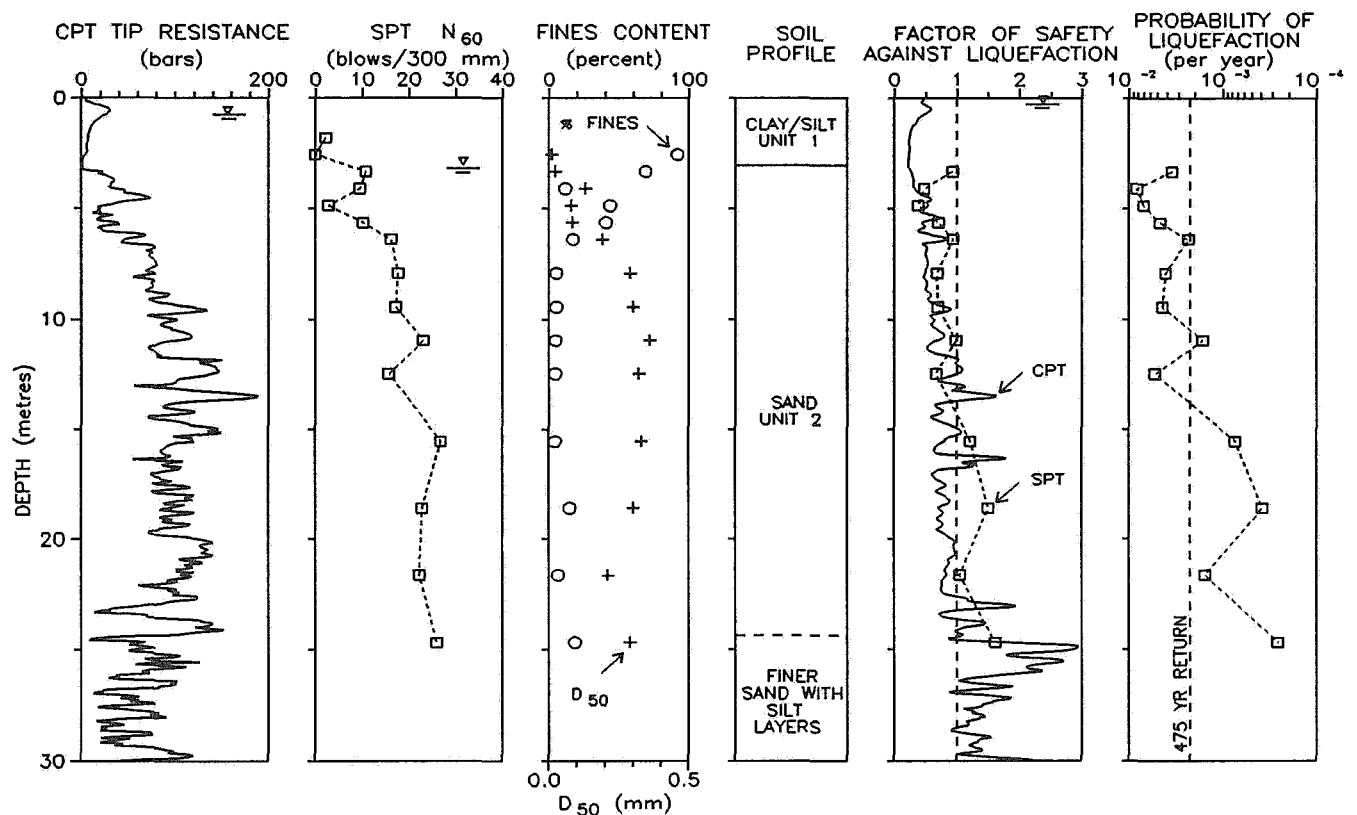


Fig. 6 In-situ Test Data and Liquefaction Potential at Location A

acceleration is 0.3g [8]. This A_{max} value was used in Eq. (1), together with "local" r_d values considered appropriate for Fraser delta soils [9].

The CRR is primarily dependent on soil density and can be determined from empirical correlations with penetration resistance developed by Seed et al. [6] and others. For this study, both the SPT blow counts (N_{60} values) and the CPT tip resistances were used to estimate the CRR. For the SPT, the correlations of Seed et al. [6] were used, while for the CPT, the correlations of Shibata and Teparaksa [10] were used. Appropriate corrections for groundwater table, SPT hammer energy, grain size and earthquake magnitude were considered.

The calculated factors of safety against liquefaction are plotted versus depth in Figs. 6 and 7 for Locations A and B, respectively. The results indicate that extensive liquefaction will occur down to about 14 m depth under the design earthquake ground motion ($M7$; $A_{max}=0.3g$). The CPT-based results suggest even more extensive liquefaction than the SPT-

based results, consistent with the more conservative correlations of Shibata and Teparaksa [10].

The probabilistic liquefaction analysis was done using a modified version of the PROLIQ2 program [11]. This simple probabilistic method combines the Cornell-McGuire method of hazard analysis and Seed's simplified method of liquefaction assessment to calculate the probability of liquefaction. The modified version, PROLIQ3, considered local soil amplification effects as suggested by Idriss [12] for different earthquake magnitudes at soft soil sites. Based on SPT N_{60} , the computed profiles of probability of liquefaction per annum versus depth are shown in Figs. 6 and 7. The results of the analysis indicate that the probabilities of liquefaction in the top 12 m depth are much higher than the annual probability of exceedance of 0.0021 (1 in 475 years) adopted by the NBCC for conventional structures. These results are also in agreement with the results from the deterministic liquefaction analysis.

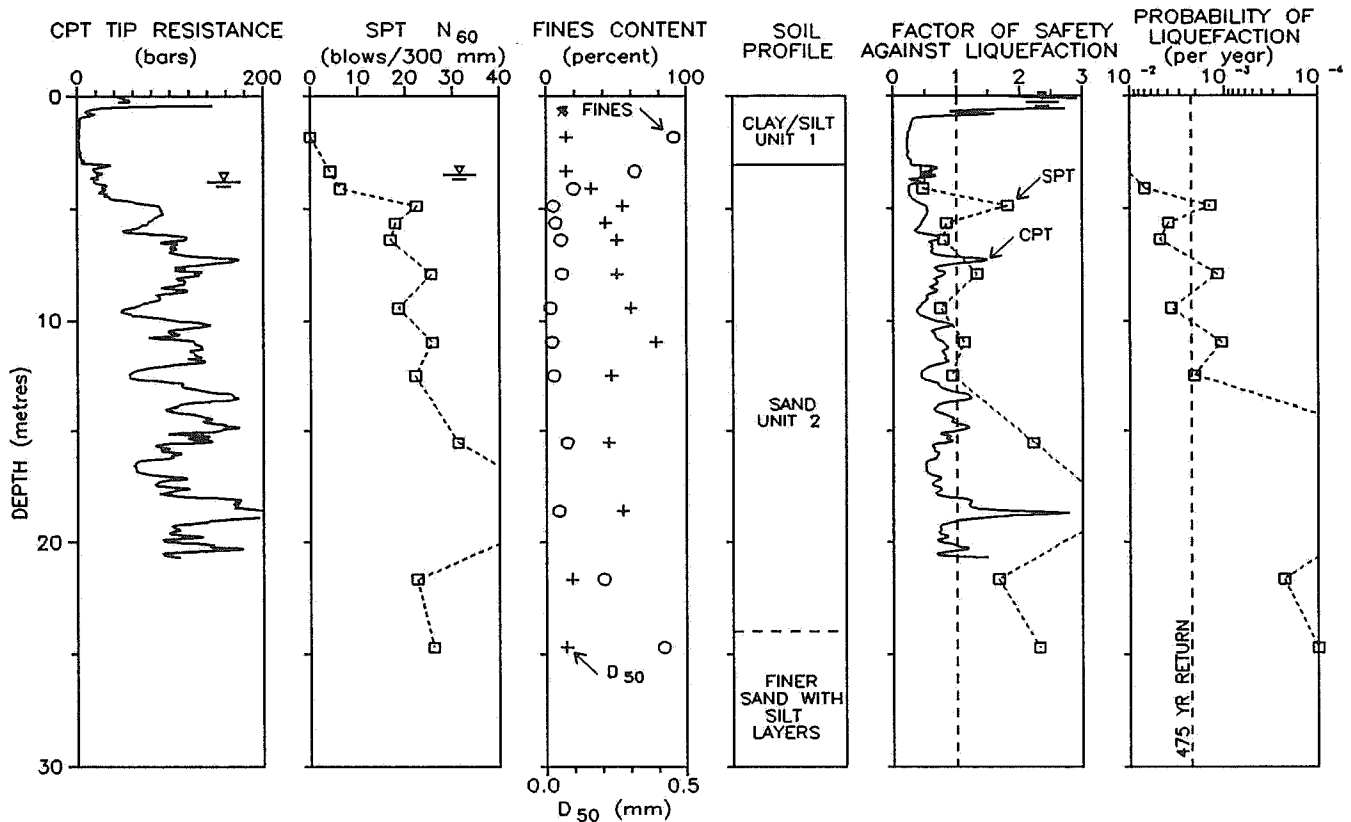


Fig. 7 In-situ Test Data and Liquefaction Potential at Location B

Remedial Measures

As discussed earlier, the sand fill and the Unit 2 sands at the Kwantlen site were densified using the dynamic compaction procedure in order to reduce the liquefaction risk and to allow the proposed structure to be founded on spread footings. Fig. 8 compares the CPT tip resistances and the calculated factors of safety against liquefaction before and after ground densification in the vicinity of Location A. It can be seen that there has been a significant reduction in the liquefaction potential in the upper 10 to 12 m. Some liquefaction may still occur below the densified zone. This deep liquefaction may cause some differential settlement, but should not cause bearing capacity failure or collapse of the structure. Some gravel drain columns were placed through the densified soil, using the vibro-replacement technique, in order to allow dissipation of excess pore pressures which might build up below the densified zone during a major earthquake.

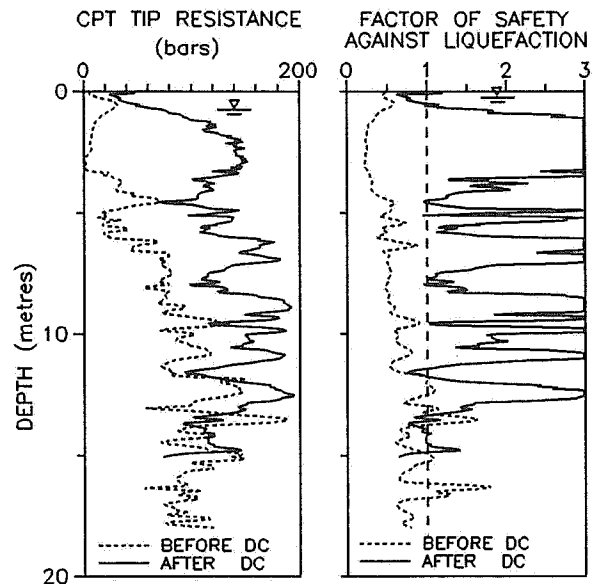


Fig. 8 CPT Profiles and Liquefaction Potential Before and After Dynamic Compaction (DC)

Conclusions

The numerous sand dykes observed during foundation excavation at the Kwantlen site are believed to have been caused by earthquake-induced liquefaction. The sand dykes originated from a shallow sand unit and cut into or through an overlying 3 m thick clay/silt crust. The grain sizes of the sand dyke materials fall within the gradation envelope of the source sands, and, in fact, are similar to the grain sizes of samples from the upper looser zones of the sand unit. Analyses of liquefaction potential, using both deterministic and probabilistic approaches and based on in-situ penetration tests conducted at the sand dyke locations, confirm that the upper portions of the sand unit, down to about 12 m depth, are susceptible to liquefaction when subjected to ground motions even below the NBCC design earthquake motion.

Acknowledgements

The authors thank Macleod Geotechnical Ltd., Klohn Leonoff Ltd. and Geological Survey of Canada for their support during the study. The assistance of the following companies and institutions during the field and laboratory investigations is gratefully acknowledged: Kwantlen College, Foundex Explorations Ltd., University of British Columbia In-Situ Testing Group, SDS Drilling Ltd., Conetec Investigations Ltd., Mud Bay Drilling Ltd., B.C Hydro and IsoTrace Laboratory. The drafting assistance of Mr. F. Chow, Klohn Leonoff Ltd., is also acknowledged.

References

- [1] Clague, J.J., Naesgaard, E. and Sy, A. 1992. Liquefaction Features on the Fraser Delta - Evidence for Prehistoric Earthquakes? Submitted to Canadian Journal of Earth Sciences.
- [2] Clague, J.J., Luternauer, J.L. and Hebda, R.J. 1983. Sedimentary Environments and Postglacial History of the Fraser Delta and Lower Fraser Valley, British Columbia. Canadian Journal of Earth Sciences, 20: 1314-1326.
- [3] Clague, J.J., Luternauer, J.L., Pullan, S.E. and Hunter, J.A. 1991. Postglacial Deltaic Sediments, Southern Fraser river Delta, British Columbia. Canadian Journal of Earth Sciences, 28: 1386-1393.
- [4] Basham, P.W., Weichert, D.H., Anglin, F.M. and Berry, M.J. 1982. New Probabilistic Strong Seismic Ground Motion Maps of Canada - A Comparison of Earthquake Source Zones, Methods and Results. Earth Physics Branch, Open File 82-33.
- [5] Sy, A., Henderson, P.W., Lo, R.C., Siu, D., Finn, W.D.L. and Heidebrecht, A.C. 1991. Ground Motion Response for Fraser Delta, British Columbia. Proceedings 4th International Conference on Seismic Zonation, Stanford, California.
- [6] Seed, H.B., Tokimatsu, K., Harder, L.F. and Chung, R.M. 1985. The Influence of SPT Procedures in Soil Liquefaction Resistance Evaluations. ASCE J. Geotech. Eng. Div., 111, 12: 1425-1445.
- [7] ASTM Standard D4633-86. Standard Test Method for Stress Wave Energy Measurement for Dynamic Penetrometer Testing Systems.
- [8] Idriss, I.M. 1990. Response of Soft Soil Sites during Earthquakes. H. Bolton Seed Memorial Symposium Proceedings, 2: 273-289.
- [9] Richmond Task Force. 1991. Earthquake Design in the Fraser Delta: Geotechnical Aspects. 26pp.
- [10] Shibata, T. and Teparaksa, W. 1988. Evaluation of Liquefaction Potentials of Soils using Cone Penetration Tests. Soils and Foundations, 28, 2: 49-60.
- [11] Atkinson, G.M., Finn, W.D.L. and Charlwood, R.G. 1986. PROLIQ2, A Computer Program for Estimating the Probability of Seismic Liquefaction including both Areal and Fault Sources. Dept of Civil Eng., University of British Columbia.
- [12] Idriss, I.M. 1991. State-of-the-Art Presentation at the 2nd Inter. Conf. on Recent Advances in Geotech. Earthquake Eng. and Soil Dynamics, St. Louis, Missouri.

Seismic Response of Deep Stiff Clay Deposits

Jonathan D. Bray

*Dept. of Civil Engineering
Purdue University, West Lafayette, Indiana*

Jean-Lou Chameau

*Dept. of Civil Engineering, Georgia Institute of Technology
Atlanta, Georgia*

Soumitra Guha

Purdue University, West Lafayette, Indiana

ABSTRACT

The localized patterns of heavy damage during the 1989 Loma Prieta earthquake demonstrate the importance of understanding the seismic response of deep clay deposits. In the Oakland area, peak ground accelerations were amplified by a factor of 2 to 4, and spectral accelerations at some frequencies were amplified by a factor of 3 to 6. Although the soft Young Bay Mud deposits are often cited as the "culprit" of amplified ground motions, significant soft clay deposits are not present at the strong motion sites in the Oakland area. Preliminary one dimensional wave propagation analyses, as well as the results of recent studies of the influence of soil conditions on ground motions during earthquakes, suggest that deep stiff clay deposits may influence ground motions much more significantly than previously considered.

Introduction

The 1985 Mexico and the 1989 Loma Prieta earthquakes provided well-documented evidence of the importance of local ground conditions on ground shaking and damage patterns. In many cases, deep clay deposits amplified the levels of shaking produced at the ground surface during these events. For example, as a result of these site specific effects during the 1989 Loma Prieta earthquake, well over half of the economic damage and more than 80 percent of the loss of life occurred on considerably less than one percent of the land area within 80 kilometers of the fault rupture zone [1]. High levels of ground shaking and damage were typically observed along the edge of the San Francisco Bay where the Bay Clay deposits (both Young Bay Mud and Old Bay Clay) were significant. Old

Bay Clays are the silty clay deposits comprising a significant part of the San Antonio and Alameda formations [2].

Considerable effort has been devoted toward developing analytical techniques for evaluating the seismic response of soil deposits. Practicing engineers often employ these analytical procedures in the evaluation of potential seismic hazards at project sites. Yet, the accuracy and reliability of seismic response analyses are highly dependent on the characterization of the sub-surface conditions and the evaluation of the dynamic properties of critical soil strata. Whereas recent investigations motivated by the damaging seismic response of soil deposits during earthquakes have provided valuable insights regarding the seismic response of specific soil deposits (e.g. San Francisco Young Bay Mud), the characteristics and effects of stiffer

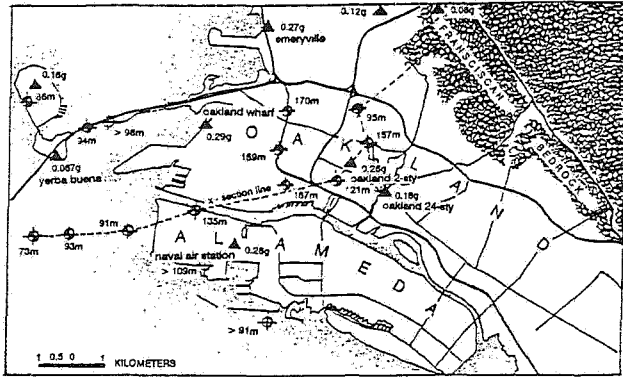


FIG. 1 -- Recorded peak ground accelerations and depth to bedrock in the Oakland area; after Rogers [7]

deposits such as the deep San Francisco Old Bay Clay deposits have received very little attention.

Observed Seismic Response of Deep Clay Deposits

The strong shaking of the 1989 Loma Prieta earthquake produced heavy damage in the Oakland area. In addition to the dramatic collapse of the Cypress Structure (I-880), over 2000 buildings in the Oakland area were damaged. The five strong motion stations in the Oakland area recorded peak horizontal accelerations in the range of 0.18g to 0.29g (Fig. 1). The 0.18g and 0.26g peak accelerations were recorded at the ground floor level of 24 story and 2 story buildings, respectively. The other sites recorded free field motions. As shown in Fig. 2, established ground motion attenuation relationships which provide peak horizontal bedrock acceleration values versus distance from the zone of energy release do a reasonably good job of fitting the recorded peak acceleration data at most sites ("soft soil" sites are not included). The mean recorded peak accelerations in the Oakland area, however, are consistently over three standard deviations greater

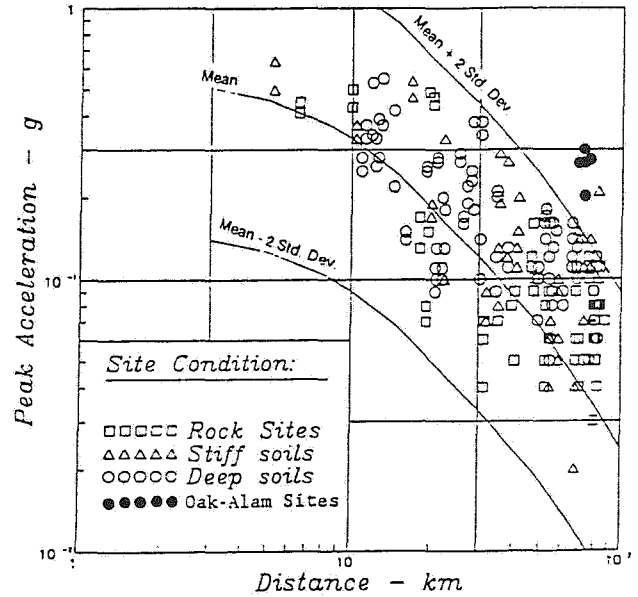


FIG. 2 -- Peak ground accelerations recorded during the 1989 Loma Prieta earthquake and Joyner and Boore [3] attenuation relationship

in magnitude than that predicted by the Joyner and Boore [3] attenuation relationship.

Although the soft Young Bay Mud deposits are often cited as the primary cause of the abnormally high peak accelerations recorded during the 1989 Loma Prieta earthquake, this is clearly not the case for the majority of the high peak accelerations recorded in the Oakland area. Of the five recorded motions in this area, only the Alameda Naval Air Station instrument is situated atop a significant deposit of Young Bay Mud (approximately 15 to 20 m thick). In contrast, soil borings indicate that the other four sites have insignificant Young Bay Mud deposits (less than 3 m thick). In fact, the two story office building strong motion station in downtown Oakland recorded a peak surface acceleration of 0.26g, although no Young Bay Mud deposits exist in this area.

Previous studies of the influence of soil conditions on recorded ground motions during earthquakes identified the adverse effects of deep soft clay

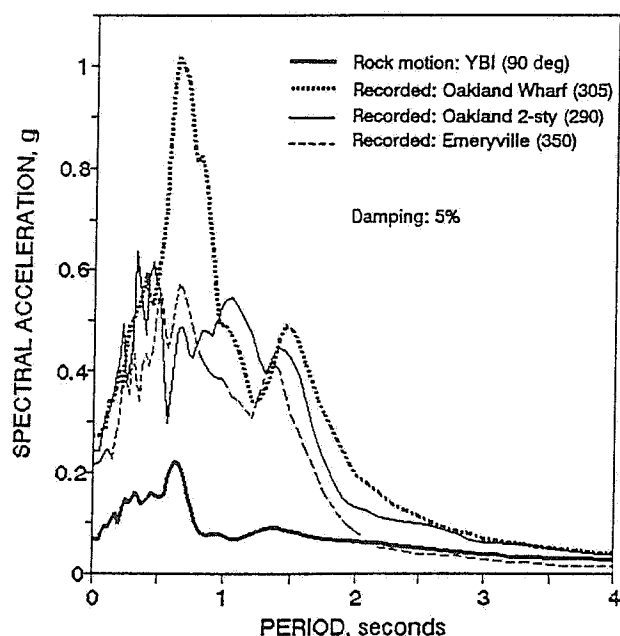


FIG. 3 -- Response spectra for three deep soil sites in the Oakland area: 1989 Loma Prieta earthquake

deposits [4]. Consequently, much effort has been devoted toward characterizing the geometric distribution and the dynamic soil properties of a number of soft clays. The results of these studies also suggest, however, that deep clay deposits that are medium stiff to very stiff in consistency may significantly amplify ground motions. After an in-depth study of the response of Young Bay Mud, alluvium and rock sites during major Loma Prieta aftershocks, Hough and others concluded that the Young Bay Mud is not solely responsible for site amplification effects, but that the underlying unconsolidated sediments can greatly amplify earthquake shaking [5].

In addition, a number of studies suggest that local topographic features may focus strong motion energy and amplify ground motions [6]. The geology in the San Francisco Bay area is quite complex, yet it appears reasonable and a number of deep soil borings suggest that the Franciscan bedrock unit underlying the thick quaternary deposits of the East

Bay area varies considerably in depth across the area [7]. Alternate periods of erosion and deposition have produced buried canyons in the bedrock. Hence, three dimensional effects on the propagation of seismic waves may be significant in the Oakland area because of the local geology.

Amplification of Strong Motions at Deep Clay Soil Sites

The amplification of higher period ground motions is one of the most critical effects of the seismic response of clay soil sites. Whereas this effect is recognized at Young Bay Mud sites, it has not received as much attention at deep stiff clay sites. The response spectra of ground motions recorded at three "non-Young Bay Mud" sites in Oakland, however, show considerable spectral amplification of long period motions (Fig. 3). If the stiffer clay deposit is sufficiently deep, longer period ground motions can be produced at deep stiff clay sites. A rough estimate of a site's predominant period can be calculated by the formula: $T_s = 4D/V_s$, where T_s = predominant period, D = thickness of soil, and V_s = average shear wave velocity of the soil. For example, at Young Bay Mud sites where the thickness of the clay ranges from 12 to 24 m and the average shear wave velocity ranges from 90 to 180 m/sec, the site's predominant period is estimated to be in the range of 0.25 to 1.0 seconds. Likewise, at deep Old Bay Clay sites where the thickness of the clay ranges from 30 to 90 m and the average shear wave velocity ranges from 200 to 500 m/sec, the site's predominant period is estimated to be in the range of 0.25 to 1.5 seconds. Hence, deep stiff clay sites have the potential for producing heavy damage in a wide range of buildings (2 to 15 story) having predominant periods close to that of the underlying deposit.

TABLE 1 -- Site coefficients recommended
by the 1988 UBC

Type	Description	S Factor
S ₁	A soil profile with either: (a) A rock-like material characterized by a velocity greater than 2,500 feet per second or by other suitable means of classification, or (b) Stiff or dense soil condition where the soil depth is less than 200 feet.	1.0
S ₂	A soil profile with dense or stiff soil conditions, where the soil depth exceeds 200 feet.	1.2
S ₃	A soil profile 40 feet or more in depth and containing more than 20 feet of soft to medium stiff clay but not more than 40 feet of soft clay.	1.5
S ₄	A soil profile containing more than 40 feet of soft clay.	2.0

The 1988 Uniform Building Code recognizes the significant influence of soft clay sites greater than 12 m thick on the ground motions and damage observed during earthquakes. The site coefficient for soil characteristics (S factor) is increased to 2.0 for the "soft soil" profile S₄ (see Table 1; a S factor of 1.0 is used at "rock" sites). On the other hand, a 90 m thick deposit of stiff Old Bay Clay could be categorized as soil profile S₂ with an S factor of only 1.2. The seismic response of the deep stiff Old Bay Clay sites during the 1989 Loma Prieta earthquake with spectral acceleration amplification factors on the order of 3 to 6 (Fig. 3) suggest that we may be currently underestimating the seismic hazard at these sites.

The recorded motions at well-documented sites throughout the East San Francisco Bay area during the 1989 Loma Prieta earthquake provide an excellent opportunity to use the observed performance as a field laboratory to test the current practice in earthquake engineering. In particular, this study will utilize the recorded motions at three sites: (a) the Oakland Outer Harbor Wharf, (b) the Oakland 2-story office building, and (c) the Emeryville Pacific Park Plaza to evaluate the reasonableness of one-dimensional seismic response analysis and to investigate the sensitivity of the analytical results to variations in the dynamic soil properties.

Site Characterization

The seismic response of soil deposits is dictated primarily by geometric considerations (e.g. thickness of the deposit, irregular topographic conditions) and by the soil's dynamic properties (i.e. shear modulus and damping characteristics). The shear modulus (G) gives an indication of the stiffness of the soil system, whereas the damping ratio (λ) provides a measure of the soil system's ability to dissipate energy under cyclic loading. In soils, both of these dynamic properties depend greatly on the shear strain level. In fact, the shear modulus and damping ratio versus shear strain relationship is highly nonlinear within the shear strain range of 10⁻³% to 0.1% which is the range of primary interest to the earthquake engineer.

Soil boring logs and shear wave velocity measurements coupled with general reports of the subsurface conditions in the Oakland area as well as established dynamic soil property correlations provide valuable insights regarding site characterization [8,9]. Previous studies have performed a sufficient number of tests to adequately characterize the dynamic properties of Young Bay Mud and cohesionless soils, however, this is not the case for the deeper Old Bay Clay deposits. The majority of geotechnical investigations in the Oakland area have terminated their boreholes at shallower depths. Additional work is required to adequately characterize the spatial distribution and dynamic soil properties of the deeper soils. Ongoing research by the writers is attempting to address this shortcoming.

Notwithstanding the shortcomings noted above, sufficient data is available to develop preliminary characterizations of the three strong motion sites studied. Soil borings have been completed at all three sites through field work conducted

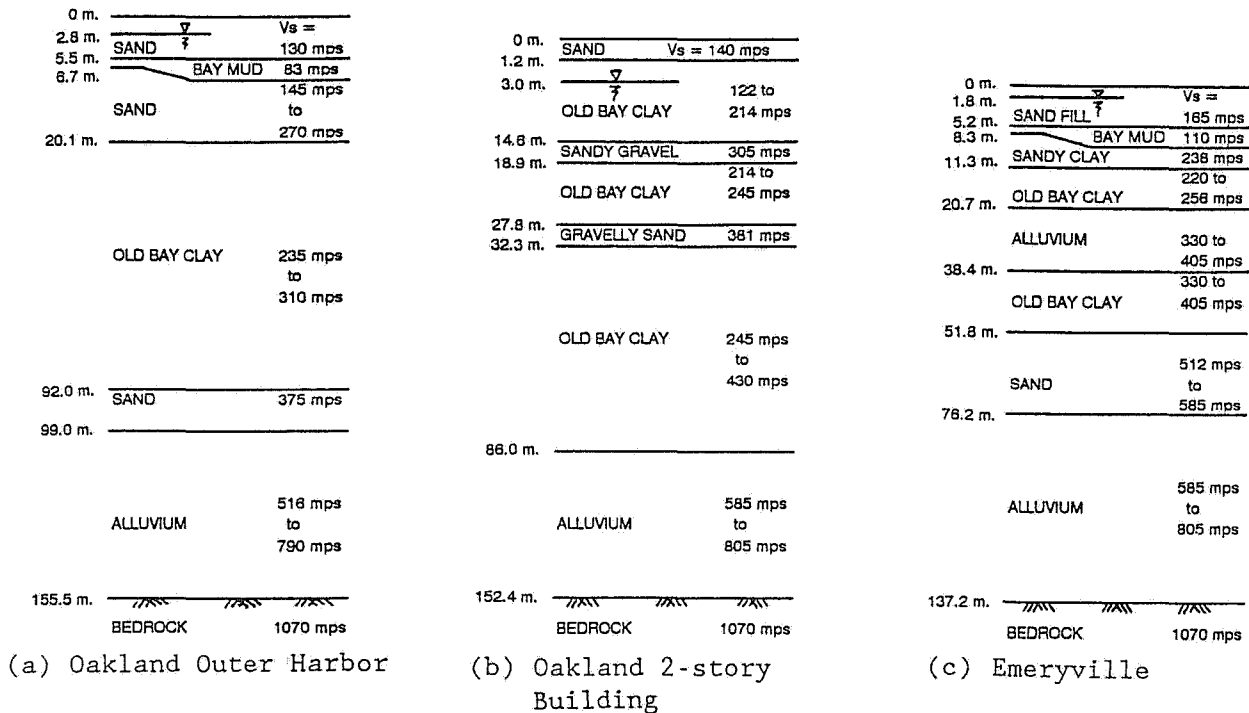


FIG. 4 -- Soil profiles used in dynamic response analyses

by the U.S. Geological Survey and initial testing on retrieved soil samples as well as some seismic shear wave velocity measurements have been performed. Using this information, the generalized soil profiles shown in Fig. 4 have been developed.

The subsurface conditions at the Oakland Outer Harbor site are known with the most confidence. The boring was terminated in competent bedrock at a depth of 155 m. Sufficient sampling was performed to characterize the principal soil horizons and in situ shear wave velocity measurements were conducted. Drilling near the Oakland 2-story building and Emeryville strong motion sites was terminated at depths of approximately 61 m before reaching bedrock. Previous borings terminated in the underlying bedrock near these sites were used to estimate the depth to bedrock. Previous seismic response analyses suggest that their results are fairly insensitive to variations in the subsurface conditions below depths of about 75 m. Shear wave velocity and

engineering properties correlations were employed to estimate the dynamic soil properties of the soil at these sites since shear wave velocity measurements were not available.

The shear wave velocity estimates define the "small strain" ($<10^{-4}\%$) dynamic shear modulus values required in the seismic response analyses, but the strain-dependent modulus reduction and damping relationships must be established. The nonlinear, strain-dependent moduli and damping for the Old Bay Clays were modeled using the relationships proposed by Vucetic and Dobry [10]. The nonlinear dynamic soil properties of Young Bay Mud, the deep alluvium, and cohesionless soils were modeled using relationships proposed by Seed and others [11,12].

Wave Propagation Analysis

The program SHAKE [13] was employed to investigate the seismic response of the three strong motion sites in the Oakland

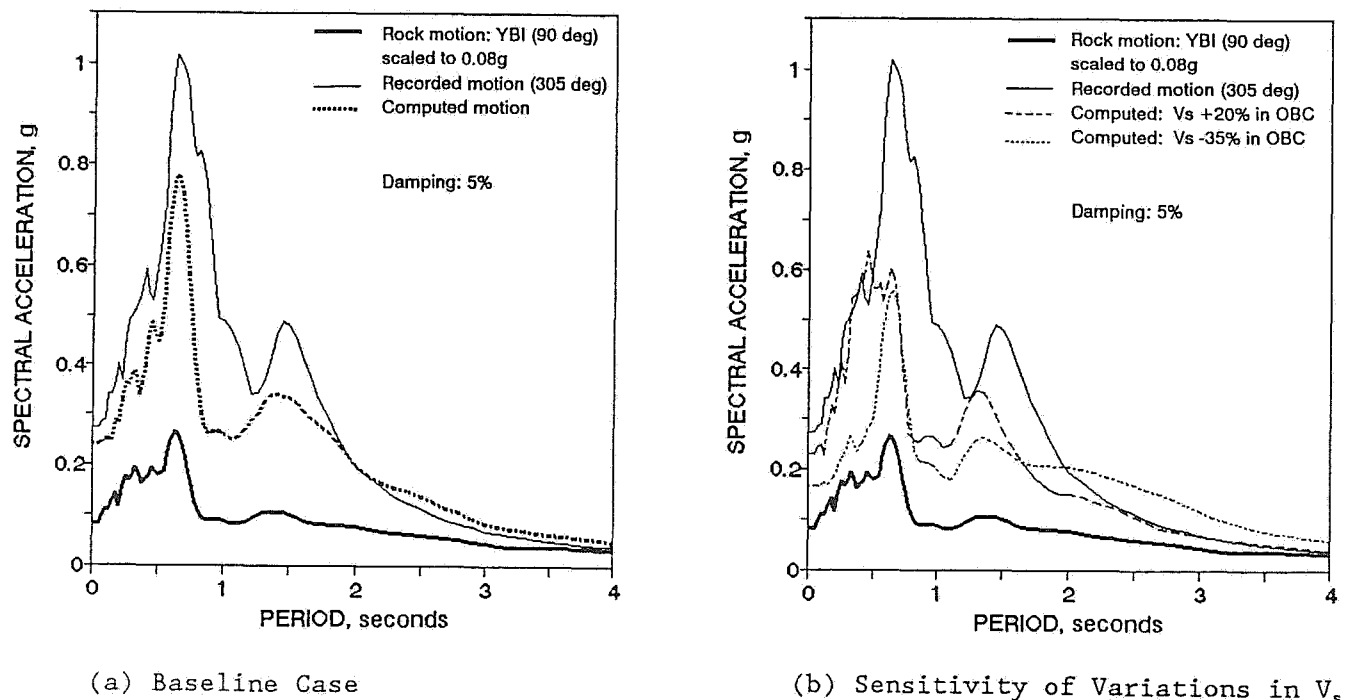


FIG. 5 -- SHAKE computed response spectra: Oakland Outer Harbor

area during the 1989 Loma Prieta earthquake. SHAKE calculates seismic site response based on the vertical propagation of shear waves through a one-dimensional column of soil. The analysis is suitable for level ground conditions which is appropriate at these three sites, however, it fails to capture the three-dimensional effects that the irregular buried bedrock topography may have produced in the Oakland area. SHAKE utilizes the equivalent linear method to model nonlinear dynamic soil moduli and damping as a function of shear strain.

Representative results of the one-dimensional wave propagation analyses of the Oakland Outer Harbor strong motion site are shown in Fig. 5. Available strong motions recorded at nearby "rock" sites were assessed and the Yerba Buena Island rock motion was judged to be most representative showing a higher concentration of energy at higher frequencies (>1.4 Hz) in the motion. The peak ground acceleration was slightly lower

than at the other "rock" sites so the acceleration time record was scaled to a more representative peak acceleration of 0.08g. As shown in Fig. 5(a), the 1-D seismic response analysis was able to capture the tendency of this deep stiff clay site to amplify motions, and the computed response spectra is in fair agreement with the recorded motion. The computed peak ground acceleration and maximum spectral acceleration were roughly 20% below that of the values recorded. A better match was obtained if the input rock acceleration time record was scaled to a peak acceleration of 0.10g, but this magnitude was judged to be an upper bound value rather than representative value.

Previous studies suggest that the results of dynamic analyses are sensitive to minor variations in the strain-dependent damping relationships, but reducing the level of damping in the Old Bay Clay had very little effect on the computed response spectra. In addition, modifying the level of "effec-

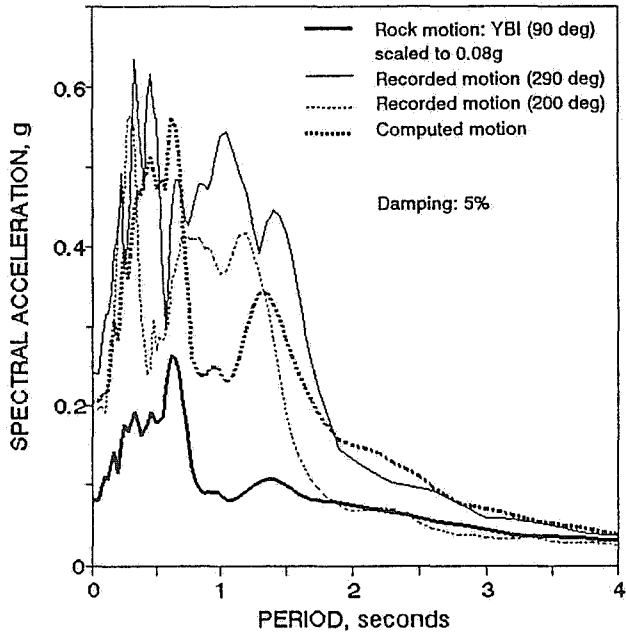


FIG. 6 -- SHAKE computed response spectra: Oakland 2-story Building

tive" strain (0.35 to 0.55) used in SHAKE to select the equivalent linear, strain-dependent moduli and damping had a minimal effect on the computed motion. Minor variations in the shear wave velocity used to establish the "small strain" shear moduli in the Old Bay Clay deposits did, however, produce significant variations in the computed response (Fig. 5(b)). Hence, the computed motions at these deep stiff clay sites during the 1989 Loma Prieta earthquake were strongly dependent on the selection of reasonable dynamic soil properties, especially the shear moduli values which influence the predominant period of these soil profiles.

Analysis of the strong motions at the Oakland 2-story building site are complicated by the fact that these motions are not free field motions but were recorded at the ground floor of a structure. The two horizontal recorded motions differ appreciably (Fig. 6). The SHAKE computed motion, however, fits the general trends indicated by the

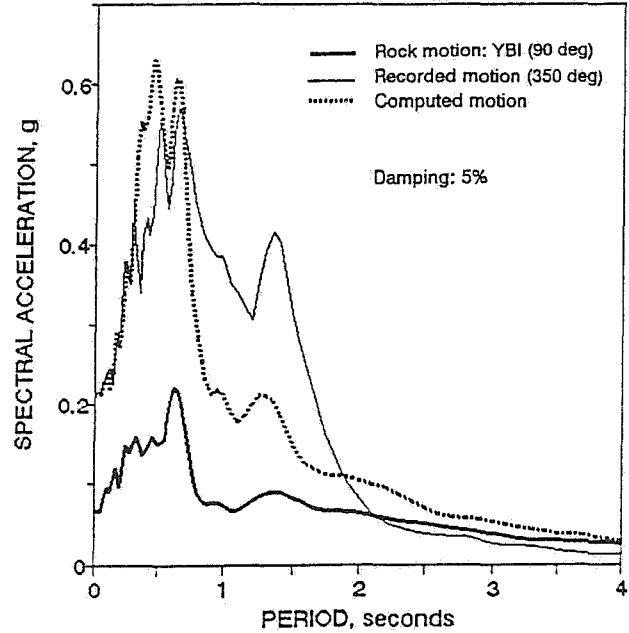


FIG. 7 -- SHAKE computed response spectra: Emeryville

the recorded motions, except at frequencies near 1 Hz. Near this frequency, the spectral accelerations predicted by the level ground, free field, 1-D seismic response analysis is less than half of that indicated in the recorded motions.

The results of the Emeryville seismic site response analyses show a similar tendency of underestimating the recorded motions at periods within the range of 1 to 1.5 seconds (Fig. 7). Up to periods on the order of one second, the agreement between the computed and record responses is excellent.

Conclusions

Previous studies in the San Francisco Bay Area as well as other parts of the world have focused on investigating the seismic response of soft clay deposits and potentially liquefiable fills and sand deposits. At a number of sites in the Bay area without significant

deposits of these materials, however, the 1989 Loma Prieta earthquake produced high peak ground accelerations and considerable spectral amplification of long period motions. It appears that deep stiff clay deposits were principally responsible for these abnormally high ground motions. This finding is important as deep stiff clay deposits exist in many earthquake prone areas around the world.

Overall, the seismic response analyses were able to provide reasonably accurate predictions of the motions recorded at three deep stiff clay sites in the Oakland area during 1989 Loma Prieta earthquake. The 1-D analyses provided good approximate predictions of the peak ground accelerations and captured the general response of the sites at most frequencies. At frequencies near 1 Hz, however, the computed response significantly underestimated the observed response at these sites. It is not known if this is a failure of the analytical procedures or if soil-structure interaction or 3-D effects produced higher spectral accelerations in the recorded motions near this frequency. The results of seismic response analyses are quite sensitive to the characteristics of the input rock motions so it is likely that the use of the Yerba Buena motion as the input motion may have also contributed to this discrepancy. Finally, the results of the analyses were sensitive to the dynamic soil properties of the Old Bay Clay, especially its shear wave velocity or small strain shear modulus.

Acknowledgements

The authors wish to thank the researchers at the U.S. Geological Survey at Menlo Park, CA, especially Jim Gibbs and Tom Fumal who allowed us to participate in their drilling program, Dr. Fernando Reyna of Purdue University who initiated the preliminary dynamic analyses, and Mr. Steven Dickenson of

U.C. Berkeley who provided useful data. Partial support to recover soil samples from the USGS drilling program was provided by the National Science Foundation under grant No. BSC-9003473.

References

- [1] Seed, R.B., et al. (1990), "Preliminary Report on the Principal Geotechnical Aspects of the October 17, 1989 Loma Prieta Earthquake", Rpt. No. UCB/EERC-90/05, Univ. of Calif., Berk., April, 137 pp.
- [2] Trask, P.D. and Rolston, J.W. (1951), "Engineering Geology of San Francisco Bay, California", Bull. of the Geol. Soc. of Amer., Vol. 62, pp. 1079-1110.
- [3] Joyner, W.B. and Boore, D.M. (1988), "Measurement, Characteristics and Prediction of Strong Ground Motion: State-of-the-Art Report", Proc., Spec. Conf. on Earthquake Engrg. and Soil Dyn. II, ASCE, 102.
- [4] Seed, H.B. (1986), "Influence of Local Soil Conditions on Ground Motions and Building Damage During Earthquakes", The Eighth Nabor Carrillo Lecture, Mex. Soc. for S M, XIII, Mazatlan, Mexico, Nov. 22.
- [5] Hough, S.E., et al. (1990), "Sediment-Induced Amplification and the Collapse of the Nimitz Freeway", Nature, MacMillan Mag., Ltd, pp. 853-855.
- [6] Aki, K. (1988), "Local Site Effects on Strong Ground Motion", Proc., Spec. Conf. on Earthquake Engrg. and Soil Dynamics II, ASCE, pp. 103-155.
- [7] Rogers, J.D. (1991), "Site Stratigraphy and Its Effects on Soil Amplification in the Greater Oakland Area During the October 17, 1989 Loma Prieta Earthquake", Proc., Sec. Inter. Conf. on Rec. Adv. in Geotech. Eq. Eng. and Soil Dyn., St. Louis, March 11-15.
- [8] Dickenson, S.E. and Seed, R.B. (1992), "Correlations of Shear Wave Velocity and Engineering Properties for Soft Soil Deposits in the San Francisco Bay Region", Rpt. No. UCB/EERC-92/XX., Univ. of Calif., Berkeley. in press.
- [9] Goldman, H.B. Ed. (1969), "Geologic and Engineering Aspects of San Francisco Bay Fill", Calif. Div. Mines & Geology; Spec. Rpt. 97, 130p.
- [10] Vucetic, M. and Dobry, R. (1991), "Effect of Soil Plasticity on Cyclic Response", Geotech. Engrg., ASCE., Vol. 117, No. 1, Jan., pp. 89-107.
- [11] Sun, J.I., et al. (1988), "Dynamic Moduli and Damping Ratios for Cohesive Soils", Report No. UCB/EERC-88/15, Univ. of Calif., Berk., Aug..
- [12] Seed, H.B., et al. (1984), "Moduli and Damping Factors for Dynamic Analyses of Cohesionless Soils", Univ. of Calif., Rpt. No. UCB/EERC-84/14, Berk.
- [13] Schnabel, B., Lysmer, J. and Seed, H.B. (1972), "SHAKE, A Computer Program for Earthquake Response Analysis of Horizontally Layered Sites", EERC Rpt. 72-12, Univ. of Calif., Berkeley, Dec.

Seismic Hazard Analysis for San Juan, Puerto Rico

R.J. Deschamps

Purdue University, West Lafayette, Indiana

D.R. Putz

*Haley & Aldrich
Rochester, New York*

K.G. Sutterer

*Georgia Institute of Technology
Atlanta, Georgia*

Introduction

The island of Puerto Rico is surrounded by seismically active zones with significant potential for large or great earthquakes. These zones feature different but related tectonics. Regardless, the active depths, recurrence relations, nature of source, and perceived potential for large events are dissimilar for each case.

San Juan (pop. 426,600) is on the north coast of Puerto Rico, near the northeast corner of the island (Figures 1). This paper summarizes a preliminary study of the seismicity of the San Juan, Puerto Rico area.

Local Geology

The general geology of the island of Puerto Rico is summarized in detail elsewhere [1,2,3]. The geology of the San Juan area features slightly deformed marine limestone, marl, and claystone dipping gently northward. This region contains widespread karst areas. Surficial deposits include blanket sands; eolinianite and marine calcarenite along the north coast; and alluvial, swamp, delta, piedmont, beach, and dune deposits. The depth to limestone bedrock is variable, ranging from 0 to 50 feet. Large landslide deposits are present in some areas.

Regional Tectonics

Puerto Rico is located along the northeast edge of the Caribbean continental plate. The Puerto Rico Trench, centered 60 km north of San Juan, is a combined subduction and strike/slip zone where the American plate is being subducted beneath the Caribbean plate (Figure 1).

Although Puerto Rico is known to be a part of the Caribbean plate, there is a substantial zone of downward faulting 58 km south of the island [2,4] (Muertos Trough - Figure 1). With the island of Puerto Rico moving upward with respect to the rest of the Caribbean plate, it is actually an isolated piece of the Caribbean plate. Other significant tectonic features

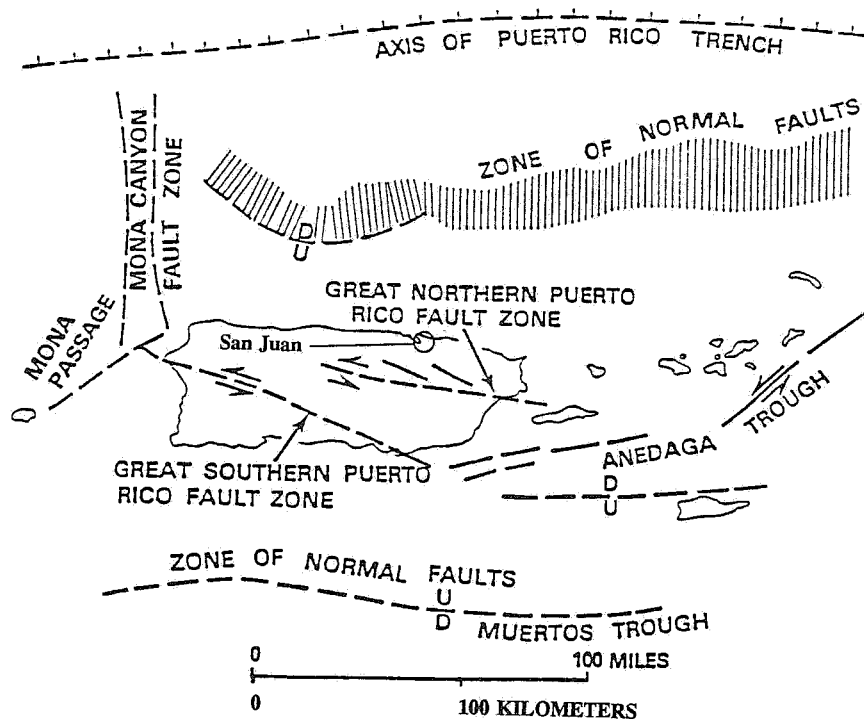


Figure 1. Puerto Rico and surrounding tectonics.

are the Anegada Trough and the Mona Canyon [2,4] (Figure 1). The Mona Canyon area is structurally complex, and its exact nature is unknown, although recorded earthquakes are generally deep (60 to 150+ km). It is believed to be an extension of the Great Southern Puerto Rico Fault Zone[4]. The Anegada Trough extends from south of Puerto Rico to beyond the Virgin Islands, and features steep scarp features. The origin and nature of this area of complex faulting is also unknown, although the area is known to be a seismic source[4].

Regional Seismicity

Molinelli [5] suggested four zones around the island that represent potential earthquake

sources: the Puerto Rico Trench, the Mona Passage/Mona Canyon area, the northern flank of the Muertos Trough, and the Anegada Trough. Of these, the Muertos is believed to represent the lowest seismic risk. The Puerto Rico Trench is believed to represent the most likely source of a great earthquake ($M > 8$), but Molinelli suggests the combined Mona Passage/Canyon, Anegada Trough, and Muertos Trough together represent a seismic risk to San Juan comparable to the Puerto Rico Trench.

McCann and Sykes [6] suggested earthquake magnitudes > 7.5 for areas all around Puerto Rico. der Kiureghian and Ang [7] suggested approximate return periods for various accelerations and Modified

Mercalli intensities on the island (Table 1).

TABLE 1 -- Estimated Mercalli intensities, accelerations and return periods for Puerto Rico.

RETURN PERIOD (years)	MODIFIED MERCALLI INTENSITY	ESTIMATED MAX. ACCELERATION (g)
50	VII	0.15
90	VII-VIII	0.18
100	VII-VIII	0.19
200	VIII	0.25
450	VIII-IX	0.33
500	IX	0.35

(after der Kiureghian and Ang, 1975)

Hazard Analysis

The numerical analyses summarized herein are based on seismic records collected by accelerographs, or surmised using conversions from the Modified Mercalli intensity. Although seismographs were in use in some areas throughout the 1900's, the distance between recorders prevented accurate collection of data for smaller events. The advent of accelerographs in the 1950's increased the practicality of many recording stations. Thus, most of the detailed records available fall within the past 30 to 40 years. Effective recording networks were not active for northern Caribbean earthquakes until the 1960's, and a Puerto Rico network was not in place until the mid 1970's [8]. Consequently, most of the data is confined to large events, and the smaller events have not been fully recorded until at least the 1960's and into the mid 1970's. No major events have occurred in the area of Puerto Rico in this time

span, so the Number of Events versus Magnitude relationship could be skewed. However, the historic information described by McCann and Sykes [6], der Kiureghian and Ang [7], and Molinelli [5] were also incorporated in this study.

Data Base

The data base for the numerical analyses was provided by the National Geophysical Data Center/NOAA in Boulder, Colorado. This data base included all recorded earthquakes in the Puerto Rico area. The plotted data is shown on Figure 2. The data available for each event included at least the location and time of occurrence, and also usually included the magnitude (by one or several scales) and depth. Most of the older data (pre 1974) was often incomplete, with depth and magnitude of somewhat questionable accuracy. The data also included codes for assessing the accuracy of the data, and these reflected the reduced accuracy of the older data.

The supplied data base was sorted using a computer program to 1) remove events without magnitude information, 2) select only data within certain designated quadrilaterals and 3) select events only within a certain range of magnitudes. Although the regional tectonics described above was helpful in selecting seismic sources, the depth of the events' source area were considered critical in selecting the radial distance from the site to the source. Consequently, a computer program was written to sort the earthquake data by depth. These

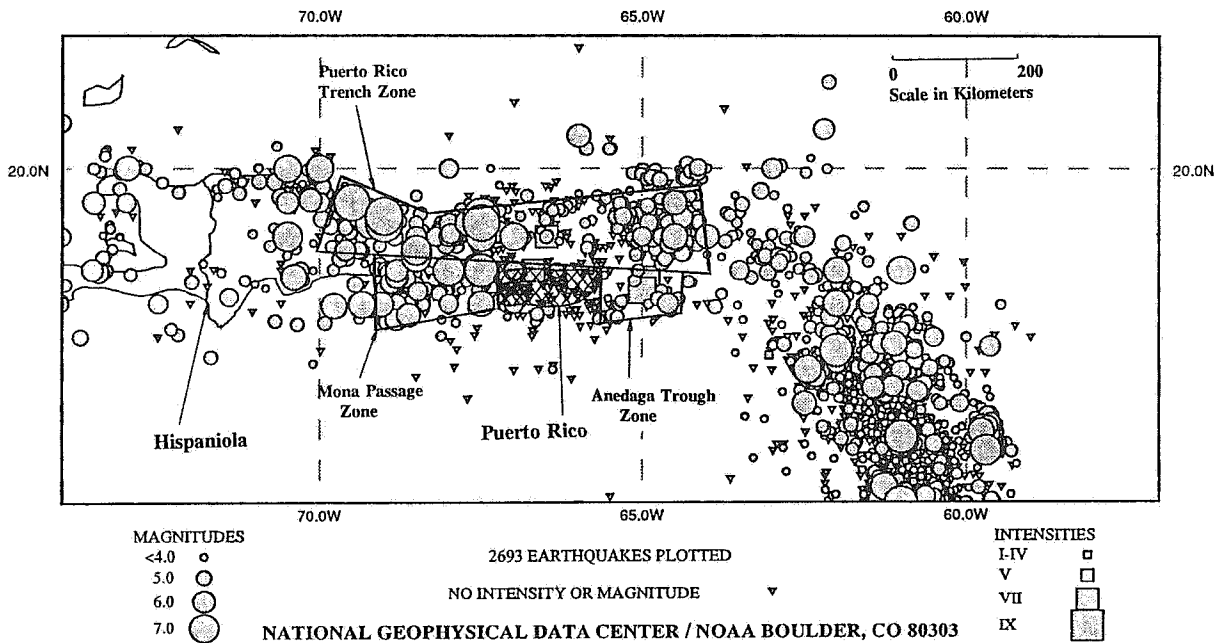


Figure 2. Regional earthquake activity and designated area sources.

efforts revealed some patterns that were used to assist in selection of source areas for the hazard analysis. This will be covered in the next section.

Seismic Sources

Three seismic sources were selected for this assessment as having the highest level of activity and the largest events within a 300 km radius of San Juan. These are the Puerto Rico Trench (PRT), the Mona Passage/Mona Canyon area (MP), and the Anegada Trough area (AT). The zones are shown on Figure 1. Generally, the three sources have significant earthquake hypocenters located between depths of 40 and 75 kilometers (Figure 3). The Puerto Rico Trench and Anegada Trough sources have some low magnitude earthquakes at shallower depths. The Mona

Passage has several earthquakes with magnitudes up to 6.1 at depths greater than 75 km.

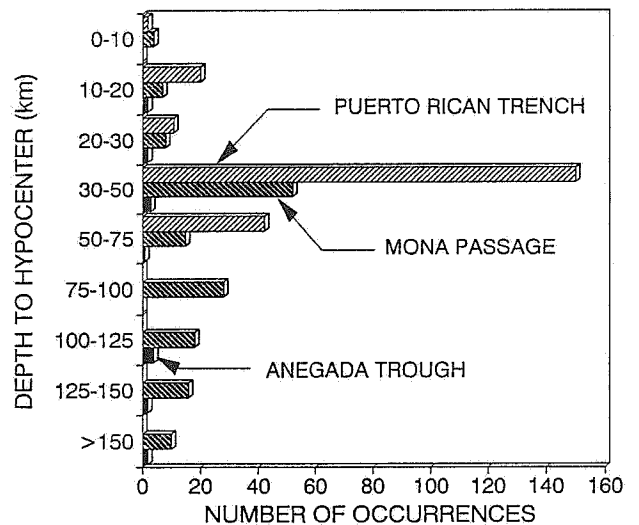


Figure 3. Earthquake occurrences sorted by depth.

Although there were a significant number of events immediately beneath the island, all of these were very small events insignificant to the numerical portion of this hazard assessment.

Recurrence Relationship

All events greater than magnitude 4.0 were selected to develop the recurrence relations. In this study, a period of the last 84 years was selected as a representative time interval. Several preliminary attempts to develop recurrence relations for the past 15 to 25 years had little effect on the recurrence relationships summarized below, and since selecting shorter time periods would eliminate several large events in the early and mid 1900's, the longer time period was employed. Linear regression was used to assign a recurrence relation to each of the data sets. The natural log of the Occurrence versus Magnitude relationship was found as follows, with slope (m) and intercept (b):

SOURCE	<u>m</u>	<u>b</u>
PRT	1.08	9.85
MP	0.87	8.38
AT	1.66	10.27

The regression analysis for the Anegada Trough data resulted in an unusually high slope (m). However, this relationship did adequately represent the data, so these coefficients were used for this study. The recurrence relation developed for the Puerto Rico Trench was considered questionable due to the presence of an area of

inactivity immediately north of Puerto Rico. This inactive zone was recognized by Molinelli [5], and McCann and Sykes [6] as a seismic "gap" capable of producing a great earthquake of $M > 8$. However, the lack of data for this area hinders reliable modelling of the recurrence relation for the zone. This is why the area was included with the more active western and eastern reaches of the Puerto Rico trench.

Inclusion of the inactive zone with the other PRT zones could unconservatively skew the hazard study, as this would result in less events distributed over a larger area. For this reason, an area correction was applied to the recurrence relation for the Puerto Rico Trench to represent some increased risk from this source. The area correction consisted of a multiplier of 1.2 on the intercept value (b) for the recurrence relation, providing:

SOURCE	<u>m</u>	<u>b</u>
PRT (unmodified)	1.08	9.85
PRT (modified)	1.075	10.03

Both of these recurrence relations were considered in the next phase of the study.

Attenuation Function

Numerous functions have been published to attempt to model the attenuation of ground motion with distance from a seismic event. There are no reasonable attenuation functions for earthquakes in the Puerto Rico area, since they are not

believed to be pure subduction zone events in most cases. Yet the events are significantly deeper than those in California for which many attenuation functions have been developed. A subduction zone relationship was selected as the best models readily available for the data considered herein. The model selected is that by Kawashima [9]. This relationship is applicable to subduction zone earthquakes with depths up to 60 kilometers, and is summarized as:

$$y = a 10^{bM} (\Delta + 30)^d$$

where

y = Peak ground acceleration
in gals

M = Japanese Magnitude

Δ = Epicentral distance in km

The coefficients selected for this study, based upon local geology of the San Juan area were:

$$\begin{aligned} a &= 2407 \\ b &= 0.216 \\ d &= -1.178 \\ \sigma_{\log y} &= 0.226 \end{aligned}$$

The Attenuation versus Distance relation for a magnitudes 7.5 event is shown on Figure 4.

Probability of Occurrence in San Juan

The Purdue University program PUHAZ [10] was used to develop probability of occurrence data for accelerations due to events at any or all of the sources. The program requires an attenuation function, recurrence relationship, and the location of each source. PUHAZ assumes uniform seismic risk within a

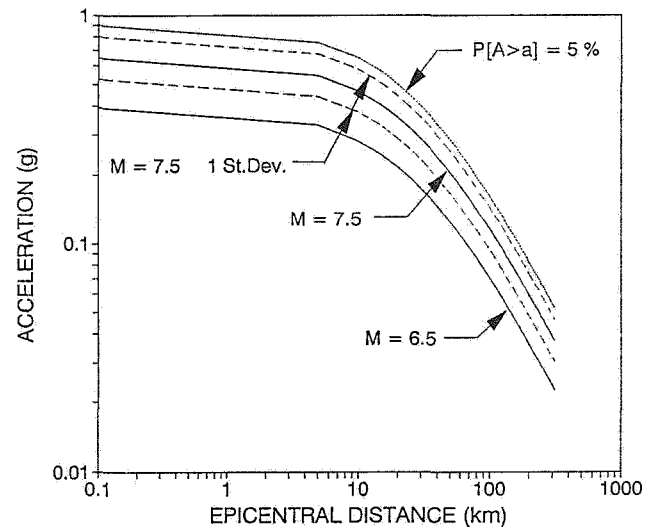


Figure 4. Kawashima acceleration attenuation relationship.

designated source area, and assumes occurrences follow a Poisson distribution. The program searches for earthquakes in circular bands emanating from the site of concern. A given seismic source will contribute a mean rate of occurrence of events equal to the fraction of the source contained in the distance band times the mean rate of occurrence for the source [10]. The findings of the hazard studies using PUHAZ are summarized in Figures 5 and 6. The Probability of Occurrence with a 50 year design life for specific accelerations is shown in Figure 6. For comparison, the Probability of Occurrence versus Acceleration relationship for the modified data is also included in this figure. This relationship demonstrates only a modest increase in acceleration values when the modified Puerto Rico Trench recurrence relation is used for the region immediately above San Juan.

The results of the above numerical analyses are considered approximate, as the time span for data collection is significantly less than the estimated return period for the larger events. This represents a limitation to any similar numerical method. However, if the recurrence relations can be estimated as linear with perhaps an upper bound, then the lack of large events should not be considered a large contribution to error. Conversely, the attenuation functions selected can have a significant affect on the conclusions to the study, and there are no assured models for this type of seismic activity.

The seismic gap north of San Juan in the Puerto Rico Trench is critical to the hazard assessment. The lack of data in this area prevents even the necessary first step of modelling, that is the selection of a recurrence relation. So despite the usefulness of the procedure described herein, engineering judgement is still an important factor. The findings and recommendations of McCann and Sykes [6] and Molinelli [5] should be considered in the hazard assessment. If a magnitude 7.5 event were to occur in the "seismic gap" zone within the Puerto Rican Trench, estimated ground accelerations on the order of 0.3 g are possible in San Juan as compared to the 0.15g estimated by this study. McCann and Sykes [6] suggested a return period on the order of 200 years for this zone. The most recent event believed to originate in this zone was in 1787 and was of a Modified Mercalli intensity VIII to IX.

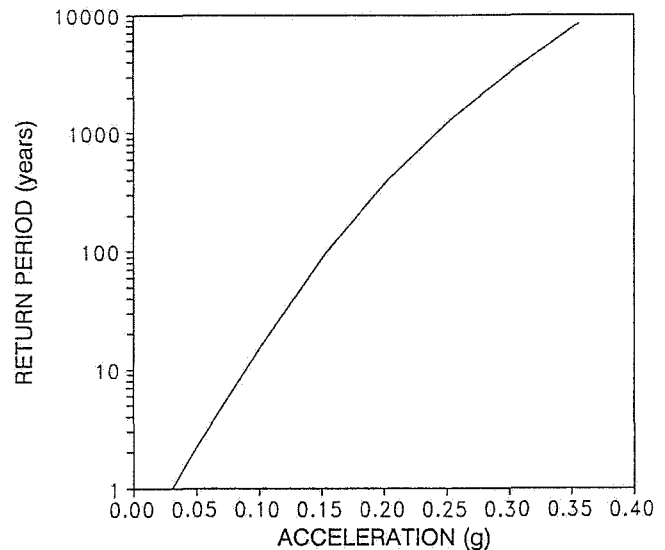


Figure 5. Ground acceleration and return period.

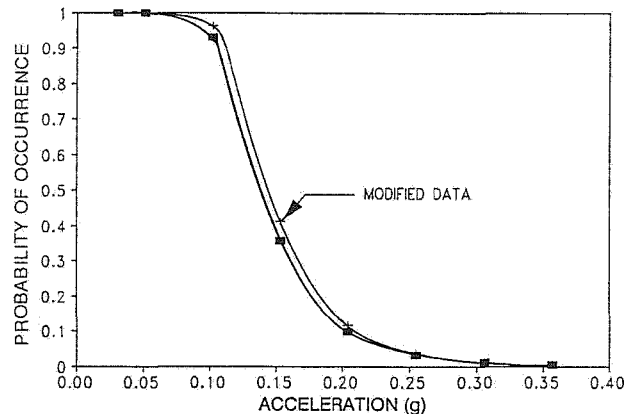


Figure 6. Probability of occurrence versus acceleration for 50 year time span.

Therefore, a 50 year design life should at least consider the possibility for 0.3g ground accelerations in parts of San Juan, although this study suggests accelerations of 0.15 to 0.2g could generally be used with confidence. Naturally, a site-specific study employing subsurface data in a free-field

analysis is recommended to assess acceleration and frequency variation in surficial soils.

Summary

The island of Puerto Rico and the city of San Juan are located in a seismically active region, and there is significant risk of large and possibly "great" earthquakes in this area in the next 50 years. Seismic design should account not only for the risks associated with the numerical analyses summarized herein, but also should consider the risks associated with near sources that cannot be modelled with the existing data.

References

- [1] Briggs, R.P., (1964) "Provisional Geologic Map of Puerto Rico and Adjacent Islands", USGS, Misc. Geologic Investigations Map I-392.
- [2] Hays, W.W., (1985) "Fundamentals of Geology and Regional Geology for Solving Earthquake Engineering Problems in the Puerto Rico Area," Proceedings of Conference XXX - A Workshop on Reducing Potential Losses from Earthquake Hazards in Puerto Rico" USGS Open File Report 85-731.
- [3] Mattson, P.H., (1966) "Geological Characteristics of Puerto Rico," Continental Margins and Island Arcs, Geol. Survey Canada Paper 66-15.
- [4] McCann, W., (1985) "The Earthquake Hazards of Puerto Rico and the Virgin Islands," Proceedings of Conference XXX ... (see [2]).
- [5] Molinelli, J., (1985) "Earthquake Vulnerability Study for the Metropolitan Area of San Juan, Puerto Rico," Proceedings for Conference XXX ... (see [2]).
- [6] McCann, W. and Sykes, (1984) "Subduction of Aseismic Ridges Beneath the Caribbean Plate: Implications for the Tectonics and Seismic Potential of the Northeastern Caribbean" Jour. of Geophysical Research, Vol. 89.
- [7] der Kiureghian, A. and Ang, H.S. "A Line Source Model for Seismic Risk Analysis," CivilEngineering Studies, No 419.
- [8] Dart, R.L. et. al. (1977) "Puerto Rico Seismic Network Data Report of Earthquakes Located by the Program HYPO and Hypoellipse," USGS Circular 821.
- [9] Joyner, W.B. and Boore, D.M. (1988) "Measurement, Characterization, and Prediction of Strong Ground Motion," Proc. ASCE Specialty Conf. of Earthquake Engineering and Soil Dynamics.
- [10] Chameau, J.L. (1990) "PUHAZ.FOR - User's Manual," Purdue University Internal Report.

Session 3B
Seismic Hazards
(continued)

1. Collection and review of available information on the geology and seismic history of Vancouver Island and definition of a study area;
2. Selection and stereoscopic interpretation of airphotos within the study area; and
3. Reconnaissance level field inspection of some features of interest.

Study Area

The selected study area comprised approximately 13,000 km² of central Vancouver Island (Fig. 1). This area included the preferred epicentre of the 1946 earthquake and all known major fault zones within a large region surrounding the epicentre.

Geology

A summary of geological mapping of Vancouver Island was prepared in 1977 by Muller [2]. Since then, interpretations of the regional geology have been updated, based on advances in theories of local lithospheric plate interaction and on the results of detailed mapping and deep seismic reflection studies carried out as part of the LITHOPROBE program. Results of the recent work pertinent to this study are summarized in references [3 to 7]. The major fault zones identified on Vancouver Island are shown on Figure 1.

Based on typical empirical relationships between earthquake magnitude, and fault area, length and displacement [e.g. 8], an earthquake with the characteristics of the 1946 earthquake (a magnitude of about 7, at a depth of approximately 30 km) would

have a fault area in the order of 700 km², a rupture length between 18 km and 35 km and a displacement of 0.9 m.

Eleven of the major fault zones and 2 minor fault zones within the study area were identified as having sufficient dimensions to theoretically produce an earthquake of about magnitude 7 or greater. The locations of the surface traces of these fault zones are shown on Figure 1 and their geological characteristics are summarized in Table 1.

The faults include normal, thrust, wrench and strike-slip types, with traces ranging in length from 35 to 100 km. They trend roughly northwest-southeast, or north-south, or a combination of these directions, consistent with the overall structural trend of Vancouver Island. Dips of these faults at the surface are generally high angle, varying from 60 degrees to vertical. Non-vertical dips are to the east or west. Geological evidence indicates that past movement along the fault zones ranges up to 2000 m.

Seismicity

The seismicity of Vancouver Island has been reviewed by Rogers [9]. The seismic record for the central island region is interesting because, although there is very little low level seismicity, there have been 4 earthquakes from M5.7 to M7.3 since 1918 (Fig. 1 and Table 2). Although these earthquakes are likely related to subduction of the Juan de Fuca Plate below the North America Plate, the exact causative mechanism is not known. They are, however, not subduction events, and instead occur within the continental lithosphere overlying the subducted oceanic crust.

The largest earthquake, the M7.3 event of June 23, 1946, caused numerous landslides,

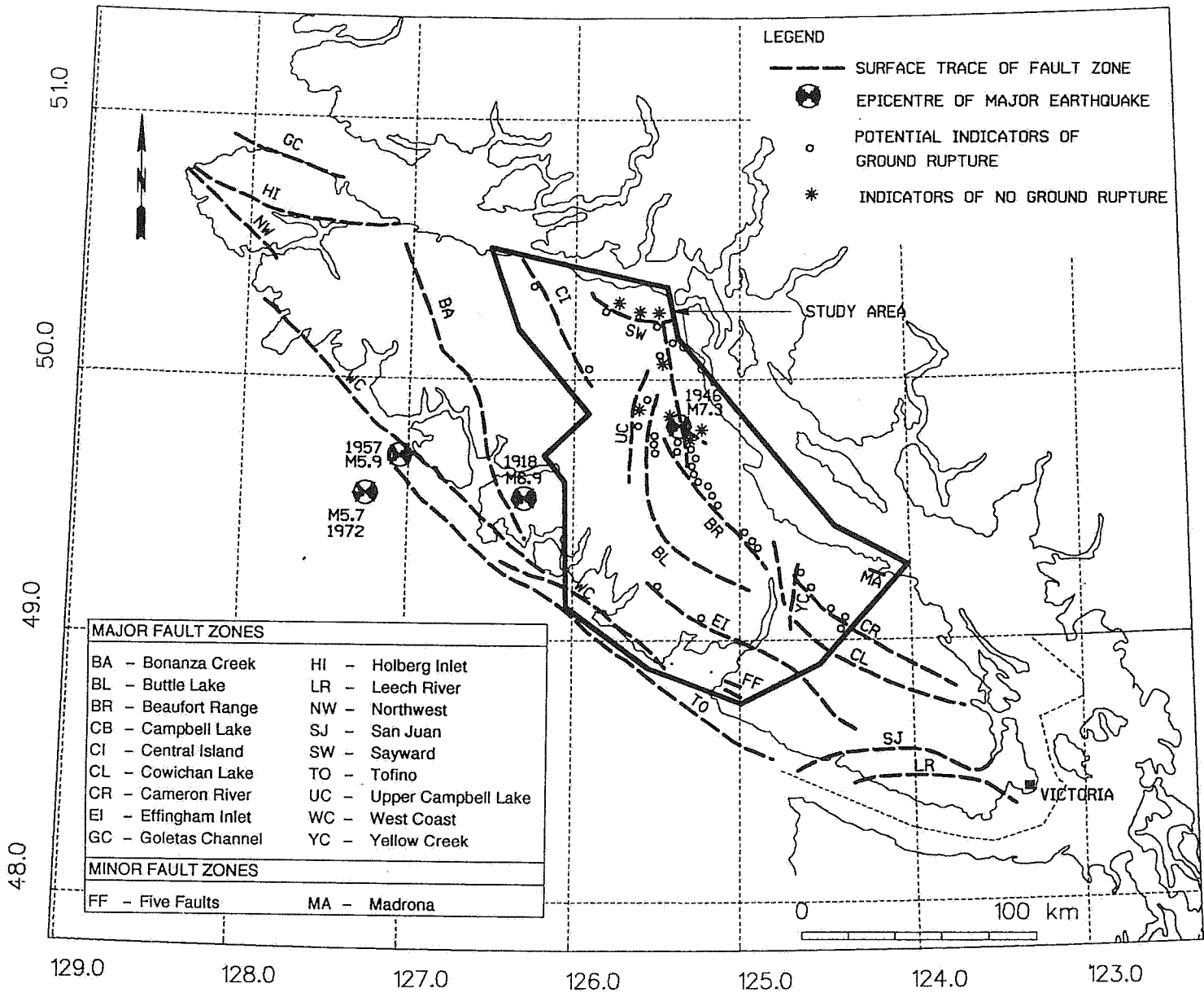


FIG. 1 - Major fault zones on Vancouver Island, major recorded earthquakes near study area, and potential indicators of ground surface rupture or no ground surface rupture within study area.

TABLE 1: SUMMARY OF GEOLOGICAL FAULT ZONE DATA

Fault Zone	General Location	Type of Fault	Length of Trace		Trend of Trace	Type of Trace	Number of Branches	Surface Dip	Estimated Separation	Minor Faults/Splays
			(map area)	(total)						
MAJOR FAULT ZONES										
Beaufort Range	Follows Cruickshank Canyon, southeastward along Toma Creek and along the southwest escarpment of Beaufort Range	Thrust and Wrench	70 km	70 km	320 – 340°	Sinuuous	1 in north 2 in south	65–90° NE	>1500 m	
Cowichan Lake	West of Horne Lake southeastward towards Cowichan Lake	Thrust	55 km	130 km	330° in north 310° in south	Arcuate	2, in places 3	65–70° NE	1500 – 2000 m	Lucy Lake Splay in the north
Yellow Creek	Southward from Horne Lake, through a portion of Cameron River valley, and follows a series of north-south creeks	Strike Slip	35 km	35 km	355 – 005°	Straight-braided	2	90°	500 – 1000 m	
Cameron River	From northwest of Horne Lake southeastward along Cameron River to Dunsmuir Creek	Thrust and Wrench	55 km	130 km	325° in north 310° in south	Arcuate braided	2 main branches	60°NE –90°	1000 m	
Buttle Lake	From Upper Quinsam Lake southward along Buttle Lake then southeastward across Great Central and Sproat Lakes	Normal	100 km	100 km	350–010° in north 310–340° in south	Arcuate offset in places	1 in north 2 in extreme south	near 90°		Arbutus Summit Fault Zone in the south
Campbell Lake	From Elk Bay southward across Campbell Lake to Piggott Creek and maybe connects (en echelon) with BRFZ. Anderson Lake Splay follows its and Dove Creek	Normal ?	65 km	65 km	345–005°	Arcuate	1			Anderson Lake Splay in the south, CBFZ could be an extension of BRFZ
Upper Campbell Lake	Southward from Campbell Lake across Upper Campbell Lake and parallel and east of Wolf Creek	Normal	45 km	45 km	060° in north 005° in south	Arcuate	1			
Effingham Inlet	Southeastward from Tofino Inlet across Effingham and Alberni Inlets towards Nitinat River	Thrust	80 km	100 km	300° in north 290° in centre 310° in south	Sinuuous	1 in north 3 in centre 1 in south	60–80° NE	>1000 m	Several unnamed splays near Alberni Inlet. Called Harrison Creek FZ south of Alberni Inlet
West Coast	Subparallel to west coast approximately 2 to 5 km inland	Strike Slip ?	55 km	175 km	315–320°	Straight-sinuuous	1			
Central Island	Southeastward from near Robson Bight to northeast of Victoria Peak. May continue to UCFZ	Normal	60 km	60 km	310–330°	Straight	2, in places	90°	300–600 m	
Sayward	Southeastward from Johnstone Strait to Seymour Narrows – Discovery Passage	Normal (Thrust?)	70 km	70 km	300–320°	Straight	1	90°	500 m?	
LESS MAJOR FAULT ZONES										
Madrona Point	Two parallel branches trending southeastward across Nanoose Peninsula	Thrust	8 km	8 km	310°	Straight-arcuate	2 parallel branches	NE	>300 m	
Five Faults	Subparallel faults trending east-west south of Alberni Inlet and east of Barkley Sound	Normal and Thrust	4–13 km	4–13 km	260–280°	Straight-arcuate	5 sub-parallel faults	90°	<500 m	Ritherdon Creek Fault Carnation Creek Fault Santa Maria Fault Christie Bay Fault Rousseau Lake Fault

soil displacements and liquefaction over a large area [10, 11, 12]. No ground surface ruptures along faults were reported, although Hodgson [10] thought that a beach on Comox Lake may have slumped into the lake due to a "tectonic drop". However, since much of the epicentral region was sparsely populated and heavily forested at the time, the lack of reported surface rupture cannot be considered conclusive.

Initially, the earthquake epicentre was generally interpreted to be in Georgia Strait, between Vancouver Island and the mainland. In 1983 Rogers and Hasegawa [13] re-evaluated the 1946 earthquake and placed the epicentre on east-central Vancouver Island (Fig. 1), with an uncertainty of about 20 km, and a depth of about 30 km. They concluded that surface rupture was a possibility, although Rogers has subsequently noted [pers. comm.] that the small number of aftershocks suggests that the earthquake was relatively deep, which reduces the possibility of surface rupture. Fault plane solutions favour right lateral strike-slip motion on a northwest striking plane. This solution coincides with the surface trace of the Beaufort Range Fault Zone, one of the longest faults on Vancouver Island.

A triangulation network in the epicentral area that had first been surveyed in 1935 was resurveyed in 1978. It was found that distortion of the network over the 43 year interval could be interpreted as approximately 1 m right lateral movement and 2.5 m normal slip on the Beaufort Range Fault Zone [14]. Slawson [pers. comm.] also noted certain local features along the fault trace that could be interpreted as possibly resulting from ground surface rupture.

TABLE 2
Major Earthquakes of Central Vancouver Island

DATE	LOCATION	ESTIMATED DEPTH	MAGNITUDE	REF.
Dec. 6 1918	N49.47 W126.24	15 km	6.9	[15]
June 23 1946	N49.76 W125.34	30 km	7.3	[13]
Dec. 16 1957	N49.65 W127.02	30 km	5.9	[15]
July 5 1972	N49.5 W127.2	25 km	5.7	[16]

Method of Study

For the airphoto study, primary emphasis was placed on the 1946 earthquake. It is the largest Vancouver Island earthquake on record, it has been the subject of several other relevant studies and it occurred recently enough that both pre- and post-earthquake airphotos were available. It was recognized though, that surface rupture could also possibly have occurred during other earthquakes, including those predating the historic record.

Due to uncertainty in the preferred location of the 1946 earthquake epicentre, the Beaufort Range Fault was not the only potential source. Thus, in the vicinity of the epicentre, all known fault zones identified as having sufficient dimensions to theoretically generate a magnitude 7+ earthquake were selected for airphoto interpretation.

The primary criterion for selection of airphotos was the date of photography; dates as close as possible to June 1946 were required. Other criteria included airphoto coverage, scale and quality. Airphotos from both Provincial and Federal Government agencies were considered.

The post-June 1946 airphotos along the

surface trace of each of the selected fault zones were initially interpreted. Usually the first set of airphotos taken after June 1946 was used. In some instances, several sets of airphotos of the same area, taken in different years and at different scales, were interpreted. Any features of interest identified on post-June 1946 airphotos were reinterpreted and visually compared to pre-June 1946 airphotos.

A number of geomorphic features of particular interest were then inspected in the field. No subsurface investigations were carried out at any of these features.

Airphoto Interpretation and Field Investigation

The blocks of airphotos used for the study, their origin, date, approximate scale and quality are summarized on Figures 2a and 2b. The pre-1946 airphotos were taken

between 1929 and 1945 and varied in quality and scale. By coincidence a block of airphotos, of relatively good quality and at a scale of approximately 1:21,000, was taken in the vicinity of the epicentre of the 1946 earthquake one month after the event. Other post-June 1946 airphotos used varied in quality and scale, and dated up to the year 1957. In total, approximately 825 stereopairs were interpreted along the surface traces of the 11 major and 2 minor fault zones.

Many, but not all, of the fault zone traces exhibited some geomorphic expression on the airphotos, including:

- distinct canyons, escarpments, shorelines and river and creek valleys; and
- alignment of smaller drainages, small lakes, low lying poorly drained areas and subdued linear depressions.

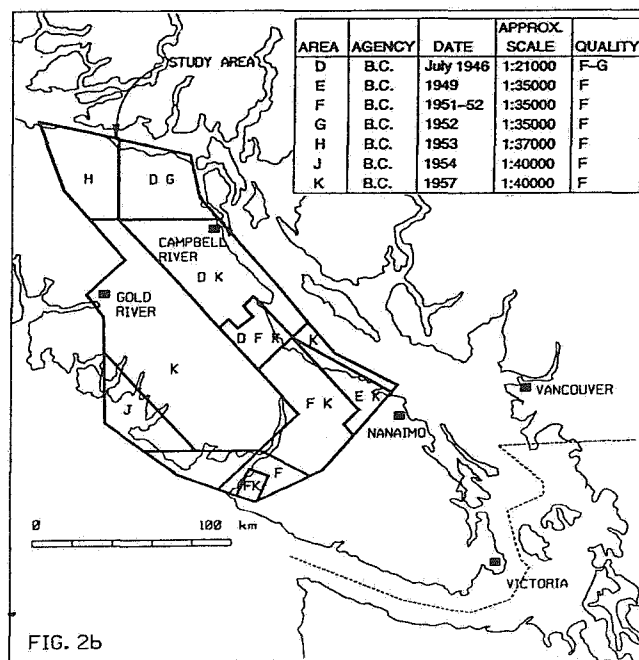
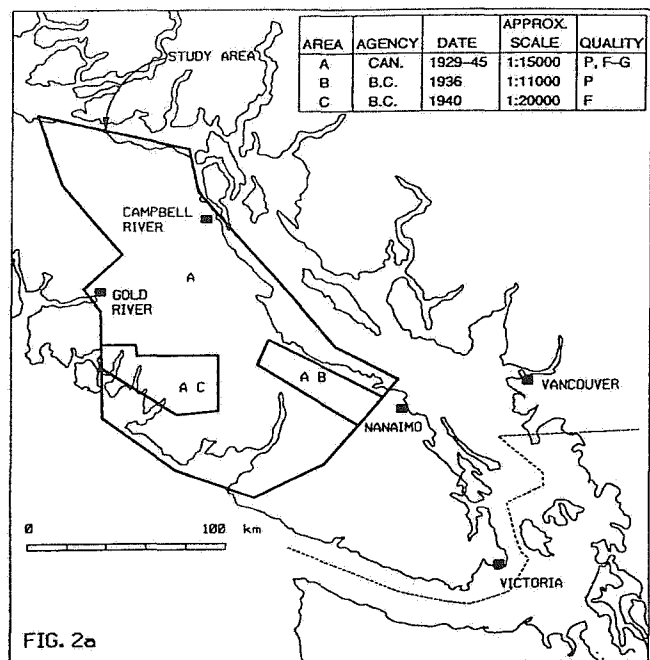


FIG. 2 - Blocks of airphoto coverage. Fig 2a: pre-1946 earthquake, and Fig 2b: post-1946 earthquake.

Numerous geomorphic features interpreted on the post-June 1946 airphotos were potential indicators of ground ruptures resulting from the 1946 earthquake. These features included:

- fresh-looking linears, fractures, scarps, and antislope features;
- a series or alignment of linears, scarps and gullies;
- aligned and offset drainages;
- a concentration of fresh-looking recent slope failures; and
- irregular distinct geomorphic features.

These features were coincident, subparallel, perpendicular and/or at irregular angles to the fault traces.

A total of 32 such geomorphic features were interpreted along the fault zones (Figure 1). The majority are concentrated along the Beaufort Range Fault Zone and along other fault zones in the vicinity of the 1946 epicentre. Figures 3a and 3b show examples of some of these features.

Most such features appeared to be identical on both the pre- and post-June 1946 airphotos. In 3 cases, however, logging and/or the poor quality of airphotos prevented confirmation. No evidence of recent ground ruptures was observed during the followup field inspections.

There were 8 geomorphic features interpreted which indicate that no ground rupture occurred along certain sections of fault zones during the 1946 earthquake. All were interpreted from relatively good quality July 1946 airphotos at a suitable

scale. Most of these features are relatively close to the epicentre and include:

- snow and ice on alpine lakes along the Beaufort Range and Campbell Lake fault zones that do not appear in any way disturbed;
- organic surface mats covering swampy areas adjacent to the Campbell Lake and Sayward fault zones that show no indication of recent disturbance;
- relatively loose deposits on the floodplain of Campbell River that show no evidence of recent disturbance; and
- the relatively dense network of logging railways straddling the Campbell Lake and Sayward fault zones that show no evidence of recent misalignment.

Figures 4a and 4b show examples of some of these features.

Limitations of the Study

There are several limitations to the methods used. The dates of the airphotos, their scale and quality were not always optimal. At the time the airphotos were taken, much of the study area was heavily forested. The precise surface trace of the faults could not always be identified in the photos. Forty years had passed between the time of the 1946 earthquake and the time of the field inspection. Notwithstanding these limitations, it is felt that the methods were suitable for the purpose of the study.

Conclusions and Recommendations

Based on this study, plus reports published shortly after the event, it is unlikely that

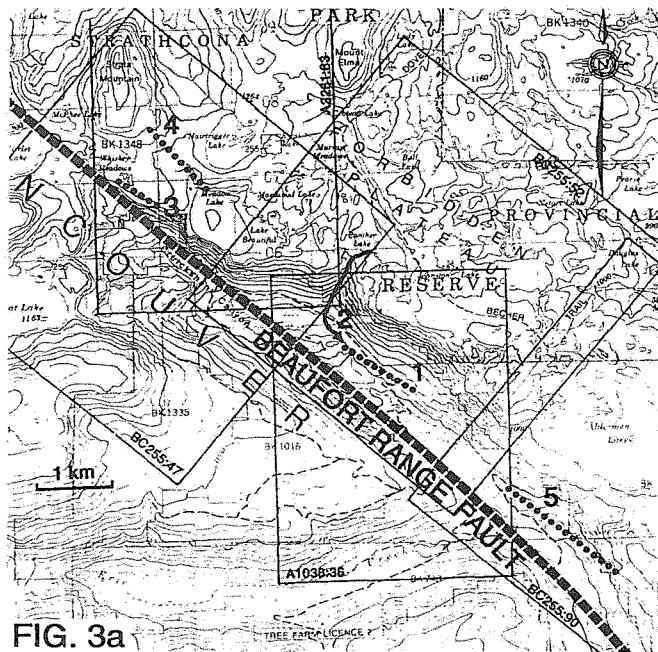


FIG. 3a

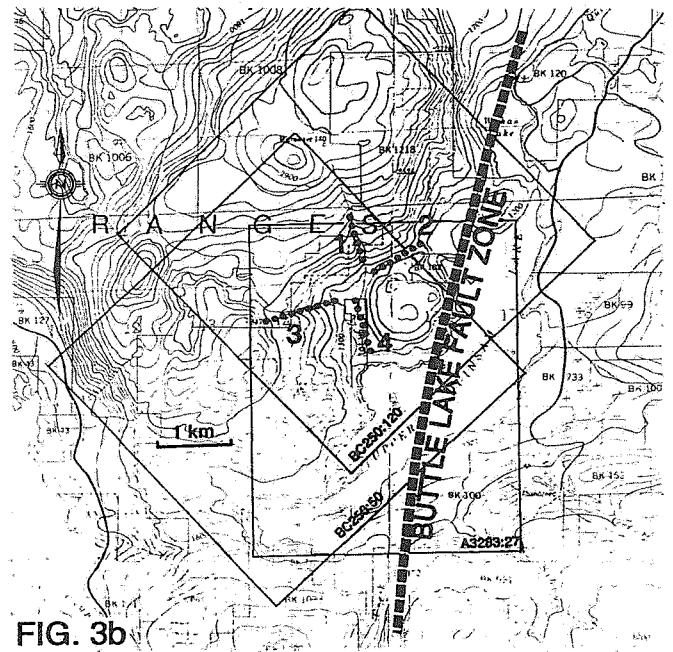


FIG. 3b

FIG 3 - Typical features possibly indicative of recent ground surface offset. Fig 3a: Beaufort Range Fault Zone, map ref. NTS 92F/11. Large antislope scarp (1), aligned with short reach of creek (2); fresh-looking scarp (3). Other lineations are: linear clearing of trees (4); lineation ending in small rock canyon (5). Fig 3b: Buttle Lake Fault Zone, map ref. NTS 92F/13. Distinct lineations (1 to 4) forming a conjugate fracture system, with no. 2 appearing as a very fresh-looking scarp in both 1946 and 1931 photos.

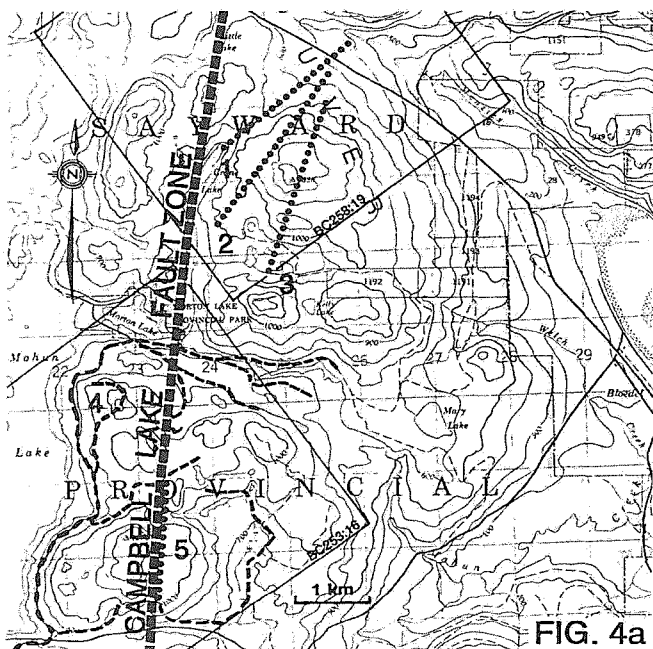


FIG. 4a

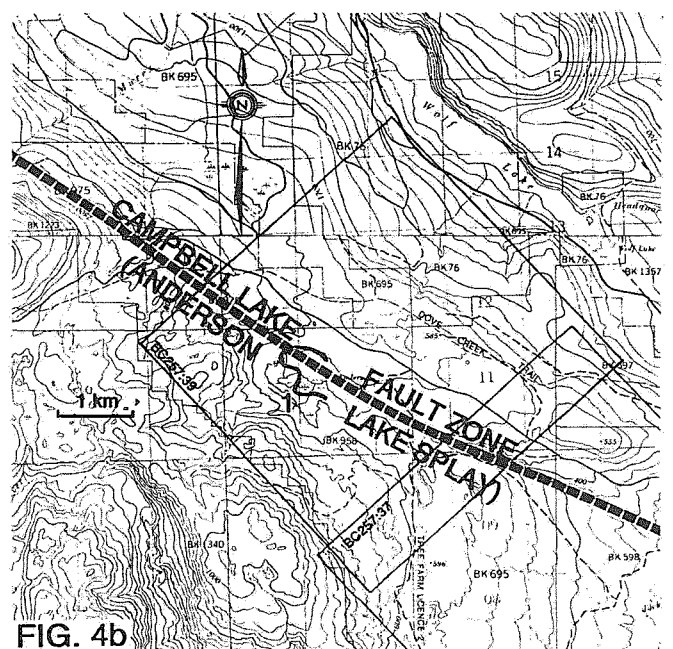


FIG. 4b

FIG 4 - Typical features indicative of no recent ground surface offset. Fig 4a - Campbell Lake Fault Zone, map ref. NTS 92K/3. Distinct fractures (1 to 3) subparallel to fault, with no observable recent offset; logging railways and trails (4), mostly in use in 1946, with no observable or reported offset. No. 5 is a linear that follows the trace of the fault. Fig 4b - Anderson Lake Splay of Campbell Lake Fault Zone, map ref. NTS 92F/11&14. Surface organic mat on swamp (1) overlying fault trace is undisturbed in July 1946 photos.

extensive ground surface rupture occurred as a result of the 1946 earthquake. Without additional more detailed studies, however, localized rupture cannot be entirely ruled out. It is possible that various local geomorphic features are related to earthquakes, either the 1946 event or earlier events, but these features could also be produced by other conditions or phenomena. In any case, this study did not identify the specific geologic source of the 1946 earthquake.

In the western USA, surface rupture has generally occurred for most historical shallow earthquakes of magnitude M6.5 to M7 or larger, although deeper events may not cause surface rupture. To date, there are no documented cases in Western Canada of surface rupture during an earthquake, but the local historic record is short.

In other parts of the world, paleoseismic studies have been successfully used to extend the historic record and to identify faults that have been active in the Quaternary. In addition to airphoto studies, many other methods such as low sun angle techniques can be useful. Very little work of this nature has been carried out in Western Canada. It is recommended that such studies be considered for various regions of British Columbia, for example where there have been strong earthquakes, or where there are known geomorphic features that could indicate surface ruptures. Some of the faults and features studied in this project would be candidates for further study.

Acknowledgements

The authors would like to acknowledge G.C. Rogers, W.H. Mathews and W.F.

Slawson for their contributions to this study. Thanks also to the staff at the BC Airphoto Library in Victoria, BC and the National Airphoto Library in Ottawa, Ontario. The approval of BC Hydro to publish this paper is also acknowledged.

References

1. VanDine Geological Engineering, 1987. Central Vancouver Island airphoto study; Report to BC Hydro, March 1987, 82p.
2. Muller, J.A., 1977. Geology of Vancouver Island; Geol. Sur. Canada, Open File 463, 3 sheets.
3. Yorath, C.J., Clowes, R.M. et al, 1985. LITHOPROBE - Phase 1: southern Vancouver Island: preliminary analyses of reflection seismic profiles and surface geological studies; Geol. Sur. Canada, Paper 85-1A, pp 543-554.
4. Yorath, C.J., Green, A.C. et al, 1985. LITHOPROBE, southern Vancouver Island: seismic reflection sees through Wrangellia to the Juan de Fuca plate; Geology, V. 13, pp 759-762.
5. Dom, K., 1986. The Beaufort Range Fault Zone in the Alberni area, B.Sc. Thesis, Dept. of Geol. Sciences, U. of British Columbia, 35 p.
6. Sutherland-Brown, A., Yorath, C.J., Anderson, R.G. and Dom, K. 1986. Geological maps of southern Vancouver Island, LITHOPROBE 1; Geol. Sur. Canada, Open File 1272, 10 maps.
7. Campbell, R.B., Dodds, C.J., Yorath, C.J. and Sutherland-Brown, A., 1992. Insular Belt; in The Cordilleran Origin

- in Canada, Geol. Sur. Canada, Geology of Canada No. 4, Chap. 17, in press.
8. Slemmons, D.B., 1977. Faults and earthquake magnitude; U.S. Army Corps of Engineers, Waterways Experiment Station, Misc. Paper S-73-1, Rpt. 6.
 9. Rogers, G.C., 1983. Seismotectonics of British Columbia; PhD Thesis, Dept of Geophysics and Astronomy, U. of British Columbia, 247 p.
 10. Hodgson, E.A., 1946. British Columbia earthquake, Jour. Royal Astr. Soc. of Canada, V. 40, pp 285-319 plus plates.
 11. Mathews, W.H., 1979. Landslides of central Vancouver Island and the 1946 earthquake, Bull. Seis. Soc. Am., V. 69, pp 445-450.
 12. Rogers, G.C., 1980. A documentation of soil failure during the British Columbia earthquake of 23 June 1946, Can. Geotech. Jour., V. 17, pp 122-127.
 13. Rogers, G.C. and Hasegawa, H.S., 1978. A second look at the British Columbia earthquake of 23 June 1946, Bull. Seis. Soc. Am., V. 68, pp 653-675.
 14. Slawson, W.F. and Savage, J.C., 1979. Geodetic deformation associated with the 1946 Vancouver Island, Canada earthquake; Bull. Seis. Soc. Am., V. 69, pp 1487-1496.
 15. Cassidy, J.F., 1986. The 1918 and 1957 Vancouver Island earthquakes, M.Sc. Thesis, Dept of Geophysics and Astronomy, U. of British Columbia.
 16. Rogers, G.C., 1976. The Vancouver Island earthquake of 5 July, 1972, Can. Jour. of Earth Sci., V. 13, pp 92-101.

Large Landslides on Vancouver Island, British Columbia

D.F. VanDine

*VanDine Geological Engineering
Victoria, British Columbia*

S.G. Evans

*Geological Survey of Canada
Ottawa, Ontario*

Abstract

As the first phase of Energy, Mines and Resources Canada's long term plan to assess the potential landslide response of Vancouver Island to future earthquakes, an airphoto-based inventory of the island's large landslides was carried out. A total of 34 landslide features, estimated to have involved in excess of 1 million m³ of material, were identified and designated as priority sites for future field investigation. In addition, 40 other smaller, but substantial landslide features, were recorded. All of the 34 priority landslides are located on the northern 2/3s of Vancouver Island. All but one lie in either the North Vancouver Island Ranges or West Vancouver Island Fiordlands physiographic regions - both regions of rugged mountainous terrain that have been subjected to glacial oversteepening. The Karmutsen volcanics are associated with 65% of the priority landslide sites. Rock slides are most common (50%), followed by rock-fall avalanches (32%), then rock slumps (18%). The most common estimated area of ground disturbance is in the range of 200,000 m² (41%). The majority of the landslides (68%) lie within the Coastal Western Hemlock biogeoclimatic zone which is subject to more than 2500 mm of precipitation annually. It is estimated that 56% of the priority landslides occurred more than 100 years ago, 18% occurred 50 to 100 years ago and 26% occurred within the past 50 years. Of the 26%, or 9, most recent events, 6 of them may be associated with the 1946, 7.3 magnitude Vancouver Island earthquake.

Introduction

This paper summarizes the methods and results of an inventory of large landslides on Vancouver Island, British Columbia [1]. This inventory is the first phase of Energy, Mines and Resources Canada's longer term plan to assess the landslide response of the island, and the west coast of Canada, to future earthquakes. As such, the study also investigated, in general terms, the relationship between the locations of past large landslides, physical settings, and where possible, past seismic activities.

Two previous inventories of landslides of portions of Vancouver Island have been carried out. Mathews [2] presented a summary of an inventory of landslides of central Vancouver Island, which he inferred were the result of the 1946 Vancouver Island earthquake. Howes [3]

included an inventory of rock slides and rock slumps in his terrain inventory of northern Vancouver Island. Roger's documentation of soil failures resulting from the 1946 earthquake did not include landslides [4].

During regional geological mapping of portions of Vancouver Island, a number of geologists noted, or inferred, landslides in their study areas. Examples of such references include Gunning [5] and Fyles [6]. Additional references to existing landslides on Vancouver Island appear in a variety of other publications.

Scope and Method

This study covered all of Vancouver Island including the major neighbouring islands (Figure 1). For the purpose of this study, large landslides are defined as those involving in excess of an estimated 1 million m³ of material. Significant landslides, but estimated to be less than 1 million m³ in volume, were also considered.

Types of landslides included in the inventory were rock-fall avalanches, rock slides and rock slumps. Areas of ongoing rock falls, soil slides, debris slides and debris flows, which although common on the island, usually have involved a volume of material much less than 1 million m³.

The study was carried out in three stages. All available references to known large landslides were collected and reviewed in Stage 1. In addition, discussions were held with geologists and engineers familiar with Vancouver Island.

Stage 2 involved 3 phases of airphoto interpretation. Phase 1 was a stereoscopic interpretation of approximately 700, 1:60,000 to 1:70,000 scale, 1986 and 1987 airphotos of the entire Vancouver Island. Any feature that had the appearance of a large landslide on these small scale airphotos, and all rock slide and rock slump features identified in Howes [3], were catalogued.

In Phase 2 all features identified in Phase 1 were re-examined on the most recent, largest scale airphotos available. The dates of the most recent airphotos ranged from 1970 to 1987. The scales of these airphotos varied from 1:10,000 to 1:20,000. From Phase 2 the features were then divided into 3 groups:

Priority A: Landslide features estimated to involve in excess of 1 million m³ of material, plus significant landslide features with an estimated volume less than 1 million m³. Because it is difficult to estimate volumes from airphotos, most landslide features with an estimated area of ground disturbance greater than 50,000 m², were included in the Priority A group.

Priority B: Landslide features usually smaller than those in Priority A, plus areas of large ongoing rock falls and associated talus deposits. Because of space constraints, this paper will not discuss Priority B landslides further. The reader is referred to VanDine Geological Engineering [1].

Very small landslides and other features that were misinterpreted as landslides on the small scale airphotos were discarded from further investigation.

Phase 3 of Stage 2 involved an examination of all Priority A landslide features using airphotos from different years in an attempt to age bracket the date of occurrence of the landslides. This phase was not carried out where it was obvious that the landslide had occurred well before the earliest available airphotos (approximately 1946).

The following information was summarized for each of the Priority A landslide features: location and approximate location of the main scarp; type and area of ground disturbance; physiographic region, biogeoclimatic zone and annual precipitation; estimated age; a brief description and references.

The common characteristics of the Priority A landslide features were analyzed in Stage 3. An attempt was made to relate the date of occurrence of these events with the known past seismic activity of Vancouver Island.

This study was based largely on the stereoscopic interpretation of BC government airphotos available at the BC Airphoto Library, Victoria, BC. No field checking was carried out. As with any such study, the results are therefore dependent on the availability, scale and quality of the airphotos.

Physical Setting of Vancouver Island

Vancouver Island is the largest island on the west coast of North America. It stretches for approximately 450 km in a northwest-southeast direction between 48°20'N and 50°40'N and between 123°10'W and 128°30'W. Although it is

approximately 125 km at its widest point, the average width is only 70 km. The total land area is approximately 32,000 km².

Physiographically, the island can be divided into 11 regions (Figure 1) [7]. Approximately 75% of the land mass is composed of the three mountainous physiographical regions: North Vancouver Island Ranges, South Vancouver Island Ranges and West Vancouver Island Fiordland. The remaining 25% are made up of plateaux, highlands, lowlands and basins.

The regional bedrock geology of Vancouver Island has been compiled at a scale of 1:250,000 by Muller [8]. The majority of the mountainous regions of the island are underlain by the mid to upper Triassic Karmutsen Formation volcanics (muTR K), the lower Jurassic Bonanza Formation volcanics (1J B) and Jurassic granitic intrusives (Jg). During the Pleistocene Epoch, glacial activity steepened, and in some cases oversteepened, many of the mountain slopes.

Rogers [9] and Cassidy [10] have most recently reviewed the regional seismicity of Vancouver Island. Since 1899, when records were first kept, six earthquakes with magnitudes 5.3 or greater have been recorded on or near Vancouver Island. Their epicentres and magnitudes are shown on Figure 1. The epicentres of all but the 1946 earthquake are located along the west coast of the island.

Biogeoclimatic zones relate the climate and the ecosystem. For Vancouver Island the biogeoclimatic zones have been summarized on a 1:500,000 scale map prepared by Nuszdorfer et al [11]. Most of the mountainous regions of the island lie within the Coastal Western Hemlock or Mountain Hemlock zones. The highest peaks fall within the Alpine Tundra. The Coastal Hemlock Zone is characterized by abundant annual rainfall and mild temperatures. The Mountain Hemlock Zone has abundant rainfall during the summer months and abundant snowfall during the winter months. The Alpine Tundra Zone has a harsh climate consisting of long, cold winters with an abundant snowfall.

Farley [12] has divided Vancouver Island into 3 approximately northwest-southeast trending

annual precipitation zones. From west to east they are: >2500 mm, 1000 mm to 2500 mm and 500 mm to 1000 mm. The western 2/3s of the island is subject to >2500 mm of precipitation annually.

Results of the Study

In total 185 landslide features and/or inferred landslide features were identified during Phase 1 of the airphoto interpretation. During the re-examination of those features on larger scale airphotos in Phase 2, 111 features were discarded from further investigation. Many of these features were snow avalanche tracks, rock falls, soil slides, debris slides or debris flows and other forms of landslides too small to consider for this study. A few of the features identified in Phase 1 were found not to be related to landslides.

Of the remaining 74 landslides features, 34 were grouped into Priority A landslide features and 40 were grouped into Priority B.

The locations of the 34 Priority A landslide features are shown on Figure 1. A unique landslide number including "A", for Priority A, and second letter which refers to the 1:250,000 scale NTS topographic map, is given to each feature. The locations, characteristics, physical settings and estimated ages of movement for each landslide feature are included in Table 1. (The reader is referred to VanDine Geological Engineering [1] for further descriptions, references and references to airphotos for each landslide feature). Table 2 through Table 10 summarize the common characteristics of the 34 Priority A landslide features.

As shown on Figure 1 and in Table 2, geographically, large landslides are limited to the northern 2/3s of Vancouver Island, that is the area roughly north of the 49th parallel of latitude. Fifty per cent of the large landslides occur within the 1:250,000 scale NTS map sheet 92F.

Table 3 indicates that rock slides are the most common of the large landslide types (50%),

followed by rock-fall avalanches (32%) then rock slumps (18%). As shown in Table 4, the most common estimated area of ground disturbance by these 34 features is approximately 200,000 m² (41%).

Table 5 indicates that all but one large landslide feature lie either in the North Vancouver Island Range or West Vancouver Island Fiordland physiographic regions -- both are regions of rugged mountainous terrain and have been subjected to glacial steepening. The majority of these features (68%) are associated with the Coastal Western Hemlock biogeoclimatic zone (Table 6) and are subject to more than 250 cm of precipitation annually (74%) as shown in Table 7.

Table 8 shows that 47% of the large landslides are underlain by volcanic rock formations, 18% occurred in intrusive rock types and 27% occurred in areas where there are both volcanic and intrusive rock formations. The Karmutsen volcanics (muTR K) are associated with 65% of the large landslides.

Of the 34 large landslides, it is estimated that 56% occurred more than 100 years ago (Table 9). It is estimated that 18% occurred 50 to 100 years ago and 26% occurred within the past 50 years. The years of occurrence of the recent large landslides, whether known or inferred, are presented in Table 10. When these dates are compared to the dates of the known significant earthquakes over the same period, it appears that the 1946 Vancouver Island earthquake may have had the greatest seismic impact on the occurrence of large landslides on Vancouver Island in the recent past.

Conclusions

The majority of the large landslides on Vancouver Island have occurred in the mountainous central and northern regions of the island. These areas of high relief are also regions of abundant annual precipitation.

A large majority of these large rock-fall avalanches, rock slide and rock slumps occurred in association with either volcanic or intrusive

rock formations. The Karmutsen volcanics were associated with 65% of the landslides.

Of the occurrences in the past 50 years, the 1946 earthquake possibly has had the greatest seismic impact on slope stability.

It is difficult to conclude from this study, however, which factors of topography, geology, rainfall and/or the location and character of the past earthquakes, have been the controlling factors. The findings of this study have been discussed, in general terms, with both W.E. Mathews and D.E. Howes in light of their earlier inventories ([2] and [3] respectively). Both agree that the numbers of large landslides noted and inventoried during this present study, and the relationships of these landslides with their physical settings, are generally consistent with the findings from their earlier studies.

Acknowledgements

The authors would like to acknowledge E.G. Enegren, D.E. Howes, D.R. Lister, W.H. Mathews, G.C. Rogers and T.P. Rollerson for their contributions to this study. Thanks are also in order to Mark Poire and his staff at the BC Airphoto Library, Victoria, BC.

References

- [1] VanDine Geological Engineering, 1990: Inventory of large landslides of Vancouver Island, British Columbia; a Report to Energy, Mines and Resources Canada, Geological Survey of Canada, Contract 23397-9-1372/01-SZ, March 1990.
- [2] Mathews, W.H., 1979: Landslides of central Vancouver Island and the 1946 earthquake; Bulletin of the Seismological Society of America, V 69, p 445-450.
- [3] Howes, D.E., 1981: Terrain inventory and geological hazards: northern Vancouver Island; BC Ministry of Environment, Assessment and Planning Branch, APD Bulletin 5.

- [4] Rogers, G.C., 1980: A documentation of soil failure during the British Columbia earthquake of 23 June, 1946; Canadian Geotechnical Journal, V 17, p 122-127.
- [5] Gunning, H.C., 1933: Zebellos River area, Vancouver Island, British Columbia, Geological Survey of Canada, Summary Report 1932, Part A, p 29-50.
- [6] Fyles, J.G., 1963: Surficial geology of Horne Lake and Parksville map areas; Geological Survey of Canada, Memoir 318.
- [7] VanDine, D.F., in preparation: The Landscape of Vancouver Island; a chapter in A Layman's Guide to the Geology of Vancouver Island, H.W. Nasmith (editor), Geological Association of Canada, Pacific Section.
- [8] Muller, J.E., 1977: Geology of Vancouver Island; Geological Survey of Canada, Open File 463, 1:250,000 scale map.
- [9] Rogers, G.C., 1983: Seismotectonics of British Columbia; PhD Thesis, Department of Geophysics and Astronomy, University of British Columbia.
- [10] Cassidy, J.F., 1986: The 1918 and 1957 Vancouver Island earthquakes; M.Sc. Thesis, Department of Geophysics and Astronomy, University of British Columbia.
- [11] Nuszdorfer, F.C., Kassay, K.L. and Scagel, A.M., 1985: Biogeoclimatic Units of the Vancouver Forest District; BC Ministry of Forests, 1:500,000 scale map.
- [12] Farley, A.L., 1979: Atlas of British Columbia: People, Environment and Resource Use; The University of British Columbia Press.
- [13] Varnes, D.J., 1978: Slope movement, types and processes; Chapter 2 in Landslides, Analysis and Control, Special Report 176, Transportation Research Board, National Academy of Sciences.

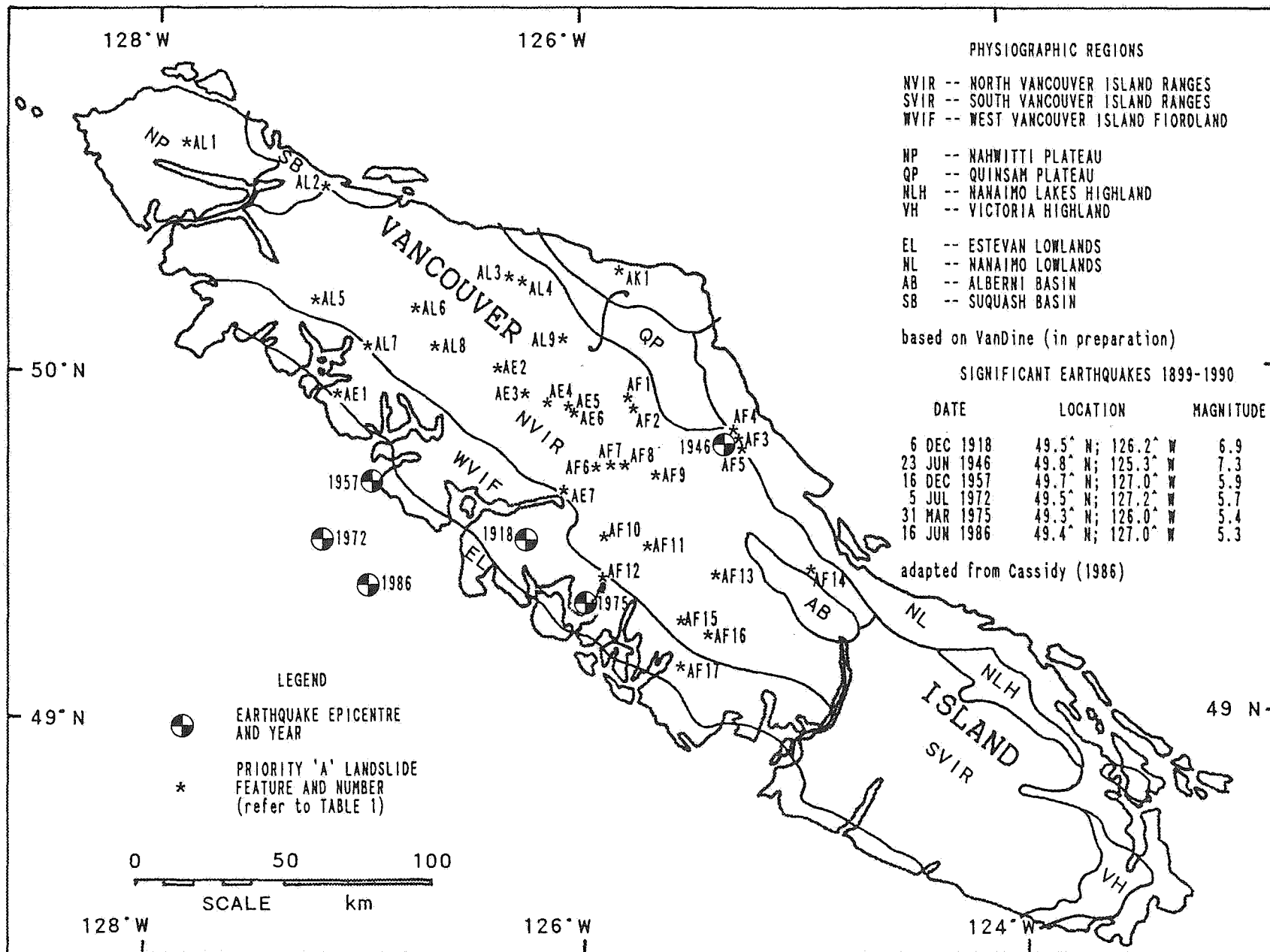


FIGURE 1--VANCOUVER ISLAND: PHYSIOGRAPHY, EARTHQUAKE EPICENTRES & LOCATION OF PRIORITY 'A' LANDSLIDE FEATURES

TABLE 1--Summary of landslide features

LANDSLIDE NUMBER	LOCATION				CHARACTERISTICS			PHYSICAL SETTING			AGE	
	GEOGRAPHIC LOCATOR #2*	NTS #3*	UTM #4*	LAT & LONG #5*	APPROX. MAINSCARP ELEV. (m) #6*	TYPE OF LANDSLIDE #7*	APPROX. AREA (*1000 m ²) #8*	PHYSIO-GRAPHIC REGION #9*	BIOGEO-CLIMATIC ZONE #10*	ANNUAL PRECIP. ZONE #11*	BEDROCK GEOLOGY #12*	ESTIMATED AGE #13*
AE1	Ship Peak	92E/14	9U	49°57'N 127°08'W	950	Rock slump	100	NVIF	CWH	>250 cm	IJ B	Ancient
AE2	Mount McKelvie North	92E/15 & 92L/02	9U	50°00'N 126°35'W	900	Rock-fall avalanche	200	NVIR	CWH	>250 cm	muTR K	Ancient/ recent
AE3	Mount Alava/Conuma Creek	92E/15 & 92E/16	9U	49°53'N 126°30'W	1200	Rock-fall avalanche	200	NVIR	MH/AT	>250 cm	muTR K	Recent 1974?
AE4	Conuma Peak	92E/16	9U	49°49'N 126°18'W	1100	Rock slide	200	NVIR	MH/AT	>250 cm	Jg	Ancient
AE5	Gold River North	92E/16	9U	49°48'N 126°02'W	900	Rock slide	200	NVIR	CWH	>250 cm	Jg/ muTR K	Ancient/ recent
AE6	Gold River South	92E/16	9U	49°48'N 126°02'W	900	Rock slide	100	NVIR	CWH	>250 cm	Jg/ muTR K	Ancient/ recent
AE7	Muchalat Inlet East	92E/09	9U	49°40'N 126°03'W	850	Rock slide	100	NVIR	CWH	>250 cm	muTR K	Ancient
AF1	Upper Campbell Lake North	92F/13	10U	49°52'N 125°39'W	600	Rock slide	200	NVIR	CWH	>250 cm	muTR K	Ancient
AF2	Upper Campbell Lake South	92F/13	10U	49°50'N 125°38'W	900	Rock slide	1,600	NVIR	CWH	>250 cm	muTR K	Ancient
AF3	Constitution Hill Middle	92F/14	10U	49°48'N 125°12'W	500	Rock slide	200	NVIR	CWH	100- 250 cm	Tg/ muTR K	Ancient
AF4	Constitution Hill North	92F/14	10U	49°49'N 125°12'W	300	Rock slump	100	NVIR	CWH	100- 250 cm	Tg/ muTR K	Ancient
AF5	Constitution Hill South	92F/14	10U	49°47'N 125°12'W	450	Rock slide	100	NVIR	CWH	100- 250 cm	Tg/ muTR K	Ancient
AF6	Butterwort Creek	92F/13	10U	49°45'N 125°53'W	1600	Rock-fall avalanche	400	NVIR	MH/AT	>250 cm	muTR K	Recent 1946?
AF7	Mount Colonel Foster	92F/13	10U	49°46'N 125°51'W	1500	Rock-fall avalanche	800	NVIR	MH/AT	>250 cm	muTR K	Recent 1946
AF8	Cervus Creek North	92F/13	10U	49°46'N 125°47'W	1600	Rock-fall avalanche	400	NVIR	MH/AT	>250 cm	muTR K	Recent 1946?
AF9	Adrian Creek	92F/12	10U	49°45'N 125°31'W	1500	Rock-fall avalanche	50	NVIR	MH/AT	>250 cm	muTR K	Old
AF10	Splendor Mountain	92F/12	10U	49°33'N 125°55'W	1200	Rock-fall avalanche	50	NVIR	MH/AT	>250 cm	Jg	Recent <1957
AF11	Mount Thelwood	92F/12	10U	49°33'N 125°42'W	1200	Rock slide	50	NVIR	MH/AT	>250 cm	Jg	Old
AF12	Moyeha Bay	92F/05	10U	49°25'N 125°56'W	400	Rock slide	200	NVIF	CWH	>250 cm	Jg/ muTR K	Ancient
AF13	Oshinow Lake	92F/06	10U	49°26'N 125°18'W	800	Rock slide	400	NVIR	CWH	>250 cm	muTR K	Ancient
AF14	Mount Joan	92F/07	10U	49°25'N 124°56'W	1100	Rock slide	1,600	NVIR	MH/AT	100- 250 cm	muTR K	Ancient
AF15	Thunderbird Creek	92F/05	10U	49°21'N 125°36'W	1000	Rock-fall avalanche	200	NVIR	CWH/MH	>250 cm	Jg/ muTR K	Recent 1957-1970
AF16	Kennedy River	92F/06	10U	49°17'N 125°27'W	750	Rock slide	400	NVIR	CWH	>250 cm	Jg/ muTR K	Recent 1970?
AF17	Clayoquot Arm	92F/04	10U	49°11'N 125°33'W	650	Rock slide	50	NVIF	CWH	>250 cm	PMns	Recent <1957
AK1	Prince of Wales Range	92K/05	10U	50°22'N 125°47'W	600	Rock slide/ avalanche	400	NVIR	CWH	100- 250 cm	muTR K	Recent 1946?
AL1	Hushamu Lake	92L/12	9U	50°41'N 127°51'W	600	Rock slump	200	NP	CWH	100- 250 cm	uTR PB	Ancient
AL2	Cluxewe River	92L/11	9U	50°35'N 127°11'W	200	Rock slide	50	NVIR	CWH	100- 250 cm	T VS	Ancient
AL3	Claud Elliot Creek	92L/07	9U	50°19'N 126°33'W	1050	Rock-fall avalanche	200	NVIR	CWH	100- 250 cm	Jg	Old
AL4	Mount Elliot	92L/07	9U	50°18'N 126°30'W	1200	Rock-fall avalanche	200	NVIR	MH/AT	100- 250 cm	Jg	Old
AL5	Kauwinch River	92L/03	9U	50°13'N 127°15'W	750	Rock slump	200	NVIR	CWH	>250 cm	Jb/ IJ B	Ancient
AL6	Wolfe Lake	92L/02	9U	50°12'N 126°46'W	1000	Rock slump	1,600	NVIR	CWH	>250 cm	uTR Q/ muTR K	Ancient
AL7	Tahsish Inlet East	92L/03	9U	50°06'N 127°04'W	450	Rock slump	200	NVIF	CWH	>250 cm	IJ B	Ancient
AL8	Kaouk River	92L/02	9U	50°05'N 126°51'W	1000	Rock-fall avalanche	800	NVIR	MH/AT	>250 cm	Jg/ uTR PB	Old late 1920s
AL9	Gerald Creek	92L/01	9U	50°07'N 126°05'W	1200	Rock slide	200	NVIR	CWH	>250 cm	muTR K	Old

* * Refer to next page for accompanying notes.

NOTES to accompany TABLE 1--Summary of landslide features

- *1* LANDSLIDE NUMBER -- First letter refers to Priority. Second letter refers to 1:250,000 scale NTS map sheet beginning with 92. Refer to FIGURE 1.
- *2* GEOGRAPHIC LOCATOR -- The closest named geographic feature.
- *3* NTS -- 1:50,000 scale National Topographic System map.
- *4* UTM -- Universal Transverse Mercator, 1000 m grid.
- *5* LAT & LONG -- latitude and longitude to the nearest minute.
- *6* APPROXIMATE MAINSCARP ELEVATION (m) -- estimated from 1:50,000 scale map.
- *7* TYPE OF LANDSLIDE -- based on Varnes [13].
- *8* APPROXIMATE AREA -- area of ground disturbance, rounded to nearest size grouping. Not to be used to calculate volumes.
- *9* PHYSIOGRAPHIC REGION -- based on VanDine [7]. Refer to FIGURE 1 and TABLE 5.
- *10* BIOGEOCLIMATIC ZONE -- based on Nuszdorfer et al [11]. Refer to TABLE 6.
- *11* ANNUAL PRECIPITATION ZONE -- based on Farley [12].
- *12* BEDROCK GEOLOGY -- based on Muller [8]. Refer to TABLE 8.
- *13* ESTIMATED AGE -- Refer to TABLE 9.

Refer to text for further details.

TABLE 2--Landslide features vs. NTS map sheet

1:250,000 NTS TOPOGRAPHIC MAP	GEOGRAPHIC CO-ORDINATES	NUMBER OF LANDSLIDES	%
92B	48°-49° N; 122°-124° W	0	0
92C	48°-49° N; 124°-126° W	0	0
92E	49°-50° N; 126°-128° W	7	21
92F	49°-50° N; 124°-126° W	17	50
92G	49°-50° N; 122°-124° W	0	0
92K	50°-51° N; 124°-126° W	1	3
92L	50°-51° N; 126°-128° W	9	26
102I	50°-51° N; 128°-130° W	0	0
TOTAL NUMBER OF LANDSLIDES		34	100

NOTE: Map sheets do not cover similar size areas of Vanc. Isl.

TABLE 3--Landslide features vs. landslide type

TYPE OF LANDSLIDE	NUMBER OF LANDSLIDES	%
Rock-fall Avalanches	11	32
Rock Slides	17	50
Rock Slumps	6	18
TOTAL NUMBER OF LANDSLIDES		34 100

NOTE: Classification of landslides based on Varnes (1978).

TABLE 4--Landslide features vs. area of ground disturbance

AREA OF GROUND DISTURBANCE (m ²)	NUMBER OF LANDSLIDES	%
50,000	5	15
100,000	5	15
200,000	14	41
400,000	5	15
800,000	2	6
1,600,000	3	9
TOTAL NUMBER OF LANDSLIDES		34 101

NOTE: Disturbed areas include both area of depletion and area of accumulation. They are intended for relative comparisons only and should not be used for volume calculations.

TABLE 5--Landslide features vs. physiographic region

PHYSIOGRAPHIC REGION	NUMBER OF LANDSLIDES	%
North Vancouver Island Ranges (NVIR)	29	85
South Vancouver Island Ranges (SVIR)	0	0
West Vancouver Island Fiordland (WVIF)	4	12
Nahwitti Plateau (NP)	1	3
Quinsam Plateau (QP)	0	0
Nanaimo Lakes Highland (NLH)	0	0
Victoria Highlands (VH)	0	0
Estevan Lowlands (EL)	0	0
Nanaimo Lowlands (NL)	0	0
Alberni Basin (AB)	0	0
Squash Basin (SB)	0	0
TOTAL NUMBER OF LANDSLIDES		34 100

NOTE: Physiographic regions based upon VanDine (in preparation). Refer to Figure 1.

TABLE 6--Landslide features vs. biogeoclimatic zone

BIOGEOCLIMATIC ZONE	NUMBER OF LANDSLIDES	%
Alpine Tundra (AT)	0	0
Mountain Hemlock/Alpine Tundra (MH)	11	32
Coastal Western Hemlock/Mt. Hemlock (CWH/MH)	1	3
Coastal Western Hemlock (CMH)	22	65
Coastal Douglas Fir (CDF)	0	0
TOTAL NUMBER OF LANDSLIDES		34 100

NOTE: Biogeoclimatic zones based on Nuszdorfer et al (1985).

TABLE 7--Landslide features vs. annual precipitation

ANNUAL PRECIPITATION (cm)	NUMBER OF LANDSLIDES	%
>250	25	74
100 - 250	9	26
50 - 100	0	0
TOTAL NUMBER OF LANDSLIDES	34	100

NOTE: Annual precipitation zones based on Farley (1979).

TABLE 8--Landslide features vs. underlying bedrock geology

BEDROCK GEOLOGY FORMATIONS	NUMBER OF LANDSLIDES	%
late Tertiary volcanics (T VS)	1	3
lower Jurassic Bonanza volcanics (IJ B)	2	6
mid/upper Triassic Karmutsen vol. (muTR K)	13	38
Jurassic island granitic intrusive (Jg)	5	15
Jurassic westcoast granitic instru. (PMns)	1	3
Tertiary granitic intrusive/vol. (Tg/muTR K)	3	9
Jurassic granitic intrusive/vol. (Jg/IJ B)	1	3
Jurassic granitic intrusive/vol. (Jg/muTR K)	5	15
Jurassic granitic intrusive/sed. (Jg/uTR PB)	1	3
upper Triassic Parson Bay sed. (uTR PB)	1	3
upper Triassic Quatsino sed./vol. (uTR Q/muTR K)	1	3
TOTAL NUMBER OF LANDSLIDES	34	101

NOTE: Refer to Muller (1977) for full descriptions of the bedrock formations.

TABLE 9--Landslide features vs. estimated age of occurrence

RANGE OF ESTIMATED AGE OF OCCURRENCE	NUMBER OF LANDSLIDES	%
Recent -- less than 50 years old	9	26
Old -- 50 to 100 years old	6	18
Ancient -- 100s to 1000s of years old	19	56
TOTAL NUMBER OF LANDSLIDES	34	100

NOTE: As determined from Phase 3 of study and from other sources.

TABLE 10--'Recent' landslides, estimated year of occurrence and years of significant earthquakes

LANDSLIDE NUMBER	ESTIMATED YEAR OF OCCURRENCE	YEAR OF SIGNIFICANT EARTHQUAKE
		1946
AF6	1946 ?	
AF7	1946	
AF8	1946 ?	
AK1	1946 ?	
AF10	< 1957	
AF17	< 1957	
		1957
AF15	1957 - 1970	
AF16	1970 ?	
		1972
AE3	1974 ?	
		1975
		1986

NOTE: Refer to TABLE 1 for details of landslides and FIGURE 1 for details of earthquakes.

The Little Doctor Lake Landslide, An Example of Coseismic Reactivation of a Landslide in Permafrost Terrain

K. Wayne Savigny

*Department of Geological Sciences, University of British Columbia
Vancouver, British Columbia*

David C. Segó

*Department of Civil Engineering, University of Alberta
Edmonton, Alberta*

Kaye L. MacInnes

*Land Resources, Indian and Northern Affairs, Canada
Yellowknife, Northwest Territories*

Two earthquakes occurred at the same location in the Nahanni region of the western Northwest Territories in 1985. The first, a M6.6 event on October 5, exceeded any previously recorded in the area. The larger M6.8 earthquake on December 23 with peak horizontal accelerations of 1.25g and peak vertical accelerations exceeding 2g [1] is the largest historical earthquake in the eastern Canadian Cordillera [2].

The North Nahanni Slide, a 5 to 7 million m³ rock avalanche triggered by the October earthquake, and a 0.1 million m³ rockfall caused by the December shock have been described elsewhere [2 and 3]. Both occurred in mountainous terrain of the Mackenzie Mountains near the epicentre. Part of a large ancient landslide situated in foothill topography 67 km east-southeast of the epicentre was reactivated at the approximate time of the December earthquake. It occurred on a gentle slope and apparently moved at high velocity. This landslide complex, referred to as the Little Doctor Lake Slide, is described here based upon a preliminary engineering geology assessment. Mechanisms that could account for reactivation of colluvium and a high velocity failure on a gentle slope are proposed. The geological setting is repeated in nearby parts of the Mackenzie Valley transportation corridor. The potential for this landslide hazard in the transportation corridor is discussed.

Site Description

The Little Doctor Lake Slide is in the southwest part of the Northwest Territories, 460 km west of Yellowknife and 420 km south of Norman Wells (Fig. 1). It is only accessible by helicopter. Linear facilities in the Mackenzie Valley transportation corridor, including the Mackenzie Highway and the Interprovincial Pipe Line

(NW) Ltd. oil pipeline are situated 60 km northeast (Fig. 1). At the time of the earthquakes, two residents lived on the northwest shore of Little Doctor Lake (Fig. 1). They reported the landslide based on second hand information from visitors who observed the fresh landslide scar on an otherwise snow-covered slope while flying to Little Doctor Lake for the Christmas Holiday.

The physiographic location is at the western limit of Mackenzie Plain near the Mackenzie Mountain front [4]. Local elevations range from a low of 100 m along Mackenzie River, to 650 m at the top of Ebbutt and Martin Hills and 1500 m in Mackenzie Mountains (Fig. 1).

The regional geology is shown on Figure 1. Rocks are Mid to Upper Cretaceous age [5] and consist of weak, fissured, grey to black claystone. They belong to the Middle Member of the Sully Formation, which is reported to contain bentonite [6]. No bentonite was found in natural exposures however, and the single *in situ* sample of claystone tested had a liquid limit of 45%, a plasticity index of 25%, and an activity of 0.75, which suggests predominantly illitic clay minerals. Regional mapping indicates bedding surfaces are flat lying to gently westward dipping near the axis of the Root River syncline (Fig. 1) [5].

The area was glaciated several times during the Pleistocene by Cordilleran and Laurentide ice sheets. The last glaciers retreated approximately 13,500 years ago leaving a blanket of till covering most of Mackenzie Plain and glaciofluvial deposits in low lying areas occupied by larger rivers and streams [7, 8 and 9]. Surficial materials overlying bedrock in undisturbed headscarp exposures range from 8 to 32 m thick and consist mainly of sandy clay till (CL). Beds of sand and

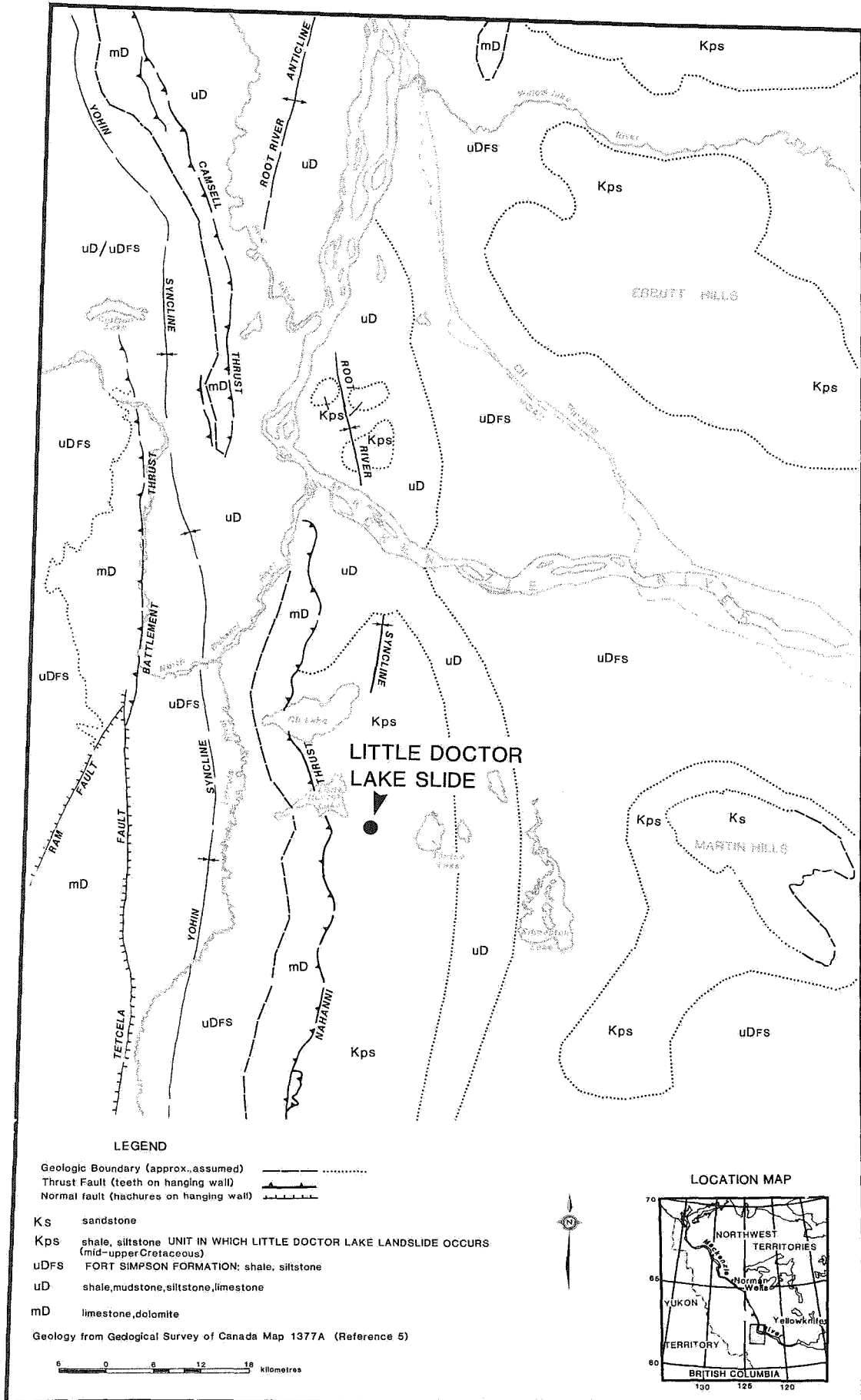


Figure 1: Location and regional geology map.

gravel (SP-GP) and lenses of clay (CI) comprise up to 15%, but are generally limited to the top one third of the surficial materials section. Natural southwest facing exposures of surficial materials are as steep as 75°.

The site lies in the discontinuous permafrost zone [10].

Little Doctor Lake Slide

A topographic map and profiles are shown in Figures 2a and 2b, respectively, and Figure 3 provides an oblique aerial view of the 1985 reactivation area and runout from the southwest. Although the slide complex is believed to have originated as one landslide, there is geomorphic evidence of multiple scarps in the source area in addition to the 1985 slide event. On this basis, the slide complex is divided into three zones as shown in Figure 2; Zones I and II represent pre-historic slide events, and Zone III the 1985 event. The estimated volume of the Little Doctor Lake Slide complex is 45 to 50 million m³. Between 4 and 5 million m³ or approximately 10% of the ancient slide was reactivated in the December 1985 earthquake.

The toe of the early post glacial slope can be estimated by projecting the eastern edge of a glaciofluvial channel beneath the slide debris (Fig. 2a). Original slopes are estimated to have been between 11° and 15°. This is consistent with natural slopes along the eastern shore of Little Doctor Lake where active instability is juxtaposed with stable slopes.

Knowledge about Zones I and II is based on airphoto interpretation, aerial reconnaissance, and profiles prepared from 1:50,000 topographic maps. Additional information for Zone III was gathered during brief site visits in May and October, 1991. The permafrost table was probed during the October visit, and a disturbed claystone sample collected was later subjected to routine laboratory index testing.

Ancient Landslides

Zone I is believed to represent the only remaining portion of the first slide event. The original slope interpreted from profile A-B (Fig. 2b) was approximately 13°. The headscarp formed at the top of the ridge and runout extended approximately 620 m from the toe. The post-failure slope measured from the top of the headscarp to the limit of runout [11] is approximately 7°. Most colluvium appears to have moved to the depositional zone. Present vegetative cover suggests

permafrost is only present in isolated parts of the depositional zone.

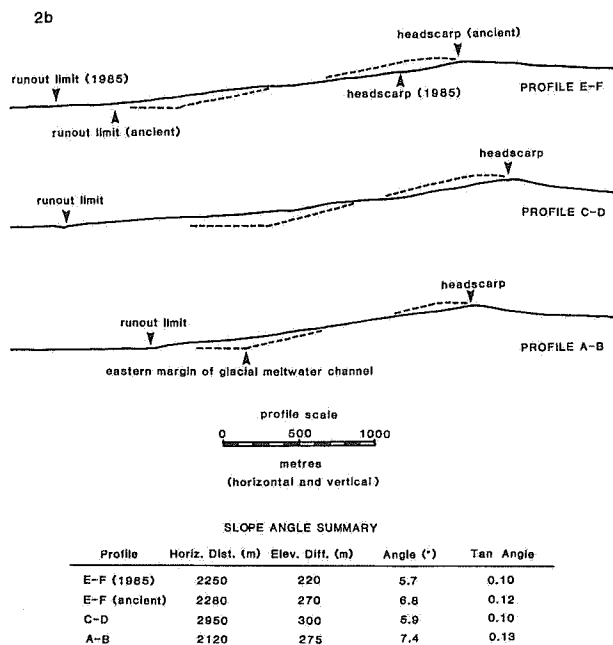
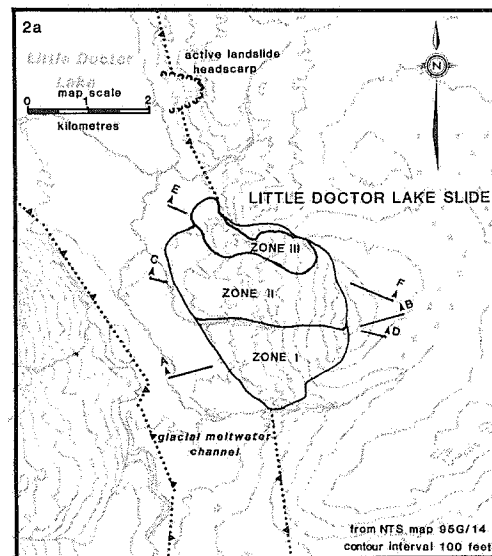


Figure 2: Little Doctor Lake Slide site map (a) and profiles (b)

Zone II represented the remainder of the ancient slide complex prior to the 1985 event. It is distinguished from Zone I by (1) a deeper failure surface, (2) a much larger runout, and (3) a greater thickness of colluvium remaining in the source area. The original slopes interpreted on profiles C-D and E-F (Fig. 2b) were approximately 15° and 11° , respectively. Either the original slide, or one or more later landslides is believed to have lowered the summit of the ridge as illustrated in Figure 2b. Runout extended as much as 1320 m from the toe. The post-failure slopes measured from the top of the lowered headscarp to the limit of runout are approximately 6° on profile C-D and 7° on profile E-F. More colluvium remained in the source area than in Zone I based on the extent to which streams are incised into the slide debris, and on natural exposures along the Zone III headscarp. Vegetation patterns suggest discontinuous permafrost is more widespread in Zone II, particularly in a 400 m wide band along the northern boundary with Zone III, and between the Zone II and III headscarps.

The pre-historic failure planes in Zones I and II probably formed along bedding surfaces dipping gently west toward the valley. The deeper failure surface in Zone II suggests two different bedrock units, likely bentonite seams, were involved. The tangent of the elevation-runout angles ranges from 0.10 to 0.13 (Fig. 2b), which is anomalously low in comparison to other large landslides [11], but not unreasonable when the large volume and the suspected presence of bentonite seams are considered. The facility for sliding and the long runout suggest the ancient landslides should be classified as rock slides-rock avalanches. The slides likely occurred in early Holocene.

1985 Landslide

Topographic profile E-F through Zone III and the upper portion of Zone II is shown in Figure 2b. The pre-1985 slide and post-1985 slide profiles are essentially the same at the scale used, except at the toe where an additional 340 m of runout distinguishes the 1985 event. The 1985 failure occurred on a gentle 7° slope. The tangent of the elevation-runout angle is 0.10. This is comparable to the lowest determined for the ancient slide, but it is unreasonably low in relation to rock slides-rock avalanches of comparable volumes [11], suggesting the 1985 event involved a highly mobile failure mechanism.

Vegetation in the central portion of Zone III consisted of low scrub growth in 1961 aerial photographs. This may have been a result of groundwater discharge or

chemistry, or small slope movements. Permafrost is believed to have disappeared from most of the Zone III source area but was present in the headscarp, changing from isolated to widespread with distance east toward the Zone II headscarp.

Two mechanisms are proposed for the 1985 landslide, liquefaction and translational sliding. The former was triggered by coseismic shaking. Translational sliding may have also been affected by seismic shaking but oversteepening in response to the liquefaction failure was likely a more significant factor. The relative importance of the two mechanisms in landslide displacements is related to the distribution and nature of ancient colluvium, and the distribution of permafrost in and around Zone III.

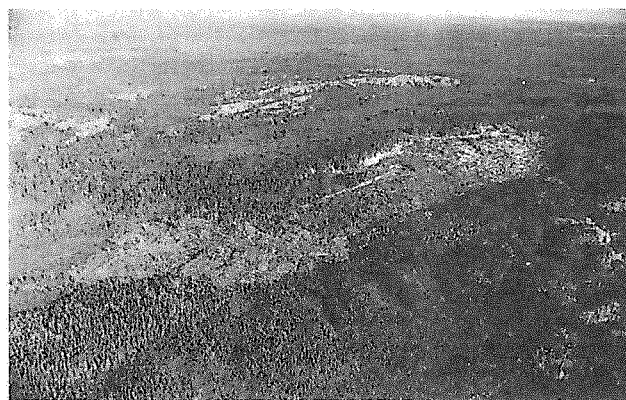


Figure 3: Oblique photograph of the 1985 reactivation area of Little Doctor Lake Slide.

Liquefaction is believed to have occurred in prehistoric colluvium which was derived mainly from glacial drift. This colluvium is estimated to have been in the order of 15 to 20 m thick in the central Zone III source area, pinching out in an upslope direction to a discontinuous veneer in the headscarp of Zone III. Its nature is predicted from examination of colluvium in the 1985 landslide scar (Fig. 4). The soil consists of sandy till mixed with discontinuous lenses and beds of sand and gravel, lenses of clay, and an increasing portion of remoulded claystone as a function of depth. A macrostructure controlled by tension cracks up to 20 cm wide at the ground surface, up to more than 3 m deep and spaced at 2 to 3 m characterized the area on both the May and October, 1991, site visits. The water table on these occasions ranged from within a few centimetres of the ground surface to more than 2 m deep. It is

proposed that the ancient colluvial soil had a similar macrostructure and that the December 1985 seismic shaking caused this structure to collapse resulting in a sudden rise in pore pressure and loss of resistance.

The 1985 landslide event also caused translational sliding, indicated by block displacements at the Zone III headscarp (Fig. 5), and east as far as the adjacent headscarp of the ancient slide (Zone II). The displacements were seated at estimated depths of 10 to 15 m in moderately disturbed claystone. It is believed this claystone was displaced for the first time in 1985, but it may also be part of the ancient colluvium sequence. The size of the displaced blocks increases from several tens of m² near the Zone III headscarp to several hectares farther east. The magnitude of displacement decreases with distance east (Fig. 6), ultimately becoming discontinuous small separations in the organic mat at the base of the Zone II headscarp. The eastern headscarp of Zone III is somewhat arbitrarily defined as the location where displaced but intact blocks moved laterally to the extent that they became separated from adjacent blocks. No fresh evidence of deformation was recognized that would suggest the block displacements post-date the 1985 event.

The 1985 landslide is classified as a liquefaction induced earthflow and rock block slide.

Discussion

The extent of liquefaction in the 1985 Little Doctor Lake Slide appears to correlate with thick, glacial-drift-derived colluvium. This is believed to have been a well-graded soil with an open, metastable structure (Fig. 4) that collapsed under seismic shaking causing a sudden increase in pore pressure, loss of resistance, and catastrophic failure. Liquefaction accounts for the anomalously long runout of the 1985 slide volume. Three variables could have precluded or reduced the susceptibility of this material to liquefaction; permafrost, seasonal frost, and low soil moisture content.

Although the area lies in the discontinuous permafrost zone, pre-slide vegetation interpreted from aerial photographs indicates permafrost had disappeared from the area that liquefied. Climate data from Fort Simpson, 100 km east of the slide, suggest most of the 1985 summer and fall experienced above average precipitation (Fig. 7). The unusually heavy October, 1985, precipitation was 30% rain and 70% snow, with average snowfalls continuing through November and December,



Figure 4: Ground surface at the approximate midpoint of the 1985 slide.



Figure 5: Displaced blocks in the 1985 slide headscarp.

1985. Although these data must be viewed with caution because of their distance from the site, they suggest seasonal penetration of the freezing front would have been slowed by the insulating blanket of snow, and antecedent soil moisture contents would have been at or above normal. Groundwater discharge, if present, would have further slowed penetration of seasonal frost and sustained high soil moisture contents.

Translational sliding at the Zone III headscarp and as far east as the Zone II headscarp probably occurred in response to the liquefaction failure. The gentle 7° slope is unusually low for sliding. This may indicate high pore pressures related to groundwater discharge. It may also indicate that lower than residual friction angles related to turbulent shear were mobilized during seismic shaking [12 and 13].

The variation in displacement magnitude associated with translational sliding in the Zone III headscarp area is attributed to two factors. First, the magnitude decreases with distance away from the oversteepened margin of the liquefied zone. This suggests higher shear stresses at the margin had a direct effect on the displacement magnitudes. Second, the magnitude was influenced by the distribution of permafrost. Displacements were greatest where airphoto evidence indicates widely separated, presumably shallow permafrost bodies. Farther east permafrost was widespread and almost certainly somewhat thicker.

The regional distribution of the Cretaceous rock unit in which the Little Doctor Lake Slide occurred is shown on Figure 1. Existing linear facilities in the Mackenzie Valley transportation corridor are a safe distance away, and landslide hazards originating in this rock unit are a negligible risk. Cryogenic and mass wasting processes in permafrost regions have the effect of increasing *in situ* void ratios, creating pervasive macrostructures, and causing unusual textural mixtures of soils, none of which, individually, may be liquefiable, but together become a hazard [14]. These factors are predicted in the literature to increase the susceptibility of thawed permafrost soils to liquefaction [15]. The Little Doctor Lake Slide is the first example known to the authors that confirms this literature prediction. Thawing of permafrost soils associated with engineered development and with climate change scenarios will undoubtedly increase risks associated with this landslide hazard.



Figure 6: Evidence of displacement behind the 1985 headscarp.

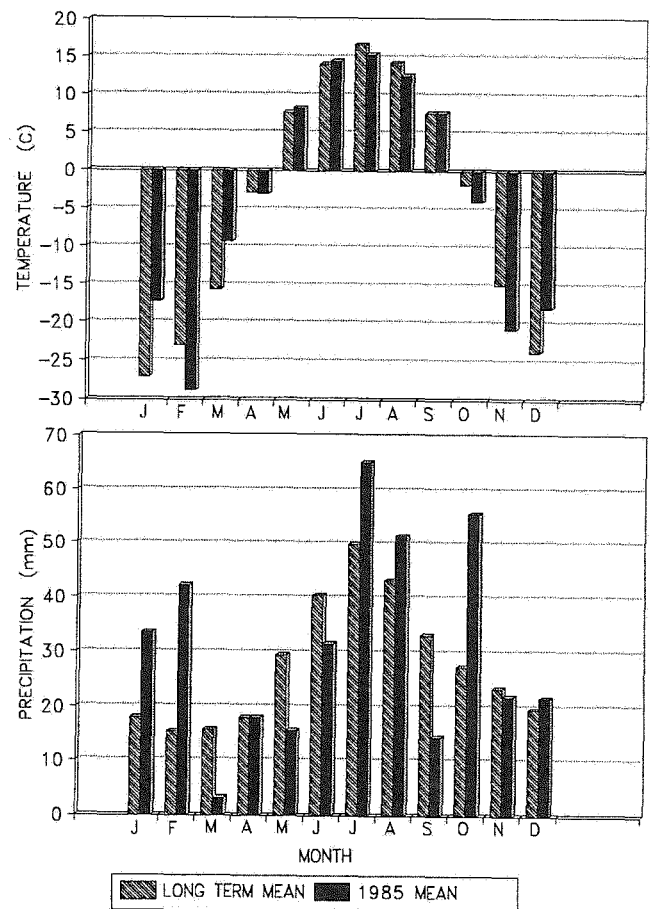


Figure 7: Temperature and precipitation data from Fort Simpson, N.W.T.

Acknowledgements

The slide was brought to the attention of one of the authors by Mr. Gus Kraus who resided at Little Doctor Lake in 1985. His enthusiasm for and knowledge of the area is gratefully acknowledged. Mr. Neil Parker of Atmospheric Environment Service provided the climate data for Fort Simpson. Financial support for this work was provided by the Northern Oil and Gas Action Plan and Land Resources Division, Department and Indian and Northern Affairs, Yellowknife. Bruce Geotechnical Consultants Ltd. provided support in preparation of the manuscript.

References

- [1] Weichert, D.H., Wetmiller, R.J., and Munro, P.. 1986. Vertical earthquake accelerations exceeding $2g$? The case of the missing peak. *Bulletin of the Seismological Society of America*, Vol. 76, No. 5, pp. 1473-1478.
- [2] Wetmiller, R.J., Horner, R.B., Hasegawa, H.S., North, R.G., Lamontagne, M., Weichert, D.H., and Evans, S.G. 1988. An analysis of the 1985 Nahanni earthquakes. *Bulletin of the Seismological Society of America*, Vol. 78, No. 2, pp. 590-616.
- [3] Evans, S.G., Aitken, J.D., Wetmiller, R.J., and Morner, R.B. 1987. A rock avalanche triggered by the October 1985 North Nahanni earthquake, District of Mackenzie, N.W.T. *Canadian Journal of Earth Sciences*, Vol. 24, p. 176-184.
- [4] Bostock, H.S. 1967. Physiographic regions of Canada. Geological Survey of Canada, Map 1245A.
- [5] Douglas, R.J.W. and Norris, D.K. 1974. Geology Sibbeston Lake, District of Mackenzie. Geological Survey of Canada, Map 1377A.
- [6] Stott, D.F. 1982. Lower Cretaceous Fort St. John Group and Upper Cretaceous Dunvegan Formation of the foothills and plains of Alberta, British Columbia, District of Mackenzie and Yukon Territory. Geological Survey of Canada, Bulletin 328, 124 p.
- [7] Craig, B.G. 1965. Glacial Lake McConnell, and the surficial geology of parts of the Slave River and Redstone River map-areas, District of Mackenzie. Geological Survey of Canada, Bulletin 122, 33 p.
- [8] Rutter, N.W. and Boydell, A.N. 1973. Surficial geology and land classification, Mackenzie Valley transportation corridor (85D, 95B (north half), 95G, I, K (east half), N, O). In, Report of Activities, Part A, Geological Survey of Canada, Paper 73-1A, pp. 239-240.
- [9] Hughes, O.L. and Duk-Rodkin, A. 1987. Relationships of Late Pleistocene landforms and deposits along Mackenzie and Richardson Mountains (abstract). 12th INQUA Congress, National Research Council of Canada, Ottawa, Programme with Abstracts, pp. 190.
- [10] Brown, R.J.E. 1967. Permafrost in Canada. Geological Survey of Canada, Map 1246A.
- [11] Scheidegger, A.E. 1973. On the prediction of the reach and velocity of catastrophic landslides. *Rock Mechanics*, Vol. 5, pp. 231-236.
- [12] Lemos, L.J.L. and Coelho, P.A.L.F. 1991. Displacements of slopes under earthquake loading. Proceedings, Second International Conference on Recent Advances in Geotechnical Earthquake Engineering and Soil Dynamics, St. Louis.
- [13] Lemos, L., Skempton, A.W. and Vaughan, P.R. 1985. Earthquake loading of shear surfaces in slopes. Proceedings: XI International Conferences on Soil Mechanics and Foundation Engineering, San Francisco, pp. 1955-1958.
- [14] Dr. P. Byrne, personal communication, 1992.
- [15] McRoberts, E.C. 1978. Slope stability in cold regions. In *Geotechnical Engineering for Cold Regions*, O.B. Andersland and D.M. Anderson, eds., McGraw-Hill Book Company, pp. 363-404.

Session 4A
Risk Assessment and
Land Use Planning

such as the mapping of natural hazards, afforestation work in the mountains, erosion control works, and the construction of protective structures in settled torrent and avalanche zones [6].

Like the Alps, the Cordilleran regions of British Columbia have been undergoing rapid economic growth for the past 100 years. The original impetus for this development was resource extraction - mining, forestry and fisheries. Currently, an expanding tourism industry is also contributing to the settlement of British Columbia's rugged natural environment.

Most of this province's land is mountainous, and as the population grows, development is increasingly occurring in areas of high relief. The greater Vancouver region is a good example of this trend; the land available for future suburban expansion is limited largely to the farmland in the lower Fraser valley and to the lower elevations of the nearby Coast Mountains. The controls on the subdivision and use of farmland makes urbanization in the Fraser Valley difficult. Therefore, much expansion is taking place on the lower mountain slopes. Hence the exposure of the population to high mountains increases yearly.

In this paper we will review some of the French and Austrian natural hazard management policies in the context of their potential applicability to cordilleran British Columbia. The Alpine countries have developed approaches and procedures of direct relevance to policy planners in montane North America.

Natural hazard mapping and management

One of the most important tools available to governments which have chosen a proactive hazard management policy is natural hazard mapping. The technical characteristics of hazard maps may be modified to suit various experts or interested citizens in a particular area. While many natural hazards are not quantifiable, experts in many countries have developed appropriately scaled means of assessing danger.

It is in Alpine Europe that some of the

best comprehensive natural hazard management policies are found. The European literature on this subject has not yet received sufficient attention from geologists, geographers, planners, and engineers in British Columbia [7].

Natural hazard mapping has been done by the governments of some Alpine European countries for decades. These mapping programs grew out of a need for effective management of the hazards posed by high mountains. The experience of these countries in this field is of interest to anyone involved in engineering, planning, land development and geography.

Natural hazard management in France

Work on French hazard mapping dates from the 1930's, when a series of floodplain maps was prepared. During the 1970's, the mapping of natural hazards and related land-use regulation was greatly extended.

1970: CLPA There was a need to reconstitute collective memory of avalanche occurrence in the French mountains. Depopulation in the Alps, which began during the industrial revolution, combined with the lack of records of natural disasters makes historical information on hazards scarce [8]. In 1970, the *Ministère de l'Agriculture* created a new series of maps to fill this need, the *Cartes de Localisation Probable des Avalanches* (CLPA): avalanche survey maps at a scale of 1/20,000. An example is the CLPA of Vallorcine (Haute Savoie) [9].

The CLPA maps were not designed for general public use, but were internal documents used by civic authorities involved in public safety and land-use planning. The mayor of the local *commune* (municipality) had to approve the maps.

The CLPA maps were clearly useful in delimiting avalanche-prone areas, but had little regulatory value since they were not formally linked to zoning or building requirements.

1974: PZEA The shortcomings of the CLPA map series led to the realization that avalanche hazard zoning regulations must be formulated in the rapidly growing

winter resort communities of the Alps and Pyrenées. Consequently, Article R. 111-3 of the national *Code de l'Urbanisme* (planning law) requires building restrictions to be in place when known natural hazards such as avalanches are present. Such areas must be delimited by prefectorial decree.

The *Plan de Zones Exposées aux Avalanches* (PZEA) process was created in 1974 to fulfil this need. Property in red zones on the map is frozen from development; blue zoned property is subjected to special construction requirements. Mapped at the scale of 1/2,000, 1/2,500 or 1/5,000, many winter resorts were mapped, such as Vallorcine (Haute Savoie) [10].

1975: ZERMOS In 1975, the *Bureau de Recherches Géologiques et Minières* began to publish, in conjunction with some French universities, the *Carte de Zones Exposées à des Risques Liés aux Mouvements du Sol et du Sous-sol* (ZERMOS) map series. Some of the leading French researchers in natural hazard mapping were commissioned to work on this series, sometimes in groups, but often alone [11]. The scale of ZERMOS maps ranged from 1/100,000 to 1/20,000. Unfortunately, these maps were not an explicit part of any land-use planning process. The cartographic techniques used in depicting natural hazards make the ZERMOS maps a valuable resource for the planner to be aware of.

1982: PER Heavy flooding in the Gironde (south of Bordeaux) and Ain (northeast of Lyon) *départements* in 1981, combined with decades of natural disasters in the Alps, caused the French government to hold an inquiry into the prevention of major natural disasters. It had become apparent that previous attempts at natural hazard cartography and management in France were insufficient in scope.

A law dealing with compensation to victims of natural disasters was passed in July 1982 (*Loi numéro 82-600*), which had two objectives:

1. the creation of a natural hazard insurance scheme, for the protection of homeowners, to be administered by existing insurance companies.
2. the prohibition of further urban expansion into areas of very high risk; the specific incorporation of preventative measures (active and passive) in the planning of both

existing communities and undeveloped areas of medium risk.

The government was obliged, under Article 5, to create a new series of natural hazard maps, called *Plans d'Exposition aux Risques naturels prévisibles* (PER). The scale of PER maps ranges from 1/10,000 in unorganized areas to 1/5,000 - 1/2,000 in urban communities, depending upon the availability of local base maps. The guidelines for the preparation of maps, including legend, scales, and colours were specified [12]. There are four maps in each PER report:

1. *Carte de localisation des phénomènes naturels* - a map of slope failures (active or potential), floodplains and geological features linked to hazards.
2. *Carte de typologie de l'occupation du sol actuelle ou en projet* - a land use map of areas of different socio-economic density, farmland, forests and cultural features.
3. *Carte des aléas* - a map indicating the risk level for known hazards.
4. *Plan d'exposition aux risques naturels prévisibles* - a land-use planning map which contains the following zones:

- . Red zone - exposed to a severe hazard or a combination of a large number of different hazards.
- . Blue zone - moderate levels of natural hazards.
- . White zone - no natural hazards.

The four maps are accompanied by an explanatory report, which includes economic and historical data on the areas which are exposed to risk, as well as data concerning the number of people in such areas. Construction and subdivision are prohibited in the red zone, and are strictly regulated in the blue zone. The report also includes a summary of past events' impact in economic terms, and information on the way in which the hazards were managed in the past (passive or active risk management). A hazard management regime is specified, including active measures where applicable. The active protective measures can include reinforcements to individual buildings, avalanche deflection barriers, check dams, and flood diversion channels. These are listed in catalogues of preventative measures to be used in the PER report [13]. The PER reports, like the PZEA, are reviewed at public meetings, and the involvement of interested parties (landowners and residents) in the mapping and zoning process is

encouraged. After approval, the maps are available for public viewing, upon application to the mayor or Prefect. An example of a PER project exists for Les Villards-sur-Thônes (Haute Savoie) [14].

Natural hazard management in Austria

Although the *Wildbach- und Lawinenverbauung* [WLV] agency had been providing mitigative measures against natural hazards on an ad-hoc basis since 1884, the need for a more comprehensive natural hazard policy in Austria became evident in the decades immediately following the second world war. From the 1950's onward, development in the mountains increased rapidly due to economic expansion and tourism. This led to an increasing demand for developable land, which was often in hazardous areas which had been free of houses for centuries. For most owners of farmland, the alluvial fans were not valuable agriculturally, yet their gravel surfaces could be used for the construction of houses. This situation (development on alluvial and debris fans) was even more pronounced in winter recreation areas. The result was extensive urban development and the inevitable occurrence of natural disasters [15]. This led to a great increase in the number of mitigative construction projects and attendant budgetary overspending.

In 1966, a law *Entsprechung auch im Katastrophen-fondgesetz* (Compensation Funds for Catastrophes) formally endorsed the principle of compensation for Austrian citizens affected by natural disasters. As a result of this entrenchment of liability and costs, prevention of disasters became urgent.

From 1884 to the 1960's, the management of natural hazards had been entrusted to the geotechnical engineers of the WLV. They were responsible for approving or rejecting requests from municipal officials for the construction of protective works. This engineering approach to hazard management, although effective, proved to be very expensive. Therefore, prevention of urban growth into dangerous areas, such as active alluvial fans, became the primary goal of the WLV in the late 1960's [16]. This change in policy direction led to the production of the first Austrian

natural hazard maps. An example of a WLV report exists for the village of Döllach im Mölltal [17].

The WLV natural hazard maps and reports are integrated into the land-use plans of local governments. Areas classified on the maps as being zones of high danger are frozen from any type of development, and areas of moderate hazard are required to meet strict construction codes. The maps are updated to reflect any large changes in the area, such as new engineering works or major forest harvesting.

Public opposition to the WLV hazard zoning maps was quite strong in the first phase of mapping, but diminished after a public input mechanism was set up in 1975. It is generally true that the communities which have approved hazard zone plans are safer, and because a lot of responsibility for construction work is transferred to the federal level (WLV), these communities are not fully liable for damage done in a natural disaster [18].

Discussion

From the experiences of two European countries, there are four key elements to a successful hazard management program:

1. nation-wide or province-wide natural hazard mapping;
2. dedication of the task of hazard management to a single agency, which can develop a body of management specialists;
3. the establishment of a comprehensive policy framework for dealing equitably with natural hazard information;
4. considerable allowance for public consultation, both during and after the establishment of hazard zones in a locality.

There are two difficult aspects - technical and political - to transferring European natural hazard management policies to B.C. The technical problem includes the task of designing a policy to fit into the existing British Columbian administrative framework. The political problem is one of obtaining sufficient "political will" to embark on a long-term program which does not produce profits or immediate benefits, unlike

other projects more commonly favoured by political leaders [19].

British Columbia

There are many weaknesses and inadequacies in the current natural hazard management policy in B.C. Regional districts and municipal governments are required, under the Municipal Act, to include information on natural hazards in each Official Community Plan. Although some hazard mapping has been done, it is not applied evenly and systematically throughout the province. Mapping for some Plans is being done by consultants and for others by the Ministry of Environment.

Currently in B.C., natural disasters are treated as "acts of God", and the major response by government is reactive. Monetary compensation to victims and expropriation of property in dangerous areas are examples of a reactive policy. This ad-hoc application of reparations unfairly burdens the many taxpayers who live in relatively safe areas. It also ignores the potential benefits of proactive management.

Existing institutional arrangements that are applicable to natural hazards are numerous, and dealt with by three levels of government. The lack of a clear mandate and "buck-passing" over the liability issue means that hazard management in British Columbia is largely ineffectual. This is probably due to a lack of understanding of the hazards issue by political leaders, and because no single agency coordinates the management of natural hazards. There is no single piece of legislation or institution in British Columbia that is designed solely to deal with the hazards posed by mass wasting.

Provincial government There are seven major weaknesses in B.C.'s provincial policies which are relevant to natural hazards:

1. There is no binding provision in the relevant legislation, requiring natural hazard mapping to be done. As a result, mapping is often not carried out until after a disaster occurs.
2. Inter-agency co-operation in natural hazard assessment is not facilitated by the present administrative structure. For example, the Ministry of Forests has

expressed concern about local governments which are attempting to regulate logging on private lands using Section 978 of the Municipal Act. The intention of this Section is to prevent natural disasters, and it would appear to be a reasonable policy for local governments to pursue, in the absence of provincial standards. Different agencies' actions and interests are apparently often in conflict.

3. The provincial government has concentrated its efforts mainly on post-destructive event and post-development mitigative measures. An increased emphasis on preventative measures would be more cost effective.

4. Public input into hazard assessment during the planning stages for new developments is minimal, yet residents of a region may have invaluable personal recollections of past natural disasters.

5. Hazard mitigation decisions may be unduly subject to political, not scientific, considerations.

6. Most of the responsibility for natural hazard assessment has been delegated by the provincial government to the regional districts and municipalities. These smaller jurisdictions are ill equipped to deal with the financial burden or political difficulties of comprehensive natural hazard assessment. Because of this, local governments usually treat natural hazard management as a liability - avoiding exercise rather than a natural hazard - avoiding exercise, as it should be. A patchwork of different levels of regulation (or no regulation) throughout the province is the result.

7. A notwithstanding clause in the Canada - British Columbia Floodplain Mapping Agreement would seem to undermine its effectiveness [20]. The agreement states that neither the provincial nor the federal governments will encourage new development in known flood areas, as designated by the series of over 200 floodplain maps. It also states that no post disaster assistance will be given to people who build new structures in designated flood areas. The notwithstanding clause allows governments to provide disaster compensation in "extraordinary circumstances". Another problem is the exclusion of Indian Reserves from this agreement, which is curious given that Indian lands are often heavily settled and may now be sold to non-Indians for residential and other purposes.

Local government The Province of British Columbia has given several legislative tools to local governments which may be used to regulate land which is subject to natural hazards. Unfortunately, much of this legislation is poorly written and some different Sections of the Municipal Act are in conflict with each other.

Section 734 of the Municipal Act requires municipal and regional Building Inspectors to act cautiously in areas which may be subject to floods, debris flows, landslides, avalanches, and rockfalls among other hazards. These areas may be identified in Official Community Plans (OCP's). Some jurisdictions have chosen to produce simple natural hazard maps for their OCP's; others provide a written description of local hazards.

Section 945(4)(b) of the Municipal Act enables local governments to designate portions of areas with Official Community Plans as development permit areas. The natural hazards which may trigger such a designation are listed in Section 976(5)(a) of the Act. Land so designated may be subject to strict site-specific regulations. Development permits are required before any building construction or subdivision of land occurs. These permits may vary the provisions of a zoning bylaw, including the permitted uses and density of occupation of land. While the development permit process is potentially a very useful management tool, it is so site-specific that very detailed (and expensive) publicly-funded geotechnical surveys would be necessary to offer reasonable hazard management prescriptions. The alternative is to have applicants for permits pay for field work at the time of application. These factors make many local governments reluctant to use this provision of the Act.

The Province of B.C. encourages local governments to enact Section 969 Floodplain Bylaws in areas designated as floodplain. Such areas are typically displayed on floodplain maps at a scale of 1/5,000, created pursuant to the Canada-British Columbia floodplain mapping agreement (these maps are not to be confused with OCP natural hazard maps). The Municipal Act states that Section 969 floodplain control bylaws cannot control or prevent subdivision in flood-prone areas; only new building

construction can be regulated. As a result, higher settlement densities in flood-prone areas cannot be prevented by this section of the Act. This program, while well intentioned, is flawed from a planning perspective.

Development in areas which are classified as potentially hazardous in OCP's is to be discouraged by the Building Inspector pursuant to Section 734(2) of the Municipal Act. A geotechnical report concerning slope stability and other physical limitations to construction may be required, and would be paid for by the landowner. Some possible conclusions of the geotechnical report involve additional expense to the landowner.

A major public relations problem for local governments which are enacting land-use regulations in response to natural hazards is the impact of such regulations on property values. Prospective buyers of property which is subject to natural hazards will benefit from information on hazards, either by acquiring the property at a lower price, or by avoiding such properties altogether. Persons already owning hazardous property may not have known about the risk when it was purchased, and may feel victimized by this situation. A natural hazard insurance scheme may go some way towards addressing these concerns.

The seriousness of these issues is increased by the imprecise delineation of potential hazard zones on many existing OCP hazard maps. Often these maps are at a small scale, and the information they contain is rudimentary. These maps are often created by government officials with unknown qualifications; the maps are often not signed and usually carry disclaimers. No attempt is generally made to quantify the degree of risk. Neither the landowner nor the Building Inspector is likely to know the actual degree of risk at any given site as expensive geological studies are not generally done in the production of these maps. The landowner is thus compelled to pay for the completion of the natural hazard assessment work which was initiated by the province, municipality or regional district.

A final consideration on the current use of OCP hazard maps is the question of liability. Municipalities and regional

districts which have knowledge of the existence of natural hazards may be liable for damage caused by destructive natural events unless specific steps are taken. This arises from the doctrine of "duty of care" which the municipal council or regional board may carry until a formal resolution or response to the hazardous conditions is made. Such a resolution may include writing letters of warning to all homeowners in known hazard areas, property expropriations, construction of mitigative works, or formally resolving to take no action due to economic constraints. A recent out of court settlement between the Village of Lions Bay (about 15 km north of West Vancouver, B.C.) and a local homeowner was apparently made because the Village council knew of the hazardous conditions but failed to satisfy "duty of care".

Municipal and regional district zoning bylaws can also be used to minimize the interaction of natural hazards and human activities. Most zoning bylaws refer to required setbacks from the "natural boundaries" of watercourses. These special setback regulations can duplicate the provisions of a Section 969 floodplain bylaw.

Natural hazard policy recommendations

1. The Provincial Government should declare natural hazard management to be an issue of Provincial importance. Major amendments to Provincial Acts should be made to ensure that effective, consistent Province-wide natural hazard management is undertaken by the Ministry of Environment. The Province should also recognize its liability in this matter, as have many European governments, thereby providing an incentive to maintain a high quality of management.
2. The Ministry of Environment should be required to undertake natural hazard mapping of a scope similar to that seen in France and Austria. These maps should be used in the Official Community Plans of local governments. Natural hazard maps should be revised upon completion of mitigative works, or upon evidence of other significant change in the area.
3. Municipal and regional governments should be compelled by the province to declare hazard sites development permit areas pursuant to Section 945(4)(b) of

the Municipal Act.

4. The B.C. government should establish a catalogue of mitigative building construction techniques for distribution to municipal and regional governments. These would be consulted when an application for a development permit in a natural hazard zone is received by local government. Guidelines for the purposes of subdivision in development permit areas should also be defined.
5. The feasibility of creating a natural hazard insurance scheme to be administered by the province and the federal government should be investigated.
6. All applications of active mitigative measures should meet cost efficiency criteria prior to the commencement of construction. Such measures should be built only after a natural hazard map for the area has been prepared. A policy for the equitable application of mitigative techniques to existing endangered communities should be established.
7. Developers should be required to pay for geotechnical reports and mitigative measures (if necessary) in the case of new construction and/or new subdivision in areas of suspected hazard.
8. If the existence or potential impact of a natural hazard can be correlated to human or economic activities, compensation to those affected should be made by the offending party.
9. More research in the field of natural hazard management should be encouraged at Canadian universities and research institutes.

References

- [1] Eisbacher, G.H.; and Clague, J.J. 1984. Destructive Mass Movements in High Mountains: Hazard and Management. Geological Survey of Canada, Paper 84 - 16. 230pp.
- [2] Aulitzky, H., editor. 1975. Hochwasser- und Lawinenschutz in Tirol. Wien: Universitäts- Verlagbuchhandlung GmbH. 412pp.
- [3] Aulitzky, H. 1974. Endangered Alpine Regions and Disaster Prevention Measures. Strasbourg: Council of Europe, Nature and Environment Series No. 6. 103 pp.
- [4] Marsh, G.P. 1874. The Earth as Modified by Human Action. New York: Scribner, Armstrong and Company. 656 pp.
- [5] Hopf, J. 1986. Personal

communication during an interview at the regional office of the Forsttechnische Abteilung für Wildbach- und Lawinenverbauung, Liebeneggstraße 11, Innsbruck, Austria.

[6] Besson, L. 1985. "Les Risques Naturels". Revue de Géographie Alpine. 73 (3). pp.321-333.

[7] Mattison, J.S. 1983. Landslide Hazard Management in British Columbia. M.R.M. Research Project, Simon Fraser University.

[8] Crecy, de, L. 1980. "Avalanche zoning in France - Regulation and technical bases". Journal of Glaciology. 26 (94). pp. 325-330.

[9] Ministère de l'Agriculture. 1974. Carte de Localisation Probable des Avalanches No. 74.05: Vallorcine - Argentière. Paris: Institut Géographique National.

[10] CEMAGREF (Centre National du Machinisme Agricole du Genie Rural des Eaux et Forêts). 1981. Plan des Zones Exposées aux Avalanches sur la Commune de Vallorcine. Grenoble: Ministère de l'Agriculture. 39 pp. including 2 maps.

[11] Pachoud, A. 1979. Carte des Zones Exposées à des Risques Liés aux Mouvements du Sol et du Sous-sol (ZERMOS) à 1/25,000, Région de Saint Gervais, Les Contamines-Montjoie (Haute Savoie); see also Olivier, G. and J. Renet. 1976. Carte ZERMOS à 1/20,000, Région de Modane (Savoie). Orléans: Bureau de Recherches Géologiques et Minières. Map and "Notice Explicative".

[12] DRM (Délégation aux Risques Majeurs). 1985a. Guide Methodologique Cartographique: Plans d'Exposition aux Risques. Paris: Service Technique de l'Urbanisme. 72 pp.

[13] DRM (Délégation aux Risques Majeurs). 1985b. Plan d'Exposition au Risque - Avalanche: Catalogue de Mesures de Prevention. Grenoble: CEMAGREF. 166 pp.

[14] RTM (Restauration des Terrains en Montagne). 1985. Plan d'Exposition aux Risques Naturels Prévisibles: Les Villards-sur-Thônes. Annecy: Préfecture de la Haute Savoie. 70 pp. and 4 maps.

[15] WLW (Wildbach- und Lawinenverbauung, Forsttechnische Abteilung für). 1984. 100 Jahre Wildbachverbauung in Österreich. Bundesministerium für Land- und Forstwirtschaft. Klagenfurt. 281pp.

[16] WLW (Wildbach- und Lawinenverbauung, Forsttechnische Abteilung für). 1986. Hochwasserschutz in Tirol. Bundesministerium für Land- und Forstwirtschaft. Wien. Supplement.

[17] WLW (Wildbach- und

Lawinenverbauung, Forsttechnische Abteilung für). 1982. Gefahrzonenplan 1982: Gemeinde Döllach im Mölltal. Wien: Bundesministerium für Land- und Forstwirtschaft. Report and 4 maps.

[18] Hattinger, H. 1987. Personal communication on the topic of WLW natural hazard maps, Bundesministerium für Land- und Forstwirtschaft, Gruppe V/B, Stubenring 12, A-1010 Vienna, Austria.

[19] Tazieff, H. 1984. "Preface". Mouvements de Terrain. Document du Bureau de Recherches Géologiques et Minières No. 83. Orléans. pp. 1-3.

[20] MoE (Ministry of Environment of British Columbia). 1988. Agreement Respecting Floodplain Mapping in the Province of British Columbia. MoE letter to local governments, File FPM-1, April 6 1988.

Engineering Decisions and Natural Hazards

S.O. Denis Russell

*Department of Civil Engineering, University of British Columbia
Vancouver, British Columbia*

Abstract

The civil engineers' largely intuitive approach to decision making in situations involving uncertainty and risk is described and compared to that of formal decision theory. Although engineers have been highly successful in dealing with risk in engineering works large and small, a better framework is needed for the collective decision making involved with natural hazards. Decision theory seems to provide such a framework, but it should be used to supplement, not replace the engineering approach.

Introduction

Although potential natural hazards can often be identified, there is always great uncertainty as to when, if ever, a hazardous event might occur, what might be its magnitude and what could be the consequences should it occur. Often the consequences can be extremely serious, including loss of life and major property damage. Many professionals are involved with the various natural hazards, but civil engineers almost always play an important role in the actions to avoid, head off or minimize the impact from such hazardous natural events.

In considering decision making, it is helpful to distinguish between three approaches:

- ordinary day to day decision making;
- the professional engineering approach;
- and the formal decision theory approach.

Civil engineers, through their training, seem to develop a particular approach to decision making in uncertain situations. This paper deals mainly with this approach, but also touches on what people do in their normal day to day decision making and outlines the formal approach of decision theory. It is suggested that for decisions involving major risks and uncertainty, such as those posed by natural hazards, a combination of all three offers the best overall approach.

Background

Day to day decision making.

In our daily decision making, we have to rely heavily on shortcuts. Our modern world has become so complex, we cannot afford to tie up our limited mental processing power on carefully considered analyses of the situation every time we have to make a decision. In a recent fascinating book

"Influence", Cialdini [1] describes the main ways in which our decision making is influenced. An example is what he calls "Social proof" - and he demonstrates that we all have strong tendencies to decide to do what other people who are like us are also doing. Another is "Deference to authority". As a species, we tend to be very deferential to those in authority - and decide to do what they want us to do.

In a sense, the shortcut methods that Cialdini describes are the antithesis of professional decision making, where we do have to carefully analyze the situation, before coming to a conclusion about what to do. However, we are all human beings and even in our professional capacities we are also influenced by the same factors as those which influence us in making decisions in our daily lives.

The Engineering Approach to Decision Making

Almost everything that civil engineers do involves uncertainty and some degree of risk. But we receive little formal training in how to deal with uncertainty. As Bella [2] points out, engineers are conditioned by their training and acquire an approach to problem solving that becomes taken for granted and almost second nature. A very strong conditioning factor in the training of engineers are the mechanics courses, which all must take. There, simplified problems, such as those involving a ladder leaning against a wall, supporting a point load, are fully specified and can be solved with a few simple principles. In this overwhelmingly deterministic world, each problem has only one right answer. Later, in design courses, safety factors are introduced, but often in the same deterministic framework. Nowadays, students also have courses in statistics and decision theory, but these are often perceived as add-ons, not central to

the main stream of engineering and thus do not seem to have much influence on engineers' thinking processes.

Considering their training, it is not surprising that many engineers take the position that if left to licensed professionals, civil engineering works can be made absolutely safe - and therefore they should be made absolutely safe. An early experience of the author's illustrates this position.

Under the broad supervision of an internationally recognized hydrologist, the author headed a small group working on the derivation of the probable maximum flood for Mica Dam on the Columbia. After the final report had been drafted by the author, the senior hydrologist revised it taking out all the qualifications and making it sound much more positive and authoritative than seemed to be justified by the poor data, the sweeping assumptions and the rather simple methods available for the analyses, at the time. In reply to a protest that it seemed unfair to present such a confident sounding report, in the circumstances, the elder statesman replied that, between us, we knew more about the hydrology of the Columbia at Mica than anyone else; that it was up to us to make the best decisions that we could; and then present them in a confident way. He asked how I would feel if I went to a doctor with a minor illness and was told that I probably just had a cold, but there was a 10% chance that I had cancer, a 5% chance that I had some other serious disease and so on. He suggested that in such a case one would never go back to that doctor again. In the same way, he said professional engineers have to "absorb" the uncertainty and present a reassuring front to their clients. The argument sounded convincing at the time; but in hindsight, it was a rather foolish and arrogant position to take. In effect it was saying that the owner

should leave the question of the safety of the dam to the professionals and rely on them to make it absolutely safe. The argument is even less tenable when dealing with natural hazards, where there is not only considerable uncertainty, but the engineers have to rely heavily on the experience and judgement of other professionals, who may not subscribe to the same ethic.

Civil engineers use two main approaches to decision making under uncertainty - safety factors and expected values. Which one is used depends mainly on the consequences of being wrong. When the consequences of failure are too serious to be tolerated, the safety factor or "bounding" approach is used. But when the possibility of failure is acceptable, then decisions are made on the basis of minimizing total expected costs. This is most often used in water resource problems and it usually results in designing for an event such as a flood with a specified probability of exceedance. By implication, if a larger flood were to occur, the structure could be expected to fail.

An example of the expected value approach is the design of culverts. On secondary roads in British Columbia, culverts are designed for the 50 year flood, the flood which is exceeded on average once in 50 years. If a culvert fails, it is replaced, but in the meantime, there are road closures and delays to traffic. However, there is usually plenty of advance warning of impending failure, so there is little danger to. Damage is thus mainly economic. From the provincial point of view, it is much more economical to replace some culverts from time to time than to design all culverts such that they would almost never fail.

In contrast to a culvert, should a major dam fail, the consequences could be catastrophic and could not be tolerated. In such cases,

everything reasonable is done to prevent potential catastrophes. For example, all major dams are designed to pass the maximum probable flood and withstand the maximum credible earthquake - the largest that could reasonably be expected to occur in the judgement of the engineers responsible.

The safety factor or "bounding" approach can best be illustrated with a structural example. If the load to which a proposed structure will be subjected is known approximately but we are sure that it will not exceed X ; and if the carrying capacity of the structure is not known with certainty but we are quite sure that it exceeds Y ; then if Y exceeds X by a suitable safety margin, we can be sure that the structure will be able to safely carry the loads imposed on it. The safety factor of course varies with the circumstances - the degree of uncertainty and the consequences of failure. Engineers receive little direct training in how to select appropriate safety factors. Instead, as they gain experience, they seem to develop this ability intuitively.

Since the consequences of failure of most civil engineering works could be very serious, if not catastrophic, the bounding approach is most often used, with the result that it becomes almost second nature. Indeed, it is so deeply ingrained, it is sometimes used in situations where it is not appropriate. As an example, if one were trying to minimize expected total costs and determined that, say, the 50 year flood should be used, then one should use his or her best estimate of that flood. But often engineers will quietly add a safety factor to their estimated value. However, although one can criticize the safety factor approach, one cannot argue with success. The vast majority of engineering structures have been designed with safety factors and function satisfactorily and safely. Failure is

so rare, it is front page news when it does occur.

The Decision Theory Approach

Decision theory offers a formal, logical way of making decisions under uncertain conditions. There is a formal methodology for drawing a decision tree, distinguishing between "chance" and "decision" events (which shows the structure of the problem at hand); assigning utility (a measure of desirability) to the tip of each branch; assigning probabilities to each branch emanating from a "chance" node; and then working backwards from the tips of the branches, computing expected utilities at the chance nodes and choosing the branch with the maximum expected utility at each decision node. The procedure is logical, rigorous, coherent and consistent. It prescribes when decisions should be made and what the decisions should be. There is also a procedure for updating estimates of the probabilities in the light of additional evidence. This is based on Bayes' theorem. Since this fits naturally with decision theory, the overall approach is often called Bayesian Decision Theory.

Unfortunately decision theory can rarely be used in practice. First of all, decision trees can quickly turn into a "bushy mess", that is become so large and complex that they become unwieldy. Next, the probabilities of the various possible events are very difficult if not impossible to estimate; and the utilities are often equally difficult to obtain. Nevertheless, decision theory is very useful at the conceptual level. It helps in separating and showing the roles of various participants in the decision making process. The decision tree lays out the structure of the problem and this should be done by the project manager or coordinator; the probabilities of the various events occurring should be provided by the

technical experts; and the utilities should be provided by the responsible officials, whether elected or appointed. If even a rough attempt is made to use decision analysis, this helps clarify the roles of the participants in the process - the study manager, the technical experts and those charged with assessing the relative desirabilities of the various possible outcomes. Otherwise, if decisions are made by the politicians alone, they are likely to be based on ignorance. Alternatively, if decisions are made by the technical experts alone, these may well be decisions that they have no right nor mandate to make.

The author had found the decision theory framework extremely helpful in dealing with complex decision situations. Having a good framework helps focus thinking and discussion. It is particularly useful if the other professionals involved in the particular situation are also comfortable with the framework. Especially if there are disagreements, a shared knowledge of the decision theory framework helps focus on their source - whether it is the structure of the problem (which is rarely the case), the relative desirability of the possible consequences (the utilities) or the probabilities of the various possible outcomes. When there is no common framework there is a tendency to argue at cross purposes. One person may be arguing about preferences while the other may be thinking about probabilities. Without a framework, it is difficult to come to agreement in such a circumstance.

Other Factors

A factor of considerable importance in dealing with potential hazards is the assignment of responsibility for the assessment and the action to be taken [3]. Engineers, like other professionals, have a

strong sense of responsibility and when responsibility is clearly designated will do everything they can to make things safe. However, when responsibility is not clearly assigned and no-one feels personally responsible, then we seem to revert to the normal decision rule of trying to do what everyone else like us is doing [1]. As an example, it is widely thought that many of the older buildings in Vancouver would be unsafe in the event of a major earthquake. If an engineer were assigned clear responsibility for ensuring the safety of a particular building (as is the case when there are major renovations) then he or she would do everything necessary to make it safe. But in the absence of such assignment, and particularly in a case like this where there is considerable uncertainty, everyone looks at what everyone else is doing. And since no-one else is doing anything about the situation, no-one feels any obligation to do so either.

Apart from civil engineers, the other main group of professionals involved with questions about natural hazards are the earth scientists - geologists, geographers, geomorphologists, hydrologists etc. As natural scientists, the latter tend to rely heavily on observations, measurements, (where possible) and descriptions of similar phenomena from elsewhere, obtained from the literature. By keeping up to date with the literature and contributing to it, earth scientists tend to be aware of experiences elsewhere and also of the latest advances in the subject. However, they also tend to have the scientists' caution and reluctance to act on or express an opinion until they are sure of their ground.

In contrast to their scientific colleagues, engineers tend to rely more on their own personal experience, on their ability to make assumptions and compute important quantities such as forces or flows and on

their general problem solving approach and less on the literature. Perhaps this comes from their training, or perhaps from a longer history of taking responsibility for very important works.

Suggested Approach

For making decisions about natural hazards, whether to do something and if so what to do, the best approach is likely to involve a group of experts. Most questions about natural hazards are too complex to be fully understood by any one person. The group should be small but should contain a civil engineer, a representative of the "owner" and other professionals with relevant expertise. It should be given clear terms of reference and clear responsibilities. Its members should all be familiar with the decision theory format, so that discussions can be held within a common framework. The natural training and instincts of the civil engineer member should ensure a safe solution. The tendency for people, to want to do the same as everyone else, especially in an uncertain situation, makes it likely that they will all agree on a common solution. However, the group has to be set up such that all members are clearly expected to act as independent professionals, since the normal human deference to authority is inappropriate in this situation. One does not want all members to simply agree with the chairman or other dominant figure in the group.

Conclusions

Civil engineers, by virtue of their training and experience have a distinctive approach to decision making in uncertain situations. The approach is largely intuitive but it is highly effective in pure engineering situations as evidenced by the fact that

engineering failures are quite rare. However, the lack of an explicit approach can lead to communication and other problems in situations where other professionals must share in the decisions - as is the case with most natural hazards. Decision theory offers a framework that can facilitate communication and discussion between professionals from different disciplines. It is believed that the best decision is likely to be made when a small group, made up of professionals from the relevant disciplines and all familiar with the decision theory format, is given clear responsibility for making the decision in question.

References

1. Cialdini, Richard B., "Influence - Science and Practice." Harper-Collins, New York, 1988.
2. Bella, D.A., "Existentialism, Engineering and the Liberal Arts." Journal of Professional Affairs, American Society of Civil Engineers, Vol 116(1), pp 309-321. 1990.
3. Russell, S.O., "Engineering and Professional Responsibilities." Jour. of Professional Affairs, American Society of Civil Engineers, Vol 116(1), pp 49-61. 1990

Evaluating Total Risk to Communities from Large Debris Flows

Graham C. Morgan
Consulting Engineer
Victoria, British Columbia

Graham E. Rawlings
Golder Associates
Vancouver, British Columbia

John C. Sobkowicz
Thurber Engineering
Victoria, British Columbia

Introduction

Alluvial and colluvial fans in mountainous areas are subject to debris flows and debris floods with potential discharges, albeit short-lived, several times greater than clear water flood discharges. On steep fans these phenomena are commonly the dominant mechanism for transporting coarse sediment. There is a need to reliably assess risk to life and property from such events and to establish the acceptability of existing or proposed land uses. There is also a need for a rational way of selecting optimum mitigative measures and sizing protective works. This paper addresses these needs.

Basic Approach

Risk to life and property from such naturally occurring hazards as rock falls, debris flows, and floods have been part of the history of Canada. Life is risky, and there is a degree of risk to life that is acceptable depending on the circumstances. Much has been written on this topic during the last decade, particularly with respect to dam safety and also natural hazards. One approach taken is to quantify risk to the life of an individual exposed to the hazard and make a comparison with other societal risks which he/she accepts or tolerates. Where populations are threatened, another approach is to quantify the risks of multiple deaths and compare with the documented risks of multiple

deaths from natural hazards in the mountainous areas of N. America and Europe (Morgan, 1990).

Risk when defined as the annual probability of loss of life of a specific individual exposed to a hazard (PDI) can be computed as follows (Pack & Morgan 1987):

$$PDI = P(H) \times P(S:H) \times P(T:S) \times P(L:T) \quad (1)$$

where:

P(H) is the annual probability of the hazardous event

P(S:H) is the probability of spatial impact (i.e. of a house) given the event

P(T:S) is the probability of temporal impact (i.e. of house occupancy) given the spatial impact, and

P(L:T) is the probability of loss of life of an individual occupant

For the purpose of this paper the product of the last three probabilities is termed "Severity". Therefore:

$$PDI = P(H) \times \text{Severity} \quad (2)$$

where:

$$\text{Severity} = P(S:H) \times P(T:S) \times P(L:T) \quad (3)$$

1 Consulting Engineer, Victoria

2 Golder Associates, Vancouver.

3 Thurber Engineering, Victoria.

Of the probabilities listed in eqn. 1, $P(H)$ is the most difficult to determine or estimate. Selection of this probability is discussed in detail in the following section.

A similar approach can be taken in quantifying risks to populations.

Selection of Probabilities of Hazardous Events, Early Methods

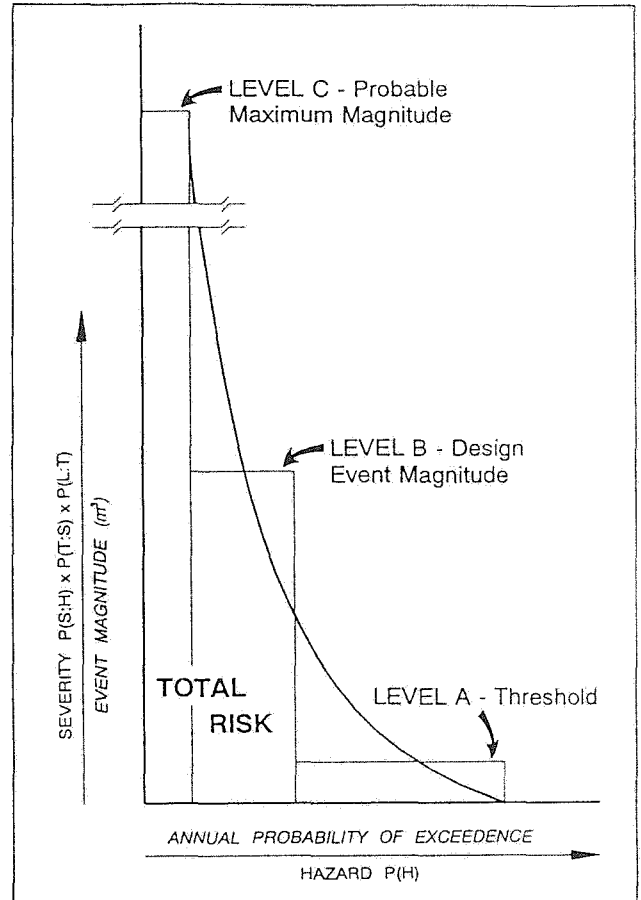
In British Columbia, in the early 1980s, a two-fold step was taken towards quantifying the probability of debris torrents (coarse, granular debris flows) which led to the design and construction of the protective works on Highway 99 (Thurber, 1983):

(a) Creeks vulnerable to debris flow (torrent) activity were ranked in order of perceived probability of occurrence. This was done by assessing a series of field characteristics, including recorded history, which were perceived by the study team to influence the proximity (in time) of the next event. This proximity was expressed in terms of the likelihood of an event occurring over the short term (i.e. the next 10 years) or within the life of a significant long term structure (such as a bridge or a house).

(b) The concept of a "design event magnitude" was developed, namely a "reasonable" upper limit was estimated for the total quantity of debris transported in a future event for a given creek. The likelihood of events equal to and less than the design magnitude was considered. This implied the acceptance of a relationship between probability of occurrence and event magnitude.

Table 1 shows the classification that resulted from this work. Although this classification was based essentially on relative probabilities of occurrence, it is important to note that the descriptions also imply probabilities in absolute terms. The work gave the use of terms such as "high" or "low" risk a more meaningful connotation.

The design event magnitude, as derived for the Highway 99 work, was found to be almost entirely dependent on the availability of debris in the creek channel including contributions from the banks. The most reliable procedure was, and is still, to undertake a detailed inspection of the creek



TOTAL RISK CONCEPT
FIGURE 1

channel and estimate a unit volume of debris (volume of debris per unit creek length or creek width times scour depth per unit creek length) along distinct reaches of the creek to arrive at a total potential debris volume (VanDine 1984). Estimated debris yield rates for various channel conditions are provided by Hungr et.al. 1984. This total potential debris volume is then "adjusted" to arrive at the design event magnitude.

Selection of Probabilities of Hazardous Events, Recent Developments

Recently considerable support has surfaced for the risk-based approach described in the previous section, particularly as applied to land-use planning and the design of structures and protective works, and it is clear that the design event magnitude approach (by itself) does not satisfy this need.

TABLE 1 -- Classification of Debris Torrents with Respect to Probability of Occurrence (Thurber 1983)

Category	Description
4. Very High	Indicates that events of less than the design magnitude can occur frequently with high runoff conditions, and the design event should be assumed to occur within the short term. It is applied to creeks that have a history of more than one event involving greater than 500 m ³ or have physical characteristics that are comparable to these creeks.
3. High	Indicates that events of less than the design magnitude will occur less frequently than under Category 4 but the design event should still be assumed to occur within the short term. It is applied to creeks that have a history of a single debris torrent. It is also applied to creeks that have no known history of events but possess several significant physical characteristics that are comparable to Category 4 creeks.
2. Moderate	Indicates that the design magnitude event should be assumed to occur during the life of a significant long term structure (such as a bridge or house). It is applied to those creeks that have significant physical characteristics that fell well within the threshold where debris torrents are possible, although not in the range of Category 4. To date these creeks have no recorded history of debris torrents, or have experienced events of uncertain origin.
1. Low	Indicates a low potential for the design magnitude event. It is applied to those creeks whose physical characteristics place them at or close to the threshold where debris torrents are possible. Although a significant debris torrent is possible during the life of a long term structure, it would require an unusually high (and thus infrequent) runoff condition.
0. "No Risk" (Very Low)	Indicates that there is virtually no potential for large debris torrents to occur although small and local torrents may occur, and torrents of varying magnitudes may develop in upper reaches and tributaries. It is applied to channel reaches whose physical characteristics fall well below the threshold where debris torrents are possible.

In 1990 a concept of total risk was developed for designing debris flow / flood control structures (Thurber 1990, Golder 1991). This concept recognises that with increasing event magnitude severity can also increase due to:

- the nature of the hazardous event changing (e.g. a debris flood could change to a rapidly moving debris flow), and
- the area of impact expanding.

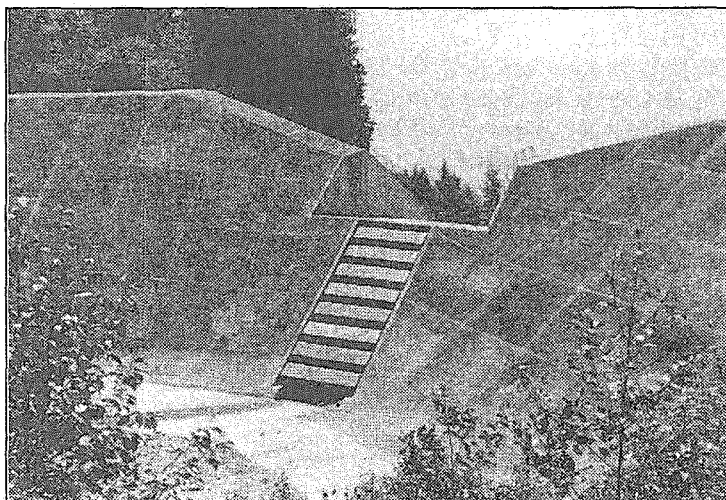
Thus at a given location there can be a relationship between the annual probability of the hazardous event and the severity of the event. This is shown on Figure 1. The area under the curve represents the total risk of loss of life from the hazard. The design event magnitude, in this context, is seen as some intermediate condition lying between a threshold magnitude (which initiates threat to life) and a probable maximum magnitude (PMM). The PMM is based on the estimated maximum channel debris yield rates and assumes that all tributaries can become active during a single event. As such

the probability of it being exceeded by a significant amount is very low.

Using this method, it is necessary to estimate the probability of occurrence of debris flows of varying magnitude. If sufficient data is available, standard techniques of frequency analysis using extreme value theory may be employed in determining recurrence intervals. However, debris flows are infrequent events and there is rarely sufficient information of suitable quality to apply frequency analysis in a rigorous manner. The estimation of recurrence intervals must largely be a matter of judgement, but frequency analysis concepts may still be used to guide this judgement. Such an approach is described in the following case history.

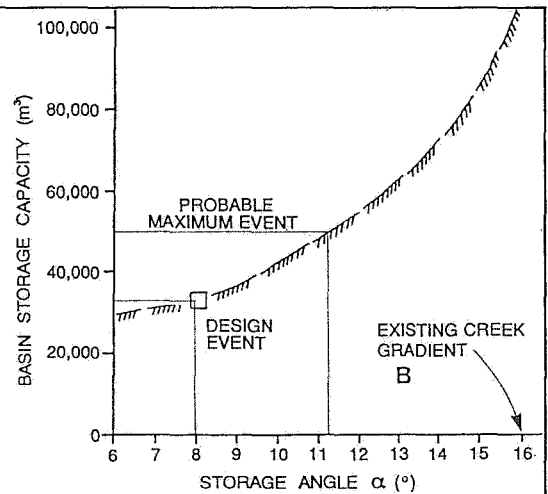
Charles Creek Revisited

Coarse granular debris flows (sometimes called debris torrents) occur on many of the creeks flowing down the 1400 m to 1800 m high mountain sides bordering the east side of Howe Sound, near Vancouver. Highway 99, the B.C. Railway, and several communities are located at the base of these mountains. In 1984 - 1987, following a series of large events involving several fatalities, a number of protective works were constructed including three large debris catchment basins. One of these basins was located on Charles Creek (Figure 2) immediately upstream of the highway and served to protect both the highway and the community along the shoreline. The basin was formed by constructing a barrier



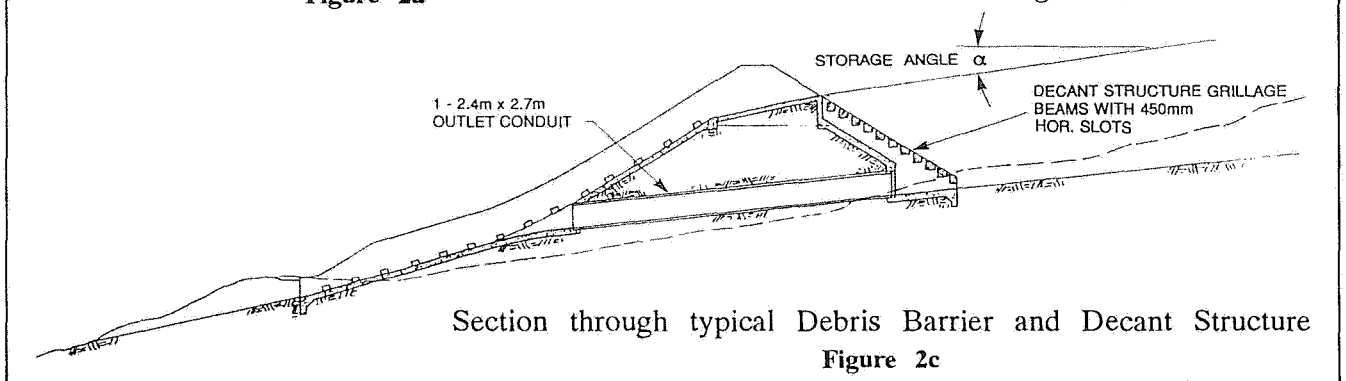
View of Charles Creek Debris Barrier from Storage Basin

Figure 2a



Basin Storage Capacity as a Function of Storage Angle

Figure 2b



Section through typical Debris Barrier and Decant Structure

Figure 2c

DEBRIS BASIN, CHARLES CREEK, HIGHWAY No. 99, B.C.

(reference Hungr, 1985)

FIGURE 2

comprising a zoned fill embankment, a central concrete decant structure, and an emergency chute on the downstream slope. The barrier is able to store a maximum depth of 12.5 m of debris. Because of the 16° creek gradient at the site, this required a 22 m high structure (to the chute sill on centre line). The construction contract was \$2.36 million.

Charles Creek has a drainage area of 1.8 km² and a total creek length including tributaries of 3500 m. A design event magnitude of 29,000 m³ was selected (Thurber 1983) and the basin was designed to accommodate 33,000 m³ at an 8° storage angle. Because of the unprecedented nature of this structure, this storage angle was conservatively selected at half the creek gradient. The creek was designated category 4 probability occurrence (Table 1), i.e. the design torrent was assumed to occur within the short term (10 years).

It is of interest to reexamine the design of the Charles Creek basin using a total risk approach. The first step is to estimate the probability that debris flows of various magnitudes will occur, that is, to construct the P(H) vs magnitude relationship shown in Figure 1. One starts by examining the known history of debris flow events, which for Charles Creek (since construction of the railway in 1956) is summarized in Table 2.

There is too little data in Table 2 to rigorously apply frequency analysis techniques, but judgement may be used to estimate recurrence intervals as follows. It is assumed that if better information were available over a longer time period, one would find

that there might be several small events each year, with an occasional moderate event, and less frequently a larger event that would impact transportation corridors and communities. One could select the largest of these events (either yearly maxima or extremal values) and order them from largest to smallest. The events shown in Table 2 would constitute the first four in this ordered list, and one could estimate a recurrence interval directly from an equation of the form:

$$R = (N + 1) / m \quad (4)$$

where:

- R = return period (or recurrence interval)
- N = number of years of record
- m = "order" of event in list

However, due to the incompleteness of the record, an alternate approach is suggested which also allows the application of some judgement. The historical data is rearranged as shown in the first 2 columns of Table 3, the range of possible debris flow magnitudes is divided into an arbitrary number of equal intervals, and the number of events whose magnitude exceeds each interval boundary is noted. If the individual events are assumed to be independent, then the maximum values should follow a binomial distribution over time, i.e. the probability of X occurrences of a debris flow exceeding magnitude M in N years would be:

$$P(X) = {}_N C_X * P(H)^X * [1-P(H)]^{(N-X)} \quad (5)$$

where:

- P(H) = expected average number of occurrences per year, i.e. the annual probability of occurrence, and

TABLE 2 -- Record of Events on Charles Creek

Date	Debris Volume, m ³	Reference / Comments
Sept. 1969	20,000 to 25,000	Volume interpreted from damage
Nov. 1972	5,000 to 10,000	Volume interpreted from damage (Total volume for 2 events)
Dec. 1981	10,000 to 15,000	Lister et. al. (1984)
Nov. 1983	15,000 to 20,000	Lister et. al. (1984)
1984 to Dec. 1991	Occasional event < 5,000	Last event in January 1991 estimated at 4,000 m ³

Table 3 -- Evaluation of Return Period for Events of Various Magnitudes
(Historical Data for Charles Creek, see Table 2)

SIZE OF EVENT (m ³ x 1000)	NUMBER OF OCCURRENCES IN EXCESS OF SIZE	RETURN PERIOD (YEARS) (Fig. 3a)	AVERAGE SIZE OF EVENT (m ³ x 1000)	RETURN PERIOD (YEARS) (Eqn. 4)
5	4	8	7	9
10	3	10	12	12
15	2	15	17	18
20	1	30	22	36
25	0	50		
50	0	500		

$$P(H) = 1 / R \quad (6)$$

The form of the binomial distribution (eqn. 5) is shown in Figure 3a for various values of R. It is a fairly simple matter to compare this information to the historical data and assign recurrence intervals as shown in the third column of Table 3. This method gives reasonable agreement with eqn. 4 (see last two columns of Table 3) but allows room for judgement concerning non-typical conditions during the period of record or missing data. The method is also applicable where no data exists and where one is relying solely on judgement in estimating P(H), which in this case is true of the PMM event.

The relationship between P(H) and event magnitude is thus illustrated in Figure 3b. Note that the return period for events in excess of the design capacity of the basin (33,000 m³) is less than 100 years, or P(H) >= 0.01. Assuming an acceptable PDI level of 1:10,000, or less (Morgan 1990) and considering reasonable values for "severity" (Eq.2), this P(H) value is unacceptably high. It is apparent that such a basin should be designed to accommodate the PMM. By reassessing the original field data, the PMM for Charles Creek has been established at close to 50,000 m³.

The capacity of a basin for a given height of barrier depends on the storage (deposition) angle of the debris (Figure 2). Hungr et.al. (1984) describe several observations of deposition angles for coarse

granular debris flows on Highway 99 and elsewhere. Deposition angles ranging between 10° and 14° have been encountered for unconfined flows, the lower angles resulting from higher discharge and/or less coarse grained events, (not to be confused with fine grained events derived from volcanic breccias, weathered rock, and fine grained soils which exhibit deposition angles as low as 6°). Since a large debris flow event comprises a spectrum of surges of varying discharges, one can expect the final deposition angle to typically fall well within this range. Furthermore the Charles Creek debris is particularly coarse grained which promotes drainage and higher deposition slopes. It is noteworthy that the 1981 and 1983 events deposited on slopes of approximately 14°. From Figure 2, the storage angle required to accommodate the PMM is a little over 11°.

Thus although we would today design the Charles Creek basin to meet an acceptable level of residual risk, the existing capacity is adequate because of the conservative storage angle assumed in the original design.

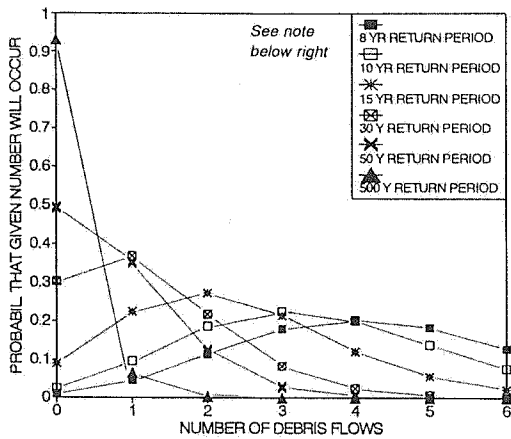
It is important to note that the basin size is governed by the need to protect the Charles Creek community. If there was no resident population, the exposure to the hazard would be substantially reduced, and the basin would need to be sized only to protect the highway crossing, and the travelling public. This changed consideration might justify the selection of a higher allowable P(H) value and

thus a decreased barrier height.

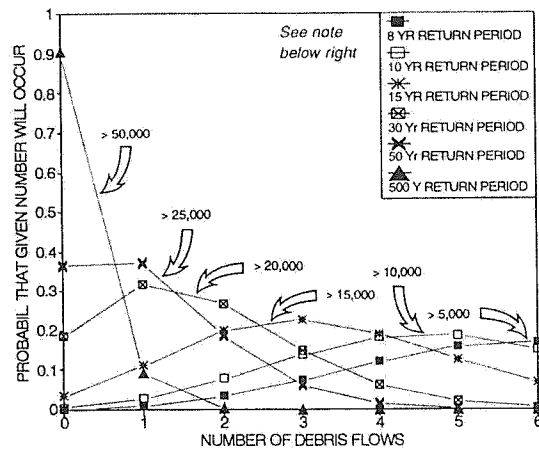
The total risk approach can also be used to predict basin maintenance costs. For example, consider a 50 year design period for the Charles Creek basin. The expected number of occurrences for events in excess of various magnitudes is given in Figure 3c, which is used to construct the cumulative

probability plot in Figure 3d. Figure 3d shows:

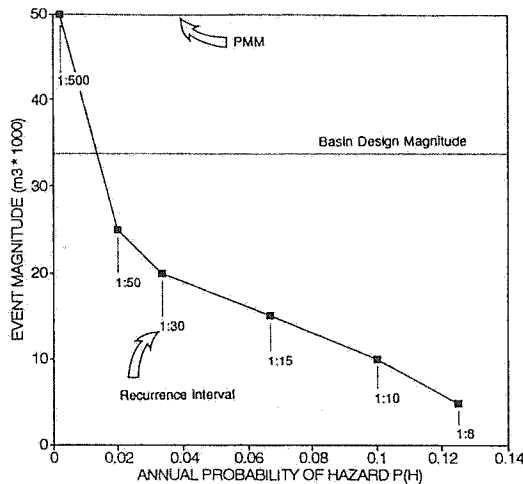
- a 50% probability (i.e. the most likely case) of a spectrum of 5 events exceeding 10,000 m³ to a maximum of 30,000 m³ plus several other lesser events in the 50 year period. This equates to a total deposition of 100,000 to 125,000 m³.



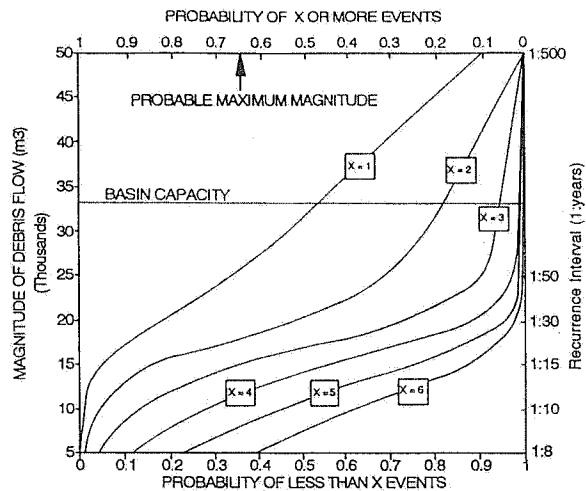
Number of Debris Flows in excess of Given Magnitude during 35 Year Period
Figure 3a



Number of Debris Flows in excess of Given Magnitude during 50 year period
Figure 3c



Annual probability of occurrence of an event exceeding specified magnitude for Charles Creek debris flows
Figure 3b



Probability of "X" Occurrences of Debris Flow Exceeding given Magnitude during a 50 Year Period
Figure 3d

CHARLES CREEK DEBRIS FLOW STATISTICAL MODELS
FIGURE 3

NOTES FOR FIG. 3a & 3c: Probabilities are given for whole values of X only. Joining lines are provided for convenience in viewing trends. Numbers arrowed to lines show range of debris flow volume judged applicable to given return period.

TABLE 4 -- Record of events on Kenyon Creek

Date	Debris Volume (m ³)	Reference / Comments
1920?	Substantial	Old Photographs
1950	8000	Eye witness Aerial photographs
1974	Minor Flow	Eye Witness
1990	20,000	Thurber (1990)

- a 90% probability (i.e. almost certain) of a spectrum of 2 or 3 events exceeding 10,000 m³ up to a maximum of 17,000 m³, plus several other lesser events in the 50 year period. This equates to a total deposition of 50,000 to 70,000 m³.

Annual clean-out of the basin is an operational requirement.

Kenyon Creek

Kenyon Creek is located near Mabel Lake some 15 km east of Enderby, B.C. and is one of several creeks in the area that experienced debris flows during a heavy storm in June 1990. The creek has a drainage area of 2 km² and about 3400 m of a total channel length of 6600 m were activated by the storm. Three debris flow events occurred involving a combined volume of 20,000 m³. The probable maximum magnitude for the post-storm condition was estimated at 29,000 m³, (Thurber, 1990).

As a result of public concern arising from the effects of the storm, the provincial government authorised a study leading to the preparation of a risk map of the area. The approach taken was to evaluate the total risk to life (Figure 1) in terms of the annual probability of loss of life of an individual resident (PDI).

The known history of previous occurrences on the creek is shown in Table 4.

Using comparable procedures to those described in the previous section, a statistical model was derived compatible with this history and the post-storm conditions in the creek. It was first necessary to estimate the probability vs event magnitude relationship shown by the histogram on Figure 1 and also in Table 5. The three event magnitudes were:

LEVEL A - the magnitude that would constitute the threshold of a significant threat to life.

TABLE 5 -- Annual probability vs debris flow magnitude for Kenyon Creek

Magnitude (m ³)	Annual Probability	Annual Probability Range
Level A: 8,000	1:33	1:20 to 1:50
Level B: 20,000	1:80	1:50 to 1:200
Level C: 29,000 (PMM)	< 1:200	< 1:200

- LEVEL B - the magnitude corresponding to the 1990 event.
- LEVEL C - the PMM.

TABLE 6 -- Allocated Probabilities for the Severity of Various Debris Flow Related Events at Kenyon Creek^c

Severity	Debris Flow		Debris Flood
	Rapid	Slow	
HIGH	1:2	1:10 ^a	1:10 ^b
LOW	-	1:100 ^a	1:100 ^b

(a) A high severity viscous flow is defined as slowly moving (<3 m/s) with a depth of >1 m. A low severity viscous flow is defined as slow moving with a depth of <1 m.

(b) A high severity debris flood is defined as a heavily sediment laden (<300 mm) flood flow exhibiting Newtonian behaviour with a velocity of >2 m/s and a depth of >0.5 m. A low severity debris flood is similarly defined except velocities are <2 m/s and depth is <0.5 m.

(c) The above probabilities assume the spatial probability P(S:H) to be 1:1 and the temporal probability P(T:S) to be 1:2; refer Eq. 1 in the text. Where the spatial probability is <1:1 (eg. where the hazard is channelized) the severity is reduced accordingly.

Note: The probabilities allocated for debris floods are based on studies of threat to life and property damage for "clean water" flood conditions as documented by FEMA 1985. The values allocated for debris flows were selected by the Study Team (Thurber, 1990).

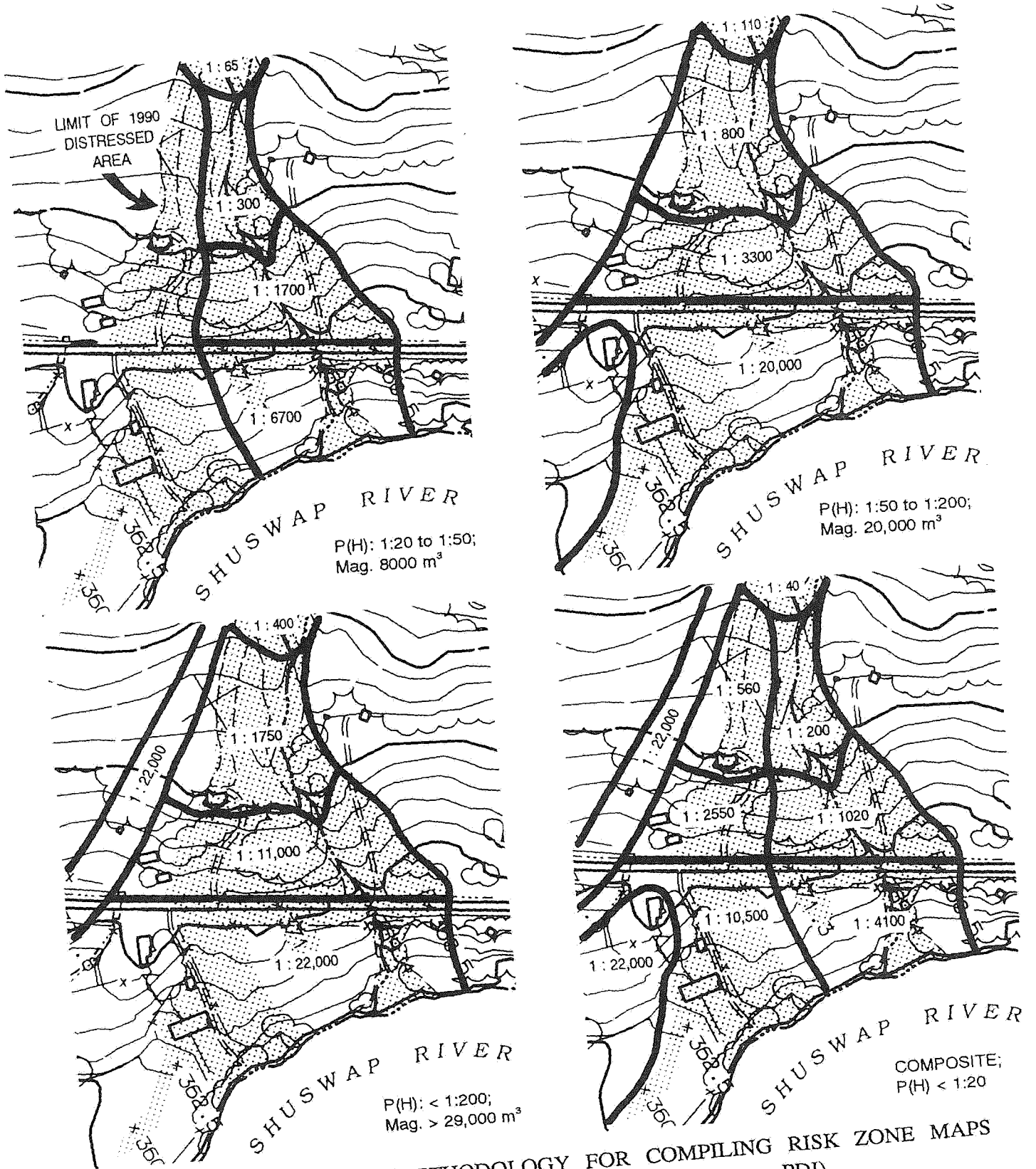
The relatively high probability allocated to the PMM was based on lack of evidence that the causative climatic and hydrologic conditions were unusual. In fact the 24 hour precipitation recorded in nearby stations suggested that the storm may not have been that unusual (i.e. recurrence intervals ranging from 2 to 50 years, not 100's of years).

The high end of the probability range for Level A (1:20) was selected by assessing the degree of disturbance of the watershed area from natural causes, (i.e. logging activities and transmission line construction), and from experience with the effect of this disturbance elsewhere.

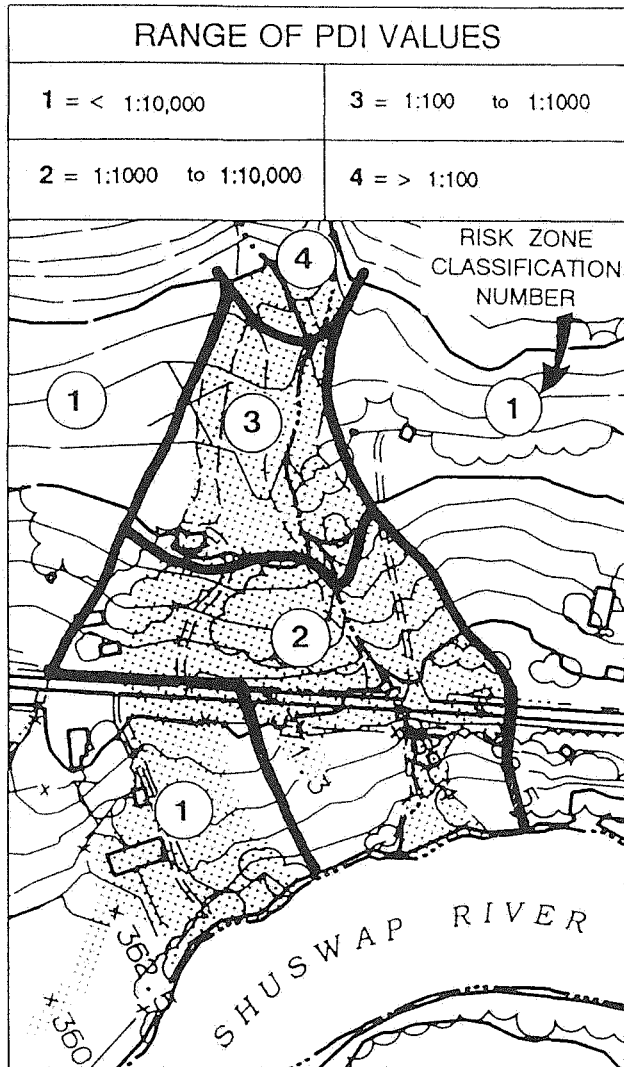
The methodology of preparing a risk map from the statistical model for Kenyon Creek is illustrated in Figure 4a. The lightly shaded area on this figure is the area covered by debris flow and debris floods during the 1990 event. The boundaries of zones exposed to a common hazard level were established for this event and this was then used as the baseline for predicting similar boundaries for the other two magnitude levels. The PDI values were evaluated for each of the zones using the severity levels summarised in Table 6. The three risk zone maps were then superimposed (i.e. the risks were summed) to produce the composite risk map shown in the bottom right of Figure 4a. The final step was to produce the risk zonation map using a code as shown on Figure 4b. The PDI ranges for this code were selected so as to facilitate decisions on the acceptability of the risks depicted by the map.

It is pertinent to note that the total risk map (Figure 4b) is not sensitive to the selection of the magnitude (severity) and probability of such extreme events as the PMM. The greater probability events appear to control even though they are less severe. In other words the area under levels A and B in Figure 1 is much greater than that under level C. Thus care should be taken in evaluating these events for use in the analysis. Fortunately our factual knowledge is usually greater at this end of the spectrum.

Analyses of this type provides a meaningful tool to regulatory agencies concerned with public safety and land development/approval processes. They can also be used for cost benefit analyses to assess the efficiency of proposed mitigative measures. For this application, a second set of



DEMONSTRATION OF METHODOLOGY FOR COMPILING RISK ZONE MAPS
(for Kenyon Creek; values shown on figures are PDI)
FIGURE 4A



maps can be compiled showing the residual risk after mitigation.

Concluding Remarks

The total risk concept provides a rational approach to evaluating risk and planning protective works in mountainous areas exposed to debris flow hazards.

The concept recognises that probability decreases with increasing event magnitude up to a probable maximum magnitude, the PMM (Fig. 1). The PMM is derived using estimated maximum channel debris

rates and assuming that all tributaries become active.

The historical record of debris flow occurrence, which forms the basis of any probability vs magnitude relationship, is commonly incomplete and in many cases must be interpreted. The procedure outlined in this paper constitutes a structure for applying necessary judgement and reaching a consensus. When extrapolating the probability vs magnitude relationship to a period well beyond the historical record, the procedure becomes less quantitative and more judgemental.

Analyses based on this concept show that where habitations are located in the runout zone of a high severity debris flow, any protective works such as catchment basins should be designed to accommodate the PMM. Where lives are not threatened or the severity of the hazard is sufficiently low as to accept a higher hazard level, the analyses permit the sizing of protective works to match the selected hazard level.

The cumulative probability plots derived during the analyses (Fig. 3d) can be used to predict maintenance costs such as basin clean-out over a selected period of time.

Risk maps (Fig. 4b) are becoming increasingly important in land use and public safety analyses. They are particularly helpful in decision making relating to:

- living with the threat of a hazard, or
- alienating land so threatened, or
- installing protective works.

The case history discussed in this paper uses the total risk concept to formulate risk maps in terms of annual probability of loss of life.

References

FEMA (Federal Emergency Management Agency), 1985. Flood Insurance Study, Guidelines and Specifications for Study Contractors

GOLDER ASSOCIATES, 1991. Geotechnical Study of Slide and Debris Flow Potential, Philpot Road, Kelowna, B.C. Unpublished report to Provincial Emergency Programme, B.C.

HUNGR O., MORGAN G.C., and KELLERHALS R., 1984. Quantitative Analysis of Debris Torrent Hazards for Design of Remedial Measures. Canadian Geotechnical Journal, Vol. 21, No.4.

HUNGR O., MORGAN G.C., VANDINE D.F., and LISTER D.R., 1985. Debris Flow Defences in British Columbia. Proceedings of Reno Symposium on Debris Flows (G.S.A. Reviews in Engineering Geology).

LISTER D.R., MORGAN G.C., VANDINE D.F., and KERR J.W.G., 1984. Debris Torrents along Howe Sound, British Columbia. IV Interim Symposium on Landslides, Toronto.

MORGAN G.C., 1990. Quantification of Risks from Slope Hazards. G.A.C. Symposium on Landslide Hazard in the Canadian Cordillera. To be Published.

PACK R.T., and MORGAN G.C., 1987. Philosophy of Landslide Risk Evaluation and Acceptance. Proceedings of 5th International Conference on Applications of Statistics and Probability in Soil and Structural Engineering, Vancouver.

THURBER CONSULTANTS, 1983. Debris Torrent and Flooding Hazards, Hwy.99, Howe Sound. Unpublished report to Ministry of Transportation and Highways, B.C.

THURBER ENGINEERING, 1990. Debris Flow Hazard Assessment, Fall Creek Slide Area. Unpublished report to Provincial Emergency Programme, B.C.

USBR (U.S. Bureau of Reclamation), 1989. Safety of Dams Program, Policy and Procedures for Dam Safety Modification Decision Making. Interim Guidelines.

VANDINE D.F., 1985. Debris Flows and Debris Torrents in the Southern Canadian Cordillera. Canadian Geotechnical Journal Vol. 22, No.1.

Session 5A
Risk Assessment and
Land Use Planning
(continued)

Return period of avalanches

In avalanche work, the return period is the average time interval within which the runout distance at a given location on an avalanche path is equalled or exceeded once. The frequency is the reciprocal of time period. Therefore, it is possible, in principle, to produce a mapping of return periods in the runout zone corresponding to different locations downslope, for example: 1, 10, 100 years corresponding to yearly probabilities: 1, 0.1, 0.01. These locations increase with distance into the runout zone as the return period increases. The factors influencing return period are related to both climate and terrain (see [2] for details).

The determination of return period may be made by three methods in order of accuracy: (1) direct, long-term observations of avalanche runout; (2) by examination of vegetation or other dateable destructive effects in the runout zone; (3) by examination of climate records and then comparing with frequencies from known avalanche paths in other areas with similar terrain, aspect and climate. These methods are discussed below.

(1) The most accurate method of determining avalanche return periods is to make direct long-term observations of avalanche runout. Even this method has uncertainty, however. The encounter probability, E , is the probability of encountering an event at least once given a return period (T) in years in a length of time (L) in years (length of exposure to risk or observation time). Since avalanche events in each year must be assumed statistically

independent of those in previous years, the encounter probability may be calculated from the binomial expansion by summing all terms beyond the first to yield the probability of at least one event over an observation period (L):

$$E = 1 - \left[1 - \left(\frac{1}{T} \right) \right]^L$$

From this equation if $L = T$ (observation period = return period), the encounter probability is about 0.65. If $L = 2T$, the encounter probability is near 0.90. For example, if the expected return period is 100 years, 200 years of careful observations would be required to be 90% confident that the 100 year avalanche has been recorded (100 years for 65% confidence). This simple analysis shows why long-term observations cannot be yet used with high confidence to specify long return period events in North America.

In general, the historical record is more reliable for determining avalanche frequency in high snowfall areas than in low snowfall areas. If an area receives frequent large snowstorms, large avalanches will occur more frequently giving greater confidence in the observations. In low snowfall areas, a short observation period may not include major avalanches. For low snowfall areas, methods (2) and (3) may have to be relied on even more to estimate major avalanche potential.

(2) If direct observations of avalanche frequency are not available, the next best method is by examination of vegetation (or other dateable destructive effects) in the runout zone. For example, by counting annual tree rings from cores, ages of standing trees may be determined. In this way, it is

possible, in principle, to produce a map of avalanche return periods for a given path in the runout zone. Other methods of dating vegetation damage are reviewed in [2].

This method is commonly applied even though it is time consuming and often several techniques must be used in concert. Usually, however, the only available reliable evidence is the outer trim-line of damaged forest which marks the maximum extent of avalanche movement on the path. Most commonly, this trim-line is associated with return periods on the order of 50-300 years.

(3) When no other information is available, avalanche frequency might be estimated by using climate records and then trying to compare with frequencies of known avalanche paths in other areas with similar terrain, aspect and climate. This method is used as a last resort and it has high uncertainty. It seems doubtful that the accuracy with respect to return period can be better than an order of magnitude.

In summary, for North American conditions where long term observations are often not available, usually method (2) must be applied. In this instance, the most common condition is that of being able to locate only the maximum extent of avalanche damage on the path. This usually provides a definition of a 'hazard line' [3] with return period of order 100 years (varying between 50-300 years). The hazard line is often found by dating vegetation or other destructive effects. When method (3) is used, the accuracy decreases and the uncertainty increases: it may be considered a last resort.

Runout estimation

The best method of locating the maximum runout position is to use field evidence such as damage to vegetation (e.g., North America) or long term historical records (e.g., in Europe). When such evidence is not available, for example in logged areas, the trend now is to use the historical record of maximum avalanche runout in a given mountain range by using terrain variables to characterize maximum runout (time period ~ 100 years) for a number of paths in that mountain range. Normally, maximum runout from at least 30 (preferably 50-100) paths [5] must be known in order to generate a predictive scheme with sufficient accuracy to be at all useful.

McClung and Mears [5] presented data from more than 50 different avalanche paths from five different mountain ranges. Their analysis (see Fig. 1) involved fitting measured maximum runout distances (using a dimensionless runout ratio) to a Gumbel distribution. The runout ratio is defined as the quotient of the horizontal runout distance (marked from the point on the avalanche path where the slope angle first declines to 10°) to the horizontal distance from the start position to the 10° point [4,5]. A significant result of the analysis is that avalanche runout distances show high variability between mountain ranges. Therefore, to apply the method in a given mountain range, a data set must be collected from that range.

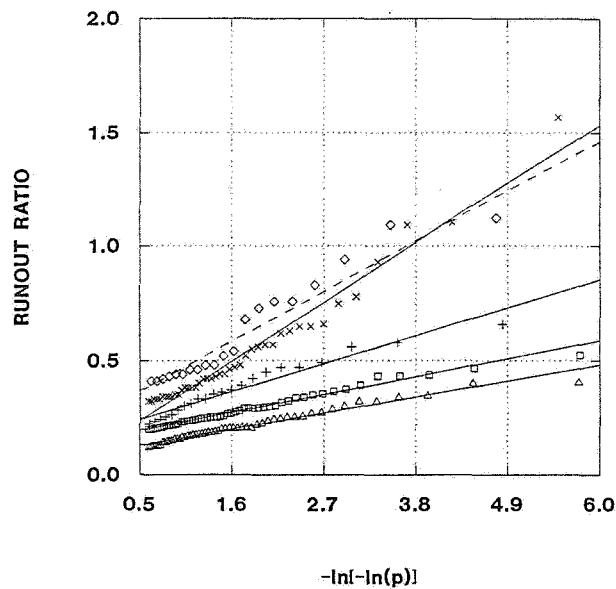


Fig. 1: Dimensionless runout ratio (see text and reference [5]) as a function of non-exceedance probability, p . (\diamond) Sierra Nevada, (\times) Colorado Rockies, ($+$) Coastal Alaska, (\square) Western Norway, (Δ) Canadian Rockies.

Impact forces

Impact forces must be estimated when construction is planned in snow avalanche terrain. Impact forces (I) are calculated as the product of flow density and avalanche speed squared: $I \sim \rho v^2$. Currently there are no recorded estimates of flow densities in connection with moving avalanches.

McClung and Schaerer [6] calculated flow densities from measured impact pressures, avalanche speeds and particle densities in avalanche deposits to give approximate estimates.

Avalanche speed data (Fig. 2) [7] show that avalanches can accelerate and decelerate rapidly at the beginning and end of motion, respectively. Given typically expected flow densities [6] it is expected that impact pressures will exceed the 30 kPa limit mentioned in Swiss zoning schemes when the avalanche speeds exceed approximately 20 m/sec. From Fig. 2 it seems evident that extremely high precision modelling would be required to define the position where the impact pressure is less than 30 kPa: for practical purposes it nearly coincides with the runout position.

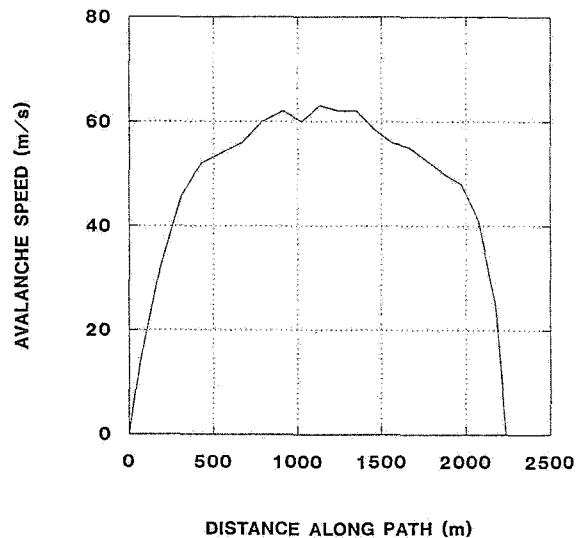


Fig. 2: Frontal speed for a large dry avalanche as a function of distance along the path.

At present, no method exists for which avalanche runout position or speeds along the incline can be calculated with precision by selecting friction coefficients in a dynamics model. The problem is simply too complex both with respect to mechanical properties of flowing snow and mechanical description of the sliding surface. (See [8] for further discussion.) In addition, modelling of the

friction implied by complex terrain element features has not been seriously attempted and the boundary conditions for the flowing snow problem are unknown.

The uncertainties with respect to impact force and speed prediction mentioned above and the fact that avalanches can decelerate very rapidly, combine to force emphasis on runout prediction in avalanche zoning schemes. Since the 30 kPa limit used to define construction zones in the Swiss zoning scheme can nearly coincide with the maximum runout position, the best policy may be to locate the maximum runout position and avoid locations upslope from it.

Zoning Scheme

In North America, direct long-term observations of runout distance are rarely (if ever) available. Usually, the only reliable evidence is the line marking maximum runout by destructive effects near the end of the path, called the hazard line [3]. The hazard line usually has an associated return period ranging from 50-300 years. When the hazard line cannot be found (for example, in disturbed areas), it may be calculated for the mountain range in question by a quantitative scheme such as in Fig. 1 as a function of the non-exceedance probability (p). For example, if $p = 0.99$, 99% of avalanche paths in the data set will have runout which will not exceed the position implied by $p = 0.99$.

Once the hazard line is located, the entire terrain profile is known for the avalanche

path for a return period of order 100 years. Given the terrain profile, it becomes possible to roughly estimate the speed profile for the maximum avalanche on the path, for example, by using the scaling model of McClung [8]. Since return period information is usually lacking, except at the hazard line, construction within the boundaries of avalanche threatened terrain should be planned based on expected impact forces for the maximum avalanche.

Summary

The proposed scheme de-emphasizes return period in avalanche land-use planning. Instead, it makes use of the historical information to estimate the hazard line position. Once the hazard line is estimated, the entire terrain profile for the maximum avalanche is defined. This makes avalanche dynamics and impact force calculations possible [8], although still not with high precision. It should be noted that the position for an impact pressure level of 30 kPa (mentioned in Swiss zoning schemes), can virtually coincide with the hazard line when the precision of current avalanche dynamics models is accounted for (note rapid deceleration depicted in Fig. 2). Therefore, it might often be that the high hazard area (red zone) and moderate hazard area (blue zone: impact pressure less than 30 kPa) of the Swiss zoning scheme would be indistinguishable when the accuracy of avalanche dynamics models is accounted for.

Acknowledgements

The ideas of A.I. Mears and K. Lied are gratefully acknowledged. H. Gubler supplied the data for Figure 2.

References

- [1] Switzerland. 1984. Directives pour la prise en considération du danger d'avalanches lors de l'exercice d'activités touchant l'organisation du territoire. Office fédéral des forêts, Institut fédéral pour l'étude de la neige et des avalanches. 23 pp. + Appendix.
- [2] McClung, D.M. and P.A. Schaerer. 1992. The Avalanche Handbook. Book in draft form.
- [3] Freer, G.L. and P.A. Schaerer. 1980. Snow Avalanche Hazard Zoning in British Columbia, Canada. *Journ. Glaciology*, 26(94):345-354.
- [4] Lied, K. and S. Bakkehøi. 1980. Empirical Calculations of Snow Avalanche Runout Distance Based on Topographic Parameters. *Journ. Glaciology*, 26(94):165-177.
- [5] McClung, D.M. and A.I. Mears. 1991. Extreme Value Prediction of Snow Avalanche Runout. *Cold Regions Sci. and Tech.* 19:163-175.
- [6] McClung, D.M. and P.A. Schaerer. 1985. Characteristics of flowing snow and avalanche impact pressures. *Ann. Glaciol.* 6:9-14.
- [7] Salm, B. and H. Gubler. 1985. Measurement and Analysis of the Motion of Dense Flow Avalanches. *Ann. Glaciol.* 6:26-34.
- [8] McClung, D.M. 1990. A Model for Scaling Avalanche Speeds. *Journ. Glaciology* 36(123):188-198.

Setbacks from the Crests of Slopes

S. Thomson, D.M. Cruden
*Department of Civil Engineering
University of Alberta*

J. de Lugt
*Department of Geology
University of Alberta
Edmonton, Alberta*

Abstract

On the Interior Plains, the crests of river valley slopes often provide an agreeable view and so are desirable sites for residential development. Unfortunately these sites may be subject to slope movements that may destroy or damage structures or services built too close to the valley crest. To avoid damage setbacks are needed. Rational setbacks, based on the ultimate angle of a stable slope, are applied to 7 case histories to assess their reliability. The method compares the angle of the slope in question with the angle of nearby stable slopes with the same geology. The stable slopes of river valleys have been abandoned, that is, there is no river erosion at the toe of the slope at present nor has there been in historic times. The geology of the slope affects its ultimate angle. For the case histories studied, ultimate angles of undisturbed bedrock slopes ranged from 6° to 17° . In overburden slopes the ultimate angle ranges from 8° to 26° . Setbacks also include an allowance for lateral erosion by the river though this factor is difficult to determine precisely. The terrain behind the valley crest is usually flat. If the terrain rises, the setback should be increased by a simply determined geometric factor; if the terrain falls the setback is decreased by a similar factor. There are several implications arising from the setback guideline. The crest areas of slopes that have reached their ultimate angle are available for development with a small setback. For any slope that has not attained its ultimate angle, the setback represents land that is not available for development without remedial work. The size of this area will depend on the height of the slope and the difference between the slope angle and the ultimate angle. Detailed geotechnical analyses and remedial work should be required before development can proceed within the setback.

Introduction

On the Interior Plains the crests of river valley slopes often provide spectacular views and so are desirable sites for residential development. Unfortunately these sites may be subject to slope movements that may damage structures or services to them. Thus there is a need for setbacks.

Setbacks to ensure long term safety of structures from slope movements have been established by theoretical or empirical methods (1, 2, 3). With the exception of analyses,

based on a detailed site investigation, most setback guidelines lack a rational basis for determining the setback distance. Also, such guidelines are site specific and their application to long reaches of a river may be prohibitively expensive.

A rational method of determining a setback based on the ultimate angles of stable slopes, was used to establish setbacks for a 20 km reach of the North Saskatchewan River between Edmonton and Fort Saskatchewan, Alberta (4, 5). This present paper applies the method to 7 case histories of damage to

structures built near the crest of valley walls in Alberta.

Methodology

The case histories involving loss or damage to structures were collected from municipal engineers, regional and local planning agencies and consulting engineering firms. All the quantities necessary to determine the setback, SG, can be determined from topographic maps and air photographs. Obviously slope heights, H, slope angles, α , and the average angle of abandoned slopes should be confirmed by a site reconnaissance which also allows a surface exploration of the site hydrogeology.

The identification of mature abandoned slopes in the vicinity of a specific slope is essential to the method for determining the setback. The ultimate slope angle, β_u , is the angle from the horizontal of abandoned slopes having similar geology, groundwater conditions and topographic position to the oversteepened slope at the site in question. Mature abandoned slopes are not presently being eroded by the river and have not been eroded for a thousand years or more. At least three abandoned slopes in the area of the slope being assessed should be located and their slope angles averaged to determine β_u .

Lateral erosion of a river is difficult to determine particularly on an engineering, as opposed to a geologic, time scale. The rate of bank erosion depends on both the material comprising the bank as well as the flow regime of the river. One site specific study, made for the North Saskatchewan River in Edmonton, suggested an average of 30 cm per year over a 100 year period (3). Although of the correct order of magnitude, erosion is episodic and much larger rates may be encountered in any given year. Tedder (4) used this rate over a 50 year period as the net lateral river erosion, E. Due to a lack of specific data on bank erosion, those slopes subject to toe erosion have been assigned an E value of 15 m. Smaller creeks show less erosion and

their slopes were arbitrarily assigned an E value of 8 m. For a given site, comparison of old air photos with the most recent will often yield an assessment of lateral erosion. Then (Fig. 1a)

$$SG = H (\cotan\beta_u - \cotan\alpha) + E \quad (1)$$

Case Histories

The work of Cruden et al. (6), on the distribution of landslides in Alberta was the basis on which the case studies were selected to give wide regional coverage. These cases are listed in Table 1 and shown on Fig. 2.

Tedder (4) suggested that the slopes within his study area could be classified into 3 types, slopes in overburden, slopes which were bedrock based and bedrock slopes where the bedrock extended more than halfway up the valley wall. This classification reflected the presence of the pre-glacial channel of the North Saskatchewan floored by pre-glacial fluvial sands and gravels in the area. Slopes entirely in overburden were cut close to the thalweg of the pre-glacial channel and drained by the gravels resulting in water tables which were generally close to the toes of the slopes. On the flanks of the pre-glacial valleys, present day slopes are based on generally impermeable bedrock raising the water table in the overlying sands to about halfway up the slope. Away from pre-glacial channels, the bedrock slopes are capped by low permeability tills and glaciolacustrine sediments, impeding recharge and resulting in water tables generally about a quarter of the way up the slope.

While the above classification does not apply to all the slopes in Alberta, (the pre-glacial succession in the Peace River Lowland is different, for instance (7)) it can be used to organize the case histories in Table 1.

Overburden Slopes

The 76th Avenue Landslide occurred on 76 Avenue near 88 Street in Edmonton and

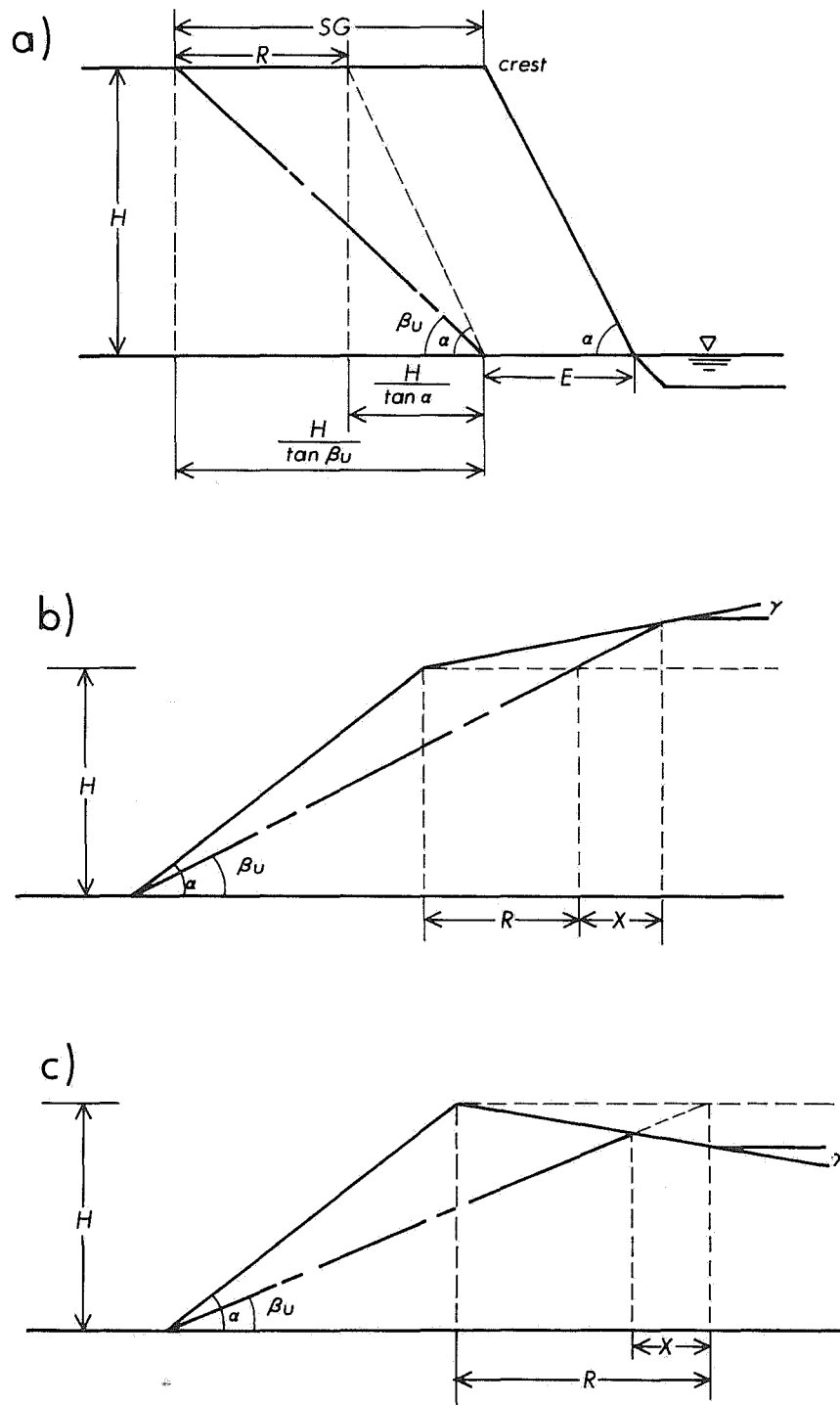


Figure 1. The contribution of erosion, E , and retrogression, R , to the setback guideline, SG , for a slope with angle, α , and height, H . a) Slope crest horizontal b) Ground rises at γ from the slope crest c) Ground falls at γ from the slope crest.

TABLE 1-- Summary of Case Histories

Slope type	Landslide	SG (R + E _n)	Distance of Structure From Crest	Approx. Crest Retreat	Comments	H (m)	β_u	α
obdn	76th Avenue Edmonton	13 m (5 + 8)	within 5 m	5 m	- 3 houses razed, slope flattened	12	11.5	12.5
obdn	MIssion Heights Grande Prairie	19 m (19 + 0)	within 10 m	7 m	- remedial work was necessary - gravel blanket, slope flattening	10	13	22
obdn	Schoendorfer Manning	32 m (17 + 15)	9 m	6 m	- the garage may have to be moved	15	26	47
obdn	Park Hill Calgary	38 m (23 + 15)	14 m	12 m	- the road was relocated and house demolished, remedial work was also necessary - horizontal drains, slope unloading toe load	30	16	20
bedrock based	Grierson Hill Edmonton	61 m (46 + 15)	?	43 m	- 16 structures affected: 2 stables, 14 houses, some were moved, others were demolished	50	17	24
bedrock based	Lesueur	66 m (51 + 15)	8 m	23 m	- the Lesueur house was removed	31	15	26
bedrock	Power Plant Medicine Hat	178 m (164 + 15)	within 18 m	16 m	- two power poles had to be moved	50	13	43

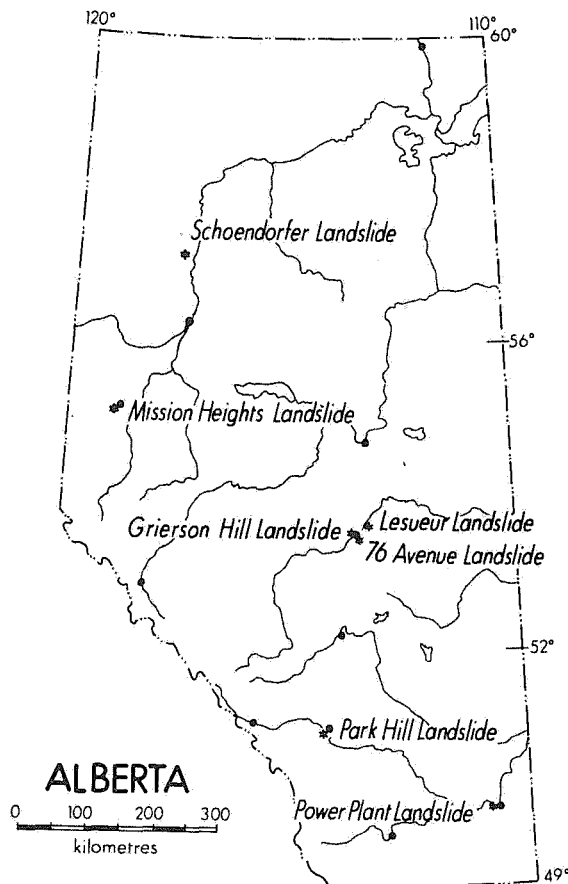


Figure 2. Location of Case Histories

resulted in the loss of 3 houses. A tributary of the North Saskatchewan River, Mill Creek, had eroded through glacial lake sediments and till to the clay shale bedrock. During the decade following World War II the area was developed and urbanization affected slope stability. In 1972 a landslide occurred and a graben formed at the crest of the slope. The scarp was tangent to the foundations of the westerly house, passed behind the middle house, and curved downhill under about a quarter of the easterly house (8). The three homes were considered unsafe for occupancy and were bought by the city. The houses were razed and the slope flattened.

This slope is classified as an overburden slope, lake sediments with till. The slide was not investigated in detail but as there was little toe erosion and steepening of the slope, a major factor may have been an increase in the

groundwater level within the slope due to local irrigation (9). The east house was within 5 m of the crest, the centre house below the crest and the west house at the crest. All three houses were within the setback guideline.

The Mission Heights Landslide occurred in 1990 in Grande Prairie. The homes in this newly developed subdivision were built in the early to mid eighties. The backyard of the centre house was extended by the placement of fill along the crest of the valley wall. The larger slide of 1990 occurred after heavy rains and affected two houses, and possibly a third located on the right flank of the slide. The scarp was within 3 m of the houses, all of which are within the guideline setback. Remedial work consisting of installation of a drainage blanket and slope flattening has been carried out.

The Schoendorfer Landslide located in the northeast of the Town of Manning, occurred in 1990 and is threatening a garage. The house on the property is built on an abandoned slope while the garage is located on an active meander slope of the Notikewin River. The 1976 air photographs show that a relatively recent slide had occurred directly below where the garage was subsequently built. It is likely that the erosion at the toe of the slope triggered the slide.

The slope is classified as an overburden slope, indicating that the groundwater level is expected to be at or near the base of the slope. The scarp of the slide, originally 9 m, is now about 3 m from the garage; well within the guideline. The most economic procedure would be to move the garage. The house is safely located.

The Park Hill Landslide occurred in 1967 in southwest Calgary, on the right bank of the Elbow River. A paved road runs parallel to the valley crest and houses front on the street on the side remote from the slope. The scarp of the

slide crossed the road to within 2 m of the house closest to the top of the slope. Because only one house was affected by the slide, it was considered most economical to remove the house and to relocate the road (10).

The valley slope in this area consists of lacustrine clayey silt with lenses and layers of sand (10). The slope was classified as an overburden slope, however the groundwater level was near the slope surface. The road and the nearest house were both within the guideline. Stabilization work in 1967 included unloading the slope and installation of horizontal drains. In 1970, following further slope movement a toe load was added.

Slopes in Bedrock

The Grierson Hill Landslide occurred in 1901 damaging seven buildings, 6 houses and a stable. Further retrogressive movements brought the totals to 2 stables and 14 houses by 1915. In some cases, threatened houses were relocated before they were actually damaged. Movements continue today, limiting development and necessitating frequent maintenance of Grierson Hill Road. Coal mining in the vicinity of Grierson Hill was the trigger of the 1901 landslide. Another factor was the high precipitation of the early 1900's. It is believed that water pressure in cracks and fissures has had a major role in re-activating the slide (11). In the 1950's a significant amount of water was pumped out of the Humberstone mine which was located directly beneath the slide area. From 1911 to 1915, the lower portion of the slope was used as a dump, accumulating up to 15 m of garbage, straw, bricks, clay and fill. The slope modifications that resulted from the extensive dumping and backfilling caused additional large slope movements. River erosion has been extreme in the area. Between 1887 and 1893 the river encroached into the bank about 15 m (14). Since that time, the outward movement of the slope has pushed the river up to 122 m from its 1893 position. The slope is bedrock-based, with the groundwater level expected in the lower half of the slope.

The total crest retreat of the Grierson Hill Landslide between 1900 and 1958 was 43 m (12) which is quite comparable to the calculated 46 m. Most of the slide area has been designated as parkland though an extensive tied back tangent wall allowed the construction of the Edmonton Convention Centre (11).

The Lesueur Landslide located on the outside bend of a meander of the North Saskatchewan River about 6.5 km northeast of Edmonton, occurred on 3 Sept. 1963. The scarp was 6 m high and exposed part of the foundation of the house. The major factor leading to the landslide was the long term erosion of the protective fluvial terrace at the base of the slope. The trigger was likely the build-up of water pressure within the slope (13) and the decrease of soil strength due to valley rebound (14). The slope is bedrock-based, with a groundwater level located in the lower half of the slope.

The initial landslide resulted in a retreat of the crest of the slope of about 12 m. In the 24 years since the slide occurred, the total retreat is close to 35 m suggesting that the 66 m is a conservative but reasonable setback guideline. The Lesueur house was built about 2 m from the crest, within the guideline.

The Power Plant Landslide occurred in 1980, on the south bank of the South Saskatchewan River in Medicine Hat. The failure produced a near vertical 150 m long scarp. Tension cracks developed adjacent to the 10-15 m high scarp, indicating that further recession was likely to occur in the relatively near future. Tension cracks formed within 2.5 m of Calgary Power utility poles, necessitating their relocation. The 1962 air photos indicated that the low level terrace to the east of the slide area extended westward, protecting the toe of the slope below the power poles. By 1980 the terrace had been completely eroded. It is likely that the destruction of this terrace led to the slope failure. MacKay and

Thomson (15) suggested that the main causes of failure are river erosion and groundwater discharge at various points within the slope.

The slope is classified as a bedrock slope with the groundwater level expected at about a quarter of the slope height. Both power poles were within 18 m of the crest, hence well within the guideline. The large setback distance is a result of the steep original slope and its height.

Discussion

In six of the seven cases presented, no damage to the structures would have occurred had they been behind the guideline. In the remaining case, the Schoendorfer Landslide, the structure is within the guideline distance but as yet has not been damaged. At the time of construction (late 1970's) the crest was 9 m from the structure, in 1990 this distance had decreased to 3 m.

For any slope that has not reached its ultimate angle, the setback from the crest represents land that is not available for development without remedial work. This area increases with the difference between the existing slope angle and its ultimate angle. In areas of high land cost, detailed geotechnical analyses of remedial work are advisable before development proceeds.

The ultimate angle of slopes is independent of the height of the slope because a mature abandoned slope has undergone considerable degradation, (1), and cohesion has decreased to zero. In the long term, the slope behaves as if it were comprised of a cohesionless material. The rate of slope retreat to its ultimate angle is not linear but is rapid in the early stages slowing down as time passes to resemble a logarithmic decay curve. Hutchinson (1) showed that the time for the London Clay to achieve an ultimate angle is in the order of 1500 years. So the setback guideline may be conservative when the life of a structure, in engineering terms, is fifty years. The problem then becomes one of assessing the amount of crest retreat remaining

from whatever stage the slope is in when development is contemplated.

In typical prairie case histories, the terrain is often horizontal at the crest of the slope. When the ground rises away from the crest of the slope at an angle γ , the retrogression, R , is increased by a factor $\tan\beta_u/(\tan\beta_u - \tan\gamma)$, (Fig. 1b). In contrast, when the ground falls away from the valley crest, retrogression, R , is decreased by $\tan\gamma/(\tan\beta_u + \tan\gamma)$, (Fig. 1c).

From all the case histories available, the ultimate slope angle of overburden slopes ranges from 8° to 26° (17 cases) for bedrock based slopes the range is from 6° to 17° (5 cases) and for bedrock slopes the range is from 7° to 14° (6 cases). The range for overburden appears large but is not unreasonable when materials range from lake clays to fluvial sands and gravels. The bedrock based and bedrock slopes have similar smaller ranges of ultimate slopes reflecting the performance of rocks varying from bentonitic mudstones to clayey siltstones.

The wide range of ultimate slope angles reinforces the need for geotechnical input to land zoning decisions. When slopes as steep as 26° may be stable and slopes as low as 7° may be unstable, the arbitrary choice of any particular slope as hazardous may be both uneconomic and dangerous. Setbacks should be established by qualified professionals. Urban centres might legislate map overlays in zoning bylaws. Less densely developed jurisdictions could simply prescribe methodologies for defining setbacks.

Conclusions

The setback has delineated a distance that appears to be prudent and effective guideline for development.

The areas adjacent to slopes that have reached their ultimate angle area are available for development, due to care being given to the influence of man.

Slopes that are not at their ultimate angle represent land unavailable for development. The applicability of the setback guideline will depend to some extent on how close the existing slope angle is to the ultimate slope angle. In any event, a detailed geotechnical evaluation is recommended.

It is suggested that the guideline presented is simple, effective and has a wide range of application. Its application will lead to a reduction in the hazards of landslides.

References

- 1) Hutchinson, J.M., 1973. The response of London Clay Cliffs to differing rates of toe erosion. *Geologia Applicata e Idrogeologica*, 8: 221-239.
- 2) Stepanek, M. and Rodier, C.E., 1980. Stability and control of slopes in Calgary. In: *Slope Stability Problems in Urban Areas*. Canadian Geotechnical Society, Toronto. 10p.
- 3) Thomson, S. and Townsend, D.L., 1979. River erosion and bank stabilization - North Saskatchewan River, Edmonton, Alberta. *Canadian Geotechnical Journal*, 16: 567-576.
- 4) Tedder, K.H., 1986. Slope stability in the North Saskatchewan River Valley. Unpublished thesis, University of Alberta, Edmonton, 254p.
- 5) Cruden, D.M., Tedder, K.H., and Thomson, S., 1989. Setbacks from the crests of slopes along the North Saskatchewan River Valley, Alberta. *Canadian Geotechnical Journal*, 26: 64-70.
- 6) Cruden, D.M., de Lugt, J.S., Lindstrom, K., and Thomson, S., 1990. Landslide Incidence In Alberta. Design and Construction Branch, Alberta Environment, Edmonton, 99p.
- 7) Cruden, D.M., Ruel, M., Thomson, S., 1990. Landslides along the Peace River, Alberta, Proceedings, 43rd Canadian Geotechnical Conference, Quebec City.
- 8) Thomson, S. and Tiedmann, C.E., 1982. A review of factors affecting landslides in urban areas. *Bulletin of the Association of Engineering Geologists*. 19-55-65.
- 9) Hamilton, J.J. and Tao, S.S., 1977. Impact of urban development on groundwater in glacial deposits. Preconference Proceedings, 30th Canadian Geotechnical Conference, Saskatoon. II: 1-35.
- 10) Hardy, R.M., Clark, J.I., and Stepanek M., 1980. A summary of case histories spanning thirty years of slope stabilization in Calgary, Alberta. In: *Slope Stability Problems in Urban Areas*. Canadian Geotechnical Society, Toronto, 24p.
- 11) Martin, R.L., Williams, E.R., and Balanko, L.A., 1984. The Grierson Hill Slide, Edmonton, Alberta. 37th Canadian Geotechnical Conference. Canadian Geotechnical Society, Toronto, pp. 125-133.
- 12) Pennell, D.G., 1969. Residual strength analysis of five landslides. Ph.D. Thesis, University of Alberta, Edmonton, 166p.
- 13) Thomson, S., 1971b. The Lesueur Landslide, A failure in Upper Cretaceous clay shale. Proceedings, Ninth Annual Engineering Geology and Soils and Engineering Symposium, Boise, ID. pp. 257-287.
- 14) Matheson, D.S. and Thomson, S., 1973. Geological implications of valley rebound. *Canadian Journal of Earth Sciences* 10: 961-978.
- 15) MacKay, C., and Thomson, S., 1980. Slope instability along the South Saskatchewan River and tributaries in the vicinity of Medicine Hat, Alberta. Report to Alberta Environment, Design and Construction Division, Geotechnical Branch, 123p.

J. Vaunat, S. Leroueil and F. Tavenas
Hazard and risk analysis of slope instability
Paper to be found on page 397

A Seismic Risk Assessment Methodology for Comparative Assessment of Multiple Sites

R.S. von Sacken

*Public Works Canada
Vancouver, British Columbia*

K.W. Savigny

*Department of Geological Science, University of British Columbia
Vancouver, British Columbia*

I. Olsen

*Bruce Geotechnical Consultants Inc.
Vancouver, British Columbia*

G. Davy

*Public Works Canada
Vancouver, British Columbia*

Introduction

Indian and Northern Affairs Canada is concerned about the potential risks to native communities in the British Columbia Region should an earthquake occur. As a first step in mitigating the potential effects of such an event, a methodology was developed to assess relative risks among various communities in the region [1]. Evaluation of structural deficiencies in existing facilities, scheduling of mitigative work, implementing appropriate land-use zoning and establishing emergency response plans will be undertaken according to an unbiased priority rating that emerges from application of the methodology.

This paper provides a description of the methodology [1]. Two communities are evaluated to illustrate how it is utilized. Possible extensions involving the use of a personal computer and spreadsheet software are considered.

The authors are grateful to Public Works Canada and Bruce Geotechnical Consultants Inc. for

permission to publish this material and for providing assistance with preparation of the manuscript.

Scope

The methodology provides a basis for evaluating site specific conditions that could exacerbate the effects of an earthquake. These include:

- Geological conditions in each community;
- hydraulic or hydrogeologic conditions in each community;
- natural and man-made features that could have a direct, adverse impact on the community or access to it; and
- other conditions or factors outside the community that could have an indirect, adverse impact on it.

A risk assessment matrix provides a quantitative and unbiased basis for evaluating relative risk among a number of communities in the region.

Weighting factors are used to account for loss of life, loss of property, and security of access.

Risk Assessment Matrix Technique

General Approach

Airphoto interpretation and terrain analysis (API) are expedient, cost efficient ways of classifying surficial materials and landforms [2, 3] as a preliminary step in earthquake hazard and risk assessment. API is traditionally followed by on-site surficial and subsurface investigations, detailed engineering assessment of the materials, and, where necessary, mitigative action to reduce risk associated with specific earthquake hazards. The cost increases dramatically as programs advance from API to field phases. Where several communities in widely separated locations are being considered, it is clearly beneficial if, through the use of API, priorities for *in situ* evaluation can be established in an unbiased way.

Broster and Bruce [4] used a matrix technique for comparative evaluation of widely-separated borrow sources. The same concepts are used here to develop a risk assessment matrix. This affords rapid and unbiased assessment of the relative susceptibility of various communities to earthquake hazards at very little cost. The matrix is designed to highlight geological conditions, which are delineated from API, and earthquake hazards having significant risks in terms of casualties, property loss and loss of access. The matrix is easily adopted to spreadsheet recording and analysis. Hence, the initial framework of the matrix is easily adjusted as additional communities are studied, as *in situ* investigations and mitigative work are completed, or in response to a seismic event where predicted and observed performance are not in accord.

Matrix Framework

There are two fundamental ways of evaluating the susceptibility of a site to earthquake damage. The first consideration is site geology, particularly soil conditions which are described in the form of terrain units as part of API. The second is the potential for coseismic impact which combines the exposure of the site to well known earthquake hazards and seismic hazard zoning prescribed in the National Building Code of Canada.

Terrain Units

Terrain units are elucidated on the basis of API by delineating areas in each community where soil and/or rock conditions are uniform. It is desirable for all API to be undertaken by the same individual. In practice, however, the API for a large number of communities could be undertaken by several individuals, possibly in different agencies. The most important guideline for interpreters to follow is to keep the number of terrain units as small as possible by using very general, textural based descriptions such as 'SAND: silty, loose' or 'CLAY TILL: silty'. This guideline provides for optimum conformity in the work done by different individuals without compromising its accuracy and attendant value in developing the matrix.

Since each community is relatively small, the magnitude of any given seismic event will not change and seismic hazards can be expected to have a consistent level of risk anywhere the same terrain unit is present. The intensity of the event will vary however, in relation to soil or rock conditions as expressed by terrain units. For example, a saturated, loose deltaic silty sand may liquefy while the event is only moderately detectable on adjacent terrain consisting of a veneer of clay till over rock.

The risk assessment matrix framework is

illustrated in Figure 1. The terrain units are entered in rows. Because different communities have different numbers of terrain units it is necessary to normalize the terrain unit totals outside of the matrix by dividing by the number of terrain units. The line where this calculation is made is shown in Figure 1.

Potential for Coseismic Impact

The potential for coseismic impact is related to several variables. Earthquake hazards and seismic hazard zoning are included in the risk assessment matrix. At a later time the seismic design of engineered structures is an important variable that could be added to the matrix.

The major earthquake hazards include:

- surface faulting (ground rupture)
- ground shaking
- ground failure
 - liquefaction
 - slope movement:
 - flow (liquefaction and flow to a free face)
 - spread (liquefaction below a brittle crust and flow to a free face)
 - slump (rotational movement on a shear surface)
 - slide (translational movement on a shear surface)
- flooding
 - tsunami
 - seiche
 - indirect (breach of an engineered fluid containment structure or breach of a natural dam)

EARTHQUAKE EFFECTS TERRAIN UNIT NUMBER	SURFACE FAULTING	GROUND SHAKING	GROUND FAILURE				FLOOD			TERRAIN UNIT SUBTOTALS	
			LIQUEFACTION	SLOPE MOVEMENT			TSUNAMI	SEICHE	INDIRECT		
				FLOW	SPREAD	SLUMP					SLIDE
WEIGHTING	1	10	10	5	5	5	5	3	2	1	
			x								
			y								
TERRAIN UNIT TOTAL											
NORMALIZED TERRAIN UNIT TOTAL											
SEISMIC RISK FACTOR											

Fig.1 Seismic Risk Assessment Matrix

The relative importance of each of the earthquake hazards is developed in the matrix by weighting. The overall range of weighting is arbitrarily set at 1 to 10, with 10 being most significant. The range and assignment of weighting values are both subjective however, and the possibility of modifying one or both as more communities are studied or as more scientific data emerge is the advantage afforded by the matrix technique. The following are the criteria considered in assigning weights to the earthquake hazards:

1. Documented level of risk;
2. exposure (*ie.* the whole terrain unit or only a portion); and
3. casualties and property damage vs. property damage only.

The following are the assigned weights for each earthquake effect:

• surface faulting	1
• ground shaking	10
• ground failure	
liquefaction	10
slope movement	
flow	5
spread	5
slump	5
slide	5
• flooding	
tsunami	3
seiche	2
indirect	1

The numbers are entered as a row immediately above the terrain unit row entries such that each weight number appears directly below the corresponding earthquake hazard (Fig.1).

Seismic Zoning

The evaluation of regional seismic hazards for the purposes of the National Building Code of

Canada is the responsibility of the Geological Survey of Canada. Seismic zoning is derived from statistical analysis of past earthquakes and from advancing knowledge of Canada's tectonic and geological structure. Zones are classified according to the most powerful ground motion that is expected to occur in an area with a given probability. A 10% probability of exceedence over 50 years is the standard used in the National Building Code [5].

In an effort to keep the matrix framework as straightforward as possible, seismic zoning is expressed in the matrix evaluation as zone number values that correspond to the zone rather than ground motion. As the zone number applies to the whole of each individual community, it is accounted for outside the matrix. The line where this calculation is made is shown on Figure 1. The calculation will be considered further in the examples that follow.

Ranking of Earthquake Effects

The ranking is a subjective rating assigned to express the anticipated severity of the earthquake effects in terms of detailed knowledge of soil and rock conditions within each terrain unit. The overall range is arbitrarily set at 0 to 3. It could be argued that this is duplication of weighting, but to counter this consider examples from two widely separated locations each having a 'SAND' terrain unit. At one site the sand is of fluvio-deltaic origin and is very thick. It is fine grained and silty, moreover, it is saturated to near the ground surface. At the second location, the sand is a product of sorting by wave action and marine (longshore) transport. The sand is fine to medium grained with some gravel and very little silt, the water table is expected to be several metres below the ground surface, and the deposits rest on rock or glacial drift. The susceptibility of the sand at the first location to ground shaking (specifically, ground

amplification of seismic energy) and liquefaction is greater than at the second location. This is accounted for by the ranking value. The ranking also enables hazards that are not applicable to be eliminated.

Matrix Development

The following steps are followed in developing the matrix:

Step 1: Assemble all available information from published maps and reports and unpublished data available from various government agencies.

Step 2: Collect air photos at a scale of approximately 1:10,000 and complete an API of the community using reference materials on soil conditions collected in Step 1.

Step 3: Enter terrain unit numbers in the left column of the risk assessment matrix.

Step 4: In the box that represents each individual terrain unit/earthquake hazard a line separates x and y values as shown in Figure 1. The x value is the ranking and the y value is the product of x and the weighting for the respective earthquake hazard. Possible combinations of the x and y values from the box in which they are shown in Figure 1 are:

x	y
0	0
1	10
2	20
3	30

Step 5: The y values are numerically

totalled along each row to determine the terrain unit subtotals. When the terrain unit subtotals are compared, a clear indication of the terrain unit having the highest seismic risk in each community emerges.

Step 6: The sum of the terrain unit subtotals determines the terrain unit total.

Step 7: The terrain unit total is normalized by dividing by the number of terrain units. The normalized value provides a way of comparing different communities regardless of seismic zoning.

Step 8: The normalized value is multiplied by the seismic zone number for the community to determine the seismic risk factor. The seismic risk factor provides a method of comparing earthquake risk after accounting for regional differences in seismic hazard set out in the National Building Code of Canada.

Since the initial development, slight modifications were made to the original matrix to include a summary of the physiographic data of the reserve and terrain classification of each terrain unit for the pilot projects [2,3].

Pilot Projects

To begin the seismic risk assessment process, fourteen communities were chosen for evaluation. These are:

	Indian Reserve (I.R.)	Seismic zone number
*	Alert Bay 1A	6
*	Masset 1	6
*	Skidegate 1	6

*	Tsulquate 1	6
*	Bella Bella 1	5
*	Dolphin Island 1	5
*	East Saanich 2	5
	Ittatsoo 1	5
*	Kitasoo 1	5
	Marktosis 15	5
*	Port Simpson 1	5
	Sliammon 1	5
	South Saanich 1	5
	Tsahaheh 1	5

The selection of these communities was based on two criteria, both are arbitrary but obviously significant factors: (1) the number of permanent residents must be 250 or greater, and (2) the location of the reserve must fall within seismic zone 5 or 6.

Preliminary airphoto interpretation and terrain analysis were performed prior to field investigation. Reconnaissance ground truthing was undertaken for nine of the fourteen sites (see reserves with asterisks). Efforts were concentrated on the northern and more isolated communities where there was little or no surficial geological information available. Field checking was carried out mainly to confirm some of the terrain units identified through API and was limited to accessible natural exposures of soils and rock.

Available geological data and results from terrain analyses were combined to produce a terrain map for each reserve. The risk assessment matrix was also incorporated as part of the legend in order to centralize as much information as possible on the same map sheet. The seismic risk assessment of two of the fourteen communities is presented in this paper as case examples: Tsahaheh Indian Reserve 1 and Skidegate Indian Reserve 1.

Tsahaheh I.R. 1

Figures 2a and 2b show the terrain map and risk assessment matrix of Tsahaheh I.R. 1, respectively. Tsahaheh is located northwest of Port Alberni, Vancouver Island, bordering Somass River. The relief of the reserve is subdued to gently rolling. Bedrock is close to or at the surface in the central portion of the reserve, where the highest elevation is approximately 60 m above sea level. This site was not field checked.

Five terrain units were identified for this reserve (Figs.2a and 2b). Terrain unit 1 consists of shore, deltaic and alluvial deposits of the Salish Sediments, which are composed of silt, clay, sand and some gravel [6]. Terraced fluvial deposits of the Capilano Sediments make up terrain unit 2, which consists of gravel and sand. These two terrain units are the main sources of aggregates in the area. Terrain unit 3 is comprised of a discontinuous veneer of Capilano Sediments overlying bedrock. These consist of varied stony clay to gravel, sand and silt, commonly less than 1.5 m thick. The same materials are underlain by Vashon drift in terrain unit 4. Thick marine or glaciomarine silt, with some clay and stony clay of up to 10 m make up terrain unit 5.

The rank values assigned to each terrain unit for each earthquake hazard reflect the anticipated severity. For example, ground shaking (i.e. amplification of ground motion) is expected to be worse in terrain units containing finer materials which include sandy and silty units such as terrain units 1 and 5, while the other three units either contain higher coarser fraction or are thin and underlain by relatively stable material such as bedrock. For liquefaction, terrain units 1, 4 and 5 have non-zero rank values. Terrain unit 5 consists mainly of thick silt, and based on its vicinity to McCoy Lake, it is expected to be at least partially saturated,

hence a rank value of 2 was given.

Since the reserve is located closely to Port Alberni (within 3 km), the only city in Canada with recorded damages caused directly by tsunami waves, Tsahaheh can potentially be affected by a tsunami. The 1964 Alaskan earthquake (M8.4) generated waves of up to 4 m high¹ which caused significant flooding and damages to the city of Port Alberni and surrounding areas including the Ahahswinis I.R.1, which borders the western limit of Port Alberni (Marshall Macklin Monaghan, 1986). Numerical modelling shows that tsunami waves of possibly 3 to 8 m high can occur in the Alberni Inlet (Dunbar *et al.*, 1989). If a sufficiently large tsunami occurs, terrain unit 1 within Tsahaheh will have the highest potential of being affected, hence a rank of 3. Terrain unit 2 was given a value of 1, as it may be partially affected.

Comparison of the terrain unit subtotals, shown in the last column of the risk assessment matrix in Figure 2b, suggests that terrain units 1 and 5 represent the worst ground conditions within Tsahaheh.

Skidegate I.R.1

The terrain map and risk assessment matrix for Skidegate I.R. 1 are shown in Figures 3a and 3b, respectively. Skidegate is located along the east coast of Graham Island, Queen Charlotte Islands. Topographic relief on the reserve is moderate on the north side to slightly more mountainous in the south. The reserve can be accessed via regular flights and ferry services to and from Sandspit on Moresby Island.

Five terrain units were identified. The majority of the reserve is covered by varying thickness of stony clay till (terrain units 4 and 5), from a thin veneer (of less than 2 m thick) to over 20 m. The clay till in terrain unit 4 is compact and slightly moist. It consists of stones and gravel embedded in a dense silty to clayey matrix with very minor sand. At the southern limit of the reserve, the clay till in terrain unit 5 is known to be sandwiched by two fairly thick layers of sand and gravel, underlain by bedrock at a depth of 20 m. The sand and gravel at this location provided the community a source of aggregates which is now depleted. Bedrock is found discontinuously at or near the surface at higher elevations and in much of the southern half of the reserve. A number of rock quarries are located within and around the reserve property.

A major fault is located just north of the reserve [9,10], along which movement commonly occurs. Terrain units 3 and 4 continue northward toward this fault (not shown in Figure 3a). Faulting may occur in these terrain units due to displacement of this fault, hence, a rank value of 1 is assigned under the column of surface faulting.

Ground shaking is expected to be worst in terrain unit 1, which consists of alluvial fan deposits of sand and silt. Saturation of this unit caused by tidal fluctuations and the finer grain size render the possibility of liquefaction. In this regard, the materials in other units are not loose, fine grained nor saturated enough to be a problem. Slumping of terrain units 1 and 3 is possible. Terrain unit 3 is believed to be a raised beach, consisting of mainly gravelly sand, underlain by terrain unit 4 (clay till) or bedrock.

Comparison of the terrain unit subtotals, unit 1 appears to be the most problematic. Submarine slumping and erosion along the shore,

¹ Tsunami crest height, above normal tide level.

inundation of parts of terrain unit 2 and possibly unit 4 may arise, if significant instability of terrain unit 1 occurs. Terrain units 2, 4 and 5 have the same subtotal, suggesting that the degree of susceptibility to damage would be similar.

Taking the seismic zone designation into consideration, the seismic risk factors for Tsahaheh and Skidegate are 193 and 177.6, respectively. These values are considered to be moderately high; they also demonstrate that, although Skidegate is located in a higher seismic zone (6), it has a slightly lower seismic risk factor than a seismic zone 5 community. Tsahaheh is considered relatively more susceptible to damage as a result of a large earthquake.

References

- [1] Bruce Geotechnical Consultants Inc. 1991. Earthquake preparedness - Development of a risk assessment methodology for native communities in the British Columbia Region. Public Works Canada, DIAND Technical Services, Report #5054. 12 p.
- [2] British Columbia Ministry of Environment. 1988. Terrain Classification System for British Columbia. Manual 10, Revised Edition. Recreational Fisheries Branch and Surveys and Resource Mapping Branch. 90 p.
- [3] Cruden, D.M. and Thomson, S. 1987. Exercises in Terrain Analysis. The Pica Pica Press. Edmonton, Alberta, Canada. 185 p.
- [4] Broster, B.E. and Bruce I.G. 1990. A site selection case study using terrain analysis in conjunction with an evaluation matrix. Quarterly Journal of Engineering Geology, London. 23, pp.209-216.
- [5] Basham, P.W., Weichert, D.H., Anglin, F.M. and Berry, M.J. 1985. New probabilistic strong seismic ground motion maps of Canada. Bulletin, Seismological Society of America. 75, pp.563-595.
- [6] Fyles, J.G. 1963. Surficial geology of Horne Lake and Parkville map areas, Vancouver Island, British Columbia. Geological Survey of Canada, Memoir 318, Map 1111A, 142 pp.
- [7] Marshall Macklin Monaghan Limited. 1986. Development management in tsunami hazard areas of Port Alberni.
- [8] Dunbar, D., LeBlond, P.H. and Murty, T.S. 1989. Maximum tsunami amplitudes and associated currents on the coast of British Columbia. Science of Tsunami Hazards. International Journal of the Tsunami Society, 7, no.1, pp.3-44.
- [9] Geological Survey of Canada. 1981. Tectonic assemblage map of the Canadian Cordillera. Map 1505A.
- [10] Sutherland Brown, A. 1968. Geology of the Queen Charlotte Island, British Columbia. British Columbia Department of Mines and Petroleum Resources, Bulletin 54.

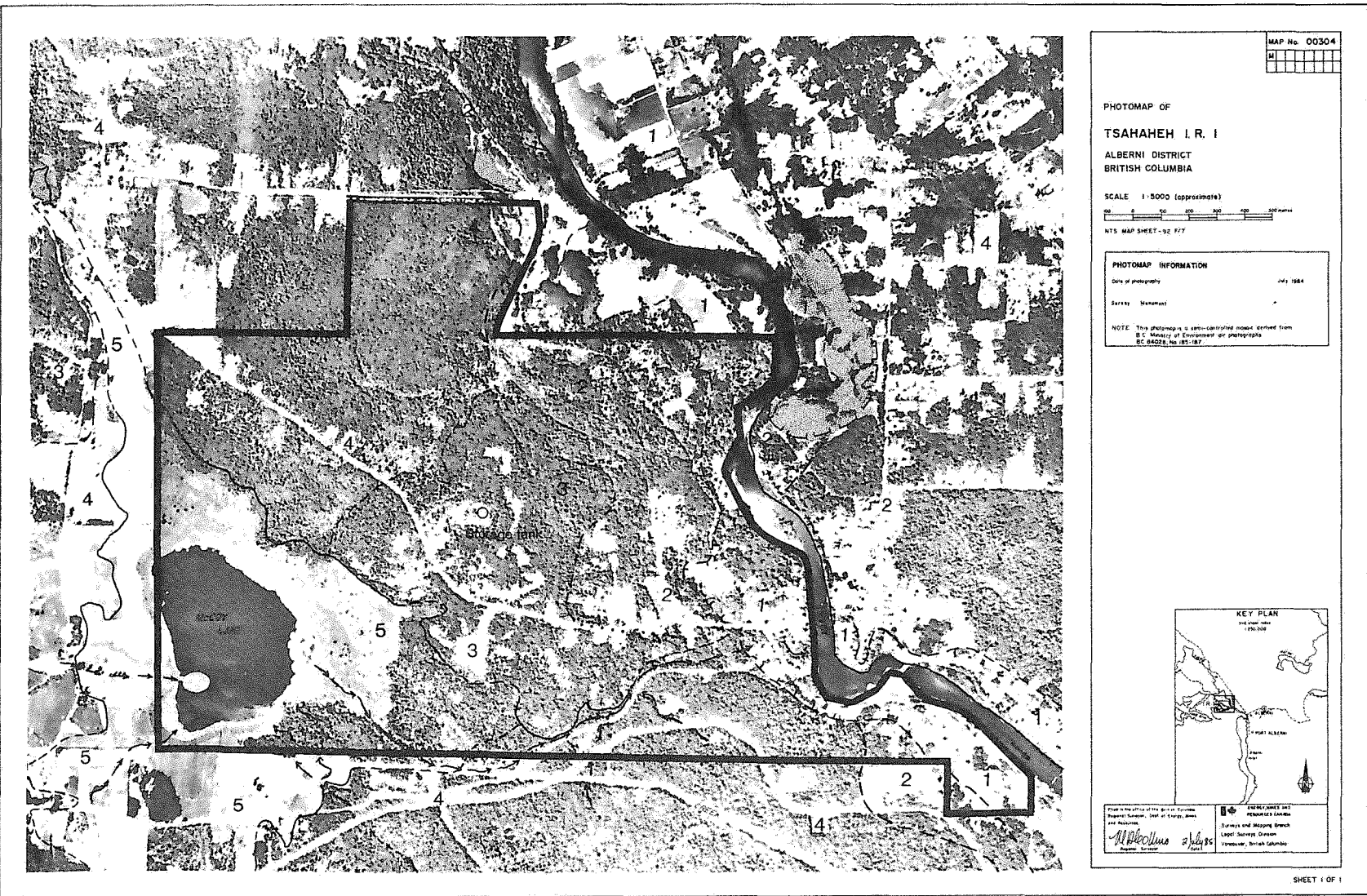


Fig.2a Terrain map superimposed onto photo-mosaic, Tsahaheh I.R. 1

BAND: Sheshaht
 RESERVE: Tsahaheh IR 1
 DISTRICT: Vancouver Island
 POPULATION: 446 (1987), 469 (1990)
 SEISMIC ZONE: 5

LAT/LONG: 49° 16' N, 124° 52' W
 NTS: 92E/7W

TERRAIN UNITS FACTOR WEIGHT	TERRAIN CLASSIFICATION	EARTHQUAKE EFFECTS										TERRAIN UNIT TOTALS	
		SURFACE FAULTING	GROUND SHAKING	LIQUEFACTION	GROUND FAILURE				FLOOD				
					FLOW	SPREAD	SLUMP	SLIDE	TSUNAMI	SEICHE	INDIRECT		
1		1	10	10	5	5	5	5	5	3	2	1	
1	ffp	0	2	1	1	1	1	0	0	3	0	1	55
2	gsft	0	1	0	0	1	1	0	1	9	0	0	23
3	gscW ^{av}	1	1	0	0	0	1	1	0	0	0	0	21
4	R gscW ^{abv}	0	1	1	1	1	1	0	0	1	0	0	37
5	M silt and clay	0	2	2	1	1	1	0	0	1	2	0	57
TERRAIN UNIT TOTALS												193	
NORMALIZED TERRAIN UNIT TOTAL												38.6	
SEISMIC RISK FACTOR												193	

SYMBOL

-  Indian Reserve Boundary
-  Terrain Unit Boundary (defined, approximated, assumed)
-  Man made/natural escarpment
-  Terrace
-  Prominent Surface Drainage
-  Sand/gravel pit

Fig.2b Seismic Risk Assessment Matrix and legend for Tsahaheh I.R.1

BAND: Skidegate
 RESERVE: Skidegate IR 1
 DISTRICT: Northwest
 POPULATION: 291 (1987), 350 (1990)
 SEISMIC ZONE: 6

LAT/LONG: 53°16'N, 131°59'W
 NTS: 103G/5W

TERRAIN UNITS	TERRAIN CLASSIFICATION	EARTHQUAKE EFFECTS									TERRAIN UNIT TOTALS	
		SURFACE FAULTING	GROUND SHAKING	LIQUEFACTION	GROUND FAILURE			FLOOD				
					FLOW	SPREAD	SLUMP	SLIDE	TSUNAMI	SEICHE		INDIRECT
FACTOR WEIGHT		1	10	10	5	5	5	5	3	2	1	
1		0	2	1	1	1	3	0	1	0	0	
sand and silt	ff ^A f	0	0	20	10	5	5	15	0	3	0	58
2		0	1	0	0	0	1	1	1	0	0	
gravel and cobble	sgk//gsW ^A	0	0	10	0	0	0	5	5	3	0	23
3		1	1	0	0	0	2	0	0	0	0	
sand	gsWt	1	1	10	0	0	0	10	0	0	0	21
4		1	1	0	0	0	0	1	1	0	2	
clay till	gfcMmh R	1	1	10	0	0	0	5	5	0	0	23
5		1	1	0	0	0	1	1	0	0	2	
till	Mh R	1	1	10	0	0	0	5	5	0	0	23

TERRAIN UNIT TOTALS 148
 NORMALIZED TERRAIN UNIT TOTAL 29.6
 SEISMIC RISK FACTOR 177.6

SYMBOL

-  Terrain unit boundary (defined, approximate, assumed)
-  Prominent surface drainage
-  Escarpment
-  Terrace
-  Steep Slope
-  Rock Quarry
-  Sand/gravel pit
-  Rip-rap

SYMBOL

-  Possible Old Landslide Area
-  Lineament
-  Excavated Area (approximated)

Fig.3b Seismic Risk Assessment Matrix and legend for Skidegate I.R.1

Session 6A
Risk in Geotechnical
Practice

usually comprises densification or drainage or a combination of the two.

The required extent of such treatment is a major concern. The zone must be sufficiently large to prevent partial decapitation from movement of the surrounding liquefied soils. It must also be such that high pore pressures from the surrounding liquefied soils do not penetrate and soften the densified zone during or after the period of severe shaking. These two aspects are examined in this paper.

Partial Decapitation

Movement in the surrounding liquefied soils could shear and partially decapitate the densified soil column if it is not sufficiently robust to resist the forces arising from such movements. Laboratory and field observations [3] suggest that the free-field displacement pattern is approximately linear within the liquefied zone as shown (Figure 1a). The maximum forces that could be applied to the densified column are the passive forces on the leading face, the drag shear forces on the sides, and the inertia force of the soil column. These must be resisted by friction forces on the base (Figure 1b). The appropriate strength to use in the calculation of these maximum forces would be the peak undrained strength of the crust and the residual strength of the liquefied sand. The residual strength could be estimated from Seed and Harder [4], but the upper rather than the lower bound strength should be considered.

While the peak undrained strength is appropriate for the stiff crust material, it is not clear that the movements would be large enough to mobilize the residual strength of the liquefied sand. The strains required to mobilize the residual strength of liquefied sand can be quite high, 5 to 50%, depending on the density of the material, and such strains are unlikely to occur unless the ground slope is greater than 5 to 10%. Such slopes would generally occur near river banks. The forces applied by the liquefied sand will therefore be less than the

maximum. However, it is likely that there will not be just one continuous layer of liquefaction but a number of layers, in which case the passive force from unliquefied sand layers within the "liquefied" zone should be considered. Numerical analyses as described by Byrne et al. [5,6] consider strain compatibility and could be used if the extent of the required densified zone based on the residual strength appears excessive.

Pore Pressure Migration

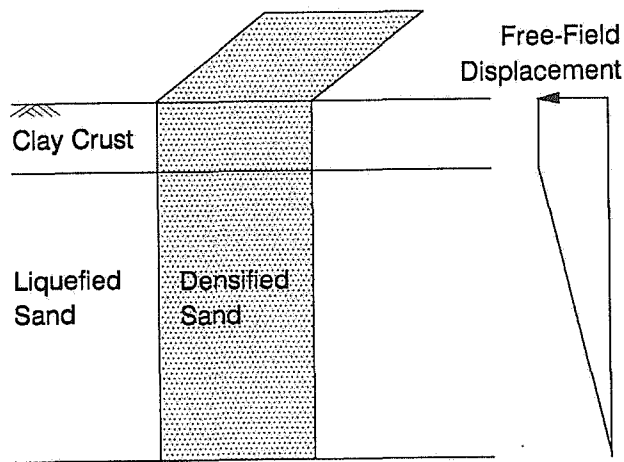
The densified column of soil will only be stable provided high excess pore pressures from the surrounding liquefied sands do not penetrate it during and after the earthquake. This is examined herein.

The high excess pore pressures are essentially generated in the undensified sand as shaking causes a collapse of the loose sand skeleton and a transfer of load to the water. A complete transfer of load to the water causes a complete loss in shear strength or liquefaction of the sand. The concern here is that these high pore pressures may penetrate and soften the densified zone and thus endanger the structure.

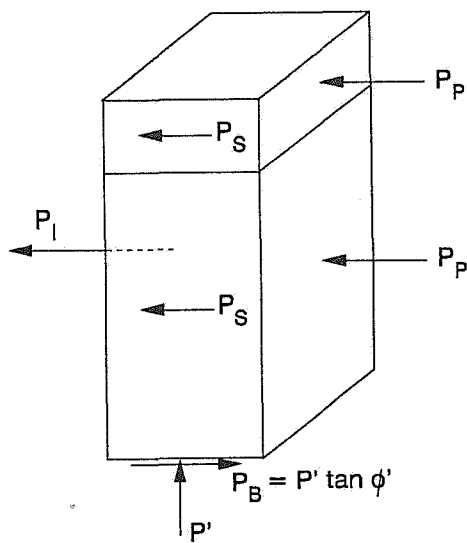
a) Conditions analyzed

A typical soil profile for Richmond was considered in the analyses. The soil profile comprises 3 m of clay crust underlain by 15 m of loose sand and followed by 5 m of dense sand as shown in Fig. 2. The earthquake is assumed to generate 100% pore pressure increase in the loose sand and 30% pore pressure increase in dense sand zones. These pore pressures are the prescribed initial conditions and redistribute and dissipate according to Biot's theory of consolidation.

Five cases were considered in order to study the effect of both the depth of densification and the drainage provisions in the densified zone. In all 5 cases a circular column of



(a)



- P_p - Passive Forces
- P_s - Drag Shear Forces
- P_l - Inertia Forces
- P_b - Base Shear Resistance

(b)

Fig. 1. Free-Field Motion and the Forces on the Densified Soil Plug

radius 10 m is considered as shown in Figure 2.

b) Analysis procedure

The redistribution and dissipation of the excess porewater pressures with time is governed by Biot's consolidation equation and was solved here using the finite element code, CONOIL-II [7]. This code considers the nonlinear nature of the sand skeleton. This is particularly important because the sand skeleton becomes very compressible at low effective stress levels when liquefaction is triggered. This low compressibility in turn means that as the liquefied sand reconsolidates, there is a large volume of water expelled which becomes a source of water that could penetrate the densified column. The material properties used in the analyses are given in Table 1.

TABLE 1: Soil properties used in the analysis

	Clay	Liquefied Sand	Dense Sand	Densified Sand With Drains	Clay With Drain
k_E	150	300	2000	2000	150
n	0.45	1.0	0.5	0.5	0.45
k_B	140	180	1200	1200	140
m	0.2	1.0	0.25	0.25	0.2
R_f	0.7	0.8	0.6	0.6	0.7
k_V (m/s)	2.5×10^{-8}	5×10^{-5}	2.5×10^{-5}	1×10^{-3}	1×10^{-3}
k_H (m/s)	5×10^{-8}	1×10^{-4}	5×10^{-5}	1×10^{-3}	1×10^{-3}

Case 1 - Densification was assumed to the full depth in the loose sand (15 m). No drainage system was assumed. This case may represent a field condition where densification is achieved using timber piles without any drainage provisions.

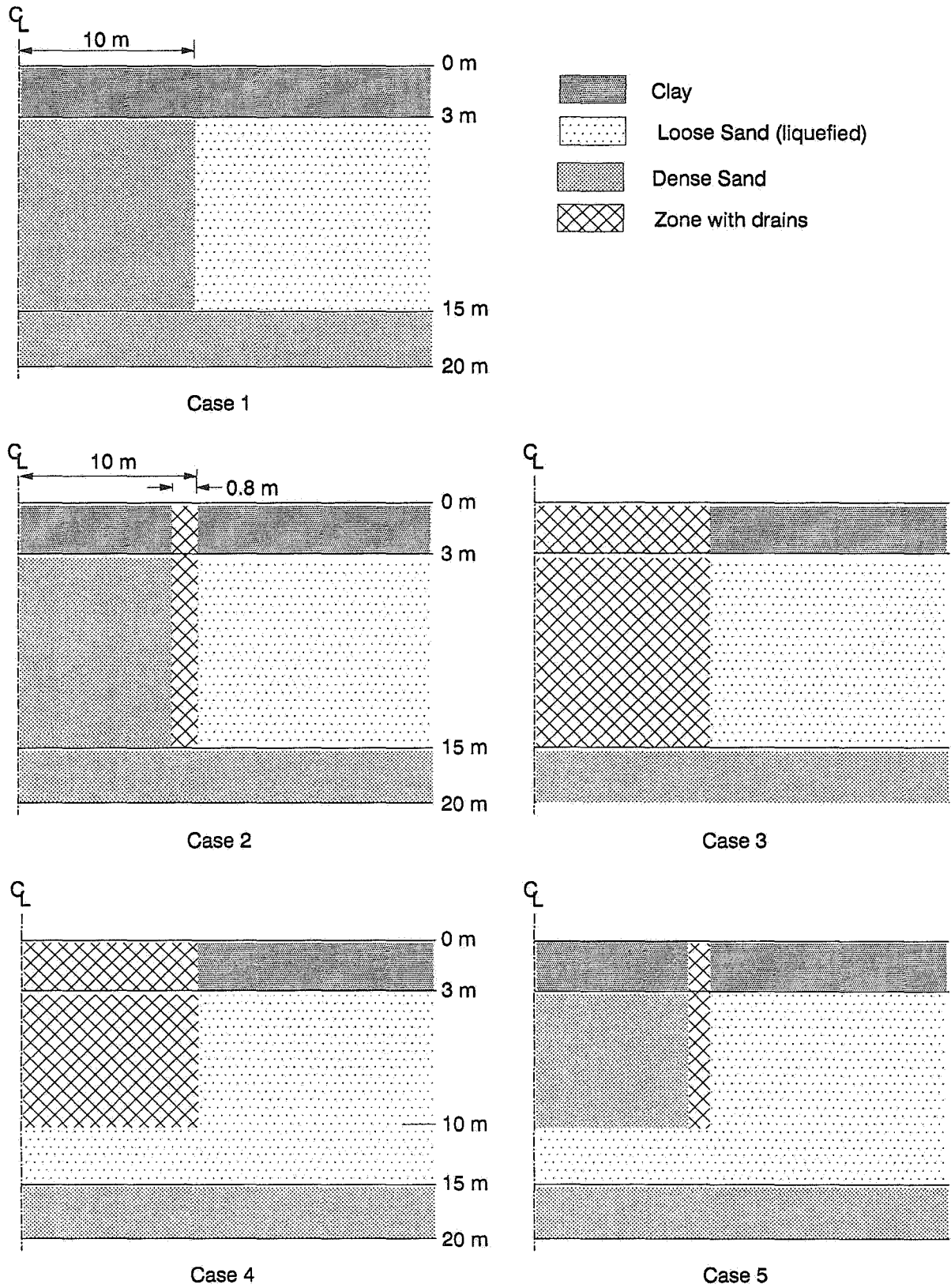


Fig. 2. Details of the Cases Analyzed

Case 2 - In this case, densification was assumed to the full depth in the loose sand together with a perimeter drainage system. This may represent a field situation where densification is achieved using timber piles with a perimeter drainage system of vibro-replacement columns.

Case 3 - In this case, densification of the loose sand was assumed to its full depth. Drainage was assumed in the densified zone. This may represent densification by vibro-replacement. In the analysis the drains were not considered on an individual basis, instead, the densified zone with drains was modelled as a soil with an equivalent permeability. The equivalent permeability can be estimated from the size and spacing of the drain and the permeabilities of the materials. The effective permeability of the clay crust was also increased due to the presence of drains.

Case 4 - This is similar to case 3, except the densification was assumed to a depth of 10 rather than 15 m in the loose sand.

Case 5 - Similar conditions as Case 2, except the densification was to a depth of 10 m in the loose sand.

Results

The excess porewater pressures at various times after the earthquake are shown in Figures 3 to 7 for all 5 cases. The excess pore pressures are shown in terms of pore pressure ratio, u/σ_{vo}' in which u is the current excess pore pressure, and σ_{vo}' is the initial vertical effective stress. $u/\sigma_{vo}' = 0$ represents zero pore pressure rise and $u/\sigma_{vo}' = 1$ represents 100% pore pressure rise or liquefaction. It is assumed that liquefaction or 100% pore pressure rise is triggered at time $t = 0$ in the loose sand. In the dense sand a pore pressure ratio of 30% is triggered at $t = 0$. The variation of the excess pore pressure ratios with time and distance from the centre of the densified zone are shown in graphs (a) and (b) in the figures. Graph (a) shows the variation at a depth of 5m and graph (b) at a depth of

10m. Graph (c) shows the excess pore pressures ratio with depth along the centreline.

Case 1 - The results for case 1 are shown in Figure 3. In this case the loose sand is densified to the full depth with no drainage provisions. It can be seen that the excess pore pressure in the surrounding untreated area migrates into the densified zone. The pore pressure ratio in the upper part of densified zone rises to 1 which means liquefaction will be triggered. However, below a depth of 6 m, liquefaction is not triggered and piles penetrating below this depth could support vertical load, although significant horizontal displacements would likely occur.

Case 2 - The results for case 2 are shown in Figure 4. This case is the same as case 1, except a perimeter drainage system is now provided. It can be seen from Figures 4 (a), (b) and (c) that a perimeter drainage system is quite effective in preventing the migration of high pore pressure from the loose zone into the densified zone. A maximum pore pressure ratio = 0.5 is predicted 1 min after the earthquake.

Case 3 - The results for case 3 are shown in Figure 5. Case 3 comprises densification and drainage to the full 15 m depth of the loose sand. It can be seen from Figure 5(a), (b) and (c) that the drains in the densified zone are very effective in preventing the high pore pressures from the surrounding liquefied zone migrating to the densified zone. The pore pressure ratio in the densified zone increases from an initial value of 0.3 at time $t = 0$, to 0.4 after 10 seconds and then reduces.

Case 4 - The predicted results for case 4 are shown in Figure 6. Only the depth of densification is different in this case from case 3. Liquefaction now occurs beneath the densified zone in the depth range 10-15 m. However, it can be seen from Figure 6 that the drainage system is very effective in dissipating all the excess pore pressures generated by the earthquake. A maximum

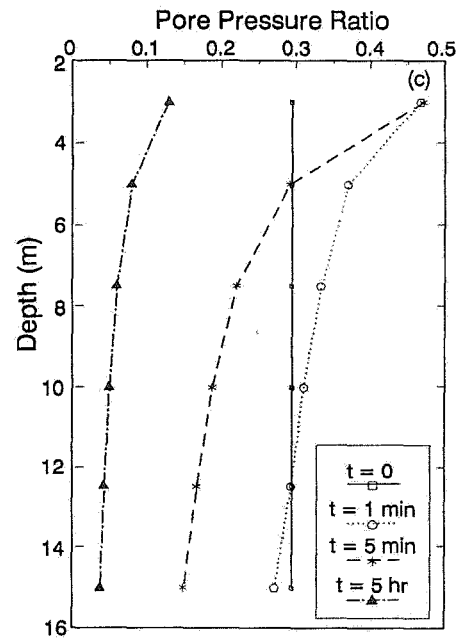
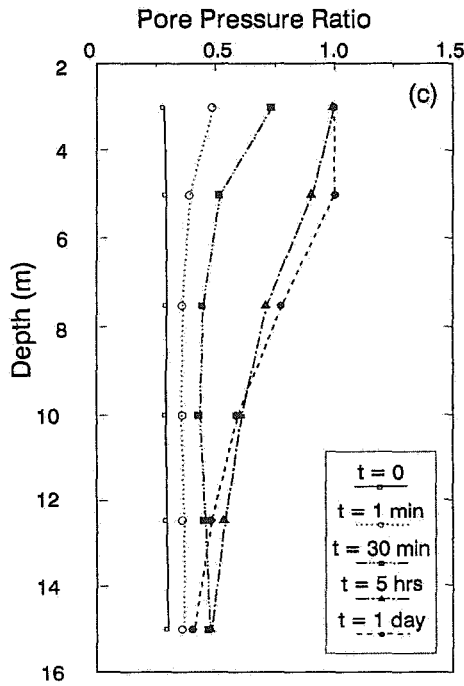
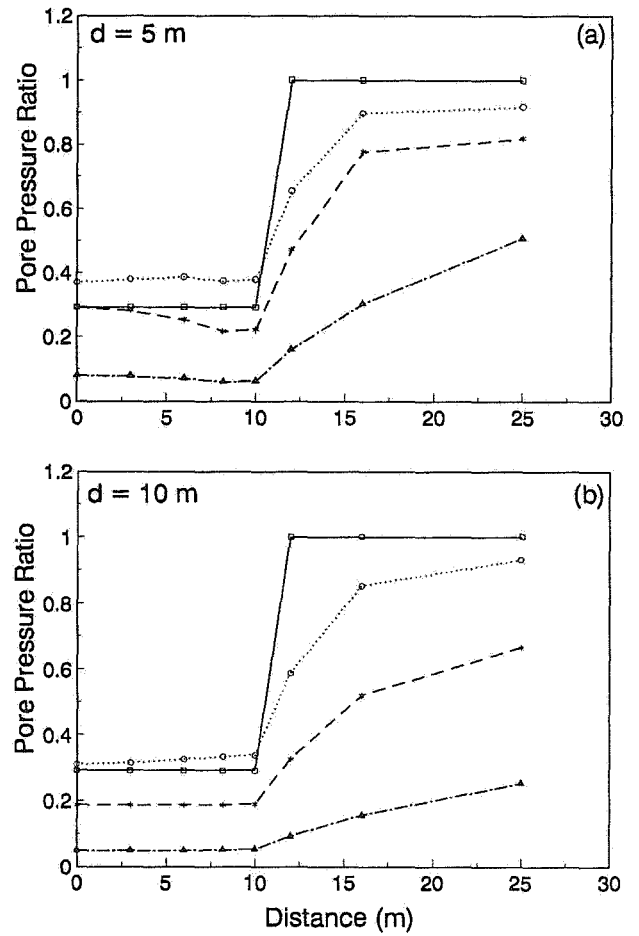
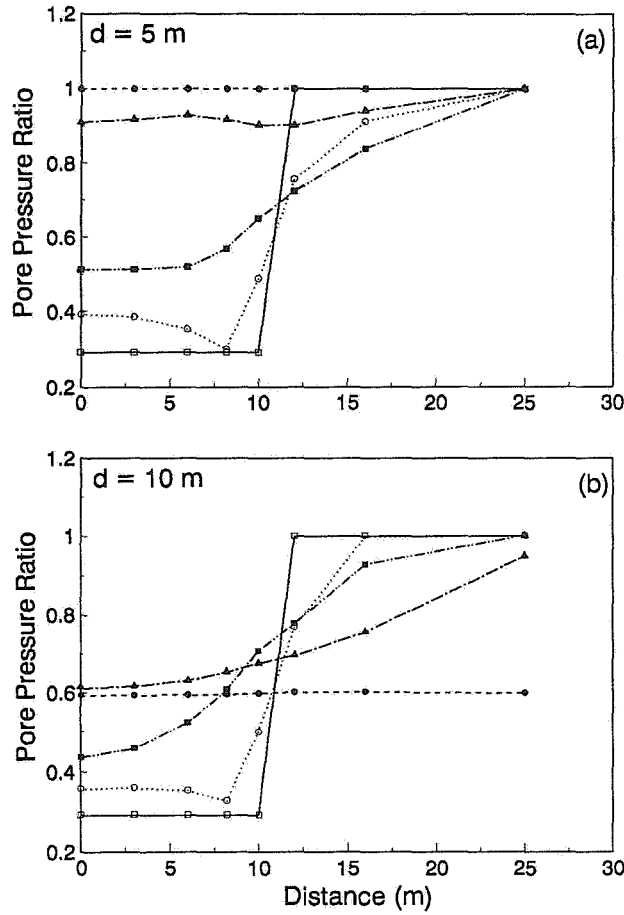


Fig. 3. Variation of Pore Pressure Ratio for Case 1

Fig. 4. Variation of Pore Pressure Ratio for Case 2

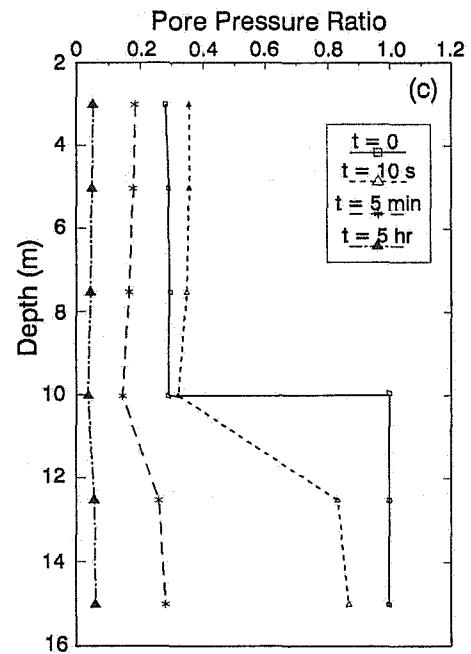
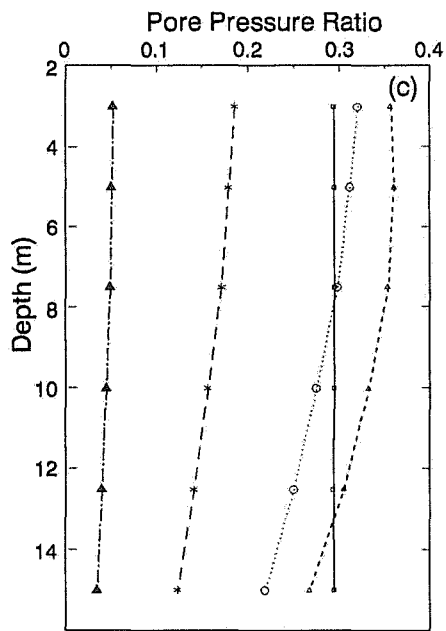
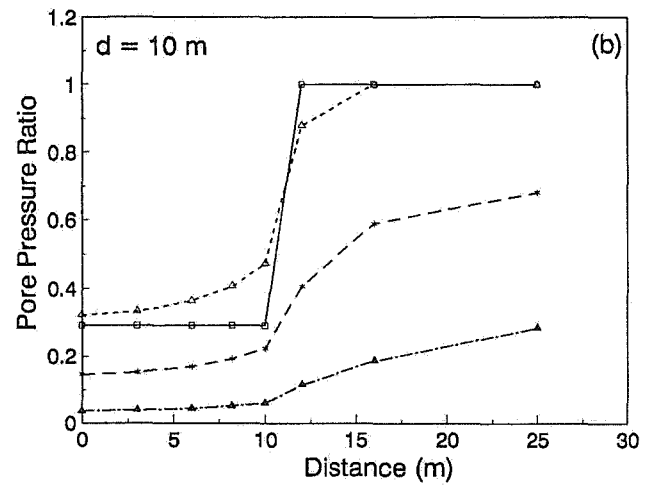
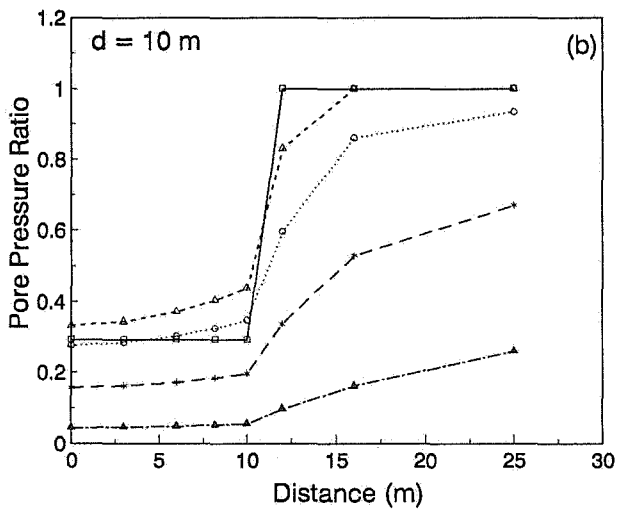
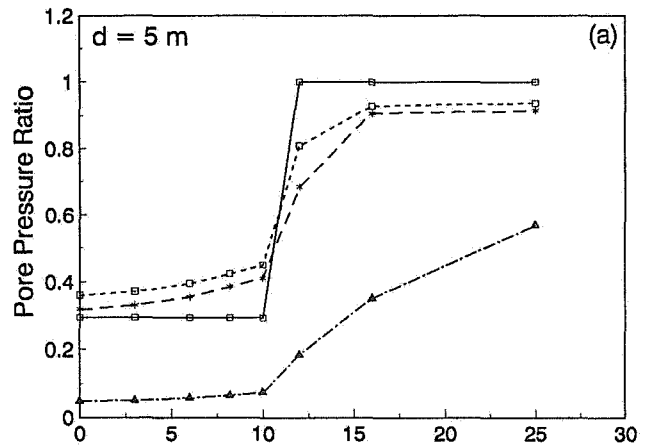
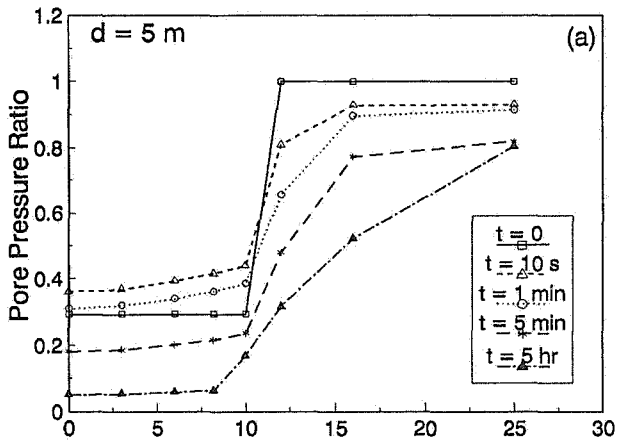


Fig. 5. Variation of Pore Pressure Ratio for Case 3

Fig. 6. Variation of Pore Pressure Ratio for Case 4

pore pressure ratio of 0.4 is predicted after 10 seconds, similar to case 3.

Case 5 - The results for Case 5 are shown in Figure 7. In this case a perimeter drainage system and densification to a depth of 10 m were provided. Because of the limited depth of densification, there are higher excess pore pressures in the deeper loose zones and larger amounts of water must escape. It can be seen that a perimeter drainage system is not adequate, and high excess pore pressures now occurs in the densified zone. A maximum pore pressure ratio of 0.7 is predicted 5 minutes after the earthquake.

Summary

The Fraser Delta is underlain by deep deposits of soil, the top 20 m of which may be susceptible to liquefaction in the event of a major earthquake. To prevent damage to major structures it is generally necessary to treat the foundation soil. Such treatment generally comprises densification and/or drainage. The major factors to consider are: (a) the treated zone must be large enough to prevent partial decapitation from movement of the surrounding liquefied soils; and (b) the high excess pore pressures in the liquefied soil must not penetrate and soften the treated zone.

The analyses show that densification alone such as could be achieved by driving timber piles will not prevent the high excess pore pressures from the surrounding liquefied soil penetrating the densified zone. Such penetration will cause 100% pore pressure rise or zero effective stress to a depth of 6 m for the conditions analyzed. Below this depth the effective stress increases and timber piles would be capable of carrying vertical load although they could be damaged by horizontal movements. Drains through the crust could significantly reduce these excess pore pressures. Perimeter drains could greatly reduce the excess pore pressures in the densified zone. The analyses show that provision of drainage within the densified zone can be very

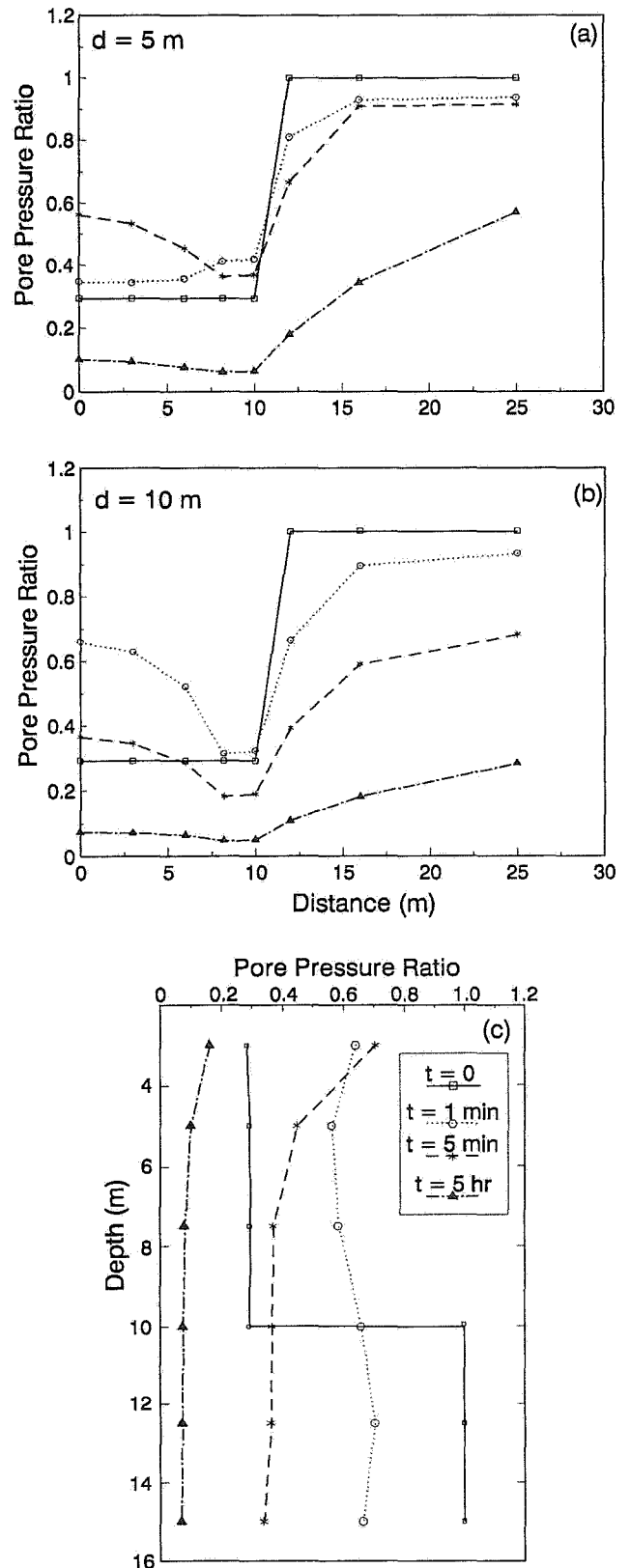


Fig. 7. Variation of Pore Pressure Ratio for Case 5

effective in preventing high excess pore pressures in the densified zone.

Acknowledgement

The authors acknowledge the financial support from NSERC and AOSTRA, and are grateful to Kelly Lamb for her typing and presentation of the paper.

References

- [1] Idriss, I., "Response of Soft Soil Sites During Earthquakes", H. Bolton Seed Memorial Symposium Proceedings, Vol. 2, pp. 273-289.
- [2] Task Force Report, "Earthquake Design in the Fraser Delta", Co-Chairmen P.M. Byrne, D.L. Anderson, Soil Mechanics Series No. 150, Dept. of Civil Engineering, University of British Columbia, Vancouver, B.C., June 1991.
- [3] Byrne, P.M., "A Model for Predicting Liquefaction Induced Displacements Due to Seismic Loading", 2nd Int. Conf. on Recent Advances in Geotechnical Earthquake Eng. and Soil Dynamics, St. Louis, Missouri, Paper 7.14, March 1991.
- [4] Seed, H.B. and Harder, L.F., "SPT-Based Analysis of Cyclic Pore Pressure Generation and Undrained Residual Strength", H.B. Seed Memorial Symposium, Proceedings, Vol. 2, 1990.
- [5] Byrne, P.M., Jitno, H., Garner, S., Lee, M. and Lou, J.K., "Analysis of Earthquake Induced Displacements of the Intake Structures, John Hart Dam", Proc. Canadian Dam Safety Conference, Whistler, B.C., 1991, pp. 97-116.
- [6] Byrne, P.M., Jitno, H. and Haile, J., "A Procedure for Predicting the Seismic Response of Mine Tailings Impoundments", Geotechnique and Natural Hazards, Canadian Geotechnical Society, May 1992.
- [7] Byrne, P.M. and Srihar, T., "CONOIL-II: A Computer Program for Consolidation Analysis of Stress Deformation and Flow of Oil Sand Masses Under Applied Load and Temperature Gradients", Dept. of Civil Engineering, University of British Columbia, Vancouver, B.C., Canada, 1989.

Behavior of Embankment Dams in Earthquakes

Robert C. Lo

Klohn Leonoff Ltd.

Richmond, British Columbia

Earle J. Klohn

Klohn-Crippen Ltd.

Vancouver, British Columbia

Abstract

The paper presents an overview of seismic behavior of embankment dams. This behavior includes: settlement, horizontal movement, cracking, pore pressure build-up, slope slumping and failure, internal erosion, seepage increases, and reservoir or impoundment breaching in the extreme cases. Relevant features of selected case histories are briefly discussed to illustrate the wide variations in observed seismic dam behavior. Empirical relations concerning seismic deformations of dam crests are reviewed and updated. Also discussed are the dam safety aspects of seismic behavior.

Introduction

Embankment and tailings dams are important hydraulic structures, and their satisfactory performance in the event of major earthquakes is critically important for the safety of downstream life and property. Case histories on the seismic performance of these structures represent a valuable database that engineers may utilize to calibrate and improve their designs [1].

This paper presents an overview of seismic behavior of embankment dams (including tailings dams). When a dam is subject to a significant earthquake, its response may include one or more of the following reactions: settlement, horizontal movement, cracking, pore pressure build-up, slope slumping and failure, internal erosion, and seepage increases. Concurrently, seiches (earthquake-generated waves) could develop in a water reservoir, or liquefaction of stored tailings could occur in the case of a tailings impoundment. Depending on the circumstances, the extreme case involves the overtopping of the dam and ensuing breach of the reservoir (or

impoundment). The paper briefly describes each of the above seismic responses and presents references to selected case histories that update and illustrate these items. Dam safety aspects under earthquake conditions are also briefly discussed.

Earthquake Impacts

Earthquake impacts on a specific dam generally increase with the earthquake magnitude and diminish with the increasing distance of the dam from the earthquake source. Other earthquake-related factors include frequency content of the earthquake and local site amplification effect. Because embankment dams are earth and rockfill structures of considerable mass, earthquake Richter magnitudes in excess of a threshold value of 5 are generally required for the earthquake to have sufficient energy and to last long enough to cause any significant dam damage.

Seismic Dam Behavior

Dam-related factors that affect its seismic performance include: the dam slopes, the position of the phreatic surface within the dam, foundation pore pressures, the static and dynamic properties of the damfill and foundation materials, the design of embankment zones, the construction quality and the maintenance care. Typical seismic dam behavior is described following with reference to selected case histories.

Crest Movement

Seismic crest movement reflects dam deformation associated with compression, lateral spreading and slope movements induced by earthquakes. Bureau et al. [2] reviewed seismic performance of earth and rockfill dams including the crest movement (settlement and horizontal movement). They introduced an Earthquake Severity Index (ESI), which reflects the influence of both the intensity and duration of the causative earthquake and is defined as:

$$ESI = A (M-4.5)^3$$

where A = peak ground acceleration at the damsite;

M = earthquake magnitude.

Bureau et al. [2] further showed an empirical relationship between the index, ESI, and the crest settlement expressed as a relative settlement ratio (crest settlement divided by dam height). This correlation plot, with data from Ref. [2] shown as solid circles, is reproduced in Fig. 1, which also contains additional data (shown as open circles) summarized in Table 1 from recent references [3 to 8]. The solid line represents the interpolated trend line through all the data points. Table 1 summarizes maximum dam crest movements reported for 1989 Loma Prieta, 1987 Edgecumbe and 1985 Michoacan earthquakes. As shown in Fig. 1, the seismic relative crest settlement is generally in the range of 0.1% to 10% (or 0.01% to 1%).

Figure 2 presents a similar plot correlating the horizontal relative crest movement (horizontal movement divided by dam height) with the

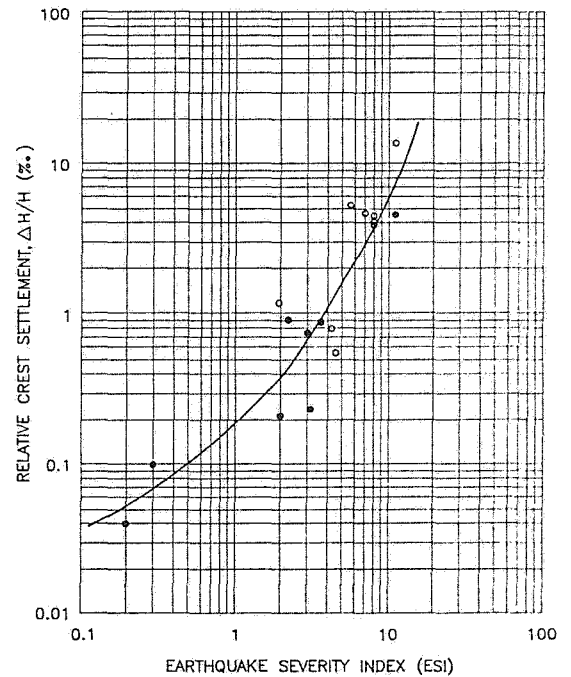


Fig. 1 Empirical Relationship Between Crest Settlement and Earthquake Severity Index (after Ref. 2)

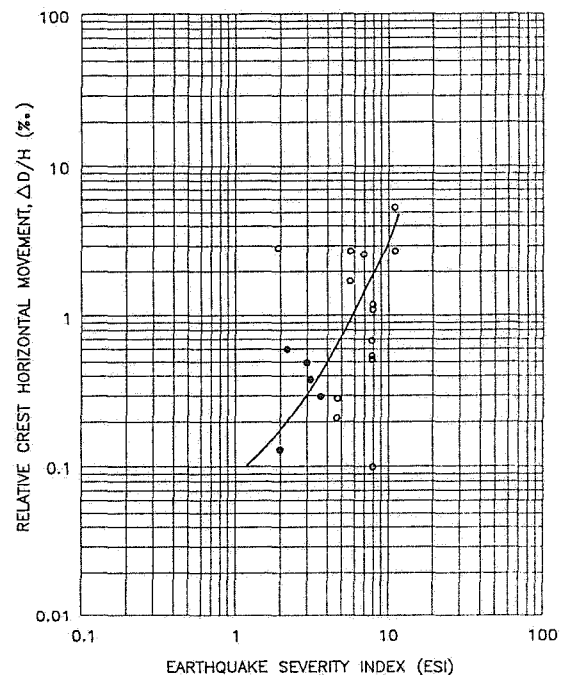


Fig. 2 Empirical Relationship between Crest Horizontal Movement and Earthquake Severity Index (after Ref. 2)

Table 1 - Seismic Dam Crest Movements and Causative Earthquake Data

Name of Dam	Location	Height of Dam H (m)	Maximum Crest Movement		Relative Crest Movement		Earthquake Date (Name)	Magnitude	Approx. Distance to Earthquake Source (km)	Peak Horiz. Ground Acceleration A (g)	Earthquake Severity Index ESI	Reference
			Settlement ΔH (mm)	Horizontal ΔD (mm)	Settlement $\Delta H/H$ (‰)	Horizontal $\Delta D/H$ (‰)						
Leroy Anderson	Calif.	71.6	40	15 (U/S) 21 (D/S)	0.56	0.21 (U.S.) 0.29 (D/S)	Oct. 17, 1989 (Loma Prieta)	7.1	21	0.26 (Observed)	4.6	3,4,5
Austrain	Calif.	56.4	762	152 (U/S) 305 (D/S)	14	2.7 (U/S) 5.4 (D/S)	Ditto	Ditto	< 2	0.6 (Estimated)	11	Ditto
Elmer J. Chesbro	Calif.	29.0	113	15 (U/S) 3 (D/S)	3.9	0.52 (U/S) 0.10 (D/S)	Ditto	Ditto	13	0.45 (Estimated)	7.9	Ditto
Guadalupe	Calif.	43.3	195	46 (U/S) 24 (D/S)	4.5	1.1 (U/S) 0.55 (D/S)	Ditto	Ditto	10	0.45 (Estimated)	7.9	Ditto
Lexington	Calif.	62.5	259	43 (U/S) 76 (D/S)	4.1	0.69 (U/S) 1.2 (D/S)	Ditto	Ditto	3	0.45 (Estimated)	7.9	Ditto
Vasona	Calif.	10.4	49	27 (D/S)	4.7	2.6 (D/S)	Ditto	Ditto	9	0.4 (Estimated)	7.0	Ditto
Matahina	New Zealand	86	100	253 (D/S)	1.2	2.9 (D/S)	Mar. 2, 1987 (Edgecumbe)	6.3	11	0.33 (Observed)	1.9	6
La Villita (Morelos)	Mexico	60	320	160 (U/S) 100 (D/S)	5.3	2.7 (U/S) 1.7 (D/S)	Sept. 19, 1985 Sept. 21, 1985 (Michoacan)	8.1 7.5	58 61	0.12 0.04 (Observed)	5.6 -	7
El Infiernillo	Mexico	148	120	-	0.81	-	Ditto	Ditto	113 116	0.09 (Estimated)	4.2 -	8

Earthquake Severity Index, ESI. The figure contains data from Ref. [2] and recent references [3 to 8]. Both upstream and downstream horizontal movement data are presented but not differentiated in Fig. 2.

A review of data presented in Figs. 1 and 2 and Table 1 suggests the following. First, the horizontal movement value is generally only a fraction of the settlement value with the following two exceptions. At Miboro Dam in Japan and Matahina Dam in New Zealand the horizontal movement value exceeds the settlement value. Secondly, although the downstream horizontal movement value is generally greater than the upstream horizontal movement value (see Table 1), cases with the reserve trend are not infrequent. Thirdly, the data for the horizontal movements in Fig. 2 seems to be more scattered than those for the settlement in Fig. 1.

Cracking

Cracks are induced by tensile or shear stresses resulting from differential settlements, relative horizontal and sliding movements. According to the orientation of the crack alignment, they are designated as longitudinal (parallel to the dam axis), transverse (perpendicular to the dam axis) or inclined (at an angle to the dam axis). Transverse cracks are more critical, because they form easy seepage paths promoting the progress of internal erosion, thus increasing the chance of uncontrolled release of reservoir water. Generally, earthquake-induced dam movements are accompanied by surficial cracks occurring at the dam crest and slopes down to limited depths with all three orientations. They occur usually at damfill or foundation zone boundaries and locations of sharp changes in geometry or material properties. Interior cracks, occurring at depth due to internal stress and strain readjustments, are much more difficult to detect. Locating the cracks and carrying out thorough repairs of embankment zones involved are essential to prevent the deterioration of an earthquake-damaged dam. Prompt actions including temporary covering of the cracks by plastic sheets to minimize water ingress are important [4,5].

For dams located in the vicinity of active faults, dam deformations (settlements and horizontal movements) and cracks directly related to fault movements require special attention.

Pore Pressure Build-Up

Data on recorded pore pressure increases induced by earthquake loadings have been gathered in recent years. These data include pore pressure increases measured in standpipe piezometers installed within the Austrian Dam [3] as well as time histories of pore pressures recorded by dynamic piezometers installed in a reclaimed sand deposits on Ohgishima Island near Tokyo [9] and in two Chilean tailings dams [10,11]. In the Loma Prieta earthquake, pore pressure increase in the clayey, sandy gravel damfill of the Austrian Dam reached 49 ft to 54 ft. When expressed as the ratio between the pore pressure rise and the overburden pressure, this increase corresponds to a ratio ranging from 0.2 to 0.3. In general, seismic pore pressure build-up is most prominent in loose sands and silts. However, cases of high pore pressure build-up in gravelly, cobbly soils were inferred during the recent Loma Prieta (1989), Borah Peak (1983), Tangshan (1976), Haicheng (1975) and Alaska (1964) earthquakes [3, 12, 13]. The coarse materials involved are relatively loose and contain significant percentages of sandy fractions.

Slope Slumping and Failure

Slope slumping and failure are generally caused by (1) loss of available shear strength due to straining or remodeling and pore pressure development, and (2) increase of driving force associated with inertial loadings. Progressive failure mechanism, pore pressure redistribution, and crack formation and its subsequent infilling with water from infiltration and seepage also contribute to slope instability. Slope failures generally occur due to the sudden and/or gradual shift of the delicate balance between the resisting and driving forces during and after the passage of earthquakes. Slope slumping and failure are usually associated with

lateral spreading, slope bulging, or slides involving shallow and/or deep failure surfaces with attendant crack development. Flow slides involving large movements are generally caused by partial or total liquefaction and/or remolding of damfill and/or foundation materials. Residual undrained shear strength of materials involved in liquefaction failures were obtained from back-analyses of case histories [14, 15, 16]. The effect of overburden pressure on the residual strength was further discussed in Refs. [17 and 18].

Internal Erosion and Seepage Increase

Earthquake induced surficial and deep cracks as well as elevated pore pressures could encourage the development of internal erosion (piping) by the continuous action of the seepage forces. Cases of earthquake-induced dam seepage increase include those reported in Refs. [3, 6, 19 and 20]. This phenomenon is particularly critical in cases involving erodible soils. Protections against piping development are: adherence to proper filter design criteria at material boundaries, incorporation of self-healing and crack-stopping materials, and construction procedures that prevent material segregation especially at contacts between material zones. Careful investigation of the cause of seepage increase, and the implementation of remedial measures including the repair of filter zones, sealing of cracks and addition of downstream inverted filters are required to control the seepage and to prevent further internal erosion.

Seiches and Tailings Liquefaction

The development of seiches, earthquake-generated waves, in a water reservoir depends on the geometry of the reservoir and propagation direction of seismic waves. Seiches tend to encroach the available freeboard as well as cause additional wave erosion of the upstream dam slope. Waves generated by slope failures along the reservoir rims including the upstream dam slope could have serious effect, if large waves are generated by the plunging of the landslide mass into the reservoir [21].

For a tailings pond, liquefaction of tailings deposits upstream of the dam could develop [Refs. 22 to 26]. The lateral extent as well as depth of the liquefied zones are functions of earthquake loadings and the distribution and properties of tailings materials as the result of their deposition and consolidation histories. Partial or full pond liquefaction would impose additional thrust force against the dam because of the transfer of intergranular pressure to pore pressure within the tailings deposits. Earthquake-generated waves in the liquefied tailings materials would have similar effect to seiches in the water reservoir.

Dam Break

Dam break is the most feared dam behavior [1, 24, 25, 26]. Potential loss of life and economic as well as environmental damage downstream emphasize the enormous consequences of such a catastrophic event.

Dam Safety

Fortunately, dam failures caused by earthquakes do not occur frequently. Many factors contribute to this favourable situation. Foremost among these are the advancement of dam engineering in design, construction, and maintenance developed by the continuous efforts of individual dam engineers and collective dam-building bodies such as the International Commission of Large Dams, dam owners and government agencies. These advancements result in better new dams possessing higher margins of safety. Furthermore, recent vigorous activities of dam-safety related inspections, investigations, reviews and rehabilitations also tend to reduce the vulnerability of existing dams. Fortuitous circumstances also play a role in reducing the chance of failure as well as the damage due to the failure. Timing of earthquake occurrences such as in daytime rather than nighttime and during periods of low reservoir levels are such examples. However, effective dam maintenance and upgrading programs and well-planned and coordinated emergency response plans are essential to enhance seismic dam

safety and mitigate potential downstream damage.

Summary

This paper presents an overview of seismic behavior of embankment dams (including tailings dams). Typical dam behavior is briefly described with references to selected cases for illustration purpose. The existing empirical database on crest settlement and horizontal movement is expanded by the addition of recent case histories. Means of enhancing seismic dam safety as well as mitigating potential downstream damage are also briefly discussed.

Acknowledgements

The authors appreciate the discussions with and assistance of Mr. Robert E. Tepel of Santa Clara Valley Water District in making available their consultant's reports.

References

- [1] Seed, H.B. 1979. Rankine Lecture: Considerations in the Earthquake-Resistant Design of Earth and Rockfill Dams. *Geotechnique* 29, No. 3, pp. 215-263.
- [2] Bureau, G., Volpe, R.L., Roth, W.H., and Udaka, T. 1985. Seismic Analysis of Concrete Face Rockfill Dams. *Proc. of Symposium on Concrete Face Rockfill Dams - Design, Construction, and Performance*, ASCE, Oct., pp. 479-508.
- [3] Harder, L.F. Jr. 1991. Performance of Earth Dams During the Loma Prieta Earthquake. *Proc. of 2nd Int'l. Conf. on Recent Advances in Geotechnical Earthquake Engineering and Soil Dynamics*, St. Louis, Mar., Vol. 2, pp. 1613-1629.
- [4] Volpe, R.L. & Associates 1990. Investigation of SCVWD Dams Affected by the Loma Prieta Earthquake of October 17, 1989. Report prepared for the Santa Clara Valley Water District.
- [5] Volpe, R.L. & Associates 1990. Repair of SCVWD Dams Affected by the Loma Prieta Earthquake of October 17, 1989. Report prepared for the Santa Clara Valley Water District.
- [6] Gillon, M.D. 1988. The Observed Seismic Behavior of the Matahina Dam. *Proc. of 2nd Int'l. Conf. on Case Histories in Geotechnical Engineering*, June, pp. 841-848.
- [7] Gonzalez-Valencia, F. 1987. Earthquake Response of La Villita Dam. *Proc. of Int'l. Conf. on The Mexico Earthquakes - 1985 Factors Involved and Lessons Learned*, pp.134-147.
- [8] Mitchell, D., Adams, J., DeVall, R.H., Lo, R.C., and Weichert D. 1986. Lessons From the 1985 Mexican Earthquake. *Can. Jour. of Civil Engineering*, Vol. 13, No. 5, pp. 535-557.
- [9] Ishihara, K. 1981. Measurements of Insitu Pore Water Pressures During Earthquakes. *Proc. of Int'l. Conf. on Recent Advances in Geotechnical Earthquake Engineering and Soil Dynamics*, Vol. 1, pp. 523-538.
- [10] Troncoso, J.H., Yasuda, S., Rodriguez, F. 1990. In-situ Measurements of Pore Water Pressures During Earthquakes. Report DIE 90-10, Departamento de Ingenieria Estructural, Escuela de Ingenieria, Pontificia Universidad Catolica de Chile.
- [11] Troncoso, J.H. 1983. Seismic Pore Water Pressures in Tailings Dams. *Proc. of 7th Panamerican Conf. on Soil Mechanics and Foundation Engineering*, June, Vol.2, pp. 641-656.
- [12] Valera, J.E. and Kaneshiro, J.Y. 1991. Liquefaction Analysis for Rubber Dam and Review of Case Histories of Liquefaction of Gravels. *Proc. of 2nd Int'l. Conf. on Recent Advances in Geotechnical Earthquake Engineering and Soil Dynamics*, Mar., Vol. 1, pp. 347-356.

- [13] Wang, W. 1984. Earthquake Damages to Earth Dams and Levees in Relation to Soil Liquefaction. Proc. of Int'l. Conf. on Case Histories in Geotechnical Engineering, Vol. 1, pp. 511-522.
- [14] Seed, R.B. and Harder, L.F. Jr., 1990. SPT-Based Analysis of Cyclic Pore Pressure Generation and Undrained Residual Strength. Proc. of H. Bolton Seed Memorial Symposium, May, Vol. 2, pp. 351-376.
- [15] Davis, A.P., Poulos, S.J., and Castro, G. 1988. Strengths Backfigured from Liquefaction Case Histories. Proc. of 2nd Int'l. Conf. on Case Histories in Geotechnical Engineering, June, pp. 1693-1701.
- [16] Seed, H.B. 1987. Design Problems in Soil Liquefaction. J. Geotech. Engrg., ASCE, 113 (8), pp. 827-845.
- [17] Lo, R.C., Klohn, E.J., and Finn, W.D.L. 1991. Shear Strength of Cohesionless Materials Under Seismic Loadings. Proc. of 9th Panamerican Conf. on Soil Mechanics and Foundation Engineering, Aug., Vol. 3, pp. 1047-1062.
- [18] Lo, R.C., and Klohn, E.J., 1990. Seismic Stability of Tailings Dams. Proc. of Int'l. Symposium of Safety and Rehabilitation of Tailings Dams, Sydney, Australia, May, pp. 90-105.
- [19] USCOLD 1988. Lessons from Dam Incidents. USA-II ASCE, pp. 64-65.
- [20] Wang, W. 1987. Lessons from Earthquake Damages of Earth Dams in China. Proc. of Int'l. Symposium on Earthquakes and Dams, Beijing, China, May, Vol. 1, pp. 243-257.
- [21] Sherard, J.L. 1967. Earthquake Considerations in Earth Dam Design. Proc. of ASCE, Vol. 93, No. SM4, July, pp. 377-402.
- [22] Rogers, J.G., Wills, C.J., and Mason, M.W. 1991. Two Sequences of Fine Grained Soil Liquefaction at Soda Lake, Pajaro River Valley, Santa Cruz County, California. Proc. of 2nd Int'l. Conf. on Recent Advances in Geotechnical Earthquake Engineering and Soil Dynamics, St. Louis, Mar., Vol. 3, pp. 151-165.
- [23] Wills, C.J., Mason, M.W. 1990. Liquefaction at Soda Lake: Effects of the Chittenden Earthquake Swarm of April 18, 1990, Santa Cruz County, California. California Geology, Vol. 43, No. 10, pp. 225-232.
- [24] Castro, G. and Troncosco, J.H. 1989. Effects of 1985 Chilean Earthquake of Three Tailings Dams. Proc. of 5th Chilean Congress of Seismicity and Earthquake Engineering, Santiago, Aug., 22 pp.
- [25] Okusa, S. and Anma, S. 1980. Slope Failures and Tailings Dam Damage in the 1978 Izu-Ohshima-Kinkai Earthquake. Engineering Geology, Vol. 16, pp. 195-224.
- [26] Dobry, R. and Alvarez, L. 1967. Seismic Failures of Chilean Tailings Dams. Proc. of ASCE, Vol. 93, No. SM6, Nov., pp. 237-260.

A Procedure for Predicting the Seismic Response of Tailings Impoundments

P.M. Byrne, Hendra Jitno

*Department of Civil Engineering, University of British Columbia
Vancouver, British Columbia*

Jeremy Haile

*Knight & Piesold
Vancouver, British Columbia*

SYNOPSIS

An analysis procedure is presented for predicting the earthquake induced displacements of a tailings impoundment. The procedure extends the simple Newmark method from a single-degree-of-freedom rigid plastic to a multi-degree-of-freedom flexible system using energy concepts. The method is applied to the proposed Kensington tailings impoundment in Alaska and the results compared with conventional Newmark analyses.

Introduction

The Kensington Project is a proposed underground gold mine located 40 miles north of Juneau, Alaska, on the east side of the Lynn Canal. The mine will require construction of a 89 m high dam to contain the tailings from the mining operations. The dam is to be constructed in stages using compacted earthfill and rockfill and a modified centreline arrangement, which differs from conventional centreline construction in that the upstream contact between the compacted fill and the tailings is inclined slightly upstream. The project is located in an area of high potential seismicity and earthquake induced liquefaction of the tailings is possible. The stability of the top portion of the dam and the potential displacements resulting from earthquake loading are therefore of extreme importance. Several cases of liquefaction induced failure of tailings dams built using the upstream construction have been reported in the literature, e.g. two

Chilean tailings dams (1), and Mochikoshi tailings dam in Japan (2,3).

Conventional limit equilibrium and Newmark analyses including hydrodynamic loading from the liquefied tailings indicated that the embankment is stable and deformations would be very small. However, because the Newmark analysis is restricted to modelling soil as a single-degree-of-freedom rigid plastic system and does not include liquefaction effects, a more detailed analysis was considered appropriate.

Deformation analyses were carried out using a pseudo-dynamic finite element procedure which allows both the inertia forces from the earthquake as well as the softening effect of the liquefied soil to be considered. The method is essentially an extension of Newmark's procedure. The procedure together with the results are presented in this paper.

Kensington Tailings Dam

The proposed tailings dam is a compacted earth/rockfill structure with an ultimate height of 89 m. The initial 50 m of embankment will be constructed as a conventional earthfill dam with a very broad crest, till core and upstream and downstream sand and gravel shell zones. Ongoing raising of the dam will be carried out as the level of the stored tailings rises, using mine waste rock and earthfill with intermediate raises placed partially onto the tailings beach, as shown on Figure 1. The resulting embankment section is referred to as a modified centreline embankment in that the upstream contact between the compacted fill and the tailings is inclined slightly upstream. It provides a cost-effective method of ongoing construction and ongoing reclamation of the downstream slope to reduce the visual impact of the embankment. The section differs from the upstream construction method as it does not rely on the tailings strength for stability, and is theoretically stable even if the tailings are fully liquefied. The concern here is that liquefaction of the slimes together with inertia effects in both the slimes and the dam could lead to large deformations and failure of the impoundment during a major earthquake.

Analyses Procedure

Prediction of earthquake induced movements of earth structures is a difficult

problem. Complex effective stress dynamic analyses procedures have been proposed (4,5) but are essentially research tools and not generally appropriate for analysis of most dam structures.

The simplest analysis procedure is that proposed by Newmark (6) in which a potential slide block is modelled as a single-degree-of-freedom rigid plastic system. Any prescribed time history of acceleration can then be applied at the base and the resulting displacements computed by numerical integration. Newmark also found that the maximum displacement at the end of the shaking period could be estimated from simple formulae by considering the earthquake to be approximated by a number of pulses.

There are two concerns when applying Newmark's simple procedure to an earth structure such as a tailings dam: (1) the soil, particularly in zones where liquefaction is triggered is not rigid plastic; and (2) the single-degree-of-freedom model does not allow the pattern of displacements to be computed. Byrne (7,8) discusses this and show a way of allowing for a general stress-strain relation as well as extending Newmark's approach to a multi-degree-of-freedom system. Basically a pseudo-dynamic finite element procedure is used in which earthquake induced displacements which satisfy energy considerations are achieved by use of a horizontal seismic coefficient. The appropriate seismic coefficient is the one which satisfies the

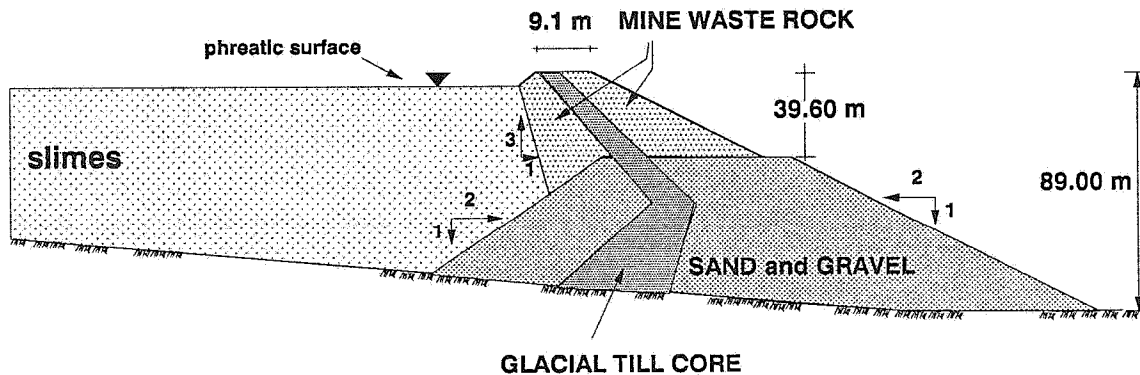


Fig. 1. Geometry and soil types of the tailings dam.

work-energy equation and is found by trial-and-error as described in (8). This approach is briefly described here. It is first applied to the Newmark problem and then extended to a general stress-strain and multi-degree-of-freedom system.

Newmark's simplified model is that of a block of mass M resting on an inclined plane of slope α , and subjected to a velocity pulse, V , relative to the base (Fig. 2a). The resulting displacement is given by

$$D = 6V^2/2gN \quad (1)$$

where D = maximum displacement, V = the velocity pulse which Newmark took as the maximum ground velocity, N = the yield acceleration, i.e., the acceleration as a fraction of "g" required to initiate yield and sliding, and g = the acceleration of gravity. The number 6 in his formula comes from considering 6 pulses of velocity V which Newmark found gave agreement with the integrated records when the ratio $N/A < 0.13$ as it usually is for practical cases of concern.

His model will now be developed in terms of work-energy and this will allow its extension to a general formulation.

The work-energy theorem states that the work done by the internal forces or stresses minus the work done by the external forces must equal the change in kinetic energy of the system, namely,

$$W_{INT} - W_{EXT} = 1/2 M V^2 \quad (2)$$

The work done by the internal forces depends on the stress-strain relations of the material and since Newmark assumed the material to be rigid plastic, the internal force or resistance is constant with displacement as shown in Figure 2b. The work done is the area beneath the resistance line. The external force is the gravity driving force, $Mg \sin\alpha$, and in this case is constant with displacement as shown in Figure 2b. The net work done is the difference between the two areas, namely

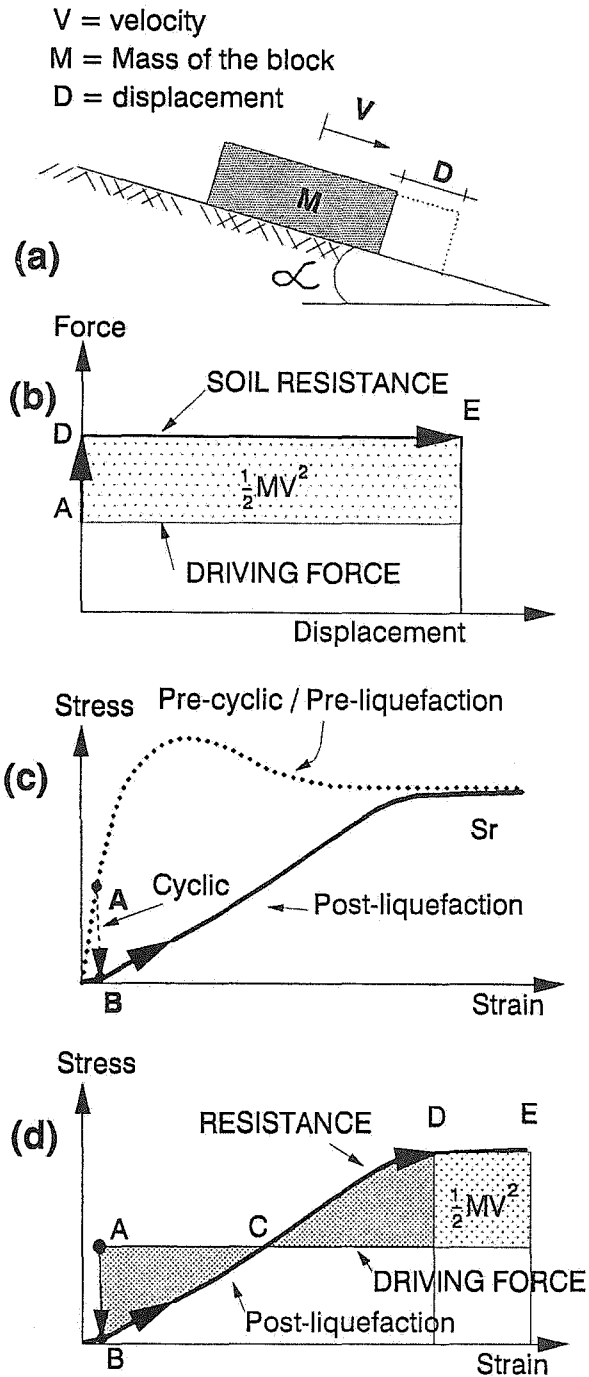


Fig. 2: (a) Block on inclined plane subjected to velocity pulse V ; (b) Work-energy, Newmark; (c) Characteristic of pre- and post-liquefaction monotonic stress-strain curves; and (d) Work-energy, extended Newmark.

the shaded area and this must equal $1/2 MV^2$.

Now $W_{INT} = (s.L)D$, where s = the shear strength of the soil and L is the length of the slide block, and $W_{EXT} = (Mg \sin\alpha)D$. Thus equation 2 reduces to

$$D(s.L - Mg \sin\alpha) = 1/2 MV^2 \quad (3)$$

or

$$D = 1/2 MV^2 / (s.L - Mg \sin\alpha) \\ = 1/2 V^2 / gN \quad (3a)$$

where the yield acceleration, N , is given by

$$N = (s.L - Mg \sin\alpha) / Mg \quad (4)$$

Equation 3 is for a single velocity pulse and when 6 pulses are considered the result is identical to Newmark's equation 1.

Soil when triggered to liquefy will not behave in a rigid plastic manner and this is examined herein. The triggering of liquefaction of loose saturated sandy soils by earthquake loading is a small strain phenomenon (7). Upon liquefaction the stress in the soil drops from A to B. Its resistance then increase with strain to a residual value, s_r , shown in Fig. 2c. The driving force from the ground slope remains constant, however, so that the system accelerates and deforms. When the strain reaches point C the material has hardened so that the stress developed is now sufficient to balance the driving stress as shown in Fig. 2d (If the driving stress exceeds the residual strength, a flow slide will occur.) However, the system has a velocity at this point and the stress continues to increase until point D is reached where the net energy ($W_{INT} - W_{EXT}$) is zero. If the system also had an initial velocity at the time liquefaction was triggered it would carry on to point E.

Comparing the rigid plastic Newmark approach with the extension to a general stress-strain relation (Figs. 2b and 2d) it may be seen that Newmark is missing the displacement from A to D. This could be a very considerable displacement since strains

of 20 to 50% are commonly required to mobilize the residual strength, s_r . However, in carrying out analyses where liquefaction is triggered only one pulse is considered appropriate, whereas Newmark considered a range of pulses up to 6 depending on the ratio N/A . So there may be compensating factors here.

For a single-degree-of-freedom system, the displacement can be computed directly from the energy equation 2 and this is described in detail in (7).

For a multi-degree-of-freedom system a finite element approach can be used. The displacements are computed from the solution of

$$[K]\{\Delta\} = \{F + \Delta F\} \quad (5)$$

where $[K]$ is the global stiffness matrix of the system, $\{\Delta\}$ is the vector of nodal displacements, $\{F\}$ is the static load vector acting on the system (gravity plus boundary loads), and $\{\Delta F\}$ is an additional load applied to satisfy the energy balance of equation 2. If $\{\Delta F\} = 0$, then for the single-degree-of-freedom, a displacement corresponding to C (Fig. 1c) would be predicted. An additional force is required to balance the energy and predict points D or E. This additional force can be considered as a seismic coefficient. However, its value is not related to the peak ground acceleration but is selected by trial and error so as to balance the energy in accordance with equation 2.

For the multi-degree-of-freedom system W_{INT} equals the work done by the element stresses and strains, and W_{EXT} equals the work done by the static load vector $= \{F\} \cdot \{\Delta\}^T$. The additional force $\{\Delta F\}$ is not included as it is merely an artifact to obtain the appropriate displacements.

The procedure has been incorporated into the finite element computer code SOILSTRESS (9) and found to give an exact agreement with Newmark when the assumptions made correspond to a single-degree-of-freedom rigid plastic system. It

gives good agreement with liquefaction induced field observations reported in (10). The procedure predicts the failure of the Lower San Fernando dam, and gives displacement predictions for the Upper San Fernando dam that are in good agreement with the measurements in terms of both the magnitude as well as the pattern of deformations. The method was used to predict possible liquefaction induced displacement of the intake structure at the John Hart Dam (8), and is currently being used by BC Hydro to estimate possible liquefaction induced displacements at Duncan Dam.

Cases Analyzed

The variables in the analyses were essentially the level of the earthquake

excitation and the location of the water table within the slimes.

Peak horizontal ground accelerations ranging from 0.2g to 0.6g were considered with corresponding peak ground velocities of 0.2 and 0.6 m/second. Tailings to the full height were examined with the water table at the surface as well as several lower levels. Only two water table conditions will be shown here: *Case 1* - Water table at the surface of the tailings; and *Case 2* - the lowest water table considered. The finite element mesh, the soil types, and the water table for these two conditions are shown in Fig. 3. It is assumed that tailings above the water table will not liquefy and that tailings below the water table will liquefy to the base of the impoundment. The zones of liquefaction are shown in Fig. 3 for both cases.

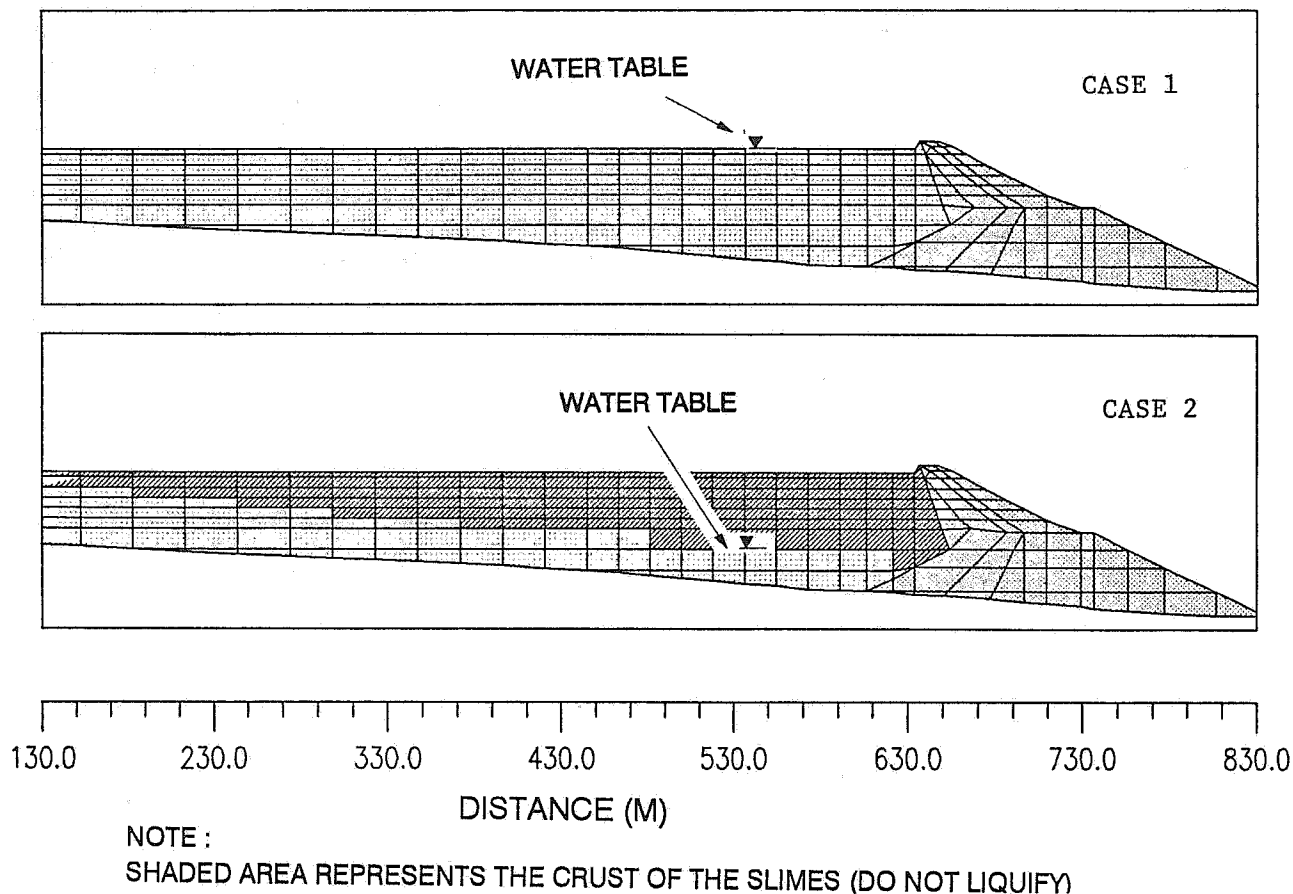


Fig. 3. Finite element mesh, soil types and groundwater conditions.

Soil Parameters Used in the Analyses

Soil parameters based on the hyperbolic model (11) were used in the analyses. The soil properties were obtained from laboratory data and the stress-strain parameters required in the analyses were computed following the method described in (11 and 12). The properties of liquefied slimes were obtained from post-cyclic monotonic triaxial test. The soil parameters used in the analyses are listed in Table 1, and are described in (11).

TABLE 1: Soil parameters used in the analyses

	Slimes	Sand/Gravel	Till
k_g	542 (4)	650	1025
n	0.50 (0)	0.50	0.50
k_b	1490	1085	1700
m	0.25	0.25	0.25
ϕ (deg)	36.5 (0)	39.0	42.0
$\Delta\phi$ (deg)	0 (0)	0	0
c (kPa)	0 (150)	0	0
R_f	0.60 (0.10)	0.60	0.60
γ_s (kN/m ³)	14.1	19.5	19.5

Note: a) Brackets indicate the properties after liquefaction

b) Pre- and post-earthquake properties for sand, gravel and compacted till are assumed identical since these soils were assumed not to liquefy.

Results

Case 1 - The predicted deformations for Case 1 with the water table at the surface of

the slimes are shown in Fig. 4. This figure shows the deformed finite element mesh magnified by a factor of 10 for a peak ground acceleration of 0.6g. This was simulated by a single velocity pulse $V = 0.6$ m/sec, $A/V=1$ was considered appropriate for the site. The liquefied slimes are predicted to undergo large horizontal movements in the "free-field", away from the face of the dam. They are constrained by the dam and move upward turning some of their kinetic energy into potential energy. Such movement of the tailings could possibly overtop the dam in the case of severe earthquake loading if the freeboard were insufficient. For the 0.6g condition, the predicted upward movement of the tailings adjacent to the dam is 1.15 m.

The predicted peak displacements of the crest of the dam are 0.48 m horizontal, and 0.09 m vertical. The maximum movement of the dam predicted from the Newmark analysis using the same soil strengths was 0.14 m. In the Newmark analysis the hydrodynamic effect of the slimes was accounted for using the Westergaard approach and considering the slimes as a heavy liquid. The Newmark value is significantly lower than 0.48 m predicted here. Predicted displacements of the dam crest for peak accelerations of 0.2g and 0.35g are listed in Table 2.

TABLE 2: Soil movements

Case	Free-board (m)	Peak Accel. m/sec ²	Dam Crest Displacement (m)		Rise in Slime Lvl. Adjacent to the Dam (m)
			Vert.	Horiz.	
1	1.5	0.2	0.09	0.24	0.71
1	4.6	0.35	0.08	0.25	0.80
1	4.6	0.60	0.09	0.48	1.15
2	1.5	0.2	0.09	0.84	0.09
2	4.6	0.35	0.11	0.67	0.15
2	4.6	0.60	0.11	0.94	0.15

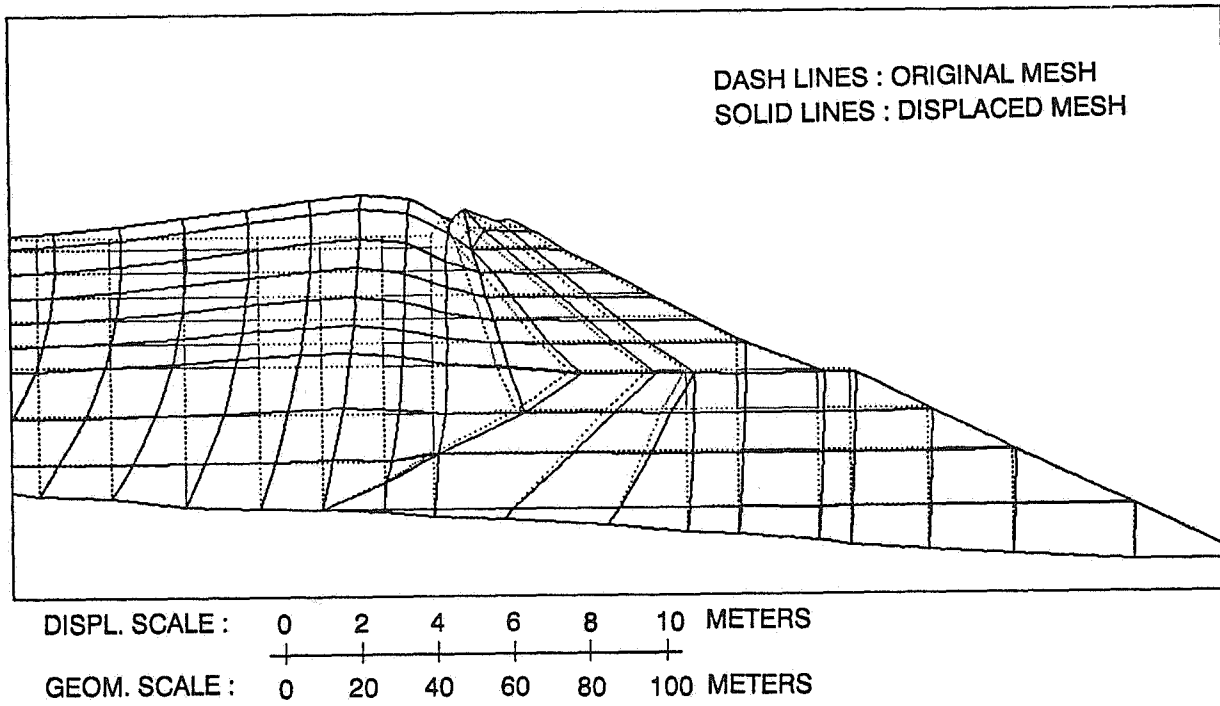


Fig. 4. Displacement pattern of the dam, Case 1.

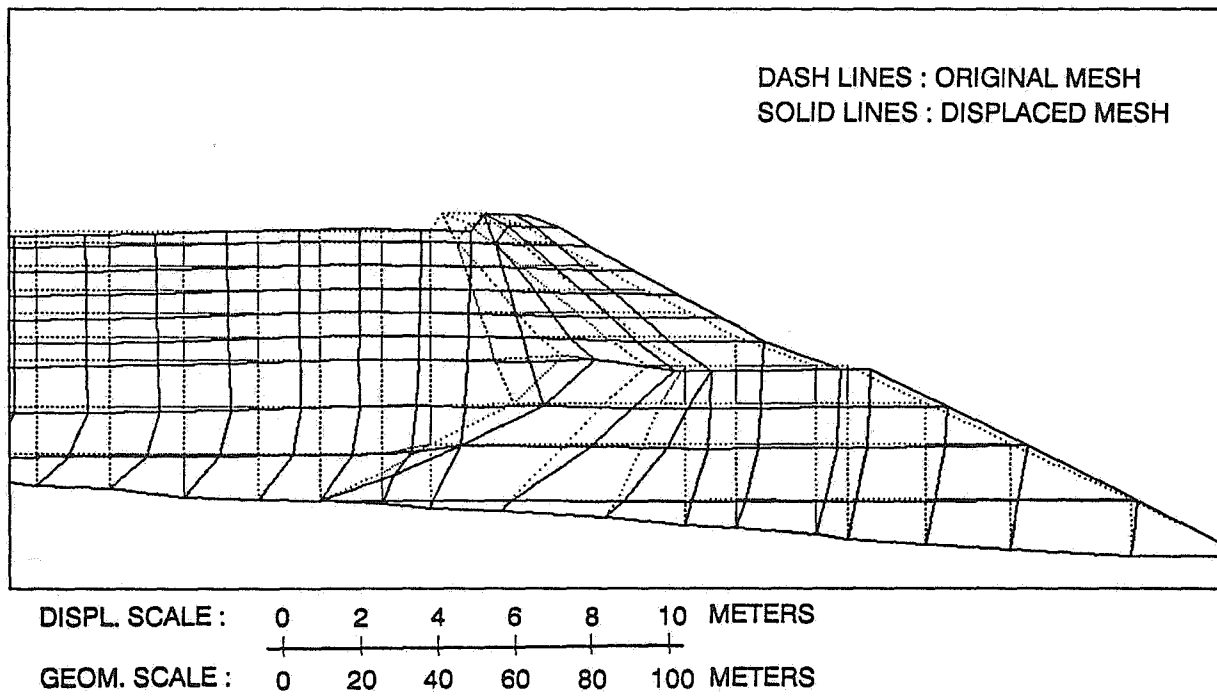


Fig. 5. Displacement pattern of the dam, Case 2.

Case 2 - The predicted deformations for Case 2 with the water table at a low level are shown in Fig. 5 for a peak acceleration of 0.6g ($V = 0.6$ m/sec). In this case only a relatively thin zone of slimes near the base of the impoundment was assumed to liquefy during earthquake shaking. The predicted displacements of the crest are 0.94 m horizontal and 0.11 m vertical. The crusted tailings essentially move horizontally with only a small surface rise.

The Newmark analysis is difficult to apply to this condition as the predicted displacement depends upon the mass of crust considered as part of the slide block.

Comparing Figs. 4 and 5, the predicted horizontal displacement values are considerably higher for the lower groundwater condition in the tailings. This, at first sight, is surprising. It results from the stiff crust above the liquefied zone acting as a battering ram and pushing the dam horizontally. When the soil liquefies to the surface, the tailings can rise and much of their kinetic energy is transferred to potential energy, thus less energy is available to push the dam horizontally and deflections are lower. The stiff crust does not rise significantly as can be seen in Fig. 5.

A summary of important soil movements for Cases 1 and 2 is given in Table 2.

Summary

An analysis procedure is presented for predicting earthquake induced displacements of a tailings impoundment. The procedure is an extension of the simple Newmark method from a single to a multi-degree-of-freedom system taking into account the softened stress-strain response of liquefied soils. The method is applied to the proposed Kensington tailings impoundment in Alaska and gives the pattern of displacement as opposed to a single displacement obtained from Newmark. The displacements are about 3 times higher than computed from the Standard Newmark and arise because

additional displacements due to the flexible nature of soil are included.

The results indicate that the structure is stable but that larger earthquake induced displacements can occur when a crust has formed over the pond.

Acknowledgements

The authors are grateful to NSERC for its financial support and to Ms. Kelly Lamb for her typing and presentation of the paper.

References

1. Dobry, R. and Alvarez, L., "Seismic Failures of Chilean Tailings Dams", *Journal of the Soil Mechanics and Foundations Division, ASCE*, Vol. 93, No. SM6, Nov. 1967, pp. 237-260.
2. Marcuson, W.F., "Liquefaction Failure of Tailings Dams Resulting from the Near Izu Oshima Earthquake, 14 and 15 January 1978", *Proc. 6th Pan American Conference on SMFE*, Vol. 2, 1979, pp. 69-80.
3. Ishihara, K., "Post-Earthquake Failure of a Tailings Dam due to Liquefaction of the Pond Deposit", *Proc. International Conf. on Case Histories in Geotechnical Eng., St. Louis*, Vol. 3, 1984, pp. 1129-1143.
4. Finn, W.D. Liam, Yogendrakumar, M., Yoshida, N. and Yoshida, H., "TARA-3: A Program to Compute the Response of 2-D Embankments and Soil-Structure Interaction Systems to Seismic Loadings", *Dept. of Civil Engineering, University of B.C., Vancouver, B.C.*, 1986.
5. Prevost, J.H., "DYNA-FLOW: A Nonlinear Transient Finite Element Analysis Program", *Rpt. No. 81-SM-1, Dept. of Civil Engineering*,

- Princeton University, Princeton, NJ, 1981.
6. Newmark, N.M., "Effects of Earthquake on Dams and Embankments", *Geotechnique*, Vol. 15, No. 2, 1965, pp. 139-160.
7. Byrne, P.M., "A Model for Predicting Liquefaction Induced Displacements", *Soil Mech. Series No. 147*, Department of Civil Engng., University of B.C., Vancouver, 1990. Also, 2nd International Conference on Recent Advances in Geotechnical Earthquake Engineering and Soil Dynamics, St. Louis, Paper 7.14, March, 1991.
8. Byrne, P.M., Jitno, H., Garner, S., Lee, M. and Lou, J.K., "Analysis of Earthquake Induced Displacements of the Intake Structures, John Hart Dam", *Proc. Canadian Dam Safety Conference*, Whistler, B.C., 1991, pp. 97-116.
9. Byrne, P.M. and W. Janzen, 1981. "SOILSTRESS: A Computer Program for Nonlinear analysis of Stresses and Deformations in Soil", *Soil Mechanics Series No. 52*, Dept. of Civil Engineering, University of B.C., December 1981, updated January 1989.
10. Hamada, M., Towhata, I., Yasuda, S. and Isoyama, R., "Study of Permanent Ground Displacement Induced by Seismic Liquefaction", *Computers and Geotechnics* 4, 1987, pp. 197-220.
11. Duncan, J.M., Byrne, P.M., Wong, K.S. and Mabry, P., "Strength, Stress-Strain and Bulk Modulus Parameters for Finite Element Analyses: Stresses and Movements in Soil Masses", Report No. UCB/BT/80-01, 1980.
12. Byrne, P.M., Cheung, H. and Yan, L., "Soil Parameters for Deformation Analysis of Sands", *Canadian Geotechnical Journal*, Vol. 24, No. 3, 1987.

Landslide Dams at Clinton Creek

M. Stepanek

*Geo-Engineering (M.S.T.) Ltd.
Calgary, Alberta*

H.F. McAlpine

*Northern Affairs Program
Whitehorse, Yukon Territories*

Clinton Creek Asbestos Mine, located some 97 km north from Dawson City (Yukon), was operated by Cassiar Mining Corporation from 1968 to 1978. The ore was extracted from the bedrock in three open pits. A total of 13 million tons of ore were milled, using a dry hammer mill process, producing approximately 1.1 million tons of asbestos fibre and almost 12 million tons of tailings. Waste rock (about 35 million m³) and dry tailings (some 7 million m³) have been deposited over the slopes adjacent to the open pits and in the mill area. Disturbance of the slopes and their loading caused permafrost degradation which, in turn, triggered massive failures of waste rock and tailings.

A failure of the rock waste dump blocked the Clinton Creek valley and formed a 73 ha lake. The creek was displaced about 25 m above the original valley bottom and cut its new channel along the interface between the waste pile and valley wall. Currently, the waste dump movements and the creek erosion appear to be in-balance. As long as an armoured section of the outlet channel remains intact, the probability of a sudden failure of this landslide dam is believed to be low.

The tailings pile, located in the Wolverine Creek valley, failed in 1974, forming a small lake. The valley blockage was almost immediately breached and asbestos tailings were carried further downstream. To control erosion, a channel with a series of rock weirs was constructed across the tailings covering the valley bottom. While this structure has operated quite well to-date, its long-term performance is questionable. The tailings pile remains unstable, the displacement of the creek upstream from the spillway continues and additional temporary blockages have occurred. The probability of a breach failure is considered to be high.

Geological Setting

Regionally, the Clinton Creek area is located within the unglaciated Yukon-Tanana Upland, within the widespread, discontinuous permafrost zone (Figure 1). The main ore bodies were located in the westerly-trending ridges on the south side of Clinton Creek. These ridges reach an elevation of 610 m a.s.l., while the valley bottom is at about elevation 400 m a.s.l.

The terrain is underlain by bedrock included within the Yukon Cataclastic Complex. Exposures in the vicinity of the mine site indicate that the geology in the area consists of two relatively complex assemblages of rock (Abbott, 1982):

- Sheared assemblage which includes ultramafic, igneous and metamorphosed rocks, such as serpentinite, diorite, amphibolite, and schist. All these rocks exhibit a strong pervasive foliation, except the ore-bearing serpentinite.

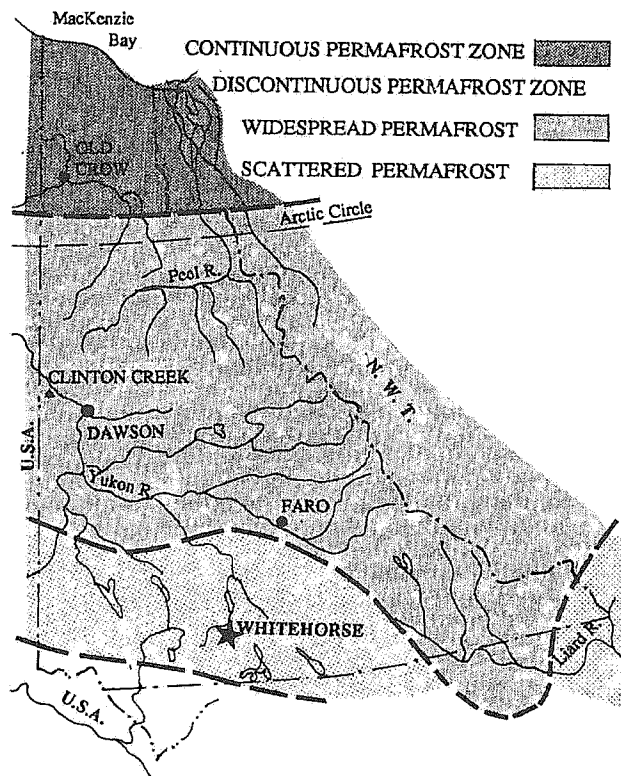


Figure 1: Location Map and Distribution of Permafrost.

- Weakly-deformed assemblage which includes shale, siltstone and sandstone, with some local phyllite and phyllonite. These strata mantle the sheared assemblage. They are thought to be of mid to upper Triassic in age.

The ore body consists of a stockwork of cross-fibre chrysolite asbestos veinlets cutting jade-green serpentine. Asbestos at Clinton Creek could be related to granitic intrusions or shearing and thrusting.

From a structural standpoint, the mine site and surrounding area are criss-crossed by a series of steep normal faults and thrust faults. The former are near-vertical and tend to bound the ore body, while the latter are of low angle and by their nature tend to occur along the contact of the two assemblages.

Bedrock exposures are scattered throughout the lower portions of the Clinton and Wolverine Creek valleys. The bedrock is mostly covered with overburden. The soil cover comprises colluvium on the slopes and alluvium in the valley bottoms. Water-laid deposits (usually classified as fluvial-lacustrine) cover the ridge where the mill was located.

Alluvial deposits in the Clinton and Wolverine Creek valley bottoms are believed to form a very weak foundation for the waste dumps, because of the presence of organics and ice-rich silts. Relatively low shear strength is also indicated for the colluvium ($\phi_r = 23^\circ$, $c_r = 0$) and weathered argillite bedrock ($\phi_r = 26^\circ$, $c_r = 0$).

Only limited information is available on permafrost conditions at the mine site. The active layer was reported to be only 0.3 to 0.5 m thick on the north-facing slopes. Segregated ice, forming large crystals and thick lenses in alluvial valley deposits and nearsurface bedrock, was commonly encountered in undisturbed ground.

Permafrost conditions reflect the energy balance between air temperature, snow and vegetation cover, as well as local micro-climate. Few measurements of the ground thermal regime are available from the mine area; however, air temperature data for Dawson (mean annual air temperature: -4.7°C) suggest that permafrost in the area should probably be classified as "warm." With ground temperatures of -4°C or greater, "warm" permafrost is sensitive to terrain and vegetation disturbances, which may result in complete permafrost degradation.

Golder Associates (1978) reported that the Clinton Creek waste dump foundation was thawed to a depth of about 10 m below the rock waste dump at that time. Temperatures of -1.0 to -1.6°C were measured at greater depths. The depth of thawed ground below the tailings pile in the Wolverine Creek valley was measured to be about 1.5 to 3.0 m.

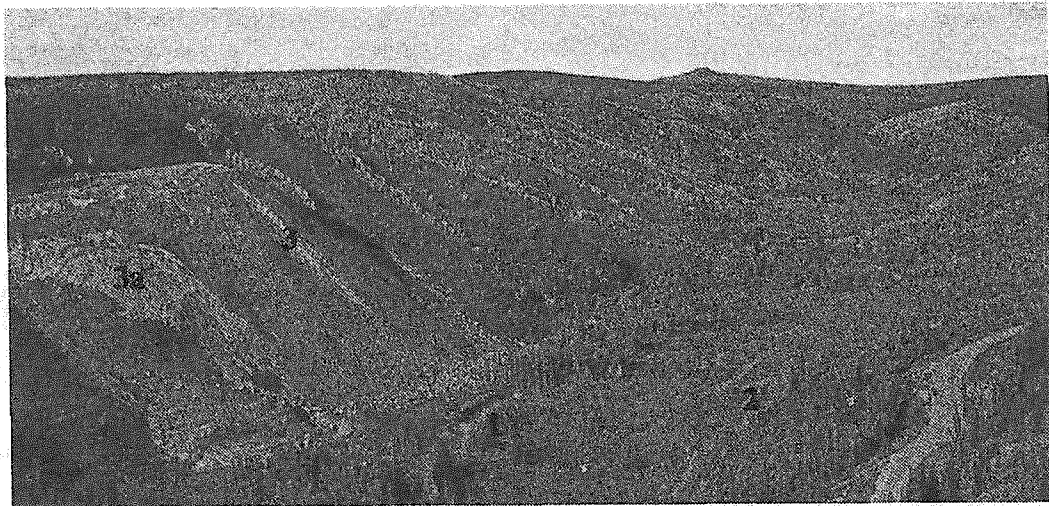


Photo 1: Clinton Creek valley in 1970, looking west. 1- original creek channel, 2- creek diversion, 3- waste dump, 3a- unstable segment of the dump.

Drainage and Hydrology

The mine area is situated some 8 km up Clinton Creek, a tributary of the Forty Mile River. Local drainages include Porcupine Creek (drainage area of 2.6 km²) and Wolverine Creek (catchment of 21.6 km²), both joining Clinton Creek in the mine area. The drainage area of Clinton Creek upstream from the confluence with Wolverine Creek is approximately 106 km², increasing to about 200 km² at its junction with the Forty Mile River.

All creeks show a wide variation in flow. Discharges range from low to zero flows during the coldest months of the winter, to high but short duration floods at the time of the spring break-up.

Flow records for these streams are limited to seasonal records by Water Survey of Canada and Northern Affairs Program, for the years 1964 to 1965 and 1978 to present, respectively. Only the Water Survey of Canada data pre-date the formation of landslide dams on Clinton and Wolverine Creeks. The magnitudes of 200 years events have been estimated, using the records from the North Klondike and Klondike Rivers, at 78 m³/s and 16 m³/s for Clinton Creek and Wolverine Creek, respectively

(Klohn Leonoff, 1986). More extreme events, commensurate with the expected life span of the landslide dams were not evaluated. Neither was such an event considered at the time of mine closure.

Clinton Creek Dam

The major portion of overburden rock from the main pit was dumped over the north facing wall of the Clinton Creek valley. Originally, the valley floor was flat-bottomed, with a width of about 240 m, and Clinton Creek meandered across the valley bottom (Photo 1). When the toe of the dump reached the valley floor, it began to spread over the low shear strength, presumably ice-rich, alluvial soils comprising the valley bottom. As more waste material was placed on the dump, the dump toe continued to spread until the valley bottom was blocked by a landslide dam (Photo 2).

The waste rock consists mainly of argillite, phyllite, platy limestone, and micaceous quartzite. Shale is commonly disintegrated into silt-sized and platy sand or gravel-sized particles, which form the matrix of this waste material.

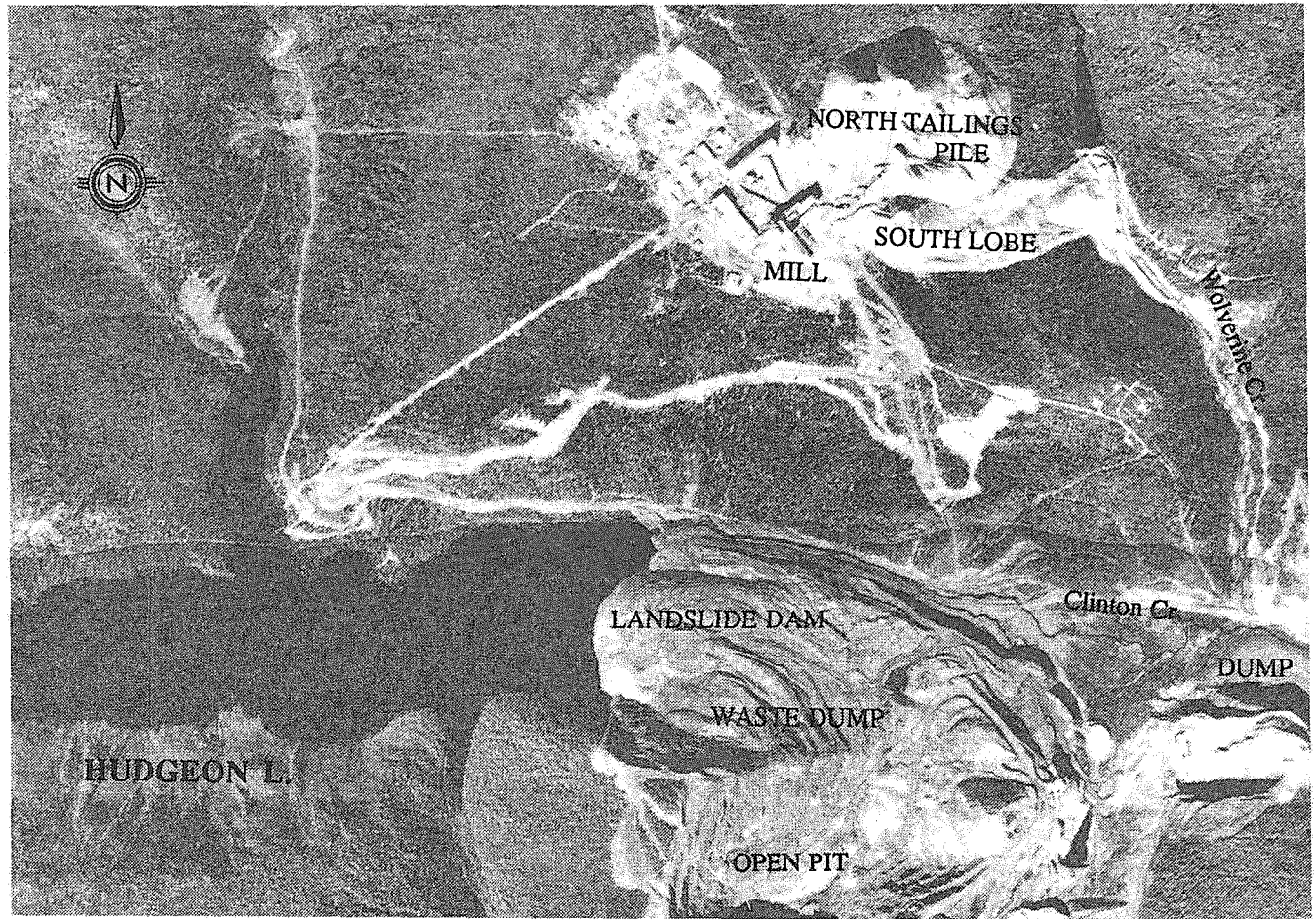


Photo 2: Aerial photograph of the mine area in 1976 showing Hudgeon Lake and blockage of the Wolverine Creek valley by the failure of the south tailings pile.

It is apparent that the steep hillside (sloping up to some 30 degrees) did not provide sufficient support to the waste rock dumped from the crest. In addition, the weak deposits forming the Clinton Creek alluvial floodplain were unable to resist the stresses imposed by a more than 140 m high waste dump. This triggered a deep-seated foundation failure, likely due to the permafrost degradation. The slide gradually advanced across the valley bottom and up onto the north valley slope. The valley blockage formed a lake (Figure 2), now known as Hudgeon Lake. The depth of water in the lake is about 26 m and its surface area is some 73 ha.

At the outlet from the lake, water flows across the waste dump along its north side. The channel, forming an incised trough bounded by waste material on the south and the valley wall on the north, has an overall gradient of about

4.5 percent and is about 0.8 km long. After its development, erosion threatened the stability of the channel and could have caused a partial breach of the valley closure. To control erosion, the mining company initially installed culverts and later a rock apron at the lake outlet. A section of rock weirs was constructed near the lake outfall in 1981. During the spring runoff in 1982, Clinton Creek escaped the rock-lined section of the channel and undercut the north valley wall. The rock-lined section was then modified and re-constructed in 1984 (Photo 3). The design included backfilling of the eroded channel and placing rip-rap along both banks of the channel. Under normal flow conditions, the armoured channel section performs well. However, the armour has not been tested by a major flood and retrogressive erosion is in progress.

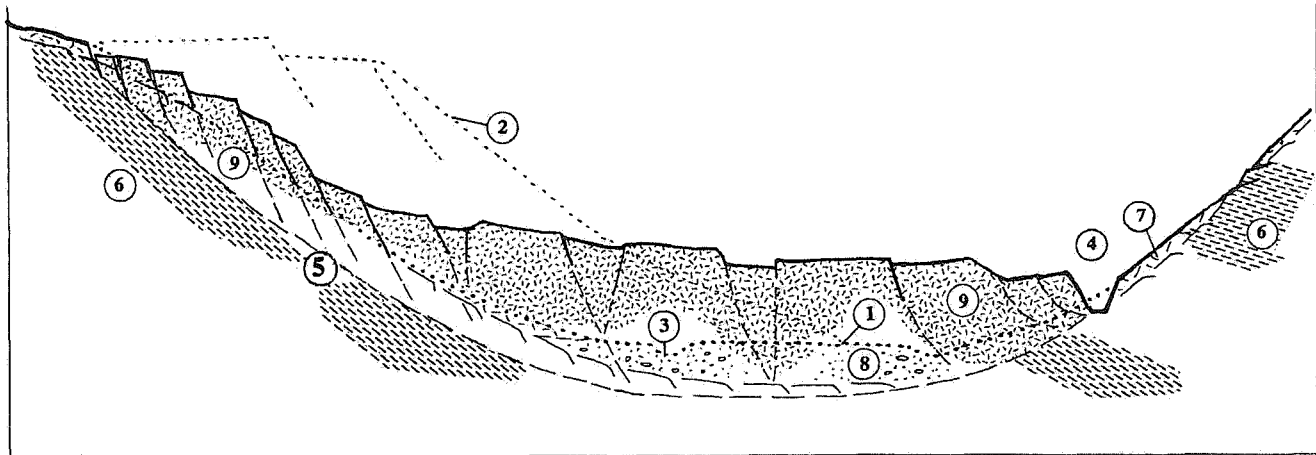


Figure 2: Clinton Creek Landslide Dam, looking upstream.
 1- original ground surface, 2- initial configuration of waste dump, 3- original creek channel, 4- present creek channel, 5- probable slip plane, 6- bedrock (shale), 7- colluvium, 8- alluvium, 9- slide debris

Dump movements were monitored between 1977 and 1986 by surveying monuments located on the dump surface and cross-channel reference lines. The horizontal rate of movement decreased from approximately 1.2 m/year in 1978 to some 0.3 to 0.6 m/year during the 1985 and 1986 monitoring seasons. The monuments were eventually destroyed and the horizontal movement is currently estimated to be in the 0.3 m/year range.

Wolverine Creek Dam

A tailings pile failure formed the small lakes in the Wolverine Creek valley (Photo 2). The tailings consist largely of serpentized peridotite, short asbestos fibre and silt to sand sized rock fragments. Tailings have been placed in two areas, which eventually formed the north and south lobes of the tailings pile. The south lobe was constructed between start-up and 1974, when a failure of the tailings pile occurred and a segment of the pile moved downslope and blocked the valley bottom, including the creek (Figure 3). Following the south pile failure, tailings were placed in the north pile until the mine shut down in 1978. The north lobe reached the valley bottom in 1985 and formed another small lake (Photo 4).

The surface characteristics of the unstable tailings piles and erratic rates of movement suggest that their failures were caused by thawing of the permafrost subgrade. It is likely that excess pore pressures developed since the ground surface slopes only at about 18 to 22 degrees in this area.

The initial valley blockage was almost immediately breached and tailings were dispersed downstream for a distance of some 2 km. The south tailings pile lobe continued to slide into the valley at a rate of some 25 m/year, spreading and increasing the volume of the valley blockage.

To control erosion and convey the creek across the landslide dam, a rock-lined outfall channel with weirs was constructed in 1978. In addition, the mining company undertook several actions designed to stabilize the piles and to prevent a sudden release and downstream transport of tailings materials. Stabilization efforts, chiefly involving partial regrading and terracing of the piles, were unsuccessful and the dumps remain unstable.

The most active areas are presently along the toe of the south pile (Photo 5) and the valley bottom in front of the north pile. The rate of horizontal movement of the south lobe is estimated to be in the range of 5 to 10 m/year. On two occasions, the southern lobe has temporarily blocked the creek channel upstream from the armoured

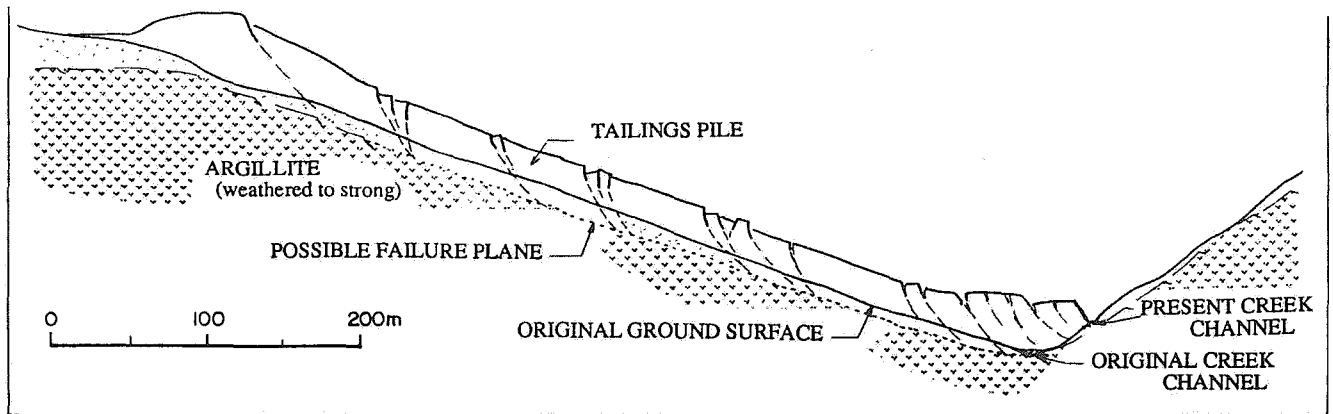


Figure 3: Schematic section of south lobe of Wolverine Creek tailings pile.

spillway. Similarly, the north lobe blocked the valley in 1985. So far, all these blockages have been breached without triggering major sediment transport.



Photo 3: View of the Hudson Lake outlet and armoured channel.

Evaluation of Hazards

The volume of the Clinton Creek waste dump volume is estimated at about 20 million m³ and the length of the landslide dam in the valley bottom is almost 0.8 km. The dam is more than 50 m high in the center of the valley.

While the waste material is heterogeneous and poorly-consolidated, a failure due to piping or collapse of the blockage is not considered likely. Approximate transverse sections of this landslide dam, a large earth fill dam (Oroville,

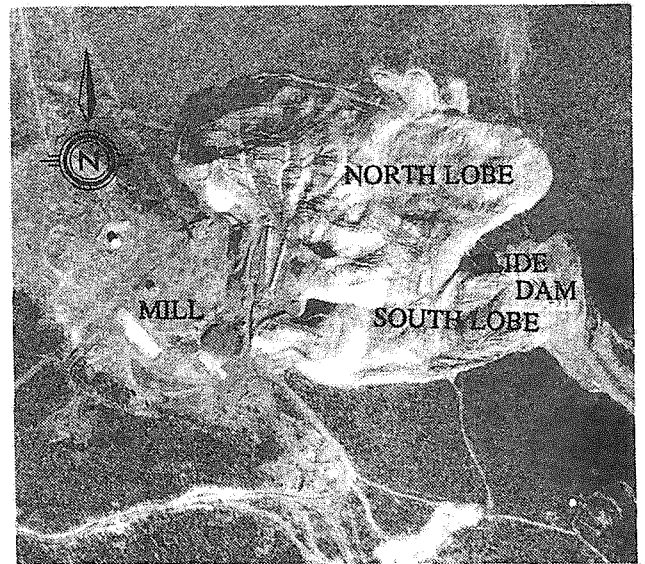


Photo 4: Aerial photograph of tailings piles in the Wolverine Creek valley, 1985.



Photo 5: South lobe of the tailings pile blocks the Wolverine Creek valley.

California) and a large moraine dam (Nostetuko, British Columbia) are compared on Figure 4. The Hudgeon Lake landslide dam is nearly as wide as the other dams, while its height is considerably smaller.

A temporary blockage of the overflow channel, due to local accelerated sloughing of the waste material, resulting in a temporary rise of the lake level and subsequent increased erosion, is considered a possible mechanism releasing large volumes of water and material. However, during the past ten years, the volume of material sliding from the waste dump into the channel has been relatively constant and, with the exception of larger blocks, readily transported further downstream. This experience validates predictions made by Klohn Leonoff (1986) in the Abandonment Plan regarding the waste dump movement and sediment transport through the overflow channel for flow events experienced to-date.

The large mass of the valley blockage, its shape and the composition of the dam material suggests that a rapid failure is unlikely. The highest risk to the stability of this landslide dam is breaching and erosion of the armoured

upstream segment of the overflow channel. It is likely that without further maintenance, stability of the outlet channel will be destroyed, resulting in accelerated erosion. This, in turn, could result in a sudden release of impounded water.

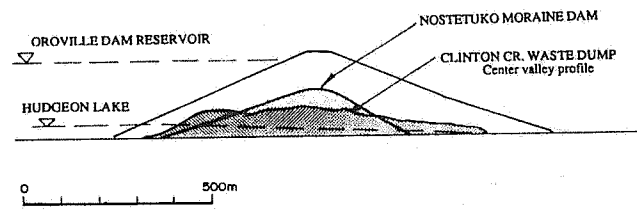


Figure 4: Schematic section of Clinton Creek Landslide Dam, Nostetuko Moraine Dam and Oroville Dam.

While the size of the landslide dam in the Wolverine Creek valley and volume of impounded water is small relative to other landslide dams (Costa & Schuster, 1988), the tailings forming this blockage are more erodible than waste rock. The volume of tailings currently blocking the valley bottom (i.e. the toe of the southern lobe) is about 1/14 of the total mass of tailings sliding into the valley.

The ongoing downslope movements of both tailings pile lobes and tailings eroded from the north lobe may fill the lower lake and form a single, relatively wide blockage. It is expected that the stream will then flow across the top of this "dam", probably confined along the east valley wall. This flow could bypass the armoured channel and breach the blockage. An assessment of the probable breach configuration, flows and sediment transport was made by Klohn Leonoff (1986), as a part of the Abandonment Plan. That analysis indicated that downstream flows would rise significantly for a distance of several kilometres from the tailings pile. The flow mechanism of sand sediment transport is difficult to predict.

Both Clinton and Wolverine Creeks, if existing armoured channels become bypassed (Photos 3 and 6), can be expected to discharge significant

INTRODUCTION

Geomorphic hazards within watersheds have been defined as any landform change, natural or otherwise that affects geomorphic stability at an isolated location and possibly further down the system (Schumm, 1988). The various hazards commonly occurring within watersheds, such as landslides, debris torrents, bank erosion and floods often occur in combination as opposed to isolated occurrences. For example, a logging operation in the upper portion of a watershed may cause a landslide adjacent to the logging road, then the downslope movement of the landslide material creates a debris torrent which moves down a steep channel and eventually drops the debris within a wide river valley resulting in diversion of flow currents and bank erosion. The short term changes during the debris torrent event (usually less than one hour) are generally followed by recurring long term events such as river bed aggradation and bank erosion. Schumm (1988) classifies hazards into three time frames:

- i) a catastrophic event
- ii) a progressive change that leads to an abrupt change; and
- iii) a progressive change with slow progressive results.

Often short term dynamic events such as landslides trigger long term river changes further down the system.

In order to understand the dynamics of various types of hazards a study framework should involve the following three space scales coupled to varying time scales as shown in Figure 1:

- i) macro-scale;
- ii) meso-scale; and
- iii) micro-scale.

The dynamics of the geomorphic hazards related to space as well as time.

SCALES OF DYNAMIC STUDIES

Dynamic processes require dynamic studies in space and time.

The study of river basin processes and hazards becomes dynamic with the involvement of macro-meso-micro scales that are also linked through time. A macro-scale study provides a broad view of geomorphic processes and features of an entire basin as well as the utilization of the basin by man. An intermediate scale of study, meso-scale, thereafter concentrates on a specific reach of river that is undergoing change while the smallest scale study, micro-scale, focuses on a local landslide or bank erosion. These studies should also be over various time spans appropriate to the geomorphic processes, for example, a study of a debris torrent entails assessment of events over a period of the order of one hour while a longer time assessment is necessary for potential glacier lake outburst floods and mapping of historical landslides. Two case studies are presented illustrating the dynamic aspects of geomorphic hazards.

DEBRIS TORRENT ALONG PATTISON CREEK BRITISH COLUMBIA

The lower Mainland region experienced a major storm between November 8 and 10, 1990. Although very significant in terms of 1 and 2 day rainfall (35 to 100 year return), the storm appears to have lacked the concentrated cells of high precipitation which are usually responsible for the generation of debris flow activity. Consequently, the predominant type of damage was due to flooding associated with the larger streams. Pattison Creek was one of a few small drainages which suffered instability during this storm (Thurber Engineering, 1990).

The debris flow was initiated by a landslide in

a small gulley at el. 940 m (Figure 2). The landslide scar is up to 50 m wide, 100 m long and 10 m deep. It occurred on a section of slope inclined on average at 25°. The side scarp reveals glacial till consisting of silty sand, gravel and cobbles.

The initial slide occurred in an area clearcut some 30 years ago, at a point where a logging road crossed the head of the gulley. However, causal connection between the occurrence of the landslide and logging is not clear. Certainly, decay of root strength, often used as an explanation of post-logging instability, could have played no significant role in this deep-seated failure. Also the cut and fill created by the road is very small compared to the depth of the sliding surface.

The most probable explanation of the slide is that the logging activity changed the surface flow and infiltration conditions at the head of a soil filled gulley. The road may have diverted surface flow from adjacent drainage paths, changing the water balance in the gulley sufficiently to raise pore-pressure and trigger sliding near the soil-bedrock contact. Such a trigger is very common on the B.C. coast, based on the authors' experience. In each case, there is an amazing contrast between the inconspicuous cause - diversion of water along a segment of an old road and the dramatic effect - a major and violent slide.

The initial slide volume was estimated as 25,000 m³. Of this total, approximately 7,000 m³ remains deposited on the base of the landslide scar. The remaining 18,000 m³ entered a small gulley and then a minor branch of the creek, stripping a wide swath of young and old forest and soil. A large part of the debris flow track below the initial slide has been eroded down to bedrock, producing more than 60,000 m³ of debris additional to that of the initiating slide.

At el. 600 m, the debris flow track widens and deflects to the left (east) on encountering a bench formed of ice contact deposits. At this point, the debris flow narrowly missed the head of the large slide scar formed during the 1960 debris flow, which is still actively eroding (Figure 2).

Below el. 600, the debris flow track follows a confined bedrock gorge to a confined alluvial fan. The peak discharge of the debris surges was probably of the order of 200 to 400 m³/s at the head of the fan.

The bulk of the debris deposited within approximately 800 m of the confined fan apex, on slopes ranging from 8° to 9°. The debris tongue in this main deposition area is up to 50 m wide and probably 2 m deep on average, containing an estimated volume of 54,000 m³. A further 30,000 m³, approximately, of finer material (afterflow) was spread over 1,250 m length of channel downstream of the main deposit. The afterflow volume was estimated by assessing the dimensions of the active flow channel existing through the debris deposition zone.

The water-sediment process during and directly after the debris torrent changed from deposition along the confined alluvial fan to one of erosion by afterflow. Of significance, is that the erosion process over the confined fan deposit will continue to supply sediment to the lower reaches of Pattison Creek and Lagace Creek which will entail annual gravel excavation if future flooding of the Hatzic Prairie floodplain is to be avoided.

In studying the impact of this geomorphic event, the scope of investigation involved assessment of about 10 km of channel as well as prediction of the consequences over the next 10 year period. This prediction into the future included the possibility of another debris torrent event especially if the older

landslide shown in Figure 2 headcuts into the 1990 landslide. If a time scale was not a part of the impact study, the community along the creek may not be prepared for another debris torrent.

GLACIER LAKE OUTBURST FLOOD IN NEPAL

As another example, consider the glacier lake outburst flood that occurred on the Sun Kosi in 1980 and was followed by a similar debris torrent flood caused by a cloudburst in 1986 (Galay, 1989). The 1980 flood caused extensive damage to the Arniko Highway (see Figure 3), destroyed three major highway bridges and took out three control gates on the diversion structure of the Sun Kosi Hydro Plant. The glacier flood was believed to be caused by piping through an end moraine originating in China (the Boquot River). However, its consequences were not studied over an extensive reach of river (macro-scale). Also the time dimension was not considered as noted by the following facts:

- i) the second destruction of the Arniko Highway in 1986 by a debris torrent means that no consideration was given to the possibility of another flood event within the lifetime of the highway. The old highway was reconstructed at the same location and was not raised above the 1980 flood levels; and
- ii) the destruction of three gates (1986) on a diversion structure used to divert water to a hydro plant did not include clear instructions for procedures to open and close during flood events. Nothing was learned from the destruction of gates during the outburst flood of 1980.

There was no short term (1 or 2 hours) acknowledgement of characteristics of debris torrent events or glacier floods on the Sun Kosi. Studies did not include the macro-meso-micro space dimensions, nor the time scale which means that the study of hazards and processes along this system was not dynamic.

DISCUSSION

Approaches to study of geomorphic hazards have generally been at isolated locations. Models of the mechanics of landslides have been developed by geotechnical specialists (Terzaghi and Peck, 1948); and Valdiya (1987), and bank erosion models were developed by Thorne (1982). These models are at isolated locations and attempts are being made to link these events through space by hazard mapping (Petak and Atkisson, 1982), but this representation generally does not adequately bring in changes with time. Some hazard maps designate the degree of hazard using terminology such as "high probability for damage" and "low probability for damage", but these terms are rarely defined numerically. This linkage of hazards in space and time is being researched (Clague, 1982; Ives, 1986) and will be receiving more attention.

CONCLUSION

Geomorphic hazards within watersheds result in changes along river systems (space dimension) as well changes with time resulting in a dynamic response to hazard events such as landslides, debris torrents, floods etc.

REFERENCES

- Clague, J.J. (1982) - "The Role of Geomorphology in the Identification and Evaluation of Natural Hazards",

Applied Geomorphology, George Allen and Unwin, London.

- Galay, V.J. (1989) - "Debris Torrents in Nepal and Use of Reliability Engineering Concepts During Redesign of River Works", Proc. ASCE Symp. Sediment Transport Modeling, New Orleans, USA.
- Ives, J.D. (1986) - "Glacial Lake Outburst Floods and Risk Engineering in the Himalaya", ICIMOD Occasional Paper No. 5, Kathmandu, Nepal.
- Petak, W.J. and Atkisson, A.D. (1982) - Natural Hazard Risk Assessment and Public Policy, Springer-Verlag, New York.
- Schumm, S.A. (1988) - "Geomorphic Hazards - Problems of Prediction", Z. Geomorph., Suppl. 67, Berlin.
- Terzaghi, K. and Peck, R.B. (1948) - Soil Mechanics in Engineering Practice, John Wiley and Sons, Inc., New York.
- Thorne, C.R. (1982) - "Processes and Mechanisms of River Bank Erosion", Gravel-Bed Rivers, John Wiley & Sons, New York.
- Thurber Engineering Ltd., 1990. Pattison Creek risk assessment. Unpublished report to B.C. Ministry of Environment, Lower Mainland Region, Nov. 21, 1990.
- Valdiya, K.S. (1987) - Environmental Geology, Tata McGraw-Hill Pub. Co., New Delhi, India.

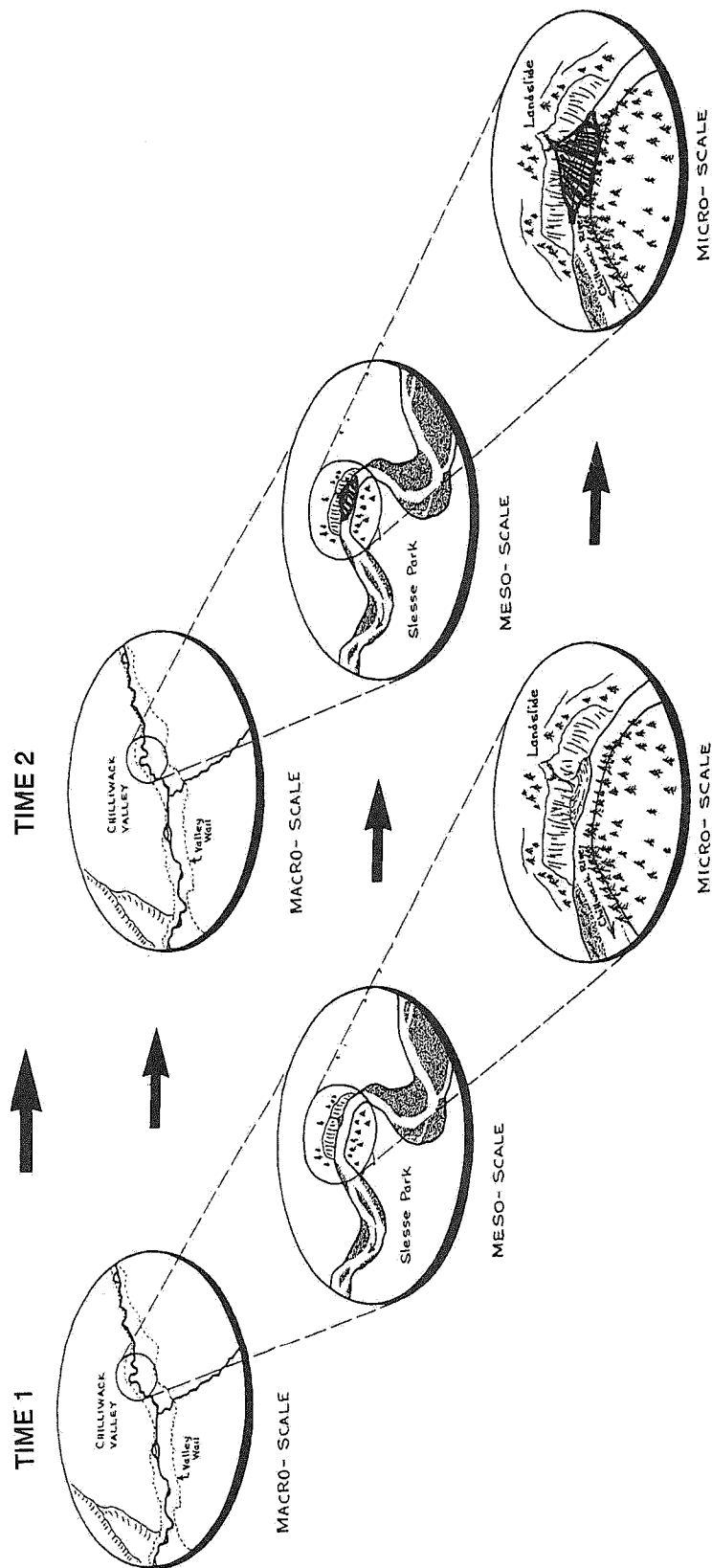


FIGURE 1
SCOPE OF GEO-HAZARD STUDIES
INVOLVING SPACE AND TIME



Figure 2
Path of Pattison Creek
Debris Torrent just bypassing
older landslide shown at left.



Figure 3

Arniko Highway - Nepal

**Highway was destroyed by debris torrent
in 1986 after being previously destroyed
by a glacier lake outburst flood in 1980.**



Figure 4

Diversion Structure on Sun Kosi - Nepal.

**The three left gates have been totally destroyed
by a debris torrent in 1986.
The three gates on the right were being opened
just prior to the flood surge.**

Precipitation Thresholds for Debris Flow Initiation in the Southern Coast Mountains of British Columbia

Michael J. Bovis & Thomas H. Millard
*Department of Geography, University of British Columbia
Vancouver, British Columbia*

Cycles of debris flow activity commonly occur during periods of prolonged, heavy frontal rainfall in the southern Coast Mountains, the most recent cycle occurring in November 1990. Although this general correspondence between rainfall and debris flows is well established, relatively little quantitative work has been conducted in the region to elucidate the details of this linkage. Only one detailed study has been conducted to date on precipitation antecedents to debris flows in this region (Church and Miles). An outstanding anomaly noted was the tendency for debris flow cycles to occur during storms of relatively low return period. However, the analysis was hampered to some extent by the general lack of precipitation data close to debris flow source areas.

In this paper, we report preliminary results from Coquitlam River basin on the meteorological conditions responsible for the November 1990 debris flows, for which we have fairly good rain gauge coverage. Back-analyses of selected debris slides which triggered debris flows in November 1990 are conducted to reconstruct the groundwater conditions at failure. Antecedent precipitation records are then used as input to a rainfall-recharge model to predict these same groundwater levels. The hydrologic model is calibrated with field permeability tests and actual records of soil-water recharge under natural rainfall conditions. We discuss the applicability of a similar model recently proposed by Keefer et al. for debris flow prediction in coastal California. The complications introduced by macro-pores (e.g. pipes) in triggering failures in Coquitlam basin are also discussed.

Characteristics of a Large Debris Flow Channel

R.J. Fannin

*University of British Columbia
Vancouver, British Columbia*

T. Rollerson

*Ministry of Forests, Vancouver Forest Region
British Columbia*

D. Hogan

*Ministry of Forests, Vancouver Forest Region
British Columbia*

D. Daust

*University of British Columbia
Vancouver, British Columbia*

Abstract

A large, active debris flow channel is located in the Tsitika Valley on Vancouver Island. While the valley is an environmentally sensitive watershed, debris flow activity at the site is a natural process of slope movement. The channel is nearly 2.5 km long from source area to depositional fan, and drops some 1000 m in elevation to the valley floor. Characteristics of the site are described with reference to the behaviour of coastal debris flows. Soils in the source area, the transportation and erosion zone, and on the depositional fan are classified with reference to particle size. An estimate of channel debris yield rate is made based on the field investigation.

Introduction

A long-term sediment monitoring program was initiated in the Tsitika River watershed in 1991 by the Ministry of Forests. In addition to monitoring the total sediment yield from the overall river basin, this program is designed to determine where sediment is produced and how it is transferred and stored within the watershed. A sediment source survey identified some 1211 sources, of which 89 were debris flows. Although this comprises only 7% of the total number of sources, preliminary estimates indicated that debris flows contribute over half of the total sediment load delivered to stream channels. The relative importance of debris flows to overall sediment production has also been documented in other coastal environments (Rood, 1984; Schwab, 1987).

One component of the monitoring program has involved characterization of a very large, active debris flow channel in the watershed. A description of debris movement on its fan is based on a survey of the channel in which the events occur. A classification of soils in the source area, in the gully and on the depositional fan is based on grain-size analysis. A video surveillance system has been installed to augment the survey data with continuing field observations of activity on the fan.

Site description

The Tsitika watershed is a part of the Nimpkish Provincial Forest, situated between Sayward River and Port Hardy on the east coast of Vancouver Island. Located in the Vancouver Island Mountain Ranges, it is an area of rugged terrain, ranging up to 1500 m in elevation. The study area was heavily glaciated during the Fraser Glaciation. Surficial soils were formed during and since the Fraser Glaciation. Drift of this glaciation includes glaciofluvial materials, till and, throughout Holocene time, colluvial materials. While the mid and lower elevation forests are dominated by Western Hemlock and Amabilis Fir, the higher elevation areas are occupied by Mountain Hemlock forests; there are limited areas of alpine tundra.

The site comprises a highly unstable gully headwall that is the major source of debris, a gully or flow channel, and a depositional fan. The active debris flow channel from source area to fan is nearly 2.5 km long. An air photograph of the site taken in 1987, Fig. 1, shows the depositional fan, the gully and the lower part of the extensive source area of the gully headwall. Debris flow activity at the site is not a consequence of forest harvesting operations. A ground survey of the site was used to develop the profile of the debris flow channel shown in Fig. 2.

The gully headwall area is approximately 650 m long. Thick glacial deposits overlying bedrock are cut by an open, deeply incised channel. Slope gradients at the back of the gully headwall are very steep, in the range 40° to 44° (85% to 95%). It comprises two distinct zones, separated by a significant rock step in a

narrow channel that is a feature of the bedrock control of the topography. The upper zone is very open, being some 25 to 100 m wide and 10 to 20 m deep, see Fig. 3. The lower zone is 15 to 30 m wide, and 4 to 17 m deep, becoming less markedly incised as it develops into the debris transport zone of the gully. Three sources of water were identified in the gully headwall area. Surface streamflow enters from the hillslope above. Groundwater flow is evident from gravels in the gully sidewalls. Snowmelt from trapped pockets in deposits of loose, unconsolidated debris is the third source.

The transportation and erosion zone is approximately 1600 m long. It is a channel of reasonably uniform cross-section, typically 10 to 15 m wide, that lies at a uniform gradient in the range 14° to 27° (25% to 50%). The transition from deeply incised channel in the gully headwall, to the main flow channel of the transportation and erosion zone, is controlled by hillslope topography and surficial soils. The upper and lower sections of this channel are quite different. Most of the upper section is scoured to bedrock, and is partially infilled with deposited boulders. Occasional levee deposits are present at curves in the path of movement. The lower section, before the gully opens out on to the depositional fan, also contains significant quantities of deposited boulders. However, erosion of the banks is occurring, and in some places trees have become lodged across the channel, impounding debris on their upstream side. Little scour to bedrock is evident. Rather the action of scour, where it occurs, is one of reworking fill material.

The gully exits from the forested hillslope on to the open slope of the valley floor, see Fig.4. The active debris fan overlies older

historic deposits. The surface of the depositional fan is 215 m long from apex to mainline roadside, some 20,000 m² in area, and lies at a uniform slope gradient of 14° (25%). Debris on the fan comprises sub-angular boulders, cobbles, and fragments of wood. Particle size sorting occurs on the fan, with larger boulders deposited near the apex. While fine sediment is washed off the surface of the fan, some fines are retained within the body of the material.

Soils

Soil samples taken from locations along the channel were classified according to the Unified Soil Classification System. The source area consists of thick deposits of glacial till overlying bedrock. The till comprises boulders and cobbles in a matrix of gravel, sand and silt. The coarse particles are sub-angular. The matrix is a well-graded material, typical of a glacial till, see Fig. 5. There are some fines in the clay-size fraction which exhibit little or no plasticity, and are likely rock flour.

Lower on the hillslope, soils in the transportation and erosion zone are more variable. Exposed cutbanks indicate the channel erodes through well-graded glacial deposits. The soil matrix includes clayey gravels and clayey silts. Near the valley floor there is evidence of fluvial sorting of the soils, with some interbedded lenses of sandy silts in deposits of colluvium.

The depositional fan comprises mainly boulders and cobbles. There are isolated deposits of fine gravels, sands and some silts. The deposits are typically sandy gravels on the upper part of the fan, and gravelly sands on the lower part of the fan.

Characterisation of debris movement

Any characterisation of debris movement in the source area, the transportation and erosion zone, and on the depositional fan must consider both the force to cause movement and the distance moved. Sidewall collapse of the glacial till into the channel, and subsequent creep of the loose material along the gully floor, are strongly in evidence. Conditions in the gully headwall suggest this downslope movement is assisted by streamflow, and to lesser extent by melt of trapped pockets of snow. Movement over long distances is less common. A levee deposit some 10 m long and 4 m high in the channel through the gully headwall observed in reach 13, at the end of the gully headwall, suggests such large events originate high in the source area, and are capable of travelling significant distances. It is likely these major events travel the complete length of the relatively steep, confined channel to the valley floor.

Morphological and vegetational evidence indicate that large changes have occurred on the surface of the depositional fan during storms that have a recurrence interval of between 10 and 20 years. The stream channel has shifted laterally across the surface of the fan during these infrequent, large magnitude storms. The contemporary channel has been in its present location since the early 1960s, approximately. A mainline log hauling road was built across the fan in 1981 and since that time there has been careful documentation of debris movement onto the road. Typically, storms which recur with a frequency of between 1 and 3 years cause minor changes to the fan that are associated with localized bank erosion.

Although these are relatively frequent events, they contribute substantial amounts of debris. The last major event in November 1990 delivered debris, in a series of pulses, onto the road. The quantity of debris on the fan was such that, following regrading of the road, the running surface was observed to be 2.5 m higher than before the storm.

Slope gradients at the back of the gully headwall are in the range 40° to 44° (85% to 95%), and are generally between 50% and 70% (27° and 35°) in this source area. The range of slope gradients in the transportation and erosion zone is between 14° and 27° (25% and 50%). The surface of the depositional fan is at a uniform gradient of 14° (25%). A review of slope gradients in gullies subject to debris flow activity on similar unlogged terrain is provided by VanDine (2), for the Howe Sound region. Initiating angles range between 20° and 57°, with steeper gradients associated with smaller drainage areas. Typically slopes greater than 10° are necessary to maintain movement of debris in a confined channel, and the average gradient (excluding any depositional fan) of events in the Howe Sound region is from 13° to 35°. The average gradient of the site in the Tsitika Valley, excluding the depositional fan, is 24°.

Deposition of material in debris flow events usually occurs at gradients less than 10°, and the range of fan angles in the Howe Sound region is 8° to 18°. The range bounds that of the site in the Tsitika Valley, which is 14°. While it is recognized that interpretation of such slope gradients is dependent on confinement of the gully, and type and water content of the debris, this comparative review of the site confirms that events initiating in the source area are

likely to travel to the valley floor and deposit on the existing fan.

The magnitude of an event may be described by the total volume of debris material transported onto the fan, expressed by a channel debris yield rate (m^3/m). Hungr et al. (1) report derived channel debris yield rates for five documented events of known magnitude in the British Columbia coast range. The values lie between 5 and 18 m^3/m . An estimation of channel debris yield rate can be made for the site in the Tsitika Valley, based on the length of the transportation and erosion zone, and with reference to the measurements of transported fill material resident in this part of the channel. As such, it does not account for any contributing material from the source area and any erosion of the flow channel by the event itself. Rather the estimation simply implies that all debris resident in the channel is deposited on the fan, and is replaced by material from the source area and additional erosion of the channel. Using this approach, which is based on a concept of storage, leads to a predicted maximum channel debris yield rate of 27 m^3/m .

Work on debris flow channel morphology in the Queen Charlotte Islands (QCI), Fannin and Rollerson (unpublished), suggests there are two quite distinct types of channel or channelized debris flows: one is characterized by channels which remain relatively steep for their entire length (gradients generally greater than 15 degrees) while the other is characterized by channels which, though steep in their initial sections, have relatively gentle gradients in their lower reaches (generally less than 15 degrees). These two main types can be subdivided into single channel and multiple channel (more than

References

- (1) Hungr, O., Morgan, G.C. and Kellerhals, R. 1984. Quantitative analysis of debris torrent hazards for design of remedial measures. *Can. Geo. J.*, 21, pp. 663-677.
- (2) VanDine, D.F. 1985. Debris flows and debris torrents in the Southern Canadian Cordillera. *Can. Geo. J.*, 22, pp.44-68.
- (3) Rood, K.M. 1984. An aerial photograph inventory of the frequency and yield of mass wasting on the Queen Charlotte Islands, B.C. B.C. Min. of Forests, Land Management Report No. 34, 55 pages.
- (4) Schwab, J.W. 1983. Masting wasting: Oct-Nov 1978 storm, Rennell Sound, Queen Charlotte Islands, B.C. B.C. Min. of Forests, Research Note No. 91, 23 pages.
- (5) Fannin, R.J. and Rollerson, T. (unpublished). Debris Flows: Some Physical Characteristics and Behaviour. A paper submitted to the *Can. Geo. J.*, January 1992.

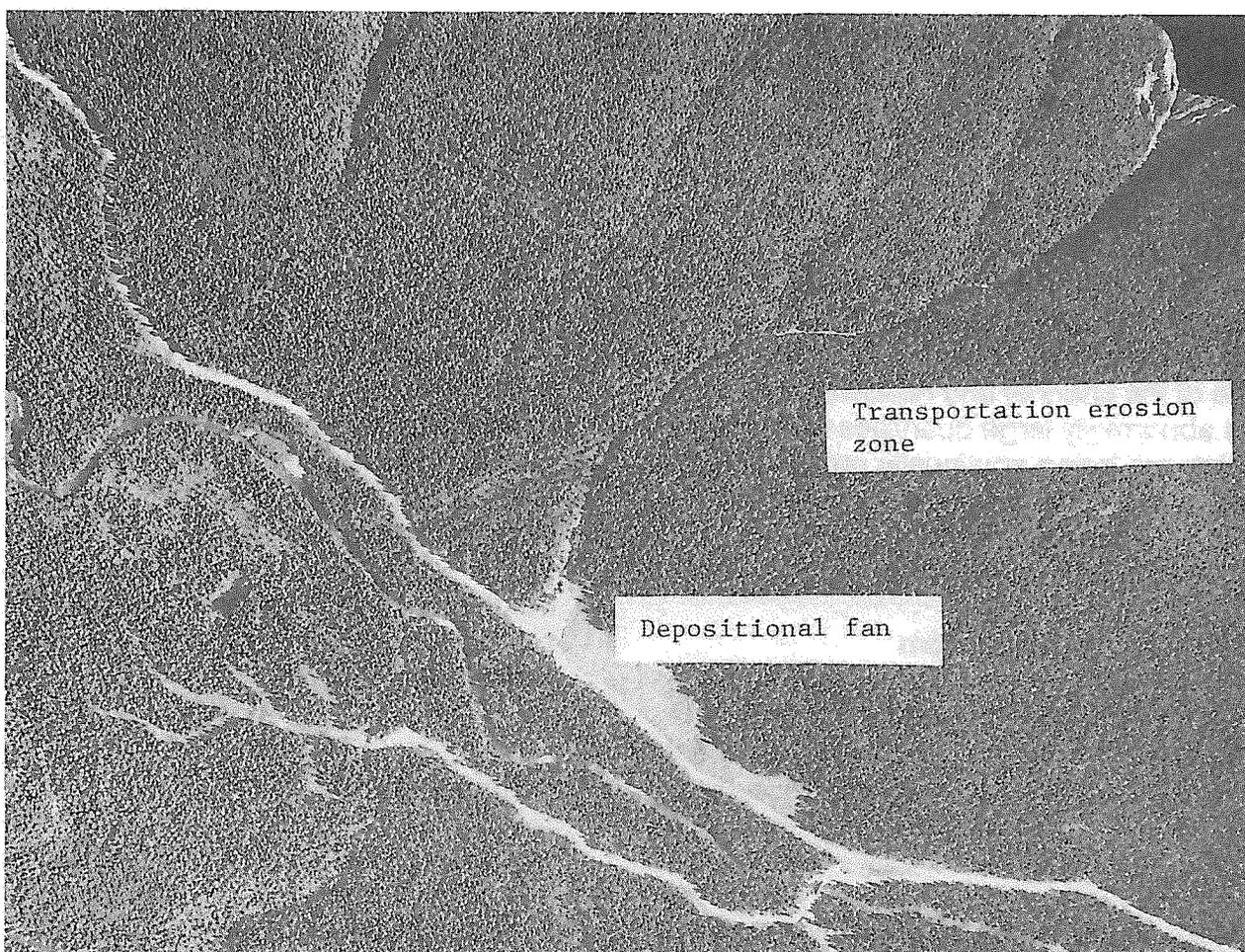


Figure 1. Air photograph of the site

one debris flow coalescing to form a larger flow) events. The two main types show somewhat different gradients in the deposition zone: the continually steep channels have a deposition of fan exhibiting an average gradient of 12° , while the steep/gentle channels exhibit an average gradient of 6° . The second type usually produces larger debris flows, with much longer runout zones (70 versus 190 meters). The characteristics of the Tsitika site would place it in the steep channel and steep fan category found in the QCI. Yet the channel is very long, hence the potential debris flow event size is large, and the runout zone is commensurately longer (200+ m). Runout length for the QCI debris flows was found to be strongly related to the size (volume) of the event. A predicted maximum debris yield rate of $27 \text{ m}^3/\text{s}$ for the Tsitika site is comparable with that of 18 events documented in similar channels in the QCI for which the mean yield is $12.4 \text{ m}^3/\text{s}$ and the standard deviation is $13.2 \text{ m}^3/\text{s}$. The large channel debris yield rate predicted for the Tsitika site is essentially a function of the large size of the channel and headwall area, and the abnormally large quantities of sediment which are being continually recruited from the deep, unstable glacial tills in the headwall area.

Video surveillance system

A video camera has been installed at the site to record activity on the depositional fan. It is used to make a daily recording, and can also capture periodic events. The control system for daily recordings comprises a timer circuit that connects directly to the circuit board of the camera through a series of relays. It allows for a recording of designated duration to be made at a designated time interval. The

existing setting of the control system is for a recording of 60 seconds duration to be made at a time interval of 24 hours. Power for the timers, the video camera and the relays is provided by a 12 V battery. The control system for periodic event recordings comprises a detector switch that is mounted some distance above normal streamflow in the channel, such that it will be triggered by passage of debris. The periodic event recording of a large debris flow moving on to the depositional fan will be used to support decisions concerning hazard control and mitigation, and to better understand sediment yield from the site.

Summary

The site is characterized by an extensive source area, a channelized transportation and erosion zone, and a large depositional fan. Soils in the source area are loose and very unstable. Water ingress is from surface and groundwater flow. The site is prone to debris flow activity and it is likely a major event will flow, without stopping, to deposit where the channel opens and the gradient flattens out onto the depositional fan. Prediction of event yield and travel distance for debris flows is facilitated by field investigation and comparison with other documented events, with emphasis placed on channel storage and channel width and gradient.

Acknowledgements

The work described in this paper has been supported by a research contract from the Ministry of Forests Research Branch. The field survey was performed by R.J. Fannin and D. Daust. Laboratory testing was performed by D.M. Raju.

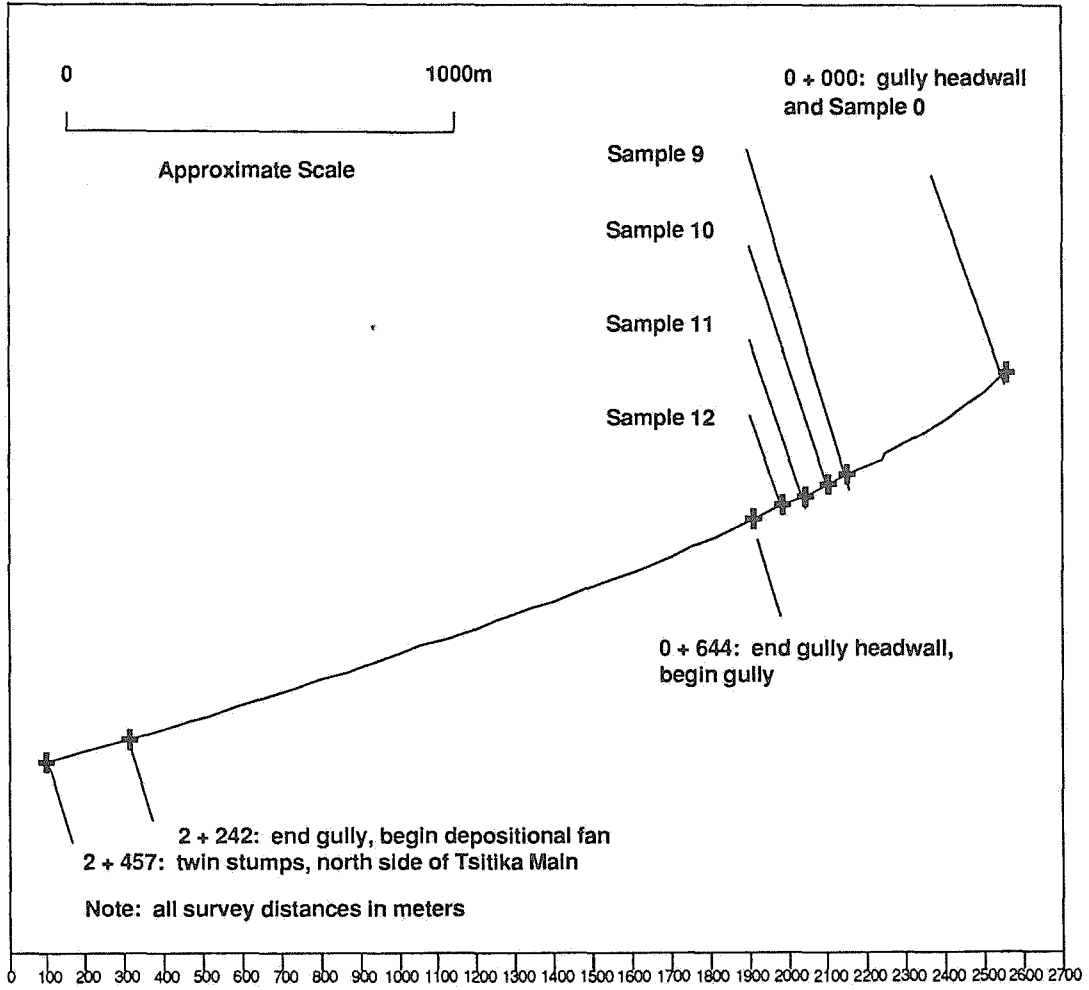


Figure 2. Profile of the debris flow channel

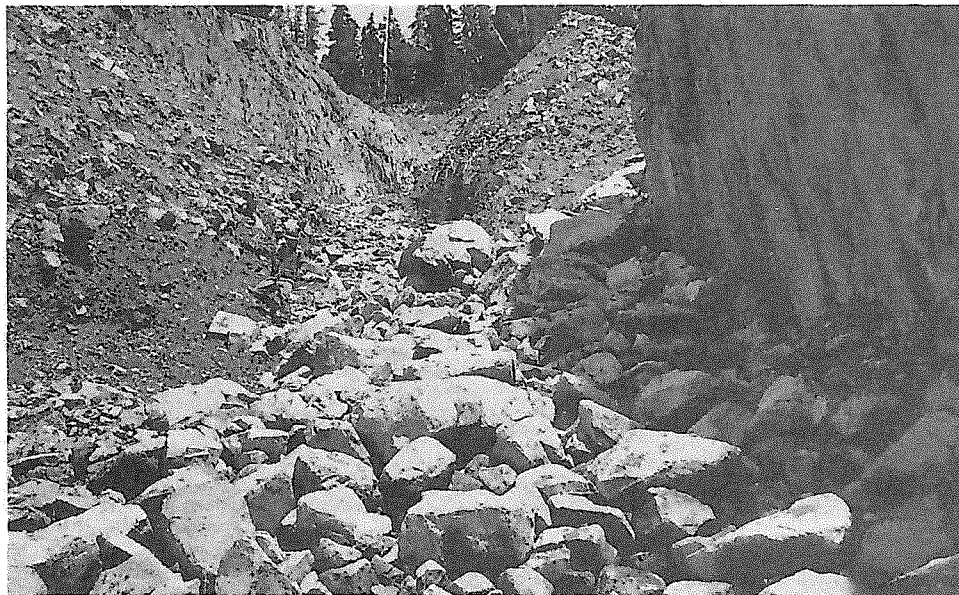


Figure 3.
Source area

Figure 4.
Soils matrix of
the source area

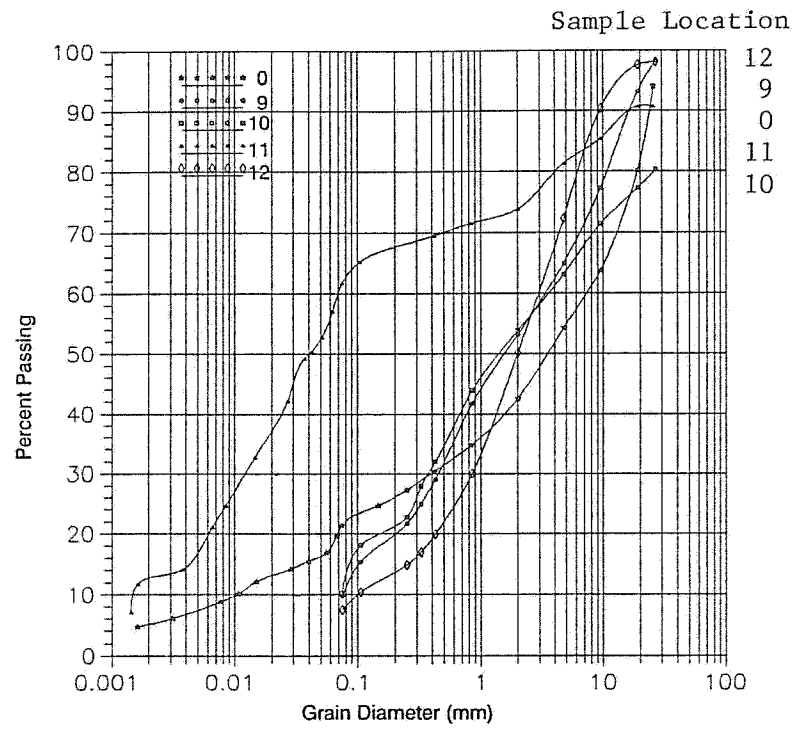


Figure 5. Depositional fan

Session 5B
Surface Hydrology and
Debris Flows
(continued)

Philpott road, a thick terrace of interbedded tills, lacustrine silts and glacial gravels typical of ice contact deposits is exposed in creek sections and slide scarps.

The overall topography of the hillside above Philpott Road is remarkably uniform and reflects an almost complete cover of colluvium overlying the bedrock and glacial deposits. As normally a high proportion of the precipitation infiltrates to recharge the groundwater system, surface streams are small and intermittent on the slopes and upper plateau. Field investigation by the authors, and earlier by a Ministry of Forests (MOF) team, showed that a poorly defined surface drainage path leads from the clearcut plateau to the area near the debris avalanche head scarp.

Broadly, the ground water regime in the slopes above Belgo Creek is simple with recharge on the plateau and higher slopes through permeable jointed bedrock, colluvium and glaciofluvial deposits, and discharge as springs on the lower slopes through coarse colluvium and glaciofluvial deposits. However, locally, the ground water system is much more complex and related to outcrop distribution, fracture patterns, and the presence of permeable sands and gravels or impermeable till.

2.2 Logging Activities

Above the crest of the hillside 300 ha were clearcut between 1983 and 1988 with conventional ground skidders used for yarding. The slopes between the cutblock and Philpott Road at the base of the mountain were selectively logged before 1959. Additionally, there are more recent local clearcut blocks including the one through which the debris avalanche passed.

Access roads to the plateau were originally constructed over 25 years ago and those to the north side of the plateau were recently deactivated with water bars. However, the older logging roads and trails constructed prior to 1963 have not been deactivated.

3.0 The 1990 Debris Avalanche

The 1990 debris avalanche travelled 800 m down the hillside above Belgo Creek on an average slope of 18° (Figure 2b). As the avalanche travelled from El. 1250 m to El. 975 m over an estimated period of 45-60 seconds, speeds were estimated to be in excess of 10 m/sec. The avalanche was triggered by local slope failures on a 35° slope some 15 m above a forest access road to the plateau area. These failures lie in an area of existing slope disturbance where mature cedar trees estimated to be in the order of 60-100 years old show deformation or tilting. Up to one metre of gravelly colluvium overlies very closely sheared and jointed bedrock in this area. Locally, smooth joints form the bedrock surface on which the colluvium rests. The thick roots of the forest barely penetrate the underlying soils and rock.

For most of the length of the avalanche the dense tree growth has been entirely removed although locally some stumps remain in their growth position. Possibly as a result of reduced energy levels at a change of slope, the avalanche split into two at elevation 1020 m, leaving an island of standing trees. Colluvial deposits, and locally non-cohesive glacial deposits, were mobilized by the failure but the dense underlying tills remained largely intact.

Debris deposition began immediately below Philpott Road where the overall slope reduces from 18° to 5° . The avalanche debris lies directly on glaciofluvial sands and gravels and test pits failed to reveal evidence of previous slide deposits. The deposited material consists of silty sandy gravel to gravelly sand with occasional cobbles and boulders, and a high proportion of organic material. The thickness reaches one metre but is 30-40 cm on average. Logs up to 60 cm diameter and 5 m length were carried to the periphery of the debris fan. Thin mud flows extended from the glaciofluvial terrace, down to the lower elevation of the Belgo Creek floodplain. All eyewitnesses attest to

the extreme mobility and fluidity of the material in the first hours after the event and report that the rescuers were wading waist deep in the deposited material.

4.0 Hydrological Effects of Logging

4.1 General

The effects of forest harvesting can be considered under several categories, principally: the effects of the logging or removal of trees; the effects of associated activities such as road building and yarding; the effects on the soil structure; and the effects on the hydrological regime and microclimate. The effects of root decay and disturbance from the construction of access trails may have weakened the soil structure and played a role in the propagation of this failure down the slope (Figure 3).

4.2 Logging and Runoff

There are numerous studies with widely varying conclusions on the effects of tree removal on runoff under average conditions. For very large floods Dyness (2) and Harr (3, 4) found that the heavy precipitation would soon saturate any unsaturated areas and make any differences in interception and runoff between cut and uncut areas negligible. On the hillside above Philpott Road the antecedent precipitation had totally saturated the area. Even two weeks after the slide, observers reported pools of standing water in the holes created by blown down trees in the area above the cutblocks. Under such conditions it is highly unlikely that the presence or absence of tree cover would have had any direct effect on runoff.

4.3 Road Construction and Runoff

Logging road construction on the plateau is considered to have caused the diversion of up to 20% additional drainage into the catchment where the debris avalanche occurred. However, it should be noted that even with this diversion, a channelized debris flow occurred in the neighbouring catchment from which the flow had been diverted. In addition to this effective increase in catchment area, the pres-

ence of the access road to the north end of the cutblock apparently diverted road and hillside drainage into the path of the debris avalanche part way down the slope. There is a possibility that this may have been instrumental in allowing a larger avalanche to develop than would have been otherwise possible.

4.4 Effects on Microclimate

In the night and early part of the morning of 12 June, snow fell at higher elevations in the general area and on the hillside above Philpott Road. However, in the forested areas this snow was caught in the forest canopy and melted as temperatures within the canopy were slightly above freezing. However, in the clearcut on the plateau, sufficient snow accumulated that a shallow cover remained over 50% of the area until around 5:30 pm despite heavy rainfall during the day. This effect was examined with a water and heat balance model by P. Beaudry in a separate study by the Ministry of Forests (5). This study found that under the prevailing temperature conditions of -1°C to 4°C snow could have accumulated at rates of 0.5 to 4 mm/hr. of water equivalent (0.5 to 4 cm/hr. snow depth) during the periods from 1:00 - 9:00 am on 12 June 1990. Thus the presence of the clearcut changed the forest microclimate sufficiently to allow significant snow accumulation when none or very little would have otherwise occurred.

5.0 Climatology

5.1 General Meteorological Conditions

The failures at Philpott Road are considered to be closely related to the weather patterns and thus a detailed analysis has been made of precipitation patterns in the area. This work extended the frequency analysis of 1-10 day precipitation by the Ministry of Forests (5) and utilized data from 13 stations in the southern Okanagan basin.

May and June 1990 were two very wet con-

secutive months throughout much of British Columbia. An October 1990 report (6) by B. Beal of the Atmospheric Environment Service (AES) summarized the situation as follows:

"For most of May an offshore ridge of high pressure maintained a fairly moist northwesterly flow over most of British Columbia. Conditions were generally unsettled with showery precipitation.

Towards the end of May (about the 22nd) the first of three vigorous "cold" low pressure systems arrived just off the Washington coast. ... Each system generated a moist southerly flow of air over the southern interior. Then as associated frontal systems moved across the interior, numerous heavy instability rainfall events were triggered. ... During the first 10 days of June, four "cold" lows migrated eastward across the province. The last "cold" low of this series culminated in the exceptional heavy rains across the interior which ended on about June 12th ..."

From an analysis of the regional precipitation patterns and local geography, the AES station at McCulloch, was chosen as the most representative of conditions on the hillside above Philpott Road. At El. 1250 m the McCulloch station is nearly at the same elevation as the plateau and only 10 km distant. Fortunately it also has one of the longer records in BC with 67 years of data available.

5.2 Frequency Analyses

5.2.1 One to Ten Day Storm Durations

From the 1 to 10 day frequency analysis of the six Okanagan Basin stations shown in Table 1, it appears that the meteorological conditions for early June 1990 had the capability of producing up to 1:100 year events. However, with respect to the Philpott Road area, the data for the Joe Rich Creek and McCulloch stations indicates that there was a multi-day event or sequence of events which had a return period of 15 to 25 years. During this multi-day event there was no one day which received more precipitation than would occur on average once

in three years. The recorded data suggests that the unusual aspect of the early June precipitation was not that there was unusually heavy precipitation on any one day, but that there was a sequence of days with heavy, but not unusual, precipitation.

5.2.2 One to Forty Day Storm Duration

As it was considered that it might take longer than 10 days to raise the piezometric pressures in the soils or bedrock to critical levels, the frequency analysis was extended from a duration of 10 days to 40 days. The precipitation amounts for the various durations were analyzed for McCulloch for both the May - June period, and for the year as a whole. For this seasonal analysis, it was found that the 1990 data was slightly outside the 95% confidence limits and was therefore excluded from the analysis. On an annual basis, the 1990 data was included in the analysis as it plotted very close to the 1982 data at the edge of the confidence limits.

On the seasonal basis the return period for the 22 day period ending on 12 June was estimated as 1:250 years. On an annual basis the maximum return period dropped to 1:100 years. In light of the long term record at McCulloch, the 95 % confidence band width was only 15% and 12% for the May-June and annual analyses, respectively. With respect to whether the 1990 event should be analyzed on a seasonal or annual basis there were three significant factors: 193 mm of precipitation fell in the June-July period in 1982 in comparison with 177 mm in 1990; over the years an extended heavy rainfall period has occurred in every month from May to December, and seasonal snowmelt contributions are of less importance for long duration periods. It was therefore concluded that the 1990 antecedent precipitation should be considered as part of an annual series with a return period of approximately 1:100 years.

5.2.3 Compounding Factors

In addition to antecedent precipitation, the occurrence of slope failures can be related to other climatological and hydrological factors which would have their own probabilities of occurrence. This would extend the return period of the 1990 debris failure event beyond the minimum of 1:100 considered appropriate for the antecedent precipitation. Such additional factors could include the combination of antecedent precipitation and a major storm event of intensity and duration of the level of the 12th of June 1992 event as discussed by Wieczorek (7), or a rain-on-snow event as described by Church and Miles (8). As the one day rainfall for 12 June had no more than a three year return period, the hydrological events preceding the debris avalanche are considered to have a combined return period of 1:300.

5.2.4 Local Storm Cells

The above conclusions are based on the precipitation records at gauged sites. As the gauges are sparsely located, local unrecorded events could also have occurred giving intense rainfall to small areas. Rainfall intensity can be important in the initiation of certain types of debris flows and a complete discussion has been given by Wieczorek (7). AES records for Kelowna show that such intense local cells were typical under the meteorological conditions of early June 1990. In fact MOF staff on their way to Philpott Road, around noon on 12 June 1990 did not encounter rain on Highway 33 from Kelowna but found it raining heavily when they turned off the highway onto Philpott Road. At 2:30 pm, the same time as the debris avalanche, a MOF road foreman found the main creek that drains the clearcut to the south of the slide area was experiencing a flash flood and at 3:30 pm the creek was described as a raging torrent.

5.3 Climate and Natural Hazards

One of the significant events of the 11-12 June 1990 period is that a snowfall of several centimetres occurred over the clearcut area on the

plateau and extended down into the forested area. This is considered to be of importance as snowmelt from rain-on-snow events, and/or rising freezing levels, are amongst the most frequently mentioned causes which can trigger debris flows. Church and Miles (8) have reviewed six of the debris flows that occurred during the 1980's in southwestern British Columbia. Their evidence is that there is no single factor, for example, antecedent precipitation, which must always be present. However, they have recognized a number of factors which have been important during particular events, including:

- Locally intense short period precipitation
- Rain-on-snow or snowmelt due to rapidly rising freezing levels
- Antecedent precipitation
- The occurrence of a triggering precipitation event. This need not be unusually large as studies show only a slight correlation between extreme 24 hour precipitation and debris failures.
- The influence of the local topography in constricting air flow and causing it to impinge on steep mountain slopes.

From their case studies, Church and Miles found that usually only one or two of the above factors were present in any given event.

From all of the discussions, it can be seen that the first four factors were likely applicable to the June 1990 event. There is a possibility that the fifth factor might also be applicable. The second factor is the only one which could have changed over time as a result of forest harvesting activity and which might have resulted in the event occurring in 1990 rather than at a previous time. With respect to this rain-on-snow event, Beaudry (5) has shown in his analysis that there likely was a significant increase in the depth of snow on the plateau above Philpott Road as a result of the clearcut. Thus the occurrence

of the rain-on-snow event and its magnitude are considered to be influenced by logging and forest management decisions on the size of clearcut. This is not to say that forest harvesting activities caused the debris slide but that they did influence one or more of the critical causative factors.

6.0 Discussion

With respect to debris flows in the Lower Mainland and along Howe Sound, Church and Miles (7) have mentioned six events from 1980 to 1983. The precipitation associated with the these events generally had durations of several hours to three days. There were two exceptions to this where the antecedent precipitation may have had an influence: (a) the Christmas 1980 events around Hope when 152% of normal precipitation fell in December and (b) the Charles Creek event of 15 November 1983 before which there were 19 days with continuous precipitation. Return periods for the precipitation associated with the event were of the order of 1:1 to 1:4 years in four cases, 1:9 years in one case and 1:100 years for the New Year's 1984 event in the Coquihalla Valley near Hope, BC.

In coastal Alaska, Sidle and Swanston (9) have reported debris failures after 24 hour precipitation with 1:1.5 to 1:3 year return periods. Sidle (10) has reported that Pierson (11) in New Zealand and Harr (12) in Oregon found failures under similar conditions. Similarly Sidle (10) reported that on the Queen Charlotte Islands, Schwab (13) had found and compared several failures in logged and unlogged areas after a major storm with a 1 in 5 year return period.

7.0 Conclusions

The 23,000 m³ debris avalanche was a first time event. However, examination of the terrain above Philpott Road shows that it is a likely area for debris flow and debris avalanche activity. The slopes are glacially oversteepened, have a cover of glacial and/or colluvial soils and are subject to seasonally heavy rainfall and snowmelt runoff. The slopes in June

1990 were also saturated by high antecedent precipitation (1:100 year) which raised pore pressures in the soil and rock. Under these conditions of existing marginal stability and saturation of the hillside slopes, rapid runoff from snow accumulation in the clearcut and from locally heavy rainfall served to initiate and propagate the debris avalanche. Although past slides had not travelled beyond the zone of initiation, this avalanche was able to propagate down the slope due to weakening of the slope by past logging activities, and due to runoff directed onto the slope from forest access roads.

Debris events in coastal British Columbia are often linked to short duration (1-3 days) rainfall with short 1-5 year return periods. In contrast the return period for this first time debris avalanche was estimated as between 300 and 1000 years based primarily on the combined probabilities of the antecedent precipitation (1:100) and the storm of 12 June 1990 (1:3) and an allowance for other factors such as locally heavy rainfall and rain-on-snow events.

ACKNOWLEDGEMENT

The authors acknowledge the permission of the Provincial Emergency Program to publish this paper. They are also grateful for the cooperation of the Ministry of Environment and Ministry of Forests Investigative Team during the study plus the helpful advice of their colleague, Mr. Graham Morgan, P. Eng.

REFERENCES

1. Golder Associates Ltd., 1991 Report to the Provincial Emergency Program on the Geotechnical Study of Slide and Debris Flow Potential Philpott Road, Kelowna, BC.
2. Dyrness, C. T., 1967. Mass soil movement in the H. J. Andrews Experimental Forest. U.S. Dep. Agric., Pac. Northwest For. Range Exp. Stn., Portland, Oreg., For. Serv. Res. Pap. PNW-42, 12pp.

3. Harr, R. D., Harper, W. C., Krygier, J. T. and Hsieh, F. S., 1975. Changes in storm hydrographs after road building and clearcutting in the Oregon Coast Range. *Water Resour. Res.*, 11(3), 436-444.
4. Harr, R. D., Levno, A. and Mersereau, R., 1982. Streamflow changes after logging 130-year old Douglas-fir in two small watersheds. *Water Resour. Res.*, 18(3), 637-644.
5. BC Ministry of Forests, 1990. Investigation into the Cause of the Destructive Debris Flow, Joe Rich - Belgo Creek area, June 12, 1990. Forest Service Investigation Team.
6. Beal, B., 1990. A Summary of the heavy rainfalls over British Columbia during the months of May and June 1990. Atmospheric Environment Service, Pacific Region.
7. Wieczorek, G. F., 1987. Effect of rainfall intensity and duration on debris flows in Central Santa Cruz Mountains, California, *Reviews in Engineering Geology*, Geological Society of America, Volume 7, pp. 93-104.
8. Church, M. and Miles, M. J. Meteorological antecedents to debris flow in Southwestern British Columbia: Some case studies. *Reviews in Engineering Geology*, v. 7 (1987): 63-79.
9. Sidle, R.C., and D. N. Swanston 1982, Analysis of a small debris slide in coastal Alaska, *Can. Geotech. J.* 19, 167-174.
10. Sidle, R. C., Pearce, A. J., O'Loughlin, C. L., 1985. Hillslope Stability and Land Use. *Water Resources Monograph Volume II, Series II*. American Geophysical Union.
11. Pierson, T. C., Piezometric response to rainstorms in forested hillslope drainage depressions, *J. Hydrol. N. Z.*, 19 (1), 1-10, 1980.
12. Harr, R. D., Water flux in soil and subsoil on a steep forested slope, *J. Hydro-l.*, 33, 37-58, 1977.
13. Schwab, J. W., Mass wasting: October-November 1978 storm, Rennell Sound, Queen Charlotte Islands, British Columbia, Publ. 91, 23 pp., Ministry of For., Victoria, Canada, 1983.

TABLE 1--

Return periods for May/June 1990 precipitation events

Meteorological Station	Return Period (years)										Date Maximum Events Ended
	1 Day Event	2 Day Event	3 Day Event	4 Day Event	5 Day Event	6 Day Event	7 Day Event	8 Day Event	9 Day Event	10 Day Event	
Beaverdell (North)	2	10	10	20	25	30	100	100	90	80	June 1 & 3
Joe Rich Creek	3	10	25	20	20	15	25	15	25	35	June 10 - 12
Kelowna Airport	60	60	40	60	40	35	30	100	50	100	June 4 & 10
McCulloch	4	10	25	35	25	15	25	25	15	25	June 11 - 13
Penticton Airport	15	15	25	25	25	25	50	35	25	50	June 3 & 10
Vernon Coldstream Ranch	100	25	35	50	35	50	>100	100	75	90	June 3

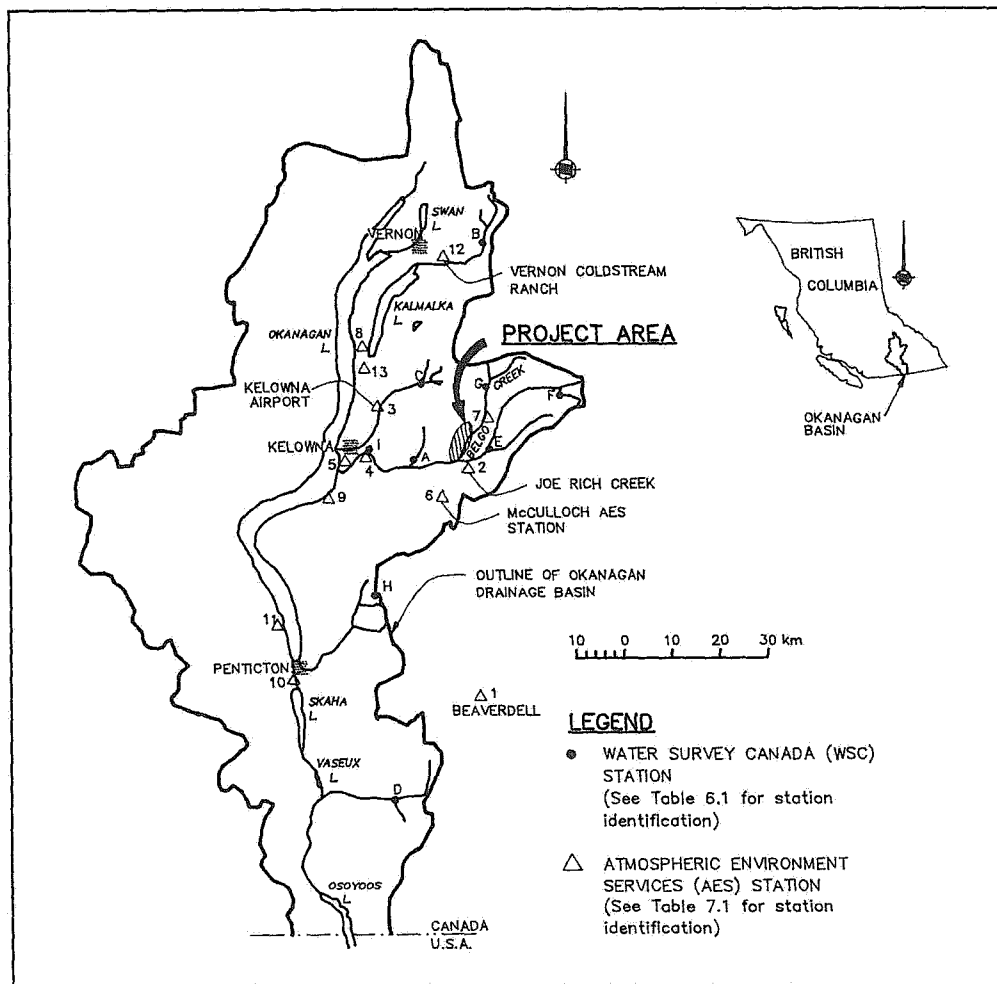


Figure 1. Location of meteorological stations in the Okanagan Basin

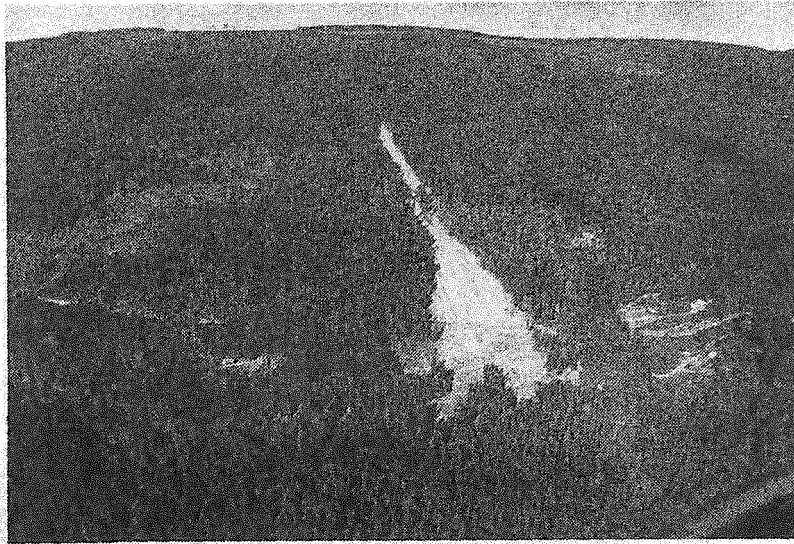


Figure 2a Debris avalanche showing clearcut areas

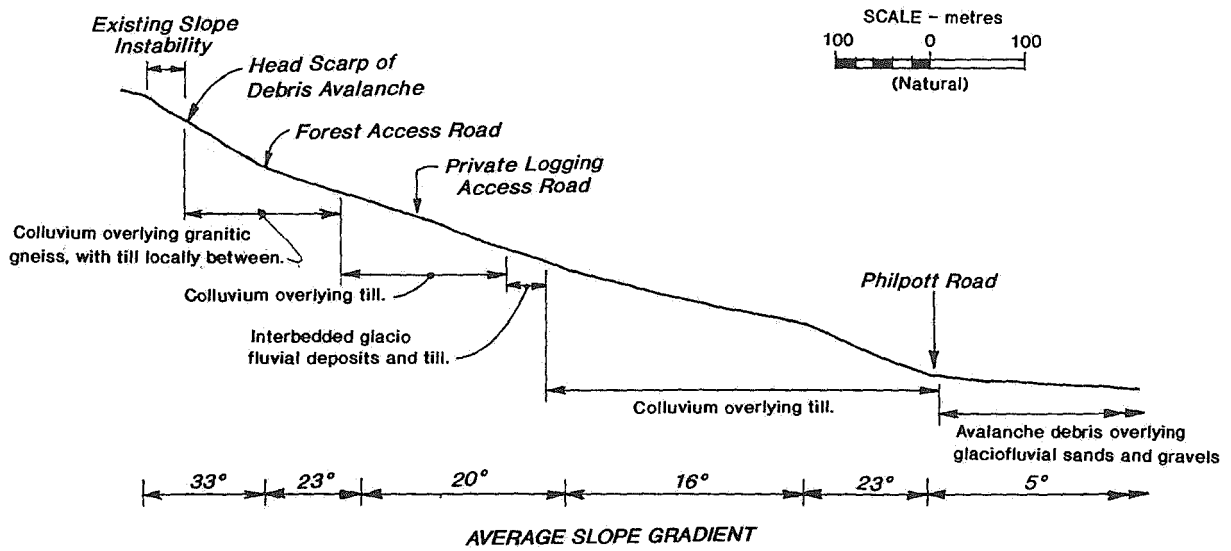


Figure 2b. Section through debris avalanche

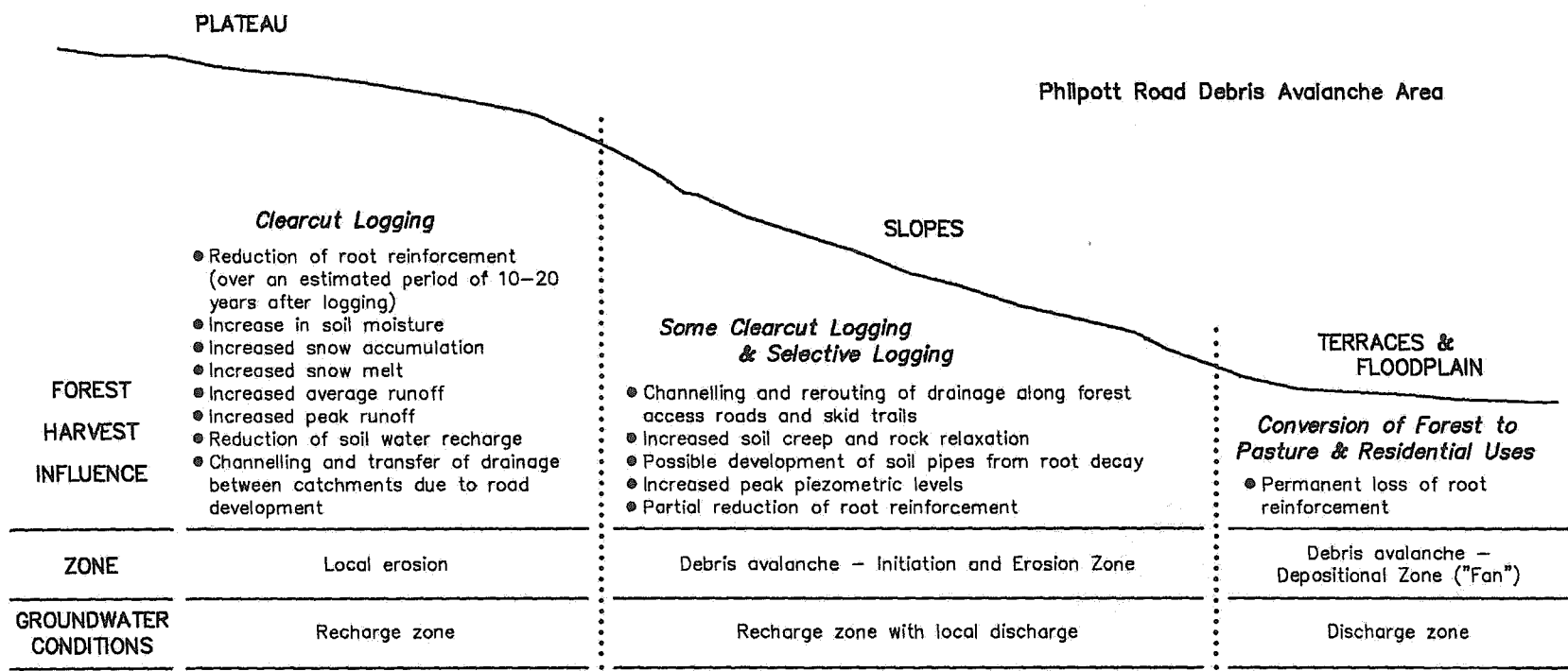


Figure 3 Schematic diagram showing influence of forest harvesting

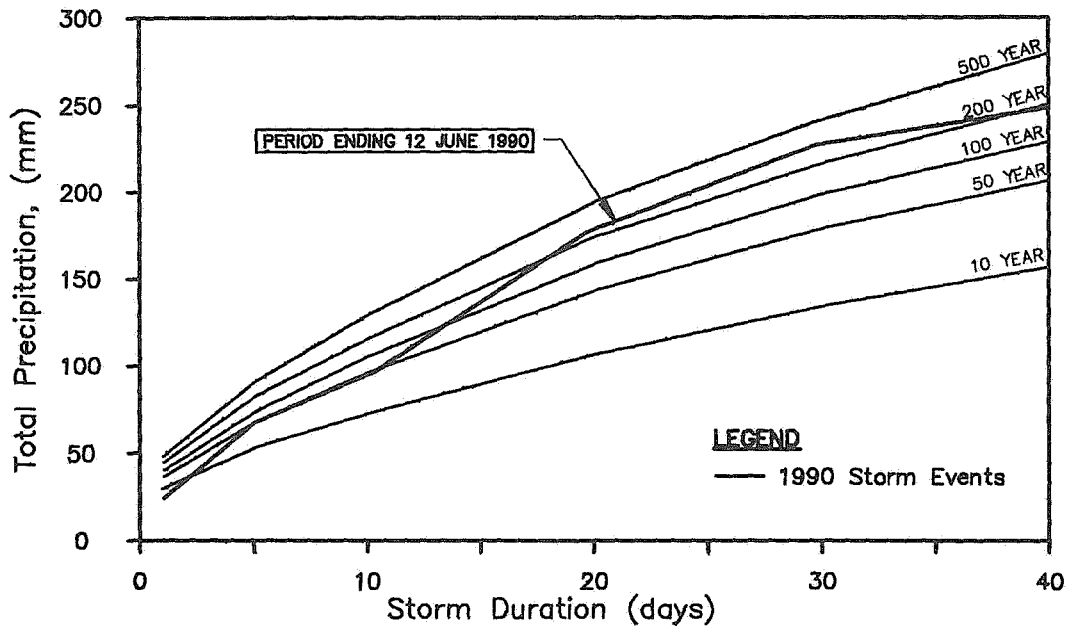


Figure 4a Precipitation-duration-frequency curve
May to June - 1 to 40 days
McCulloch Station

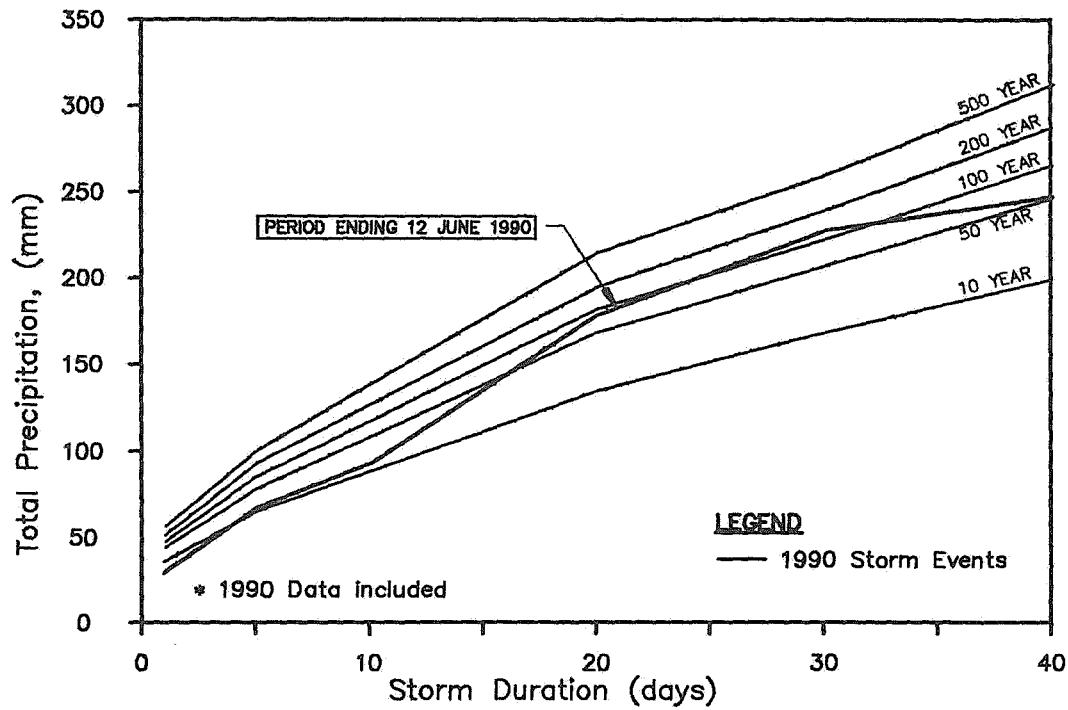


Figure 4b Precipitation-duration-frequency curve
Annual - 1 to 40 days
McCulloch Station



**Geogrid Reinforced Soil and Lock-Block Debris Deflector
for Transmission Towers:
B.C. Hydro's Revelstoke to Ashton Creek
500 kV Transmission Line
Tower No. 75/2
20 km East of Enderby, British Columbia**

B.C. Anderson,
B.C. Hydro, Vancouver, British Columbia

T.R. Haigh
*Nilex Geotechnical Products,
Burnaby, British Columbia*

C.D. Smith
*City of Vancouver, Engineering
Vancouver, British Columbia*

A. Introduction

In June of 1990, numerous debris flows occurred on a south facing mountain slope, 20 km east of Enderby, B.C., during a period of intense rainfall. A local resident measured 140 mm of rainfall in a 30-hour period. Four BC Hydro transmission towers were partially or completely destroyed by debris flows

which temporarily cut off power from the Revelstoke Dam. One of these towers, No. 75/2 of Circuit 5L75, was later rebuilt in the same vicinity. A geogrid reinforced soil and concrete block debris deflector was built in 1991 to protect this tower from future flows. See Fig. 1.

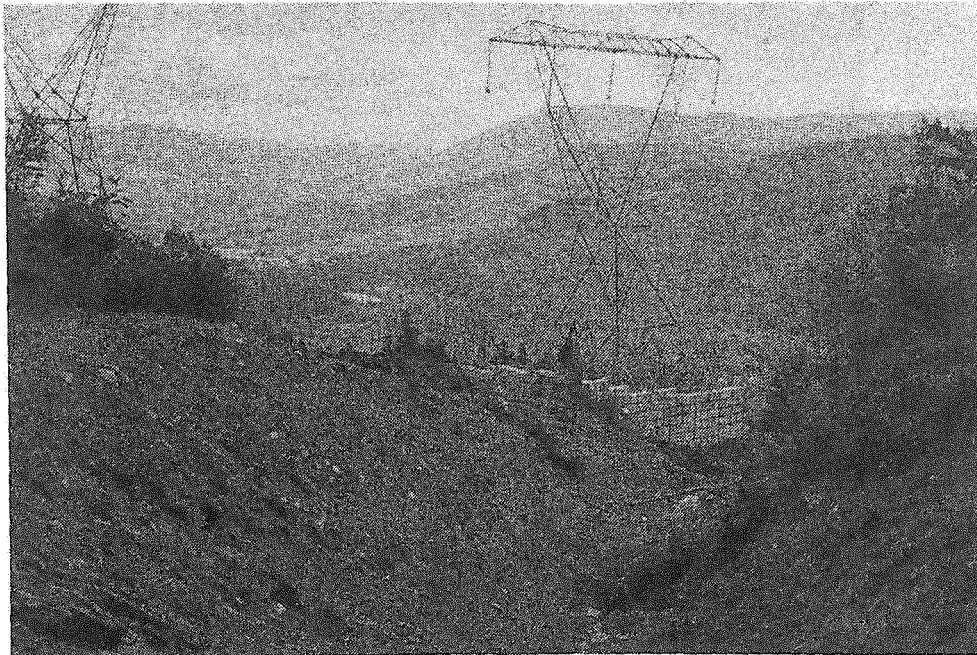


Fig. 1. Looking down channel to debris deflector at Tower 75/2.

Numerous debris flows were initiated at many locations on the mountain slope, over a width of 4 km, just west of Falls Creek and north of Mabel Lake Road. The mountain slope rises 975 m above the valley bottom, at an overall slope of about 23 degrees. The bedrock, forming the slope, consists of metamorphic rocks belonging to the Monashee Group. It is typically thinly mantled with colluvium and other surficial deposits (1 to 5 m), with few bedrock exposures. Portions of the area had been logged in the past and since covered with a dense regrowth of trees and vegetation. Several debris flows originated 2/3 of the way up the slope, in heavily treed areas, and reached Mabel Lake Road below, resulting

in the destruction of private property at the base of the slope. The larger flows were channelized (debris torrents) with many of the smaller ones being planar (debris flows)[1]. The slide debris consisted mainly of saturated, brownish, fine-grained soils, angular cobbles and boulders, and an irregular array of broken trees that were typically debarked. Some of the smaller flows, in cleared areas, might be more properly termed mudflows (mainly fine grained material), but for the purposes of this report all further references will be to debris flows. Fig. 2 shows the damaged tower with a guy wire attached to a bulldozer after the flow event in June 1990.

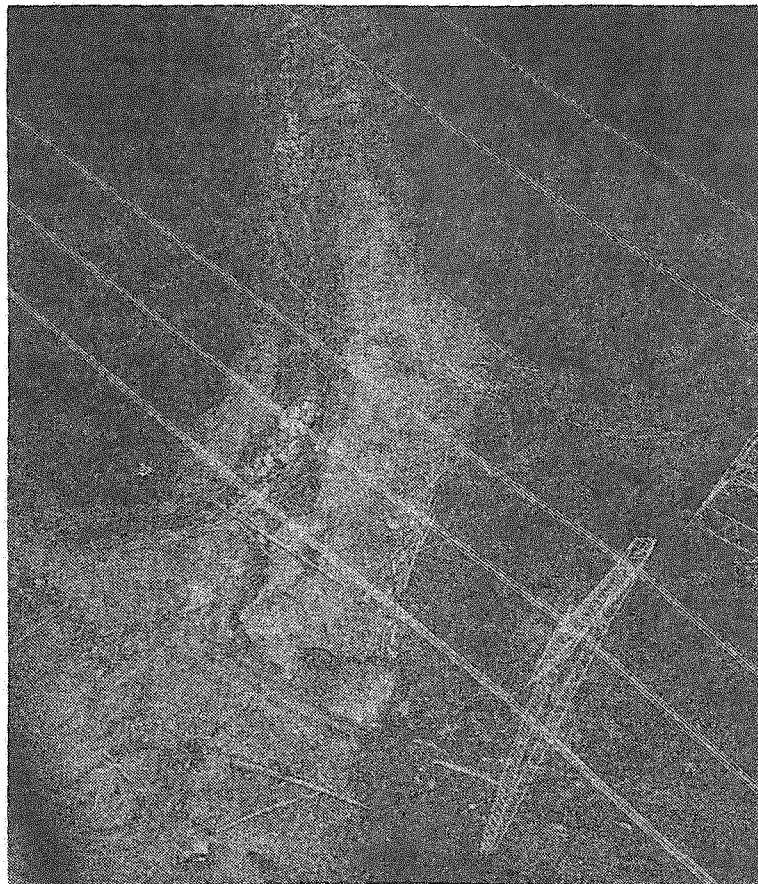


Fig. 2. Tower 75/2 had guy attached to bulldozer after debris flow.

Helicopter reconnaissance of the flow channel, above Tower 75/2, indicated that large amounts of surficial deposits still existed in the scarp area, and along much of the channel bed, creating a risk of future debris flows. The mass and height needed to divert a potential debris flow could not be created with the fine erodible soil, and there were few suitable rock outcrops nearby. There would also be the danger of run-up over a sloping embankment structure built on the 15 degree slope at the site. The best solution appeared to be, to build a high wall structure, with a concentrated mass uphill of the tower, of either, earth and cast-in-place concrete, or concrete blocks and soil reinforced with geogrids. Access to the site, several kilometres up the steep mountain slope, required off road vehicles, making cast-in-place concrete construction both difficult and expensive. A decision was made to use precast concrete Lock-Blocks which could be relatively easily transported up on tandem axle flat deck crane trucks. BC Hydro had the prior experience of constructing a similar concrete block

debris deflector at a remote site, (Tower 32/1 of Circuit 5L30), near Sechelt Creek, in 1988.

B. Design

1. General Layout

The debris deflector was designed for three loading conditions:

- 1) as a mass to deflect a large flow of fluid around the tower.
- 2) to resist individual impact from high velocity boulders and logs, and
- 3) as an every day retaining wall structure.

The debris deflector was laid out to shield the tower from debris flows with the majority of the flow being deflected off the long 19.5 metre wall along the east edge of the debris flow path. See Fig. 3.

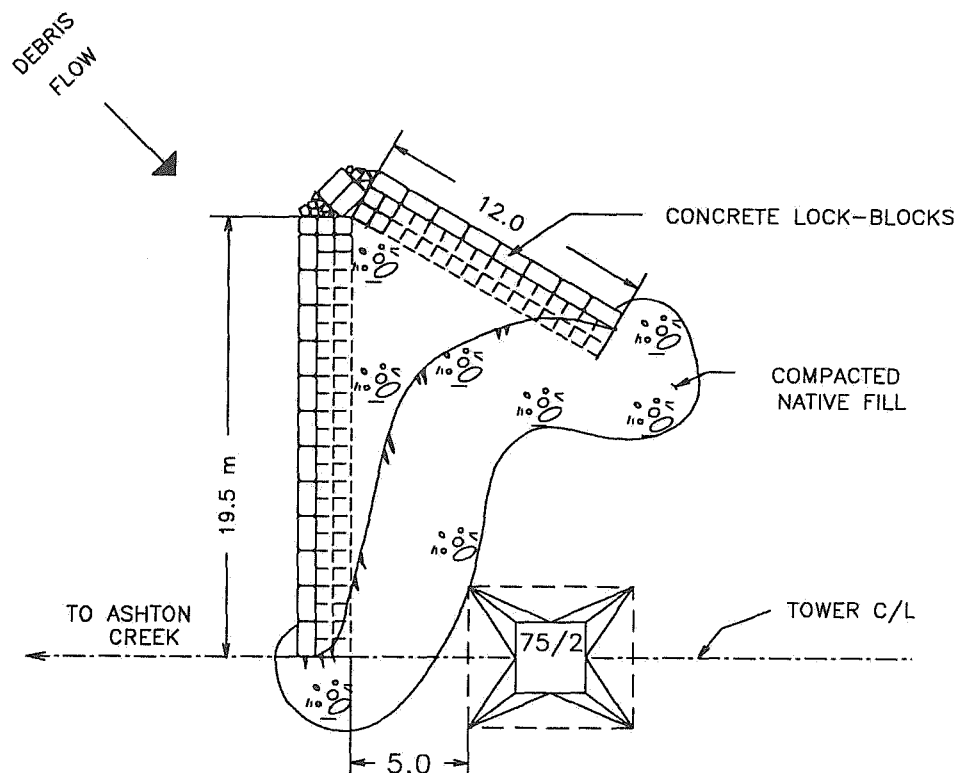


Fig. 3. Plan of Concrete Block and Earth Debris Deflector

2. Resultant Fluid Force Analysis

The main debris deflector wall was orientated at 45 degrees to the expected debris flow so the resultant force would pass through the centre of gravity of the soil/block mass. The ground slope was approximately level in the direction of the resultant force so there was no additional force component caused by the weight of the deflector itself. For calculation of sliding resistance of the deflector (soil and blocks), the soil shear strength was calculated using the Mohr-Coulomb failure criterion [2] of the soil.

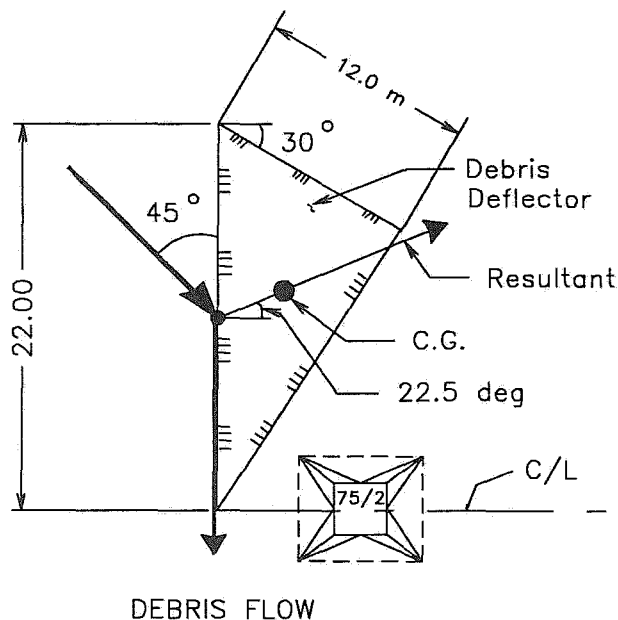
The velocity for laminar flow was approximated using a modified "Poiseuille Equation" referred to in [1]. This formula incorporates material density, ground slope, flow height, channel shape and apparent fluid viscosity. The calculated velocities appear to agree with velocities estimated from videos of debris flows.

The reference equation for velocity is:

$$V = \frac{\gamma_{\text{sat}} \sin \theta H^2}{c v}$$

Sat. unit wt.	$\gamma_{\text{sat}} = 15 \text{ kN/m}^3$
Stream gradient	$\theta = 25 \text{ degrees}$
Flow Height	$H = 3.5 \text{ metres}$
X-Sect. Coeff.	$c = 5$
App. viscosity	$v = 3 \text{ kPa}\cdot\text{s}$

Cross section coefficients given in [1] are 3 for a wide rectangular channel, 5 for trapezoidal, and 8 for a semi-circular channel. The force imparted on the structure by the debris flow was calculated using basic fluid momentum formulae [3]. It was assumed that no fluid velocity would be lost on impact (ignoring wall friction), giving more conservative design values. See Fig. 4.



Flow Velocity = 5.2 m/s
(19 km/hr)

Resultant = 1,000 kN

Total Deflector Wt. = 10,000 kN

Sliding Resistance = 3,000 kN

Factor of Safety = 3.0

Fig. 4. Resultant Flow Force Analysis for Debris Deflector

3. Retaining Wall Design

Hydraulics and impact resistance indicated the debris deflector face should be vertical, and that multiple block thickness should be incorporated near the base of the structure. The multiple block thickness was deemed more appropriate in terms of load spreading under concentrated impact loading. Aside from withstanding a frontal attack during a debris flow, the Lock-Block faced geogrid reinforced soil structure must resist gravitational forces on a long term basis from the backfill soil.

The debris deflector must be capable of resisting sliding and overturning forces, and also maintain an acceptable factor of safety in terms of global stability. Based on site conditions, geometry of the geogrid layout was chosen as 3.0 metres beyond the Lock-Block facing to provide a stable structure on this sloping terrain. No rigorous analysis of stability was carried out. However, this geogrid length to wall height ratio is consistent with other reinforced soil structures with similar siting conditions [4].

Design checks were carried out using Tensar Earth Technologies' computer program TENSVAL. The program is based on the assumption that the reinforced and retained backfills develop a Rankine active state of stress. This assumption is valid considering strain compatibility between the geogrid and reinforced soil. The program analyzes

geogrid reinforcement in terms of tension, anchorage and vertical spacing by using equations of static equilibrium; and calculates factors of safety for sliding and overturning, as well as bearing pressure for the reinforced soil mass. Based on presumptive soil properties of unit weight and angle of external friction of 20 kN/m^3 and 35 degrees respectively, and with the geogrid geometry as selected for overall stability, the computer program indicated the following factors of safety against:

- sliding	5.8
- overturning	15.4
- geogrid tension	1.9 min.

A bearing pressure of 96 kPa was calculated by the program with an eccentricity of loading equal to 0.17 m .

The Tensar geogrid to Lock-Block mechanical connection is obtained by laying the geogrid over the full width of block, with one complete transverse bar of the geogrid falling in front of the raised key-way on the block. The geogrid is forced upward into the cavity of the overlying block to provide a frictional grip, which has been determined to provide anchorage in excess of the long term allowable design load of the geogrid. Where construction takes place in cooler temperatures or where a stiffer grade of geogrid is used, it has been found beneficial to cut transverse bars (of the geogrid) only, outside of the key-way, to allow a tight fit of the key-way to develop.

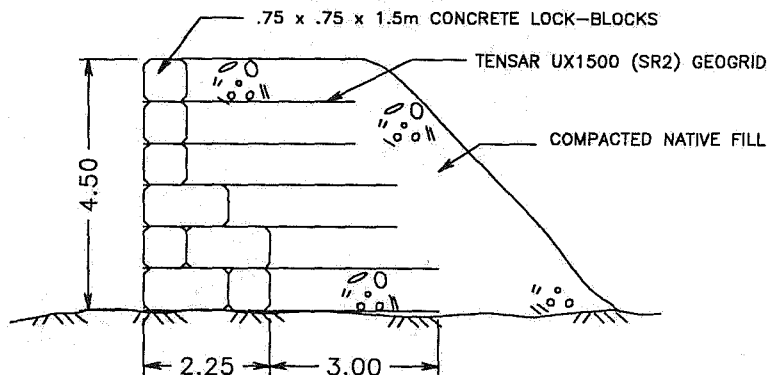


Fig. 5. Cross-section of Debris Deflector

C. Construction

The debris deflector was constructed during the period of June 24 to July 8, 1991. The work was done by BC Hydro using contracted equipment. Key staff were B.A. Tweddle (manager), R. Essery (site supervisor) and L.W. Calvert (inspector). Site grading was done with a D8 Cat bulldozer. Local borrow material, consisting of relatively clean sand and gravel, was dozed down slope. It was then placed and compacted with a Hitachi EX270LC excavator in lifts corresponding to the Lock-Block and geogrid placement. Tensar UX1500 (SR2) geogrid was cut to design lengths, laid over the block work and backfill and sandwiched into place with the next course of blocks. See Fig. 6. The sequence was then repeated with additional fill being placed over the geogrid, being careful in the fill placement to keep the geogrids from being displaced and free of wrinkles. In the lower portion of the wall, where multiple block thicknesses were incorporated, some difficulty was encountered in matching block key-ways. This appeared to be the result of slight differences in key-way tolerances and block thickness; and was likely the result of having blocks supplied from two different sources. About one-half of the Lock-Blocks came from a Kelowna

source and the other half from Vernon.

Cost of constructing the block faced geogrid reinforced soil structure was about \$70,000 in total. Based on a front face area of approximately 140 m² the costs of the individual components of the work are as follows:

<u>Item</u>	<u>Cost/m²</u>	<u>Cost</u>
Geogrid	\$ 65	\$ 9,100
Lock-Blocks	\$ 135	\$ 18,900
<u>Equip & Lbr</u>	<u>\$ 300</u>	<u>\$ 42,000</u>
Total Cost		\$ 70,000

The equipment and labour component of the costs includes transportation costs into the remote site which are quite high. The Lock-Blocks were transported, 22 at a time, from Vernon or Kelowna to the base of the mountain and then taken up to the site on tandem axle crane trucks. The remoteness of the site, in combination with multiple Lock-Block thickness and tight space constraints on the site has resulted in construction costs that are about twice the normal cost of a similar height Lock-Block/Tensar geogrid reinforced soil retaining wall. Another factor which makes the above noted unit cost of wall appear high relative to more conventional retaining structures are site grading costs and fill placement beyond the geogrid reinforced zone.

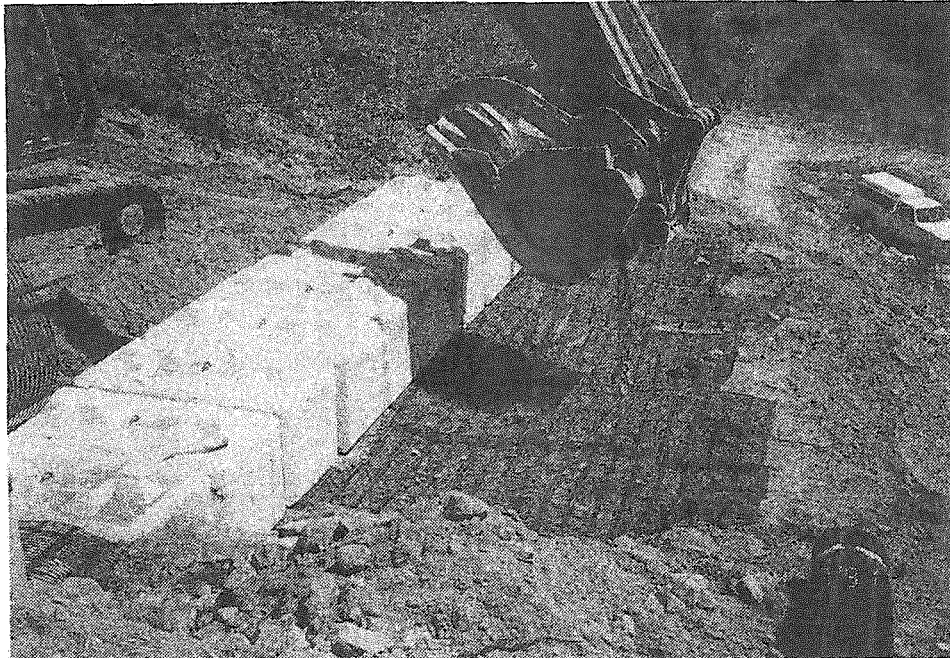


Fig. 6. Installation of Concrete Lock-Blocks and Tensar Geogrid

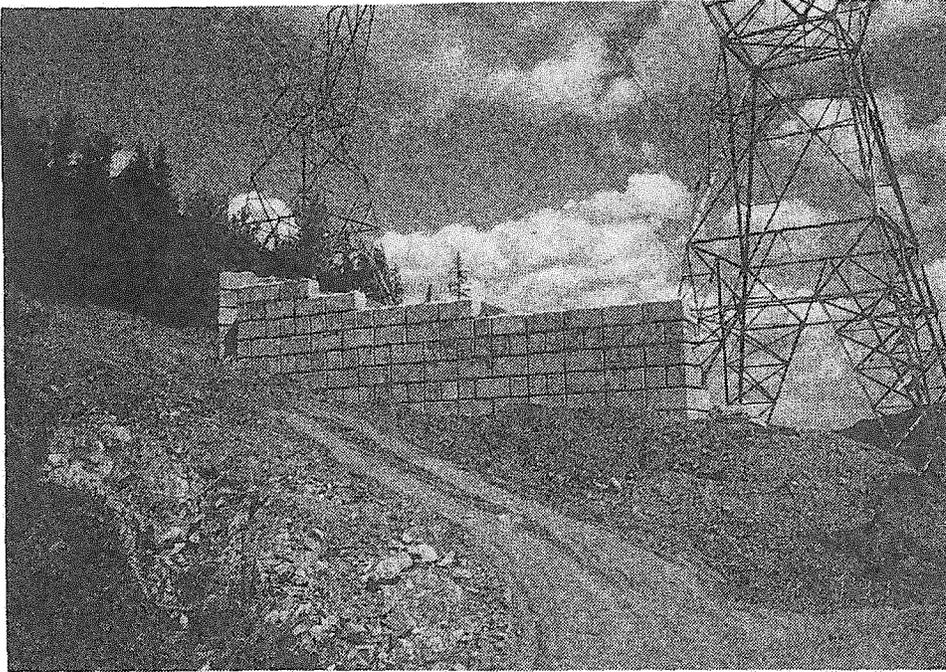


Fig. 7. Construction of debris deflector almost complete.

D. Summary and Conclusions

Design and construction details for a Lock-Block faced, Tensar geogrid reinforced soil debris deflector for transmission towers are presented. Even though debris flow events in this area are infrequent, (say every 30 years or so), the cost of \$70,000 for such a structure is justified, when compared to the \$500,000 replacement cost of the tower.

Construction costs are at least twice as high, for this deflector, when compared to similar soil retaining walls in urban areas. This is primarily due to double the quantity of blocks, remoteness of site and additional site work.

Lock-Blocks work well with the geogrids to provide a durable facing system and good interlock of the components. The high density polyethylene geogrids provide long term durability in an alkaline environment that will exist in the facing anchorage zone, and allow use of non-select site soils for backfill.

Factor of safety (5.8), when analyzed as a retaining wall, is higher than normal. This is due to global stability

considerations driving the geogrid design. The overall factor of safety for the structure against sliding during a debris flow is 3.0.

Using interlocking blocks from more than one source, can introduce some difficulties, where key-way tolerances are small to start with.

Acknowledgements

The authors acknowledge the cooperation provided by Nilex Geotechnical Products Inc.; the Production Department of the Southern Interior Region of BC Hydro, B.A. Tweddle, R. Essery and L.W. Calvert; and to D.J. Armstrong for reviewing the paper.

The opinions in this paper are those of the authors and do not necessarily represent the views of any other individual or organization.

References

1. VanDine, D.F., "Debris Flows and Debris Torrents in the Southern Canadian Cordillera", Canadian Geotechnical Journal, Volume 22, 1985.
2. Craig, R.F., "Soil Mechanics", Van Nostrand Reinhold (UK) Co. Ltd, Berkshire, England, 1985.
3. Daugherty, R.L., Franzini, J.B., and Finnemore, E.J., "Fluid Mechanics with Engineering Applications", McGraw-Hill Book Company, Toronto, 1982.
4. Haigh, T.R., Pack, R.T. and Kerr, J.R., "Tensar Geogrid Reinforced Soil Retaining Wall with Lock-Block Facing", VGS Symposium Proceedings, Vancouver, B.C., 1991.

Performance of Buried Fibre Optic Telecommunications Cable Subjected to Debris Torrent Events Coquihalla Corridor, British Columbia

M. Miles

*M. Miles and Associates Ltd.
Victoria, British Columbia*

R. Kellerhals

*Kellerhals Engineering Services Ltd.
Heriot Bay, British Columbia*

A.H. Rice

*Golder Associates Ltd.
Vancouver, British Columbia*

INTRODUCTION

In 1988 the British Columbia Telephone Company (B.C.Tel.) undertook a two year program to construct the final leg of the Telecom Canada trans-continental buried fibre optic cable telecommunications system. Known as the "Lightguide", the system crosses 750 km of mountainous terrain from Jasper, Alberta to Vancouver, B.C. A 60 km portion of the route passes through the Cascade Mountains along the Coquihalla Corridor east of Hope, B.C., an area renowned for its steep topography, high precipitation, frequent flooding, avalanches and debris torrents. The corridor has previously been used by the now abandoned Kettle Valley Railway. Presently it contains an oil pipeline, two natural gas pipelines and a four lane highway.

The Lightguide consists of a 19 mm diameter cable with a steel and polyethylene core around which a dozen hair-thin glass fibres are wound. The cable is sheathed with a steel and polyethylene wrap and placed inside a 75 mm diameter high-density polyethylene (HDPE) duct which is buried in a 10 m wide right-of-way. The Lightguide is considered to be vulnerable to damage if exposed by scour.

The authors worked with the B.C. Tel's design and construction teams during 1988 and 1989 selecting routes, evaluating risk of damage and selecting depth of cover and sag-bend setback distances for the cable. They also designed protective works and inspected construction to minimize the potential for breakage of the buried cable by debris torrents or slope instability.

This paper has been prepared in four parts. The first part of the paper reviews the inventory procedures used to identify debris torrent prone sites and to assess potential scour depths. Part 2 describes the techniques which were developed to protect the Lightguide from the debris torrent risk. The third part of the paper discusses the program for verifying scour depth predictions, sag-bend setback distances and protection work requirements.

The final section of the paper describes a number of sizeable debris torrents which crossed the Lightguide right-of-way during November 1989 and November 1990. The performance of the protective measures are reviewed and requirements for on-going monitoring and maintenance of this type of facility are discussed.

1. Physical Setting and Debris Torrent Inventory Procedure

The Coquihalla Corridor is located immediately east of Hope in south-western British Columbia. This mountainous area receives between 0.9 and over 3 m of precipitation per year and experiences frequent intense rainstorms. Previous studies (1) indicate that rainfall intensities commonly exceed threshold values which have been observed to result in debris slides or debris torrents in susceptible materials (2, 3). Debris torrents, or surges of rock, water and organic debris, have been reported on many of the small steep gradient streams in this area (4, 5). A number of studies of debris torrent hazard had previously been conducted during planning for the Coquihalla Highway (6, 7) and a variety of investigations have been undertaken to determine design parameters for containing debris torrents (e.g. 8). However, at the time of construction, no studies appear to have addressed the problem of predicting potential scour depths in debris torrent prone channels. This hazard was significant here as the Lightguide was locally the 3rd or 4th right-of-way placed through the narrow mountain valleys of the corridor. As such it was frequently forced to undesirable sites, such as the apex of debris torrent prone fans, or the top of cutslopes above an adjoining utility.

In order to address these concerns, 162 streams along the general route were classified with respect to debris torrent hazard. These initial studies were used to finalize route location and to prepare preliminary design recommendations suitable for contract tendering. As discussed in Section 2, these recommendations were subsequently refined during construction.

Items which were investigated during the inventory studies are summarized on the Coding Sheet Key (Table 1). Items of parti-

cular interest included evidence of historical debris torrent occurrence, the position of the right-of-way with respect to areas subject to deposition or erosion, the size of the existing stream channel and maximum observed depth of channel incision. Upslope land use (particularly potential logging activity) and the presence of downslope discontinuities (such as a cutslope on an adjacent right-of-way) were also factors which were specifically addressed. Test pits were available from one debris torrent prone site, but were not otherwise feasible due to access difficulties. Surficial geology information was therefore based principally on interpretation of 1:10,000 scale air photos.

On the basis of this analysis the authors were able to define which streams were subject to debris torrent events and to document the depths of channel incision at a variety of stream types and locations. This did not provide a complete basis for design as there was the potential that the incised channels we observed had partially infilled with sediment, or that changes in land use (logging, fire, construction of downslope right-of-ways) could result in more severe conditions in the future.

2. Description of Protection Measures

Design criteria

Telecom Canada guidelines stipulate that service interruption resulting from structural failure cannot exceed 2 hours per year. For this reason very stringent design standards were necessary. However, several Coquihalla Highway bridges were used as Lightguide stream crossings and it was pointless to try and apply a more stringent hydrologic design criterion than the 1 in 200 year flood used by the B.C. Ministry of Transportation and Highways. In most instances risk could not be quantified and engineering judgement,

aiming at a comparable level of security, had to be used instead.

Typical designs for debris torrent prone streams

Sag bend setback distances were specified and burial depth recommendations prepared for both the stream channel per se and the adjacent fan or flood plain surfaces. Burial depth was measured from the top (crown) of the Lightguide conduit. It was specified in multiples of 0.5 m, as this was the closest that could reasonably be controlled in the prevailing rough terrain. The maximum depth specified was 4 m, which is the limit for standard hydraulic excavators. Wherever a depth of 2 m or more was specified, the HDPE duct was placed in a steel casing. At those crossing sites where the design burial depth under the channel exceeded the burial depth specified for the adjacent fan or valley flat, the "under channel depth" was to be maintained for 2 m beyond the channel banks, with a gradual transition back to the "fan or valley flat depth".

In particularly hazardous or complicated sites, design drawings were prepared showing the location of diversion channels, catch basins, or other control measures. However at most sites where deep burial alone was considered to provide inadequate protection "standard" erosion control designs were used and are illustrated on Figure 1. The rip-rap to be used for erosion control was at least 800 mm class as defined in Table 2. The typical designs No.3 (upslope cutbank plug) and No.4 (downslope protection) were always used in combination with designs No.1 and No.2, respectively. The channel width is shown as 1 m on the typical designs, which is the minimum, and most common, value. Width was a parameter that could only be finalized after right-of-way grade construction.

TABLE 2-- Rip-rap specifications

RIP-RAP: Rip-rap shall consist of clean, hard, durable angular rock of a quality that will not disintegrate on years of exposure to water or the atmosphere, conforming to the following gradations.

PER CENT BY WEIGHT LARGER THAN	800 mm CLASS		1200 mm CLASS	
	Size (intermediate axis) (mm)	Approx. Mass (kg)	Size (intermediate axis) (mm)	Approx. Mass (kg)
80	500	250	500	250
50	800	1,000	1,200	3,400
20	1,000	2,000	1,500	6,600
0	1,200	3,400		

3. Design Verification During Construction

The contract documents allowed a period of at least 5 days between grade construction and initiation of trenching. Within this period the streams were inspected and the initial design parameters verified. This procedure was thought to be necessary as no survey data were available and hence the configuration of the completed grade could not be predicted prior to construction. This procedure also allowed the soil profile in the grade backslope to be inspected. In some locations the clearing of vegetation cover exposed historic debris torrent deposits or other indicators of past debris torrent activity.

Trenching frequently exposed debris torrent deposits (Plate 1) which allowed additional verification of design burial depth criteria. Generally the Lightguide was placed below the lower boundary of past debris torrent activity. At a few sites debris torrent deposits extended to the underlying bedrock. In these circumstances the steel casing was sometimes attached with steel dowels and concrete to the bedrock surface prior to the

placement of erosion protection.

It is interesting to compare the design burial depth with the depth of debris torrent deposits exposed in the trenching operations. Design burial depths for most high risk sites were 3 m (below the grade surface, which would correlate to a depth of 3 to possibly 5 m below the previous existing ground surface - with the smaller value generally corresponding to deeply incised, more hazardous sites). At a few exceptional sites burial depths of 4 m were recommended. Measurements of the depth of debris torrent deposits (identifiable by differing textural composition, colour and organic content) indicated maximum depths at relatively high risk sites ranged from 2.5 to 2.8 m. *[Note: The sample size is small and far from comprehensive.]* The scour depth estimates therefore appear to be of the right order of magnitude, particularly considering that the erosion protection measures should reduce scour locally at the right-of-way.

4. Post-Construction Performance

Sizeable rainstorm events occurred in the Coquihalla Valley on both November 10, 1989 and November 10, 1990. One and two-day precipitation totals at the Atmospheric Environment Service Station at Hope Airport were 93 and 198 mm in 1989 and 131 and 304 mm in 1990. Return periods for 1 to 10 day precipitation totals ranged between 2 to 10 years in 1989 and between 7 and 46 years in 1990. Estimated daily and instantaneous peak streamflow values on Upper Coquihalla River had return periods of 12 and 8 years in 1989 and 30 and 40 years in 1990. In the lower Coquihalla River, estimated daily and instantaneous peak streamflow values had return periods of 8 and 5 years in 1989 and values of 35 and 20 years in 1990. Both storms initiated a number of debris torrents with larger and more numer-

ous events occurring in 1990.

Debris torrent materials were deposited on the Lightguide right-of-way at 3 sites and, if any scour occurred, it was covered by subsequent deposition. At three other sites material was transported over the right-of-way, resulting in some loss of material from the erosion protection blanket (Plate 2). One of these events was particularly interesting as the debris torrent subsequently overtopped a berm placed to prevent debris torrents reaching the Coquihalla Highway (Plate 3). This berm, which is located perpendicularly across the debris torrent path, has a height of 6.2 m, with an upslope face of 23°. On the basis of Eq. 1

$$h = \frac{v^2}{2g} \quad \{1\}$$

where h is the run up height (m), v is the incoming velocity (m/s) and g is force of gravity (9.8 m/s^2), the minimum approach velocity of this torrent was 11 m/s. [This velocity is near the upper limit of debris torrent velocities (3 to 12 m/s) cited in reference 9]. This event carried boulders 18 m^3 in size over the top of the berm. Interestingly, boulders of up to 5 m^3 in size were deposited on the berm crest and no significant scour occurred on any portion of the berm. A similar event occurred in 1989 when a debris torrent climbed over a curved berm located 1 km downstream. [No survey data are available from this site and velocities have therefore not yet been calculated.] These observations indicate that, in some circumstances, debris torrents can pass over substantial obstacles without causing significant scour.

Discussions with B.C. Tel. personnel indicate that the Lightguide was not damaged by debris torrents associated with either the 1989 or 1990 storms. Some minor repairs to erosion protection measures were required

following the 1990 event. A cursory inspection indicated the maximum observed scour by these debris torrents was 2.8 m (on a fan not crossed by the Lightguide, but which had been cleared during highway construction). The designs discussed in this paper have therefore withstood two storms which resulted in at least 6 debris torrents crossing the Lightguide alignment. Additional monitoring is desirable to further verify the design procedures and to ensure that the debris torrent protection measures are adequately maintained. Right-of-way operation and maintenance guideline prepared for B.C. Tel. indicate that such monitoring should be done by an experienced geomorphologist or engineer to ensure that potential maintenance problems, or changes in erosion potential due to land use variations, etc., are recognized and addressed.

ACKNOWLEDGEMENTS

The successful construction of the Coquihalla Section of the Lightguide resulted from the close cooperation between the B.C. Tel staff, their consultants and the prime contractor (Argo Industries Ltd. of Kamloops, B.C.). The on-going monitoring and maintenance of the system is now the responsibility of the B.C. Tel. Lightguide Maintenance Group headquartered in Kamloops, B.C., to whom the authors are grateful for permission to publish this paper.

REFERENCES

1. Church, M. and M.J. Miles. 1987. Meteorological antecedents to debris flow in southwestern British Columbia; Some case studies. pp. 63-79. *In: Debris Flows/Avalanches: Process, Recognition, and Mitigation*. John E. Costa and Gerald F. Wieczorek, (Eds.) Geol. Soc. of America, Reviews in Engineering Geology Volume VII. 239 pp.
2. Caine, N. 1980. The rainfall intensity-duration control of shallow landslides and debris flows: *Geografiska Annaler*, v. 62A, p.23-27.
3. Innes, J.L. 1983. Debris Flows. *Progress in Physical Geography*. Vol. 7, Number 4, pp. -469-501.
4. Miles, M.J. and Kellerhals, R. 1981. Some engineering aspects of debris torrents: Canadian Society of Civil Engineering, 5th Canadian Hydrotechnical Conference, Fredericton, New Brunswick, Proceedings, p. 395-420.
5. Evans, S.G. and D.R. Lister. 1984. The geomorphic effects of the July 1983 rainstorms in the southern Cordillera and their impact on transportation facilities. *In: Current Research, Part B, Geol. Surv. of Canada, Paper 84-1B*, p. 223-235.
6. Miles, M.J., E.A. Harding, T. Rollerson and R. Kellerhals. 1979. Effects of the proposed Coquihalla Highway on the fluvial environment and associated fisheries resource. Vols. 1 & 2. Unpub. report to the B.C. Ministry of Highways and Public Works.
7. Thurber Consultants Ltd. 1985. Final Report Debris Torrent Assessment, Wahleach and Floods, Highway 1 Hope to Boston Bar Creek Summit, Coquihalla Highway. Unpublished report to the B.C. Ministry of Transportation and Highways. 27 p. plus Appendices.
8. Hungr, O., G.C. Morgan and R. Kellerhals. 1984. Quantitative analysis of debris torrent hazards for design of remedial measures. *Can. Geotech Journ.* Vol. 21, No. 4. p. 663-677.
9. VanDine, D.F. 1984. Debris flows and debris torrents in Western Canada. *Proc. 8th Can. Geotech. Colloquium, 37th Can. Geotech. Conf. & 4th Int. Symp. on Landslides*, Toronto, Canada. 82 p.

TABLE 1-- Stream inventory coding key

1: TAG #: - refers to survey tag placed in field	2: STREAM NAME: (if available)						
3: CHAINAGE STATION:							
4: AIR PHOTOS:	<table border="0"> <tr> <td>BC B.C. Govt.</td> <td>BC Prov Photo Sales</td> </tr> <tr> <td>WE Westcoast Energy</td> <td>TMC Triathlon Mapping Corp.</td> </tr> <tr> <td>MOTH Min. of Transport.& Highways</td> <td>SRS Selkirk Remote Sensing</td> </tr> </table>	BC B.C. Govt.	BC Prov Photo Sales	WE Westcoast Energy	TMC Triathlon Mapping Corp.	MOTH Min. of Transport.& Highways	SRS Selkirk Remote Sensing
BC B.C. Govt.	BC Prov Photo Sales						
WE Westcoast Energy	TMC Triathlon Mapping Corp.						
MOTH Min. of Transport.& Highways	SRS Selkirk Remote Sensing						
5: THURBER STREAM NUMBER: - from Thurber Consultants Ltd., 1985							
6: DETAILED SITE INVENTORY: - indicates if available	YES : NO						
7: PIN LOCATION is described with reference to:							
a) Stream Bank	South (pin on Hope side) North (pin on Merritt side)						
b) Distance to Stream - Horizontal distance between vegetation trim line and pin,							
c) Side of ROW	CL on the centreline U/S on upslope side of ROW D/S on downslope side of ROW ? position is uncertain						
8: BASIN AREA: where relevant, digitized from 1:50,000 scale NTS mapping							
9: STREAM SIZE: (S)mall : (M)edium : (L)arge							
10: CROSSING LOCATION:							
S non-incised on valley wall	G in a gully or incised channel						
U upper one third of fan	M middle one third of fan						
L lower one third of fan	V within a valley flat						
* modified by human action							
11: MOTH CULVERT DIAMETER: given as an indicator of stream size							
12: CHANNEL DIMENSIONS given as a range in width (m) depth (m) and slope (%); gully depths (B) base or (T) top for:							
i) active channel on row	ii) incised channel on row						
iii) active channel upstream of row	iv) incised channel upstream of row						
13: MAXIMUM OBSERVED CHANNEL INCISION (m) over the LTS ROW as measured in the field In some circumstances depths have been measured from U/S (upslope) or D/S (downslope) of the ROW							
14: UPSLOPE LAND USE - present or potential land use based on Ministry of Forests 25-yr cutting plan							
UR unlogged, recreational reserve	UN unlogged, no merchantable timber						
UM unlogged, has merchantable timber	UP unlogged, may contain merchantable timber						
UL recently logged, now 2nd growth	UB recently burned, now 2nd growth						
15: PRESENCE OF DOWNSTREAM DISCONTINUITIES AND HEIGHT (m) plus reason for occurrence							
WE Westcoast Energy	H B.C. Ministry of Transportation & Highways						
# natural drop	SS natural slope steeper than channel slope over ROW						
16: DEBRIS FLOW POTENTIAL: based on historic activity							
DN no indication of debris flows							
DD potential for debris slide or flow, ROW in deposition zone							
DI evidence of or potential for small flow or slide - scour <1.5 m							
DL evidence or potential for medium/large flow/slide - scour <2.5 m, unless noted							
* increased scour potential due to other factors present							
17: POTENTIAL SCOUR: by fluvial activity in channel or on adjacent fan or valley flat							
SN none or minor <.5 m	SI intermediate <1.5 m						
SL severe, <2.5 m, unless noted	* increased scour potential due to other factors						
18: POTENTIAL FOR MAINTENANCE EXCAVATIONS (to remove sediment accumulations)							
MN not applicable	MI may occur, unlikely to exceed >1.5 m in depth						
MS likely to occur, excavation may exceed 1.5 m below present ground surface							
19: LATERAL CHANNEL STABILITY							
CS stable	CM progressive shift across valley flat or fan						
CA sudden shift across valley flat or fan	CMA channel could shift progressively or suddenly						
20: WIDTH OF AREA SUBJECT TO SCOUR OR SEEPAGE:	referenced north or south to rebar pins where possible, or from 1:5,000 scale photos on large fans.						
21: IS AREA SUBJECT TO SCOUR CONTIGUOUS WITH THAT TO THE NORTH OR SOUTH:	YES : NO						



Plate 1. Looking along excavated trench showing base of historic debris torrent deposits (A), steel casing protecting the Lightguide (B) and pipe carrying streamflow across the right-of-way (C). The base of the debris flow deposits are 2.8 m below the elevation of the stream bed. (August 18, 1989)



Plate 3. Same location as Plate 1 showing debris torrent deposits on top of a 6.2 m high berm located downslope of the Lightguide right-of-way. Debris flow deposits in the background covered the Lightguide to a depth of at least 2 m. (April 29, 1991)

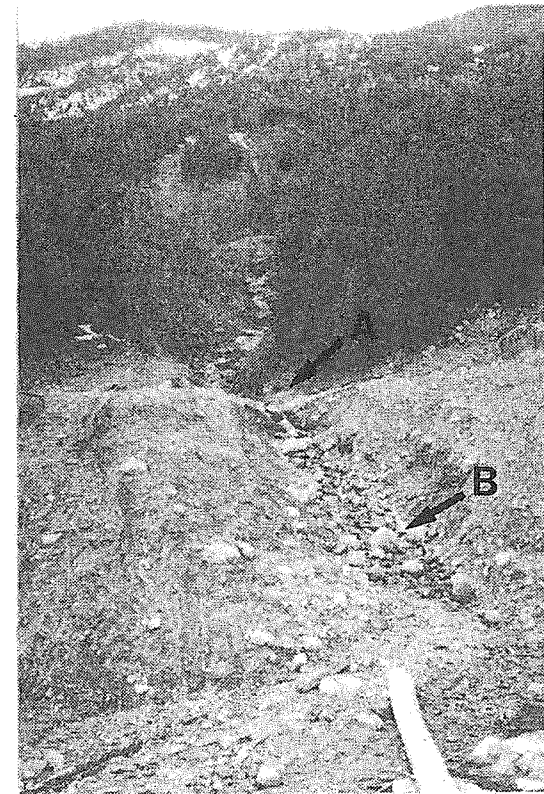
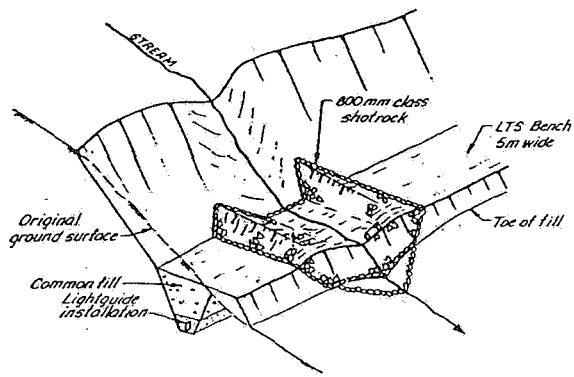
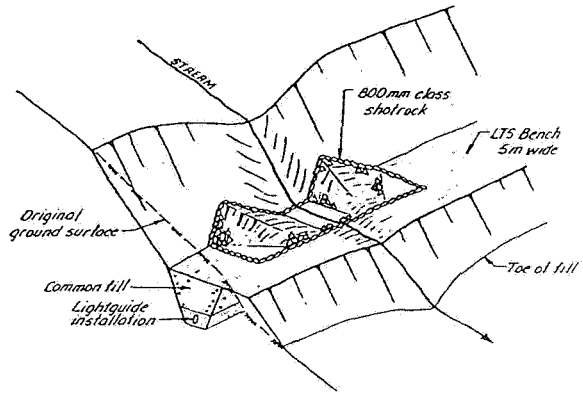


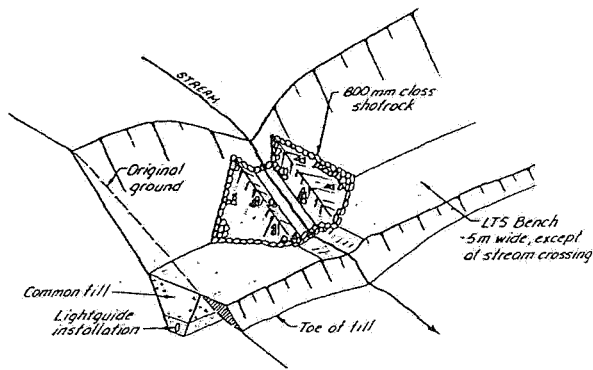
Plate 2. Same location as Plate 1, showing scour on the right-of-way (A) and unravelling of the erosion protection materials (B) following the November, 1990 debris torrent event (April 29, 1991).



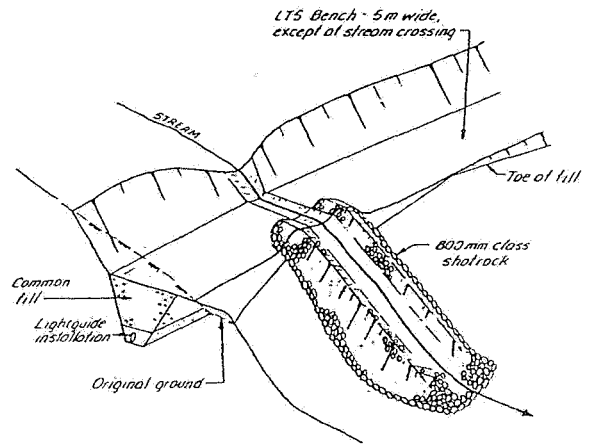
Oblique View of Type 1 Erosion Control



Oblique View of Type 2 Erosion Control



**Oblique View of Type 3 Erosion Control
Upslope Cutbank Plug**



**Oblique View of Type 4 Erosion Control
Downslope Protection**

Figure 1 : TYPICAL DETAILS – SMALL STREAM EROSION CONTROL

Relocation of Buried High Pressure Oil Pipeline Subjected to Potential Flood Hazard Coquihalla River Valley, British Columbia

A.H. Rice
Golder Associates Ltd.
Vancouver, British Columbia

L.H.E. Weran
Trans Mountain Pipe Line Co. Ltd.
Burnaby, British Columbia

K. Savage
Trans Mountain Pipe Line Co. Ltd.
Kamloops, British Columbia

M. Miles
M. Miles and Associates Ltd.
Victoria, British Columbia

INTRODUCTION

The Trans Mountain Pipeline Company Ltd. (TMPL) owns and operates a 1146 kilometre long 610 mm diameter buried high pressure oil pipeline which originates in Edmonton, Alberta and terminates in Burnaby, British Columbia. Originally constructed in 1952 and 1953, the pipeline transports crude petroleum and refinery feedstocks to both domestic and export markets. TMPL is the sole supplier of crude oil to Vancouver area refineries who depend on continuous service throughout the year. The pipeline passes through much mountainous terrain along its route⁽¹⁾. Of particular concern to TMPL in recent years has been that portion of the pipeline route which passes through the Coquihalla River Valley east of Hope, B.C. Significant channel shifting has occurred in recent years and on-going river erosion poses a potential hazard to the pipeline. Both the crude oil supply demands faced by TMPL and the companies commitment to environmental protection make river erosion damage to the pipeline an unacceptable prospect.

In November 1989, a large flood event occurred on the Coquihalla River. The oil pipeline was exposed and slightly damaged by scour in the riverbed at a crossing located approximately 15 km upstream of Hope, B.C. The exposed pipeline became a serious operating and environmental concern to TMPL. Temporary repair and protection of the pipeline was therefore carried out during September, 1990. The temporary work involved using bolt-on concrete ballast weights to prevent impact damage from mobile debris and placing bed armour downstream of the pipeline to prevent scour. During November, 1990 another large flood event occurred on the Coquihalla River. The river jumped its channel exposing and damaging the pipeline along most of its length between the two crossings. The authors carried out a study and evaluated options for long term protection of the pipeline from river erosion damage. Analysis of changes in river bed elevations led to the conclusion that not only was the exposed crossing at risk of damage but that the crossing immediately upstream was also at risk of exposure and damage as bed river degradation propagated upstream. Negotiations with regulatory agencies indicated that a long term solution to eliminating the risk of pipeline damage was required. In addition, pipeline repairs would be expected to minimize sediment production in order to protect the fisheries environment.

This paper is presented in three parts. The first part describes the impact of the two large flood events which resulted in pipeline exposure. The second part outlines the studies carried out to determine the level of risk to which the pipeline might be subjected if another significant flood were to occur. The third part discusses how design decisions were made and outlines construction operations associated with the long term pipeline protection scheme which was implemented. This involved excavating a tunnel through the adjacent mountainside through which the pipeline was re-routed allowing the two river crossings to be completely eliminated.

The 1989 and 1990 Flooding

In August 1990 TMPL maintenance personnel from Hope, B.C. discovered an exposure of the 610 mm oil pipeline where it crosses the Coquihalla River at km 996.2 (see Plate 1). Inspection of available discharge records indicated that a flood event on November 10, 1989 most likely resulted in local scour and exposure of the pipeline. High water levels in the river effectively prevented observation of the exposed pipeline until the summer of 1990.

Significant changes in river morphometry have been observed in recent years in the lower Coquihalla River.⁽²⁾ These changes are thought to be related to a number of factors including: increased sediment load introduced by tributary streams and channel shifting; localized straightening of the river channel due to highway construction resulting in increased river slope and greater potential for channel incision; and channel confinement between long linear rip rap banks placed to protect various right-of-ways which tends to increase water velocities and scour potential. The net effect of these factors at the site was to increase the potential for both local scour and channel incision during large flood events.

Recognizing the historical tendency for the Coquihalla River to experience floods in the late fall and early winter (see Figure 1) TMPL determined that immediate repair and protection of the pipeline was required. With the fall months approaching quickly, the available options were limited. There was insufficient time to deepen the crossing and a proposal to attempt to control scour by placing large quantities of channel armour at the crossing site was opposed by regulatory agencies. A temporary repair was implemented in September 1990. The river was routed around the site by excavating a diversion channel and constructing a cofferdam using 1 cu.m sandbags (see Plate 2). Instream work could then be carried out (see Plate 3). This involved placing small quantities of bed armour immediately downstream of the crossing and attachment

of bolt on concrete weights to protect the pipeline from debris impact (see Plate 4). This repair was acceptable to both the regulatory agencies and TMPL only because it was known that permanent repairs and protection would be undertaken in 1991.

On November 10, 1990, another sizeable flood event occurred on the Coquihalla River. During this flood the river jumped its bank at the km 996.0 crossing just upstream of the exposed pipe. The river rapidly developed a new channel between the two crossings along the existing pipeline right-of-way. The river was pushed back into its original channel using heavy equipment and large quantities of riprap. Subsequent inspection revealed that the top of the pipeline had been exposed for a distance of over 125 m (see Plate 5). The resulting small dents and gouges were significant enough to require the complete replacement of the damaged pipeline.

Assessment of Risk

In order to confirm qualitative risk assessments an examination of the historical variation in precipitation and runoff was carried out to determine the magnitude of the events which resulted in the 1989 and 1990 pipe exposures. Analyses were conducted with both precipitation data from the vicinity of Hope, B.C. and streamflow data from the Coquihalla River.

The determination of the average return period for the 1989 and 1990 flood events was complicated by the shift in location of the Hope weather station in 1973 and by the relocation of the Coquihalla stream gauging site after it was destroyed by a flood in 1984.

Analysis of precipitation data indicated the maximum return period associated with the November, 1989 rainfall event was about 10 years. The maximum return period associated with the November, 1990 rainfall event was about 50 years. These return periods are smaller than those published in previous studies⁽³⁾ which did

not take into account the effect of relocating the Hope weather station. This result is important as it suggests that the damaging floods did not result from exceptionally large precipitation events. It is interesting to note that analysis of regional data suggests that there may be a trend towards higher 24 hour precipitation intensities in the Hope area (see Figure 2).

In order to determine the magnitude of the 1989 and 1990 flood events, a frequency analysis of annual maximum daily and instantaneous discharges were undertaken for the Coquihalla River.

The magnitude of annual maximum daily discharges observed several kilometres downstream of the site are shown on Figure 3. The November 1989 flood was on the order of a 10 year event while the November 1990 flood had larger return periods on the order of a 35 year event. These return periods are similar to those predicted from the multi-day precipitation totals.

These results indicate that recent floods have not been exceptionally large events and much larger floods must be expected. The level of risk of future damage to the pipeline was sufficiently high to warrant implementing appropriate protection measures.

Remedial Design and Construction

Measures to adequately mitigate the possibilities of serious pipeline damage and potential service interruption without reburying or moving the pipeline could not be identified. Three options were examined from technical, environmental and economic perspectives. These were:

- 1) reconstruction of the km 996.2 crossing and deepening of the pipeline along the 125 m which had been exposed in November 1990 (cost estimate \$950,000);
- 2) reconstruction of both the km 996.2 and the km 996.0 river crossings and the

125 m of pipe between them (cost estimate \$1,124,800); and

- 3) relocation of the pipeline into a tunnel through an adjacent rock bluff, effectively eliminating both crossings (cost estimate \$1,200,000).

Both the first and second options posed a technical concern. Channel stability at the site was considered to be potentially problematic. Analysis indicated that more than 1 metre of bed degradation had occurred at the km 996.2 crossing over a ten year period. Channel downcutting also appeared to be progressing upstream towards the km 996.0 crossing. Adoption of option 1 would be a stop gap measure, while both options 1 and 2 required extensive in stream work. Although sediment control and subsequent fish habitat mitigation could be carried out⁽⁴⁾, the environmental concerns would still be an issue in obtaining approval to conduct this work. On the basis of this analysis a decision was made to select option 3.

Relocation of the pipeline into a tunnel involved laying approximately 500 metres of new pipeline and 120 metres of tunnel excavation. Advantages of this option which could not be accurately quantified in the economic analysis included:

- 1) ready access to the pipeline;
- 2) allowance within the tunnel for a second pipeline installation; and,
- 3) certainty that river erosion hazards would never again pose a risk to this section of pipeline.

The tunnel was designed as an inverted U-shape with a width of 2.5 metres and a height of 3.0 metres. Drilling and blasting, pattern rock bolts, mesh and shotcrete were used for crown support. The invert was bedded with sand and the pipeline, fabricated outside the tunnel, was installed on rollers (see Plate 6). All work was completed and the new pipeline was in operation by September 1991.

The abandoned pipeline which is still in the river, will be removed in the summer of 1992.

ACKNOWLEDGEMENTS

The authors wish to acknowledge the support of the Trans Mountain Pipe Line Company Ltd. throughout the project, the cooperation of the National Energy Board and the British Columbia Ministry of Environment and the exemplary performance of Emil Anderson Construction Company Ltd. of Hope, B.C. who undertook both the temporary and permanent repairs at the site.

1. Savigny, K. Wayne & Rinne, Norman, F. 1991: *Assessment of Landslide Hazards along a Pipeline Corridor in Mountainous Terrain of Southwestern British Columbia*, 44th Can. Geotech. Conf., September 30, 1991.

2. Miles, M.J. et al., 1979: *Effects of the Proposed Coquihalla Highway on the Fluvial Environment and Associated Fisheries Resource, Vols. 1 & 2*; unpub. rep. to Ministry of Highways and Public Works, January, 1979.
3. Coatta, A. 1990. *November 1990 heavy rains in southern British Columbia*. Unpublished report, Pacific Region, Atmospheric Environment Service, Weather Services Directorate, Environment Canada, 5 p.
4. Nicholson, B.C., Plummer, R.L., Conlin, B.H. and Rice, A.H., 1989. *1988 Environmental Engineering Design Award, British Columbia Telephone Company Lightguide Project*. The B.C. Professional Engineer, Volume 40, Number 5, pp. 11 to 14.

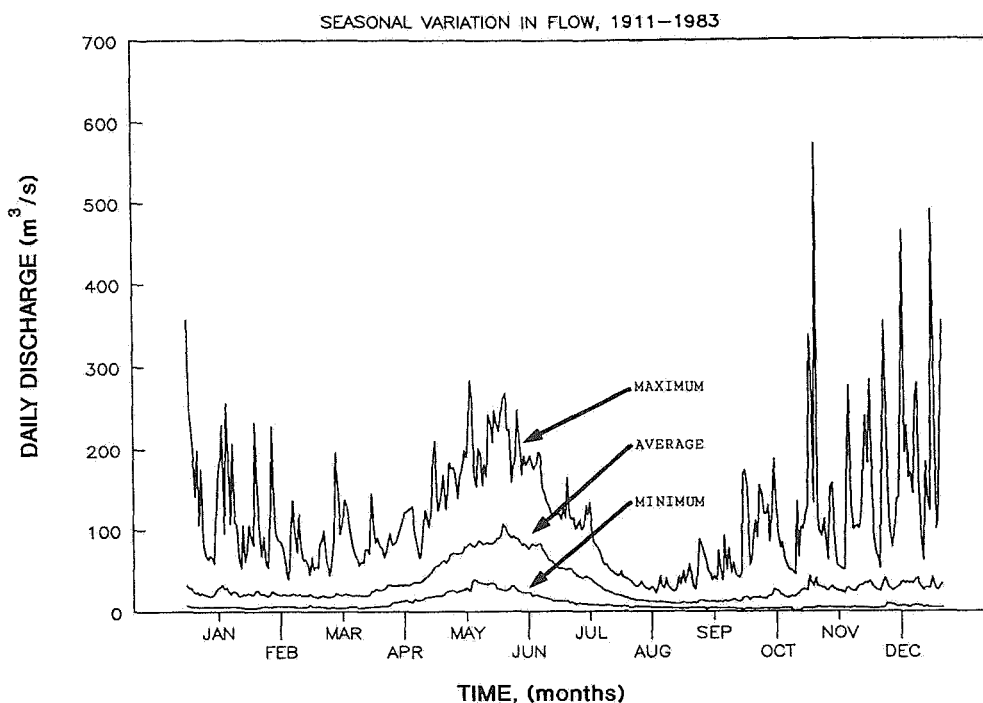


Figure 1 - Seasonal variation in discharge, Coquihalla River near Hope.

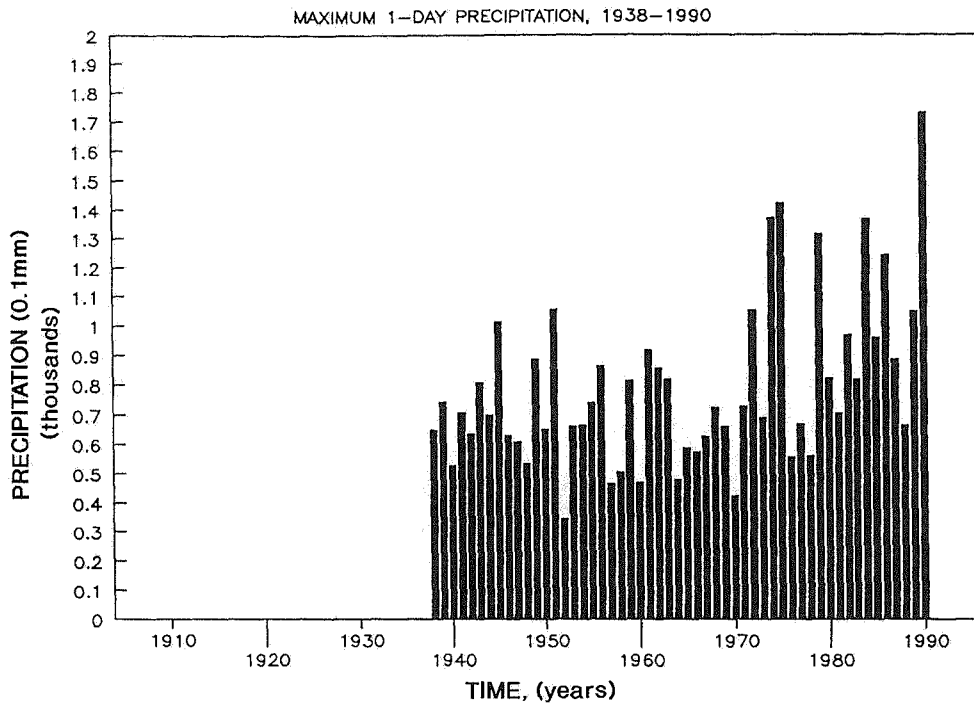


Figure 2 - Historical variation in maximum 1 day precipitation, Hope plus Hope Airport stations.

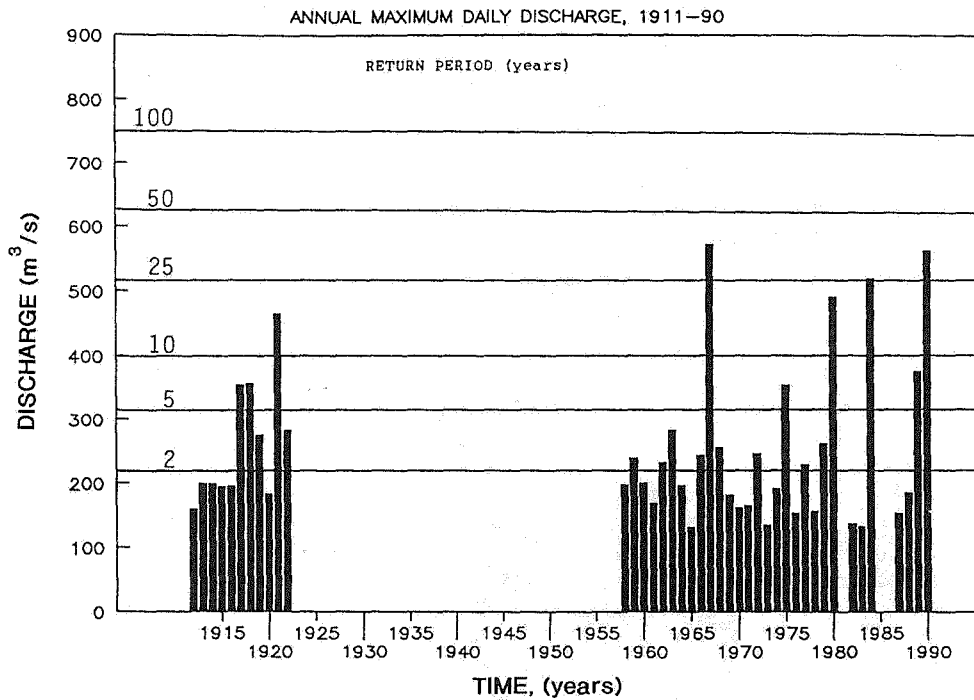


Figure 3 - Historical variation in annual maximum daily discharge, Coquihalla River near Hope plus Coquihalla River above Alexander Creek.

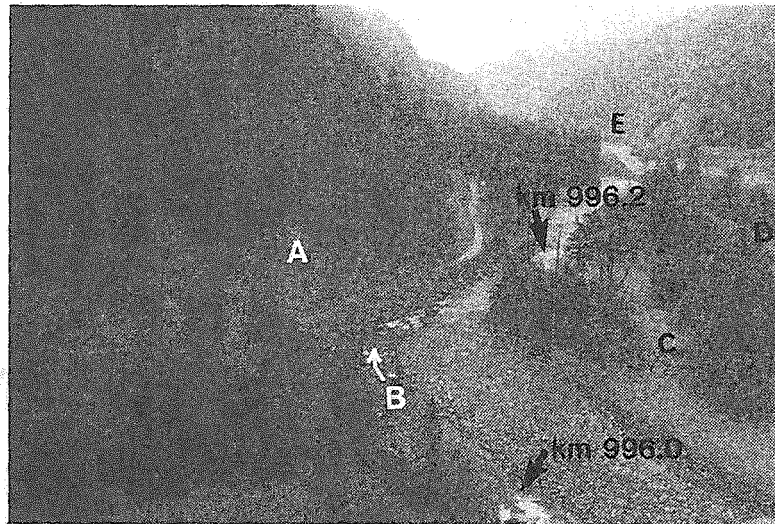


PLATE 1

Aerial perspective of the site looking downstream along the Coquihalla River towards Hope, B.C. Note congested nature of the corridor. The letters denote the following features: A - Rock bluff; B - Coquihalla River; C - TMPL right-of-way washed out by November 1990 flood; D - Location of Westcoast Energy Inc. natural gas pipeline right-of-way; E - Coquihalla Highway.

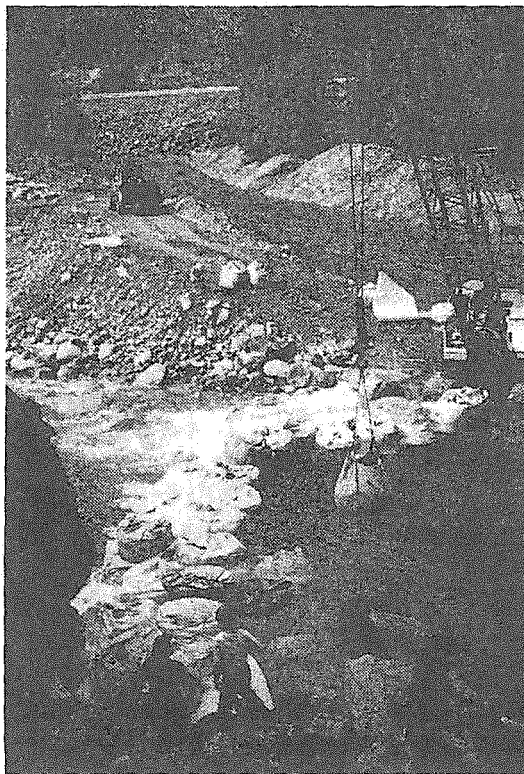


PLATE 2

Cofferdam construction to route river flow away from exposed pipeline along excavated diversion channel, August, 1990.

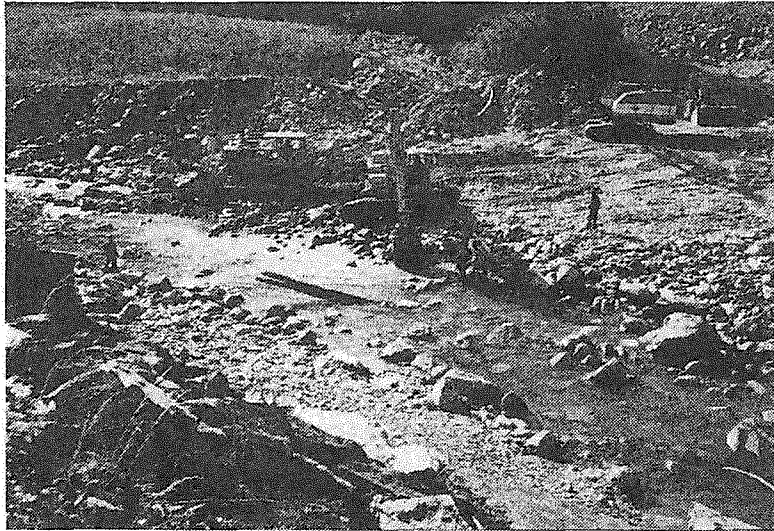


PLATE 3

Instream temporary repair and protection work underway, September 1990.
Note exposed pipeline just downstream of partially buried log.



PLATE 4

Completed temporary repair and protection work consisting of bed armour and
bolt on weights, October, 1990.

July-August Flood Events

July and August are usually known as months of good weather and as vacation time in most northern hemisphere temperate climate countries. Surprisingly, the history of extreme hydrological events in these countries shows that they are also months for damaging and dangerous flooding from extreme rainfall events.

In southwestern British Columbia, intense summer storms of small areal extent are the norm. These storms are commonly used in design for small catchments, such as municipal storm drainage systems. Summer storms of large areal extent (covering several tens to several thousands of square kilometers) are, however, very unusual. However when they do occur they are usually extremely damaging.

One of the earliest documented floods in Vancouver's history was on September 6, 1906, and was described in the Daily Province newspaper. The flood was described as "the worst in 10 years", with "the city road under three feet of water for hundreds of feet". Precipitation records for Vancouver PMO station showed a peak rainfall of 79.5 mm for the 24 hour period preceding the flood.

Jones (1) reported a "mudflow" generated on the Cheekeye River near Squamish in August 1958 following a "heavy rainstorm". In discussing mudflows, Jones concluded: "the magnitude and frequency is unpredictable, as their occurrence appears to depend upon sudden abnormal rainstorms rather than upon normal autumn rainfall peaks".

Similar conditions caused flooding in southwestern BC in July 1972. Schaefer (2) reported on the magnitude of the storm

(261 mm of rain in 48 hours) on Hollyburn Ridge during July 11-12, 1972, when parts of the Upper Levels Highway, under construction at the time, were washed out. This storm was of large areal extent, and review of the synoptic weather charts showed that it was associated with a stalled low pressure zone over the Pacific (personal conversation, M. Church). Flooding occurred extensively in the Lower Mainland area, including the Chillwack River basin.

Evans and Lister (3) reported seven unusually large floods in the Fraser Valley and in Revelstoke Park in July 1983.

In northern Europe summer storm damage is not uncommon. Very warm föhn winds blowing over Jostelden glacier on August 14, 1979, caused "the worst flooding in living memory" in western Norway. The flood transported giant boulders, see NCE (5). The flood on the river Lyn in southwestern England during the night of August 14-15, 1952 was caused apparently by a rain event of extraordinary intensity and duration. . During a 24 hour period, 143 mm of rain fell on the 61 km² basin. Homes that were at least 200 years old next to the river in the village of Lynmouth were destroyed, killing 34 people, see Delderfield (6). One author (PRBW) was visiting the area on vacation when the flood occurred. Another author (NAS) recently visited the area, and noted that the boulder bed from the flood is still visible. Slides will be shown during our verbal presentation. The name Lynmouth is derived from the Anglo Saxon word "Llynna" meaning torrent.

In Italy, the secondary dam of the Zerbino reservoir in the Appenines near Genoa was destroyed by flooding on August 13 1935, with the loss of 111 lives. The storm that caused the flooding was extraordinarily large (525 mm of precipitation in 6 hours).

In the Alps, occasional extreme summer storms are known to occur, and have been documented. In Austria, Stiny (7) has described the history of their occurrence during a period of more than 1000 years.

In Switzerland, a particularly interesting case study occurred on August 7, 1978, reported by Brushin et al (8). Much of Ticino, the only Swiss province south of the Alps, was devastated by the greatest floods ever known in the area. The mean annual discharge of the Melezza River (basin area 140 km²), just upstream of the Palagnedra dam is 6.3 m³/s. During the August 1978 deluge, the peak discharge was estimated to be 3000 m³/s. Large sections of earth and forest peeled off the mountain flanks and fell into the reservoir. Some 2 Mm³ of sand, gravel and logs swept into the pool, the logs jamming the spillway. The dam was entirely overtopped, and suffered major damage at its downstream toe. Although rainfall intensities were not the highest recorded, the storm covered an exceptionally large region, with the 200 mm isohyet encompassing an area of about 200 km².

Damage to the Melezza River catchment and the associated Palagnedra dam were photographed by one of us (NAS) in 1978.

Fitzsimmons Creek, Flooding and Bed Elevation Changes

Fitzsimmons Creek drains a region of the southern Coast Mountains that is steep, and prone to slope failures of various kinds. A report by Jackson et al (9) provides insight into the fascinating range of conditions existing in the region. To quote: "Streams entering the main valley flow from glacier-clad mountains and upland basins, through gorges flanked by bedrock and late Pleistocene sediments, and onto entrenched

debris fans on the valley floor. During extreme rainstorms and/or periods of rapid snowmelt, these streams may transport very large amounts of sediment, in part as a result of slumps and debris avalanches in their upper reaches".

A section for Fitzsimmons Creek (Figure 1) shows the range of gradients that occur in main channel bed. Note that these gradients are not steep enough to set off or maintain debris torrents, although tributary streams draining the sides of the valley exhibit periodic debris torrents, which carry material directly into the main channel.

The infrastructure development for Whistler Village (bridges, roads and buildings) have all been built on the alluvial fan reach of Fitzsimmons Creek. This was identified as an alluvial fan in 1977 by H.W. Nasmith, Thurber Consultants (10), before the start of construction, and planning for the Village was handled diligently. A well set back training berm was built, and is presently being extended along the fan to the north, as the built up area of the village grows. The Creek was thought to be geotechnically hazardous, and a report by Skermer and Russell (11) identified debris-laden floods, of the sort that subsequently occurred in August 1991, as being the most likely hazard.

The basin area of Fitzsimmons Creek where it enters Green Lake is 93 km². The basin covers a large range of altitudes (630 m to 2600 m), and during most of the year precipitation falls on a river basin that is either all snow covered, or is snow covered at the highest elevations, and bare at the lowest elevations. During rare summer events, temperatures are high enough that the precipitation falls on an entirely snow free catchment (with the exception of small areas of glaciers).

Flow gauging on Fitzsimmons Creek started very recently, in early 1992, and no records are yet available. Precipitation measurements have been made at Alta Lake, 1.5 km. west of the Village, since December 1976. The 10 and 100-year return period, 24-hour, precipitation events for this station are 62 mm and 91 mm respectively. Data from short term rain measurements on Whistler mountain show that the precipitation at 1800 m. elevation is about 40% greater than the precipitation at Alta Lake. This infers representative storm precipitation amounts for the mountain of about 87 mm and 128 mm for 10 and 100-year events respectively.

Events that have been known to have caused significant flooding in Fitzsimmons Creek have all been in the recent past, because the area was settled recently. The highest rainfall totals for maximum 48-hour periods from the Alta Lake rain gauge were:

Dec 25-26 1980, 100 mm
 Oct 30-31 1981, 90 mm
 Nov 09-10 1990, 97 mm
 Aug 29-30 1991, 103 mm

The rainfall totals for maximum 24-hour periods from the Alta Lake gauge were:

Nov 10, 1990: 72 mm (15-year return)
 Aug 30, 1991: 76 mm (20-year return)

The response of Fitzsimmons Creek during the flood of August 1991 compared to the flood of November 1990 was dramatically more severe. The August 1991 flood flow exceeded the channel capacity by a large factor causing large flows to pass over the floodplain. The extensive damage caused to vegetation on the floodplain, and the large amount of debris and bed material added to the floodplain was witness to the fact that

the flood was of large return period, probably in the range 50-80 years. The fact that the return period of the rainfall event that caused the extreme flooding on August 29-30, 1991, was only medium was not surprising or inconsistent. Before and during the event almost the whole catchment was snow free, and was not buffered by a snow pack, enabling very fast runoff to occur, causing the extreme flooding.

We routed an example 48-hour storm, with a peak precipitation of $76 \times 1.4 = 107$ mm in 24 hours through the Fitzsimmons Creek basin using Clark's method, see Bedient and Huber, (12). The calculation showed that the peak instantaneous flood was $120 \text{ m}^3/\text{s}$, and the daily average maximum flood was $100 \text{ m}^3/\text{s}$. This instantaneous flood magnitude was about twice the channel full capacity of Fitzsimmons Creek. Measurements of the flood at Green Lake outlet based on Green Lake peak water surface elevations and a rating curve for the lake outlet, with a flow allowance for contributions from other tributaries to Green Lake, confirmed this flow magnitude.

Observations of the bed of Fitzsimmons Creek were made before and after the flood in the alluvial fan reach (where there are ten bridge crossings), and in the high gradient canyon reach upstream of the fan. The most spectacular changes to the channel bed and floodplain occurred in the canyon reach.

This is a reach of average gradient about 12%, with the flow in a channel about 10 to 12 m wide, and a valley floor width (channel and floodplain) about 40 to 50 m wide. The river flows predominantly north, and is deflected from the east side of the canyon to the west side and back again, by the bedrock walls. During flood times, movement of large boulders in the 1 to 1.5 m diameter

range is facilitated by a large sand fraction in the bed-load. The large boulders are "rafted" along in the heavy sand-water fluid matrix.

Photography of parts of this reach was done by one of us (PRBW) only 10 weeks before the flood (on June 22), and by another of us (NAS) in 1988. Concerns existed about the stability of a logjam that existed about 100 m upstream of the Blackcomb pump station intake, and the logjam was carefully photographed. Eight days after the flood, on September 7, 1991, the reach was photographed again, with care being taken to line up photographs from the same locations as in June 1991, with the zoom lens at the same magnification. Evidence about bed elevations during the flood was also collected from sand and small floating debris that had lodged either on the sides of the canyon walls, or lodged on large debris and trees that had not been moved by the flood.

The results showed that extraordinarily large changes had occurred in bed elevations during and after the flood. Immediately upstream of the old logjam site, the bed elevation rose about 1.5 m during the flood due to an apparent overload of bed material (mostly sand and boulders) mixed with large logs and trees. During the tail of the flood, the creek eroded its own deposits, and within eight days the bed level had eroded to an elevation that was 4.5 m lower than the elevation in June 1991. At the old logjam site, during a period of several years prior to June 1991, a secondary channel had developed on the east side of the jam, see Figure 2. A dead fir tree standing at the side of the channel survived the flood and served as a useful measure of the increase of bed elevation. During the flood, the secondary channel was infilled with 2.5 to 3 m of bed material. The logjam was completely carried away and/or smothered by new bed material

and debris. At Blackcomb Mountain pump station intake immediately downstream of this reach, photographic comparisons showed that the bed had risen about 2.5 m during the flood, and had fallen within 8 days of the flood to the same level that existed before the flood.

Post Flood Remedial Work

The post flood remedial work consisted of gravel and debris removal, the repair of bridges, the reinstatement of sanitary and potable water services, and the repair of the water intake for the Blackcomb Mountain snow-making equipment.

One week after the flood, a land and air reconnaissance of the floodplain and the upper watershed of Fitzsimmons Creek was carried out by us, on behalf of Whistler Resort Municipality. This was to provide advice on the flood damage, and to identify any possible situations such as logjams or landslides that could hamper the cleanup operations.

The initial response involved the restoration of the channel capacity in the 1 km reach just upstream of and adjacent to the Whistler Village. Excavation equipment was brought in to remove the logjams at bridges and to construct a diversion channel to facilitate debris removal operations. A local survey company was retained to provide cut stakes for the excavator operators in order to restore the channel thalweg and channel banks to pre-flood conditions and to determine the actual quantity of sediment washed down during the flood.

Temporary sanitary sewer and potable water services were provided for residents affected by the flood. A local gas company was

on-site to evaluate the damage to the scoured gas lines crossing the creek.

Five bridges were damaged and consequently closed to traffic, necessitating vehicle and pedestrian traffic re-routing.

Most of the bridges sustained varying amounts of erosion and scour damage to their supports.

A structural engineer specializing in bridges evaluated the safety of all 10 bridges. One two lane wooden bridge, Nancy Green Bridge, was damaged so severely that it was deemed unsafe and was torn down and replaced with a Bailey bridge.

The most upstream of the bridges (Skier Bridge), located at the commencement of the fan, failed by washout of the east embankment and the resulting collapse of the east side deck (see Figure 3). This washout was caused by severe aggradation of the Creek bed during the peak of the flood, causing high velocity water to be able to impinge on unprotected soil and erode the toe of the fill embankment.

A major step in the cleanup operation was to establish a modus operandi to facilitate the removal of 128,000 m³ of gravel and about 1,000 trees within the 4 km floodplain of Fitzsimmons Creek. The initial operation was expanded to provide the ability to remove 500 to 700 truck loads of material per day working six days a week.

Upon completion of channel excavation, broken rock, riprap bank protection (maximum diameter of 1.5 m), placed at a 2 horizontal to 1 vertical slope, was installed to restore damaged banks and to enhance vulnerable areas.

The removal of gravel and debris from the channel and the installation of rock riprap

took seven weeks at an approximate cost of \$2.8 M. In addition, bridge reconstruction and restoration of essential services plus park land damage totalled approximately \$0.9 M.

Conclusions

Several valuable lessons and inferences were gathered from observations of the large flood event that occurred on Fitzsimmons Creek on August 29 to 30, 1991. These were:

- 1). Record magnitude floods for mountain Creeks may be caused by mid- and late-summer conditions of rain storms falling on wholly snow-free land surfaces, rather than by the well documented rain-on-snow events.
- 2). In mountain Creeks with large contributions of sediment from the sides of the river channel, the channel and floodplain rapidly choke with sediment during the early and peak stages of the flood. This causes large amounts of temporary aggradation, of 2 meters or more. During the recession of the hydrograph, the channel bed is eroded to close to its level before the flood, leaving large quantities of new material on the floodplain.
- 3). In engineering design, e.g. highway fill embankments near Creeks, it is important to build rip-rap protection very high, to accommodate not only the flood discharge, but also the fact that the bed of the channel may rise a great deal during the peak of the flood. Computed water surface elevations for flood design must allow for this infilling of the bed. The conventional wisdom that Creeks erode their beds during the flood peak may not apply to many mountain Creek situations.

4). For the routine operation of gauging stations in mountain Creeks, the rating curve will change during the rising and peak stages of the flood. At the end of the flood, the rating curve may return to close to the pre-flood rating. This change may occur during a period as short as one day to a few days only, so that in many cases it is unlikely that the change will be documented by gauging technicians. For this reason, instantaneous flood peaks obtained from water level recorders may give values that are much too high.

References

1. Jones, W.C., 1959. Cheekye River Mudflows. B.C. Department of Mines report, Victoria, B.C.
2. Schaefer, D.G., 1983. Storms. The B.C. Professional Engineer, December.
3. Evans, S.G., and Lister, D.R., 1984. The Geomorphic Effects of the July 1983 Rainstorms in the Southern Cordillera and Their Impact on Transportation Facilities. Current Research, Part B, Geological Survey of Canada, Paper 84-1B.
4. Schermerhorn, V.P., 1967. Relations between Topography and Annual Precipitation in Western Oregon and Washington. Water Resources Research, No. 3.
5. NCE, 1979. Melting Ice-Cap Floods Nordic Valley. New Civil Engineer International, September.
6. Delderfield, E.R., 1953. The Lynmouth Flood Disaster, E.R.D. Publications Ltd., Exmouth, Devon, England.
7. Stiny, J., 1938. Über die Regelmäßigkeit der Weiderkehr von Rutschungen, Bergstürzen and Hochwasserschäden in Österreich. Geologie und Bauwesen. Jahrg. 10. Heft 1, März. Springer, Vienna.
8. Bruschin, J., Bauer, S., Delley, P., and Trucco, G., 1982. The Overtopping of the Palagnedra Dam. Water Power & Dam Construction, January.
9. Jackson L.E., M. Church, J.J. Clague and G.H. Eisbacher., 1986. Slope Hazards in the Southern Coast Mountains of British Columbia. Geological Society of America, Cordilleran Section, Annual Meeting, Vancouver, B.C., May 6-10, 1986. Field Trip No. 4 Guidebook.
10. Thurber Consultants Ltd., 1977. Fitzsimmons Creek, Whistler, B.C., Geotechnical Review of Landslides and Debris Flows. Unpublished report to the Land Management Branch, B.C., Department of Environment.
11. Skermer, N.A. and Russell, S.O., 1987. Geotechnical Hazards Assessment of Fitzsimmons Creek, for Resort Municipality of Whistler. Steffen Robertson and Kirsten (B.C.) Inc., Report 64501.
12. Bedient P.B. and W.C. Huber, 1988. Hydrology and Floodplain Analysis. Addison Wesley Publishers, 650 p. (See Page 293).

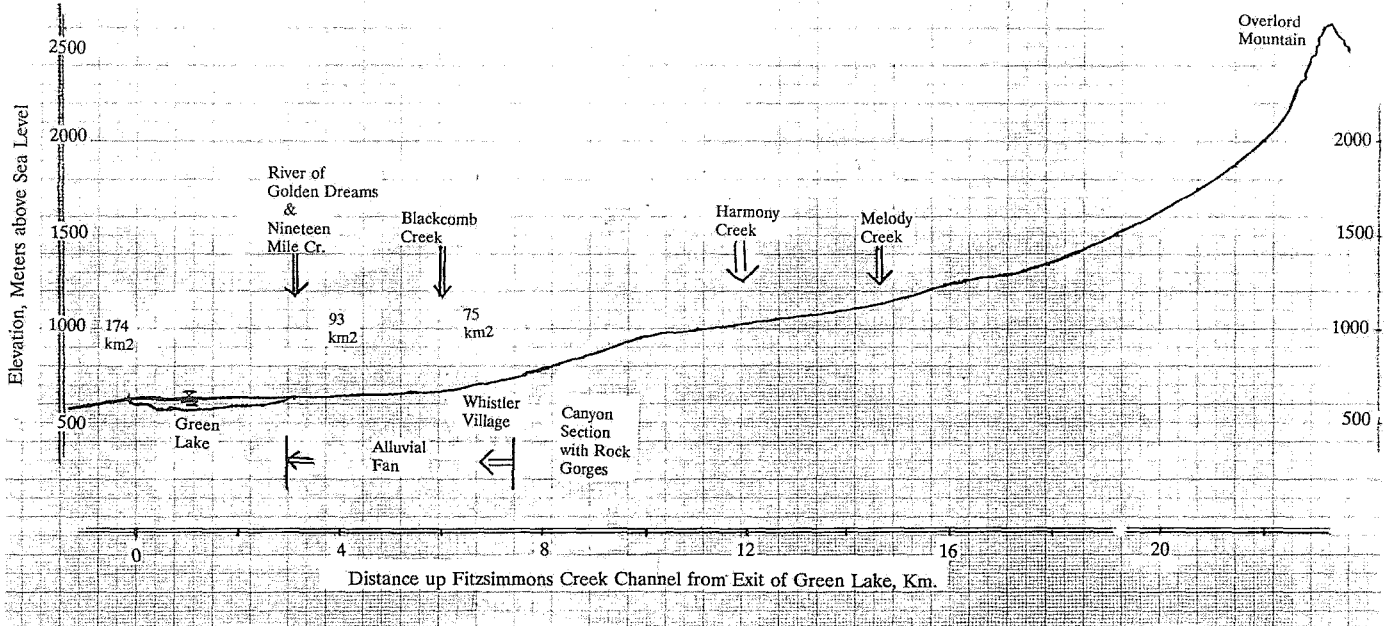


Figure 1. Profile of Fitzsimmons Creek, Whistler, British Columbia

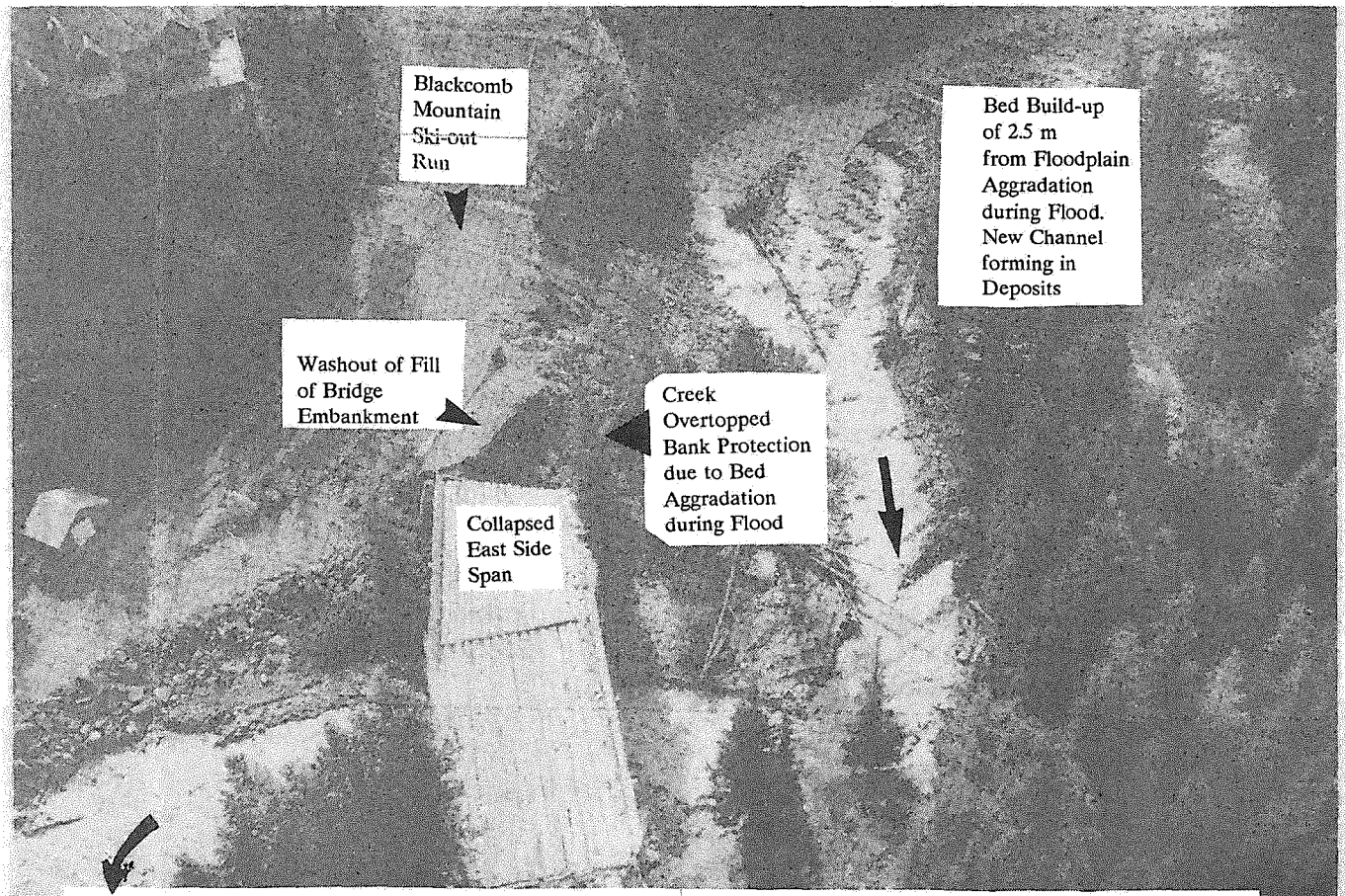


Figure 3. Failure of Fill Embankment and Abutment of Skier Bridge, Whistler, B.C.

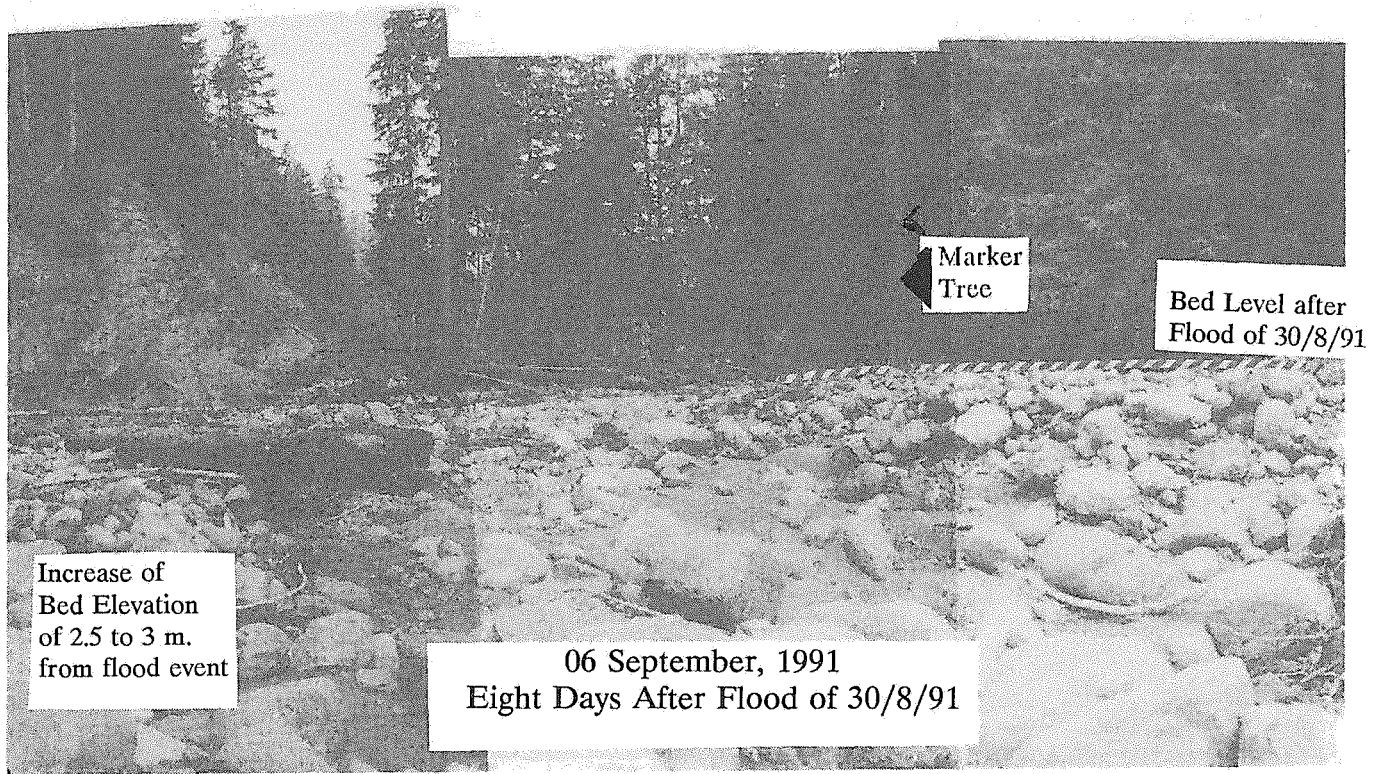


Figure 2. Bed of Fitzsimmons Creek in Canyon Section, 450 m Upstream of Skier Bridge

Patterns and Styles of Sedimentation, Erosion and Failure, Fraser Delta Slope, British Columbia

B.S. Hart

*Pacific Geosciences Centre
Sidney, British Columbia*

D.B. Prior

*Atlantic Geosciences Centre
Dartmouth, Nova Scotia*

T.S. Hamilton, J.V. Barrie & R.G. Currie

*Pacific Geoscience Centre
Sidney, British Columbia*

Abstract

The Geological Survey of Canada has initiated a multi-year, multi-component study of the Fraser Delta slope. In this paper we outline our current understanding of the geological processes active in this environment, based on the results of recent marine geological and geophysical surveys. We have identified complex patterns and styles of sedimentation, erosion and substrate failure. Much of the slope along Roberts Bank is erosional, whereas deposition from suspended plumes occurs on the Sturgeon Bank slope. Instability occurs on a variety of spatial and temporal scales. Portions of the slope adjacent to present or former river mouth positions can be the site of submarine channel and failure complexes. Larger features, apparently failure-related, tens of metres thick remain enigmatic. These results raise process-related issues which need to be addressed by geotechnical studies of the slope deposits.

Introduction

The Fraser Delta is the largest delta on Canada's Pacific Coast. In close proximity to the largest urbanized area on that coast, it is the site of much human activity and development. To ensure that societal uses of the offshore portions of the delta are undertaken safely, efficiently and with minimal disruption to or risk from the environment, it is vital that the geologic processes active in this environment be understood. With these concerns in mind, the Geological Survey of Canada has begun a program which concentrates on the subaqueous portions of the delta. The objectives of this multi-component study include the characterization of the surface morphology, internal structure and stability of the delta slope and substrates of the adjacent Strait of Georgia. The concerns of BC Hydro for foreshore installations and submarine cables have led to its joint participation in these study programs.

Subaqueous delta slopes are the sites of a variety of sedimentary and post-depositional processes. Slope failure in such an environment can be initiated by a variety of factors and the morphologic evidence for submarine slope failures is equally varied [1]. The definition of the spatial distribution, three dimensional geometry and age of disturbed sediments is a precursor to focused geotechnical investigations. Of key importance is the clarification of the relationship between sediment physical properties, the forces required to initiate failure and the dynamics of the moving mass once during failure and downslope transport.

This paper describes the sedimentary framework of the Fraser Delta slope, the relatively steeply dipping (typically 2-4°) portion of the delta between the edge of the flat-lying intertidal zone and the axis of the Strait of Georgia. Previous studies of this region [e.g. 2, 3] have suggested that a variety of instability processes may have occurred in this setting. Our aim here is to

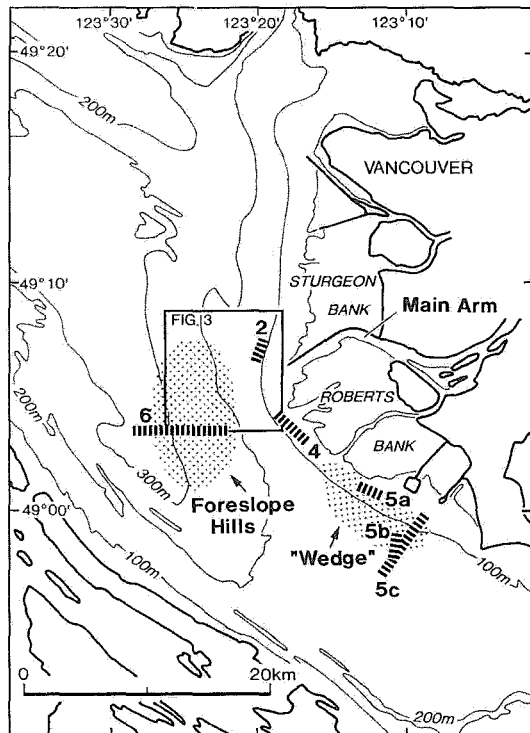


Fig. 1. Location of study area showing location of profiles shown in Figures 2-7.

characterize the geologic processes (sedimentation, erosion, failure) inferred to be presently or formerly active in this environment. We emphasize that the work is ongoing, and many questions remain.

Study Area

The Fraser is the largest river on the Pacific Coast of Canada. The delta formed at its mouth has a subaerial extent of approximately 1000 km², with growth of the present delta into the Strait of Georgia (Fig. 1) occurring entirely since the last glaciation [4]. Hamilton [5] has described the principal stratigraphic components underlying the central Strait, and mapped their distribution. He demonstrated that the postglacial deltaic sediments have been deposited on an erosional surface developed on deformed Tertiary bedrock and Quaternary deposits of marine and glacial origin, and are in places over 200 m thick.

At present, about 80% of the river discharge is through the Main Arm; this distributary is the only riverine source of sand [6]. Earthquakes with magnitudes as large as 6.5 to 7.0 can be expected to affect adjacent portions of the continental margin as frequently as every 10 to 20 years [7].

Methods

Several surveys of the Fraser Delta slope and adjacent Strait of Georgia have been conducted over the past decade. The results presented here are based primarily on the results of three cruises conducted in 1991 (PGC 91-01, 91-04, 91-08). In all, geophysical surveying has included collection of over 1200 km of high-resolution seismic records (Huntec Deep Tow Seismic) collected with fully corrected 100 kHz side-scan sonar imagery of the seafloor, and over 5000 km of airgun seismic profiles (of which about 2500 km is near or on the delta slope), generally with accompanying 3.5 kHz high-resolution sub-bottom profiling systems. Over 50 vibrocores, gravity and piston cores have been collected adjacent to the delta.

Interstitial gas, manifest as "acoustic turbidity", adversely affects both resolution and penetration of high-resolution seismic systems over much of the delta slope. Such gas is common in many deltaic environments and is attributed to bacterial degradation of buried organic matter within the sediment column. The acoustic effects of gas are frequency dependant, such that low frequency seismic systems are affected less than higher frequency sub-bottom profiling systems.

Styles and patterns of sedimentary and post-depositional processes presented in the following sections are interpretations based on seismic facies analysis [e.g. 8], accompanied by analysis of side-scan sonar images of the seafloor. These results are checked against core information wherever possible. Future work will test these interpretations and provide constraints on possible alternatives.

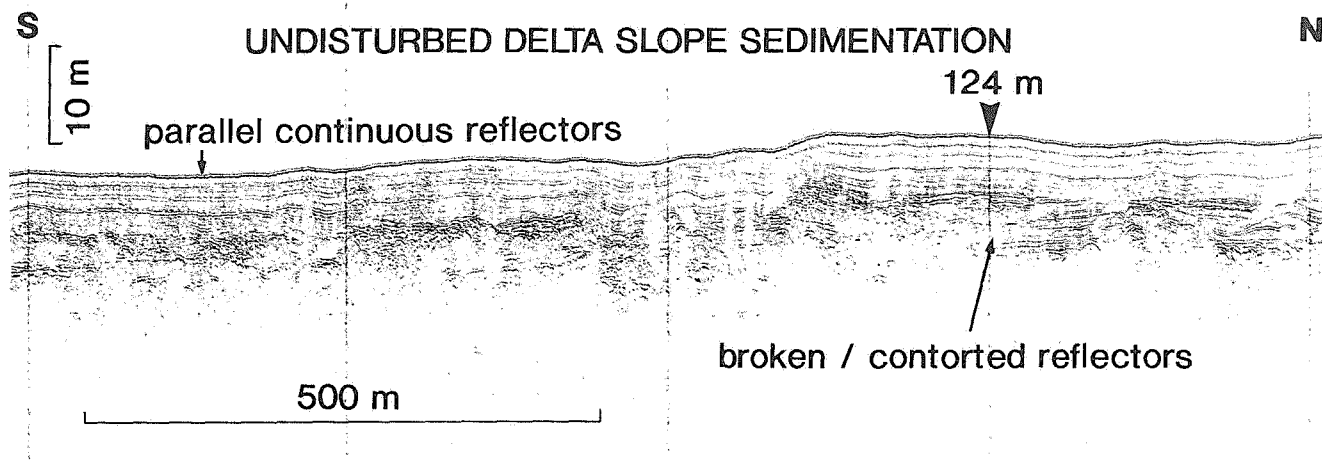


Fig. 2. Hunttec high-resolution seismic record showing parallel continuous reflectors typical of undisturbed delta slope sediments.

Sedimentation and Erosion

Sedimentation in delta slope settings is primarily from river mouth suspension, or by failure-derived gravity currents (see below). Rates of sediment accumulation or erosion are determined by the interplay of settling rates from suspension and strength of bottom currents at any one site. On the Fraser Delta, the course of the main river channel is known to have shifted by several kilometres in historical times prior to jetty construction [e.g. 9] and previous, more substantial changes of the river mouth position would have significantly altered patterns of slope sedimentation and erosion.

Parallel continuous reflectors, conformable with the seafloor, are observable on high-resolution seismic profiles of much of the delta slope (Fig. 2). Cores from these regions typically consist of massive muds, although sand (sometimes present as discrete laminae) is present in some cores from the upper portions of the slope. The mud is thought to represent undisturbed delta slope sediments, deposited from suspended sediment plumes. Such deposits are characteristic of the delta slope along Sturgeon Bank, and the axial portions of the strait. Comparison of profiles of ^{137}Cs concentrations in cores from this area with the fallout record can be used to measure sedimentation rates. Calculated values of $1\frac{1}{2}$ - 2 cm per year

are typical of the slope north of Sand Heads [see also 10]. Integration of high-resolution seismic data and measured sedimentation rates suggests that these areas have remained stable for the past few hundred years.

Zones of erosion are suggested by the truncation of seismic reflectors at the seafloor. They represent sites where deposition has ceased, due to changes in sediment supply (e.g. shifting of the river mouth position) or altered hydrodynamic conditions (e.g. shifting current patterns). The absence of measurable concentrations of ^{137}Cs in cores can also be used to infer that they were taken from zones of non-deposition or erosion. The combined evidence of these two techniques suggests that the delta slope adjacent to Roberts Bank is dominantly erosional.

A subaqueous dune field (sandwaves and megaripples) attests to the transport of sand by bottom currents along a portion of the delta slope adjacent to Roberts Bank [11]. Bedform migration is dominantly to the W to NW, sub-parallel to flood tidal currents. Side-scan sonar observations indicate that high voltage cables, lain on the seafloor in 1956, are partially exposed between sandwaves, attesting both to the absence of fine-grained sediment deposition and the mobility of the bedforms. The evidence suggests therefore that the delta slope adjacent to Roberts Bank, located south of the Main Arm, is scoured by flood tidal

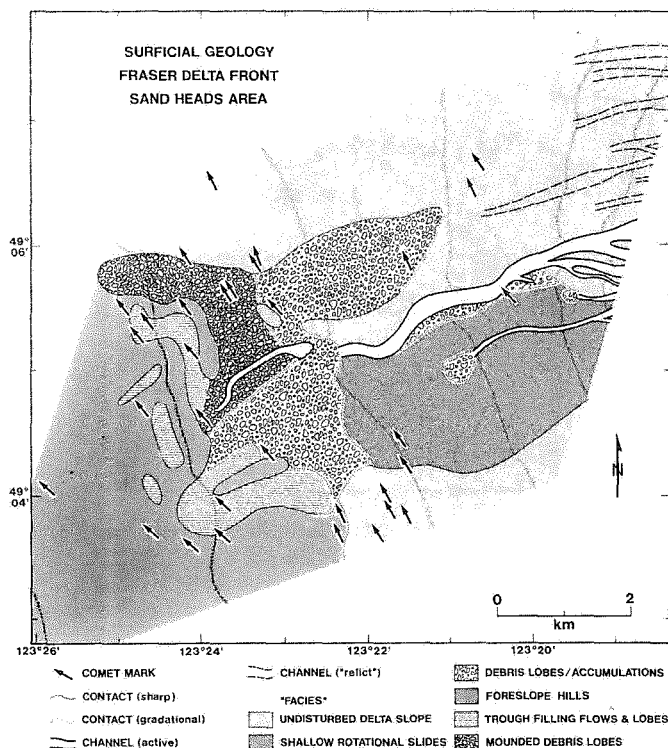


Fig. 3. Surficial geology map of submarine channel and failure complex seaward of Main Arm. The slope is dissected by a series of "active" and "relict" submarine channels, with sandy density flow deposits at the base of the active channels. Further explanation provided in [12].

currents which prevent accumulation of delta slope muds there.

Slope Instability

A submarine channel and failure complex has developed on the delta slope immediately seaward of the Main Arm (Fig. 3). The largest submarine channel has a depth of incision which decreases downslope from over 35m on the upper slope to 3m at the 200m isobath. Channel width is typically about 250m, but varies. This channel is characterised by steep erosional walls over much of its length and sandy sediments on its floor [see also 13]. Sandy debris flow deposits ("debris accumulations"), characterised by chaotic reflectors on high-resolution seismic records, cover an area of nearly $6 \times 10^6 \text{ m}^2$ at the base of the channel. Turbidite sands are present further downslope. Both types of gravity flow deposits apparently originated as failures at the mouth of

the Main Arm [e.g. 13]. An area of over $7 \times 10^6 \text{ m}^2$ of the upper slope south of the main submarine channel is comprised of shallow rotational slide blocks involving the upper few metres of the sediment column.

Other submarine channels, associated with base of slope turbidites and debris accumulations, can be found incised into the delta slope seaward of other former and modern river distributaries (e.g. Fig. 4). The channels probably originated when the associated river channel acted as a major sediment source to the upper portion of the delta slope. The channel floors are now generally muddy, the walls are smooth, and seismic stratigraphic relationships suggest that they are being infilled and are therefore no longer active.

The internal structure of the delta slope along the southern part of Roberts Bank is complex. Discontinuous, "contorted" parallel reflectors, in places erosionally truncated at the seafloor, are present

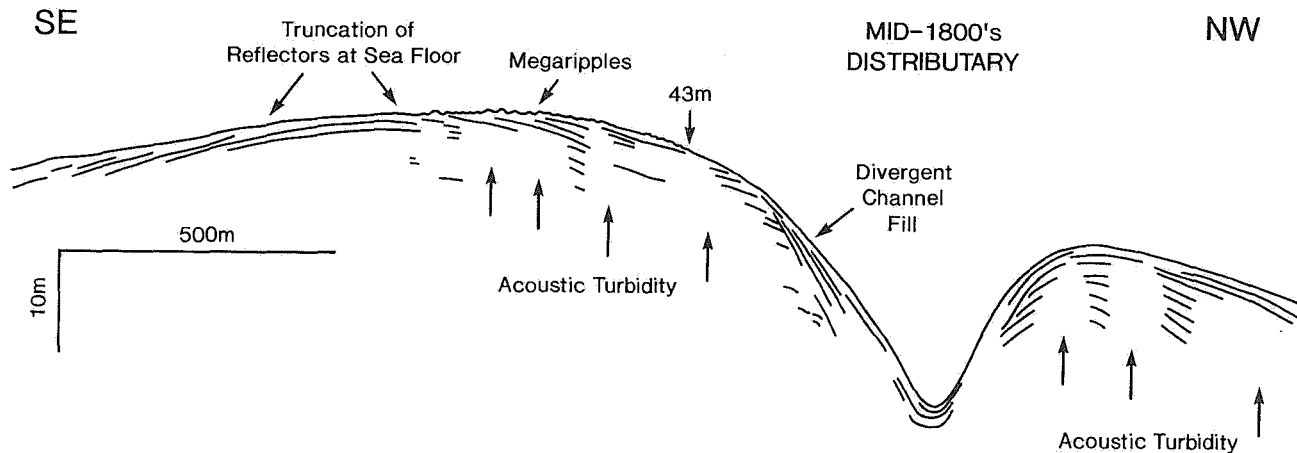


Fig. 4. Interpretation of Huntco high-resolution seismic profile showing delta slope channel cross-section on Roberts Bank, seaward of former main channel position in mid-1800's [9]. Note truncation of reflectors at the seafloor, and divergent geometry of channel fill muds.

beneath the sandwave field (Fig. 5a). Vibrocores through the sandwaves and into the underlying sediments indicate that the latter are comprised of interbedded sandy and muddy units which are not in equilibrium with the present current regime in this area. Their acoustic character on seismic records is substantially different from that of sediments of bathymetrically equivalent portions elsewhere on the Fraser Delta.

Chaotic reflectors, probably representing mass failure deposits, underlay at least 20 km² of the seafloor at the base of the Roberts Bank slope (Fig. 5b). Attenuation of high-resolution seismic signals by the overlying sandwave field obscures the relationship between the chaotic reflectors and the contorted parallel reflectors further upslope. However, airgun seismic profiles collected from this area in November 1991 [14] indicate that the two form part of a "wedge" of deltaic deposits, locally over 40m thick, which pinches out along and downslope (Fig. 5c). Given the problems associated with obtaining acoustic images of the detailed internal structure of the wedge (due to interstitial gas and the sandy nature of the sediments), our understanding of this complex remains limited at present. One possible explanation is that the entire wedge may represent failure deposits (with reflector

coherence degrading downslope from less to more highly disturbed sediments) emplaced either as a single massive event, or a series of relatively minor events.

The "Foreslope Hills", a region of elongate hills and troughs at the base of the slope in the central strait, have formed the object of several previous studies [e.g. 3, 15]. The internal structure of the hills, as seen on newly acquired airgun seismic data from this area [14] (Fig. 6) clearly indicate that the hills comprise distinct blocks, in places fault bounded. The blocks can be over 50 m thick, and comprise the middle to upper portion of the postglacial sediment column. Stratification within each block dips upslope - in direct contrast to reflection patterns observed on undisturbed portions of the delta slope such as Sturgeon Bank. This structural style is not compatible with previous interpretations that the Foreslope Hills are the product of compressional folding [2] or slumping followed by remoulding and deposition [3]. One possible explanation is that the hills represent rotational slipping of cohesive sediments generated by downslope extension [e.g. 16]. Efforts are under way to map and interpret the three-dimensional geometry of the Foreslope Hills system.

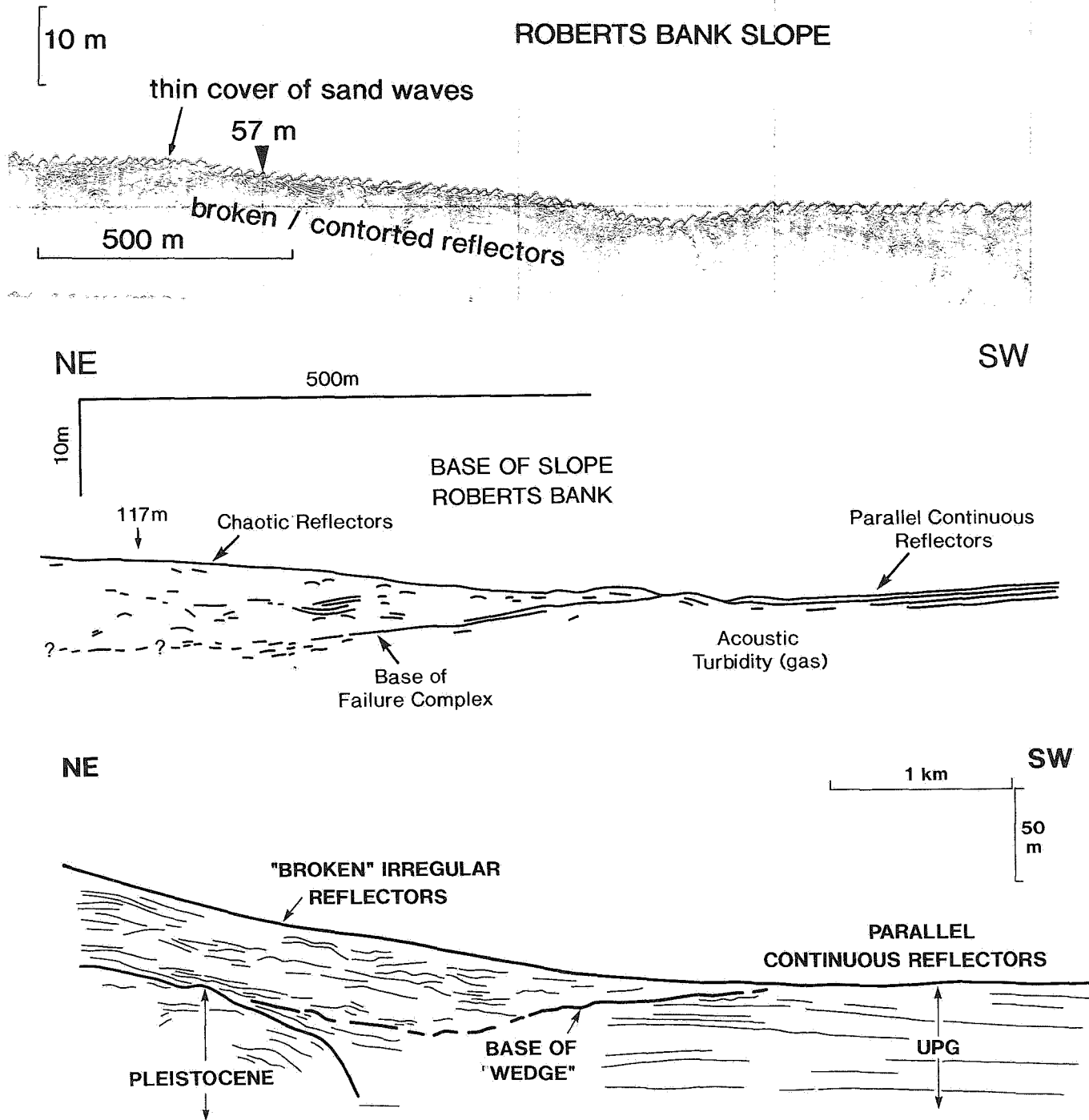


Fig. 5. a) Huntex high-resolution seismic profile over sandwave field showing "thin skin" of sandwaves over contorted parallel reflectors. b) Interpretation of Huntex high-resolution seismic profile of failure deposits (chaotic reflectors) at base of southern Roberts Bank slope. Chaotic reflectors overlie parallel continuous reflectors. c) Interpretation of airgun seismic record of Roberts Bank slope showing wedge-like feature, at least the upper portions of which are failure deposits.

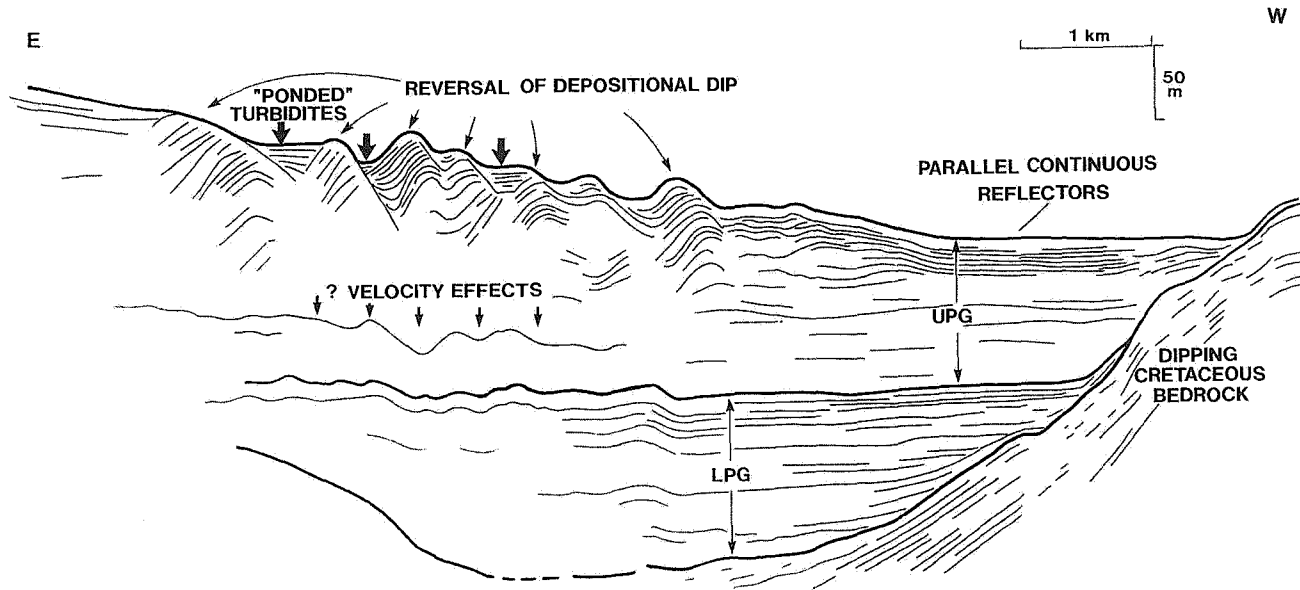


Fig. 6. Interpretation of airgun seismic profile showing internal structure of Foreslope Hills. See [14] for further description.

Summary and Future Directions

The work summarized in this paper indicates that the Fraser Delta slope is characterized by marked spatial variability. The delta slope adjacent to Roberts Bank is dominantly erosional, whereas suspended sediment plumes deposit mud on the northern part of the delta slope adjacent to Sturgeon Bank. The location of the Main Arm (the principal sediment source) and the strength of the flood tidal currents along the Roberts Bank slope appear to be the principal factors currently controlling these patterns of sedimentation and erosion.

Within this depositional framework, we have identified distinctive morphological components which suggest that slope failure has occurred on several spatial and temporal scales. Much of the evidence for failure appears to be associated with present or former river mouth positions although two large features, comprising tens of meters of the sediment column, remain enigmatic. Continued geological investigations, consisting primarily of mapping and age dating of failure deposits, will provide additional information which can be used to constrain the distribution, three-dimensional geometry and historical development of failure-related features

on the Fraser Delta slope.

The newly acquired geological data raises several new slope stability issues which must be further addressed by definition of the geomechanical properties of the slope sediments through *in situ* testing, coring, boreholes and modelling. It is anticipated that these studies will help clarify the relationship between the sediment's physical properties, the interplay of forces required to initiate failure, and the rheology of the moving mass once failure has occurred. Integration of the geotechnical and geological components will enhance our ability to predict the stability of specific portions of the Fraser Delta slope in response to various external forcing mechanisms (e.g. earthquake loading).

References

1. Prior, D.B. and Coleman, J.M., 1984. Submarine slope instability. In: D. Brunsten and D.B. Prior (eds.), *Slope Instability*. John Wiley and Sons Ltd., New York, 419-455.
2. Luternauer, J.L. and Finn, W.D.L., 1983. Stability of the Fraser River delta front. *Canadian*

- Geotechnical Journal, 20, 606-613.
3. Hamilton, T.S. and Wigen, S.O., 1987. The Foreslope Hills of the Fraser Delta: Implications for tsunamis in Georgia Strait. *International Journal of the Tsunami Society*, 5, 15-33.
 4. Clague, J.J., Luternauer, J.L. and Hebda, R.J., 1983. Sedimentary environments and postglacial history of the Fraser Delta and lower Fraser Valley, British Columbia. *Canadian Journal of Earth Sciences*, 20, 1314-1326.
 5. Hamilton, T.S., 1991. Seismic Stratigraphy of Unconsolidated Sediments in the Central Strait of Georgia: Hornby Island to Roberts Bank.; Geological Survey of Canada, Open File 2350.
 6. Milliman, J.D., 1980. Sedimentation in the Fraser River and its estuary, southwestern British Columbia (Canada). *Estuarine and Coastal Marine Science*, 10, 609-633.
 7. Rogers, G.C., 1982. Some comments on the seismicity of the northern Puget Sound -Southern Vancouver Island region. In: J.C. Yount (ed.) *Earthquake hazards of the Puget Sound region*, Washington State. U.S. Geological Survey, Open File Report, 21p.
 8. Bouma, A.H., Stelting, C.E. and Feeley, M.H., 1983. High resolution seismic reflection profiles. In: *Seismic Expression of Structural Styles* (A.W. Bally ed.); American Association of Petroleum Geologists, *Studies in Geology Series #15*, V. 1, (1.2.1) 1-23.
 9. Johnston, W.A., 1921. Sedimentation of the Fraser River delta; Geological Survey of Canada, Memoir 125, 46p.
 10. Moslow, T.F., Luternauer, J.L. and Kostaschuk, R.A., 1991. Patterns and rates of sedimentation on the Fraser River delta slope, British Columbia; In: *Current Research, Part E*; Geological Survey of Canada, Paper 91-1E, 141-145.
 11. Luternauer, J. L., 1980. Genesis of morphologic features on the western delta front of the Fraser River, British Columbia - status of knowledge; In: *The Coastline of Canada*, S.B. McCann (ed.); Geological Survey of Canada, Paper 80-10, 381-396.
 12. Hart, B.S., Prior, D.B., Barrie, J.V., Currie, R.G. and Luternauer, J.L., *submitted*. A river mouth submarine channel and failure complex, Fraser Delta, Canada. *Sedimentary Geology*.
 13. Kostaschuk, R.A., Luternauer, J.L., McKenna, G.T. and Moslow, T.F., *in press*. Sediment transport in a submarine channel system: Fraser River delta, Canada; *Journal of Sedimentary Petrology*.
 14. Hart, B.S., Horel, G., Olynyk, H.W. and Frydecky, I., *in press*. An airgun seismic survey of the Fraser Delta slope. In: *Current Research, Geological Survey of Canada, Paper*.
 15. Tiffin, D.L., Murray, J.W., Mayers, I.R. and Garrison, R.E., 1971. Structure and origin of Foreslope Hills, Fraser Delta, British Columbia. *Bulletin of Canadian Petroleum Geology*, 19, 589-600.
 16. Wernicke, B. and Burchfiel, B.C., 1982. Modes of extensional tectonics. *Journal of Structural Geology*, 4, 105-115.

Surface Water Waves Generated by Submarine Landslides

L. Jiang & P.H. Leblond

Department of Oceanography, University of British Columbia
Vancouver, British Columbia

ABSTRACT

Underwater landslides are a common source of small scale tsunamis in coastal areas. Theoretical and experimental studies on surface waves induced by underwater landslides are scarce. We develop a numerical model to study the coupling of a submarine landslide and the surface waves which it generates. A formulation of the dynamics of the problem is presented, where the landslide is treated as a Bingham-plastic flow and the water motion is assumed to be irrotational. Long wave approximation is adopted for both water waves and the mudslide. The resulting differential equations are solved by a finite-difference method. We present the numerical results for the mudslide surface variations, the surface elevations and the distribution of the horizontal velocity of the slide. The solution of the viscous fluid model can be derived as a special case of the present solution.

1. Introduction

Many small, but locally destructive, surface waves have resulted from underwater landslides with sufficient displaced volume. A major submarine landslide occurred April 27, 1975, in Kitimat Inlet, B.C., Canada, generating water waves with a height of up to 8.2m [1]. The duration of the slide was estimated to be (0.5-2) minutes. *Karlsrud* and *Edgers* [2] reported that an underwater landslide which occurred in the fjord near Sandnessjoen, Norway, generated a flood wave of (4-7)m in height and broke the electric power lines across the fjord. *Miloh* and *Striem* [3] studied the extreme changes in the sea level along the coast of Levant, Israel, and found that a recession of the sea occurred more often than a flooding of the shore. Such events may have been caused by mud slumping on the continental slope. Recently discovered evidence of slumping at the foot of the Fraser River, B.C., Canada, has created some apprehension about the possibility of a tsunami in the Strait of Georgia [4]. Therefore, a better knowledge of the phenomenon is of great significance to the technological development of offshore resources exploration and protection.

Various models have been proposed to study the

phenomenon of submarine landslides. Most of them are one-dimensional and can be classified into three classes: (1) viscous models [5,6], (2) visco-plastic models [7,8], (3) frictional models [9]. Much less work, however, has been done regarding the mechanical characteristics and the behavior of a submarine landslide and the tsunamis triggered by it [10]. All the previous studies on submarine landslides were based upon the assumption of a rigid lid at the water surface, or under the deep water assumption (the mudslide can not be felt by the free surface). There has been little investigation on the interaction between an underwater landslide and the surface waves which it generates.

The problem of surface water waves generated by an underwater landslide is poorly understood because there is a lack of both theoretical research and accurate observational data. *Miloh* and *Striem* [3] proposed an empirical evaluation method to study the waves induced by an underwater landslide. They assumed that the slide potential energy is partially converted into the surface wave energy. Their main parameter was the energy transfer ratio which was assumed to be less than 2%. In addition, they postulated that a major solitary wave, followed by a few small waves that can be neglected, was

generated. Equating the wave energy to the transferred part of the landslide energy yields the desired result of wave height, which can give a rough appraisal of a risk in practical cases. In *Miloh and Striem's* method the energy estimation relies on an almost arbitrary value of the energy transfer ratio and on the assumption of a single solitary surface wave profile.

Wiegel, et al., [11] conducted two-dimensional experiments in which the effect of a falling slide in a wave tank was analyzed. In the experiments, rigid bodies of several shapes, sizes, and weights were allowed to drop vertically or to slide down inclines of several angles (24° - 90°), in water of various depths, from several heights above the bottom. It was found that a crest is always formed first downwards from the slope, followed by a trough from one to three times the amplitude of the first crest, followed by a crest with about the same amplitude as the trough. The magnitude of the amplitudes depended primarily upon the submerged weight of the body but also upon the depth of submergence. The transfer ratio, relating to the net potential energy release to the wave energy, was of the order of 1%-2%. The sliding bodies used in *Wiegel's* [11] experiments were rigid blocks; they can not adequately simulate underwater mudslides whose surface is constantly changing while flowing down a slope.

Jiang and LeBlond [12] presented a numerical model for calculating surface waves which are produced by an underwater landslide, in which the slide is treated as incompressible viscous flow. Submarine sediments in different places may have different rheological behaviour, mostly as a consequence of the chemical composition, the grain size distribution, silt charge, etc.. Many laboratory tests on the rheological properties of coastal sediments [13] indicate that the Bingham fluid model is a good fit to the measured rheograms. Therefore similar analysis of the surface wave generation by a submarine Bingham-plastic slide appear wanting.

In this paper, a numerical model is presented to investigate water waves generated by underwater landslides on a gentle uniform slope in shallow water. The landslide material is treated as an incompressible Bingham plastic fluid. The long wave approximation is employed for both the water wave and the mudslide. The long wave approximation is valid only for small slope, so a

slope with angle of 1° - 5° is considered. A formulation of the governing equations of the mudslide and the surface waves is presented. It is assumed that water and mud are initially at rest and that the mud starts flowing down the slope at $t=0$. Surface waves produced by a mudslide with an initial parabolic shape are calculated by a finite difference method.

2. Bingham Model for The Submarine Landslides

A Bingham fluid (also called viscoplastic fluid) is one in which no deformation takes place until a specified stress (called the yield stress or the Bingham stress) is applied to the fluid, after which the deformation is driven by the excess of the stress beyond the yield stress. The stress-strain relation of a Bingham fluid is shown in Fig.1.

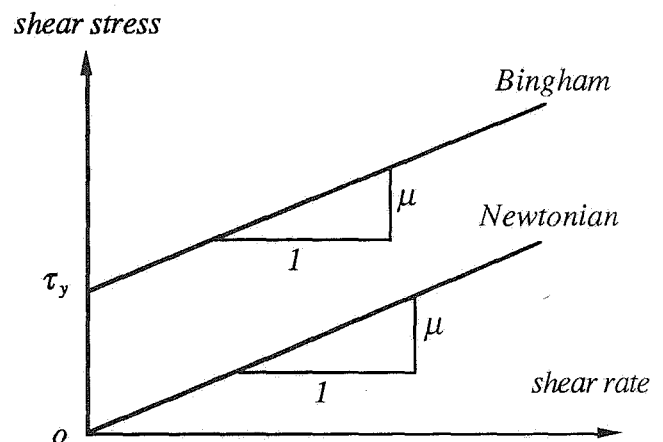


Fig.1 The stress-strain relation of Bingham fluid

For one-dimensional shear flow of a Bingham fluid, the stress-strain relation is

$$\mu \frac{\partial u}{\partial z} = 0, \quad \text{if } |\tau| < \tau_y, \quad (1)$$

$$\mu \frac{\partial u}{\partial z} = \tau - \tau_y \operatorname{sgn}\left(\frac{\partial u}{\partial z}\right), \quad \text{if } |\tau| > \tau_y. \quad (2)$$

where τ_y is the Bingham yield stress, μ is the coefficient of dynamic viscosity. The constitutive equations (1)-(2) can be used only if the flow is laminar.

The nonlinear constitutive relation (1)-(2) lead to two distinct zones in the flow (see Fig.2): the shear zone and the plug zone. In the shear flow, the shear stress exceeds the yield stress and the velocity U_s must vary in z . In the plug flow, the stress is smaller than the yield stress and the velocity U_p must be uniform in z .

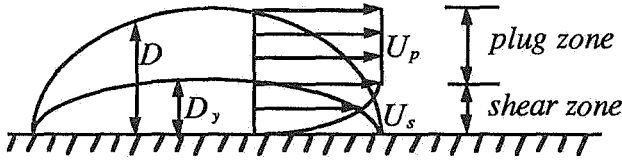


Fig.2 Velocity distribution of a Bingham flow

Consider a layer of visco-plastic mud flowing down a rigid impermeable slope inclined at a small angle θ with respect to the horizon (see Fig.3). Let the x -axis start from the upper margin of the slope, coinciding with the still water level and be directed to the deep sea. The z -axis is positive upward. We considered a river (at $x < 0$) with a depth of h_1 to avoid a mathematical singularity at the shore, and also a deep sea with a depth of h_2 to make the model more practically consistent. The free surface is designated as $z = \eta(x,t)$, and the sloping bottom as $z = -h_s(x)$. By the long wave approximation, the horizontal lengthscale is much greater than the vertical lengthscale and the velocity is essentially in the x -axis direction. The pressure within the mud layer can be assumed to be hydrostatic.

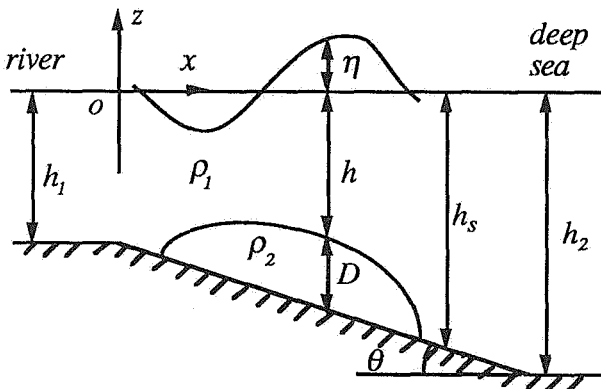


Fig.3 Definition sketch of the mudslide and the waves

The longitudinal momentum equation for the entire mud layer is

$$\rho_2 \frac{DU_m}{Dt} = (\rho_2 - \rho_1)g \sin \theta - \frac{\partial p}{\partial x} + \frac{\partial \tau}{\partial z},$$

$$-h_s(x) \leq z \leq -h(x,t). \tag{3}$$

where $U_m(x,z,t)$ is the horizontal particle velocity in the mud layer, τ is the shear stress in the mud, ρ_1 and ρ_2 denote the densities of water and mud respectively, $h(x,t)$ is the depth of the water and $p(x,z,t)$ denotes the pressure in the mud layer, which can be expressed as

$$p(x,z,t) = \rho_1 g(\eta + h) - \rho_2 g(z + h),$$

$$-h_s(x) \leq z \leq -h(x,t) \tag{4}$$

We neglect the tangential stress on the water-mud interface because the viscosity of water is much smaller than that of the mud, and the basal shear of the mudflow is much greater than the interfacial shear [14]. The corresponding boundary conditions are: zero-shear on the water-mud interface, and the non-slip condition on the bottom, i.e.,

$$\tau = 0, \quad \text{at } z = -h(x,t), \tag{5}$$

$$U_m = 0, \quad \text{at } z = -h_s(x). \tag{6}$$

Integrating (3) with respect to z and substituting (4) and (5) yields the shear stress distribution through the entire mud layer

$$\tau = (z + h) \left\{ \rho_2 \frac{DU_m}{Dt} + \rho_1 g \frac{\partial \eta}{\partial x} - (\rho_2 - \rho_1)g \left(\alpha + \beta - \frac{\partial D}{\partial x} \right) \right\}$$

$$-h_s(x) \leq z \leq -h(x,t). \tag{7}$$

where $\alpha = \tan \theta$, $\beta = \sin \theta$.

At the bottom, $z = -h_s(x)$, the shear stress is

$$\tau_b = -D \left\{ \rho_2 \frac{DU_m}{Dt} + \rho_1 g \frac{\partial \eta}{\partial x} - (\rho_2 - \rho_1)g \left(\alpha + \beta - \frac{\partial D}{\partial x} \right) \right\}. \tag{8}$$

For an underwater landslide starting from rest, it

is obvious that $|\tau_b|$ must exceed the yield stress τ_y for the slide to initiate, i.e., the fluid moves downslope if

$$(\rho_2 - \rho_1)g(\alpha + \beta - \frac{\partial D}{\partial x}) - \rho_1 g \frac{\partial \eta}{\partial x} \geq \frac{\tau_y}{D}, \quad (9)$$

and the fluid moves upslope if

$$(\rho_2 - \rho_1)g(\alpha + \beta - \frac{\partial D}{\partial x}) - \rho_1 g \frac{\partial \eta}{\partial x} \leq -\frac{\tau_y}{D}. \quad (10)$$

The slide does not initiate if $|\tau_b| < \tau_y$, or

$$\tau_y > D\{(\rho_2 - \rho_1)g(\alpha + \beta - \frac{\partial D}{\partial x}) - \rho_1 g \frac{\partial \eta}{\partial x}\} > -\tau_y. \quad (11)$$

At the yield surface the shear stress is equal to the yield stress, i.e.,

$$\tau = \tau_y \text{sgn}(U_p), \quad \text{at } z = -(h_s(x) - D_y(x, t)). \quad (12)$$

where $U_p(x, t)$ represents the plug velocity in the plug zone, $D(x, t)$ is the total thickness of the mud flow and $D_y(x, t)$ is the thickness of the shear zone.

The momentum equation in the plug zone can be obtained from (3), substituting (4),

$$\begin{aligned} \rho_2 \frac{DU_p}{Dt} = & (\rho_2 - \rho_1)g(\alpha + \beta - \frac{\partial D}{\partial x}) - \rho_1 g \frac{\partial \eta}{\partial x} \\ & + \frac{\partial \tau}{\partial z}, \\ & -(h_s(x) - D_y(x, t)) \leq z \leq -h(x, t). \end{aligned} \quad (13)$$

Integrating (13) with respect to z and substituting boundary condition (5) yields the shear stress distribution through the plug zone

$$\begin{aligned} \tau = (z + h) \left\{ \rho_2 \frac{DU_p}{Dt} + \rho_1 g \frac{\partial \eta}{\partial x} \right. \\ \left. - (\rho_2 - \rho_1)g(\alpha + \beta - \frac{\partial D}{\partial x}) \right\}. \end{aligned} \quad (14)$$

Substituting boundary condition (12), (14) reads

$$\begin{aligned} \rho_2 \frac{DU_p}{Dt} = & (\rho_2 - \rho_1)g(\alpha + \beta - \frac{\partial D}{\partial x}) - \rho_1 g \frac{\partial \eta}{\partial x} \\ & - \frac{\tau_y \text{sgn}(U_p)}{D - D_y}. \end{aligned} \quad (15)$$

For the shear flow, the velocity is dependent in z , equation (3) reads

$$\begin{aligned} \rho_2 \frac{DU_s}{Dt} = & (\rho_2 - \rho_1)g(\alpha + \beta - \frac{\partial D}{\partial x}) \\ & - \rho_1 g \frac{\partial \eta}{\partial x} + \mu \frac{\partial^2 U_s}{\partial z^2}. \end{aligned} \quad (16)$$

where μ is the dynamic viscosity of the mud, $U_s(x, z, t)$ represents the shear velocity which satisfies the following boundary conditions:

$$\begin{aligned} U_s(x, z, t) = U_p(x, t), \\ \text{at } z = -(h_s(x) - D_y(x, t)), \end{aligned} \quad (17)$$

$$\frac{\partial U_s}{\partial z} = 0, \quad \text{at } z = -(h_s(x) - D_y(x, t)), \quad (18)$$

$$U_s = 0, \quad \text{at } z = -h_s(x). \quad (19)$$

For a steady visco-plastic flow on a uniform slope, the left-hand terms of (16) vanish and the vertical distribution of the velocity in the shear zone is parabolic. Here, we assume that the mudslide rapidly reaches its equilibrium velocity [7, 8, 14] so that we may use a vertical parabolic distribution for the shear velocity, $U_s(x, z, t)$, which satisfies (17)-(19),

$$U_s(x, z, t) = U_p(x, t) \left\{ 2 \frac{z + h_s}{D_y} - \left(\frac{z + h_s}{D_y} \right)^2 \right\}. \quad (20)$$

Integrating (16) with respect to z from $z = -h_s(x)$ to $z = -(h_s(x) - D_y(x, t))$ and substituting (20) yields the governing equation of the shear flow

$$\begin{aligned} \rho_2 \left(\frac{2}{3} D_y \frac{\partial U_p}{\partial t} - \frac{1}{3} U_p \frac{\partial D_y}{\partial t} + \frac{8}{15} U_p D_y \frac{\partial U_p}{\partial x} \right) = \\ \left\{ (\rho_2 - \rho_1) \left(\alpha + \beta - \frac{\partial D}{\partial x} \right) - \rho_1 \frac{\partial \eta}{\partial x} \right\} g D_y - \frac{2\mu}{D_y} U_p \end{aligned} \quad (21)$$

Conservation of mass in the entire mud layer requires

$$\frac{\partial D}{\partial t} + \frac{\partial q}{\partial x} = 0, \quad (22)$$

where $q(x,t)$ is the volume flux of the mudflow:

$$\begin{aligned} q(x,t) &= U_p(D - D_y) + \int_{-h_s}^{-(h_s - D_y)} U_s(x,z,t) dz \\ &= \frac{1}{3} U_p(3D - D_y). \end{aligned} \quad (23)$$

For a uniform mud layer on an underwater slope with no elevation at the water surface, it can keep static at the threshold of downslope flow under the condition $\tau_b = \tau_y$. Using the expression of the shear stress at the bottom, (8), we obtain the critical thickness of mud at which the mud can stay stationary on a slope with inclination θ ,

$$D_c = \frac{\tau_y}{(\alpha + \beta)(\rho_2 - \rho_1)g}. \quad (24)$$

Thus a uniform mud layer can remain stationary on a slope if its thickness D is smaller than D_c . In contrast, a Newtonian fluid can achieve the state of static equilibrium only when the bed is horizontal and the depth constant.

We choose the initial maximum mud thickness, D_0 , as the vertical length scale, $[H]$; the initial mud length, L_0 , as the horizontal length scale, $[L]$; and the horizontal velocity scale $[U] = (g'[L])^{1/2}$. We adopt the following dimensionless variables

$$(x^*, z^*, t^*) = ([L]^{-1}x, [H]^{-1}z, \sqrt{g'/[L]}t), \quad (25)$$

$$(\eta^*, D^*, D_y^*, D_c^*, h^*) = [H]^{-1}(\eta, D, D_y, D_c, h), \quad (26)$$

$$(U_m^*, U_p^*, U_s^*) = [U]^{-1}(U_m, U_p, U_s). \quad (27)$$

where the variables with an asterisk are dimensionless and g' is the reduced gravity, defined as

$$g' = \frac{\rho_2 - \rho_1}{\rho_2} g. \quad (28)$$

With (25)-(27), the governing equations (15), (21) and (22) take on the form, with the asterisks being omitted,

$$\begin{aligned} \frac{\partial U_p}{\partial t} + U_p \frac{\partial U_p}{\partial x} &= \alpha + \beta - \varepsilon \frac{\partial D}{\partial x} - \frac{\varepsilon}{r-1} \frac{\partial \eta}{\partial x} \\ &\quad - \frac{(\alpha + \beta)K}{D - D_y} \text{sgn}(U_p), \end{aligned} \quad (29)$$

$$\begin{aligned} \frac{2}{3} D_y \frac{\partial U_p}{\partial t} - \frac{1}{3} U_p \frac{\partial D_y}{\partial t} + \frac{8}{15} D_y U_p \frac{\partial U_p}{\partial x} \\ = D_y \left(\alpha + \beta - \varepsilon \frac{\partial D}{\partial x} - \frac{\varepsilon}{r-1} \frac{\partial \eta}{\partial x} \right) - \frac{2}{\varepsilon R} \frac{U_p}{D_y}, \end{aligned} \quad (30)$$

$$\frac{\partial D}{\partial t} + \frac{\partial q}{\partial x} = 0, \quad (31)$$

where

$$\varepsilon = \frac{[H]}{[L]}, r = \frac{\rho_2}{\rho_1}, K = \frac{D_c}{[H]}, R = \frac{\rho_2 [H] \sqrt{g'[L]}}{\mu}.$$

3. Shallow-water Wave Equations with Ground Motion

For waves on a gentle slope in shallow water, we adopt the long wave approximation, i.e., the vertical lengthscale is much smaller than the horizontal lengthscale. Thus the water motion is essentially in the x -axis direction and the pressure distribution in the water can be assumed hydrostatic. The dynamic equations for nonlinear shallow-water waves induced by the general motions of an impermeable seabed are

$$\frac{\partial(\eta + h)}{\partial t} + \frac{\partial}{\partial x} [u(\eta + h)] = 0, \quad (32)$$

$$\frac{\partial u}{\partial t} + u \frac{\partial u}{\partial x} + g \frac{\partial \eta}{\partial x} = 0. \quad (33)$$

where $u(x,t)$ is the horizontal velocity of the water motion.

Using the same length scales and velocity scale as those used for the mudslide and remembering $h(x,t) = h_s(x) - D(x,t)$, (32) and (33) in dimensionless variables read, with the asterisks being omitted,

$$\frac{\partial \eta}{\partial t} = \frac{\partial D}{\partial t} - \frac{\partial}{\partial x}(uh_s) - \frac{\partial}{\partial x}(u\eta) + \frac{\partial}{\partial x}(uD), \quad (34)$$

$$\frac{\partial u}{\partial t} = -\frac{\epsilon r}{r-1} \frac{\partial \eta}{\partial x} - u \frac{\partial u}{\partial x}. \quad (35)$$

4. NUMERICAL SOLUTIONS

Assume the mud is initially at rest and has a parabolic surface (see Fig.4), i.e.,

$$D(x,0) = D_0 \{1 - [2(x - \bar{x}) / L_0]^2\}. \quad (36)$$

where, \bar{x} is the initial x-coordinate of the center of the mud, $\bar{x} = (x_1 + x_2) / 2$, x_1 and x_2 are the initial x-coordinates of the rear and front margins of the mud; $L_0 = x_2 - x_1$, is the initial length of the mud and D_0 is the initial maximum mud thickness.

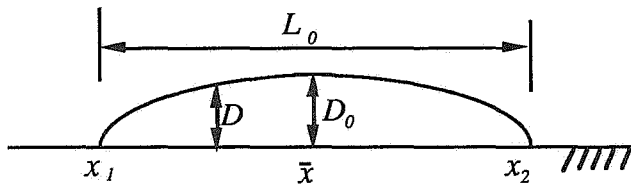


Fig.4 Definition sketch of initial mud surface

Given the slope angle and the typical parameters of the mud (the density, the viscosity and the yield stress) and the initial positions of the mudflow, we calculated $\eta(x,t)$ and $u(x,t)$ for the waves and $D(x,t)$, $D_y(x,t)$ and $U_p(x,t)$ for the mudslide by numerically solving the governing equations with a finite-difference method, in which the forward difference in time and the backward difference in space are used in the discretized equations. Two small artificial viscosities (of the form $\mu_a \partial^2 u / \partial x^2$, with μ_a the artificial viscosity; for the mudslide, $\mu_a = 0.001-0.006$; for the waves, $\mu_a = 0.025$) were introduced in the discretized equations for the water motion and for the mudslide to avoid numerical instabilities.

In the following numerical calculations, we considered a initial parabolic mud surface with height/length ratio of $\epsilon = D_0 / L_0 = 0.0087$, starting on a gentle uniform slope with inclination $\theta = 2^\circ$.

We employed the following typical parameters ranges: the density ratio of mud and water $r = 2.0$; the Reynold number R_e , defined as $R_e = \epsilon R$, is 87; the equilibrium thickness of the mud layer $D_c = (0.05-0.5)D_0$. We considered a river (at $x < 0$) with depth $h_1 = 0.5D_0$ and a deep sea with depth $h_2 = 12.5D_0$. The initial position of the mudflow is indicated by the parameter $\kappa = D_0 / h_0$, where $h_0 = h_s(\bar{x})$. We presented the results for the case where $\kappa = 2/3$.

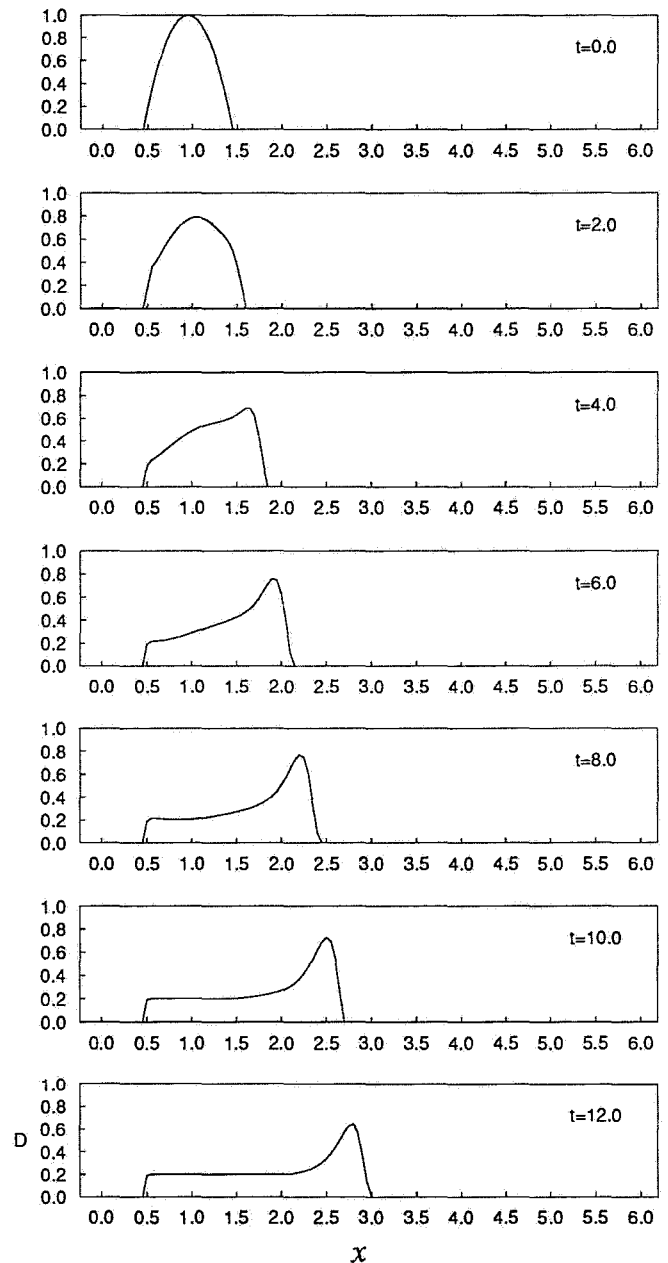


Fig.5 Variation of the mud surface, $D_c = 0.2$

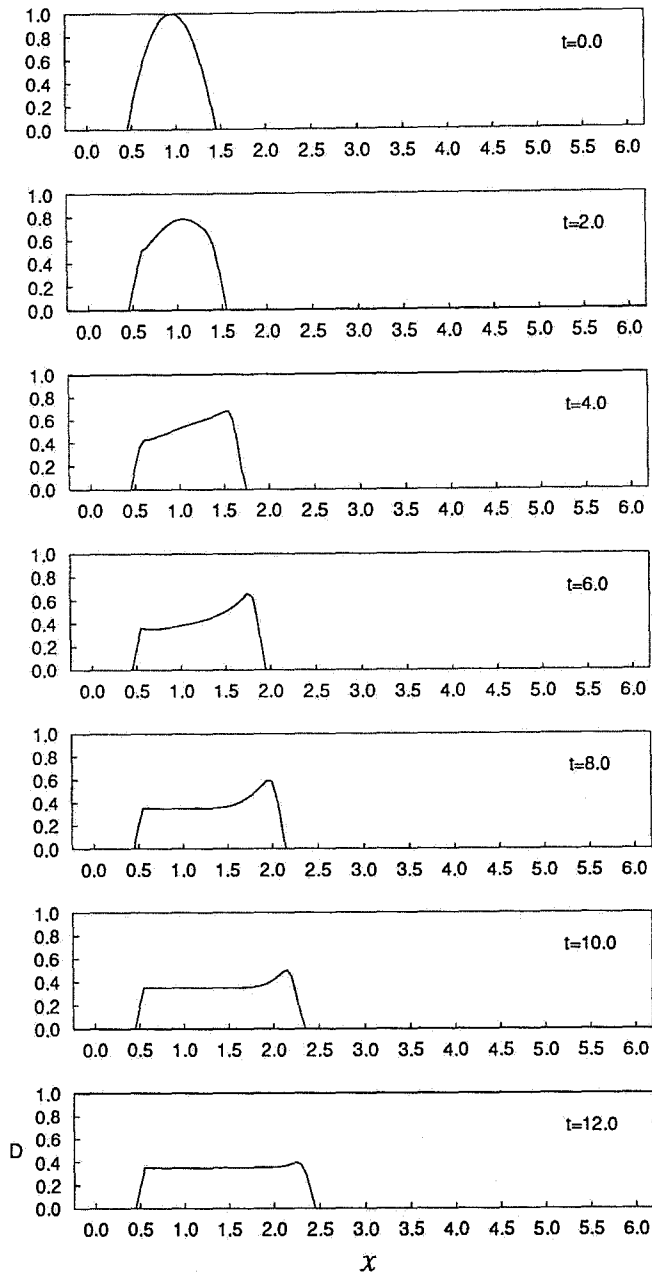


Fig.6 Variation of the mud surface, $D_c=0.35$

Figures 5 and 6 show the successive positions of the mud surface for $D_c=0.2$ and $D_c=0.35$ respectively. The results indicate that the plasticity of the mud slows down the flow speed of mud significantly. The run-out distance of a Bingham mudslide is limited. The slide will stop on the slope until the shear stress acting on the bottom of the slide is smaller than the yield stress. This is very different from the flow pattern of a viscous fluid flow which will spread very far from its original site on the slope until the capillary force dominates the flow.

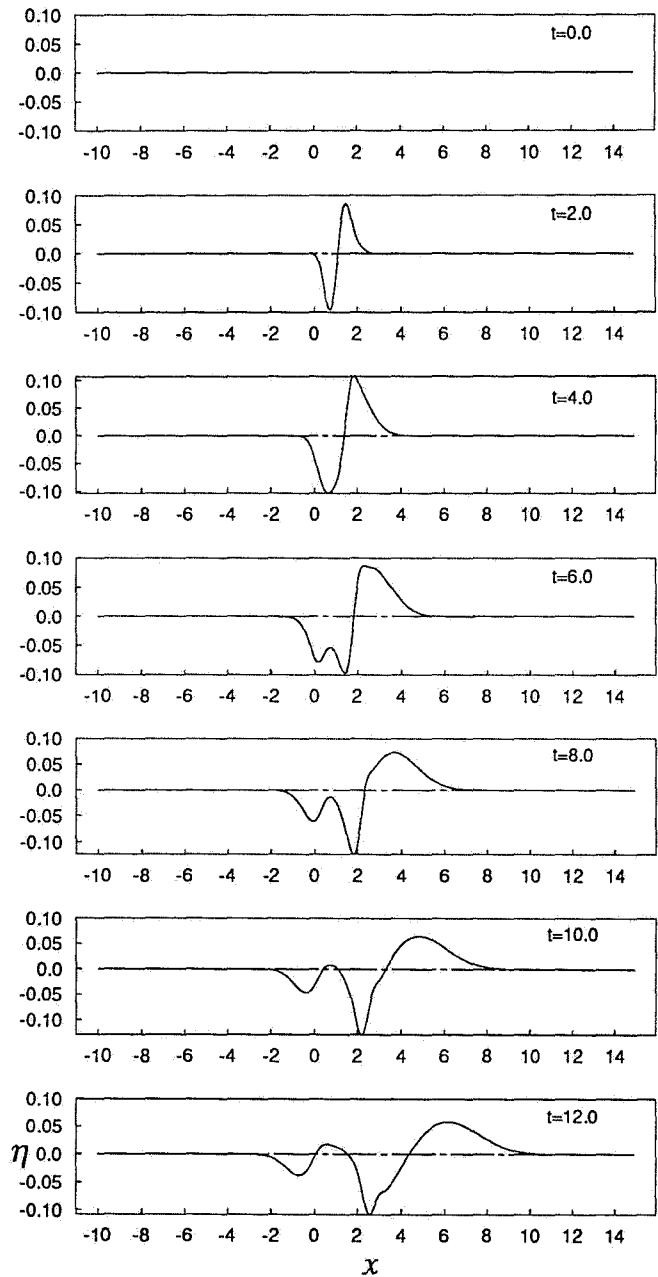


Fig.7 Evolution of surface waves, $D_c=0.20$

Figures 7 and 8 illustrate the evolution of the surface waves generated by the underwater mudslide under the conditions specified in Figs. 5 and 6. Three major waves are produced: the first wave is a large crest which propagates into deeper water from the slide site; the second wave is a trough following the crest as a forced wave propagating with the speed of the slide front. The third wave is a small trough which propagates shoreward. The fact that a trough propagates toward the shore coincides qualitatively with the observation [3] that a recession

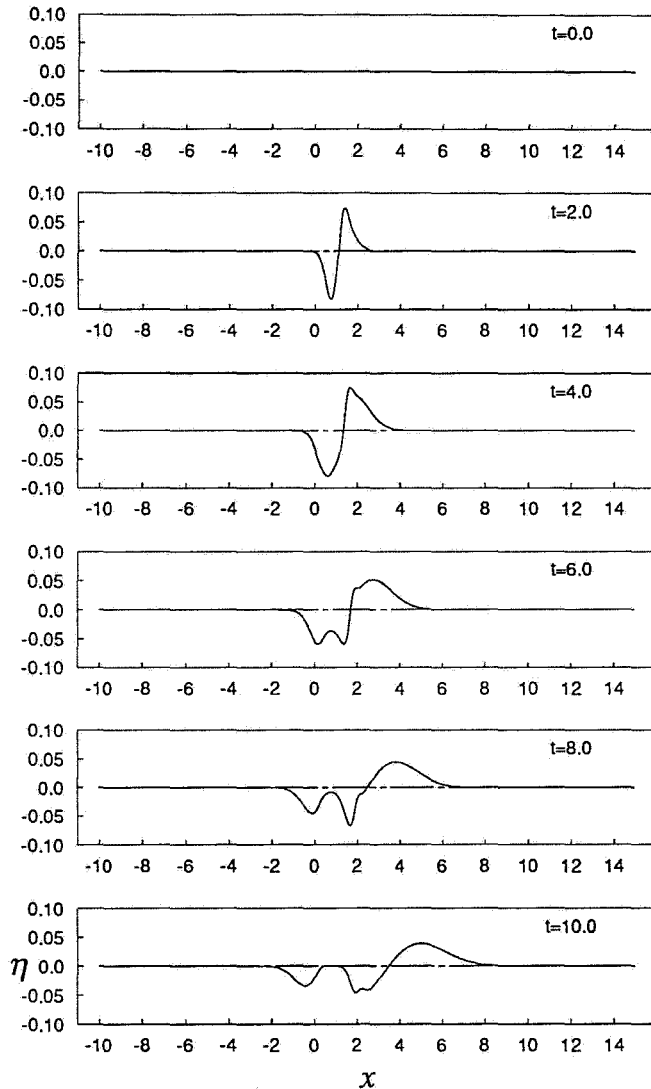


Fig.8 Evolution of surface waves, $D_c=0.35$

of the sea occurs as a result of the mud slumping on the continental slope. The parameter D_c (indicating the effect of the yield stress) has significant effect on the height of surface waves. The slide with larger D_c (i.e., larger yield stress) flows slower and generates smaller waves.

5. Concluding Remarks

We have presented a formulation of the dynamics of a Bingham-plastic submarine mudslide coupled with the surface waves which it generates, flowing on a gentle uniform slope. The numerical results show that the mudslide and the waves are significantly affected by the yield stress of the mud.

Acknowledgments. This study was supported by a strategic grant from the Natural Sciences and Engineering Research Council of Canada.

References

- [1] Murty, T.S., 1979, Submarine slide-generated water waves in Kitimat Inlet, British Columbia, *J. Geophys. Res.*, Vol.84, 7777-7779.
- [2] Karlsrud, K., and Edgers, L., 1980, Some aspects of submarine slope stability, *Marine Slides and Other Mass Movements*, Saxov, S., ed., 61-81.
- [3] Miloh, T., and Striem, H.L., 1978, Tsunami effects at coast sites due to offshore faulting, *Technophysics*, Vol.46, 347-356.
- [4] Hamilton, T.S., and Wigen, S.O., 1987, The foreslope hills of the Fraser River Delta: Implication of tsunamis in Georgia Strait, *Science of Tsunami Hazards*, Vol.5, 15-33.
- [5] Johnson, A.M., 1970, *Physical Process in Geology*, San Francisco, Freeman, 557pp.
- [6] Trunk, F.J., Dent, J.D. and Lang, T.E., 1986, Computer modeling of large rock slides, *J. Geotech. Engrg.*, Vol.112, No.3, 348-360.
- [7] Edgers, L., 1981, Viscous analysis of submarine flows, *Norwegian Geotechnical Institute*, Report 52207-3, 21p.
- [8] Liu, K.F., and Mei, C.C., 1989, Slow spreading of a sheet of Bingham fluid on an inclined plane, *J. Fluid Mech.*, Vol.207, 505-529.
- [9] De Matoes, M.M., 1988, Mobility of soil and rock avalanches, PhD Thesis, Univ of Alberta.
- [10] Locat, J., Syvitski, J.P., Norem, H., Hay, A.E., Long, B., LeBlond, P.H., Schafer, C.T., and Brugnot, G., 1990, Une approche a l'etude de la dynamique des coulées sous-marines: le project ADFEX. *43e Conference Canadienne Geotechnique*, Quebec, Canada.
- [11] Wiegel, R.L., 1955, Laboratory studies of gravity waves generated by the movement of a submerged body, *Trans. Am. Geoph. Un.*, Vol.36, 759-774.
- [12] Jiang, L., and Leblond, P.H., 1991, The coupling of a submarine slide and the surface waves which it generates, submitted to *J. Geophys. Res.*
- [13] O'Brien, J.S., 1988, Laboratory analysis of mudflow properties, *J. Hydraulic Engrg.*, ASCE, Vol.114, No.8, 877-887.
- [14] Mei, C.C., and Liu, K.F., 1987, A Bingham-plastic model for a muddy seabed under long waves, *J. Geophys. Res.*, Vol.92, 14581-14594.

Numerical Modeling of Physical Aspects of Submarine Debris Flows

F. Moutte, J. Locat & P. Therrien
 Département de Géologie, Université Laval
 Sainte-Foy, Québec

Abstract : Debris flows may cause material damage, and sometimes, human death. So as to protect ourselves against debris flows - and other flows or avalanches - we have to calculate velocity, height, run-out distance and pressure of these flows.

This paper deals with physical aspects of debris flows that we want to put in a finite elements model. The basic equations that we use in the model are the constitutive equations of a CEF-fluid which describe the stress tensor of non-Newtonian fluids as studied by Criminale, Ericksen and Filbey. We introduce a model of shear stress at the bed of the flow and on the upper boundary.

All these assumptions may contribute to a numerical model which should be able to predict the evolution of submarine and subaerial avalanches, and debris flows.

Résumé : Les coulées de débris peuvent provoquer des dommages matériels et parfois causer des pertes humaines. Pour se protéger des coulées de débris, et des autres coulées ou avalanches, on se doit de calculer la vitesse, la hauteur, la distance d'écoulement et le champs de pression de ces coulées.

Cet article expose certains aspects physiques des coulées de débris que nous désirons simuler par un modèle aux éléments finis. Les équations de base sont issues du tenseur des contraintes d'un fluide non-Newtonien du type CEF-fluid qui a été étudié par Criminale, Ericksen and Filbey. Nous introduisons un modèle de contraintes de cisaillement au niveau du lit et de la couche supérieure de la coulée.

Toutes ces hypothèses devraient conduire à un modèle numérique susceptible de prédire l'évolution des avalanches sous-marines et sub-aérienne et, des coulées de débris.

A debris flow is a heterogeneous gravity-driven mass movement that involves water-charged and coarse-grained

material flowing, more or less rapidly on open hillslopes or in preexisting channels. The slope where the flow occurs can be divided into three parts : the starting zone where the phenomenon is initiated, the run-out zone and the run-down zone where material is deposited [1].

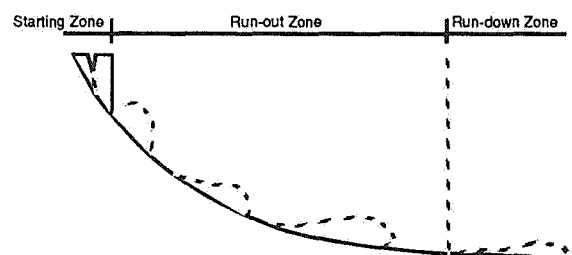


Figure 1. Description of a debris-flow between the starting zone and the run-down zone

There are several conditions which are conducive to a debris flow initiation (earthquake, over-load, over-saturation of soil, etc.). These conditions generally modify material characteristics such as yield strength, viscosity, density and pore pressure and thus a mass can reach the instability conditions. A computational treatment of the starting zone needs special program tools such as Knowledge-Based Systems or Geographic Information Systems.

The run-out zone may be seen as a zone where part of the initial energy will be transformed into heat or velocity. We can study this part mainly with physical equations (equations of momentum, conservation of mass, constitutive equations,...).

Once all of the energy has been transferred, the flow stops in the run-down zone. Several statistical models already exist for snow avalanches and might be adapted to debris flows.

In the following, we pay attention only to the run-out zone, in particular to the basic physical model and its

mathematical expressions and to the numerical model.

Physical Model

In experimental studies and investigations of incompressible non-Newtonian fluids it is usual to introduce three viscometric functions : a viscosity function η , a primary normal stress ψ_1 and a secondary normal stress ψ_2 . These viscometric functions should appear in the general constitutive equations. Though the literature of continuum models provides several constitutive equations for flowing materials, a fairly simple model which explicitly exhibits all three viscometric functions has been proposed by Criminale, Ericksen and Filbey [2]. The equations representing the CEF-model are

$$\sigma_{ij} = -p \delta_{ij} + 2 \eta d_{ij} + (2 \psi_1 + 4 \psi_2) d_{ik} d_{kj} - \psi_1 \{ d_{ij,t} - w_{ik} d_{kj} + d_{ik} w_{kj} \}$$

where δ_{ij} is the Kronecker tensor.
 η , ψ_1 , ψ_2 are scalar valued functions measuring shear and are identical to the viscometric functions.
 d_{ij} is the deformation tensor
 $d_{ij} = \frac{1}{2} [v_{i,j} + v_{j,i}]$
 $d_{ij,t}$ is the material derivative of d_{ij} .
 w_{ij} is the spin tensor $w_{ij} = \frac{1}{2} [v_{i,j} - v_{j,i}]$

The first term of this tensor represents the isotropic stress, the second term represents the viscosity and the third and fourth term represent the viscoelasticity.

Stress Tensor and Constitutive Equations

A set of constitutive equations has been proposed by Norem *et al.* [3] to model flowing granular materials. These constitutive equations mix a CEF-model and a reduced plasticity model of Oldroyd-Bingham.

$$\sigma_{ij} = - (p_u + p_e) \delta_{ij} \quad \text{isotropic stress}$$

$$+ 2 (\tau_s + p_e \tan \phi) \frac{1}{\dot{\gamma}} d_{ij} \quad \text{plasticity}$$

$$+ 2 \rho m \dot{\gamma} d_{ij} \quad \text{viscosity}$$

$$+ \rho (2 v_x - 4 v_y) d_{ik} d_{kj} - \rho v_x \{ d_{ij,t} - w_{ik} d_{kj} + d_{ik} w_{kj} \} \quad \text{viscoelasticity}$$

where p_u is the pore pressure

- p_e is the pressure transferred through the grain lattice or effective pressure
- τ_s is the yield strength
- ϕ is friction angle
- $\dot{\gamma}$ is the measure of shear and is defined by $\dot{\gamma} = \sqrt{2 d_{ij} d_{ij}}$
- ρ is the density
- m , v_x , v_y are viscosity parameters

The first four terms¹ of this tensor represent a simple Oldroyd-Bingham² model, the last three terms originate from the CEF-model. This material model has predominantly viscoplastic behaviour.

Norem *et al.* have made other assumptions ; specifically, for the velocity field : $v_x = v_x(y)$, $v_y = 0$, $v_z = 0$. Thus the constitutive equations yield the following stresses :

$$\sigma_x = p_e + p_u + \bar{\rho} (v_x - v_y) \left(\frac{\partial v_x}{\partial x} \right)^r \quad (1)$$

$$\sigma_y = p_e + p_u - \bar{\rho} v_y \left(\frac{\partial v_x}{\partial x} \right)^r \quad (2)$$

$$\sigma_z = p_e + p_u \quad (3a)$$

$$\tau_{xy} = \tau_s + p_e \tan \phi + \bar{\rho} m \left(\frac{\partial v_x}{\partial x} \right)^r \quad (4)$$

$$\tau_{xz} = \tau_{yz} = 0 \quad (3b)$$

where $\bar{\rho}$ is the average density of the flowing material
 r are exponents and depend on flow criteria (assumed equal to 1 for submarine flowslides)

Actually, the yield strength of the material is expressed by $\tau_s + p_e \tan \phi$. The first term, τ_s , is pressure-independent and assumed not to be especially equal to zero. The second term, which depends on pressure and friction angle, is a Coulomb friction. According to Savage and Sayed [4] and Hungr and Morgenstern [5] the dynamic friction angle is very close to the internal static friction angle.

¹That is to say the isotropic stress and the plasticity.
² $\sigma_{ij} = -p \delta_{ij} + 2 \mu_{ijkl} \frac{1}{\dot{\gamma}} d_{kl} + 2 \eta_{ijkl} d_{kl}$ is the complete Oldroyd-Bingham stress tensor

Studies on induced stresses in flowing granular materials had been made by Bagnold [6] & [7]. Bagnold found both a dispersive pressure in Oy direction and dynamic shear stress due to interparticular contacts. The exponent, r, is equal to 1 in macro-viscous flows and 2 in inertial flows.

The pressure transferred through the grain lattice, τ , may be found by applying equation (2), so the effective pressure is defined by the overburden pressure, dispersive pressure and pore pressure.

Pore Pressure and Acting Forces

Since the pore pressure plays a decisive part in submarine flows, it is very important to discuss and evaluate it. In materials liquified by blasting, pore pressure may have values 50 percent above the hydrostatic pressure. After Hutchinson and Bhandary [8] excessive pore pressure is assumed to be dissipated by consolidation.

The pore pressure may be seen as the sum of pressure due to water above the submarine flow, excessive pore pressure and atmospheric pressure, thus we have :

$$p_u = p_a + \rho_f g (H - y) \cos \alpha + \Delta u \rho_f g (h - y) \cos \alpha \quad (5)$$

- where p_a is the atmospheric pressure
- Δu is excessive pore pressure expressed as the ration to hydrostatic pore pressure within the flow
- ρ_f density of the interstitial flow
- H height of the water level
- h height of the flow
- g gravity
- α inclination of the slide path

The acting forces on our control volume are : force due to gravity, forces due to stresses acting on the vertical and finally shear stresses on the top and the bottom of the flow. The stresses acting in the vertical plane are normal stresses and pressure acting on the top of the flow. The shear stresses acting on the top and the bottom of the flow needs more investigation and will be explained in the next section.

Boundary conditions

Boundary conditions at the bed and at the upper layer consider frictions, modeled by shear stresses, between the flow and bed, and between the flow and the upper water.

At the upper layer, since the flow has a small thickness to length ratio we may assume these shear stresses to be comparable with those acting on flat plates moving into a more or less undisturbed fluid [9] & [10]. For turbulent flow over a flat rough plate the shear stress along the plate is defined by the following empirical equation

proposed by Schlichting [11].

$$\tau_h = \frac{1}{2} \left(2,87 + 1,58 \log \frac{x}{k} \right)^{-2,5} \bar{\rho} V^2 \quad (6)$$

- where k is the roughness length
- V is the undisturbed fluid velocity

The roughness length may be determined as Bagnold expressed it using wind-blow sand in his model. 'k' would be likely to lie between the ripple length and the grain size, that is to say between .001 and .1 meter.

While the boundary conditions at the upper layer was shown essentially to depend on the velocity of the dense slide, boundary conditions at the bed depend strongly on the material properties of the bed and the dense slide. We have to divide conditions into two groups : beds in which plasticity shear strength exceeds dynamic stress of the flow (non-erosive beds) and the opposite condition (erosive bed).

Since materials of submarines flow slides consist of the same type as bed materials, it is quite reasonable to assume that slip will not occur in slides. Yet, the roughness of the boundary may be considerably different from the flowing material roughness, and this could induce slip velocity. In the case of non-slip velocity the shear stress at the bed may be calculated by constitutive equations. For slip velocity conditions, Norem *et al.* [9] assumed the shear stress to be expressed by :

$$\tau_b = (\bar{\rho} - \rho_f (1 + \Delta u)) gh \cos \alpha \tan \phi_b + \bar{\rho} s v_b \quad (7a)$$

- where τ_b is the shear stress at the bed
- ϕ_b is the Coulomb friction angle at the bed interface
- s is a roughness parameter
- v_b is the velocity at the bed

If the bed consists of a softer material, the transferred shear stresses may exceed the shear strength of the bed material and, consequently, erosion may occur. In this case shear stress at the bed may be expressed by :

$$\tau_b = (\bar{\rho} - \rho_f (1 + \Delta u)) gh \cos \alpha \tan \phi_b \quad (7b)$$

If there is erosion, we have to pay attention to the expression of the equation of momentum in the mathematical model.

Mathematical Model

The mathematical model consists of expressions of physical assumptions with physical laws of conservation, and behaviour. We have chosen a differential control volume to explain these laws, we shall apply all the physical assumptions on this control

volume.

The flow is assumed to be two-dimensional, and we shall try to express the velocity as a function of x, y and t and the height of the flow as function of x and t.

Definition of the finite control volume and first equations

The chosen differential control volume is fixed in the Ox direction, but its height is allowed to vary in such a way that its upper surface coincides with the upper layer of the dense flow, and this at all times.

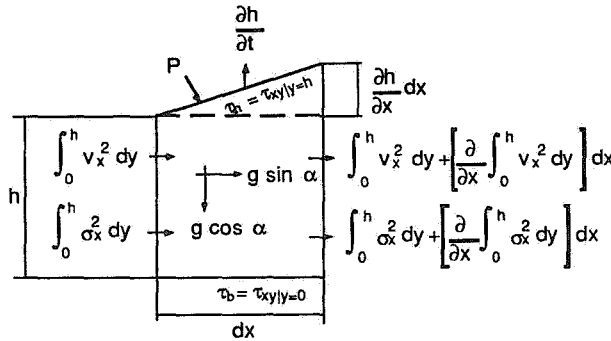


Fig. 2 : The chosen differential control volume. Forces acting on this control volume are represented on each surface of the volume. These forces are essentially gravity, compression (normal force in the Ox direction), effects of hydrostatic pressure, and finally stresses on the top and the bottom of the control volume.

By considering the flow at any given moment through the differential control volume, the momentum equation is :

$$\frac{\partial}{\partial t} \int_0^h \bar{\rho} v_x dy + \frac{\partial}{\partial x} \int_0^h (\bar{\rho} v_x) v_x dy = \sum_{\text{Control Volume}} f_x \quad (8)$$

The first integral considers the rate of change of momentum of mass within the control volume, the second one represents net transport. Forces on the right hand side of the equation is the components of the forces acting in the Ox direction.

By considering the flow at any moment through the differential control volume, the equation of continuity is :

$$\frac{\partial}{\partial x} \int_0^h v_x dy + \frac{\partial h}{\partial t} = 0 \quad (9)$$

This equation expresses that height varies only due to

variation of velocity through the control volume.

Expression of the acting forces and the velocity profile

As written before, the acting forces are gravity, stresses acting on the vertical and stresses on the top and the bottom of the flow. We express them in the Ox direction, so we have :

$$f_x = \begin{aligned} & (\bar{\rho} - \rho_f) g h \sin \alpha && \text{gravity} \\ & - \frac{\partial}{\partial x} \int_0^h \sigma_x dy && \left. \begin{array}{l} \text{stresses acting on the vertical} \\ + p_1 \frac{\partial h}{\partial x} \end{array} \right\} \\ & + p_1 \frac{\partial h}{\partial x} \\ & - \tau_h \\ & - \tau_b && \left. \begin{array}{l} \text{stresses on the top and the bottom} \end{array} \right\} \end{aligned}$$

where p_1 is the pressure acting on the upper boundary

Let us express each of these components. Study of the steady flow [3] & [1] with constant height helps us to express stresses¹ in the control volume. Acceleration in the Oy direction can be neglected², thus the normal stress σ_y is given by expression from steady flow study. The constitutive equations (1) and (2) give that

$$\begin{aligned} \sigma_x &= \sigma_y - \bar{\rho} v_x \frac{\partial v_x}{\partial y} \\ &= P_a + (\bar{\rho} - \rho_f) g (h - y) \cos \alpha \\ &\quad + \rho_f g (H - y) \cos \alpha - \bar{\rho} v_x \frac{\partial v_x}{\partial y} \end{aligned}$$

So the acting forces on the control volume may be expressed as :

$$f_x = \begin{aligned} & (\bar{\rho} - \rho_f) g h \sin \alpha \\ & - (\bar{\rho} - \rho_f) g \cos \alpha h \frac{\partial h}{\partial x} + \frac{\partial}{\partial x} \int_0^h \bar{\rho} v_x \frac{\partial v_x}{\partial y} dy \\ & - (\tau_h + \tau_b) \end{aligned} \quad (10)$$

To continue, we have to express the velocity profile. Once again, the steady flow study helps us to express it. Norem et al [1] assume velocity distribution may be given by a sinusoidal function.

¹In the steady flow conditions we may express σ_y and τ_{xy} as function of h and y , thus we have :

$$\begin{aligned} \sigma_y &= P_a + (\bar{\rho} - \rho_f) g (h - y) \cos \alpha + \rho_f g (H - y) \cos \alpha \\ \tau_{xy} &= (\bar{\rho} - \rho_f) g (h - y) \sin \alpha - \tau_h \end{aligned}$$

²This assumption induces a kinematic condition.

$$v_x(y) = v_1 \sin \left(\frac{\pi}{2} \frac{y}{h} \right) - v_2 \frac{y}{h} \quad (11)$$

where v_1 and v_2 are velocity control parameters

Finally we may express the acting forces on the control volume as :

$$\begin{aligned} f_x = & (\bar{\rho} - \rho_f) g h \sin \alpha \\ & - (\bar{\rho} - \rho_f) g \cos \alpha h \frac{\partial h}{\partial x} \\ & + \bar{\rho} v_x \left(\frac{2}{\pi} v_1 - \frac{1}{2} v_2 \right) \frac{\partial h}{\partial x} \\ & - (\tau_h + \tau_b) \end{aligned} \quad (12)$$

At this point, the main fundamental equations and physical principles of our subject have been developed. We are going to combine them to produce the final system.

Final System

This mathematical problem in the general case has 3 unknown functions of abscissa x and time t :

$h(x,t)$	the height of the flow
$v_1(x,t)$	a velocity control point
$v_2(x,t)$	a velocity control point

We have to find 3 equations to solve this problem. One which derives from assumptions on acceleration in the Oy direction is the kinematic condition at the upper boundary, the two others are given by the equation of continuity and the momentum equation.

In the previous paragraph, we approximated acceleration in the Oy direction. Furthermore, the corresponding velocity can be neglected, this means that :

$$v_y(h) = \frac{Dh}{Dt} = \frac{\partial h}{\partial t} + v_x|_{y=h} \frac{\partial h}{\partial x} \approx 0$$

Thus

$$\frac{\partial h}{\partial t} + [v_1 - v_2] \frac{\partial h}{\partial x} = 0$$

Now, we can explain the final system of 3 necessary equations² :

$$\frac{\partial h}{\partial t} + [v_1 - v_2] \frac{\partial h}{\partial x} = 0 \quad (I)$$

$$1 v_x(y) = v_1 \sin \left(\frac{\pi}{2} \frac{y = h}{h} \right) - v_2 \frac{y = h}{h} = v_1 - v_2$$

²We emphasize in bold font unknown functions of the system

$$\frac{\partial h}{\partial t} + \frac{\partial}{\partial x} \left\{ \frac{2}{\pi} h v_1 - \frac{1}{2} h v_2 \right\} = 0 \quad (II)$$

$$\begin{aligned} & - \bar{\rho} \frac{\partial}{\partial t} \left\{ \frac{2}{\pi} h v_1 - \frac{1}{2} h v_2 \right\} \\ & + \bar{\rho} \frac{\partial}{\partial x} \left\{ \frac{1}{\pi} h v_1^2 - \frac{8}{\pi} h v_1 v_2 + \frac{1}{3} h v_2^2 \right\} \\ & + \left\{ (\bar{\rho} - \rho_f) g \cos \alpha h - \bar{\rho} v_x \left(\frac{2}{\pi} v_1 - \frac{1}{2} v_2 \right) \right\} \frac{\partial h}{\partial x} \\ & + (\bar{\rho} - \rho_f) g h \sin \alpha - (\tau_h + \tau_b) = 0 \end{aligned} \quad (III)$$

with

$$\tau_h = \frac{1}{2} \left(2,87 + 1,58 \log \frac{x}{k} \right)^{-2,5} \bar{\rho} v^2$$

$$\tau_b = \begin{cases} [\bar{\rho} - \rho_f (1 + \Delta u)] g h \cos \alpha \tan \phi_b + \bar{\rho} s v_b \\ [\bar{\rho} - \rho_f (1 + \Delta u)] g h \cos \alpha \tan \phi_b \end{cases}$$

Next, we have to transform this mathematical into a finite element model and solve the discrete system we shall product.

Numerical Model

In finite element method, we have to solve three different questions [12]. What is the actual dimension of the model? What is the type of mathematical system? What is the lowest order derivative?

Answering each of these questions gives us a watermark to build the model, that is to say to choose the finite element and the most stable numerical scheme. Since the unknown functions in the previous mathematical system are functions of abscissa x and time t , this model is a 1D-space model. A short study of the mathematical model shows us a non-linear hyperbolic system, and finally the lowest order derivative is 1.

We are now going to discuss every aspect of the numerical model. First of all, we overview the formulation, then we present aspects of finite element choice and gridding and finally we speak about the numerical scheme.

Formulation

From equations (I), (II) and (III) we can express a system of non-linear partial differential equations such as :

$$[C(u)] \{\dot{u}\} + [k(u)] \frac{\partial}{\partial x} \{u\} + \{f(u)\} = 0$$

$$\text{where } \{u\} \text{ is } \begin{Bmatrix} h \\ v_1 \\ v_2 \end{Bmatrix}$$

$$\{\dot{u}\} \text{ is } \frac{\partial}{\partial t} \{u\}$$

We note $L(U)$ the differential operators of this system. The finite element method helps us to transform this system to :

$$W = \int_{\text{domain}} \psi (L(u) + \{f\}) dV = 0$$

$$= [C(u)] \{\dot{u}\} + [K(u)] \{u\} + \{F(u)\} = 0$$

Thus we eliminate the ∂x differential operator in our expressions [13]. As usual in finite element methodology, we express 'W' as a sum of virtual works on each finite element of the grid and then we have to assemble matrices and vectors of each element on global matrices (M, K) and the vector F of our problem and resolve this final discrete system.

Finite element and Gridding

Since our model is a 1D-space model and the lowest order derivative is 1, we need neither special finite elements nor complex or high precision finite elements. Thus we choose the fairly simple two nodes finite element over which we can define C^0 continuity shape functions¹ [12].

We shall use a reference element which is described in a local referential and transformed in the actual referential. So we shall have to apply a grid on our profile description. The main given of this model is a profile of the run-out zone. Since Nature is not as simple as an Euclidian mathematical space, we have to keep information on discontinuities. Thus we shall use special blending functions to discretize our profile. Such functions as Hermite, Bézier or B-spline functions are easily usable² to discretize and keep discontinuity information.

Numerical Schemes

We have to resolve two numerical problems, first of all our model is a non linear system and it is a time dependent model. Consequently, we have to use a numerical method to discretize time differential operator

¹In this case, shape functions are $N_1(x) = \sqrt{1-x^2}$ and $N_2(x) = \frac{x+1}{2}$ with $-1 \leq x \leq 1$

²Hermite and Bézier blending functions are easier to compute than B-spline functions

and a numerical method to solve the non linear component of the system.

Actually, these two numerical schemes are linked, but we are going to present the numerical method to solve the non linear component of the system and then aspects of time discretization.

The main assumption in non-linear solution techniques is that U is undoubtedly convergent. Thus we may approximate C, K and F at any iteration to evaluate U. If we know U_t^j and $U_{t+\Delta t}^j$, we shall evaluate $U_{t+\Delta t}^{j+1}$ as

following :

$$\left[C \left(U_{t+\Delta t}^j \right) \right] \left\{ \dot{U}_{t+\Delta t}^{j+1} \right\} + \left[K \left(U_{t+\Delta t}^j \right) \right] \left\{ U_{t+\Delta t}^{j+1} \right\} + \left\{ F \left(U_{t+\Delta t}^j \right) \right\} = 0$$

$$\text{where } \left\{ \dot{U}_{t+\Delta t}^{j+1} \right\} \text{ is } \frac{\left\{ U_{t+\Delta t}^{j+1} \right\} - \left\{ U_t \right\}}{\Delta t}$$

We shall do this, while the condition of convergence is untrue.

In order to resolve the time component, we shall use the very well-known and useful finite difference Lax-Wendroff's³ numerical scheme [14] [15] & [16]. This scheme is well-suited to hyperbolic systems. This scheme is a two-step scheme, *i. e.* we have to evaluate $U_{(n,t+\frac{\Delta t}{2})}$ by using $U_{(n-1,t)}$ and $U_{(n+1,t)}$ and then we evaluate $U_{(n,t+\Delta t)}$ with $U_{(n,t)}$ and $U_{(n,t+\frac{\Delta t}{2})}$.

We can express the global algorithm of this numerical model.

```

loop on time steps
  loop on number of elements (n = NELT)
    U_{n,t+\Delta t}^0 = Lax-Wendroff { U_{1..n,t}, U_{1..n,t+\frac{\Delta t}{2}} }
    while not convergence on U_{n,t+\Delta t}^j
      iterate on U_{n,t+\Delta t}^j
    U_{n,t+\Delta t}
  end of resolution

```

³So called Taylor-Galerkin scheme in finite element method [16]

Discussion

This numerical model should improve a finite difference model carried out by Norem *et al.* [1]. Actually, this model introduces in the computation the pore pressure as a function of time, and the shear strength.

Although we would like to be able to consider pore pressure as a function of both time and space, we cannot, practically speaking. The physical model does not allow us to. Since we use the equation of continuity, we cannot introduce aspects of overthrusting in our model. But we should work on this in order to improve this model.

Finally, not all the boundary conditions are entirely explained, and before we compute this model we have to analyze them.

Acknowledgement

The authors are grateful to the reviewers for their patience, useful comments and suggestions. We want to thank Harald Norem and Bonsak Schieldrop from the Norges Geotekniske Institutt and Fridtjov Irgens from Universitetet i Trondheim who gave us information on the physical assumptions and carried out the physical model of this numerical model.

References

- [1] Norem, H., Schieldrop, B., 28 February 1991
"Stress analyses for numerical modeling of submarine flowsides"
Internal Report n° 522090-10 NGI, Norges Geotekniske Institutt, 26 pp
- [2] Criminale, W. O. Jr, Ericksen, J. L., Filbey, G. L. Jr, 1958
"Steady shear flow of non-Newtonian fluids"
The John Hopkins University - Baltimore Maryland USA
- [3] Norem, H., Irgens, F., Schieldrop, B., 1986
"A continuum model for calculating snow avalanche velocities"
Avalanche Formation, Movement and Effects
Proceedings of the Davos Symposium - September 86, Swiss
International Association of Hydrological Sciences, n° 162, 1987
- [4] Savage, S. B., Sayed, M., 1984
"Stresses developed by dry cohesionless granular materials in annular shear cell"
Journal of Fluid Mechanics,
Vol 142., pp 391-430
- [5] Hungr, O., Morgenstern, 1984
"High velocity ring shear tests on sand"
Géotechnique, Vol 34, pp 415-421
- [6] Bagnold, R.A., 1954
"Experiments on a gravity-free dispersion of large solid spheres in a Newtonian fluid under shear"
Proceedings of the Royal Society, Series A, n° 255, pp 49-63
London
- [7] Bagnold, R.A., 1956
"The flow of cohesionless grains in fluids"
Philosophical transactions of the Royal Society ,
Vol 249, n° 964, pp 235-297
London
- [8] Hutchinson, J. N., Bhandary, R. K., 1971
"Undrained loading : a fundamental mechanism of mudflows and other mass movements"
Géotechnique, Vol 21, pp 353-358
- [9] Norem, H., Irgens, F., Schieldrop, B., 1989
"Simulation of snow-avalanche flow in run-out zone"
Annals of Glaciology, Vol 13, pp 218-225
- [10] Norem, H., Locat, J., Schieldrop, B., 1990
"Physics and modeling submarine flowslides"
Marine Geotechnology
- [11] Schlichting, H., 1958
"Boundary layer theory"
Pergamon Press, New York [London - Paris], 523 pp
- [12] Zienkiewicz, O. C., Taylor, R. L., 1989
"The finite element method : basic formulation and linear problems"
MacGraw-Hill, Fourth Edition, Vol 1, ISBN 0-07-084174-8, 648 pp
- [13] Dhatt, G., Touzot, G., 1984
"Une présentation de la méthode des éléments finis"
Collection Université de Compiègne (France), deuxième édition, ISBN 2.00924-0, 543 pp.
- [14] Wendroff, B., White, A. B., 1989
"A supraconvergent scheme for nonlinear hyperbolic systems"
Computers and Mathematics with Applications,
Vol 18, n° 8, pp 761-767.

- [15] Donéa, J., Laval, H., 1988
"Application de la méthode des éléments finis à la dynamique des fluides"
in "Aspect théoriques et numériques de la dynamique des structures"
Collection de la direction des Études et Recherches d'Électricité de France
Eyrolles, ISBN 0399-4198, pp 1-57

- [16] Donéa, J., Quartapelle, L., Selmin, V. ,1987
"An Analysis of time discretization in the finite element solution of hyperbolic problems"
Journal of Computational Physics, Vol 70, n°2,
pp 463-499

Viscosity, Yield Strength, and Mudflow Mobility for Sensitive Clays and Other Fine Sediments

Jacques Locat

Groupe de Recherche en Géologie de l'Ingénieur (GREGI)
Université Laval, Sainte-Foy, Quebec

Abstract: Recent developments in the evaluation of the viscous behavior of muds has led to the incorporation of viscosity measurements in the evaluation of mudflow mobility for fine grained materials. Most of previous evaluation of flow properties were derived from back calculated flow events so that the viscosity was a sort of free parameter adjusted to fit observations. The paper present various relationships that can be used in evaluating the mobility of mudflows which will help to limit the number of free variables during the computation.

These findings were included in a more detailed study of mudflow mobility for the case of St. Jean Vianney (Québec) in sensitive clays and for an alpine-type mudflow at La Valette (Alpes Maritimes, France).

Résumé: Des développements récents ont permis une meilleure mesure en laboratoire des paramètres viscosimétriques des coulées boueuses. La plupart des données de viscosité et seuil d'écoulement étant dérivées de l'analyse à rebours de coulées de boues, les relations proposées dans cet article devraient aider à l'étude de leur mobilité surtout en limitant le nombre de variables libres dans le calcul.

Les résultats sont appliqués à une étude plus détaillée de deux coulées boueuses: une à St-Jean-Vianney (argiles sensibles, Québec) et l'autre à La Valette (Alpes Maritimes, France).

INTRODUCTION

Debris flows are quite common in nature and represent one of the major threat to human life or property [1, 2]. It is an important hazard for which not only the occurrence or location must be predicted but also and very importantly its extent and velocity. Debris flows can peak at velocities as high as 20 m/s and can reach out at distances many kilometers away from the origin [3, 4]. The environments in which debris flows can be found are numerous: from

the sensitive clay plain to the alpine terrain and in deltaic subareal environments or on the deep sea floor. Only very few cases have been investigated for which velocity profiles and run out distances could be estimated or calculated [5, 6]. Over the last 10 years, some emphasis have been put on the laboratory determination of viscous flow properties of yield stress fluids such as remolded soils [7, 8]. It is difficult to directly measure, in the field, the viscous behavior of debris flows and when viscosity and yield strength data were obtained from back calculated events, it appears that differences between back calculated and measured values could be as much as four orders of magnitude. In many field evaluations, the viscous parameters are set to be the free variables. With the availability of laboratory measurements, one could then provide input data for yield strength and viscosity so to help improving modeling techniques and their use.

This paper concentrates on looking at the development of simplified relationships between index parameters for soils and their flow behavior with the objective of using them in mudflow mobility evaluation. The soils that have been tested are all fine-grained sediments (see Table 1) so that the relationships developed in this paper are, for the present, limited to clayey soils for which the water content is at or above the liquid limit.

FLOW PARAMETERS

Soils which present viscous behavior can be classified according to their particular behavior for various shear rate conditions (Figure 1). The main difference between newtonian and non-newtonian behavior is the presence of a yield strength which represents an initial resistance to flow. Most of the soils tested present either a flow behavior close to that of a Bingham or a pseudo plastic fluid. The general flow behavior can be represented by the following equation:

$$\tau = \tau_c + \eta \dot{\gamma}^m, \quad \tau \geq \tau_c \quad (1)$$

where τ is the yield stress, τ_c the yield strength, η the viscosity and γ the shear rate. For $m < 1$ the fluid behaves as pseudoplastic, for $m > 1$ as a dilatant, and when $m = 1$ as a Bingham fluid. For the general relationships presented hereafter, all soils are considered to behave as a Bingham fluid and the viscosity is thus measured from the slope of the last portion of the yield stress/shear rate curve taken as a straight line which intercepts the yield stress axis at a value defined as the yield strength (τ_c).

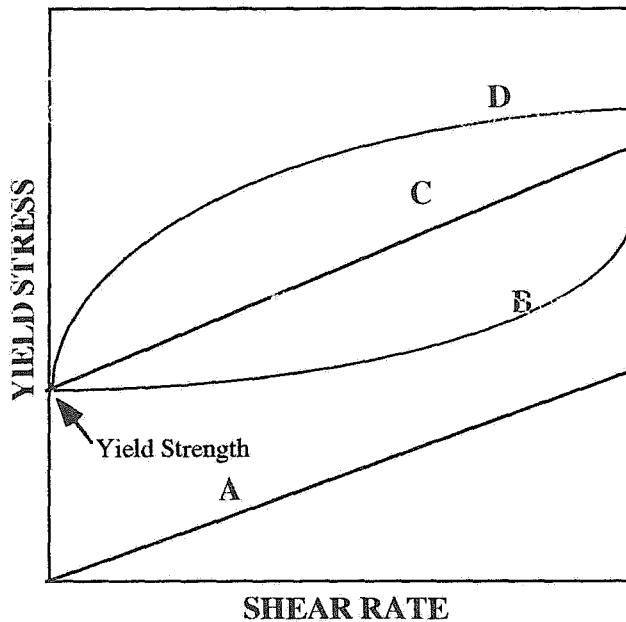


Figure 1. Typical flow curves for yield stress fluids: (A) Newtonian, (B) dilatant, (C) Bingham and (D) pseudo plastic (modified from Nguyen and Boger [9]).

The flow parameters have been obtained on various soils with a couette type viscometer (HAAKE, model RV-12) that can operate at shear rates as high as 1200 rpm but only on silt and clay mixtures. The procedure followed for measuring the viscous behavior of the soil as previously been described by Locat and Demers [7]. Before any measurement at a given shear rate, the soil is sheared at the highest shear rate possible so to ensure that the soil microstructure is always in the same condition before testing it at that particular shear rate. It is interesting to note here that, for the instrument used, the shear rate of 100 rpm is equivalent to a field velocity of about 10 m/s. In that sense, most of the measurements in the laboratory are taken at a velocity close to that of field conditions. For a full treatment on measuring flow properties of yield stress fluids, the reader is referred to the recent work of Nguyen and Boger [9].

SOILS TESTED

Soils tested in this programme came from various regions. The La Valette soil has been taken from the matrix of a debris flow which occurred in 1988 in the Alpes Maritimes (France). The Beaufort soil is from the Beaufort Sea area from a site where thaw problems were expected so that the flow properties of the sediment were of interest. The Cambridge soil is from a core collected at Cambridge Fjord, Baffin Island at a water depth of 400 m. Soils of that area have not been studied in details but have similar characteristics to the sensitive clays of Eastern Canada as it also come from glaciated pre-Cambrian terrain. The Saguenay soil as been taken from the Saguenay Fjord and the St-Alban soil from that locality just east of Québec City; this later soil being typical of leached sensitive clays.

Various soil properties have been assembled in Table 1 which illustrates the range in grain size and plasticity index. It must be noted that the La Valette soil as been sieved to retain only the portion lower than 100 μm . Water content values are for field conditions at the time of sampling.

TABLE 1. Physico-chemical characteristics of the various soils (SAG: Saguenay; LAV: La Valette; BEAU: Beaufort; CAM: Cambridge; STA: St. Alban)

	SAG	LAV	BEAU	CAM	STA
w (%)	59-70	20-35	35	76	46
w _p (%)	26-29	21-25	26	31	19
w _l (%)	59-70	37-41	52	64	36
I _p (%)	33-41	16-17	26	33	17
SS ¹	28-63	25-29	57	38	52
S ²	24-28	-	20	33	0,3
CF ³	65-85	25-35	30	40	46

1: Specific Surface Area, in m^2/g

2: Salinity, in g/L

3: Clay Fraction (%)

Soils tested present a liquidity index/remolded shear strength relationship that is quite uniform for the type of material used. The good relationship is partly due to the forcing of the measurement of liquid limit with the fall cone at a remolded shear strength of 1070 Pa. Values of the remolded shear strength for soils above a liquidity index of 3,0 were estimated with the relationship proposed by Locat and Demers [7]:

$$C_{u_r} = \left(\frac{19,8}{I_L} \right)^{2,44} \quad (2)$$

where the remolded shear strength (C_{ur}) is computed in kPa. Results for most soil samples are shown in Figure 2.

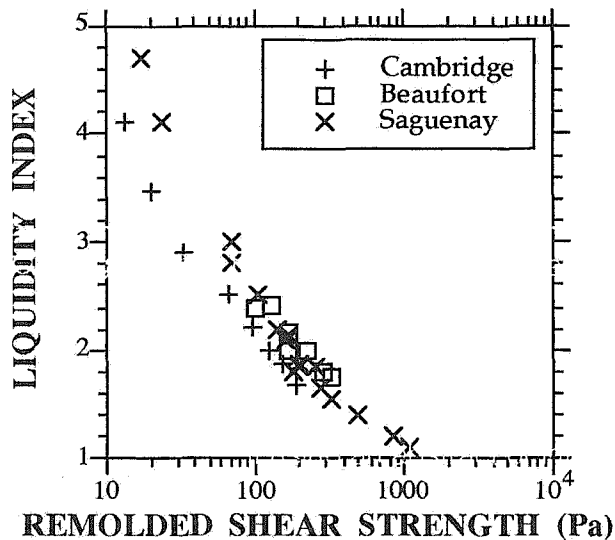


Figure 2. Relationship between the remolded shear strength and the liquidity index for some soil samples tested.

FLOW BEHAVIOR IN THE LABORATORY

The flow behavior of all soils was tested at various water content (or liquidity index) but only results for a liquidity index at about 4.0 (Figure 3) and about 2.0 (Figure 4) are presented here.

The La Valette and Beaufort soils have a distinct behavior compare to the others with a more pronounce pseudoplastic yield stress/shear rate curve. On the opposite, the Cambridge, St. Alban and Saguenay samples have a flow behavior closer to that of a Bingham fluid. For both extreme values of liquidity index, the differences are maintained. Even if the flow behavior is different from soil to soil, it has been considered that applying a Bingham model would still provide a good first estimate of both the viscosity and the yield strength. The viscosity and yield strength will be computed as indicated above.

The St. Alban soil presents a very low yield strength and viscosity at a liquidity index of about 2 (Figure 4). This behavior has been observed before for very sensitive clays that is those marine that have been leached to a low

salinity. The effect of the salinity on the St. Alban soil have been illustrated by Locat and Demers [7].

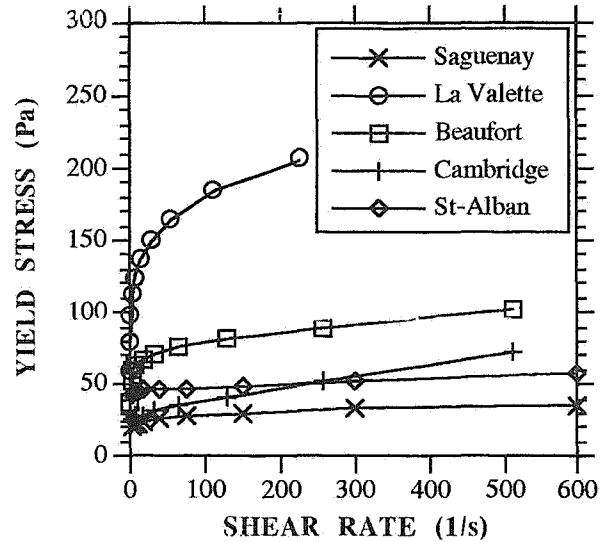


Figure 3. Yield stress and shear rate results for soils prepared at a liquidity index of about 4.0 (Saguenay: 3.85; La Valette: 3.8; Beaufort: 3.2; Cambridge: 4.1; St. Alban: 4.2).

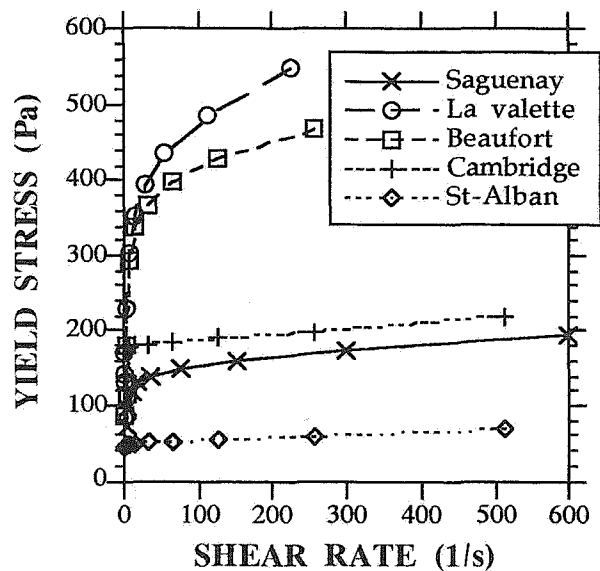


Figure 4. Yield stress and shear rate results for soils prepared at a liquidity index of about 2.0 (I_L values are as follows: Saguenay: 2.09; La Valette : 2.34; Beaufort: 1.99; Cambridge: 1.97; St. Alban: 2.12).

By inspection of Figures 3 and 4, it can be seen that for an equivalent liquidity index, coarser soils will tend to have a higher viscosity.

One can also observed that at about the same liquidity index, the yield strength of soils can differ on the basis of their grain size but as the soil is finer, the yield strength values tend to be quite similar for at the same liquidity index.

When the various soils are compared on the basis of their liquidity index it is possible to obtain a significant relationship between easily measurable index properties such as the liquidity index (I_L) and the flow parameters. As it will be shown later, these relationships have been observed by many other authors and particularly O'Brien [2], O'Brien and Julien [10], and Wildenrath and Williams [11]. Only for the soils tested, various useful relationships can be derived from Figures 5, 6 and 7. The data related to the Aspen soils will be discussed later.

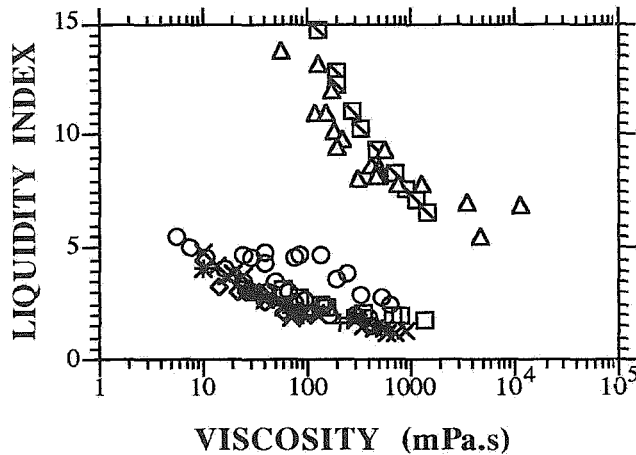
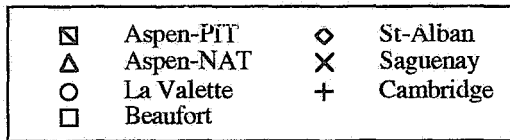


Figure 5. Relationship between liquidity index and viscosity for the soils tested.

The relationship between the liquidity index and the viscosity can be written to help predicting the viscosity of a remolded clayey soil such as:

$$\eta = \left(\frac{6.98}{I_L}\right)^{4.63} \quad (3)$$

Similarly, we can relate also the yield strength to the liquidity index by the following relationship:

$$\tau_c = \left(\frac{7.926}{I_L}\right)^{4.07} \quad (4)$$

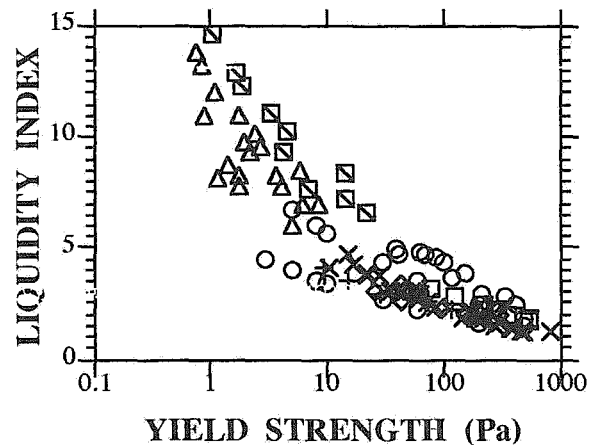
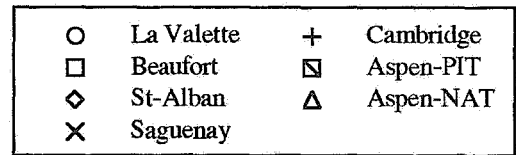


Figure 6. Liquidity index and yield strength for soils tested.

Another useful relationship related to Figure 7 is between both flow parameters, which for the sensitive clays can be written as:

$$\tau_c = 3.068 \eta^{0.773} \quad (5)$$

The first two relationships with the viscosity have a correlation coefficient just above 0.7 while Eq. 5 has a correlation coefficient of 0.9.

The La Valette soil shows the greatest variation. It is related to changes in the grain size of the samples that were analyzed for two different series. Although the clay fraction only differs by about 10%, its effect on the flow properties is quite significant. Such departure has also been previously noted for sensitive clays that had been submitted to an increase in salinity resulting in an apparent increase in the grain size distribution cause by flocculation [7]. For clayey soils, these differences are compensated when one relates viscosity and yield strength as soils with a higher yield strength will tend to have a higher viscosity. All together, even if some variation is present between various soils, for a given sample, the

relationship is usually quite consistent over a wide range of water content values.

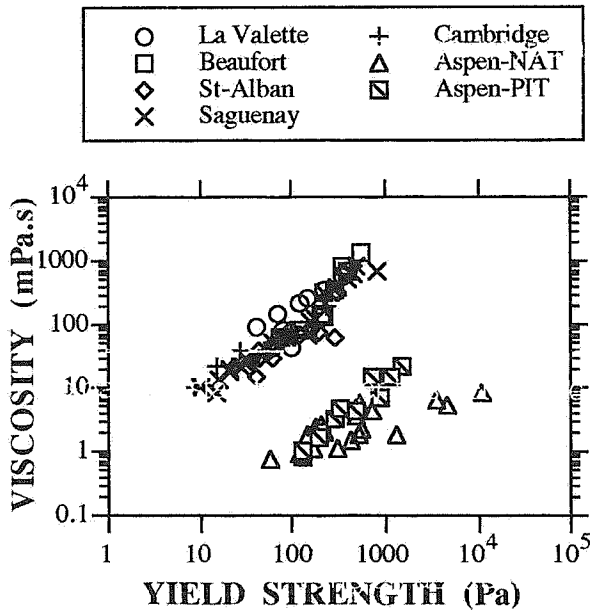


Figure 7.. Viscosity and yield strength relationship for soils tested.

The above correlations are for clayey soils. Often debris involve coarser material with a matrix that has some plasticity. This is the case for many debris flows in California [2] and for mudflows in tailing dams [12]. To better illustrate the effect of the grain size on the observed differences between the coarser and finer soils, results of O'Brien [2] have been used and presented in Figures 5, 6 and 7. O'Brien's results are presented originally in terms of volumetric concentration rather than liquidity index, which is often the case in fluid mechanics. The following relationships have been derived from those of O'Brien [2] to express the volumetric concentration (c_v) in terms of the water content (w) and specific gravity of the soil particles (G_s):

$$c_v = \frac{\left[\left(\frac{1+w}{1+G_s w} \right) G_s \right] - 1}{G_s - 1} \quad (6)$$

Doing this, it is possible to rewrite Eq. 6 to develop an expression for the water content:

$$w = \frac{1 - c_v}{c_v G_s} \quad (7)$$

Equation 7 can then be used to compute the water content and then the liquidity index of a given soil.

The data taken from O'Brien [2] is from soil samples that have a low plasticity. The Aspen-NAT sample has a liquid limit of 25%, a plasticity index of 6% and a clay fraction of 27% while the Aspen-PIT sample has a liquid limit of 32% and a plasticity index of 11% for a clay fraction of 31%. Flow parameters for the Aspen soils were also obtained with a couette type viscometer and for comparable range in shear rates.

The first observation is that Aspen soil was tested at values of liquidity indices much greater than those of this work. It is worth noting here that for a liquidity index of about 6, the Aspen soil exhibit a viscosity that is about 3 orders of magnitude greater than that for the clayey soil. With water content approaching 100%, these soils have a very large amount of water relative to low liquid limit. This can also explain some of the discrepancy observed on measuring the viscosity of the matrix of some debris flows and indicates how important it is to identify what is the matrix material and how representative is the laboratory sample in relation with the *in situ* material.

Comparing the Aspen soil to the others suggests that coarser soils would have a higher viscosity, at a given liquidity index, but a relatively lower yield strength. Here, the yield strength can be seen as the equivalent of the cohesion parameter that would tend toward zero as the granular behavior is more pronounced. On the other hand, it is quite interesting to observe that the relationship for the yield strength is quite coherent with other data. This argument is hereafter to propose a more general relationship for the yield strength of silt and clayey soils that would appear to be valid over a wide range of water content:

$$\tau_c = \left(\frac{11.425}{I_L} \right)^{3.148} \quad (8)$$

Further improvements of this relationship would be to take into account soils below their liquid limit as to verify the validity of Eq. 8 at these lower values.

FLOW BEHAVIOR IN THE FIELD

In order to look at the use of these flow parameters determined in the laboratory, back analyses of two case histories are presented. The first one is related to the St. Jean-Vianney slide that took place in 1971 in Québec. This case has been previously analyzed by Edgers and Karlsrud [6] who provide the topographic (Figure 8) and thickness data for the flow (average of about 13 metres and a velocity around 7 m/s). The starting zone corresponds to the toe of the slope before failure and the end zone is at the Saguenay River.

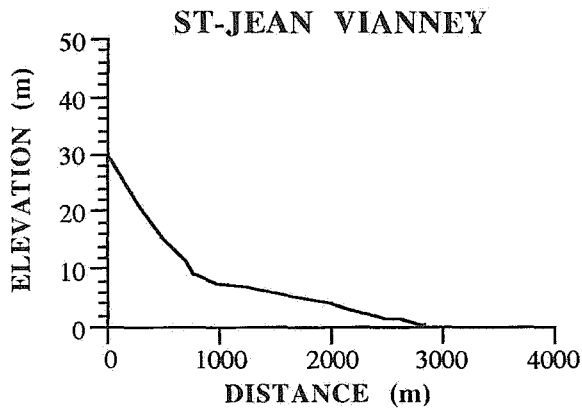


Figure 8. Surface flow profile at St. Jean Vianney.

The La Valette site has been introduced earlier and the topographic (Figure 9) and thickness data (between 5 and 10 metres) are taken from Colas and Locat [13]. The starting zone is located at a narrow section of the stream and the end zone is located at a dam build for protection purposes. The cascade is a place where and old erosion barrier had been erected. This sudden increase in steepness will help to accelerate the flowing mass at that point.

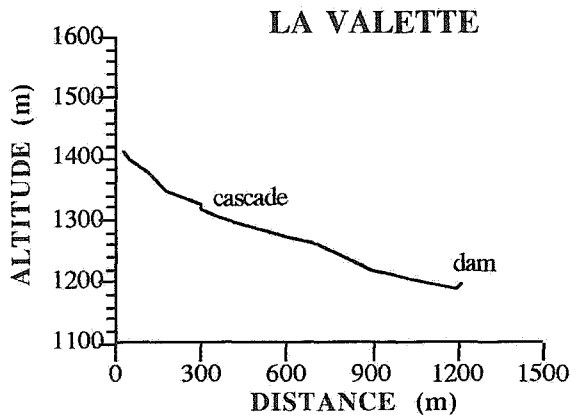


Figure 9. Surface flow profile at La Valette.

The numerical software has been taken from Edgers and Karlsrud [6] who have provided an analysis of the debris flow with the use of a program called "VIFLOW". This software solves the one dimensional flow equation of a Bingham fluid in terms of the velocity (v) which is computed as a function of the slope angle (β), the effective unit weight (γ'), the flow height (h), the viscosity and the yield strength with the following equation:

$$v = F_0 + (v_0 F_0) \left(\frac{-\delta t}{a} \right) \quad (9)$$

where:

$$a = \frac{(2\gamma' h \sin \beta + \tau) (\gamma' h \sin \beta - \tau)}{6\eta h \gamma' \sin^2 \beta} \quad (10)$$

and

$$F_0 = \frac{(2\gamma' h \sin \beta + \tau) (\gamma' h \sin \beta - \tau)}{6\eta h (\gamma' \sin \beta)^2} \quad (11)$$

The value of the initial velocity (v_0) has been set to 0. This program has been used to back calculate the viscosity and yield strength for various case histories. The adjustment of the parameters is done by fitting the observed velocity and run out distance. In such a case, the viscosity and the yield strength are acting as a free variable.

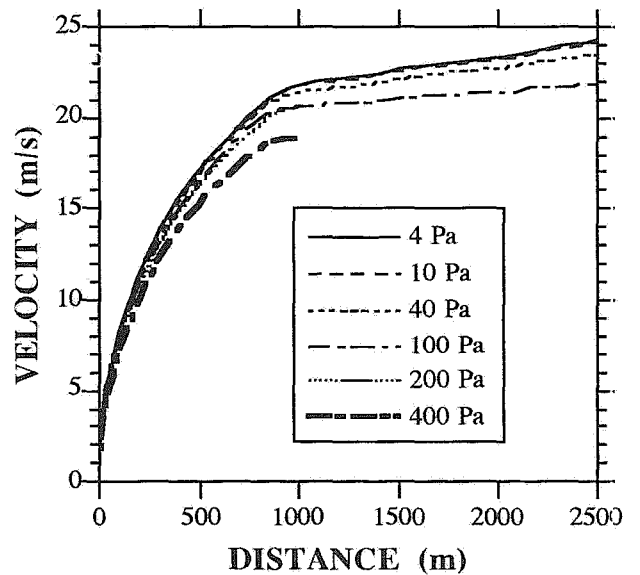


Figure 10. Velocity/distance profiles for the case of St. Jean Vianney for various values of the yield strength (values of yield strength vary from 4 to 400 Pa for a viscosity of 100 mPa.s and an effective unit weight of 6 kN/m³)

For St. Jean-Vianney, the initial computation [6] provided a fit to the run out distance and thickness for viscosity values of 810 000 mPa.s which, for this soil at a liquidity index of about 2 (as a minimum estimate) is really too high, especially for a sensitive clay with a very low electrolyte content. In this case, the flow can be considered as a one-phase flow so that the flow parameters are determined in the laboratory on samples that are representative of the flowing mass. They had estimated the

velocity at about 7 m/s. From the known values of the liquidity index, the viscosity should be at about 100 mPa.s and the yield strength between 100 and 200 Pa. With a viscosity of 100 mPa.s and various yield strength values a sensitivity analysis was carried for St. Jean-Vianney and the results are shown in Figure 10. We can see that even with a yield strength of 400 Pa, the velocity still reach a value as high as 18 m/s but stops suddenly as the plug flow thickness is reached.

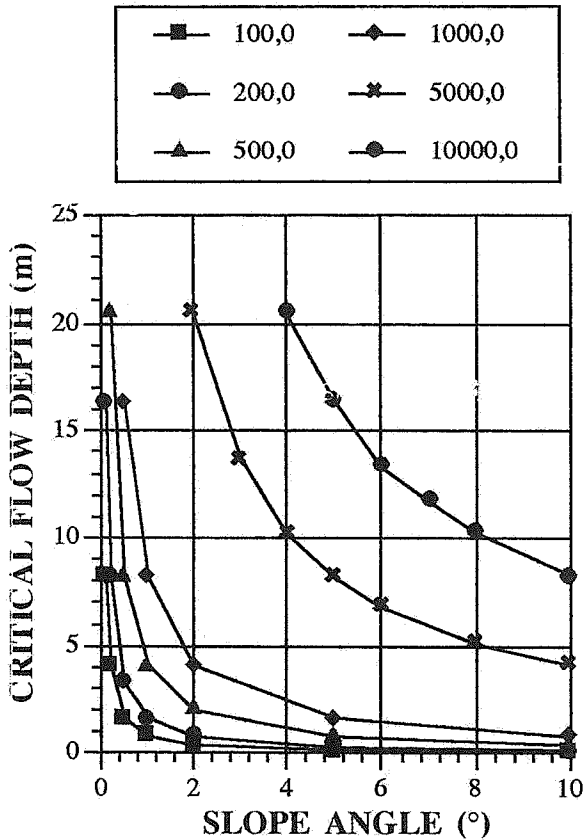


Figure 11. Slope angle and critical flow depth for various values of the yield strength (at an effective unit weight of 6 kN/m^3).

Plug flow conditions are met when the angle of the slope is such that a critical depth (H_c) is reached. This is evaluated according to the following equation:

$$H_c = \tau / (\gamma' \sin \beta) \quad (12)$$

The sensitivity of this criteria is very important to any change in the slope angle (Figure 11).

For the case of La Valette, the situation is quite different. The material has flowed at a liquidity index close or less than 1 and at velocity not exceeding few metres per second. VIFLOW has been used here with very contrasting

variables in terms of viscosity. If one estimate that the average water content at the time of flowing was such that the liquidity index of the matrix was between 0.8 and 1.5, Eq. 3 and Eq. 4 can be used for a first estimate of both the viscosity and the yield strength. Using these equations yields a range of 1235 mPa.s to 22 685 mPa.s for the viscosity and 876 Pa to 11 312 Pa for the yield strength (597 Pa to 2980 Pa when using Eq. 8). Figure 11 illustrates the sensitivity of the computation to both the viscosity and the yield strength, for the La Valette case. In order to reach a low velocity a high yield strength must be used. The use of the laboratory results appears to provide some fair estimates of the run out distance and velocity.

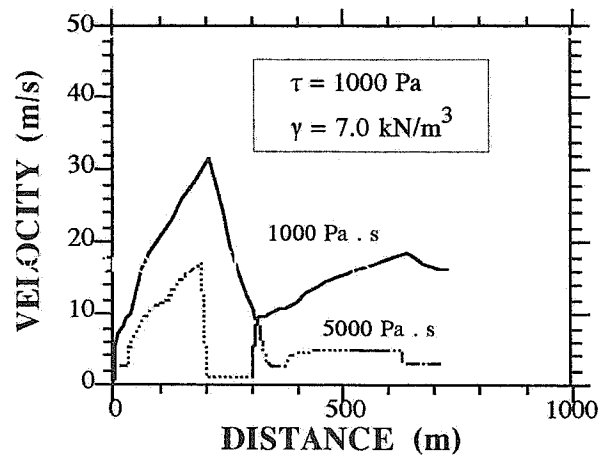


Figure 12. Velocity/distance profiles for the La Valette case at various viscosity (given in Pa.s) for a yield strength of 1000 Pa.

The flow at La Valette had stopped on a slope of about 7° and at a thickness of about 5 m which, from Figure 11, would indicate a yield strength of about 4000 Pa. The flow had also stopped at about a mid distance between the cascade and the dam (Figure 9) which corresponds to a distance of about 800 m. Computation shown in figure 12 and 13 show that the model is quite capable to predict where the flow will stop. However, the viscosity values are rather high. Here, the channeling effect was quite important and this is not taken into account in the model.

DISCUSSION AND CONCLUSION

There are still some major difficulties in both measuring the flow properties of yield stress fluids, particularly those with a two phases component. In the laboratory, problems are often encountered when one wishes to measure coarse soil (gravel or even sand).

Still, as we proceed further in developing flow property measurement it will bring about a reduction in the amount

of free variables in the system so that better control on the adequacy of numerical models will be possible.

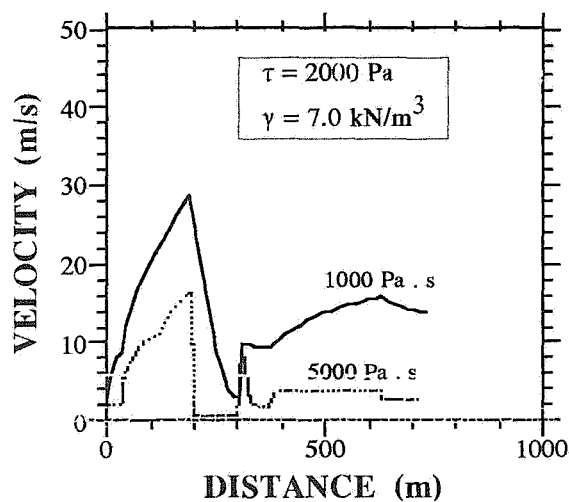


Figure 13. Velocity/distance profiles for the La Valette case at various viscosity (given as Pa.s) for a yield strength of 2000 Pa.

It is believe that the relationship presented here are of practical use if they can be at least define on a case by case basis. Still, and particularly for the yield strength, these general relationships do provide a first estimate of flow properties when no other techniques are readily available. More case histories need to be investigated and more laboratory data compiled in order to achieve a broader picture specially to appreciate the differences between cohesive and non-cohesive soils.

ACKNOWLEDGMENTS

This work represents the compilation of many reports produced by students and researchers of the Groupe de Recherche en Géologie de l'Ingénieur of Université Laval (GREGI). This research is supported by a grant from NSERC.

REFERENCES

- [1] Cruden, D.M., Thomson, S., Bornhold, B.D., Chagnon, J.-Y., Locat, J., Evans, S.G., Hegimbottom, J.A., Moran, K., Piper, D.J.W., Powell, R., Prior, D., and Quigley, R.M., 1989. Landslides: extent and economic significance in Canada. *In: Landslides and Economic Significance* (Brabb and Harrod ed.), Balkema, Rotterdam, pp.:1-23.
- [2] O'Brien, J.S., 1986. Physical processes, rheology and modeling of mud flows. Ph. Thesis, Colorado State University, 155 p.
- [3] Johnson, A.M., and Rodine, J.R., 1984. Debris flows. *In: Slope Instability. Edited by D. Brunsten and D.B. Prior.* Wiley, New York, N.Y., pp. 257-262.
- [4] VanDine, D.F., 1985. Debris flows and debris torrents in the Southern Canadian Cordillera. *Canadian Geotechnical Journal*, 22: 44-68.
- [5] Karlsrud, K., and Edgers L., 1982. Some aspects of submarine slope stability. *In: Marine Slides and Other Mass Movements. Edited by S. Saxev and J.K. Nieuwenhuis, NATO Conference Series, Series IV: Marine Sciences, vol. 6, pp.: 61-81.*
- [6] Edgers, L., and Karlsrud, K., 1982. Soil flows generated by submarine slides - Case studies and consequences. Norwegian Geotechnical Institute, Publication 143, pp.: 1-10.
- [7] Locat, J., and Demers, D., 1988. Viscosity, yield stress, remolded strength, and liquidity index relationships for sensitive clays. *Canadian Geotechnical Journal*, 25: 799-806.
- [8] Torrance, J.K., and Pirnat, M., 1984. Effect of pH on the rheology of a marine clay from the site of the South Nation River landslide of 1971, Canada. *Clays and Clay Minerals*, 32: 384-390.
- [9] Nguyen, Q.D., and Boger, D.V., 1992. Measuring the flow properties of yield stress fluids. *Annual Review in Fluid Mechanics*, 24: 47-88.
- [10] O'Brien, J.S., and Julien, P.Y., 1988. Laboratory analysis of mudflow properties. *ASCE, Journal of Hydraulic Engineering*, 114: 877-887.
- [11] Wildemuth, C.R., and Williams, M.C., 1984. Viscosity of suspensions modeled with a shear-dependent maximum packing fraction. *Rheological Acta*, 23: 627-635.
- [12] Jeyapalan, J.K., Duncan, J.M., and Seed, H.B., 1983. Investigation of flow failures of tailings dams. *ASCE, Journal of Geotechnical Engineering*, 109: 172-189.
- [13] Colas, G., and Locat, J., 1992. Analyse de la mobilité de la coulée boueuse de La Valette, Alpes Maritimes, France. *Laboratoire des Ponts et Chaussées, Paris, (sous presse).*

Hazard and Risk Analysis of Slope Instability

J. Vaunat and S. Leroueil

Department of civil engineering, Université Laval, Sainte-Foy, Quebec

F. Tavenas

McGill University, Montréal, Québec

Introduction

The appraisal of stability conditions for an existing slope requires qualitative and quantitative data from geology, hydrology, geomorphology, hydrogeology and soil mechanics. These data are considered at geological, regional and local scales. To produce a stability diagnosis at the slope scale, it is necessary to extract from all these data, significant informations about the present mechanical conditions of the slope and their evolutions with time. To be able to decide what measures — remedial works, people evacuation... — have to be taken, the movement consequences and the cost of the measures must be considered. In order to do it, a method based on risk analysis has been developed and is used as a reasoning frame in an expert system. This approach is presented here and applied to a slope in the Rivière Blanche valley in the Province of Québec.

Hazard and risk analysis

Risk analysis aims at evaluating the occurrence probability of a phenomenon and at studying its consequences. The phenomenon is called the danger, the occurrence probability the hazard and the consequences the risk.

Varnes [1984] defined the total natural risk as the set of damages resulting from the occurrence of a natural phenomenon. Its evaluation requires the determination of:

- 1) the natural hazard or the phenomenon occurrence probability within a given area and a given time period;
- 2) the risk elements or the elements potentially damaged by the phenomenon;

- 3) the vulnerability of each element represented by a damage degree comprised between 0 (no loss) and 1 (total loss) depending on the magnitude of the occurring phenomenon;
- 4) the specific risk equal to the product of the hazard by the vulnerability and defined for each element;
- 5) the total risk which integrates all the specific risks.

The French risk exposure maps (PER) program put the risk elements into 4 categories: goods, activities, persons and social functions (Asté [1991]). These elements can suffer consequences directly from the phenomenon or from induced phenomena such as dammed river, cut highway, environment degradation... Thus, the total risk depends strongly on the values, but also on the triggering order of the specific risks. Its evaluation requires a good assessment of the movement and its magnitude, of the limits of the endangered area and of the considered time period.

The notion of danger defined by Einstein [1988] is used to describe both the phenomenon and the concerned area. A phenomenon considered in a landslide problem is time-evolutive and may be split into the mechanism or pre-failure evolution, the failure itself and the movement or post-failure evolution. The failure corresponds either to the development of the whole failure surface or to the overcoming of an acceleration threshold value in creep movements and spreads. In order to assess the vulnerability of an element, a magnitude is assigned to the danger and represented by two energy components: the mass, and the velocity of the moving material. A last danger characteristic which could be added is the "activity" defining how far the present state is from the failure. This "activity" is linked to the hazard.

The danger is evaluated by a synthesis of stability/instability discriminant factors. A distinction is made between causal factors which are generating the failure process and revealing factors which indicate the present "activity", but do not contribute to the failure process. Among the causal factors, the PER methodology distinguishes the factors of predisposition and the triggering or aggravating factors (Champetier de Ribes [1987]). From a mechanical point of view, the factors of predisposition give informations about the present state and the response of the slope when modifications of this state are caused by triggering factors.

Fig.1 presents the frame of the whole risk analysis, including the hazard analysis. A landslide which took place on April, 19th 1975 at St. Ambroise is used to illustrate the existing links between the different components of the hazard and risk analysis. To do this, slope conditions are considered before the landslide.

St. Ambroise is located at the toe of the Laurentian mountains. The stratigraphy of the site consists in a 3m thick upper layer of sand and gravel underlain by a layer of grey clay with shells up to a depth of 38m. This material has a significant silt fraction, a liquid limit of about 30, a low plasticity index in the order of 10, a liquidity index higher than 3, an undrained shear strength increasing with depth from 20kPa at 5m to 35kPa at 17m and a remolded shear strength lower than 1kPa (Grondin [1978]). The considered slope was located on the outside bank of a meander where signs of important erosion were observable. The height of the slope was 20m and the average inclination was about 25°. One year before the event, a small landslide involving two 10m thick slices occurred in this area, in springtime .

Lebuis studied this region in 1977. The sedimentary environment consists in a basal permeable layer of till or fluvio-glacial sediment, a thick layer of marine sensitive clay and a more permeable upper layer of sand, gravel or weathered clay. The slopes along the river have relatively low inclinations due to past movements but become steeper when a sand layer protects the bank toe from stream erosion. Due to recharges through outcrops on the Laurentian hillsides, artesian conditions are often present in the basal layer.

Observations of neighbouring slopes (Lafleur and Lefebvre [1980]) showed a typical permanent groundwater regime characterized by a water table at a depth of about 3m, a downward gradient value of 0.2 under the crest of the slope and an upward toe gradient value of 0.15. In periods of heavy infiltration by rain or snow-melt, the water table rises

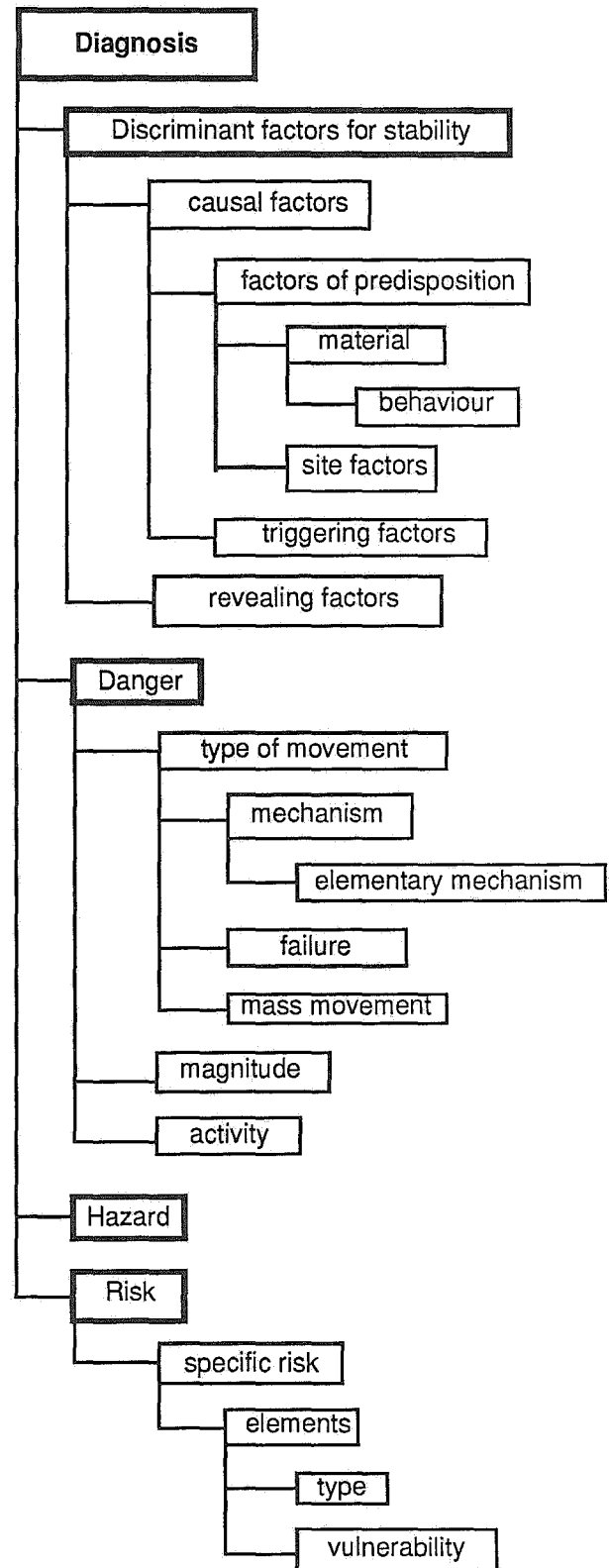


FIG. 1 -- Components of slope stability risk analysis

up to the ground surface. The river level varies strongly in springtime and the erosion is very active, especially along the outside banks of the meanders. Three types of movements were observed along the river: superficial slides of the vegetal cover, slumps or rotational slides in clay or sand layers and retrogressive landslides. As observed by Lebuis [1977], among the 25 earthflow scarps with a size varying between 10 000m² and 780 000m² and an estimated occurrence since a date comprised between 9500B.P. and 4000B.P., 7 were located in a 5.5km long section containing the considered slope. Two months before the St. Ambroise landslide, a small retrogression involved an area of 70m by 45m 460m upstream.

The instability revealing factors along the Rivière Blanche are the presence of fissures and earth rolls in the slopes, the natural removal of vegetal cover at some places and the presence of recent landslide scarps.

Determination of discriminant factors for stability

This step consists in selecting among the set of available data for the site and the region those that are determinant for the stability. These factors can be classified into causal factors of predisposition, triggering causal factors and revealing factors.

The causal factors of predisposition are the site characteristics that determine the slope behavior when one or several triggering factors occur. The set of these factors is divided into two groups: the group containing informations about the materials and their behavior, and the group containing informations about the general morphology of the site. The factors of predisposition are first selected on the basis of the general knowledge of the qualitative behavior of the materials. Depending on this qualitative behavior and on the geomorphology of typical failures in the considered geological area, other factors of predisposition reflecting the slope morphology can be defined.

The determinant material in case of St. Ambroise is the grey clay. With a liquid limit lower than 40 and a remolded shear strength lower than 1 kPa (Lebuis *et al.* [1983]), this material is sensitive to remolding. This material is also erodable under the action of hydraulic forces.

Two types of landslides can be observed along the Rivière Blanche valley: rotational landslides and retrogressive landslides. As presented by Tavenas [1984], initial rotational landslides are essentially controlled by the height of the slope, the inclination of the slope and the pore pressure regime; the subsequent slides are essentially undrained and will depend mostly on the undrained shear strength, on the liquid limit and on the remolded shear strength of the clay. In addition to the material characteristics, there are geomorphological factors:

- 1) the presence of the basal artesian layer and the upper recharge layer which are together controlling the pore pressure values;
- 2) the topography of the slope that controls the initial failure and the possibility of retrogression by backscarp instability.

The presence of shells beds is not considered as preponderant because of their discontinuous distribution.

The triggering factors are temporary factors the occurrence of which above a threshold value can initiate failure. These factors are classified into four groups corresponding to four possible modifications of the slope stability conditions: modification of the pore pressure regime, modification of shear strength parameters by for example chemical action, modification of geometry by erosion, human action or other movement and modification of external loads by loading at the top, unloading at the toe, dynamic loading.... At this stage, the triggering factors are selected not because of their influence on the slope stability but because of their possible occurrence.

In the St. Ambroise case, the regional study indicates two triggering factors: the river erosion at the toe of the slope and the infiltration by rain and snow-melt. The first is acting in a progressive manner and the second is considered as aleatory with some distribution in the year.

The revealing factors are of two types: factors at the slope scale related to the behavior of the material closed to failure (creep deformations, tensile fissures,...) and regional factors given by the occurrence of past failures in the area. The regional factors are taken in account to detect that a failure mechanism is acting while the factors at the slope scale are used to define the "activity", i.e to situate the present stability conditions relatively to failure.

There is high density of landslides near the St. Ambroise slope let consider an active erosion along the Rivière Blanche valley. At the slope scale, apparently, the only revealing factor before the

occurrence of the considered landslide was a small landslide which occurred in 1974. As no debris of this landslide stayed in the river bed, a toe erosion of the steep backscarp continued.

Inventory of possible dangers

This step aims first at determining the possible dangers which depend on the existing combinations between factors of predisposition and triggering factors. The respective contribution of these factors to the type of danger can be assessed by three approaches applied separately or mixed together: the regional geomorphological considerations, the deterministic slope stability analyses and the statistical analysis. In the present study, only the geomorphological approach is used.

Along the Rivière Blanche, the existence of two types of movement (simple rotational landslides and retrogressions) indicates that several combinations of causal factors exist. Furthermore, these two types of movement were observed at the same site, which indicates that at least two combinations of the triggering factors, infiltration and erosion, exist and influence the failure mode. The importance of infiltration is evidenced by Fig. 2 presented by Lafleur and Lefebvre in 1978. Maximal landslide frequencies appear during spring and autumn, when, due to heavy rain and/or snow melt, the water table is at its higher level.

The observation of different sizes of landslides along the Rivière Blanche valley, in the same sedimentary environment indicates a limited influence of the material behavior on the magnitude of the slide. It thus appears that the important factors for the magnitude of a movement are the triggering and morphological factors (topography and long term pore pressure regime).

Once the different dangers determined, the following elements have to be characterized for each danger: the mechanistic process towards failure and the activity, the failure itself and the induced movements with their magnitude.

The mechanistic process depends, in a deterministic way, on the causal factors as a whole. For a given stratigraphy and a given triggering factor, only one mechanism, called elementary mechanism, may develop. If there is only one triggering factor, the hazard is related to the occurrence of this triggering factor. When several

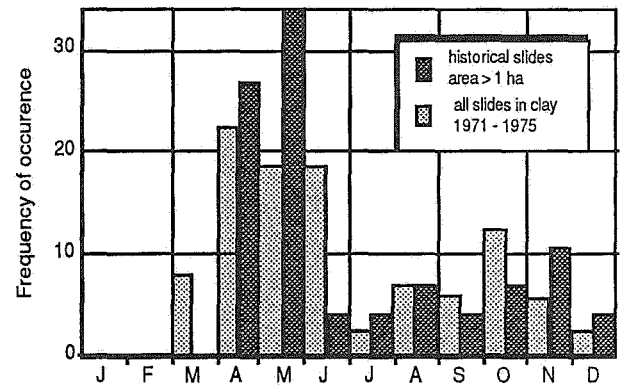


FIG. 2 -- Annual distribution of landslides in Québec (after Lafleur and Lefebvre [1978]).

triggering factors are interrelated, several mechanisms may exist. In such a case, the stability is difficult to assess in terms of occurrence probability of the different triggering factors. It is then necessary to integrate all these variables within one coefficient. The hazard is evaluated in relation with the value of the coefficient. An occurrence mode — aleatory, periodic or progressive — is assigned to the elementary mechanisms in order to determine the hazard.

In the case of the St. Ambroise landslide, two dangers were evidenced: simple failure and retrogressive landslide. A simple rotational landslide failure mode is governed by masses equilibrium along a well-defined failure surface and the mechanism is associated to the driving and resisting moments. The presence of both an erodable material and an active erosion implies a first elementary mechanism: an increase of shear stress in the clay mass. This mechanism is progressive. A second mechanism is the shear strength variation due to pore pressure changes. It depends on the frozen state of the slope, the duration and the intensity of rain, the swelling response of the mass as described by Kenney *et al.* [1980]. This mechanism thus can be considered as aleatory. The whole mechanistic evolution of the slope towards failure is the result of the interaction between these two elementary mechanisms, as indicated in Fig. 3. A classical stability analysis taking into account the type of failure and the variables controlling the mechanism are generally appropriate to evaluate the possibility of a simple failure.

To tackle the second danger, that is retrogression, Tavenas [1984] proposed four criteria: the occurrence of an initial landslide, the existence of a

continued backscarp instability in undrained conditions, the ability for the debris to be remolded and the ability for the debris to flow when remolded. In this case, there are three elementary mechanisms: a mechanism leading to an initial landslide, a mechanism of continued backscarp instability and a mechanism of clay liquefaction by remolding. The mechanism of initial landslide has just been studied. The stability of the backscarp is essentially undrained and is controlled by its height, the presence and the importance of the counterweight applied by the debris and the undrained shear strength of the clay. As indicated by Mitchell and Markell [1974] and by Carson [1977], a $\gamma H / C_u$ larger than 4 or 6 is necessary to initiate a retrogressive landslide. The mechanism of liquefaction necessitates an energy sufficient to remold the clay and conditions such that the remolded clay is liquefied. As shown by Tavenas *et al.* [1983], these conditions are usually fulfilled in clays with a liquid limit less than 40% and an undrained remolded shear strength less than 1 kPa or a liquidity index less than 1.2.

The failure is characterized by the shape and the dimensions of the failure surface. As indicated before, the shape depends on both the factors of predisposition and the triggering factors. For a given site, the dimensions are function of the simultaneous occurrence of different triggering factors. They are bounded by factors of predisposition, such as, for example, the presence of a rock outcrop. When more than one triggering factor occur, a method using a coefficient, for example, a coefficient of safety, is necessary to assess these dimensions.

The shape of the initial landslide failure surface in a homogeneous cohesive material is generally circular, but its depth varies depending on the existing pore pressures. Low pore pressures in the clay mass and an active erosion (A on Fig. 3) give steeper slopes and superficial slides while high pore pressures (B and C on Fig. 3) generally involve larger volumes of soil in the landslides. A stability analysis in effective stresses is appropriate to define the depth of the surface. In the St. Ambroise area, Lebus [1977] observed one or two simple slides having a thickness of about 10m.

For the retrogression, the final shape of the failure surface is composed of a floor of low inclination and a backscarp of reduced height. To study the dimensions of the failure, the method consists in:

- 1) defining the maximal area which could be affected, on the basis of topography and spatial repartition of the material which could liquefy. At St. Ambroise, the mass of

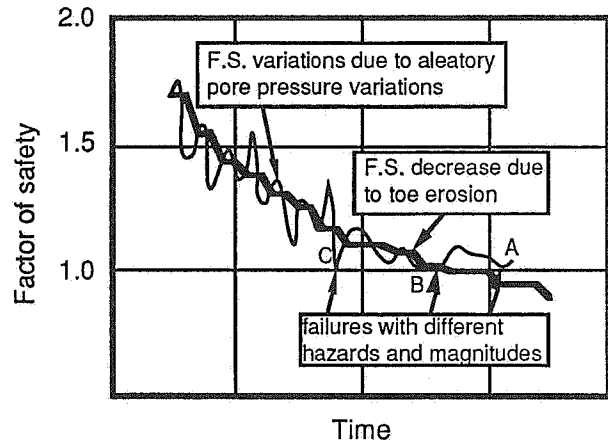


FIG. 3 -- Schematic variations of failure conditions due to erosion and infiltration .

clay which could be involved in a retrogressive landslide is comprised between an old earthflow crater on one side and a gully on the other side. It is thus limited to a corridor, about 150m wide. As previously mentioned, the material is prone to liquefy in all the area.

2) correlating within this area the retrogression distance using the relationships proposed by Mitchell and Markell [1974] or Carson [1977] (Fig. 4).

From this figure, the stability number at St. Ambroise is of about 10 and the distance of retrogression could be extremely important, as high as 2km. It is worth noting however that the distance of retrogression observed in the area is generally smaller than 500m.

The movement of the failed mass is characterized by a remolding degree of the material and by the kinematics of the mass, which is often simply described by an average velocity and a distance travel. It depends on the failure characteristics, the topography and the material characteristics.

In the St. Ambroise case, the slope is 20m high. Using a relationship proposed by Tavenas *et al.* [1983] between the energy which dissipates in the initial landslide and the remolding index defined as $(C_u - C_{ux}) / (C_u - C_{ur})$ where C_u is the undrained shear strength, C_{ur} the remolded shear strength and C_{ux} the shear strength of partly remolded material, the remolding index of the failed mass is evaluated to 70% which indicates an almost total evacuation of the debris. The distance of travel could be limited by the opposite bank of the river,

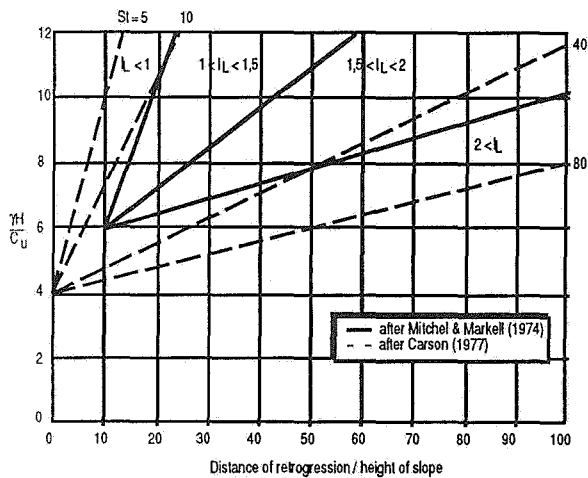


FIG. 4 -- Earthflow chart (from Tavenas *et al.* [1983]).

but the remolded material could be evacuated by the river stream.

The "activity" is the last element to define. The terms fossilized movement, past movement, present movement and potential movement can be used to qualify this "activity". A more quantitative parameter is the distance to failure which can be determined on the basis of the evolution of the revealing factors.

In St. Ambroise, there are no informations available on the "activity" of the slope itself. But Lebuvis *et al.* [1983] made an interesting regional compilation which can be used to assess the "activity". They plotted height versus inclination for a variety of slopes presenting stable and instable signs; they also found a good correlation with a circular stability analysis in effective stresses, when using $c' = 7 \text{ kPa}$, $\phi' = 31^\circ$ and hydrostatic pore pressures (Fig. 5). The considered slope appears to be very close to failure.

Appraisal of magnitudes and hazard

The **magnitude** is characterized by the volume and the average velocity of the mass in movement. Its upper limit is generally controlled by site effects and factors of predisposition but the value itself depends also on triggering factors. At St. Ambroise, as in most landslides in sensitive clays, the velocity cannot be determined, but is

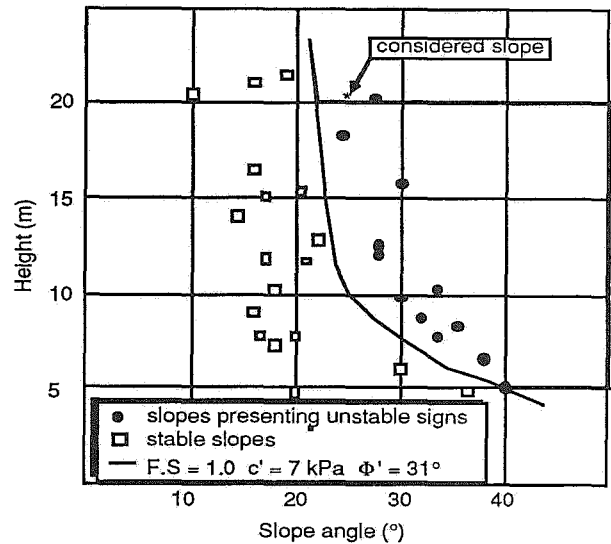


FIG. 5 -- Heights and angles of the clay slopes in the St. Ambroise area (from Lebuvis *et al.* [1983]).

known as being extremely high, whatever the type of slide. The dangers can thus be characterized only on the basis of the volume of soil involved.

The **hazard** is only a function of the occurrence of triggering factors above given thresholds. With the determination of the danger, the type of failure and movement, the area considered and the magnitudes are known. The remaining factor for hazard calculation is the time period considered. Indeed, depending on the different occurrence modes for the elementary mechanisms, the hazard can vary for different time periods.

For the initial landslide at the St. Ambroise site, where progressive mechanism of erosion is active, the failure is certain at a date which is a function of the present stability conditions of the slope and the erosion rate. For evaluating the erosion rate for the Ottawa river, Williams *et al.* [1979] used a correlation between the retrogression distance of the bank crest, the retrogression distance of the bank toe, the bank angle, and the occurrence of landslides. This approach allows a quantification of the recurrence period and an estimation of the remaining time prior failure. Unfortunately, data on the bank retrogression along the Rivière Blanche were not available. The hazard is also controlled by pore pressures and their variation with time. However, as previously indicated and shown on Fig. 5, the slope is rather unstable and small pore pressure increases could trigger the landslide.

Risk forecast

The types of the risk elements are first compiled within the endangered area. This area includes the area directly threatened and areas concerned by induced phenomena.

At the site of St. Ambroise, the risk is very limited. A simple landslide would not have consequences. A retrogressive landslide would affect only agricultural lands. The only major risk in case of a retrogressive movement would be a damming of the river stream, an inundation of agricultural lands and of the local road situated 800m upstream.

The vulnerability of each element is very difficult to assess with only a number from 0 to 1. An element can have a value, can be the centre of an activity and contain people. It is thus preferable to consider real losses. These losses can be total or partial; the damage degree of an activity may be evaluated by the cost of substitution; the number of threatened persons can measure the risk for people.

At St. Ambroise, the vulnerability could be easily evaluated: the value of the destroyed agricultural area and the substitution cost of their agricultural function, such as food purchase for animals; the clearing works of the dammed river and the substitution cost for water supply of farms located downstream; the inundation cost which represents the temporary losses of the agricultural activities and the substitution cost of road cut.

The specific risk is defined as the product of hazard by vulnerability. For the direct damages, the hazard is that of the initial movement. For the damages due to induced phenomena, a new hazard must be assessed. When overlapped phenomena exist, each phenomenon has its proper factors of predisposition and is triggered by previous phenomena. The factors of predisposition control 1) the possible occurrence for the phenomenon; 2) the threshold for the magnitude of the previous phenomenon which could induced the considered one. The hazard of the new phenomenon is then equal to the hazard of the triggering phenomenon multiplied by a reducing coefficient depending on the factors of predisposition.

The farm lands directly damaged at St. Ambroise have a specific risk equal to the retrogression hazard multiplied by the possible losses. The river damming is an induced phenomenon for which the topography and the river stream are the factors of

predisposition and the retrogression the triggering factor. A condition exists between the stream flow and the retrogression velocity to prevent the debris to be carried down the stream before forming a dam. This additional condition gives a hazard of river damming lower than the hazard of retrogression.

The total risk is evaluated with a classification of the different elements in terms of decreasing importance as it is made at Honk-Kong (Brand [1988]). This list gives the upper and the lower limits of the total risk.

Such a list can be made at St. Ambroise. The total risk includes:

- 1) agricultural lands with a high specific risk, because of a high value of the hazard;
- 2) water supply difficulties and inundated lands, with a moderate risk because of limited consequences;
- 3) one local road cut with a low risk because of low hazard;

No human lives are endangered. Because of small consequences, the risk can be described as low, despite of the high hazard .

Conclusion

The presented hazard analysis is based on two main points: the first is the distinction between factors of predisposition and triggering factors, the second is the methodology of mechanism investigation which defines the danger and the hazard. All the informations on the geometry of the slope, on its initial stability conditions, on the behavior of the materials and on "external actions" are used to define the mechanical process.

The mechanisms are correlated in a deterministic way with factors of predisposition and triggering factors. The mechanisms determine the type of failure and the type of movement. The occurrence mode of the mechanisms in relation with the occurrence mode of the triggering factors and the type of soil mass response gives the probabilistic assessment of the hazard. When more quantitative evaluations, such as magnitude, endangered area and hazard evaluations are needed, the distinction between factors of predisposition and triggering factors is not sufficient. It is then necessary to investigate the controlling variables of the triggering factors and their thresholds. When only one triggering factor exists, the hazard is correlated with it. When several triggering factors exist, the hazard is a function of a coefficient integrating all the variables.

The risk analysis takes into account the chain of induced phenomena, natural or not, each phenomenon having its proper factors of predisposition, triggering factors, danger, hazard and risk. The risk quantification is given by a classification of all the specific risks, from the higher to the lower.

At St. Ambroise, the factors of predisposition were the topography and the sensitive clay. The triggering factors were the erosion and the pore pressure variations. The danger to be considered was a retrogression on a distance which could be of about 500m. The hazard is very high. The elements of risk may be agricultural land loss and inundation consequences. The risk thus is low. In fact, a landslide happened there with a retrogression of 350m; the damages were limited to the destroyed area. A temporary inundation deprived farms of water during one day.

The application of this analysis in the scope of an expert system should be pointed out. Expert systems use qualitative as well as quantitative data and are thus appropriate for risk analysis. In the expert system XPENT described by Faure *et al.* [1992], the diagnosis is built in three central reasoning modules: one defining factors of predisposition and triggering factors, a second considering the mechanisms in relation with a base describing qualitatively material behaviors, and a hazard module.

Acknowledgements

The authors are thankful to D. Demers who provides the most part of references and data about the St. Ambroise case.

Bibliography

- Asté, J.P. [1991]. personal communication.
- Brand, E.W. [1988]. Special lecture: landslide risk evaluation in Hong-Kong. Proc. of the 5th Int. Symp. on Landslides, Lausanne, Vol.2, pp. 1059-1074.
- Carson, M.A. [1977]. On the retrogression of landslides in muddy sediments. Can. Geot. Journ., Vol.14(4), pp. 582-602.
- Champetier de Ribes, G. [1987]. La cartographie des mouvements de terrains: des ZERMOS aux PER. Bull. de Liaison du LCPC, Vol. 150-151, pp. 9-19.
- Einstein, H.H. [1988]. Special lecture: Landslide Risk Assessment Procedure. Proc. of the 5th Int. Symp. on Landslides, Lausanne, Vol.2, pp. 1075-1091.
- Faure, R.M., Mascarelli, D., Vaunat, J., Leroueil, S., Tavenas, F. [1992]. Present state and development of XPENT, expert system for slope stability problems. Proc. of the 6th Int. Symp. on Landslides, Christchurch, in print.
- Grondin, G. [1978]. Etudes des caractéristiques des argiles du Québec et critères d'identification des argiles extra-sensibles. MSc. Thesis, Univ. de Sherbrooke, Québec, Canada.
- Lafleur, J., Lefebvre, G. [1978]. Influence des écoulements souterrains sur la stabilité des pentes naturelles d'argile. Min. Energie et Ressources, Québec, rap. DP-609, 354p.
- Lafleur, J., Lefebvre, G. [1980]. Groundwater regime associated with slope stability in Champlain clay deposits. Can. Geot. Journ., Vol.17(1), pp. 44-53.
- Lebuis, J. [1977]. Les zones exposées aux coulées argileuses dans la région de St. Ambroise de Kildare. Min. Energie et Ressources, Québec, rapport interne, 47p.
- Lebuis, J., Robert, J.M., Rissmann, P. [1983]. Regional mapping of landslides hazard in Québec, Proc. Symp. on slopes on soft clays, Linköping, SGI Report No. 17, pp. 205-262.
- Mitchell, R.J., Markell, A.R. [1974]. Flowslides in sensitive soils. Can. Geot. Journ., Vol.9(1), pp. 11-31.
- Tavenas, F., Flon, P., Leroueil, S., Lebuis, J. [1983]. Remolding energy and risk of slide retrogression in sensitive clays. Proc. Symp. on slopes on soft clays, Linköping, SGI Report No. 17, pp.423-454.
- Tavenas, F. [1984]. Landslides in Canadian Sensitive Clays — A State-of-the-Art. Proc. of the 4th Int. Symp. on Landslides, Toronto, pp 141-153.
- Varnes, D.J. and the IAEG Commission on Landslides and other Mass Movements on Slopes Landslides hazard zonation: a review of principles and practice. Unesco, Paris.
- Williams, D.R., Romeril, P.M., Mitchell, R.J. [1979]. Riverbank erosion and recession in the Ottawa area. Can. Geot. Journ., Vol.16(4), pp. 641-650.

Landslides and River Damming Events Associated with the Plinth Peak Volcanic Eruption, Southwestern British Columbia

S. Evans

Geological Survey of Canada, Ottawa, Ontario

Abstract

The flank eruption of Plinth Peak within the Mount Meager volcanic complex, at about 2350 y BP, deposited the Bridge River ash up to 550 km to the east-northeast of the vent and is the most recent major volcanic eruption in the Garibaldi Volcanic Belt of southwestern British Columbia. A radiocarbon-controlled chronology of deposits in the Lillooet River valley in the vicinity of Plinth Peak is being constructed and has revealed a complex series of events associated with the eruption. A major pre-eruption landslide deposit (est. vol. $> 50 \times 10^6 \text{m}^3$) has been mapped in Salal Creek, a northerly tributary of the Lillooet River. It extends 5 km from the Lillooet River up to el. 1158 m and has also been mapped at scattered locations in the Lillooet Valley. The lithology of the deposit suggests a source on Plinth Peak but the deposit is overlain by Bridge River Tephra. Eruptive products of the Plinth Peak event include tephra, pyroclastic flow and debris flow deposits overlain by a welded breccia. The initial eruption was closely followed by a second major landslide, a debris avalanche from Plinth Peak (est. vol. $2\text{-}4 \times 10^8 \text{m}^3$). Its debris filled the Lillooet valley and dammed the river. Debris flow deposits possibly related to the breach of the debris dam are found up to 6 km downstream. The landslide events were followed by an eruption of a small lava flow into the bowl created by the landslides and initial eruption. Sediments deposited during subsequent damming events, up to at least 900 y BP, are found in the Lillooet River valley upstream of Plinth Peak.

Introduction

The Garibaldi Volcanic Belt (Fig. 1; Green et al. [1]) of southwestern British Columbia is the northward extension of the Cascade Volcanic Belt (Scott, [2]). Quaternary volcanic rocks of the Garibaldi Group occur in three major centres, viz. Mt. Garibaldi, Mount Cayley, and Mount Meager (Fig. 1). All three centres currently support glaciers or ice caps, have large accumulations of pre-historic debris associated with them (Read [3, 4]; Hardy et al. [5]; Evans and Brooks [6]) and have experienced major historical landslides (e.g. Moore and Mathews [7]; Hardy et al. [5]; Jordan [8]; Clague and Souther [9]; Smith and Patton [10]; Evans [11]). The occurrence of these landslides has resulted in the natural damming of major rivers in the Belt as documented by Evans [12] and Brooks and Hickin [13]. The high

incidence of historic landslides has led Evans [14, 15, 16] to suggest that the Belt is the most landslide prone environment in the Canadian Cordillera.

The present paper reports on field work carried out in the Mount Meager volcanic complex where the most recent eruption in the Belt occurred in the first millennium B.C (Read [3, 4]). The eruption took place on the north east side of the complex on the north east flank of Plinth Peak (el. 2679 m) and deposited the so-called Bridge River tephra (Nasmith et al. [17]; Mathews and Westgate [18]) in an easterly plume up to at least 550 km from the source vent (Fig. 1).

The paper enlarges on previous work by Read [3, 4] and Stasiuk and Russell [19, 20]. Its object is to document the occurrence of catastrophic landslides and associated river damming events in the Lillooet valley below Plinth

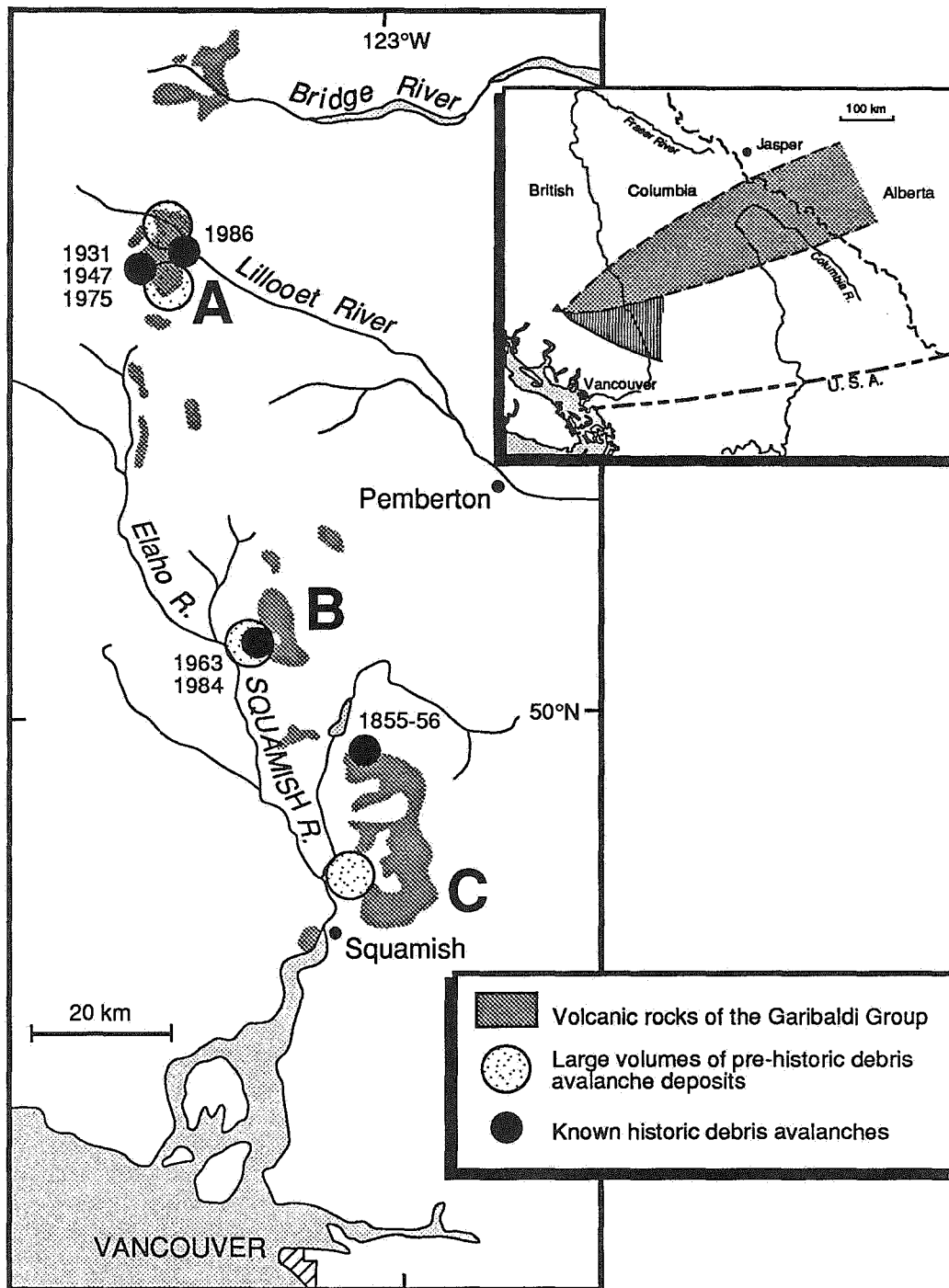


FIGURE 1. Map of Garibaldi Volcanic Belt, southwestern British Columbia, showing main volcanic centres (A: Mount Meager; B: Mount Cayley; C: Mount Garibaldi), location of large volumes of pre-historic debris avalanche deposits, and the location and dates of known historic debris avalanches (after Evans and Brooks, [6]). Inset map shows plume of Bridge River Tephra extending eastward from Plinth Peak which resulted from eruption at ca. 2350 y BP (after Mathewes and Westgate [18]).

Peak prior to, directly after, and significantly later than the 2350 y BP eruption. It also identifies gaps in the current data base of radiocarbon dates obtained for these events.

The focus of the present work is timely in view of increased logging and recreation activities in the region as well as renewed interest in geothermal energy potential within the complex (e.g. Nevin [21]).

Landslides in the Mount Meager volcanic complex

Most if not all slopes developed on Quaternary volcanic rocks within the Mount Meager complex show evidence of slope movement. A wide range of landslide types exists within the complex (Jordan, [8]; Jordan and Slaymaker [22]). Evans [11] has described the 1986 rock avalanche from the north side of the peak of Mount Meager. The detached mass of Pleistocene rhyodacite had an estimated volume of $0.5 \times 10^6 \text{m}^3$.

Large rock avalanches have occurred on the south side of the volcanic complex. For example, a massive rock avalanche of unknown age originated in Quaternary andesitic flows on the south face of Pylon Peak and descended Angel Creek spreading out in the Meager Creek valley. The debris covers an area of 5km^2 . Assuming an average thickness of 20m the volume is in the order of $100 \times 10^6 \text{m}^3$.

Exposures of a pre-historic debris avalanche deposit are found on Devastation Creek near its confluence with Meager Creek on the west side of the volcanic complex. In historical times the effect of a major landslide at Devastation Glacier was reported by Carter [23]. Carter and his fellow climbers noted the deposits of a large rock / debris avalanche from the flanks of The Devastator. The landslide was thought to have occurred in October 1931 since a large flood (probably due to a breaching of a landslide dam) in Meager Creek had been noted at that time by a local trapper.

In 1947 aerial photographs fresh landslide debris is evident on the surface of Devastation Glacier. The landslide involved Pleistocene andesitic flows and pyroclastics. The landslide is assumed to have taken place in 1947 because the debris does not show any distortion due to glacier movement. The volume of the 1947 landslide is estimated to be in the order of $2 - 4 \times 10^6 \text{m}^3$.

On July 22, 1975 a complex series of landslide events took place at Devastation Glacier when approximately $13 \times 10^6 \text{m}^3$ of altered Quaternary pyroclastic materials and glacier ice was lost from the west flank of Pylon Peak (Smith and Patton [10]). The events were initiated by a rockslide which continued down Devastation Creek valley as a high velocity debris avalanche up to 7 km from its source. Four men were killed by the landslide. The debris avalanche was followed by a major debris flow formed from the talus deposits of ice and soft rock which had collected in a portion of the rockslide scar. Both slides travelled roughly the same distance. The debris avalanche also triggered a major secondary slide on the western flank of The Devastator.

Pre-eruption landslide in the Lillooet Valley

Scattered exposures of what is interpreted to be a landslide deposit are found in the Lillooet River valley in the vicinity of the confluence with Salal Creek (Fig. 2). At location E it attains a thickness of over 35 m. The deposit extends up Salal Creek for 5 km to el. 1158 m (Location F in Fig. 2) and consists of massive blocks of rhyodacite, typical of the Plinth Assemblage, in a pulverised matrix. The diffuse boundaries of the deposit and the thick vegetation cover, make it difficult to outline the extent of it in detail. Further, some uncertainty exists as to the source of the deposit but it is likely to have originated on the north east flank of Plinth Peak. The landslide dammed Salal Creek and formed a lake upstream of el. 1158 m. Laminated silts and clays deposited in the lake have yielded organic material for radiocarbon dating currently underway. Where exposed in Salal Creek and the Lillooet valley the landslide deposit is covered by Bridge River tephra (Fig. 2).

The landslide preceded the eruption of Bridge River tephra by a long enough period to allow the development of a paleosol on the debris surface beneath the tephra.

Eruptive products from Plinth Peak

The products associated with the 2350 y BP Plinth Peak eruption, termed the Bridge River assemblage by Read [3], have been described in detail by Read [3, 4] and Stasiuk and Russell [19, 20]. They include Bridge River tephra consisting of air fall pumice, pyroclastic flows,

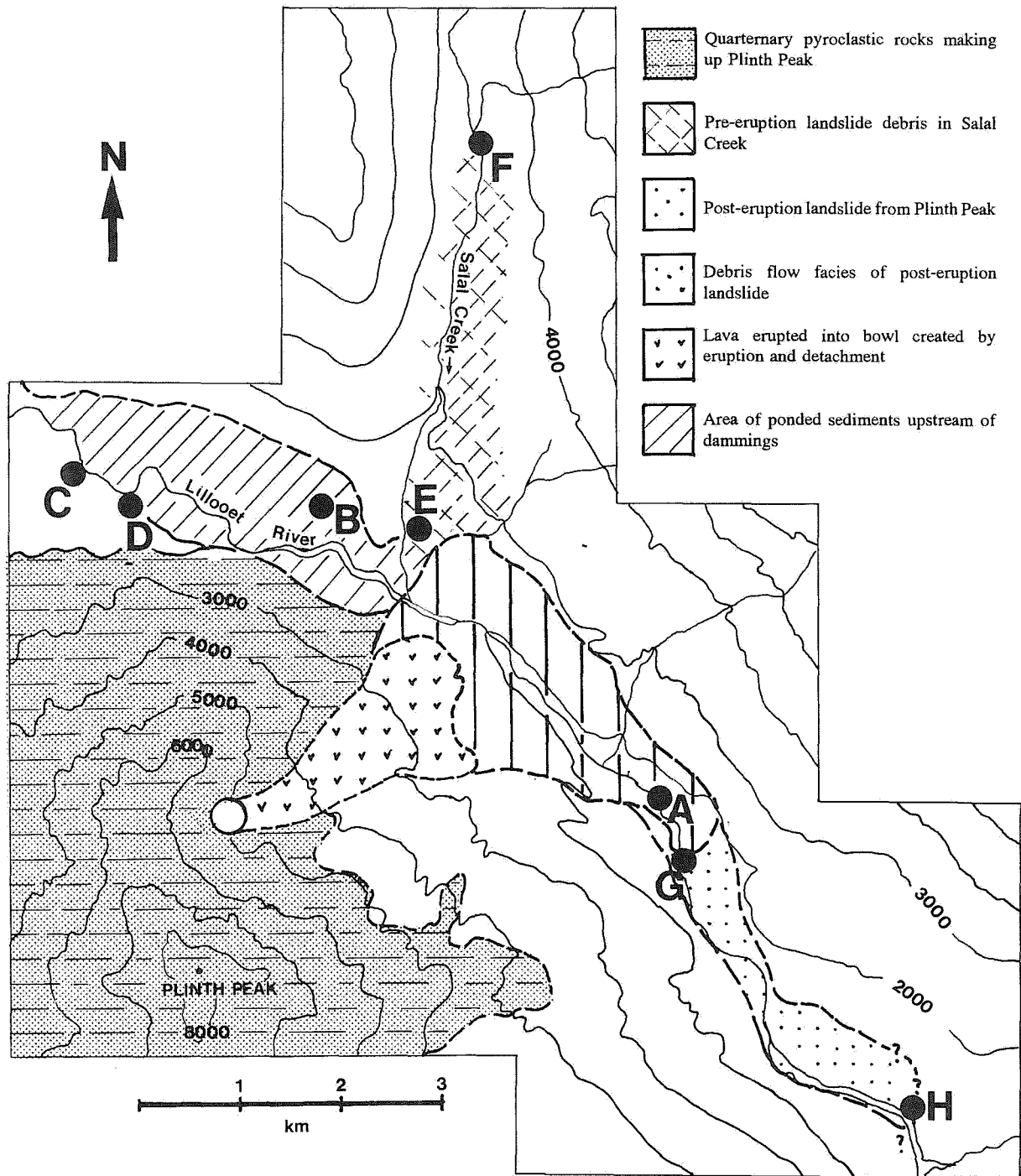


FIGURE 2. Map of Plinth Peak and vicinity showing extent of eruptive products, landslide debris and exposures mentioned in the text. Geology of Plinth peak after Read [3]; surface geology of Lillooet valley based on field mapping in 1989 and 1991 and is preliminary only. Contours are in feet.

and multiple flows of a resistant vitroclastic breccia. Later debris flows contain massive blocks of the vitroclastic breccia.

The tephra buried and charred trees on the Lillooet valley floor which are preserved in their growing positions (Fig. 3).

Radiocarbon dates from these trees have allowed precise dating of the tephra emplacement (Table 1). A sample collected by Read [24] from the centre of one of the trees yielded a date of 2500 ± 50 (GSC-2571) which when corrected for the age of the tree, which was estimated at 150 years, gives a date of 2350 ± 50 (Read [24]). Samples collected from the outer surfaces of trees in this investigation, gave dates of 2300 ± 90 (GSC-5190; Fig. 3) and 2410 ± 100 (GSC-5203).

Post-eruption landslide from Plinth Peak

In the Lillooet Valley adjacent to the river channel the vitroclastic breccia is overlain by a thick debris avalanche deposit (Fig. 2) which attains a thickness of at least 150 m. Further up the valley side slopes the deposit overlies Bridge River Tephra. The debris consists of large blocks in a finer matrix and covers an area of about 4 km^2 . It has an estimated volume in the order of $2\text{-}4 \times 10^8 \text{ m}^3$. The geometry of the deposit indicates that it blocked the Lillooet River up to el. 760 m, i.e. 75 metres above its present upstream channel.

Despite hazardous traverses over exposures in the deposit no organic materials have been recovered from the landslide debris to allow its dating. It is assumed that the landslide debris was emplaced immediately after the vitroclastic breccia since no weathering of the breccia surface is evident, and in most exposures the contact is sharp and clean. It is probable that it emanated from the steeper parts of Plinth Peak upslope of the vent at approximately 1500 m which were destabilised by the eruption.

As at the Mount Cayley prehistoric debris avalanche accumulation, described by Evans and Brooks ([6]), distal margins of the debris avalanche are difficult to define since they are transitional to debris flow facies downstream of location G in Fig. 2 which extend to at least location H in Fig. 2. These deposits may represent the result of catastrophic breaching of the dam created by the post-eruption landslide from Plinth Peak. No tephra

occurs on top of the deposit.

A small lava flow (Fig.2) was erupted into the bowl created by the detachment of the debris avalanche.

Later damming events in the Lillooet Valley

Upstream of Salal Creek, sediments formed by the damming of the Lillooet River are exposed in eroding river banks and form the flat marshy area of this part of the Lillooet Valley (Fig. 2). The sediments suggest a low energy environment in contrast to the present high energy fluvial environment of the Lillooet. They vary from fine sands and laminated silts to layered gravels and contain a large variety of organic remains including wood fragments and charcoal. Dating of some of these remains has yielded a perplexing result (Table 1) which is still being evaluated on the basis of more detailed dating of the sediments currently underway. In contrast to the expectation that the sediments are related to the damming of the Lillooet River by the products of the Plinth Peak eruption, and/or the post-eruption landslide at about 2350 y BP, the dates indicate much younger damming events at 1860 ± 50 (GSC-5278) and 1090 ± 50 (GSC-5370).

GSC-5278 is from a tree stump still in growing position rooted on a debris avalanche deposit and which was drowned by the rising waters in the landslide dammed lake. The nature and location of the dam responsible for ponding the Lillooet upstream of Salal Creek at about 1860 y BP has not as yet been ascertained. GSC-5370 is from near the top of the ponding sequence.

A damming at 900 y BP is indicated by dates 900 ± 60 (GSC-3498) and 890 ± 90 (GSC-4290), obtained by P.B. Read and P. Jordan from a debris avalanche diamicton exposed just upstream from Salal Creek. According to Read [23], the debris avalanche emanated from between 1525 and 2125 m on the NE flank of Plinth Peak, fell to about the 670 m in the Lillooet valley, and climbed the opposite side of the valley to about 940 m. The 900 y BP event blocked the Lillooet River and sediments deposited in the ponding are exposed upstream.

TABLE 1: Radiocarbon dates from deposits in the Lillooet River valley near Plinth Peak

GSC Lab. No.	Collector	Date	Material and enclosing deposit	Location in Fig. 2
<u>Lillooet River Canyon</u>				
GSC-2571	P.B. Read	2500±50 ¹	Charred tree buried by Bridge River tephra	A
GSC-5190	S.G. Evans	2300±90	Charred tree buried by Bridge River tephra	A
GSC-5203	S.G. Evans	2410±100	Charred tree buried by Bridge River tephra	A
<u>Upstream of Salal Creek</u>				
GSC-3498	P.B. Read	900±60	Log in debris avalanche diamicton	B
GSC-4290	P. Jordan	890±90	Log in debris avalanche diamicton	B
GSC-5278	S.G. Evans	1860±50	Tree in ponded sediments	C
GSC-5370	S.G. Evans	1100±50	Log in ponded sediments	D

¹ Sample taken from centre of tree; date corrected to 2350±50 for approximate age of tree

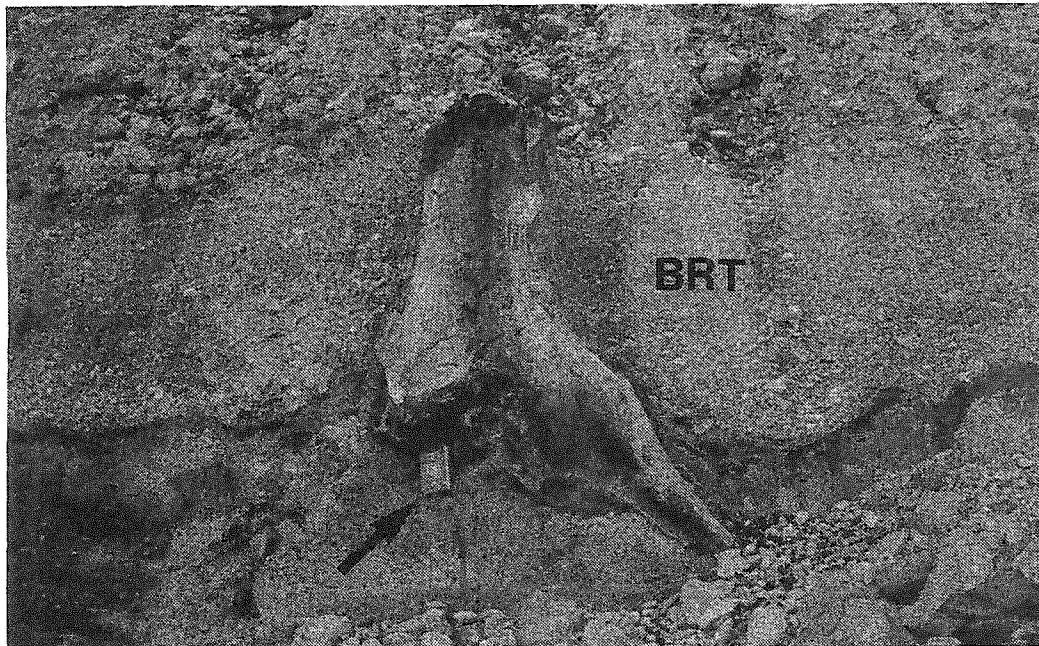


FIGURE 3. Tree stump in growing position buried by Bridge River Tephra (BRT) in Lillooet River canyon (location A in Figure 2). Wood sample from outer surface of tree yielded a radiocarbon age of 2300±90 (GSC 5190). Note field book (arrowed) for scale.

Conclusions

This paper contributes to evidence currently accumulating that numerous large-magnitude pre-historic debris avalanches have occurred in the volcanic centres of the Garibaldi Volcanic Belt, an area of southwest British Columbia which is of considerable strategic importance.

The most recent eruption took place in the Belt within the Mount Meager volcanic complex at Plinth Peak at about 2350 y BP and deposited the Bridge River tephra.

In this work evidence has been presented that major debris avalanches from Plinth Peak occurred before the eruption, directly after the eruption, and on more than two occasions up to at least 900 y BP. These landslides resulted in multiple dammings of the Lillooet River which may have breached in a catastrophic manner, similar to that inferred for the 1931 event in Devastation Creek noted above.

The hazard implicit in these findings are important to consider in future resource and possible energy development in the Upper Lillooet River valley. Work on landslide hazard in the Garibaldi Volcanic Belt continues.

Acknowledgements

I am grateful to Shane Dennison, Eugene MacDonald, and Matthew Evans for assistance in fieldwork in the Lillooet Valley - Plinth Peak area.

References

[1] Green, N.L., Armstrong, R.L., Harakal, J.E., Souther, J.C., and Read, P.B. 1988. Eruptive history and K-Ar geochronology of the Late Cenozoic Garibaldi Volcanic Belt, southern British Columbia. *Geological Society of America, Bulletin*, **100**: 563-579.

[2] Scott, W.E. 1990. Patterns of vulcanism in the Cascade Arc during the past 15,000 years. *Geoscience Canada*, **17**: 179-182.

[3] Read, P.B. 1977. Geology of the Meager Creek geothermal area, British Columbia. Geological Survey of

Canada Open File 603.

[4] Read, P.B. 1990. Mount Meager Complex, Garibaldi Belt, southwestern British Columbia. *Geoscience Canada*, **17**: 167-170

[5] Hardy, R.M., Morgenstern, N.R., and Patton, F.D. 1978. Report of the Garibaldi Advisory Panel. Unpublished report B.C. Department of Highways, Victoria, B.C.

[6] Evans, S.G. and Brooks, G.R. 1991. Prehistoric debris avalanches from Mount Cayley volcano, British Columbia. *Canadian Journal of Earth Sciences*, **28**: 1365-1374.

[7] Moore, D.P. and Mathews, W.H. 1978. The Rubble Creek landslide, southwestern British Columbia. *Canadian Journal of Earth Sciences*, **15**: 1039-1052.

[8] Jordan, P. 1987. Impacts of mass movement events on rivers in the southern Coast Mountains, British Columbia: summary report. Water Resources Branch, Inland Waters Directorate, Environment Canada, Report IWD-HQ-WRB-SS-87-3, 62 p.

[9] Clague, J.J., and Souther J.G. 1982. The Dusty Creek landslide on Mount Cayley, British Columbia. *Canadian Journal of Earth Sciences*, **19**: 524-539.

[10] Smith, H.R. and Patton, F.D. 1984. Comparison of the Devastation Glacier slide with other high velocity debris flows. 4th International Symposium on Landslides, Abstract volume, p.96.

[11] Evans, S.G. 1987. A rock avalanche from the peak of Mount Meager, British Columbia. *In* Current Research, Paper 87-1A, Geological Survey of Canada, Paper 87-1A, p. 929-933.

[12] Evans, S.G. 1986. Landslide damming in the Cordillera of western Canada: in *Landslide Dams. Processes, Risk and Mitigation*, ed. R.L. Schuster, American Society of Civil Engineers, Geotechnical Special Publication No. 3, pp. 111-130.

[13] Brooks, G.R., and Hickin, E.J. 1991. Debris avalanche impoundments of Squamish River, Mount Cayley area, southwestern British Columbia. *Canadian Journal of Earth Sciences*, **28**: 1375-1385.

[14] Evans, S.G. 1984. The landslide response to tectonic assemblages in the southern Canadian Cordillera.

Proceedings, IV International Symposium on Landslides. Toronto, 1: 495-502.

[15] Evans, S.G. 1990a. Landslides in the Cordillera ; an overview. Program with Abstracts, v. 15, Geological Association of Canada / Mineralogical Association of Canada, p. A38.

[16] Evans, S.G. 1990b. Massive debris avalanches from volcanoes in the Garibaldi Volcanic Belt, British Columbia. Program with Abstracts, v. 15, Geological Association of Canada / Mineralogical Association of Canada, p. A38.

[17] Nasmith, H., Mathews, W.H., and Rouse, G.E. 1967. Bridge River Ash and some other Recent ash beds in British Columbia. Canadian Journal of Earth Sciences, 4: 163-170

[18] Mathewes, R.W. and Westgate, J.A. 1980. Bridge River tephra: revised distribution and significance for detecting old carbon errors in radiocarbon dates of limnic sediments in southern British Columbia. Canadian Journal of Earth Sciences, 17: 1454-1461.

[19] Stasiuk, M.V. and Russell, J.K. 1989. Petrography and chemistry of the Meager Mountain volcanic complex, southwestern British Columbia. Geological Survey of Canada, Paper 89-1E, p. 189-196.

[20] Stasiuk, M.V. and Russell, J.K. 1990. The Bridge River Assemblage in the Meager Mountain volcanic complex, southwestern British Columbia. Geological Survey of Canada, Paper 90-1E, p. 227-233.

[21] Nevin, A.E. 1991. Geothermal projects at Mount Meager, British Columbia - history, geology, power marketing, and implications for the U.S. Cascades. Washington Geology, 19: 34-37.

[22] Jordan, P. and Slaymaker, O. 1991. Holocene sediment production in Lillooet River basin, British Columbia: a sediment budget approach. Geographie physique et Quaternaire, 45: 45-57.

[23] Carter, N.M. 1932. Exploration in the Lillooet River watershed. Canadian Alpine Journal, 21: 8-18.

[24] Read, P.B. 1983. Meager Creek Series. In W.Blake (Ed.) Geological Survey of Canada, Radiocarbon Dates XXIII, Geological Survey of Canada Paper 83-7, pp.20-21.